



An Introduction to Hydraulic Testing in Hydrogeology

Basic Pumping, Slug, and Packer Methods

William W. Woessner, A. Campbell Stringer
and Eileen P. Poeter

*An Introduction to Hydraulic
Testing in Hydrogeology
Basic Pumping, Slug, and Packer Methods*

The Groundwater Project

William W. Woessner

*Emeritus Regents' Professor of Hydrogeology
University of Montana
Missoula, Montana, USA*

A. Campbell Stringer PG

*Principal Hydrogeologist
NewFields
Missoula, Montana USA*

Eileen P. Poeter PE

*Emeritus Professor of Geological Engineering
Colorado School of Mines
Golden Colorado, USA*

***An Introduction to Hydraulic
Testing in Hydrogeology
Basic Pumping, Slug, and Packer Methods***

*The Groundwater Project
Guelph, Ontario, Canada
Version 3, March, 2024*

All rights reserved. This publication is protected by copyright. No part of this book may be reproduced in any form or by any means without permission in writing from the authors (to request permission contact: permissions@gw-project.org). Commercial distribution and reproduction are strictly prohibited.

Groundwater-Project (The GW-Project) works are copyrighted and can be downloaded for free from gw-project.org. Anyone may use and share gw-project.org links to download GW-Project's work. It is not permissible to make GW-Project documents available on other websites nor to send copies of the documents directly to others. Kindly honor this source of free knowledge that benefits you and all those who want to learn about groundwater.

Copyright © 2023 William W. Woessner, A. Campbell Stringer, and Eileen P. Poeter
(The Author/s)

Published by the Groundwater Project, Guelph, Ontario, Canada, 2023.

An Introduction to Hydraulic Testing in Hydrogeology: Basic Pumping, Slug, and Packer Methods / William W. Woessner, A. Campbell Stringer, and Eileen P. Poeter
352 pages
ISBN: 978-1-77470-090-7
DOI: <https://doi.org/10.21083/978-1-77470-090-7>.

Please consider signing up for the GW-Project mailing list to stay informed about new book releases, events, and ways to participate in the GW-Project. When you sign up for our email list it helps us build a global groundwater community. [Sign up](#).

APA (7th ed.) Citation:

Woessner, W. W., Stringer, A. C. & Poeter, E.P. (2023). *An introduction to hydraulic testing in hydrogeology: Basic pumping, slug, and packer methods*. The Groundwater Project. <https://doi.org/10.21083/978-1-77470-090-7>.



Domain Editors: Eileen Poeter and John Cherry

Board: John Cherry, Richard Jackson, Ineke Kalwij, Everton de Oliveira and Eileen Poeter

Steering Committee: John Cherry, Allan Freeze, Paul Hsieh, Ineke Kalwij, Douglas Mackay, Stephen Moran, Everton de Oliveira, Beth Parker, Eileen Poeter, Ying Fan, Warren Wood, and Yan Zheng.

Cover Image: National Water Services LLC., Paoli, IN, USA

Table of Contents

TABLE OF CONTENTS	IV
THE GROUNDWATER PROJECT FOREWORD	IX
FOREWORD	X
PREFACE	XI
ACKNOWLEDGMENTS	XII
OVERVIEW	1
1 INTRODUCTION	2
2 TYPES OF HYDRAULIC TESTS	4
2.1 PUMPING TESTS.....	5
2.2 SLUG TESTS.....	6
2.3 TESTING WITH PACKERS.....	6
2.4 TEXT ORGANIZATION	6
PART 1: PUMPING TESTS	7
3 CONCEPTUALIZING GROUNDWATER FLOW TO WELLS	8
3.1 DEVELOPMENT OF THE CONE OF DEPRESSION UNDER TRANSIENT CONDITIONS	8
3.2 THE CONE OF DEPRESSION UNDER STEADY-STATE CONDITIONS	12
4 SETTING A PURPOSE, DESIGNING, AND CONDUCTING A PUMPING TEST	15
4.1 PURPOSE.....	17
4.2 COMPILING AND INTERPRETING EXISTING DATA SETS	17
4.3 PUMPING AND OBSERVATION WELL DESIGN AND CONSTRUCTION DATA	19
4.3.1 <i>Design of Pumping and Observation Wells</i>	19
4.3.2 <i>Observation Well Spacing</i>	22
4.4 PUMPING TEST COMPONENTS AND DESIGN	23
4.4.1 <i>Selecting the Pumping Rate</i>	23
4.4.2 <i>Selecting the Duration of the Pumping Test</i>	23
4.4.3 <i>Choosing a Pump and Power Supply</i>	24
4.5 WATER LEVEL AND DISCHARGE MEASUREMENT SCHEDULES.....	25
5 TEST EXECUTION AND DATA ANALYSIS	28
5.1 MEASURING AND RECORDING WATER LEVELS	28
5.2 ESTABLISHING BASELINE CONDITIONS AND WATER LEVEL TRENDS	32
5.3 METHODS TO MEASURE AND MAINTAIN A PUMPING RATE	32
5.4 DATA ANALYSIS	35
5.4.1 <i>Correcting Water Level Data</i>	35
5.4.2 <i>Determining the Test Pumping Rate for Analysis</i>	37
5.5 NOTES FOR SUCCESSFUL TEST EXECUTION.....	37
6 MATHEMATICS OF FLOW TO A PUMPING WELL	39
6.1 USING POLAR COORDINATES	39
6.2 DEVELOPMENT OF EQUATIONS DESCRIBING AQUIFER RESPONSES TO PUMPING	39
6.2.1 <i>Confined Aquifers</i>	40
6.2.2 <i>Unconfined Aquifers</i>	42
6.3 GENERAL ASSUMPTIONS USED TO DEVELOP ANALYTICAL WELL HYDRAULIC EQUATIONS.....	44

7	THEIM STEADY-STATE ANALYTICAL MODELS FOR PUMPING CONFINED AND UNCONFINED AQUIFERS	47
7.1	STEADY-STATE CONDITIONS IN A CONFINED GROUNDWATER SYSTEM	47
7.2	STEADY-STATE CONDITIONS IN AN UNCONFINED AQUIFER	50
7.3	AN OPPORTUNITY TO WORK WITH STEADY-STATE PUMPING TEST DATA	56
8	TRANSIENT ANALYTICAL MODEL FOR PUMPING OF A FULLY CONFINED AQUIFER	57
8.1	FORMULATION OF THE THEIS EQUATION	57
8.2	USING THE THEIS EQUATION TO PREDICT DRAWDOWNS IN TOTALLY CONFINED AQUIFERS	64
8.3	COMPUTING T AND S FROM HYDRAULIC TEST DATA USING THE THEIS METHOD	65
8.3.1	<i>Theis Curve Matching Method</i>	65
8.3.2	<i>Cooper-Jacob Straight Line Method</i>	70
8.3.3	<i>Cooper-Jacob Distance-Drawdown Method</i>	74
8.3.4	<i>Analyzing Recovery Data</i>	78
8.3.5	<i>Variable Discharge Pumping Test</i>	82
8.3.6	<i>Applicability Of Methods Presented in this Section</i>	83
8.4	AN OPPORTUNITY TO WORK WITH PUMPING TEST DATA FROM A CONFINED AQUIFER	85
9	TRANSIENT ANALYTICAL MODELS FOR PUMPING IN A LEAKY CONFINED AQUIFER	86
9.1	FORMULATION OF EQUATIONS TO ADDRESS LEAKY CONFINED CONDITIONS	86
9.2	HANTUSH-JACOB SOLUTION (LEAKY CONFINED-NO WATER RELEASED FROM AQUITARD STORAGE)	88
9.2.1	<i>Formulation of the Hantush-Jacob Equation</i>	88
9.2.2	<i>Predicting Drawdown in Leaky Confining System with the Hantush-Jacob Equation</i>	90
9.2.3	<i>Pumping Test Data from a Confining Aquifer with a Leaky Confining Bed Without Additional Water Released from Aquitard Storage</i>	91
9.2.4	<i>Hantush-Jacob Curve Matching Method for a Pumping Test in a Confining Aquifer with a Leaky Confining Bed Without Water Released from Aquitard Storage</i>	92
9.2.5	<i>Hantush Inflection-Point Method for a Pumping Test in a Confining Aquifer with a Leaky Confining Bed Without Water Released from Aquitard Storage</i>	94
9.3	HANTUSH EQUATION FOR A LEAKY CONFINED SYSTEM WITH WATER RELEASED FROM CONFINING BED STORAGE ..	99
9.3.1	<i>Using the Hantush Equation to Predict Drawdown in Leaky Confining Units with Water Released from Confining Bed Storage</i>	102
9.3.2	<i>Hantush Curve Matching Method to Compute T and S from a Pumping Test in Leaky Confining Unit with Aquitard Storage</i>	104
9.4	AN OPPORTUNITY TO WORK WITH PUMPING TEST DATA FROM A LEAKY CONFINED AQUIFER	107
10	TRANSIENT ANALYTICAL MODELS FOR PUMPING AN UNCONFINED AQUIFER	108
10.1	APPROXIMATING THE RESPONSE OF PUMPING UNCONFINED AQUIFERS USING THEIS APPROACH	108
10.1.1	<i>Pumping Test Analysis</i>	111
10.2	FORMULATING EQUATIONS TO REPRESENT THE DELAYED YIELD RESPONSE	113
10.3	FORMULATING DELAYED YIELD ANALYSIS	116
10.3.1	<i>Mathematical Development of a Delayed Yield Analysis Method</i>	117
10.4	COMPUTING T AND S FROM AQUIFER TEST DATA	120
11	EFFECTS OF WELL INTERFERENCE, BOUNDARIES, AND AQUIFER ANISOTROPY ON DRAWDOWN ...	126
11.1	WELL INTERFERENCE	126
11.2	USING SUPERPOSITION TO REPRESENT SIMPLE BOUNDARY CONDITIONS	130
11.2.1	<i>Image Well Methodology</i>	133
11.2.2	<i>Linear Impermeable and Recharge Boundaries</i>	133
11.3	DEVELOPMENT OF CONES OF DEPRESSION IN ANISOTROPIC HETEROGENEOUS MATERIAL	138

11.4	AN OPPORTUNITY TO USE WELL HYDRAULICS TO EVALUATE WELL INTERFERENCE IN THE PRESENCE OF A RECHARGE BOUNDARY	140
12	ESTIMATING HYDROGEOLOGIC PROPERTIES USING A SINGLE PUMPING WELL	141
12.1	SPECIAL CONSIDERATIONS WHEN USING DRAWDOWN DATA FROM A PUMPING WELL.....	141
12.1.1	<i>Partial Penetration</i>	143
12.1.2	<i>Well Loss and Using Step-Drawdown Tests to Assess Loss</i>	147
12.1.3	<i>Well Interference</i>	157
12.1.4	<i>Other Conditions that Effect Pumping Well Drawdown</i>	157
12.2	DRAWDOWN AND RECOVERY CURVE-MATCHING METHODS FOR A SINGLE PUMPING WELL.....	158
12.2.1	<i>Analyzing Time-Drawdown Data</i>	158
12.2.2	<i>Analyzing Recovery Data</i>	160
12.3	STEADY-STATE APPROXIMATION OF TRANSMISSIVITY	162
12.4	PERFORMANCE TESTS, SPECIFIC CAPACITY DATA, AND ESTIMATING T	165
12.4.1	<i>Cautions when Using Performance Test Results</i>	165
12.4.2	<i>Methods to Estimate Transmissivity from Performance Tests</i>	166
12.4.3	<i>Using Specific Capacity to Estimate Transmissivity Assuming Steady-State Conditions</i>	167
12.4.4	<i>Using Specific Capacity Data to Estimate Transmissivity Assuming Transient Conditions</i>	167
12.4.5	<i>Basic Equations Relating Specific Capacity to Transmissivity</i>	170
12.5	AN OPPORTUNITY TO EVALUATE HYDROGEOLOGIC PROPERTIES USING DATA FROM A PUMPING WELL	172
13	USING SOFTWARE TO ANALYZE HYDRAULIC TEST DATA WITH A PUMPING WELL	173
13.1	PUMPING TEST ANALYSIS SOFTWARE PACKAGES	174
13.2	DATA PLOTTING AND CURVE-MATCHING METHODS	177
	PART 2: SLUG TESTS	180
14	ESTIMATING HYDROGEOLOGIC PROPERTIES USING A SINGLE UNPUMPED WELL.....	181
14.1	THE SLUG TEST	181
14.2	PERFORMING A SLUG TEST.....	184
14.2.1	<i>Assessing the Hydrogeologic Setting and Well Construction</i>	184
14.2.2	<i>Special Considerations for Water Table Systems</i>	185
14.2.3	<i>Free Exchange of Water with the Formation</i>	186
14.2.4	<i>Raising and Lowering the Water Level</i>	188
14.2.5	<i>Recording Water-Level Change</i>	190
14.2.6	<i>Test Repeatability</i>	191
14.3	FIELD DATA: OVERDAMPED, UNDERDAMPED AND CRITICALLY DAMPED WATER-LEVEL RESPONSES TO SLUG TESTS 191	
14.4	METHODS TO INTERPRET OVERDAMPED SLUG TESTS	194
14.4.1	<i>Hvorslev Slug Test Method</i>	194
14.4.2	<i>Bouwer and Rice Slug-Test Method</i>	202
14.4.3	<i>Cooper-Bredehoeft-Papadopulos Slug-Test Method</i>	206
14.4.4	<i>KGS Slug Test Method</i>	212
14.5	METHOD TO INTERPRET UNDERDAMPED SLUG TESTS.....	217
14.5.1	<i>Development of Type-Curve Equations</i>	219
14.5.2	<i>Unconfined-High-K Bouwer and Rice Model</i>	222
14.5.3	<i>Confined – High-K Hvorslev Model</i>	222
14.5.4	<i>Transitional Slug-Test Responses</i>	224
14.6	SOFTWARE AVAILABLE TO ANALYZE SLUG TESTS.....	224
14.7	AN OPPORTUNITY TO EVALUATE HYDROGEOLOGIC PROPERTIES USING SLUG-TEST DATA.....	225
	PART 3: PACKER TESTS	226

15	BASIC HYDRAULIC TESTING WITH PACKERS	227
15.1	THE PACKER TEST.....	227
15.1.1	<i>Selecting the Test Interval</i>	229
15.1.2	<i>Setting up the Packer System</i>	230
15.2	TESTING METHODS AND ANALYSES.....	231
15.2.1	<i>Slug Tests</i>	232
15.2.2	<i>Constant-Rate Pumping Tests</i>	232
15.2.3	<i>Constant-Head Injection/Withdrawal Test</i>	232
15.2.4	<i>Step-Rate Injection Test (Lugeon Test)</i>	234
15.2.5	<i>Drill-Stem Test</i>	239
16	SPECIAL CONSIDERATIONS FOR CHARACTERIZING LOW-PERMEABILITY SYSTEMS, AQUITARDS	240
16.1	PROPERTIES OF AQUITARDS.....	240
16.2	TEST METHODS USED TO ESTIMATE AQUITARD PROPERTIES.....	242
16.2.1	<i>Internal Methods</i>	243
16.2.2	<i>External Methods</i>	246
17	WRAP-UP	253
18	EXERCISES	255
	EXERCISE 1.....	256
	EXERCISE 2.....	257
	EXERCISE 3.....	259
	EXERCISE 4.....	260
	EXERCISE 5.....	261
	EXERCISE 6.....	262
	EXERCISE 7.....	264
19	REFERENCES	265
20	BOXES	276
	BOX 1 SAMPLES OF GRAPH PAPER FOR CURVE MATCHING METHODS.....	276
	BOX 2 ESTIMATING STORATIVITY AND SPECIFIC STORAGE (Ss).....	279
	BOX 3 IMAGE WELL THEORY APPLICATION WHEN TWO LINEAR BOUNDARIES ARE PRESENT.....	285
	BOX 4 PRODUCTION WELL EFFICIENCY.....	288
	BOX 5 AQTESOLV.....	290
	BOX 6 AQUIFERTEST V12.....	292
	BOX 7 AQUIFER ^{WIN32} V6.....	297
	BOX 8 SOFTWARE USED TO ANALYZE SLUG TESTS.....	300
	BOX 9 LABORATORY METHODS USED TO DETERMINE HYDRAULIC PROPERTIES OF AQUITARDS AND LOW PERMEABILITY FORMATIONS.....	302
	<i>Box 9.1 Falling Head Permeameter (modified from Box 4.3 of Woessner and Poeter (2020))</i>	302
	<i>Box 9.2 Triaxial Permeability Test</i>	303
	<i>Box 9.3 Consolidometer</i>	304
	BOX 10 REPRODUCTION OF FIGURES FROM ROWE AND NADARAJAH (1993) CORRECTION FACTORS.....	307
	BOX 11 AQTESOLV SOLUTIONS TO EXERCISES.....	309
	<i>Box 11.1 AQTESOLV Solution for Exercise 2</i>	309
	<i>Box 11.2 AQTESOLV Solution for Exercise 3 a and b</i>	312
	<i>Box 11.3 AQTESOLV Solution for Exercise 5</i>	315
	<i>Box 11.4 AQTESOLV Solution for Exercise 7</i>	316
21	EXERCISE SOLUTIONS	317
	SOLUTION EXERCISE 1.....	317

SOLUTION EXERCISE 2	320
SOLUTION EXERCISE 3	328
SOLUTION EXERCISE 4	332
SOLUTION EXERCISE 5	337
SOLUTION EXERCISE 6	342
SOLUTION EXERCISE 7	347
22 ABOUT THE AUTHORS	350
MODIFICATIONS TO ORIGINAL RELEASE	A

The Groundwater Project Foreword

At the United Nations (UN) Water Summit held on December 2022, delegates agreed that statements from all major groundwater-related events will be unified in 2023 into one comprehensive groundwater message. This message will be released at the UN 2023 Water Conference, a landmark event that will bring attention at the highest international level to the importance of groundwater for the future of humanity and ecosystems. This message will bring clarity to groundwater issues to advance understanding globally of the challenges faced and actions needed to resolve the world's groundwater problems. Groundwater education is key.

The 2023 World Water Day theme *Accelerating Change* is in sync with the goal of the Groundwater Project (GW-Project). The GW-Project is a registered Canadian charity founded in 2018 and committed to the advancement of groundwater education as a means to accelerate action related to our essential groundwater resources. To this end, we create and disseminate knowledge through a unique approach: the democratization of groundwater knowledge. We act on this principle through our website, <https://gw-project.org/>, a global platform, based on the principle that

“Knowledge should be free, and the best knowledge should be free knowledge.” Anonymous

The mission of the GW-Project is to promote groundwater learning across the globe. This is accomplished by providing accessible, engaging, and high-quality educational materials—free-of-charge online and in many languages—to all who want to learn about groundwater. In short, the GW-Project provides essential knowledge and tools needed to develop groundwater sustainably for the future of humanity and ecosystems. This is a new type of global educational endeavor that is made possible through the contributions of a dedicated international group of volunteer professionals from diverse disciplines. Academics, consultants, and retirees contribute by writing and/or reviewing the books aimed at diverse levels of readers from children to high school, undergraduate and graduate students, or professionals in the groundwater field. More than 1,000 dedicated volunteers from 127 countries and six continents are involved—and participation is growing.

Hundreds of books will be published online over the coming years, first in English and then in other languages. An important tenet of GW-Project books is a strong emphasis on visualization; with clear illustrations to stimulate spatial and critical thinking. In future, the publications will also include videos and other dynamic learning tools. Revised editions of the books are published from time to time. Users are invited to propose revisions.

We thank you for being part of the GW-Project Community. We hope to hear from you about your experience with the project materials, and welcome ideas and volunteers!

The GW-Project Board of Directors

January 2023

Foreword

The subject matter of this book, hydraulic testing, is foundational to nearly all groundwater investigations because the tests provide values of transmissivity (which can be used to estimate hydraulic conductivity). Hydraulic conductivity and hydraulic head are the two most important parameters in groundwater science. When conducted under transient conditions, hydraulic tests also provide values for storativity or specific yield.

Hydraulic testing involves estimating values of hydraulic parameters—primarily hydraulic conductivity—from field observations of changes in hydraulic head. These changes result from withdrawal or injection of water at measured rates out of or into boreholes in geologic media. This parameter estimation process is underpinned by mathematical models representing head changes in response to withdrawal or injection of water. Conditions in the field always have complexity that cannot be represented fully in the models. Thus, conceptualizations of hydrogeologic conditions need to be simplified to develop mathematical solutions. Given these simplifications, the parameter values obtained from the process are appropriately regarded as estimated, not measured, values in the normal use of the word ‘measurement’.

It is common for the assumptions underlying the model simplifications to be overlooked such that inappropriate models are applied to test data resulting in poor estimates of the parameters. This book provides clear concise explanations that can help groundwater professionals avoid misapplying models to hydraulic test data.

The extraction of parameter values from hydraulic tests involves uncertainty and those who become experts in this endeavor, which is a combination of art and science, have accumulated valuable experience in interpreting hydraulic test results. This book introduces the most important mathematical models that are the heart of hydraulic testing in groundwater practice. In addition, it provides guidance on designing hydraulic tests. All the concepts related to hydraulic testing are expressed in diagrams to facilitate visualization of hydrogeologic conditions and in graphs to illustrate system response to hydraulic testing.

The authors of this book, William Woessner, Emeritus Regents’ Professor of Hydrogeology, University of Montana, A. Campbell Stringer, Principal Hydrogeologist, NewFields, Montana, and Eileen Poeter, Emeritus Professor of Geological Engineering, Colorado School of Mines bring over 60 years of academic teaching and research experience, and a combined 90 years of applied hydrogeology consulting to the production of this book.

John Cherry, The Groundwater Project Leader
Guelph, Ontario, Canada, September 2023

Preface

All groundwater investigations (including resource investigations, development of water supplies, and identification and remediation of contaminated sites) require deriving field-based values of basic hydrogeologic properties such as hydraulic conductivity, transmissivity and storativity. In the earlier Groundwater Project book *Hydrogeologic Properties of Earth Materials and Principles of Groundwater Flow* (Woessner & Poeter, 2020) groundwater principles and parameters were defined. Discussion of methods to determine parameters focused on laboratory methods and referenced field hydraulic testing methods but did not provide details on application. This book is a companion to that earlier work, as well as a standalone document that provides foundational methods used to generate field-scale representations of common hydraulic parameters. The book presents a conceptual view of how hydraulic testing methods such as the pumping tests, slug tests, and testing with packers are applied, as well as the advantages and limitations of the underpinning analytical solutions. The book focuses on methods addressing simplified confined, leaky confined and unconfined groundwater systems. It explains how curve-matching of field test data to analytical models is used to interpret test results. Though software for analyzing hydraulic test data is briefly discussed, some of which include choices of several additional analytical models and one-button automated analysis, this book emphasizes basic concepts, principles, and methods. For application of available software, the reader is sent to the program websites and documentation. The main body of text along with many illustrations, examples, and exercises with solutions provide the reader with the information needed to correctly apply hydraulic testing and analytical methods. The authors bring over 60 years of academic teaching and research experience, and an additional 90 years of applied hydrogeology consulting to the production of this book.

Acknowledgments

We deeply appreciate the thorough and useful reviews of and contributions to this book by the following individuals:

- ❖ John Wilson, for review, New Mexico Tech, USA;
- ❖ Garth van der Kamp, for review, University of Saskatchewan, Canada;
- ❖ Christopher Neville, for review, S.S. Papadopoulos & Associates, Inc., USA;
- ❖ Kamini Singha, for review, Colorado School of Mines, USA;
- ❖ Thomas Osborne for assistance in setting content and editing, HydroSolutions Inc., USA;
- ❖ Robert Sterrett for assistance in setting content and editing, RJS Consulting, Inc., USA; and,
- ❖ David Rugh for assistance with content related to and editing borehole hydraulic testing, NewFields, USA.

We are grateful for Amanda Sills and the Formatting Team of the Groundwater Project for their oversight and copyediting of this book.

OVERVIEW

This book introduces how hydraulic testing is used to derive field-scale values of hydrogeologic properties using three basic hydraulic testing methods: pumping tests, slug tests, and packer tests. The introductory material describes the response of the groundwater system to testing and approaches used to analyze test data. Section 1, *Introduction*, states the goal, provides a general definition of hydraulic testing, and describes the response of a groundwater system to testing. Section 2, *Types of Hydraulic Tests*, defines three types of hydraulic testing applied by hydrogeologists and concludes with a subsection explaining the organization of the remainder of the book. The overview section is followed by three parts: *Pumping Tests*, *Slug Tests*, and *Packer Tests*.

For students and professionals who are new to the topic of hydraulic testing emphasis should be placed on reading the material provided in the Part 1, *Pumping Tests*, Sections 1 through 11 and Part 2, *Slug Tests*, Section 14. Practitioners more familiar with hydraulic testing will find much of the material presented in Parts 1 and 2 similar to material they have been exposed to previously. Practicing hydrogeologists will likely be interested in the content of Section 12 that addresses methods used to analyze tests of a single pumping well; Section 13 that describes the use of software to analyze pumping tests; Section 15 about methods to conduct and analyze packer tests; and Section 16 that summarizes methods to determine hydraulic properties of low permeable material.



Pumping Test



Slug Test



Testing with Packers

These images show examples of equipment set up used for pumping, pneumatic slug, and testing with packers. The photography is used with permission: pumping test (Newfields-Missoula, MT, USA), slug test (geoprobe.com), and packer test (<https://www.usgs.gov/media/images/photograph-usgs-hydrologists-and-packers-well-testing>).

1 Introduction

This book provides the basic theory and tools needed to assist readers in understanding the responsible application of hydraulic testing methods to generate field-scale hydrogeologic properties of groundwater systems. We describe methods used to conduct pumping tests, slug tests, and open borehole testing with packers, analyze test results, and use results to forecast future responses of groundwater systems to the extraction or injection of water. The material in this book is supported by extensive literature covering hydraulic testing. This includes newly published groundwater books and copies of original works available for free on the [Groundwater Project website](#)[↗] (e.g., *Groundwater Storage in Confined Aquifers*, Wang, 2020; *Transient Groundwater Hydraulics*, Glover, 1974; *Ground-water Hydrology and Hydraulics*, McWhorter & Sunada, 1977; *Groundwater*, Freeze & Cherry, 1979; *Analysis and Evaluation of Pumping Test Data*, Kruseman & de Ridder, 2000). Additional literature includes hydrogeology textbooks (e.g., Walton, 1970; Fetter, 2001; Schwartz & Zhang, 2003; Kasenow, 2001; Todd & Mayes, 2005; Weight, 2019), and numerous free federal, state, and local agency publications (e.g., [Ground-Water Hydraulics](#)[↗]; Lohman, 1972). This book summarizes and condenses much of the material found in these references and provides detailed descriptions of field methods and hydraulic testing data analysis techniques.

The magnitude and extent of water level changes observed during hydraulic tests reflect the distribution of storage and transmission properties of the saturated material being tested. Hydrogeologists rely on hydraulic testing to evaluate well performance and to characterize the groundwater system including values of hydraulic conductivity, transmissivity, and storativity, as well as recharge sources, rates of leakage between geologic units, and the presence of local boundary conditions. Results of testing are used to predict the response of the groundwater system to changes in pumping and recharge and to assess contaminant movement.

Hydraulic tests can be conducted using a single pumping well, a pumping well with observation wells, and in open boreholes. Hydraulic tests usually include measuring changes in water levels over time. Water levels during some hydraulic tests reach steady state. Analysis of both transient and steady-state water-level data can yield estimates of hydrogeological properties. Hydraulic tests can be performed on aquifers that freely yield water to wells, and in lower permeability units such as aquitards and fractured rock systems. Testing can also include the pumping of multiple wells to investigate the interaction and interconnection of groundwater in complex geological settings.

Methods described in this book focus on the application of analytical solutions derived from governing equations, stated initial conditions, and boundary conditions. Once mastered, standard analytical techniques can be applied to a wide variety of hydraulic testing settings.

It is assumed the reader has a general knowledge of hydrogeology such as is covered in the Groundwater Project book *Hydrogeologic Properties of Earth Materials and Groundwater Flow* [↗](#) (Woessner & Poeter, 2020). Additional hydrogeologic terms used in this text will be defined when introduced.

2 Types of Hydraulic Tests

There are three main types of field-scale hydraulic tests: pumping tests, slug tests, and testing with packers (Figure 1). Pumping tests involve pumping or injecting water from/to a well. Slug tests involve quickly raising or lowering the water level in a well bore without pumping. Testing with packers involves isolating intervals in open boreholes using an inflatable bladder and displacing borehole water. Hydraulic tests are commonly referred to as aquifer tests, where aquifers are saturated geologic materials that store and transmit water in sufficient quantities and rates such that they can be sources of water for humans (Woessner & Poeter, 2020). Despite that terminology, they are also commonly used to characterize hydrogeologic properties of less permeable units that do not meet the definition of an aquifer. Hydraulic tests are sometimes referred to as “pump tests.” Though this is used as an abbreviated term for a pumping test, the wording indicates a test of the pump (e.g., is it working, what sustained yield can it produce, and so on) as opposed to an evaluation of subsurface properties. In units where head is above the ground level, an uncapped well in the unit may flow without the use of a pump. Hydraulic testing of flowing wells will be referred to as a pumping test in this book because natural conditions are “pumping” the well. Thus, pumping test is the preferred term used in this text.

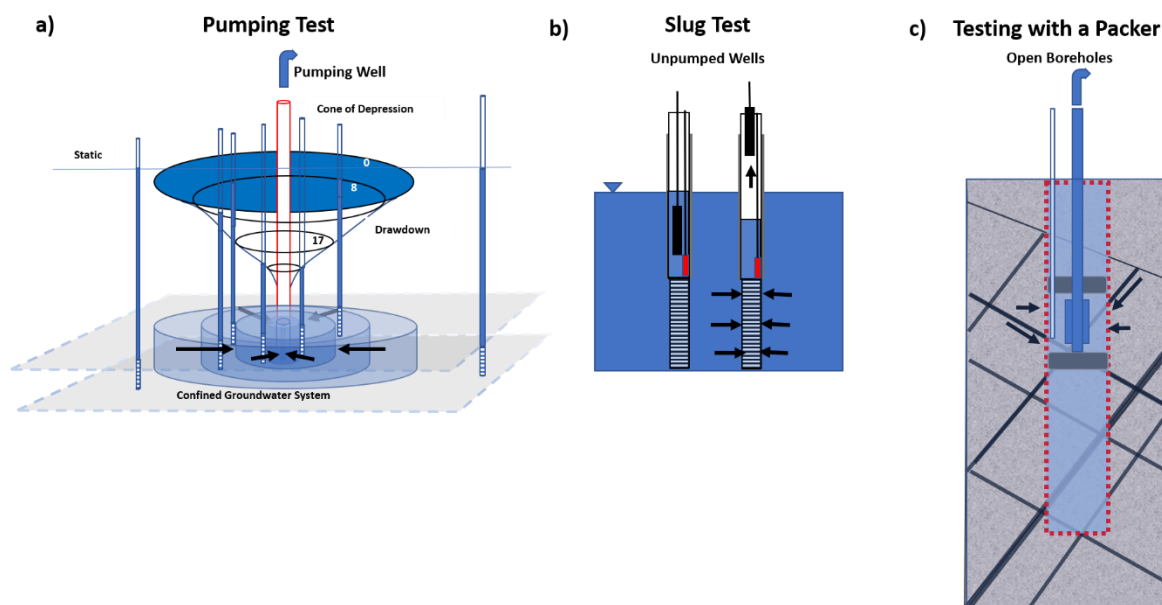


Figure 1 - Schematic of three types of hydraulic tests. Black arrows indicate the direction of groundwater flow. a) Pumping test where a well in a groundwater system is pumped and the change in water levels are observed in the pumping well and observation wells (smaller-diameter surrounding wells). The potentiometric surface at a specific time during the test is shown to represent the drawdown (initial water level minus pumping-induced water level). This drawdown is called the cone of depression. b) Slug test where a solid cylinder is inserted or removed from a well causing an abrupt change of water level in the well, then the water level recovery is monitored over time. c) Testing with packers in an open borehole where a section of an open borehole (red dashed lines) intersecting fractures (blue and gray intersecting lines) of a rock in a groundwater system is isolated with packers (gray rectangles). The interval between the packers is pumped and water levels are monitored through time.

2.1 Pumping Tests

When a well is pumped, water levels in the pumping well and adjacent groundwater system decrease over time. This decrease is referred to as *drawdown* (Figure 1). Drawdown is defined as the difference between the beginning (initial or static) water level in a well and the water level at some time after pumping has begun (a positive value). Events unrelated to the pumping may affect water levels in the aquifer, thus the so-called static water level needs to be adjusted to the level that would exist if the other events did not occur, so in this book the static water level is referred to as the corrected static water level. Drawdown generally increases as the well is pumped until the system reaches a steady state or withdrawal from other wells in the vicinity decreases. In some pumping tests, water is pumped into the test well (injected) at a prescribed rate instead of water being pumped from the well. In this case, water levels in the formation rise from initial levels—and instead of drawdown, the water levels drawup (i.e., have negative drawdown). Pumping tests are typically conducted in one well while monitoring water levels in one or more unpumped observation wells, but sometimes pumping tests are conducted using a single well with no monitoring wells.

Time-drawdown data are collected from each well included in the test, and analytical or numerical methods are used to generate information on the hydrogeologic properties of the system. Pumping tests can be conducted using constant and/or variable pumping rates, or a constant drawdown. Though packer testing within an open borehole can include pumping, they will be described in a section on packer methods (Section 15).

Constant-rate tests (the most common type of pumping test) are designed to maintain discharge at a continuous rate throughout the test, which simplifies data analysis (as discussed in later sections of this book). Although it is practically difficult to maintain a constant discharge rate, this approach is preferable because using a variable pumping rate requires a more complex analysis. Specifically designed variable-rate pumping tests are used to estimate formational properties and quantify how the well design and pumping rate affect the magnitude of drawdown in the pumping well. In some settings, such as when a well flows under natural conditions at the surface and discharge declines over time, or when water is extracted at a variable rate to maintain a constant water level over time, then a constant drawdown method is used to analyze the results for estimation of hydrogeologic properties (e.g., Lohman, 1972).

Hydraulic testing sometimes involves pumping multiple wells to investigate how other pumping wells or observation wells respond to stresses located over a specific area. For example, given a complex fractured-bedrock groundwater system in which mine dewatering is planned or potential water supply is being explored, use of multiple pumping wells can evaluate the interconnectedness of the system.

2.2 Slug Tests

A slug test is performed by rapidly displacing water in the well and observing the recovery of the water level over time (Figure 1b). The water can be displaced by inserting or removing an object or, in a low hydraulic conductivity material, by pumping water from the well, as long as the pumping is brief relative to the recovery. Different analytical methods are available for analyzing the test data depending on the well design and water-bearing unit types (e.g., confined, or unconfined). Slug tests can be performed on small-diameter wells in which pump installation is problematic. Slug tests may also be chosen to evaluate low- and high-yielding groundwater units and at locations with contaminated groundwater, where pumping tests are impractical because discharge cannot be disposed of economically.

2.3 Testing with Packers

Uncased boreholes can be tested using packers. The test isolates a portion of the borehole using a single packer or a set of double packers (Figure 1c). The interval of interest is then tested using pumping, injection, or slug methods. These tests involve monitoring head changes over time in response to the addition or extraction of water and are analyzed using analytical and numerical methods.

2.4 Text Organization

The remainder of this book is organized into three parts discussing each method in detail: Pumping Tests, Slug Tests, and Testing with Packers. A final section addresses approaches used to characterize low-permeability formations such as aquitards. Each part begins with conceptual models of how testing affects different types of groundwater systems (e.g., confined, leaky, unconfined). This text is followed by a description of test methodologies. Data analyses are framed by describing the theoretical mathematical foundation and available analytical methods used to estimate hydrogeological properties. Examples demonstrating the data analysis process are presented within the text. Linked boxes provide additional detail on some subjects. A notation section is not included because each variable is defined in each section following the equation in which it is used. The book concludes with a summary/wrap up, a set of problems including their solutions, and references.

PART 1: PUMPING TESTS

Part 1 includes Sections 3 through 13 and focuses on hydraulic tests that use a pumping well to perturb the water table or potentiometric surface in the target formation.

- Section 3 describes how groundwater systems respond to a pumping well.
- Test design and methods used to conduct a pumping test with observation wells are described in Section 4.
- Section 5 describes test execution and data collection.
- Section 6 provides mathematical foundation required to analyze pumping test results.
- Sections 7 through 10 describe analysis of steady-state and transient pumping test data sets under confined, leaky confined, and unconfined conditions. More specifically, analyses of confined and unconfined steady-state conditions are described in Section 7; while Sections 8, 9, and 10 describe transient pumping of fully confined, leaky confined, and unconfined aquifers, respectively.
- Section 11 addresses how pumping multiple wells under various boundary conditions influence pumping test results.
- Section 12 describes additional considerations required to analyze data when pumping tests are conducted using only one well.
- Section 13 describes how specialized software is used to analyze pumping test results.



This photograph shows a pumping test being conducted in an unconfined sand and gravel aquifer in the Bitterroot valley, Western Montana, USA. The photograph is used with permission from Montana Bureau of Mines and Geology (2023).

3 Conceptualizing Groundwater Flow to Wells

This section describes the conceptual framework of the mechanics of groundwater flow to a pumping well. Once a well is installed and the pumping system set up, the pump is started and water flows up the outflow pipe to the land surface. The flow of groundwater to a well is induced because the pump extracts water from the well bore drawing down the water level in the well. This sets up a hydraulic gradient between the water level in the well (lower hydraulic head) and the adjacent groundwater system (higher hydraulic head). Groundwater flows in response to a decrease in the hydraulic head because groundwater moves from areas of the higher hydraulic head to lower hydraulic head (i.e., high groundwater elevations to low groundwater elevations as referenced to a common elevation datum, generally mean sea level). This is discussed by Woessner and Poeter (2020). While this difference in hydraulic head is maintained by pumping, water flows from the adjacent groundwater system into the well.

3.1 Development of the Cone of Depression Under Transient Conditions

The region surrounding a pumping well where water levels are drawn down by pumping is referred to as the cone of depression. Maps, cross sections, and 3D representations of the cone of depression can be plotted using head or drawdown values (Figure 2). Drawdown is computed by taking the static head in a well (corrected for background influences on head) minus the measured head at a time since the pumping began (Figure 2). Flow to the well is radial under isotropic and homogeneous conditions (i.e., where hydrogeologic properties are constant and the same at all points within the hydrogeologic system being investigated; Woessner & Poeter (2020)). Drawdown occurs in the pumping well, observation wells and any other wells within the cone of depression. Transient conditions exist when pumping induces continuing drawdown over time. Water levels in the pumping well and in nearby unpumped observation wells decrease rapidly when pumping starts, then the rate of drawdown slows as the test progresses (Figure 3).

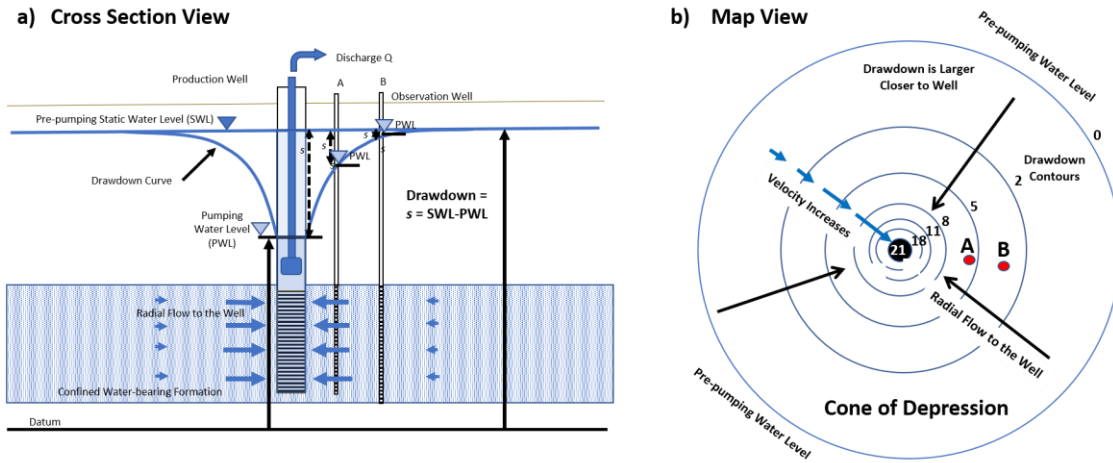


Figure 2 - Groundwater flow to a pumping well penetrating an isotropic and homogeneous confined aquifer.

- a) Cross-sectional view of the response of water levels (vertical black arrows) in the pumping well and surrounding observation wells. The decline in water levels represented by a potentiometric surface is shown as a drawdown curve. The groundwater velocity in the confined aquifer is highest near the well (large black vectors).
- b) Map view of the drawdown distribution around a pumping well. Numbers represent values of drawdown in units of length. A and B, located at the red dots, are unpumped observation wells. The zone of measurable drawdown is referred to as the cone of depression, which is centered at the pumping well (black dot). The flow of water (blue arrows) to the well is radial and equal in all directions when the aquifer is isotropic and homogeneous. Velocity (black vectors) increases from the outside edge of the cone of depression where the hydraulic gradient is very small to the pumping well where the gradient is large.

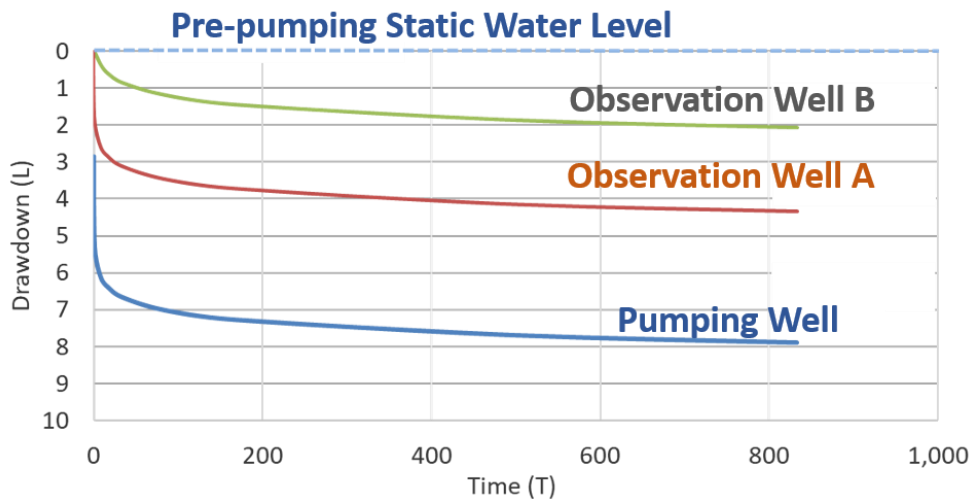


Figure 3 - Schematic of the changes in drawdown with time for a pumping well and the two observation wells shown in Figure 2 where Well A is closer to the pumping well than Well B. Drawdown values are plotted on arithmetic scales. Positive numbers represent potentiometric surface decline. Drawdown has dimensions of length (e.g., units of m, ft, and so on) and time may be in units of seconds, minutes, hours, or days depending on the length of the test and properties of the system tested. Conceptually, in a confined isotropic and homogeneous system under a constant pumping rate, the rate of drawdown is logarithmic with time, and drawdown is greatest at the pumping well. Drawdown at the observation wells begins sometime after pumping starts and is less in observation wells located farther from the pumping well.

Water levels in the pumping well begin to recover (rise) after pumping stops. With time, water levels begin to recover in observation wells within the cone of depression, with

recovery occurring first in wells nearest to the pumping well. Once the pump is shut off, water within the cone of depression continues to flow toward the well under the pumping-created hydraulic gradients. As water is no longer being extracted from the pumping well, groundwater from the surrounding aquifer region replenishes aquifer storage, and water levels begin to recover. Recovery is rapid at first, then slows as hydraulic gradients within the cone of depression decrease (Figure 4). Similar patterns are observed in observation wells.

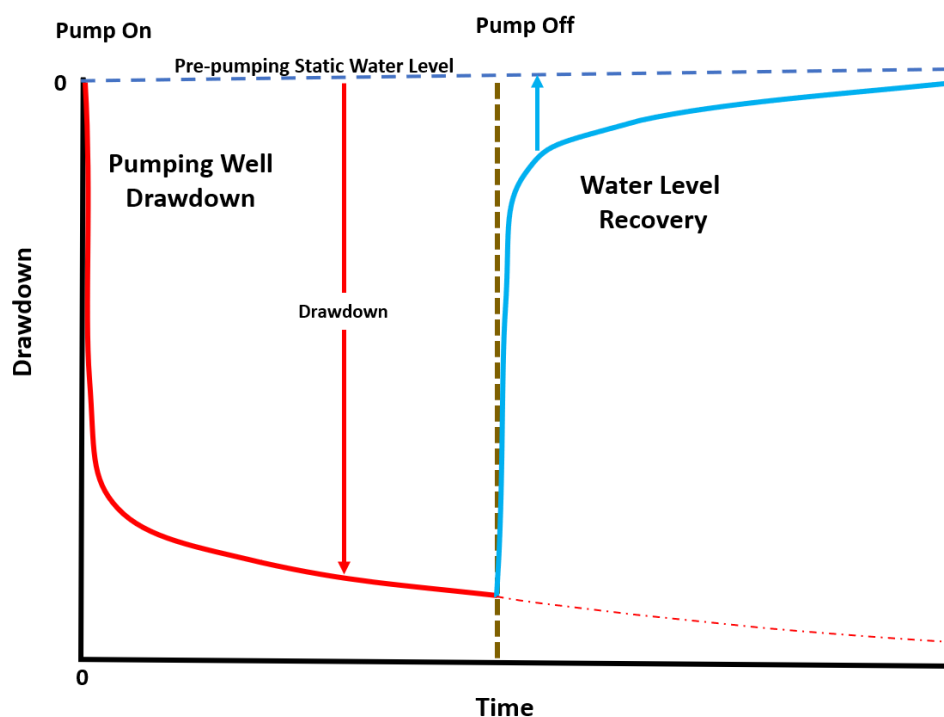


Figure 4 - Illustration of drawdown and recovery for a pumping well discharging at a constant rate. The dashed blue line represents the corrected static water level. The red line is the drawdown during pumping. The brown vertical line represents the time when the pump is turned off. The blue line shows the recovering water levels after the pumping has ended. The vertical blue arrow shows the residual or unrecovered drawdown. The dot-dashed red line is the projected drawdown that would continue to occur if the pump was not turned off.

The background water level is rarely static because it is subject to the influence of other features connected to and within the groundwater system (e.g., pumping of nearby wells; changing water levels in bodies of surface water such as a stream, lake, or ocean; recharge from precipitation). Consequently, water levels need to be recorded for some time prior to the start of pumping and for some time after the end of pumping, to infer the trend and correct the static water level for rises and falls of the background water levels during the test. Corrections for variation in the background water level may need to be applied when analyzing the test as discussed in Section 5.

Water pumped from a well in a confined aquifer is released from storage as the head declines due to compaction of the water-bearing unit and expansion of stored water as pressure decreases (Woessner & Poeter, 2020). The unit is not physically dewatered, rather

the drawdown cone forms in the potentiometric surface and the hydrogeologic unit remains confined. During recovery, the observed decrease in drawdown is caused by water reentering storage as the increased pressure expands the water-bearing unit and compresses the water within the unit. The recovery is rapid at first and slows with time.

When an unconfined unit is pumped, water levels decline as water flows to the wellbore and a cone of depression develops in the water table (Figure 4). In contrast to a confined system, a portion of the aquifer is physically dewatered as water drains by gravity from saturated pores and the water table elevation declines over time. Water released from storage is a combination of water released from elastic storage as in the confined system (compression of the matrix and expansion of the water), and water that drains from saturated pores as the water level declines. The drawdown is rapid at first then slows with time. In some settings at early times after pumping begins, drainage of water from the capillary fringe and vadose zone recharges the aquifer temporarily slowing the decline of the water table elevation. As pumping continues, drawdown resumes its earlier logarithmic rate of change. Specifics of pumping unconfined aquifers are discussed in Section 10.

Pumping reduces the saturated thickness of an unconfined aquifer at and near the well as the cone of depression expands over time. Under isotropic and homogeneous conditions and with a fully penetrating production well, groundwater flow is radial to the well and mostly horizontal (Figure 5). Near the well, however, where pores have drained, flow parallels the sloping water table. In this region, vertical flow occurs (Figure 5a).

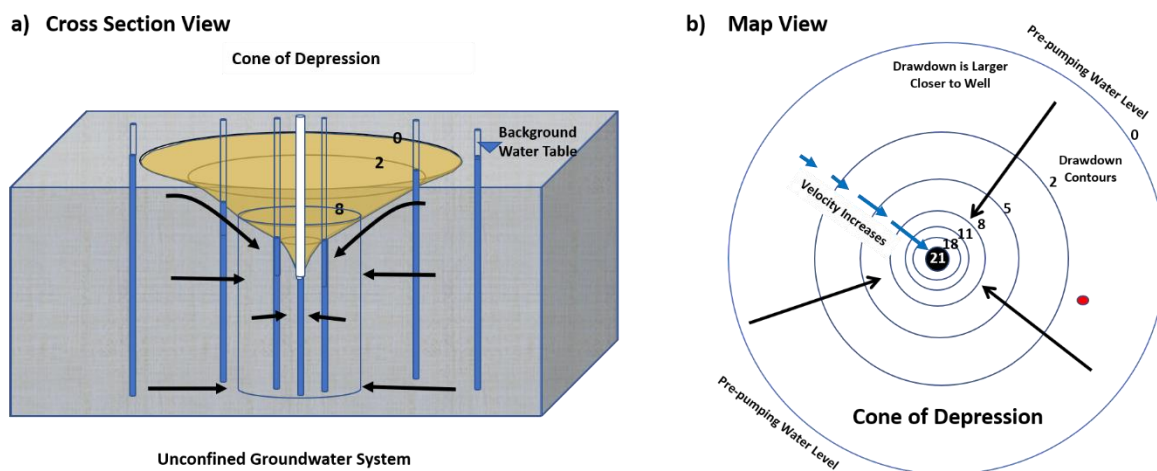


Figure 5 - Schematic of the cone of depression in the water table of an unconfined aquifer. The aquifer is assumed to be isotropic and homogeneous, and the wells fully penetrate the aquifer.

- Schematic of a cone of depression showing drawdown data at surrounding observation wells and the pumping well. The blue-gray block represents a fully saturated portion of the unconfined aquifer. The light brown shaded area represents the portion of the aquifer dewatered during pumping. Flow (represented by arrows) to the well is radial. Near the pumping well a vertical flow component is present as flow parallels the curved water table.
- A map view of the cone of depression plotted as drawdown. The flow (black arrows) is radial. Numbers represent values of drawdown in units of length. Gradient increases with proximity to the pumping well (drawdown contours are closer together). The velocity (blue vectors) increases as groundwater moves from the edge of the cone to the center. The red dot represents an observation well.

Under ideal conditions, the rate of drawdown decreases with time. This is because the volume of confined aquifer material in the cylinder below the cone of depression forming in the potentiometric surface increases with time by the square of the radius of the cone of depression. Water is withdrawn at the same rate over time, but the cylindrical volume contributing water grows as the cone of depression expands. Thus, less drawdown is required to yield the same amount of water from storage. The volume of the cylinder of aquifer material below the cone of depression is $h\pi r^2$ where h is the thickness of the confined aquifer and where r_1 is the radius of the cone at Time 1 and r_2 is the radius at Time 2 as shown in Figure 6.

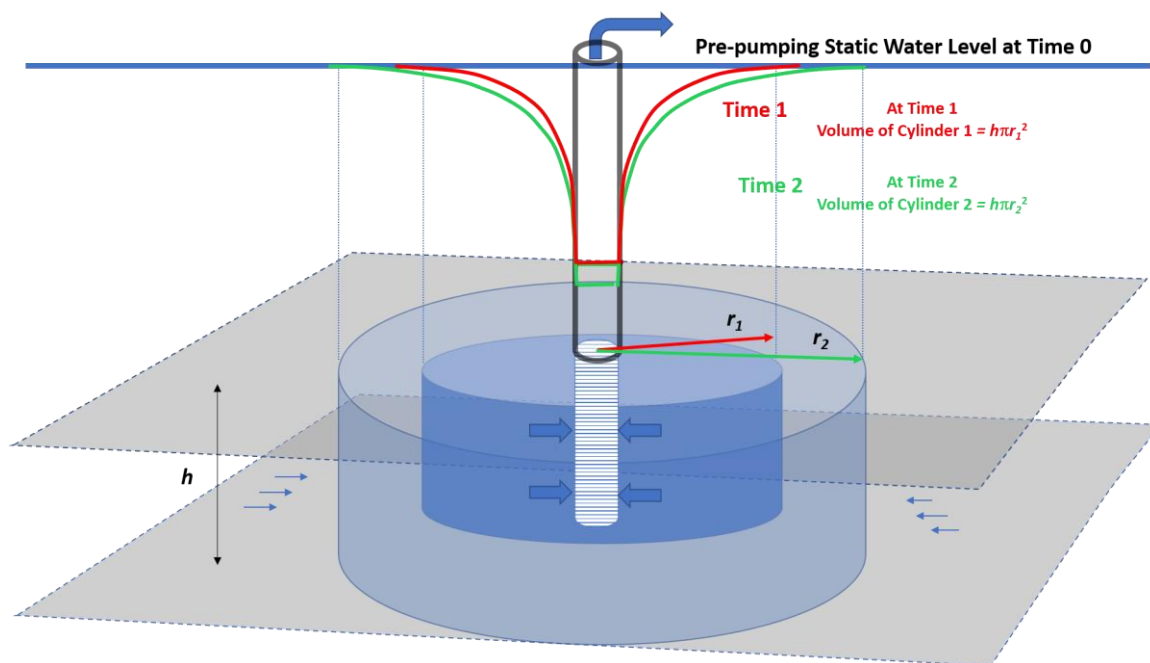


Figure 6 - As the duration of pumping increases in this isotropic and homogeneous confined aquifer the rate of water-level decline decreases (Figure 3) due to the increasing volume of aquifer contributing water to the pumped well. A rapid decline in head occurs in the early period of pumping. At Time 1 the volume of water that has been pumped from the well was derived from the release of water stored in the aquifer as controlled by the storativity (S) of the aquifer within the dark blue cylinder of radius r_1 in the confined unit. S is a dimensionless number reflecting the volume of water produced for one unit of drawdown per one unit of area. Thus, the volume released from the aquifer after a period of pumping is the product of three entities: S , the average drawdown over the area of the cone of depression, and the surface area defined by the perimeter of the cone (i.e., $Volume = S(\text{Average Drawdown})(\text{Area})$). A drawdown cone is also shown at Time 2 after pumping twice as long at the same constant rate. Because the pumping is constant and for the same duration, the same volume of water is released from storage between Time 1 and Time 2 throughout the light blue cylinder of radius r_2 and this zone has the same storativity (S). The drawdowns between Time 1 and Time 2 are smaller than between Time 0 and Time 1 because the same volume of water is yielded from a larger area.

3.2 The Cone of Depression Under Steady-State Conditions

If as a well is pumped and drawdown ceases (i.e., the heads within the cone of depression are not changing with time) the system has reached a steady-state condition. At steady state the constant flow of water from the well originates from a recharge source that is intercepted by the cone of depression.

Steady-state conditions most commonly occur in confined groundwater systems when leakage from aquitards and aquifers that overlie or underlie the confined system, or from a boundary—such as a transmissive fault or lake in direct communication with the aquifer—provides water to the aquifer being pumped (Figure 7). Water levels stop declining (Figure 8) when the leakage rate (water entering the pumping unit) becomes equal to the pumping rate (Figure 9). In an unconfined system, steady-state conditions occur when an adjacent recharge source equals the discharge rate at the well (Figure 9). As the water levels defining the cone of depression are not changing with time, none of the discharge water originates from the release of stored water within the aquifer being pumped. Instead, it is derived from external sources.

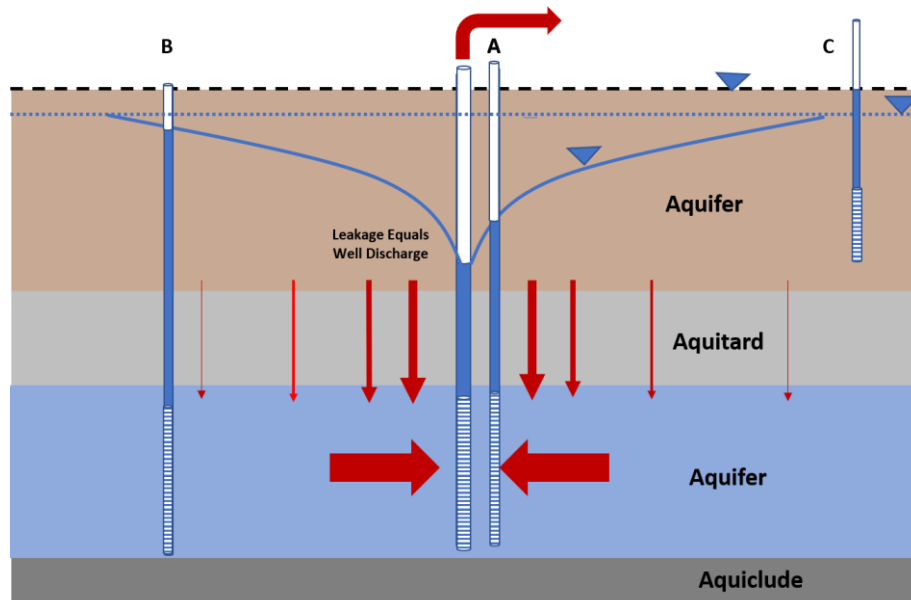


Figure 7 - Steady-state conditions for a well pumping in a confined aquifer (blue). The dashed blue line is the corrected static water level for the confined aquifer and the dashed black line is the corrected static water level for the overlying aquifer. The overlying confining bed (aquitard) is sufficiently permeable such that as the cone of depression forms in the confined aquifer, vertical gradients between the overlying aquifer/aquitard and the pumped aquifer allow leakage to the pumped aquifer (vertical red arrows). In this example, leakage rates equal the pumping rate, drawdown in the aquifer being pumped has ceased, and the cone of depression is no longer expanding. Schematic drawdown curves for the pumping well and observation wells A and B are shown in Figure 8.

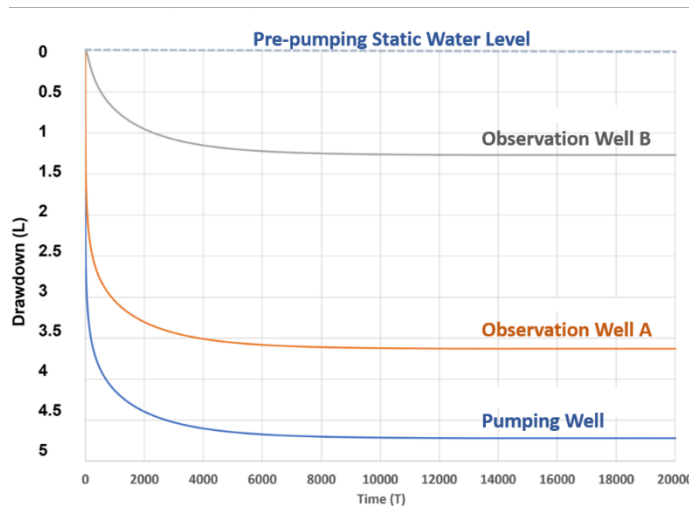


Figure 8 - Schematic of the occurrence of steady-state conditions during pumping of a confined aquifer that over time captures a recharge source that equals the well discharge. Drawdown in the pumped well and observation wells ceases, that is the water levels stabilize. Well, locations are shown in Figure 7. Drawdown has dimensions of length (e.g., units of m, ft) and time may be in units of seconds, minutes, hours, or days depending on the length of the test and properties of the system tested.

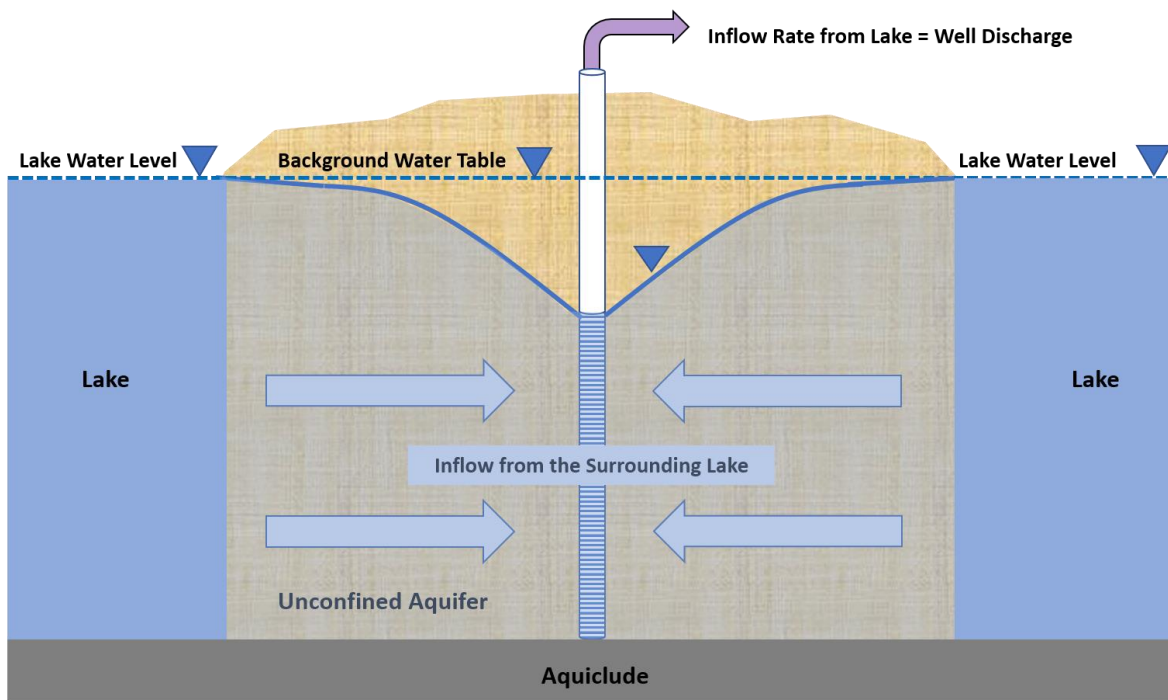


Figure 9 - Illustration of steady-state conditions in an unconfined groundwater system where pumping occurs at the center of a circular island surrounded by a lake. Inflow from the lake equals the pumping well discharge rate. As a result, drawdown stops, no water is released from storage, and all water comes from the lake.

4 Setting a Purpose, Designing, and Conducting a Pumping Test

Procedures to design and conduct pumping tests are described in many hydrogeology and engineering textbooks, government publications, and elsewhere in scientific literature. Some useful examples of guidelines are provided by the United States Environmental Protection Agency (Osborne, 1993), British Standard (2003), Standards Australia (2006), Washington State Department of Ecology (2020), and the book *Groundwater and Wells* (Sterrett, 2007). The American Society for Testing and Materials (ASTM) has at least 13 documents describing standard procedures that should be used to conduct and analyze pumping tests. A list of these ASTM documents is provided in a document produced by the United States Nuclear Regulatory Commission (2015). The approaches and methods described herein for conducting successful pumping tests are based on guidelines such as those cited above as well as professional experience. A flow chart of the key components for setting up and conducting a pumping test is shown in Figure 10.

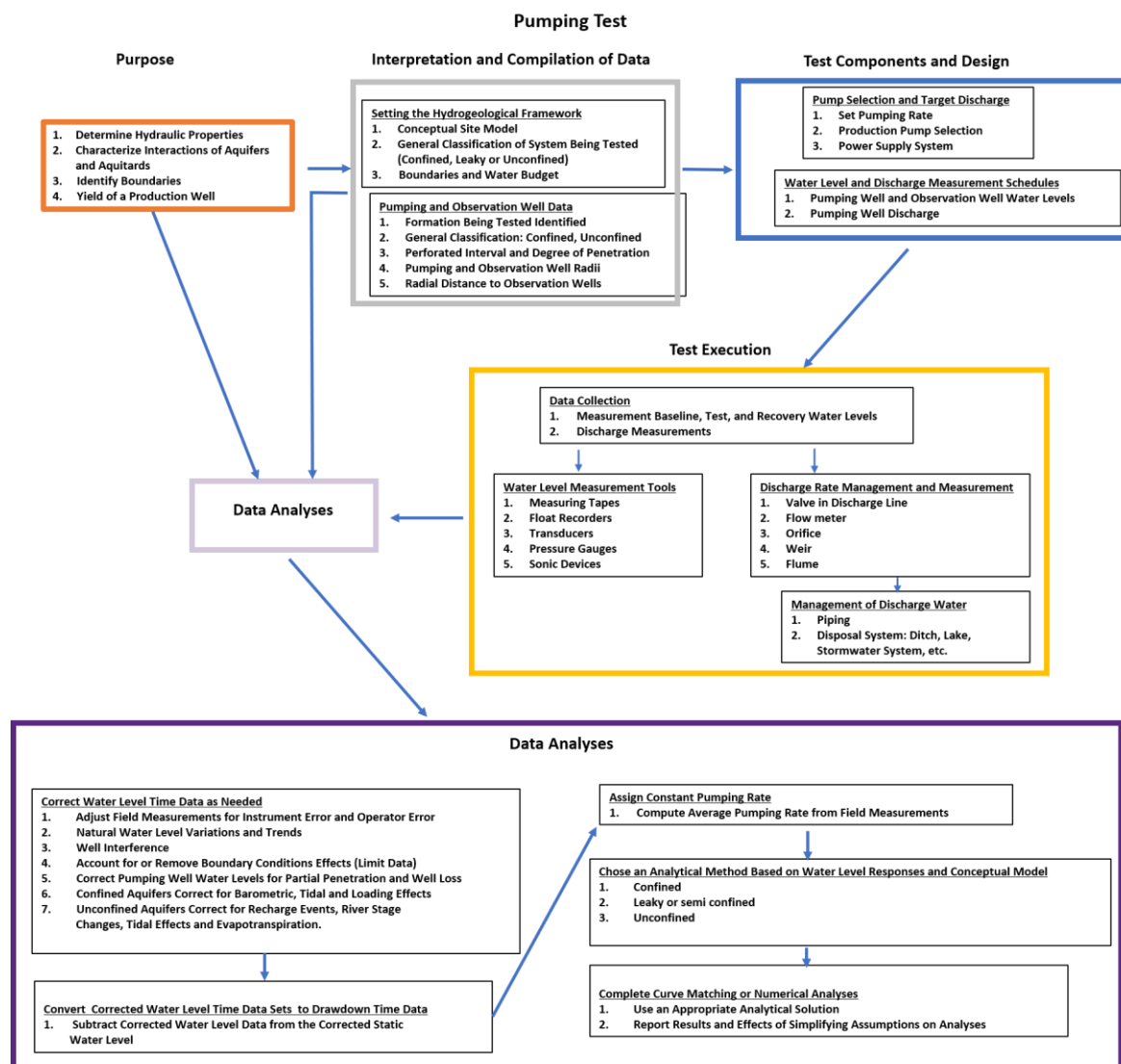


Figure 10 - Development of information and data required to plan, execute, and analyze a pumping test.

- a) The first step is to identify site and regional hydrogeologic conditions that will affect test design and resulting interpretation. A hydrogeologic conceptual model of the site and region is developed. This process includes collecting and interpreting geologic and hydrogeologic information including specifics on existing water bearing units and wells. The second step is to design the pumping test. Hardware requirements are identified, then pumping rates and test duration are planned. Next, measurement schedules are developed including monitoring of background water levels before and after testing. The third step is to initiate the test including pretest data collection and well instrumentation. The test is executed, while drawdown, time, and discharge data are recorded. When pumping stops, recovery water levels are recorded along with continued background water level recording. Once the test is complete the conceptual model and observed water level and pumping data are processed to determine hydrogeologic properties of the tested formations.
- b) Data analysis includes several steps. First the measured water level data are organized and corrected to remove influences that are not related solely to the formational properties at the test site. Next drawdown is computed. The pumping discharge records are reviewed, and a constant pumping rate assigned. The drawdown, time, and discharge data, along with the hydrogeologic, pumping, and observation well data, are used to choose and apply an appropriate analytical method. Curve matching and or numerical analyses are executed. Results and limitations are reported.

4.1 Purpose

A clear purpose is required to design and conduct a pumping test. Most often, pumping tests are conducted to determine the magnitude and distribution of field-scale hydrogeologic properties (K , T , and S). In some settings the purpose may be establishing how aquifers and confining units respond to pumping and to quantify the hydraulic properties of the less permeable confining units. Pumping tests can also be designed to determine whether the hydrogeologic unit is bounded and how the boundaries affect drawdown response over time. In some settings, pumping tests are conducted on production wells to determine sustainable yields for prescribed production schedules. Identifying the purpose is the first step in designing a pumping test (Figure 10).

4.2 Compiling and Interpreting Existing Data Sets

When designing a hydraulic test, the groundwater professional should first collect and analyze a wide variety of site and regional hydrogeologic information (Figure 11). This process includes reviewing available literature, evaluating local geologic and groundwater conditions, and formulating a general water budget for the site under investigation.

The better one understands the hydrogeologic setting, the more likely a pumping test will be successful. This understanding includes:

- the sequence and extent of hydrogeologic units,
- the presence of physical and hydrogeologic boundaries,
- estimates of the hydrogeologic properties of water-bearing units and aquitards,
- estimates of groundwater flow directions and rates,
- potential for the interconnectedness of units,
- sources, locations and rates of recharge and discharge,
- the design and yield of existing wells, and
- a groundwater budget for the area,

all of which facilitates determination of an appropriate pumping rate and duration for the test. The resulting hydrogeologic conceptual model frames the design and execution of the planned pumping test. Additional guidance on formulating a hydrogeologic conceptual model is provided by Woessner and Poeter (2020). In some settings, not all the components listed in Figure 11 are readily available. When information is limited, efforts should be focused on obtaining and analyzing topographic maps, geologic maps and cross sections, weather trends, as well as identifying locations of known water features, quantifying existing water uses, and reviewing available hydrogeologic publications related to the area of study.

Data Used to Construct a Hydrogeological Site Model

Physical framework

Topographic maps showing the stream drainage network, surface water bodies, landforms, cultural features, and locations of structures and activities related to water

Geologic maps of surficial deposits and bedrock

Hydrogeologic maps showing extent and boundaries of aquifers and confining units

Maps of tops and bottoms of aquifers and confining units

Saturated thickness maps of unconfined (water table) and confined aquifers

Average hydraulic conductivity maps for aquifers and confining units and transmissivity maps

for aquifers

Maps showing variations in storage coefficient for aquifers

Estimates of age of groundwater at selected locations in aquifers

Hydrologic budgets and stresses

Precipitation data

Evaporation data

Streamflow data, including measurements of gain and loss of streamflow between gaging stations

Maps of the stream drainage network showing extent of normally perennial flow, normally dry channels, and normally seasonal flow

Estimates of total groundwater discharge to streams

Measurements of spring discharge

Measurements of surface water diversions and return flows

Quantities and locations of interbasin diversions

History and spatial distribution of pumping rates in aquifers

Amount of groundwater consumed for each type of use and spatial distribution of return flows

Well hydrographs and historical head (water-level) maps for aquifers

Location of recharge areas (areal recharge from precipitation, losing streams, irrigated areas, recharge basins, and recharge wells), and estimates of recharge

Chemical framework

Geochemical characteristics of earth materials and naturally occurring groundwater in aquifers and confining units

Spatial distribution of water quality in aquifers, both areally and with depth

Temporal changes in water quality, particularly for contaminated or potentially vulnerable unconfined aquifers

Sources and types of potential contaminants

Chemical characteristics of artificially introduced waters or waste liquids

Maps of land cover/land use at different scales, depending on study needs

Streamflow quality (water-quality sampling in space and time), particularly during periods of low flow

Figure 11 - Data used in building hydrogeologic conceptual models (Alley et al., 1999).

The hydrogeologic conceptual model should include both the regional setting and site-specific conditions. This model is then used to identify the likely behavior of the unit being tested and the surrounding geologic units. Using the hydrogeologic conceptual model, the nature of the water-bearing unit can be interpreted (e.g., confined, unconfined, leaky), the likelihood of impermeable or recharge boundaries impacting drawdowns assessed, ideal locations and construction of test and observation wells estimated, and the type of analytical tool that may best fit resulting test results proposed.

4.3 Pumping and Observation Well Design and Construction Data

Pumping tests should include observation wells but can be performed using a single pumping well if necessary. Use of unpumped observation wells produces more reliable results because it is difficult to accurately measure drawdown in the aquifer via the pumping well bore due to wellbore storage issues early in the testing period and head losses that occur when water flows through the screen and along the bore that contains the pump, pipes, and wires. Also, observation wells provide information regarding storage properties of the aquifer and the spatial variation of hydraulic properties.

Often, pumping and observation wells can be selected from existing wells completed in the target unit, otherwise wells can be specifically installed for the test. Typically, existing wells (including domestic, municipal, industrial and/or irrigation wells) are used, when possible, as constructing a new pumping well is costly.

4.3.1 Design of Pumping and Observation Wells

Well construction logs should be reviewed prior to selecting an existing pumping well for the test. In many regions, driller's logs are filed with regulatory agencies when wells are constructed (Figure 12). These provide information on the stratigraphy encountered during drilling, notes on when water bearing units were intersected, a short pumping test (performance test), borehole and casing diameters, location and type of grouting, and the position of perforated intervals in the well casing.

If wells need to be installed to perform a pumping test, standard practices described by Sterrett (2007) should be applied (Figure 13). The Groundwater Project book *Domestic Wells: Introduction and Overview* (Drage, 2022) provides a good discussion of drilling techniques used to install domestic wells. Ideally, pumping wells should include a screened or perforated interval that fully penetrates the aquifer and be of sufficient diameter to accept a pump that will produce the desired yield for the planned pumping test. Water supply wells are typically screened across the zones observed to yield the highest discharge rates during drilling, and often a filter or gravel pack is placed between the well screen—or perforated casing—and the borehole wall adjacent to this zone (Figure 13). A well is generally considered fully penetrating if at least 80 percent of the aquifer thickness is screened because this makes it possible to obtain approximately 90 percent or more of the maximum yield that could be obtained if the entire aquifer was screened (Kruseman & de Ridder, 2000).

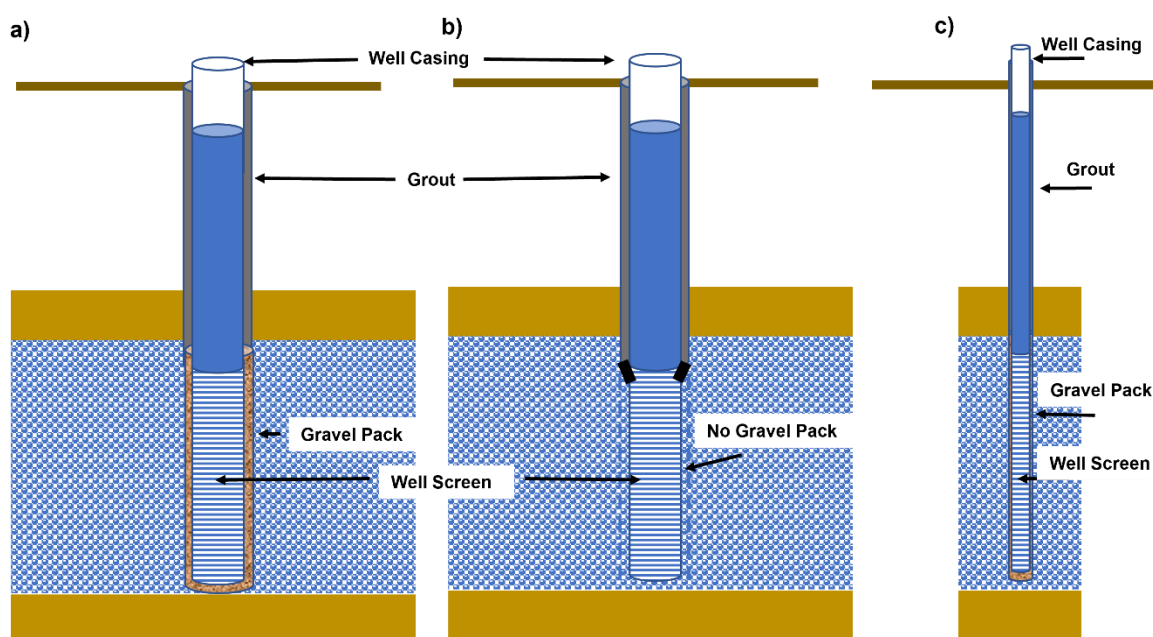


Figure 13 - Schematics representing ideal designs of production and observation wells with fully penetrating screened intervals, at least 80 percent of the thickness (Kruseman and de Ridder (1992)).

- Production well with steel casing that is grouted with cement or bentonite to the top of the gravel pack. The well consists of a solid casing and an attached screen interval set in a borehole. A gravel pack surrounds the screen. The annulus around the remainder of the casing is filled with grout.
- A production well where the perforated interval is a slightly smaller diameter than the well casing. The telescoping screen is set in an open hole and not surrounded by a gravel pack. The remainder of the borehole above the screen is grouted.
- Observation well set in a borehole. Typically, the screened interval is attached to a steel or PVC casing and a gravel or sand pack is installed around the screen. The remainder of the borehole is grouted to the surface.

Ideally, observation wells also should be installed with screened intervals equal to or greater than 80 percent of the test unit thickness (Kruseman & de Ridder, 2000). However, this is rarely done for cost reasons. The length of the observation well screen is not important when the pumping well screen fully penetrates the tested unit or observation

wells are located outside of the zone impacted by partial penetration effects, as discussed in Section 12. Well casing must be of sufficient diameter to accept water-level monitoring devices. Generally, diameters greater than 25 mm will accept transducers and mechanical tapes (Sterrett, 2006).

Observation wells need to be in good communication with the formation being tested. Newly constructed wells should be developed after they are installed using methods described by Sterrett (2007). Taylor and Alley (2001) recommend that wells should be hydraulically tested before used as observation wells to assure the perforated interval is not damaged or plugged with silt or fouled with bacteria such that it is not optimally responding to head changes. Depending on the well construction: pumping, bailing, or slug testing (Section 2) can be used to assess if wells are in good communication with the geologic material being evaluated by hydraulic testing.

4.3.2 Observation Well Spacing

The spacing of pumping and observation wells is driven by the purpose of test. For a successful pumping test, pumping-induced drawdown at observation locations must generally be both measurable and exceed the magnitude of other influences on water levels (e.g., low-permeability boundaries, surface water bodies, other pumping wells, irrigation, precipitation recharge, and barometric pressure changes). Observation well spacing should be based on the estimated radius of influence of the pumping during the test. The radius of influence is estimated using analytical equations (presented in Sections 7-10) that forecast drawdown based on the designed pumping rate, hydrogeologic unit type, hydraulic characteristics, and the duration of the test.

General guidance for placement of monitoring wells is provided by Sterrett (2007). In unconfined aquifers, he suggests observation wells be placed no further than 30 to 90 m from the pumping well. In confined aquifers they should be placed within 90 to 200 m of the pumping well. These general guidelines are based on the concept that the large storage coefficient of unconfined systems corresponds to a smaller zone of influence. However, as mentioned above, pumping rates, transmissivities, storativities, and test duration all affect the extent of the cone of depression.

The USEPA Aquifer Test Guidance (Osborne, 1990) suggests when one observation well is used it should be spaced 15 to 90 m from pumping well. Osborne (1990) states that when multiple observation wells are used, they should be placed in a line at varying distances from the well or “...along rays perpendicular to the pumping well.” If boundaries are expected to influence the test, then observation wells should be located near the boundaries. Ideally, observation wells should also be located outside of the anticipated zone of influence to monitor natural and anthropogenic induced changes to the water levels. He also notes that if anisotropic conditions are present, monitoring wells should be placed to reflect the likely pattern of anisotropy.

4.4 Pumping Test Components and Design

In preparation for conducting the pumping test, the desired pumping rate and test length, the type and capacity of the pump used to stress the groundwater system, and the power supply should be identified.

4.4.1 Selecting the Pumping Rate

Planning the target discharge rate for the test is partly dependent on the thickness, extent, and hydraulic properties of the hydrogeologic unit being pumped, the hydraulic constraints of the pump selected, and the anticipated duration of the test. The target pumping rate is usually based on either the target well yield (in the case of a water supply well), the capacity of the pump or preliminary calculations of the estimated maximum drawdown in the pumping well (for example, pumping at 2,000 L/minute will likely draw the pumping well-water level down 30 m over 6 hours of pumping). The likely amount of drawdown for a prescribed test period can be estimated using reported field values of transmissivity (T) and storativity (S) for units of similar lithology and thickness, or at other locations where the water-bearing unit was tested. These data are substituted into analytical or numerical models to compute drawdowns for selected yields and a user specified test duration.

Another approach is to conduct one or more short pumping tests or step-drawdown tests prior to conducting the main test. When little is known about how the formation will respond to pumping, these tests may be performed to observe drawdown versus time at different pumping rates. Step-drawdown testing is discussed in Section 12.4. In brief, it involves pumping the well at a few different rates for a short period of time and monitoring the water levels for a short period of time. For example, sequentially pumping the well at 500 L/min, 2000 L/min, and 5,000 L/minute with each step lasting 30 to 60 minutes. Based on the step-drawdown test results, an optimum pumping rate for a long-term pumping test can be estimated as described in Section 12. When nearby observation wells are also monitored, water-level trends near the end of the test in the pumping well and at observation wells can be extrapolated to estimate drawdown values at the end of the planned test. A second approach to estimating drawdown at the end of the planned test is to apply analytical tools to compute aquifer property values and then calculate the response of the hydrogeologic unit to the planned pumping rate.

4.4.2 Selecting the Duration of the Pumping Test

The length of a pumping test (which will also be the length of time for monitoring recovery after pumping stops) is dependent on the stated purpose. Principally, tests are conducted to determine the hydraulic properties of the tested water bearing unit, T and S . Other tests may be designed to determine if steady-state conditions will occur (e.g., Kruseman & de Ritter, 2000) or if distant boundaries exist that will affect long-term well performance and the magnitude of drawdowns.

Drawdown should be measured after the pumping has stopped (time-recovery data) until water levels have recovered to within 90 percent of the corrected static water level at the beginning of the test. This typically occurs over the same length of time that pumping occurred (total test time for a 2-hour pumping test would be about four hours). Longer tests are usually required to account for aquitard leakage and the delayed water-level response commonly seen in unconfined systems. USEPA guidelines recommend pumping tests should last at least 24 hours with water level recovery data collected in the following 24-hour period, resulting in a 48-hour test period (Osborne, 1993).

It may be desirable to examine if pumping will result in water-level changes reaching steady-state conditions. Such pumping tests may require days to weeks to complete. Kruseman and de Ritter (2000) caution that inexperienced hydrogeologists may interpret that steady-state conditions have occurred when the drawdown rates become small yet the cone of depression is still expanding. A true steady-state condition is not realized until a recharge boundary or confining bed leakage equals the pumping rate. In unconfined systems delayed yield causes water levels to appear to stabilize, however, this is a temporary condition that can last minutes, hours, or days. Otherwise, the cone of depression keeps expanding, though slowly. It is recommended that pumping tests of unconfined aquifers should last up to three days in an attempt to avoid misinterpreting drawdown responses (Kruseman & de Ritter, 2000). Often regulatory requirements related to identifying the response of the groundwater to the pumping of a production well are conducted for a period of 72 hours (with a similar period of recovery data collected).

In some cases, information on the location of boundaries and how they influence well discharge as well as the size and shape of the drawdown cone is an additional desired outcome of a pumping test. Depending on the distance of the boundary from the pumping well, a pumping period longer than the suggested 24-hour period may be needed. Once again, the appropriate pumping time can be estimated by computing estimates of the position of the drawdown cone at various times.

4.4.3 Choosing a Pump and Power Supply

In some systems a hand pump, bailer, or bucket may provide sufficient flow for a low-flow pumping test if a relatively constant discharge rate can be maintained by such methods. However, that is difficult to achieve except in very low hydraulic conductivity materials.

Generally, a submersible pump or line shaft turbine pump is used to perform higher-rate pumping tests. The pump used to provide the desired yield should be selected based on the target flow rate, the manufacturer's pump efficiency curve, the well diameter and depth, the length of the screened or perforated interval, and the anticipated maximum drawdown in the well. USEPA guidance suggests selected pumps should have a capacity that is 20 percent higher than the test pumping rate (Osborne, 1993).

The available drawdown in the pumping well must be considered (Figure 14) when selecting a pumping rate. If the drawdown associated with the desired discharge rate exceeds the available drawdown, a lower rate must be used. As illustrated in Figure 14 not all the head above the pump intake is available to provide specified yields because pumps require a few meters or more of water level above the pump intake (operating head) to prevent the introduction of air into the pump that causes a reduction of discharge. Adequate water circulation around the pump is required to prevent overheating. Pump operating heads vary with individual pumps. Pump operation manuals should be consulted to determine efficient operating head values in order to assure sufficient available drawdown will persist during the test.

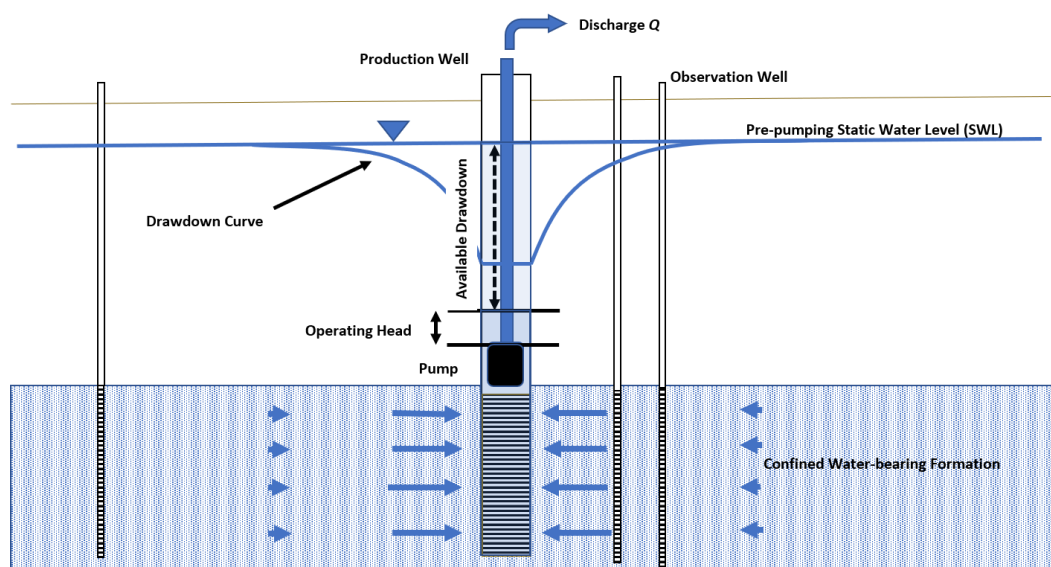


Figure 14 - Schematic of a pumping well showing the available drawdown and pump operating head. When pumping commences, available drawdown decreases. In settings with large water columns (i.e., static water level well above the pump level), the available drawdown is greater than in situations where static heads are closer to pump intake levels. Pumps require some operating head (depth of water over the pump) to generate an uninterrupted supply of water. If the water level declines below the operating water level the water will entrain air which reduces flow rates and causes cavitation in the pump. Pump operating manuals should be consulted to determine the minimum operating head when assessing the available drawdown needed to complete a test.

Operation of the selected pump also requires a reliable power source. Commonly, electrical power supplies or generators are used to operate submersible or line shaft turbine pumps. If power is interrupted during the test, it may be necessary to terminate the test and allow water levels to recover to near pre-test levels and then start over. Brief interruptions in power that occur later in the test can be compensated for by pumping at a calculated higher rate so that the average rate remains unchanged. However, a reliable power source and pump are key components of successful pumping tests.

4.5 Water Level and Discharge Measurement Schedules

A schedule for measuring water levels at the pumping well and observation wells should be developed before initiating the test. Pumping causes water levels in pumping

and nearby observation wells to respond rapidly at first and then more slowly as the test proceeds (often a logarithmic trend). The initial changes in water levels must be measured frequently as techniques used to analyze field data often rely on early-time data trends. Most often researchers suggest measuring the water level changes as rapidly as possible in the pumping well and nearby observation wells in the first 30 minutes to an hour of the initiation of each drawdown and recovery period. Less frequent measurements are required the longer the pump is operated. When transducers are used to record water level changes, they can be programmed to measure water levels every fraction of a second if needed. If measurements are being completed by hand (e.g., mechanical, or electronic tapes) it is recommended that measurement intervals follow a logarithmic pattern. Sterrett (2007) provides information on the minimum number of data points required to create a useful water level data set (Table 1).

Table 1 - Minimum drawdown measurement time intervals for pumping and observation wells (modified from Sterrett, 2007; Kruseman and de Ridder, 2000).

Pumping Well	
Time Since Pumping Started (or Stopped) (min)	Time Intervals Between Measurements (min)
0-5	0.5-1.0
5-15	1
16-60	5
60-12	20
120 to termination of test	60
Observation Well	
Time Since Pumping Started (or Stopped)	Time Intervals Between Measurements
0-2 min	Approx. 10 sec
2-5 min	30 sec
5-15 min	1 min
15-50 min	5 min
50-100 min	10 min
100 min-5 h	30 min
5 h to 48 h	60 min
48 h to 6 days	Every 8 h
6 days to shutdown	Once a day

Flow rates should be recorded with sufficient frequency to document a constant rate or to monitor planned rate changes (Duffield, 2022). Most often pumping tests are conducted using a constant pumping rate. Kruseman and de Ridder (1994) recommend checking and adjusting the flow rate at least once every hour. USEPA guidance suggests that a planned constant pumping rate should not vary more than five percent. Though no standard pumping rate monitoring schedules are commonly used, discharge measurements should be collected every 10 minutes in the first few hours of a pumping

test and then every 20 to 40 minutes for the next three or four hours. As the drawdown rate slows, monitoring intervals can be extended. These recommendations are based on the use of standard electric pumps that operate at a constant number of revolutions per minute.

5 Test Execution and Data Analysis

The following subsections describe the components of setting up and completing a pumping test. This includes methods to measure water levels during pumping and recovery, monitoring baseline water level conditions and trends, measuring, and maintaining a pumping rate, and managing discharge water.

5.1 Measuring and Recording Water Levels

Water levels are measured to establish pre- and post-testing water level trends, as well as during both the pumping and recovery phases of pumping tests. Water levels can be measured with several manual and automated devices, some of which are installed in the wells for the entire test (Figure 15).

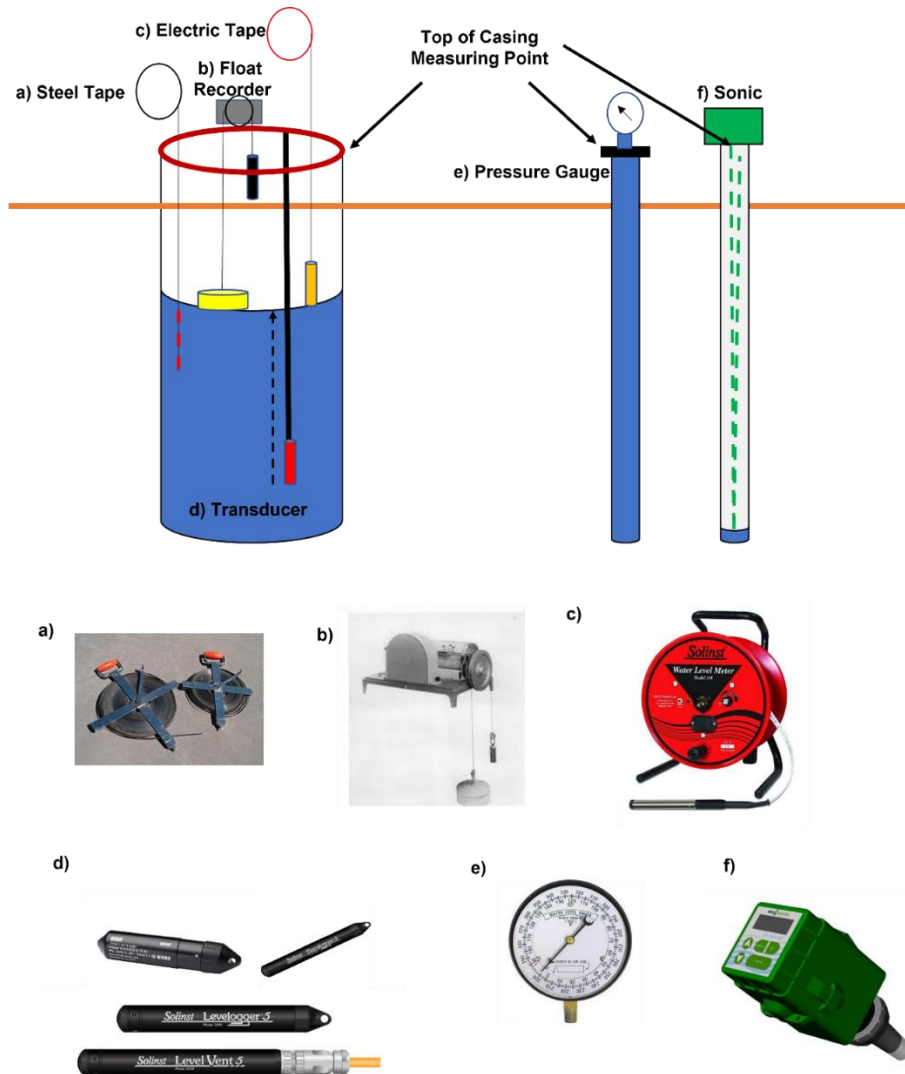


Figure 15 - Groundwater level monitoring methods. The diagram shows how each measuring device would be used in a well.

- a) Steel graduated tape with the measuring end chalked with carpenter's chalk (https://aces.nmsu.edu/pubs/_m/M118/welcome.htm).¹
- b) An older technology float recorder using a pen and paper chart records water level changes and time. The initial water level below the top of the casing is determined and used to convert water level changes recorded on the chart to changes in head.
- c) An electric tape used to measure water levels sends a signal to the tape case once the probe contacts the water. The tape is graduated, and a direct water-level reading is taken at the measuring point (e.g., <https://www.solinst.com/>).²
- d) Transducers are submerged below the static water level and record changes in the pressure of the overlying column of water over time (pressure decreases as drawdown occurs). An initial measurement of the static water level is recorded at installation and used to convert pressure changes to water levels. Transducers come either sealed to the atmosphere (absolute pressure) or vented to the atmosphere. Unvented (sealed) transducers require simultaneous collection of barometric pressure (e.g., Solinst barologger) readings. These data are used to make corrections to recorded water levels (measurements include water level changes and barometric changes) (e.g., <https://www.solinst.com/>; www.onsetcomp.com).³
- e) Observation wells where the water level is above the top of the casing can be closed in with a valve outfitted with a pressure gauge or a pressure transducer. The changes in pressure are recorded during pumping and converted to length measurements (although the gauge shown reads feet of water directly) www.Grainger.com/.⁴
- f) A sonic water level meter is used most often for deep wells, wells with partial obstructions and/or not perfectly straight wells. A sound pulse travel time is used to measure the water level (e.g., <https://enoscientific.com/well-watch-670/>).⁵

Manual measuring tapes can be used to monitor water levels (Figure 15). Graduated electronic water level meters (or electric tapes) indicate the depth to water below a measuring point (usually the top of casing) when a sensor contacts the water surface, and a circuit is completed resulting in a beep or light. The tape reading at the measuring point is the depth to water. One or more electric tapes are usually on site to periodically measure background water levels in pumping and observation wells during a test. When multiple electronic water level tapes are used, they should be calibrated to a steel tape or reference electronic water level tape that is used as a standard. Each tape used may have its own individual correction factor relative to the standard tape. Some water level data may need to be corrected for instrument error.

If only a steel tape is available, it can be used to determine water levels. A steel graduated tape with the end portion of the dry tape marked with chalk or water-soluble ink is lowered into the well and then held at a designed measuring point (top of casing) at an even measurement mark (e.g., 15 m). The tape is then retrieved, and the amount of wet tape recorded. The depth to water from the top of casing is obtained by subtracting the length of wet tape from the measuring point value. If multiple steel tapes are used during a test, they should be standardized. When using only measuring tapes to record test water level changes, the timing of measurements is dependent on the speed at which the tape can be deployed, the water level read, and the time and level data recorded. Rapid measurement during early periods of pumping and recovery are often difficult to capture using measuring tapes, especially when steel tapes are applied. Thus, other devices such as pressure transducers are recommended.

Water level data may need to be corrected for operator error. This is quantified when an operator consecutively measures the background water levels in a single well multiple (at least three) times. Assuming these water level measurements represent a single value, the mean water level and error are computed. The recorded error is the operator error for the field personnel reporting the data. All water level data collected by that operator includes the computed error.

Older float recorders can also be used to record water levels in monitoring wells that are not outfitted with pumps or other piping that would prevent installation of a float and counterweight (Figure 15). Typically pens controlled by the float record water level changes over time on paper charts. Clock mechanisms can be mechanical or electrical. A reference initial water level is measured and recorded prior to the initiation of the test and several times during the test. Float recorder water levels are corrected using hand measured water level data when they do not agree. For the most part, float recorders have been replaced with transducers.

Pressure transducers are suspended with a cable to a depth below the anticipated decline in maximum level of drawdown (Figure 15). Transducers measure the pressure exerted by the column of water above the transducer at the start of the test and then the

decrease in pressure as drawdown occurs. Pressure transducers have specified submerged operational ranges within which they are designed to operate (e.g., 0 to 5 m, 5 to 10 m, 10 to 25 m, 25 m to 50 m, etc.). Transducers should be selected for test wells to match their published operational range and sensitivity. For example, if the water level in the pumping well is anticipated to change 20 m during a test, a transducer with a range of 5 m to 25 m should be used. However, for the same test an observation well located 100 m from the pumping well that is anticipated to change about 7 m would have a transducer installed with a range of 5 to 10 m. The relationship between the background water level and the water level height over the transducer is established by measuring the water level at the start of the test using a calibrated electronic water level measuring tape. It is recommended that water levels are periodically measured manually during the test and used to collaborate/correct transducer records as needed.

Transducers are often set to record measurements using fixed time intervals (e.g., every second, 1 min, 10 min, etc.) or at variable time intervals following a logarithmic trend. Many transducers and cables include air tubes open to the atmosphere (vented), but some do not (absolute or unvented). If transducers are not open to the atmosphere, they are paired with an on-site micro-barometric sensor. The barometric data are used to correct the water levels as the unvented transducers record the combined barometric change and water level change during operation.

A mechanical pressure gauge or pressure transducer can be used to monitor water levels in observation wells where the total head is greater than the elevation of the top of the casing (Figure 15). Gauge specifications including ranges, accuracy, and precision are provided by manufacturers.

Sonic meters work by transmitting a sound wave into the well and measuring the time it takes for the pulse to return after reflecting off the water surface. The distance is calculated using the speed of sound and time. Sonic meters are operated at the top of the well casing and do not physically touch the water surface (Figure 15). They are useful in wells with deep water levels (100s of meters), when wells have partial obstructions, and where casings are angled. Some meters are hand operated and others can be programmed to collect water level data over time. It should be noted that accuracy and precision of sonic meters is typically less than that of electronic water level measuring tapes (e.g., 0.03 m versus 0.003 m). Manufacturers specifications should be reviewed, and error bars included with water level data. If conditions allow steel tape or electronic water level measurement tapes to be deployed, sonic measurement records can be calibrated to standard water level values.

5.2 Establishing Baseline Conditions and Water Level Trends

Pre-test water levels should be measured prior to the initiation of the pumping test. The baseline data are used to document on-going regional water level changes and determine if other pumping wells in the area are impacting background water levels (well interference). An observable rise or fall in water levels may also be caused by natural variation in recharge and discharge and/or barometric effects.

Water levels in the pumping and observation wells should be monitored for at least 48 hours before the test to establish natural regional trends. When nearby pumping wells are causing water level changes at the test site they should be shut off prior to testing and remain off during testing.

Barometric pressure changes influence heads within confined and semi-confined aquifers. If tested formations are confined, a micro-barometric sensor should also be operated during the entire test to examine if some small water-level changes are the result of variations in atmospheric pressure (e.g., Todd & Mays, 2005; Wang, 2020). Though small changes in confined water levels due to changes in barometric pressure may be masked by large changes in test water levels at early times, they may become significant if test water level changes are small (Clark, 1967). Barometric effects do not affect unconfined aquifer heads as the water table is open to the atmosphere. Also, some hydrogeologic systems located near areas effected by ocean tides may show responses to the changing tides in the water level data (e.g., Todd & Mays, 2005).

When variations in pumping test water levels occur that are not directly related to formational properties, observed drawdown data need to be corrected for these perturbations prior to analysis (e.g., Todd & Mays, 2005; Kruseman & de Ridder, 2000; Sterrett, 2007).

5.3 Methods to Measure and Maintain a Pumping Rate

Discharge should be monitored frequently during a test to document variations in pumping rates. As described earlier, because standard electric submersible or line shaft turbine pumps operate at a constant number of revolutions per minute, observed initial discharge rates tend to decline over time as the head in the well declines. This is because as drawdown occurs the pump must lift water from a greater depth affecting the pump efficiency. Though variable-rate pumping tests can be conducted, most pumping tests are designed as constant-rate discharge tests. If a constant-rate test is planned, a method to maintain a constant pumping rate must be deployed. Typically, a valve is included in the pump discharge line that is not fully open when the test begins and set to deliver the target discharge rate (Figure 16). As the test proceeds, the valve can be opened to adjust the discharge rate as needed. When rates vary during a constant-rate test, an average weighted discharge is often computed to represent the test pumping rate.

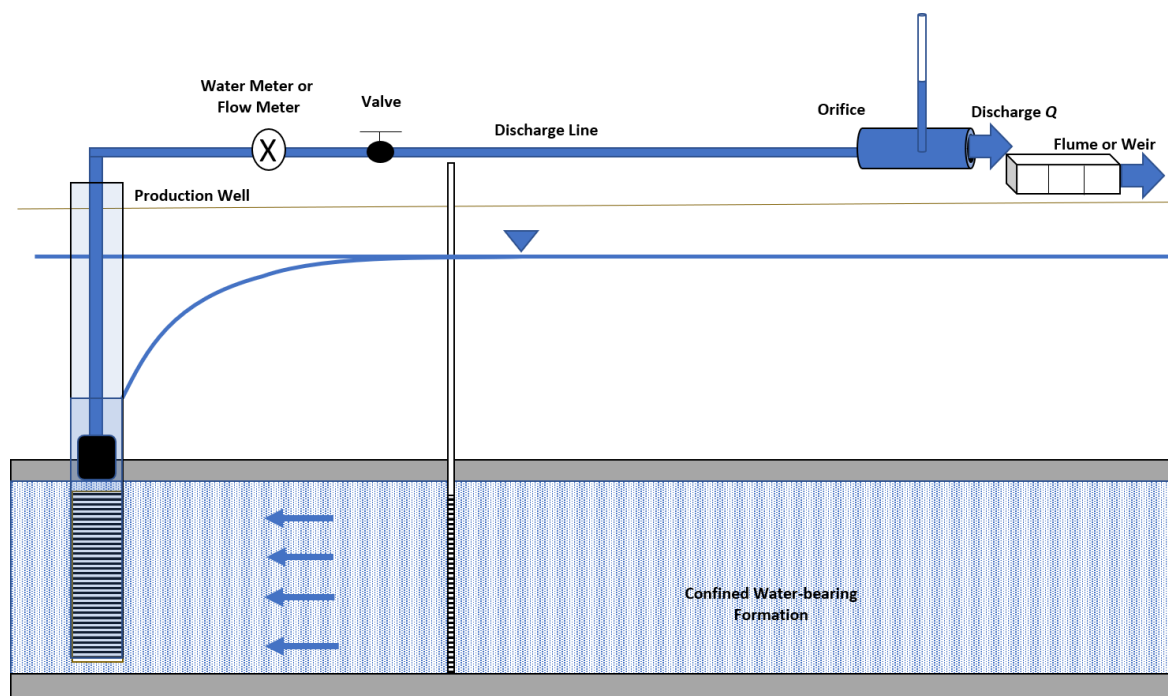


Figure 16 - Methods to monitor and control discharge: To reduce the number of variables when analyzing pumping test data, it is desirable to have the pumping rate remain constant. This requires measuring the discharge rate accurately. It is also important to have the ability to adjust the pumping rate as needed. In this example a valve is installed in the discharge line so that it can be opened to compensate for a decrease in flow rate as the water level in the well declines. If pumps with variable frequency drives are available, the pumps can be programmed to maintain a constant discharge rate.

Given the difficulty of maintaining a constant discharge rate, the use of an electric pumps with a variable frequency drive can dramatically improve the quality of the test data. These specialized pumps maintain a constant discharge rate by increasing the revolutions per minute when discharge decreases. A discharge monitoring schedule should still be followed to assure proper operation of the variable frequency drive pump. If a line shaft turbine pump is powered with a diesel motor with speed adjustment, discharge rates can be maintained by increasing or decreasing the pump rotation speed.

The discharge rate can be monitored using an in-line water meter or flow meter placed in the discharge pipe. The discharge pipe and flow meters should be assembled to ensure accurate readings. Discharge pipes must be full and the meter installed several pipe diameters distant from sources of turbulence such as bends or valves. Meters (especially older models) should be independently calibrated and checked prior to or during the test. Other discharge-rate measurement devices include orifice meters, flumes, and weirs installed at the end of discharge pipe. (Figure 16). For low pumping rates, a volumetric measurement can be made by frequently timing how long it takes to fill a bucket or drum of known volume (for example, it takes three minutes to fill a 20-L bucket, flow rate is $Q = 20 \text{ L} / 3 \text{ minute} = 6.7 \text{ L/minute}$). Extra time and personnel may be required to oversee the discharge rate measurements and adjustments when orifices, weirs, or flumes are used.

Because pumping tests often produce large volumes of water (e.g., a well operating at 4,000 L/minute pumped for 8 hours delivers 1,920,000 L of water), a plan is needed to

manage the volumes of water produced during the pumping test. Depending on the regulations in the local of the test it may be necessary to acquire water rights to pump and discharge the water which may take time as well as create additional expense, so this should be addressed well in advance of the testing date. Further, it may be necessary to secure an environmental permit to discharge the pumped water. There are four major physical concerns that require consideration during planning and design of the test.

1. Water discharged to the surface may infiltrate and become artificial recharge to the unit being tested. This recirculation would slow the rate of observed drawdown, making observed water level changes inaccurate.
2. Discharging substantial volumes of water near the production well can flood the operational area making data collection difficult. Discharging water off-site could have adverse effects on off-site property.
3. Discharge of high flow rates can cause significant erosion at the point of discharge.
4. If the water being withdrawn is contaminated, plans for proper containment and disposal are required.

To avoid Concern #1, discharge must be routed away from the test area to eliminate the possibility of recharge within the radius of influence (drawdown cone). In unconfined aquifers, water must be conveyed via hose, pipe, ditch, storm sewer, or surface water feature beyond the radius of influence of the pumping well. The radius of influence can be estimated based on transmissivity estimates and basic analytical equations. If a deep confined aquifer is being pumped, under most conditions, infiltrating pump discharge may not impact test results. Under these conditions it may be feasible to infiltrate the discharge to the shallow subsurface via a pit or trenches without affecting water levels within the confined hydrogeologic unit being tested. However, if possible, the discharge should be piped away from the site.

Concern #2 can usually be avoided by conveying the discharge away from the test area. This often requires many meters of discharge pipe or hose. In some cases, a municipal drainage system, or a nearby surface-water feature, may handle the water. In arid areas, a lined evaporation pond may be able to dispose of the pumped water. Affected off-site property owners should be consulted to obtain permission and avoid adverse effects.

Concern #3 can be alleviated by discharging directly into large surface water bodies or infiltration galleries or constructing energy dissipation structures at the ultimate point of discharge (e.g., Thompson and Kilgore, 2006).

Concern #4 may be resolved by capturing contaminated water and processing it before release. However, when large volumes of water are produced containing or treating discharge water may be cost prohibitive and other testing methods not requiring pumping should be considered (Section 14, Slug Testing).

5.4 Data Analysis

Following test completion, time-drawdown and time-discharge rate data must be generated (Figure 10) in a form usable for test analysis. Data may need to be corrected for instrument accuracy errors and operator errors. It may also be necessary to correct the data for water-level changes not directly related to the pumping test such as precipitation events and additional drawdown (or drawup) due to changes in the pumping rate of nearby wells. The first step is to correct the collected water level data, then compute drawdown.

5.4.1 Correcting Water Level Data

Most hydrogeologists convert transducer data to equivalent water levels and then correct the data for barometric effects, and for natural pre-pumping water level trends and well interference responses. However, they rarely report instrument and operator errors that affect raw water level measurements. These conditions should also be accounted for when water level data are corrected, and drawdown computed. A discussion of water level corrections that addresses a number of factors including accounting for instrument and operator error follows.

Correction for instrument and operator errors are presented using the following example. Assume a water level measured during a constant rate pumping test at 100 minutes is 25.870 m below the top of the casing monitoring point. This measurement is recorded using electronic water-level measuring tape #2 of the three tapes used to record water level changes at the site. This tape was calibrated to a standard steel tape and found that the readings should be uniformly reduced by 0.006 m (instrument error): $WL = 25.870 \text{ m} - 0.006 \text{ m} = 25.864 \text{ m}$. The operator attempted to quantify how precisely she could measure the water level and took three measurements of the background water level in this well before pumping was initiated: 20.545 m, 20.549 m, and 20.543 m. This results in an average water level of 20.547 with a range of 0.002 to -0.004 m. Thus, the operator error was expressed as a standard deviation is 0.003 m. So, the water level measured by an operator using electric tape #2 is 25.864 with a standard deviation of 0.003 m. The background water level is reported as follows.

$$20.547 \text{ m} \pm 0.003 \text{ m} (\text{average}) - 0.006 \text{ m} (\text{instrument error}) = \\ 20.541 \text{ m} \pm 0.003 \text{ m} (\text{background})$$

The drawdown is calculated as follows.

$$25.864 \text{ m} \pm 0.003 \text{ m} (\text{operator error}) - 20.541 \text{ m} \pm 0.003 \text{ m} (\text{operator error}) = \\ 5.323 \text{ m} \pm \text{error}$$

The error computed when adding or subtracting is determined as follows.

$$(\text{error}_1^2 + \text{error}_2^2)^{0.5} = ((0.003)^2 + 0.003^2)^{0.5} = 0.004 \text{ m}$$

The reported drawdown at 100 minutes is then 5.323 m \pm 0.004 m. Though rarely done the computed drawdown value should be plotted with error bars. At scales typically used to

compute time-drawdown data, small error bars will be difficult to depict and are usually omitted.

The example above illustrates how to correct water level measurements assuming only measurement and operator errors are present. This is rarely the case. A number of other conditions can also affect observed water levels and require adjustment (correction) of the water level data before drawdown attributed to only the formational properties can be computed.

1. **A naturally occurring trend in water levels occurring before and during the time test period.** For example, if the pre-pumping water level was declining at a rate of 0.25 m per day then starting with the background water level at the beginning of the test, water level data would need a correction of $(0.25 \text{ m/d})(1 \text{ d}/1440 \text{ min}) = 0.00017 \text{ m/minute}$ as the test proceeds. For example, at 100 minutes since the beginning of the test, the background water level would have declined $(100 \text{ min})(0.00017 \text{ m/min}) = 0.017 \text{ m}$, so the measured water level at 100 minutes would have to be corrected by adding 0.017 m to the measured water level (the measured water level reflects the natural declining rate).
2. **Starting or stopping of pumping from nearby wells.** When the cone of depression of a pumping well that is not used for the test overlaps an observation or pumping well used for the test, additional drawdown occurs as explained in Section 11. This will be recorded as an anomalous increase or decrease of drawdown. If these events are short lived, the field water level trend prior to the disturbance can be extended and the observed water level data corrected by substituting water levels for the trend before interference occurred.
3. **Recharge or impermeable boundary effects.** Recharge or impermeable boundaries can slow or increase drawdown rates (respectively) in the pumping well or observation wells. When the goal is to generate time-drawdown data for analyses, these records can be truncated as trends change and the early data used in analyses. Another option is to analyze the data using image well theory as described in Section 11.
4. **Well construction effects.** The rate of drawdown measured in the pumping well can be influenced by well construction design (fully or partially penetrating screens) and turbulence as water enters the well bore and flows to the pump (well loss). Both conditions result in greater drawdown than if the wells were 100 percent efficient (i.e., neither condition was present). Corrections are needed before drawdown can be computed. Corrections for partial penetration and well loss are presented in Section 12. Delay of drawdown in the pumping well may be caused by storage in the well bore. This is a problem because many analysis techniques assume the well bore to have infinitesimal diameter such that pumped water is immediately removed from the aquifer. In the field, water initially comes from water stored in the well bore before impacting the aquifer

causing drawdown to proceed more slowly than the theoretical model represents. This is particularly problematic when there is a relatively low discharge rate from a large diameter well.

5. **Barometric pressure, tidal, and direct loading effects on confined systems.** Observation well drawdown in confined aquifers can also be affected by these influences. Correction methods are described in references such as Todd and Mays (2005). Transducer data need to be calibrated to water level measurements and instrument errors using manufacturer's specifications. In addition, if the transducers are unvented, corrections for changes in barometric pressure during the test period are required (Todd & Mays, 2005). An example of manufacturer's information is provided by Solinst™ at this [link](#)[↗].
6. **Effects of local recharge events (rainstorms), changing river stage, tidal changes, and diurnal evapotranspiration from phreatophytes on unconfined aquifers.** These effects can influence observed water levels in unconfined systems (e.g., Todd & Mays, 2005). Water level data exhibiting these effects during a pumping test require correction prior to calculating drawdown.

Corrected water level data are then used to compute drawdown data. The resulting time-drawdown data are used to compute aquifer properties.

5.4.2 Determining the Test Pumping Rate for Analysis

Discharges measured during the pumping test are used to calculate the effective discharge rate for analysis of time-drawdown data. The pumping rate, time, and, if required, the new adjusted rate, are recorded on the data sheets during a test. When a constant-rate test is conducted, the effective rate is computed from time-weighting the measured pumping rates and then computing an average pumping rate. If gauge accuracy is known, error can be assigned.

An example of computing a time-weighted average pumping rate is provided in this paragraph. A 2-hour pumping test is designed at a rate of 3,740 L/minute (L/ min). However, a constant rate was not obtained during tests, which is not unusual. Assume that the discharge measurement record is 3,710 L/min at 10 minutes, 3,751 L/min at 20 min, 3,741 L/min at 30 min, 3,750 L/min at 60 min, and 3,731 L/min at 120 min. The time-weighted average rate is computed as $((3,710 \text{ L/min} \times 10 \text{ min}) + (3,751 \text{ L/min} \times 10 \text{ min}) + (3,741 \text{ L/min} \times 10 \text{ min}) + (3,750 \text{ L/min} \times 30 \text{ min}) + (3,731 \text{ L/min} \times 60 \text{ min})) / (120) \text{ min} = 3,737 \text{ L/min}$.

5.5 Notes for Successful Test Execution

Completing a successful aquifer test requires careful planning and coordination. It helps to remember that if a test is started and conditions are such that early-time drawdown data are not being collected rapidly enough (Table 1) or the pumping rate is varying such that a planned constant discharge rate is not occurring, it is best to stop the test and restart it once water levels have recovered. The test is restarted when measurement frequency

issues are resolved and a method to stabilize the pumping rate has been implemented. This will increase the time and costs needed to complete the test, but it is better to correct these issues than spend the time and money to complete a long, poor-quality pumping test.

6 Mathematics of Flow to a Pumping Well

This section discusses the mathematics describing groundwater flow to a pumping well. When the properties of a horizontal hydrogeologic unit are isotropic and homogeneous, and perforations of the pumping well fully penetrate the unit (Figure 17), flow to a pumping well is horizontal and radial (equal in all directions). Calculus is used to describe hydraulic responses to partial differential equations that are useful for forecasting the effect of pumping on groundwater systems and deriving field scale parameters such as T and S from pumping tests.

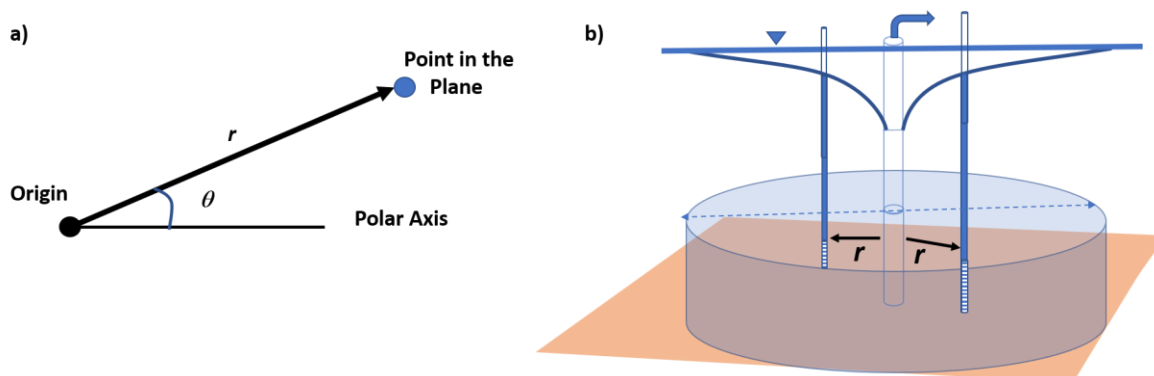


Figure 17 - Radial flow to a well described using polar coordinates. a) Polar coordinates are defined as the radial distance from the origin to a point in a plane with the angle, θ , measured counterclockwise from a horizontal polar axis. b) The radial distance (r) from the pumping well (origin) to two observation wells penetrating a confined aquifer (represented by the light blue shaded cylindrical volume) is illustrated. The cylinder represents the portion of the aquifer impacted by pumping. The cylinder diameter is represented by a dashed blue, double-arrow line. The orange square represents the impermeable aquifer base.

6.1 Using Polar Coordinates

Radial flow can be described using a polar coordinate system, where r is the radial distance from an origin (a pumping well) to an observation point (Figure 17). The position of the observation point is defined by r and an angle, θ , measured from a horizontal axis (polar axis) in a counterclockwise direction (Figure 17). When conditions are isotropic and homogeneous, the water bearing unit is horizontal, and the open area of the pumping well fully penetrates the unit, the angle θ becomes unimportant as all flow is horizontal and thus is the same on every radius (Fetter, 2001).

6.2 Development of Equations Describing Aquifer Responses to Pumping

Equations developed to relate the hydrogeologic properties of earth materials in a groundwater system to the changes in hydraulic head when the aquifer is pumped, are founded on Darcy's Law and the conservation of mass (water). These general governing equations are presented in the Groundwater Project book *Hydrogeologic Properties of Earth Materials and Groundwater Flow* (Woessner & Poeter, 2020). The equations describe factors

controlling the movement of groundwater in confined and unconfined water bearing units under steady-state and transient conditions, and in isotropic, anisotropic, homogeneous, and heterogeneous settings.

The flow of groundwater to wells under a variety of conditions can be represented by these same governing equations (Woessner & Poeter, 2020). When conditions are defined by linear mathematical differential equations, and specific mathematical boundary and initial conditions are applied, calculus solution techniques result in algebraic equations referred to as analytical solutions or analytical models.

The governing equations for confined and unconfined aquifers form the basis for development of analytical solutions describing the flow of water to a pumping well. A wide variety of analytical solutions that predict the corresponding water level response to pumping in both steady-state and transient conditions are documented in the literature. However, in almost all cases, basic formulations are limited to radial flow in an isotropic and homogeneous hydrogeologic unit that is considered unbounded (i.e., of infinite lateral extent). Other boundary conditions can be specified in some cases. These simplifying conditions reduce the mathematical challenges encountered when solving and formulating an analytical solution.

6.2.1 Confined Aquifers

The development of analytical solutions for pumping conditions starts with the governing equations that describe steady-state and transient flow in two dimensions (i.e., in horizontal x - and y -cartesian coordinates) in a homogeneous and isotropic confined groundwater system. Transmissivity, T , describes the ease with which water moves through an aquifer and is defined as the product of hydraulic conductivity and aquifer thickness. Given their two-dimensional nature, they are applicable to essentially horizontal flow. Equation (1) describes steady conditions and Equation (2) describes transient conditions.

$$0 = \left(\frac{\partial^2 h}{\partial x^2} + \frac{\partial^2 h}{\partial y^2} \right) \quad (1)$$

$$S \frac{\partial h}{\partial t} = T \left(\frac{\partial^2 h}{\partial x^2} + \frac{\partial^2 h}{\partial y^2} \right) \quad (2)$$

where:

S = storativity (dimensionless)

h = hydraulic head (L)

t = time (T)

T = transmissivity (L^2T^{-1})

x,y = coordinates (L)

These two-dimensional equations in cartesian coordinates (x,y) can be converted into polar coordinates by recognizing $r = (x^2 + y^2)^{0.5}$ as shown in Equations (3) and (4).

$$0 = \left(\frac{\partial^2 h}{\partial r^2} + \frac{1}{r} \frac{\partial h}{\partial r} \right) \quad (3)$$

$$S \frac{\partial h}{\partial t} = T \left(\frac{\partial^2 h}{\partial r^2} + \frac{1}{r} \frac{\partial h}{\partial r} \right) \quad (4)$$

where:

S = storativity (dimensionless)

h = hydraulic head (L)

t = time (T)

T = transmissivity (L^2T^{-1})

r = radial distance from the origin (the pumping well) (L)

Additional documentation on the derivation of Equations (3) and (4) is provided in the work of Lohman (1972, in the section presenting partial differential equations for radial flow).

Formulating the steady-state and transient equations, Equations (5) and (6) respectively, in terms of drawdown (s) for any r value is presented in many documents (e.g., Loaiciga, 2009).

$$0 = \frac{1}{r} \frac{\partial s}{\partial r} + \left(\frac{\partial^2 s}{\partial r^2} \right) \quad (5)$$

$$\frac{S}{T} \frac{\partial s}{\partial t} = \frac{1}{r} \frac{\partial s}{\partial r} + \left(\frac{\partial^2 s}{\partial r^2} \right) \quad (6)$$

where:

s = drawdown = $h_{\text{corrected-static}} - h_t$ (L)

$h_{\text{corrected-static}}$ = initial water level prior to pumping corrected for background variations (L)

h_t = water level at time t since the pumping started (L)

r = radial distance from the center of the pumped well to the observation well (L)

t = elapsed time since the start of pumping (T)

T = transmissivity (L^2T^{-1})

S = storativity (dimensionless)

Equations (3), (4), (5), and (6) are referred to mathematically as linear differential equations and can be solved using calculus techniques. They are the basis for the development of an analytical equation describing the response of confined aquifers to pumping. Additional factors can be added to these equations to account for other groundwater sources and sinks such as leakage at a constant rate or the constant discharge of water from a pumping well (negative value of w) as in Equations (7) and (8).

$$0 = \left(\left(\frac{\partial^2 h}{\partial r^2} + \frac{1}{r} \frac{\partial h}{\partial r} \right) + w \right) \quad (7)$$

$$S \frac{\partial h}{\partial t} = T \left(\left(\frac{\partial^2 h}{\partial r^2} + \frac{1}{r} \frac{\partial h}{\partial r} \right) + \frac{w}{T} \right) \quad (8)$$

where:

- S = storativity (dimensionless)
- h = hydraulic head (L)
- t = time (T)
- T = transmissivity (L^2T^{-1})
- r = radial distance from origin (pumping well) (L)
- w = source or sink term (LT^{-1})

6.2.2 Unconfined Aquifers

The two-dimensional governing equation representing essentially horizontal steady-state and transient flow in a homogeneous and isotropic unconfined groundwater system are shown in Equations (9) and (10). These equations are based on the assumptions that the water table is the top of the aquifer (i.e., drainage of pores in the capillary fringe is negligible) and elastic storage is negligible (i.e., water comes from drainage of pores below the water table and not from expansion of water or compression of the aquifer). Head values are measured from the horizontal base of the unconfined unit to the water table thus represent the saturated thickness as well as head.

$$0 = \frac{\partial^2 h^2}{\partial x^2} + \frac{\partial^2 h^2}{\partial y^2} \quad (9)$$

$$S_y \frac{\partial h}{\partial t} = \frac{K}{2} \left(\frac{\partial^2 h^2}{\partial x^2} + \frac{\partial^2 h^2}{\partial y^2} \right) \quad (10)$$

where:

- S_y = specific yield (dimensionless)
- h = hydraulic head measured from the base of the aquifer (L)

- K = hydraulic conductivity (LT^{-1})
 t = time (T)
 x,y = Cartesian coordinates (L)

In radial coordinates these equations become Equations (11) and (12).

$$0 = \left(\frac{\partial^2 h^2}{\partial r^2} + \frac{1}{r} \frac{\partial h^2}{\partial r} \right) \quad (11)$$

$$S_y \frac{\partial h}{\partial t} = \frac{K}{2} \left(\frac{\partial^2 h^2}{\partial r^2} + \frac{1}{r} \frac{\partial h^2}{\partial r} \right) = \frac{K}{r} \frac{\partial}{\partial r} \left(h r \frac{\partial h}{\partial r} \right) \quad (12)$$

where:

- S_y = specific yield (dimensionless)
 h = hydraulic head measured from the base of the aquifer (L)
 K = hydraulic conductivity (LT^{-1})
 t = time (T)
 r = distance from origin (pumping well) (L)

Additional factors can be added to these equations to account for other groundwater sources and sinks such as leakage at a constant rate into an unconfined aquifer under steady-state or transient conditions as shown in Equations (13) and (14).

$$0 = \left(\frac{\partial^2 h^2}{\partial r^2} + \frac{1}{r} \frac{\partial h^2}{\partial r} \right) + \frac{2}{K} w \quad (13)$$

$$S_y \frac{\partial h}{\partial t} = \frac{K}{2} \left(\left(\frac{\partial^2 h^2}{\partial r^2} + \frac{1}{r} \frac{\partial h^2}{\partial r} \right) + \frac{2w}{K} \right) \quad (14)$$

where:

- S_y = specific yield (dimensionless)
 h = hydraulic head measured from the base of the aquifer (L)
 K = hydraulic conductivity (LT^{-1})
 t = time (T)
 r = distance from origin (pumping well) (L)
 w = source or sink term (LT^{-1})

Though these differential equations describing radial flow in an unconfined system are properly stated, they are also mathematically nonlinear. These governing equations cannot be easily converted to analytical solutions using standard calculus methods (Fetter, 2001). As a result, numerical methods are commonly used to simulate groundwater flow to wells in unconfined aquifers (e.g., Anderson et al., 2015). Transient analytical equations associated with basic methods to graphically solve unconfined hydraulic testing results are formulated using an approximation of Equation (12) that is linearized with the confined formulation, and a condition that the drawdown in the unconfined system is small at observations points such that hydraulic properties are constant. This is accomplished by taking h outside of the derivative of the right-hand side of Equation (12) and substituting b for h to derive Equation (15).

$$S_y \frac{\partial h}{\partial t} \cong \frac{Kb}{r} \frac{\partial}{\partial r} \left(r \frac{\partial h}{\partial r} \right) = T \left(\frac{\partial^2 h}{\partial r^2} + \frac{1}{r} \frac{\partial h}{\partial r} \right) \quad (15)$$

where:

- S_y = unconfined storativity (specific yield) (dimensionless)
- h = head measured as the difference between the water table elevation and the elevation of the horizontal base of the unconfined aquifer (L)
- t = elapsed time since the start of pumping (T)
- K = hydraulic conductivity (LT^{-1})
- b = saturated thickness measured from the base of the aquifer to the water table at the pumping well (L)
- r = radial distance from the center of the pumped well to the observation well (L)
- T = Kb , unconfined aquifer transmissivity (L^2T^{-1})

Section 10 discusses this approach where specific analytical models describing pumping unconfined systems are presented.

6.3 General Assumptions Used to Develop Analytical Well Hydraulic Equations

Several simplifying assumptions are required to generate workable analytical solutions from linear differential equations. Such equations are used to forecast the effect of pumping on production and observation well water levels. The resulting analytical solutions are powerful, but their use has limitations as they are simplified to represent ideal conditions that are not usually satisfied in the real world.

Many textbooks list the general assumptions used to formulate standard analytical hydraulic test equations (e.g., Freeze & Cherry, 1979; Fetter, 2001; Kasenow, 2001). In this

book we use a modified version of those listed in Fetter (2001) including twelve general assumptions.

1. **A confining layer underlies the geologic unit being pumped.** This assumption states no water moves vertically upward from the underlying formations.
2. **Geologic units being pumped are essentially horizontal.** This assumption eliminates the need to account for flow that is not horizontal.
3. **The geologic unit being pumped has infinite lateral extent.** This assumption eliminates the presence of boundary conditions that could limit the expansion of the cone of depression (e.g., impermeable or recharge boundaries).
4. **The potentiometric surface and water table are stable (do not change with time) prior to pumping, and all subsequent changes in the potentiometric surface and water table are a result of pumping.** This assumption eliminates the complications of having the background water level fluctuate prior to the start of pumping or during pumping. Under these conditions the potentiometric surface and water table are initially static, and all drawdown is caused by the pumping well. This removes those variations in drawdown that may be created by nearby pumping wells or natural water level variations (e.g., recharge, discharge, barometric, or tidal effects).
5. **The geologic unit being pumped is isotropic and homogeneous.** This assumption means that hydrogeologic properties such as K , T , S , and S_y are uniform and constant. Under these conditions the cone of depression will be symmetrical.
6. **Flow in the pumped formation is radial.** This assumption allows radial flow theory and mathematics to be applied. It also says observation wells located at different radial distances from the pumping well do not have to be in a straight line to describe how pumping affects water levels at various distances from the pumping well.
7. **Flow in the pumped formation is essentially horizontal.** This factor eliminates the need to account for vertical flow and the resulting more complex mathematics.
8. **Darcy's law governs groundwater flow.** This assumption allows governing equations based on the validity of Darcy's Law to be used to formulate the required mathematics (i.e., groundwater flow is laminar, as discussed by Woessner and Poeter (2020)).
9. **The viscosity and density of the groundwater is constant.** This assumption eliminates the need to account for variations in viscosity and density which cause K to vary and produce gradients in addition to the hydraulic gradients caused by pumping the well. This assumption requires that temperature and

dissolved solute concentration are reasonably uniform throughout the aquifer over the time period when the equation is applied. Again, formulating a solution that includes these factors requires additional mathematical rigor.

10. **The observation and pumping wells are screened over the entire geologic unit being tested and are 100 percent efficient.** The fully screened assumption assures that the flow of the water in the geologic unit is horizontal. The 100 percent efficient requirement means there are no frictional nor turbulent head losses as water enters the pumped well. This is important because head loss causes water levels to be lower in the pumped well than in the aquifer immediately adjacent to the well, whereas the equations assume the head in the pumping well is equal to the head in the aquifer at the locations of the well. The 100 percent efficient requirement also means there is no skin effect. A skin is a zone in the formation around the borehole that has been altered as a result of drilling, often due to drilling fluid permeating the pores of the formation and decreasing hydraulic conductivity in the zone. Observation wells are not pumped so they do not have losses due to friction or turbulence although they may have a skin that may limit the rate of water level response to pumping.
11. **The location of the pumping well can be represented as a single point that has an infinitesimal diameter.** This assumption simplifies the mathematics of calculating the drawdown at a distance, r , from the pumping well and eliminates the need to consider the effect of water stored in the well bore, a condition that would impact the drawdown observed in the pumping well (referred to as casing/wellbore storage effects).
12. **The well discharge is constant.** This factor eliminates the need to define the well discharge as a variable entity in the mathematical solution.

Analytical well hydraulic equations can be thought of as tools to describe how any selected well discharge affects the head distribution in the hydrogeologic unit being pumped. Analytical solutions provide continuous solutions. This means under steady-state conditions (Section 7) they can be used to generate an estimate of drawdown at any location in the problem domain as defined by the radial distance from the pumping well. When equations are transient (Sections 8-12), they describe conditions at any location and time since pumping started.

Sections 7 through 12 develop analytical equations that describe how wells effect water levels in confined and unconfined units under steady-state and transient conditions. These equations can be applied to estimate drawdown resulting from pumping of a well at a specified rate when hydrogeologic properties are known. These equations are also used to analyze pumping test results and compute hydrogeologic property values from the time/drawdown data for the hydrogeologic units pumped.

7 Thiem Steady-State Analytical Models for Pumping Confined and Unconfined Aquifers

Steady-state conditions occur when water levels stop changing within the cone of depression during a pumping test. Steady state is an equilibrium condition. Steady state occurs when the expansion of the cone of depression is limited by a recharge boundary condition that provides a source of water to the pumping well other than water stored in the aquifer and creates a steady condition when the inflow rate is equal to the extraction rate of the well (Figures 8 and 9). When steady-state conditions occur, water is not being released from storage in the unit being pumped. Thiem (1906) developed equations that describe steady-state conditions during pumping confined and unconfined units. These are known as the Thiem equations.

A well may need to be pumped for a long period before the cone of depression expands sufficiently to capture recharge sources that equal the well discharge rate and thus stabilize the heads. Tests may require pumping over several days or weeks before reaching a steady state. When recharge sources are not encountered *pseudo-steady-state* conditions may be observed. This refers to conditions where drawdown rates become minimal with long pumping times. Steady-state equations are often applied to these conditions to estimate hydraulic conductivity and transmissivity.

7.1 Steady-State Conditions in a Confined Groundwater System

The general assumptions listed under the discussion of the development of analytical solutions in Section 6 are applied when developing equations to represent steady-state pumping conditions. An additional condition is applied stating that drawdown has reached equilibrium as the cone of depression ceases to expand as pumping continues.

The steady-state mathematics are based on Darcy's Law and the conservation of mass. Under steady-state conditions the gradients within the cone of depression do not change over time. With radial flow, the discharge at any given radial distance from the pumping well is equal to the hydraulic conductivity (K) times the cross-sectional area ($2\pi rb$), times the gradient ($-dh/dr$) at that radial distance from the pumping well (Figure 18).

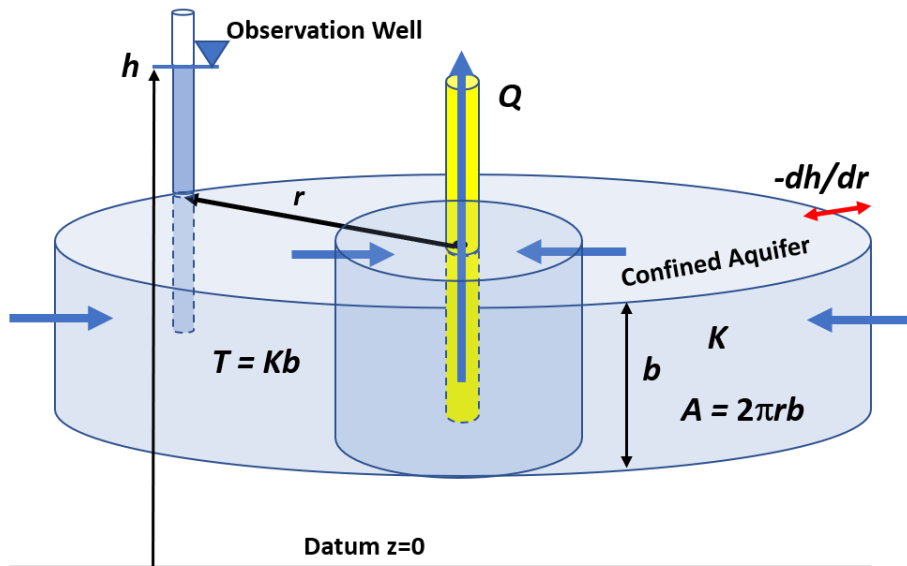


Figure 18 - The radial flow of water through a cylindrical area within the steady-state cone of depression in an isotropic and homogeneous system. The well discharge, Q , is constant as it passes through each circumferential cross-sectional area, A , defined as $2\pi rb$. The hydraulic conductivity is represented by K . The steady-state gradient ($-dh/dr$) is constant at each r .

Darcy's Law is the equation describing steady-state flow in an isotropic and homogeneous confined aquifer as shown in Equation (16).

$$\frac{dh}{dr} = \frac{Q}{2\pi Tr} \quad (16)$$

where:

- h = total head measured from a datum (L)
- r = radial distance to an observation well (L)
- Q = constant pumping rate, negative for withdrawal (L^3T^{-1})
- T = confined aquifer transmissivity (Kb) (L^2T^{-1})
- K = hydraulic conductivity (LT^{-1})
- b = thickness of the confined aquifer (L)

Equation (16) is used to generate an analytical solution when it is constrained by conditions where the heads at two observation wells, each located at a different radial distance from the pumping well, are known as shown in Figure 19. Standard integration techniques are used to derive what is referred to the Thiem steady-state equation for pumping a confined unit.

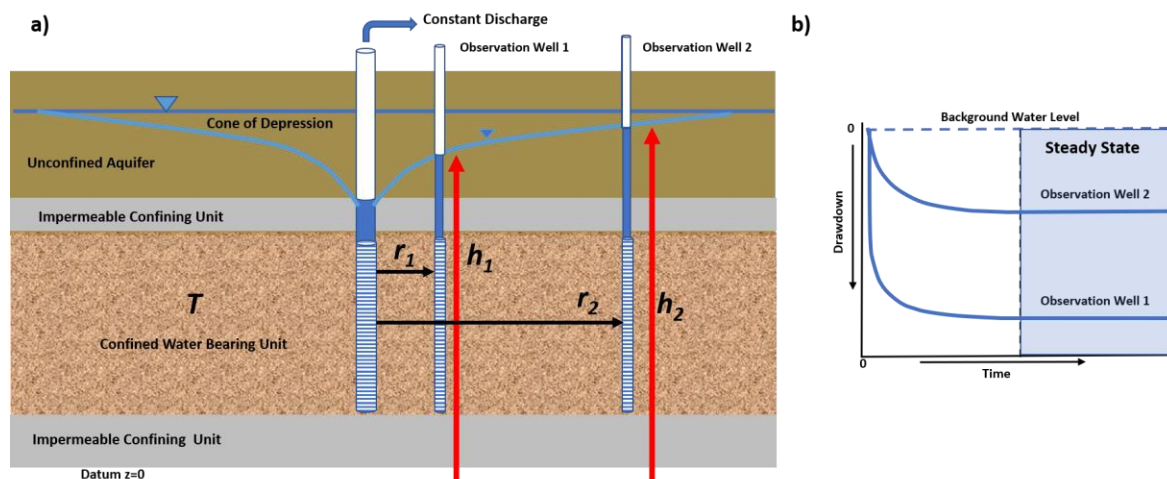


Figure 19 - Cross section of a confined aquifer and the parameters used to define steady-state conditions. a) The heads at the observation wells (red arrows) are measured from a datum. The radial distances are measured from the pumping well. b) An arithmetic plot of drawdown and time showing the drawdown reaching steady-state conditions (dashed vertical black line and blue shaded area).

The Thiem analytical solution (Thiem, 1906) for a confined aquifer is written in terms of transmissivity as shown in Equation (17).

$$T = \frac{Q}{2\pi(h_2 - h_1)} \ln\left(\frac{r_2}{r_1}\right) \quad (17)$$

where:

T = confined aquifer transmissivity (Kb) (L^2T^{-1})

Q = constant pumping rate (L^3T^{-1})

h_2 = head at observation well 2 located further from the pumping well (L)

h_1 = head at observation well 1 located closer to the pumping well (L)

r_2 = radial distance to observation well 2 (L)

r_1 = radial distance to observation well 1 (L)

Equation (17) does not include storativity of the aquifer because storage is irrelevant in a steady-state system as indicated by the steady-state groundwater flow equations. In a steady-state system, the heads are constant and no water is released from storage during pumping. The equation can be used to solve for T when a constant-discharge test includes drawdown data from two observation wells.

Example

Let us assume there is a well in a confined groundwater system pumping at 1,500 m^3/d and the heads have stopped declining after some time signaling steady-state conditions are occurring. If the head in observation well 1 at a radial distance of 55 m is 1,033 m and the head at observation well 2 at a radial distance of 150 m is 1,040 m, compute T .

$$T = \frac{1,500 \frac{m^3}{d}}{2 (3.14) (1040m - 1033m)} \ln \frac{150 m}{50 m} = 37.5 \frac{m^2}{d}$$

The Thiem equation can also be used to predict the steady-state head at an observation well located at any radial distance from the pumping well if the aquifer transmissivity, pumping rate, head, and the radial distance to one observation well are known.

7.2 Steady-State Conditions in an Unconfined Aquifer

The mathematics for steady-state flow in an unconfined aquifer are based on Darcy’s Law and the conservation of mass. Under steady-state conditions the gradient within the cone of depression does not change over time and the discharge at any radial distance (within the cone of depression) from the pumping well is equal to the hydraulic conductivity (K) times the cross-sectional area ($2\pi rh$), times the gradient ($-dh/dr$) at that radial distance. In the case of the unconfined system, the head values (h) are defined as the difference between the water table elevation and the elevation of the aquifer base (Figure 20).

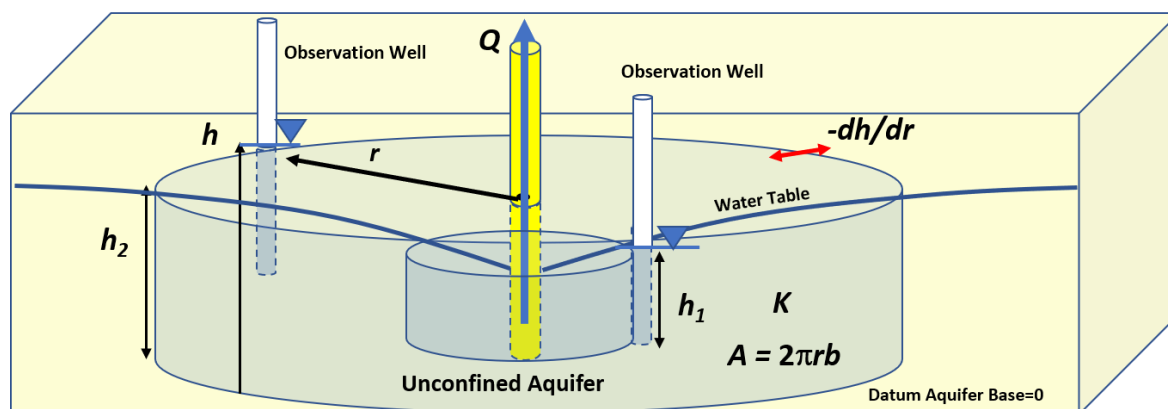


Figure 20 - The radial flow of water through a cylindrical area within the steady-state cone of depression created in an isotropic and homogeneous unconfined groundwater system when pumping a well at a constant rate. The well discharge (Q) passes through a cross sectional area ($A=2\pi rh$), of a material that has a hydraulic conductivity (K) under a gradient ($-dh/dr$) directing water to the well. The head (h) is equal to the saturated thickness measured as the water table elevation minus the elevation of the base of the unconfined system.

To formulate an analytical solution, the Thiem (1906) general assumptions are applied along with the Dupuit (1863) assumptions that the slope of the water table is equal to the hydraulic gradient and flow is horizontal (e.g., Fetter 2001; Kruseman & de Ritter, 2000). The resulting equation describes steady-state flow in an unconfined system as shown in Equation (18).

$$Q = -(2\pi rh)K \left(\frac{dh}{dr} \right) \tag{18}$$

where:

Q = constant discharge (L^3T^{-1})

r = radial distance to the pumping well (L)

h = saturated thickness of the aquifer measured from the aquifer base (L)

dh/dr = hydraulic gradient (dimensionless)

An analytical solution is derived by integration with the head in the unconfined unit defined as the height of saturation above the unconfined aquifer base, h_1 . The closer observation well is defined by values of r_1 and h_1 , and the farther observation well represented by values r_2 and h_2 (Figure 21).

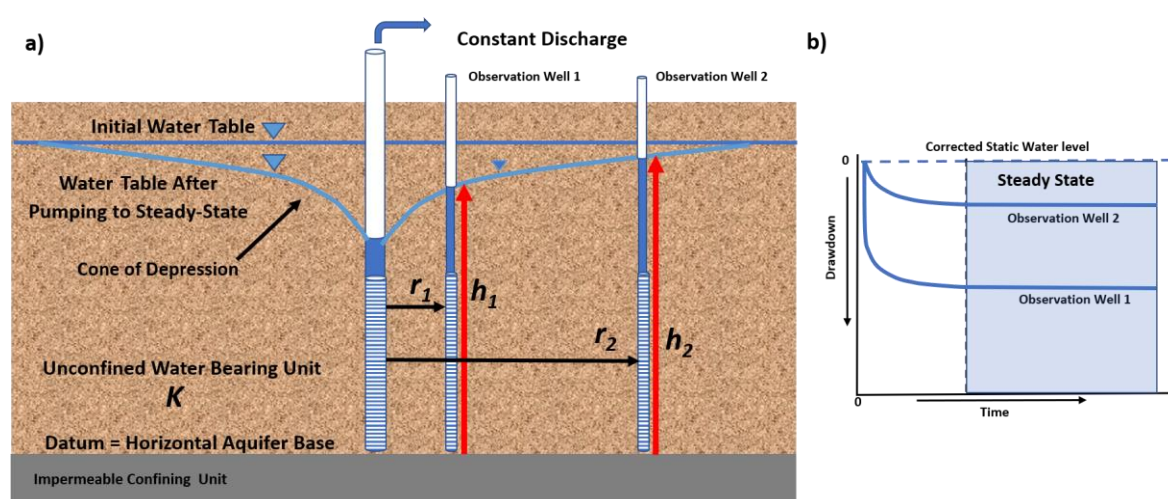


Figure 21 - Cross section of an unconfined groundwater system under steady-state conditions. a) Location of observation wells and parameters required by the Thiem equation. The saturated thickness (h) at an observation well is measured from the horizontal base of the system. b) Drawdown time curves for the observation wells. The dashed vertical line and light blue shading indicate when drawdown reaches and remains at steady state.

The resulting analytical solution is given as Equation (19).

$$K = \frac{Q}{\pi(h_2^2 - h_1^2)} \ln\left(\frac{r_2}{r_1}\right) \quad (19)$$

where:

K = unconfined unit hydraulic conductivity (LT^{-1})

Q = constant pumping rate (L^3T^{-1})

h_2 = saturated thickness at well 2 furthest from the pumping well (L)

h_1 = saturated thickness at well 1 furthest from the pumping well (L)

r_2 = radial distance to observation well 2 (L)

r_1 = radial distance to observation well 1 (L)

The use of this equation assumes that once heads have reached steady state the change in saturated thickness at observation locations are small—less than 2 to 10 percent, depending on the literature reference.

Example

Assume a well is pumping in an unconfined aquifer at 1,500 m³/d. The original saturated thickness is 30 m. After reaching steady state the saturated thickness at observation Well 1 located 37 m from the pumping well is 26.9 m. The steady state saturated thickness at observation well 2, located 147 m from the pumping well, is 29.2 m. The hydraulic conductivity can be estimated for the unconfined system using Equation (19).

$$K = \frac{1,500 \frac{\text{m}^3}{\text{d}}}{3.14 ((29.2\text{m})^2 - (26.9\text{m})^2)} \ln\left(\frac{147 \text{ m}}{37 \text{ m}}\right) = 5.11 \frac{\text{m}}{\text{d}}$$

As with the confined aquifer equation, the saturated thickness of the aquifer at any radial distance from the pumping well can be computed if the aquifer hydraulic conductivity, well discharge, and the saturated thickness at a radial distance at one observation well are known.

Again, when applying the Thiem equation for unconfined aquifers it is assumed that the head at observation wells is measured from the horizontal base of the aquifer so that it corresponds to the saturated thickness. The values of total head are not used in this equation as they are in the Thiem equation for confined groundwater systems. A common mistake is to use head values based on a datum other than the aquifer base (e.g., mean sea level). This will result in large errors in the estimated value of K .

Jacob (1963) proposed a modification of the Thiem equation for use with a water table system where drawdown becomes significant (i.e., 10 to 25 percent of the initial saturated thickness) at observation wells during testing (Figure 22). His method adjusted the observed drawdown (not saturated thickness), s_1 and s_2 , to values that would occur if no significant dewatering took place (less than 2 to 10 percent depending on the reference source: Jacob, 1950; United States Department of the Interior (USDI), 1981) as shown in Figure 22. Calculations of K and T are then computed using the Thiem representation.

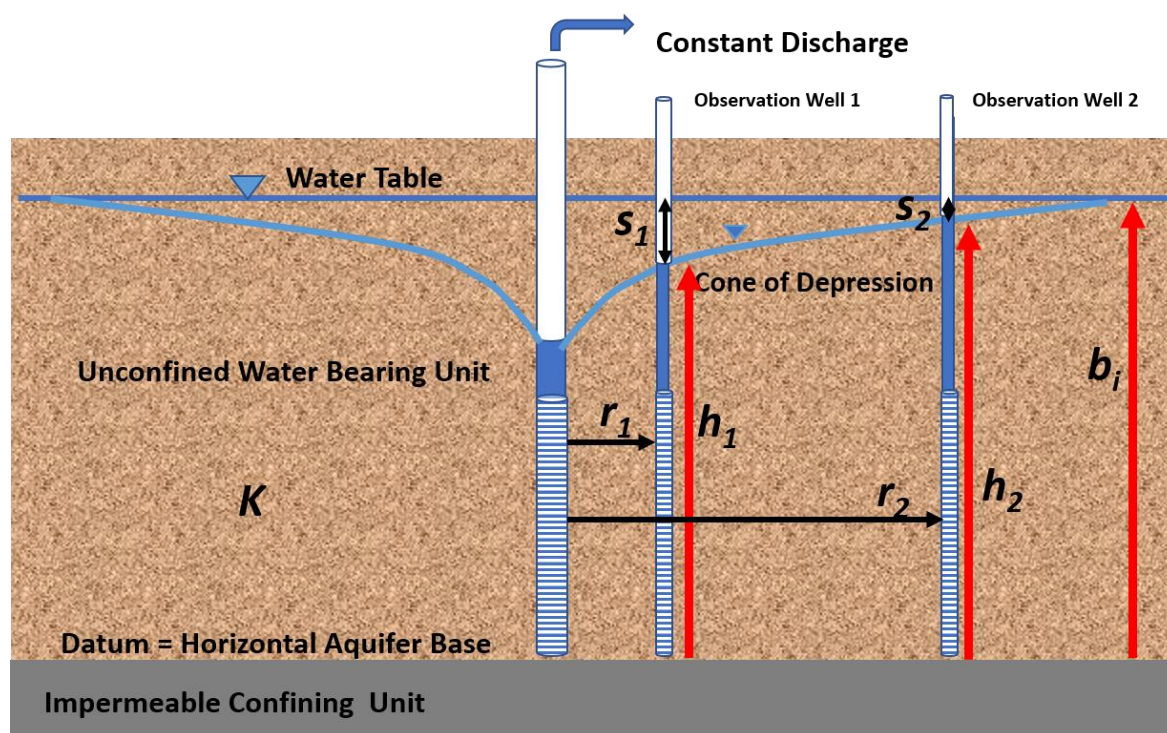


Figure 22 - The Jacob (1963) approach to estimating T for the steady-state pumping of an unconfined aquifer with significant drawdown. The drawdown at the two observation wells is s_1 and s_2 , respectively. The pre-pumping saturated thickness is represented by b_i . The saturated thickness at the observation wells is h_1 and h_2 , respectively.

Lohman (1972) presents the unconfined formulation in terms of corrected drawdown as shown in Equations (20) and (21) for K and T respectively. The log base 10 is used in Lohman's equations so it is useful to know that $\ln(x)=2.3\log(x)$.

$$K = \frac{-Q \cdot 2.3 \log\left(\frac{r_2}{r_1}\right)}{\frac{2\pi b_i \left((b_i^2 - 2b_i s_2 + s_2^2) - (b_i^2 - 2b_i s_1 + s_1^2) \right)}{2b_i}} \quad (20)$$

$$T = \frac{-Q \cdot 2.3 \log\left(\frac{r_2}{r_1}\right)}{2\pi \left(\left(s_1 - \frac{s_1^2}{2b_i} \right) - \left(s_2 - \frac{s_2^2}{2b_i} \right) \right)} \quad (21)$$

where:

- b_i = initial (pre-pumping) unconfined saturated thickness (L)
- K = hydraulic conductivity (LT^{-1})
- Q = constant discharge rate (L^3T^{-1})
- r_2 = radial distance to observation well 2 (L)
- r_1 = radial distance to observation well 1 (closest) (L)
- s_1 = drawdown at observation well 1 (closest) (L)

s_2 = drawdown at observation well 2 (L)

T = transmissivity (L^2T^{-1})

Using Equation (21) the drawdown correction is equal to $s^2/2b$. If the magnitude of the correction is small, the computed T value will not change much. The correction is recommended when the pre-pumping saturated thickness is affected by 10 to 25 percent at the measuring point (Kasenow, 2001; USDI, 1981). Kasenow (1995, 1997) developed additional approaches to correct observed drawdown data when reductions exceed 25 percent.

Example of Graphical Method

Steady-state analyses require information from a pumping test that includes the measured drawdown (corrected-static head - pumping head) at two locations (i.e., two different radial distances from the pumping well). Lohman (1972) presents a graphical distance-drawdown method using corrected drawdown to solve for T under confined and unconfined conditions. A graphical semi-log, distance-drawdown graph is shown in Figure 23. To represent confined aquifers, Equation (21) is simplified by representing the change in drawdown with distance with the change in drawdown over one log cycle of radial distance (i.e., $\Delta s_{\log-r}/(\Delta \log(r))$) to obtain Equation (22). $\Delta s_{\log-r}$ is purposefully selected as the drawdown change over one log cycle of distance so that $\Delta s_{\log-r}/(\Delta \log(r))$ becomes $\Delta s_{\log-r}$ divided by 1 (e.g., $\Delta(\log r) = \log 100 - \log 10 = 1$).

$$T = \frac{2.3 Q}{\frac{2\pi\Delta s_{\log-r}}{\Delta(\log r)}} \quad (22)$$

where:

T = transmissivity (L^2T^{-1})

Q = constant discharge (L^3T^{-1})

$\Delta s_{\log-r}$ = change in drawdown over one log cycle of distance (positive) (L)

$\Delta(\log r)$ = difference in log of radial distances that differ by one order of magnitude (dimensionless)

When drawdowns need correction for unconfined aquifer dewatering then Equation (23) is used.

$$T = \frac{2.30 Q}{\frac{2\pi\Delta \left(s - \frac{s^2}{2b_i} \right)}{\Delta \log r}} \quad (23)$$

where:

T = transmissivity (L^2T^{-1})

Q = constant discharge (L^3T^{-1})

$\Delta(s-(s^2/(2b_i)))$ = change in corrected drawdown over one log cycle of distance (positive) (L)

$\Delta \log r$ = one log cycle of radial distance (dimensionless)

b_i = initial (pre-pumping) unconfined saturated thickness (L)

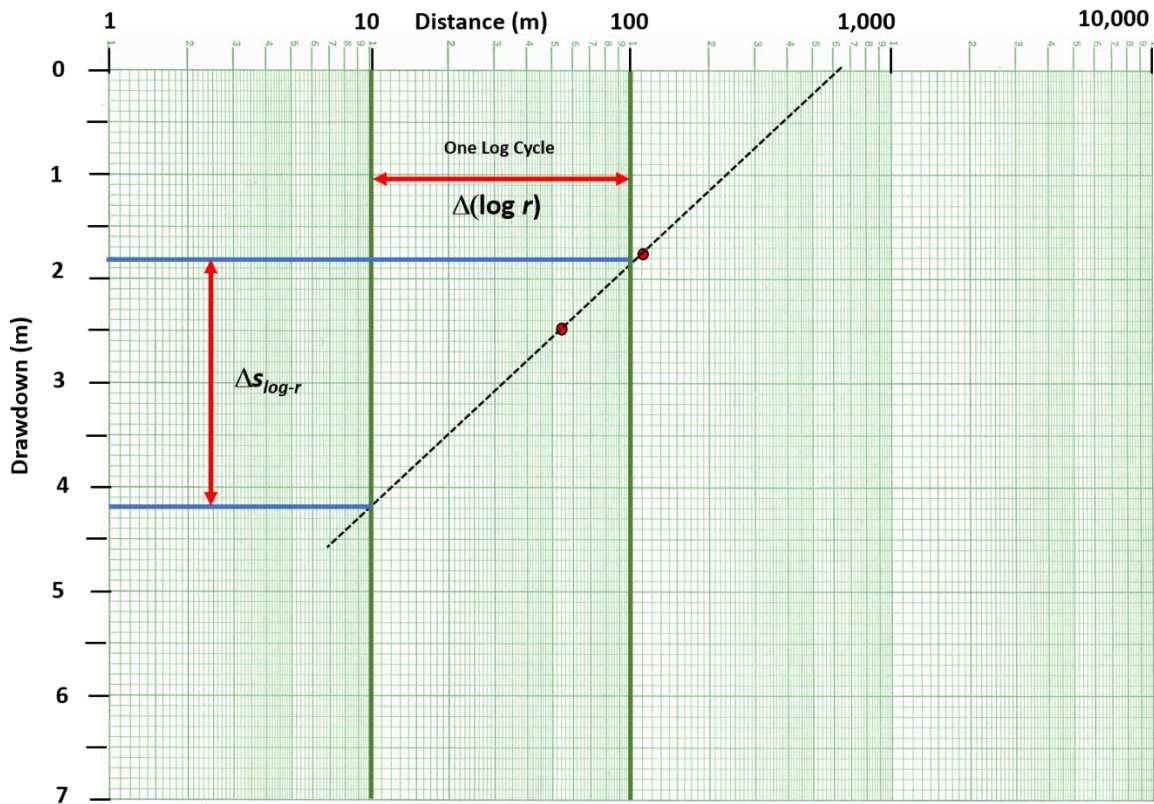


Figure 23 - Plot of the drawdown at two observation wells (red dots) after steady-state conditions were reached during a constant discharge test of a confined aquifer. The slope of the line is defined over one log cycle as $\Delta s_{\log-r} / \Delta(\log r)$ (red double arrows). $\Delta s_{\log-r} / \Delta(\log r)$ is equal to 2.4 m / 1.

Example

The distance-drawdown plot presented in Figure 23 is the steady-state drawdown observed at observation wells located 55 m and 123 m from a production well pumping at a constant rate of 1,400 m³/d. The wells fully penetrate a 24 m-thick confined sand. From the graph, $\Delta s_{\log-r} = 2.4$ m. T is computed using Equation (22).

$$T = \frac{2.3 \cdot 1,400 \frac{\text{m}^3}{\text{d}}}{2 \cdot (3.14) \cdot (4.2 \text{ m} - 1.8 \text{ m})} = 214 \frac{\text{m}^2}{\text{d}}$$

Sections 8 through 11 address the development and application of simplified analytical models that represent how groundwater systems respond to pumping and how T and S are estimated under transient conditions.

7.3 An Opportunity to Work with Steady-State Pumping Test Data

Section 7 discussed pumping tests that encounter steady state conditions. [Exercise 1](#) ↓ provides a hands-on opportunity to work with data representing steady state conditions in a confined aquifer.

8 Transient Analytical Model for Pumping of a Fully Confined Aquifer

A hydrogeologic unit is considered confined when the heads in tightly cased wells are higher than the top of the unit. The surface defining the head distribution is referred to as the potentiometric surface (Woessner & Poeter, 2020, Figure 46). The pressure in confined systems exceeds the hydrostatic pressure.

C. V. Theis (1935), with the assistance of C. I. Lubin, applied the mathematics that describe a “...continuous point source for a heat conduction problem” (Lohman, 1972), to formulate an analytical solution for flow to a well in a confined aquifer under transient conditions. Transient conditions are non-equilibrium conditions. The Theis solution (1935) describes how a confined groundwater system would react to pumping over time. This was the first transient model available for analyzing non-steady time-drawdown data sets. Prior to his work, wells would be pumped for long periods until drawdown reached steady-state or pseudo-steady-state conditions (as described in Section 7). Then drawdown versus distance data would be analyzed using the Thiem steady-state equations. Theis’s non-equilibrium analyses resulted in shorter hydraulic tests in which time-drawdown data are used to derive hydraulic properties of confined systems.

8.1 Formulation of the Theis Equation

Development of the Theis analytical solution incorporates the general assumptions described in Section 6.3 along with the following additional assumptions:

1. The confined unit is covered by overlying and underlying confining beds that are aquifuges (non-porous and impermeable, i.e., not permitting any water to leak into the aquifer).
2. The source of all water pumped from a well is derived from the instantaneous release of water from elastic storage of the unit (there is no recharge or flow of water into the cone of depression from other sources).
3. The pumping well has an infinitesimal diameter.

Figure 24 illustrates the Theis conceptual model.

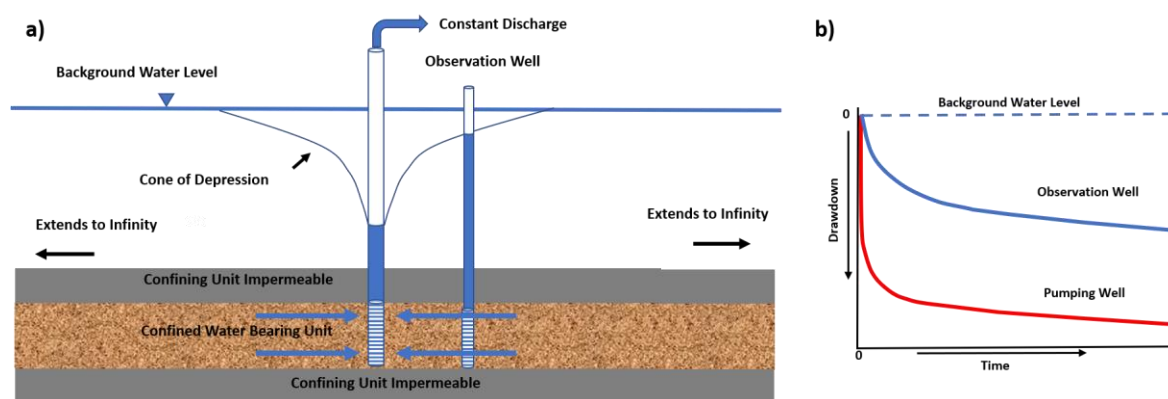


Figure 24 - Conceptual model of the Theis equation conditions describing the head response to pumping in a totally confined isotropic and homogeneous aquifer. a) Cross sectional view of a confined water bearing unit that is infinite in lateral extent as well as overlain and underlain by confining units that are impermeable. b) Schematic of the response of water level changes (drawdown from the corrected-static water level) in the pumping well and an observation well when the pumping rate is constant.

The basic differential equation, Equation (6), governing radial flow to a well in a confined systems expressed in terms of drawdown is repeated here for the reader's convenience (Loaiciga, 2009).

$$\frac{S}{T} \frac{\partial s}{\partial t} = \frac{1}{r} \frac{\partial s}{\partial r} + \left(\frac{\partial^2 s}{\partial r^2} \right) \quad (24)$$

where:

- s = drawdown, corrected pre-pumping static head minus head at time t (L)
- r = radial distance from the center of the pumped well to the observation well (L)
- t = elapsed time since the start of pumping (T)
- T = transmissivity (L^2T^{-1})
- S = storativity (dimensionless)

Equation (24) can be visualized by describing the transient radial flow in any cylindrical section within the cone of depression of a confined system (Figure 25).

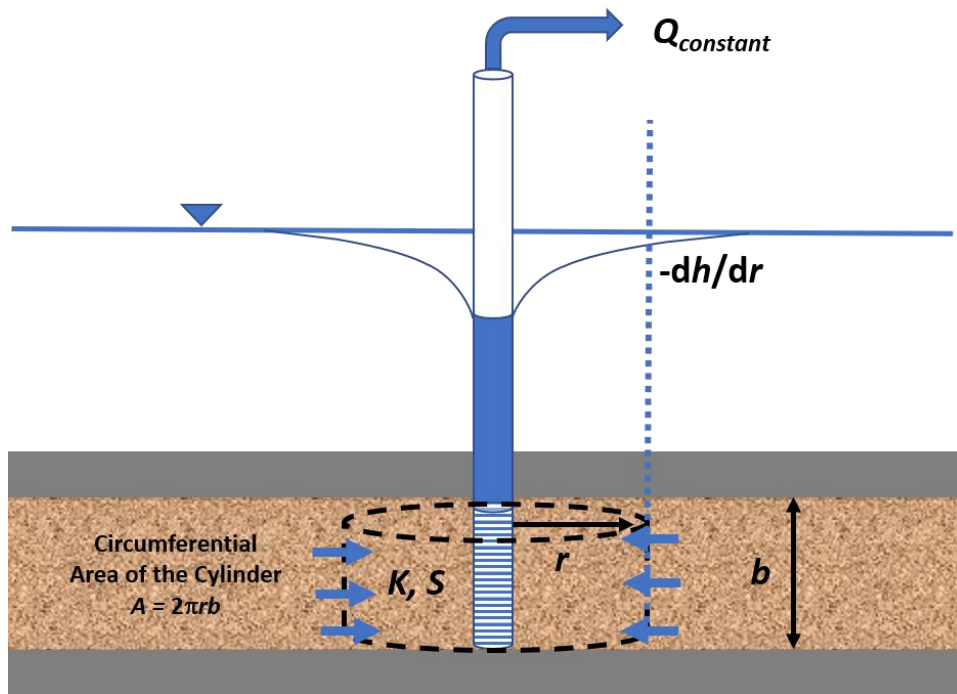


Figure 25 - Conceptualization of confined radial flow in the cone of depression during pumping at a constant rate, Q . The water bearing unit is shown in tan and the impermeable confining beds in gray. The tan patterned saturated material of thickness b is totally confined (gray confining beds). The radial discharge of groundwater, Q , through a cylinder of aquifer is shown by the blue arrows, r is the radius of the cylinder, b is the aquifer thickness, K is the hydraulic conductivity, S is the storativity, and $-dh/dr$ is the hydraulic gradient at the outer edge of the cylinder (blue dashed line). Q is equal to the product of the flow velocity at distance r from the well and the circumferential cross-sectional area ($2\pi rb$) so $Q = -2\pi r b K (dh/dr)$. As pumping progresses $-dh/dr$ varies with time and water is released from storage, $S (-dh/dt)$.

Using the basic confined radial-flow differential equation, general mathematical assumptions presented in Section 6.3, and the additional assumptions that support the Theis equation, along with specified initial and boundary conditions, an analytical solution describing the expected drawdown, s , within the cone of depression at any time after constant pumping begins was derived. Conditions include that drawdown is zero at the start of the pumping. Given that $h(r,t)$ is the head at a radial distance and time, then $h(r,0) = h_0 = 0$ for all r , where h_0 is the corrected-static head. The condition that the confined formation has infinite lateral extent is given by $h(\infty,t) = h_0$ for all t . The constant pumping rate is represented as a point sink at $r = 0$. It represents the well, which is a vertical line through the aquifer, but the two-dimensional aquifer can be represented by a one-dimensional equation given that the well fully penetrates a homogeneous horizontal layer such that at any radius (r) the drawdown is the same at all vertical positions in the aquifer. All in all, the differential equation accounting for flow and the release of water from storage as the heads change is generated using calculus techniques that are quite involved and are not described here but can be found in Loaiciga (2009).

The Theis solution formulated in terms of drawdown, s , is presented in Equation (25). The integral in Equation (25) is known as the exponential integral. Methods to approximate this integral are known and have been compiled in tables for corresponding

values of the argument, $u = r^2S/(4Tt)$. When computing u , units should result in a value of u that is dimensionless. Equation (25) is commonly written as Equation (26) with $W(u)$ inserted to represent the Theis well function (i.e., the exponential integral).

$$s(r, t) = \frac{Q}{4\pi T} \int_{\frac{r^2 S}{4Tt}}^{\infty} \frac{1}{y} \exp(-y) dy \quad (25)$$

$$s(r, t) = \frac{Q}{4\pi T} W(u) \quad (26)$$

where:

$s(r, t)$ = drawdown at a radial distance r and time t (L)

Q = constant well discharge rate (L^3T^{-1})

T = transmissivity (L^2T^{-1})

S = storativity (dimensionless)

t = time (T)

r = radial distance (L)

$W(u)$ = Theis well function (dimensionless)

$u = r^2S/(4Tt)$ (dimensionless)

A solution for the well function, $W(u) = \left[-0.5772 - \ln u + u - \frac{u^2}{2 \cdot 2!} + \frac{u^3}{3 \cdot 3!} - \frac{u^4}{4 \cdot 4!} + \dots \right]$ is an infinite series in which values in the sequence become smaller and smaller as the components are computed. Equation (27) shows the substitution for $W(u)$. Most often values of $W(u)$ are rounded to a few decimal places and only the first three or four terms of the well function equation are required to determine $W(u)$. Tables of the well function computed for values of u are readily available in the literature and can be obtained on the internet (e.g., Figure 26).

$$s = \frac{Q}{4\pi T} \left[-0.5772 - \ln u + u - \frac{u^2}{2 \cdot 2!} + \frac{u^3}{3 \cdot 3!} - \frac{u^4}{4 \cdot 4!} + \dots \right] \quad (27)$$

where:

s = drawdown (L)

Q = constant well discharge rate (L^3T^{-1})

T = transmissivity (L^2T^{-1})

$u = r^2S/(4Tt)$ (dimensionless)

t = time (T)

r = radial distance (L)

S = storativity (dimensionless)

u	$N \times 10^{-15}$	$N \times 10^{-14}$	$N \times 10^{-13}$	$N \times 10^{-12}$	$N \times 10^{-11}$	$N \times 10^{-10}$	$N \times 10^{-9}$	$N \times 10^{-8}$	$N \times 10^{-7}$	$N \times 10^{-6}$	$N \times 10^{-5}$	$N \times 10^{-4}$	$N \times 10^{-3}$	$N \times 10^{-2}$	N	
1.0	33.9616	31.6590	29.3564	27.0538	24.7512	22.4486	20.1460	17.8435	15.5409	13.2383	10.9357	8.6332	6.3315	4.0379	1.8229	0.2194
1.1	33.8662	31.5637	29.2611	26.9585	24.6559	22.3533	20.0507	17.7482	15.4456	13.1430	10.8404	8.5379	6.2363	3.9436	1.7371	0.1860
1.2	33.7702	31.4677	29.1741	26.8715	24.5689	22.2663	19.9637	17.6511	15.3586	13.0560	10.7534	8.4509	6.1494	3.8576	1.6506	0.1535
1.3	33.6842	31.3817	29.0940	26.7914	24.4889	22.1863	19.8827	17.5511	15.2785	12.9759	10.6734	8.3709	6.0685	3.7785	1.5689	0.1235
1.4	33.6251	31.3225	29.0199	26.7173	24.4147	22.1122	19.8096	17.5070	15.2044	12.9018	10.5993	8.2968	5.9955	3.7054	1.5241	0.1162
1.5	33.5651	31.2535	28.9509	26.6483	24.3458	22.0432	19.7406	17.4380	15.1354	12.8328	10.5303	8.2278	5.9266	3.6374	1.4645	0.1000
1.6	33.4916	31.1890	28.8864	26.5838	24.2812	21.9786	19.6760	17.3735	15.0709	12.7683	10.4657	8.1634	5.8621	3.5739	1.4092	0.08631
1.7	33.4309	31.1283	28.8258	26.5232	24.2206	21.9180	19.6154	17.3128	15.0103	12.7077	10.4051	8.1027	5.8016	3.5143	1.3578	0.07465
1.8	33.3738	31.0712	28.7686	26.4660	24.1634	21.8608	19.5583	17.2557	14.9531	12.6505	10.3479	8.0455	5.7445	3.4581	1.3089	0.06471
1.9	33.3197	31.0171	28.7145	26.4119	24.1094	21.8058	19.5042	17.2016	14.8990	12.5964	10.2939	7.9915	5.6906	3.4050	1.2649	0.05620
2.0	33.2684	30.9658	28.6632	26.3607	24.0581	21.7555	19.4529	17.1503	14.8477	12.5451	10.2426	7.9402	5.6394	3.3547	1.2227	0.04890
2.1	33.2196	30.9170	28.6145	26.3119	24.0093	21.7067	19.4041	17.1015	14.7989	12.4964	10.1938	7.8914	5.5907	3.3069	1.1829	0.04261
2.2	33.1731	30.8705	28.5679	26.2653	23.9628	21.6602	19.3578	17.0550	14.7524	12.4498	10.1473	7.8449	5.5443	3.2614	1.1454	0.03719
2.3	33.1286	30.8261	28.5235	26.2209	23.9183	21.6157	19.3131	17.0106	14.7080	12.4054	10.1028	7.8004	5.4999	3.2179	1.1099	0.03250
2.4	33.0861	30.7835	28.4809	26.1783	23.8758	21.5732	19.2706	16.9680	14.6654	12.3628	10.0603	7.7579	5.4575	3.1763	1.0762	0.02844
2.5	33.0453	30.7427	28.4401	26.1375	23.8349	21.5323	19.2298	16.9272	14.6246	12.3220	10.0194	7.7172	5.4167	3.1365	1.0443	0.02491
2.6	33.0060	30.7035	28.4009	26.0983	23.7957	21.4931	19.1905	16.8880	14.5854	12.2828	9.9802	7.6779	5.3776	3.0985	1.0139	0.02185
2.7	32.9683	30.6657	28.3631	26.0606	23.7580	21.4554	19.1528	16.8502	14.5478	12.2450	9.9425	7.6401	5.3400	3.0615	0.9849	0.01918
2.8	32.9319	30.6294	28.3268	26.0242	23.7216	21.4190	19.1164	16.8138	14.5113	12.2087	9.9061	7.6038	5.3037	3.0261	0.9573	0.01686
2.9	32.8968	30.5943	28.2917	25.9891	23.6865	21.3839	19.0813	16.7788	14.4762	12.1736	9.8710	7.5687	5.2687	2.9920	0.9309	0.01482
3.0	32.8629	30.5604	28.2578	25.9552	23.6526	21.3500	19.0474	16.7449	14.4423	12.1397	9.8371	7.5348	5.2349	2.9591	0.9057	0.01305
3.1	32.8302	30.5276	28.2250	25.9224	23.6198	21.3172	19.0146	16.7121	14.4095	12.1069	9.8043	7.5020	5.2022	2.9273	0.8815	0.01149
3.2	32.7984	30.4958	28.1932	25.8907	23.5880	21.2855	18.9829	16.6803	14.3777	12.0751	9.7726	7.4703	5.1706	2.8965	0.8583	0.01013
3.3	32.7676	30.4651	28.1625	25.8599	23.5573	21.2547	18.9521	16.6495	14.3470	12.0444	9.7418	7.4395	5.1399	2.8668	0.8361	0.008930
3.4	32.7378	30.4359	28.1326	25.8309	23.5274	21.2249	18.9229	16.6197	14.3171	12.0145	9.7130	7.4097	5.1102	2.8379	0.8147	0.00784
3.5	32.7088	30.4062	28.1036	25.8010	23.4985	21.1959	18.8933	16.5907	14.2881	11.9855	9.6830	7.3807	5.0813	2.8099	0.7942	0.006970
3.6	32.6806	30.3780	28.0755	25.7729	23.4703	21.1677	18.8651	16.5625	14.2599	11.9574	9.6548	7.3526	5.0532	2.7827	0.7745	0.006160
3.7	32.6532	30.3506	28.0481	25.7455	23.4429	21.1403	18.8377	16.5351	14.2325	11.9300	9.6274	7.3256	5.0259	2.7562	0.7554	0.005448
3.8	32.6266	30.3240	28.0214	25.7188	23.4162	21.1138	18.8110	16.5085	14.2059	11.9033	9.6007	7.2985	5.0000	2.7306	0.7371	0.004820
3.9	32.6006	30.2980	27.9954	25.6928	23.3902	21.0877	18.7851	16.4825	14.1799	11.8773	9.5748	7.2725	4.9755	2.7056	0.7194	0.004267
4.0	32.5753	30.2727	27.9701	25.6675	23.3649	21.0623	18.7598	16.4572	14.1546	11.8520	9.5495	7.2472	4.9482	2.6813	0.7024	0.003779
4.1	32.5506	30.2480	27.9454	25.6428	23.3402	21.0376	18.7351	16.4325	14.1299	11.8273	9.5248	7.2225	4.9236	2.6576	0.6859	0.003349
4.2	32.5265	30.2239	27.9213	25.6187	23.3161	21.0130	18.7110	16.4084	14.1058	11.8032	9.5007	7.1985	4.8997	2.6344	0.6700	0.002969
4.3	32.5029	30.2004	27.8978	25.5952	23.2926	20.9900	18.6874	16.3834	14.0823	11.7797	9.4771	7.1749	4.8762	2.6119	0.6546	0.002633
4.4	32.4800	30.1774	27.8748	25.5722	23.2696	20.9670	18.6648	16.3591	14.0593	11.7567	9.4543	7.1520	4.8533	2.5909	0.6397	0.002336
4.5	32.4575	30.1549	27.8523	25.5497	23.2471	20.9446	18.6420	16.3364	14.0368	11.7342	9.4317	7.1295	4.8310	2.5684	0.6253	0.002070
4.6	32.4355	30.1329	27.8303	25.5277	23.2252	20.9226	18.6200	16.3174	14.0148	11.7122	9.4097	7.1077	4.8091	2.5474	0.6114	0.001841
4.7	32.4140	30.1114	27.8088	25.5062	23.2037	20.9011	18.5985	16.2959	13.9933	11.6907	9.3882	7.0860	4.7877	2.5263	0.5979	0.001635
4.8	32.3929	30.0904	27.7878	25.4852	23.1826	20.8800	18.5774	16.2748	13.9723	11.6697	9.3671	7.0650	4.7667	2.5063	0.5848	0.001453
4.9	32.3723	30.0697	27.7672	25.4646	23.1620	20.8594	18.5568	16.2542	13.9516	11.6491	9.3465	7.0444	4.7462	2.4871	0.5721	0.001291
5.0	32.3521	30.0495	27.7470	25.4444	23.1418	20.8392	18.5366	16.2340	13.9314	11.6289	9.3263	7.0242	4.7261	2.4679	0.5598	0.001148
5.1	32.3323	30.0297	27.7271	25.4246	23.1220	20.8194	18.5168	16.2142	13.9116	11.6091	9.3065	7.0044	4.7064	2.4491	0.5478	0.001021
5.2	32.3129	30.0103	27.7077	25.4051	23.1026	20.8000	18.4974	16.1948	13.8922	11.5896	9.2871	6.9850	4.6871	2.4306	0.5362	0.000906
5.3	32.2939	29.9913	27.6887	25.3861	23.0835	20.7809	18.4783	16.1758	13.8732	11.5706	9.2681	6.9659	4.6681	2.4126	0.5250	0.000806
5.4	32.2752	29.9726	27.6700	25.3674	23.0648	20.7622	18.4596	16.1571	13.8545	11.5519	9.2494	6.9473	4.6495	2.3948	0.5140	0.0007198
5.5	32.2568	29.9542	27.6516	25.3491	23.0469	20.7439	18.4413	16.1387	13.8361	11.5336	9.2310	6.9289	4.6310	2.3755	0.5034	0.0006409
5.6	32.2388	29.9362	27.6336	25.3310	23.0285	20.7259	18.4233	16.1207	13.8181	11.5155	9.2130	6.9109	4.6134	2.3564	0.4930	0.0005708
5.7	32.2211	29.9185	27.6159	25.3133	23.0108	20.7082	18.4056	16.1030	13.8004	11.4978	9.1953	6.8937	4.5958	2.3377	0.4830	0.0005085
5.8	32.2037	29.9011	27.5985	25.2959	22.9934	20.6908	18.3882	16.0856	13.7830	11.4804	9.1779	6.8758	4.5785	2.3203	0.4732	0.0004539
5.9	32.1866	29.8840	27.5814	25.2789	22.9763	20.6737	18.3711	16.0685	13.7659	11.4633	9.1608	6.8588	4.5615	2.3111	0.4637	0.0004039
6.0	32.1698	29.8672	27.5646	25.2620	22.9595	20.6569	18.3543	16.0517	13.7491	11.4465	9.1440	6.8420	4.5448	2.2953	0.4544	0.0003601
6.1	32.1533	29.8507	27.5481	25.2455	22.9429	20.6403	18.3378	16.0352	13.7326	11.4300	9.1275	6.8254	4.5283	2.2797	0.4454	0.0003211
6.2	32.1370	29.8344	27.5318	25.2293	22.9267	20.6241	18.3215	16.0189	13.7163	11.4138	9.1112	6.8092	4.5122	2.2645	0.4366	0.0002854
6.3	32.1210	29.8184	27.5158	25.2133	22.9107	20.6081	18.3055	16.0029	13.7003	11.3978	9.0952	6.7932	4.4963	2.2494	0.4280	0.0002550
6.4	32.1053	29.8027	27.5001	25.1975	22.8949	20.5923	18.2898	15.9872	13.6846	11.3820	9.0795	6.7775	4.4806	2.2346	0.4197	0.0002299
6.5	32.0898	29.7872	27.4846	25.1820	22.8794	20.5768	18.2742	15.9717	13.6691	11.3665	9.0640	6.7620	4.4652	2.2201	0.4115	0.0002094
6.6	32.0745	29.7719	27.4693	25.1667	22.8641	20.5616	18.2590	15.9564	13.6538	11.3512	9.0487	6.7467	4.4501	2.2058	0.4036	0.0001816
6.7	32.0595	29.7569	27.4543	25.1517	22.8491	20.5465	18.2439	15.9414	13.6388	11.3362	9.0337	6.7317	4.4351	2.1917	0.3959	0.0001521
6.8	32.0446	29.7421	27.4395	25.1369	22.8343	20.5317	18.2291	15.9265	13.6240	11.3214	9.0189	6.7169	4.4204	2.1779	0.3883	0.0001248
6.9	32.0300	29.7275	27.4249	25.1223	22.8197	20.5171	18.2145	15.9119	13.6094							

The table (Figure 26) provides one way to obtain the Theis well function for a computed value of u . When u values do not match table u values, they are often estimated using linear interpolation between corresponding table values. As the relationship between u and $W(u)$ is non-linear a more precise method is to compute $W(u)$ using the representation shown in Equation (27). Use of the table shown in (Figure 26) can be avoided and easily replaced by directly computing a value of $W(u)$ from values of u . For example, the well function can be written as or $W(u) = -\text{Ei}(-u)$ and a number of mathematics software programs can be used to obtain the value. A free option is to use the [WolframAlpha.com equation solver](https://www.wolframalpha.com) on the Internet as shown in Figure 27.

The screenshot shows the WolframAlpha.com equation solver interface. The input field contains the equation $W = -\text{Ei}(-0.001)$. Below the input field, there are buttons for "NATURAL LANGUAGE" and "MATH INPUT". A "POPULAR" section shows various mathematical symbols like square root, cube root, and integration. The result section shows the value $6.33154\dots$ and a "More digits" button. A note at the top says "Assuming 'W' is a variable | Use as a unit instead".

Figure 27 - Use of the [WolframAlpha.com equation solver](https://www.wolframalpha.com) on the Internet to determine the value of $W(u)$. The result for $u= 0.001$ is 6.3315 which is the same value shown in the table of Figure 26.

The relationship between $W(u)$ and u is such that as u becomes smaller as $W(u)$ becomes larger. A log-log plot of what is referred to as the Theis type curve is created by plotting values $W(u)$ on a vertical log axis and values of $1/u$ on the horizontal log axis. Figure 28 shows the inverse relationship of u and $W(u)$ because $W(u)$ increases with an increase in $1/u$ (Figure 28). A log-log plot of drawdown data versus time from a field test has the same form.

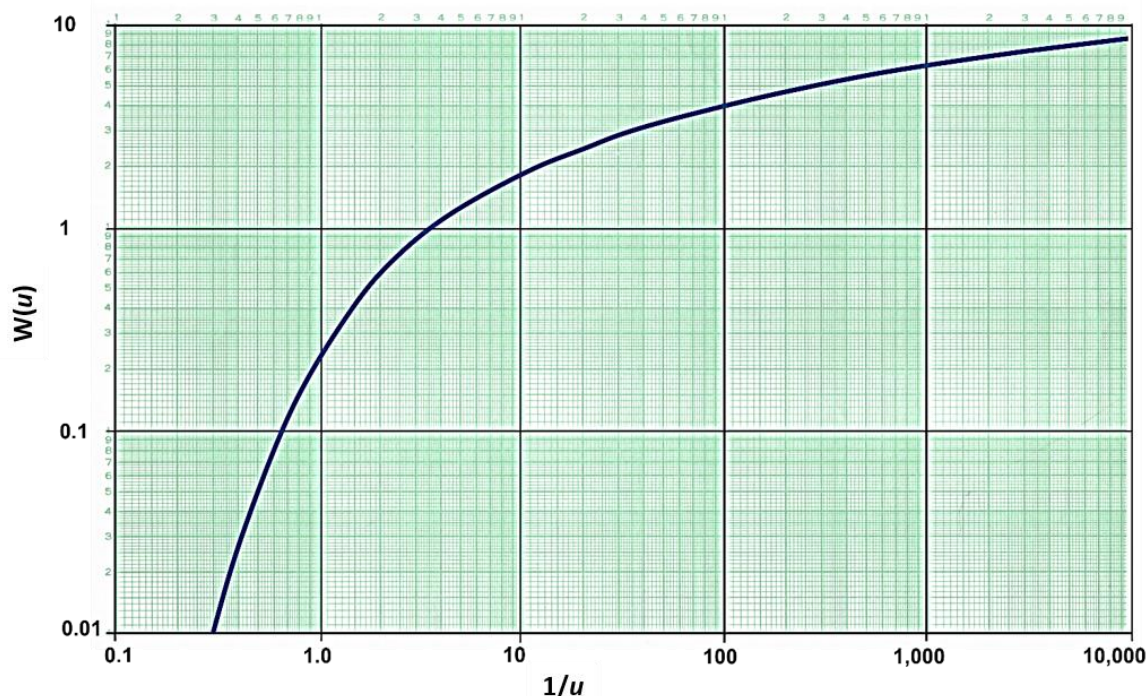


Figure 28 - The Theis type curve is a log-log plot of the Theis well function $W(u)$ for corresponding values of $1/u$.

The type curve can also be plotted as a log-log plot as $W(u)$ versus u . In that case, field data are plotted as s versus r^2/t . This representation is used by some hydrogeologists when interpreting pumping test data (e.g., Lohman, 1972). Type curves in this book are plotted as $W(u)$ versus $1/u$ which takes the same form as a plot of drawdown versus time, s versus t .

When a pumping test is conducted in a confined aquifer, the time-drawdown response is dependent on the relative values of T and S . The drawdown at a radial distance from the pumping well is inversely proportional to T and directly proportional to the pumping rate as shown in Equation (27). The relationship to S is more difficult to discern because it is inside the expression for u , but drawdown at a radial distance from the pumping well is also inversely proportional to S . For similar magnitudes of change, transmissivity has a greater influence on the total drawdown than the storativity. Figure 29 illustrates how the cone of depression profile varies under selected combinations of T and S . For a given value of S , when T increases the drawdown cone becomes broader and shallower. For a given value of T , when S increases the drawdown cone becomes narrower and deeper. Generally, as T and S increase, the cone of depression becomes shallower, whereas when T and S values decrease, the cone of depression expands and becomes deeper. These observations are useful when developing conceptual models of the likely behavior of a confined groundwater system to pumping.

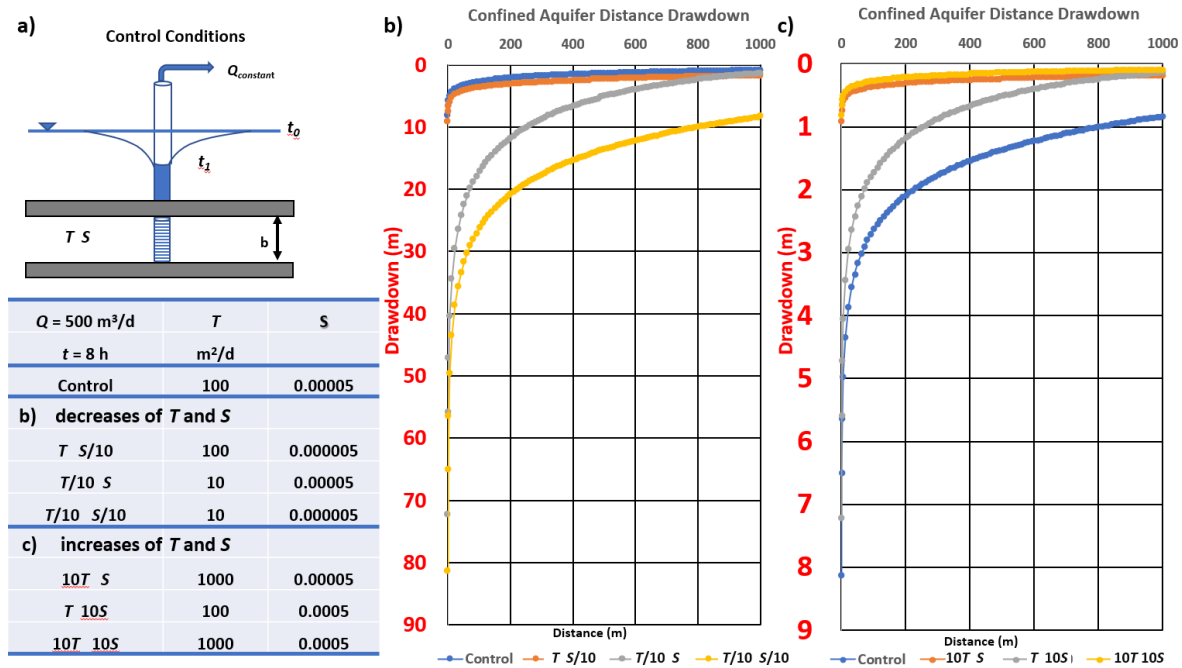


Figure 29 - Illustration of the influence of T and S on the shape and extent of drawdown when pumping an isotropic and homogeneous confined aquifer at a constant rate of $500 \text{ m}^3/\text{d}$ and observing drawdown versus distance from 0 to 1,000 m after 8 hours of pumping. Drawdown extends beyond 1,000 m after 8 hours of pumping, but the graph was truncated at 1000 m for this illustration. The pumping well is located at $r = 0$.

- a) Schematic of the control conditions and a table of the assigned variations of the control settings. A designation such as $T,S/10$ corresponds to the control value of T and the reduction of S by an order of magnitude, $S/10$.
- b) Comparison of the effect of reducing T and S by an order of magnitude plotted along with the control conditions (blue line). The vertical scale is from 0 to 90 m, and in red to help the reader notice the scale change between (b) and (c). When T and S are smaller than the control values the drawdown versus distance profile is deeper and extends further beyond the 1,000 m which is the maximum value of r that is plotted here (so there is more drawdown at $r = 1,000$ m than for the control drawdown).
- c) Comparison of the effect of increasing T and S by an order of magnitude plotted along with the control conditions (blue line). The vertical scale is from 0 to 9 m, much smaller than that of (b), and in red to help the reader notice the scale change between (b) and (c). As T and S values increase relative to the control values, the drawdown distance profile is shallower with less drawdown at the 1,000 m x-axis terminus. Drawdown versus time values were simulated using AQTESOLV V5, www.aqtesolv.com.

Section 8.2 addresses the use of the Theis analytical solution and aquifer parameters to predict drawdown.

8.2 Using the Theis Equation to Predict Drawdowns in Totally Confined Aquifers

When the properties of a fully confined aquifer are known, T and S can be inserted into the Theis equation (Equation (26)) and the drawdown for any time since pumping began can be computed at any radial distance from the pumping well.

Example

Compute the drawdown at an observation well located 300 m from a well that is pumped at a constant rate of $4000 \text{ L}/\text{min}$ ($4 \text{ m}^3/\text{min} = 5,760 \text{ m}^3/\text{d}$) for 8 hours (0.33 d) when the confined formation T is estimated at $800 \text{ m}^2/\text{d}$ and $S=0.00008$.

First u is calculated, then the corresponding Theis well function value is derived.

$$u = \frac{r^2 S}{4Tt} = \frac{(300 \text{ m})^2 0.00008}{4 \left(800 \frac{\text{m}^2}{\text{d}}\right) 0.33 \text{ d}} = u = 0.0068 \text{ or } 6.8 \times 10^{-3}$$

Again, it is important to use consistent units such that u has no units because it is a dimensionless value. Using the well function table in Figure 26, $W(u) = 4.4204$. So, the drawdown 300 m from the pumping well would be calculated as follows.

$$s = \frac{5760 \frac{\text{m}^3}{\text{d}} 4.4204}{4 (3.14) 800 \frac{\text{m}^2}{\text{d}}} = 2.53 \text{ m}$$

As a check on the table value of $W(u)$, substituting values of u into the infinite series shown in Equation (27) and only extending the calculation to the first two terms that contain u results in $W(u) = 4.4204$. This correlates with the table value.

Again, this analytical solution is for a fully confined, isotropic and homogeneous system using the general simplifying assumptions and the additional Theis assumptions. The values used in Equation (26) must have compatible units so that drawdown is reported in length units (e.g., ft, m).

8.3 Computing T and S from Hydraulic Test Data using the Theis Method

Theis (1935) developed a method to estimate values of T and S from pumping test data. Time and drawdown data are measured in an observation well and then matched to the Theis curve. The method can also be used to compute hydrogeologic properties from time-drawdown data measured in a pumping well. However, drawdown data require correction when the pumping well is not 100 percent efficient and/or is partially penetrating and/or wellbore storage is significant. These corrections are addressed in the section on using a single pumping well to estimate T and S (Section 12). When drawdown data are collected from one or more observation wells, it is not necessary to correct drawdown for well efficiency because these wells are not pumped so they are effectively 100 percent efficient.

8.3.1 Theis Curve Matching Method

Values of T and S for a fully confined groundwater system can be computed by rearranging Equation (26) to solve for transmissivity as shown in Equation (28). T is directly proportional to the constant pumping rate, Q , and the well function, $W(u)$, and inversely proportional to drawdown.

$$T = \frac{Q}{4\pi s} W(u) \quad (28)$$

where:

$$\begin{aligned}
 T &= \text{transmissivity (L}^2\text{T}^{-1}\text{)} \\
 s &= \text{drawdown (L)} \\
 Q &= \text{constant well discharge rate (L}^3\text{T}^{-1}\text{)} \\
 W(u) &= \text{Theis well function (dimensionless)}
 \end{aligned}$$

The well function is computed for the same time as the drawdown is measured by determining the argument $u = r^2S/(4Tt)$. The argument is specific to the radial distance of the observation well from the pumping well and the time at which the drawdown was measured. The equation for u can be rearranged to solve for storativity (S) as shown in Equation (29).

$$S = \frac{u4Tt}{r^2} \quad (29)$$

where:

$$\begin{aligned}
 S &= \text{storativity (dimensionless)} \\
 u &= \text{integral argument (dimensionless)} \\
 T &= \text{transmissivity (L}^2\text{T}^{-1}\text{)} \\
 t &= \text{time (T)} \\
 r &= \text{radial distance to pumping well (L)}
 \end{aligned}$$

The unknowns in Equations (28) and (29) are T and S , respectively.

The curve matching technique introduced by Theis (1935) uses the superposition of paper plots to derive match points with values of $W(u)$, $1/u$, s and t that are substituted into Equations (28) and (29) to solve for T and S . There is value in understanding how curve matching is performed. The discussions presented in this section and the following sections assume the hydrogeologist will perform curve matching using either hand or computer-generated log-log plots of pumping test results, s versus t , and the Theis type curve, $W(u)$ versus $1/u$. These curves are physically or electronically superimposed to generate required input for Equations (28) and (29). More recently, curve-matching software can mathematically generate a best fit of the observation data to the Theis curve. Most programs allow the user to visually examine the best fit and adjust the fit if needed. The use of software to generate estimates of T and S is discussed in Section 13.

The curve matching process involves plotting both the $W(u)$ versus $1/u$ (Figure 30) and the hydraulic test time-drawdown (Figure 31) on the exact same size paper using a log-log scale. Samples of log-log, semi-log, and arithmetic paper are provided in [Box 17](#). Curves can also be plotted in a spreadsheet or software program that produces log-log graphs. All variables increase from the lower lefthand corner of the graphs. A plot of the Theis type curve (Figure 30) is derived by plotting the table of values shown in Figure 26 or generating the plot by substituting values of u into the equation for $W(u)$ (i.e., the term within the brackets of Equation (27)). Some publications (e.g., Lohman 1972) provide paper

plots of several different type curves including the Theis type curve. Once again, the field data must be plotted at the same log-log scale as the type curves.

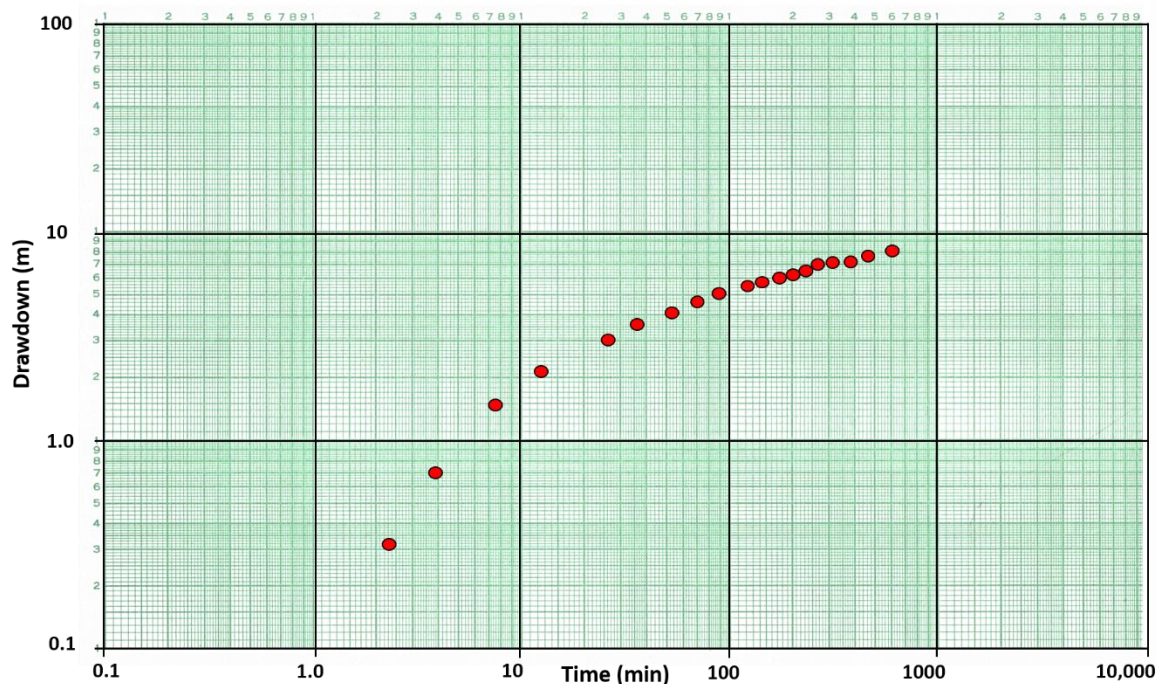


Figure 30 - Hydraulic test drawdown versus time data for an observation well plotted on 3 by 5 cycle log-log paper at the same scale as the Theis Type Curve in Figure 28. Red dots represent field data collected during a constant rate pumping test.

Once the field data are plotted, the type curve plot is placed on a light table (or glass window) and the field data plot is overlaid (superposed). If computed plots are generated with a spreadsheet program (digital), in software such as Microsoft Excel, test data plots can be modified with a degree of transparency, overlaid and matched to an underlying type curve. It is essential that the log cycles are the same size on the graph paper for the plotted data and the type curve. The field data plot is shifted around keeping the graph axes parallel until a best match of the field data with the type curve is obtained (Figure 31).

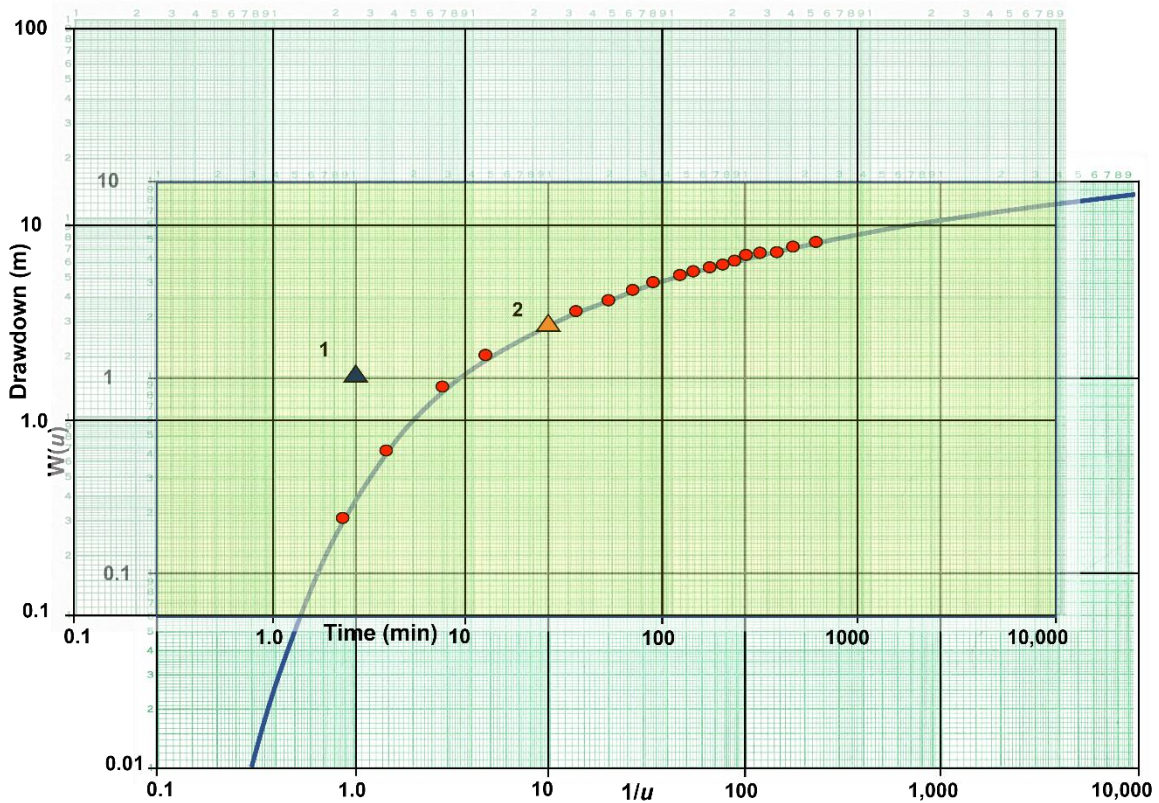


Figure 31 - Example of curve-matching methodology. Typically, when using a light table, the type curve is laid down and secured then a plot of hydraulic test data (with axes of the same scale as the type curve) is overlain so the data fits on some portion of the type curve. The axes are kept parallel. Once the match is achieved, a match point (triangle) is chosen within the overlapping fields of the graphs (light yellow shaded area). The match point does not have to be on the matched portion of the curve, it can be anywhere within the overlapping field (light yellow). At the match point, values of $W(u)$, $1/u$, s , and t are read from the graph axes. Two match points are shown in this example, both will yield equal ratios of the variables. The second match point is not needed but is used in an example calculation to demonstrate that any match point will produce the same results. Match-point values are then used in Equations (28) and (29) to compute T and S .

Within the overlapping fields of the graphs a single point is chosen to be the match point where values of s , t , $W(u)$ and $1/u$ are obtained by determining the values of the chosen point on both curves. The match point does not have to be on the portion of the type curve where the data curves were matched. Any match point within the overlapping fields will yield the same ratio of variables (Figure 31). Some investigators use a straight pin to pierce the two sheets of paper at the selected match point site. When doing this the papers can be separated so the data are more easily read from each plot. Once the values at the match point are obtained and the constant pumping rate and radial distance between the pumping well and observation well are inserted in the appropriate equations, Equations (28) and (29), the value of T and S are derived. The computation of S uses the newly computed value of T from Equation (28). The value of $1/u$ needs to be converted to a value of u . All values used in the calculations must be in the appropriate units so final values of T have dimensions of L^2T^{-1} and S is dimensionless.

The type curve fitting methodology is a standard methodology used by hydrogeologists to assess drawdown data from a single observation well. This same

approach will be used in other sections of this book. A second curve matching procedure can be applied that uses data sets from a single or multiple observation wells. In this case the type curve is plotted as $W(u)$ versus u and one or more observation well data sets are plotted as s versus r^2/t on a single graph. The match point selection process is the same as described in the preceding section. This yields values of $W(u)$, u , s , and r^2/t . These parameters are then substituted into Equation (28) to compute T and Equation (29) to compute S (where r^2/t is converted to $1/(r^2/t)$). Lohman (1972) illustrates this by using drawdowns from three observation wells on an s versus r^2/t log-log plot, then matching to the type curve and selecting a single match point to compute estimates of T and S .

Example

An example of using pumping test data to derive T and S for a totally confined groundwater system is given here using the data plotted on Figure 30. The test data are collected for an observation well located 200 m from a well pumping at a constant rate of $1.7 \text{ m}^3/\text{min}$ or $2,448 \text{ m}^3/\text{d}$.

A match point (triangle 1 in Figure 31) is selected within the two overlapping fields. At match point 1 the values of $W(u) = 1$, $1/u = 1$ ($u=1/1=1$), $s=1.7 \text{ m}$ and $t=2.7 \text{ min}$ (0.0019 d). Starting with Equation (28), T is calculated.

$$T = \frac{2448 \frac{\text{m}^3}{\text{d}}}{4 (3.14) 1.7 \text{ m}} (1) = 114.6 \frac{\text{m}^2}{\text{d}}$$

Now with an estimate of T , Equation (29) can be used to compute S .

$$S = \frac{1 (4) 114.6 \frac{\text{m}^2}{\text{d}} 0.0019 \text{ d}}{(200 \text{ m})^2} = 0.000022 \text{ or } 2.2 \times 10^{-5}$$

To illustrate that once a curve match has been achieved the location of the match point can be anywhere in the overlapping fields, we calculate T and S from the data at match point 2 on Figure 31. At match point 2, $W(u) = 1.8$, $1/u = 10$ ($u = 0.1$), $s = 3 \text{ m}$ and $t = 27 \text{ min}$ (0.019 d).

$$T = \frac{2448 \frac{\text{m}^3}{\text{d}}}{4 (3.14) 3 \text{ m}} (1.8) = 116.9 \frac{\text{m}^2}{\text{d}}$$

and

$$S = \frac{0.1 (4) 116.9 \frac{\text{m}^2}{\text{d}} 0.019 \text{ d}}{(200 \text{ m})^2} = 0.000022 \text{ or } 2.2 \times 10^{-5}$$

Reading the four values from the graph in Figure 31 at match point 2 produces a small difference in the two computed T values. This is not unexpected as there is some error in reading all four values from the graphs. When match point 1 was selected it was purposely chosen so values of $W(u)$ and $1/u$ would be clearly defined. Errors reading the s

and t values are likely and contribute to the difference in the two T values. The S values are less sensitive to u and t variation and the computed values were within roundoff errors. If the field data curve perfectly matches the type curve, then all T and S values will be identical.

When type curves plotted as $W(u)$ versus u are used with data plots of s versus r^2/t , match points will be s , r^2/t , $W(u)$ and u . Calculations are undertaken using Equations (28) and (29).

When performing curve matching, in some cases field data may poorly match the type curve for the selected analytical solution. A poor data fit may occur if one or more of the simplifying assumptions used to create the analytical model are violated (e.g., the aquifer is not isotropic and homogeneous), measurement or recording errors are introduced during field data collection, an unrecognized boundary is encountered by the cone of depression, or a constant pumping rate is not maintained. When this occurs, further analysis of the data or application of a different analytical method may be required, otherwise the results are less certain.

8.3.2 Cooper-Jacob Straight Line Method

Cooper and Jacob (1946) developed a method to analyze confined aquifer pumping tests that involves plotting hydraulic testing results without the need to curve match. Their method approximates the Theis well function, $W(u)$, with the first two components of the infinite series as shown in Equation (30).

$$W(u) \cong -0.5772 - \ln\{u\} \quad (30)$$

where:

$$u = r^2S/(4Tt) \text{ (dimensionless)}$$

The Theis Equation is then written with this substitution (Equation (31) or Equation (32)) and referred to as the Cooper-Jacob approximation (e.g., Freeze & Cherry, 1979).

$$s(r, t) \cong \frac{Q}{4\pi T} \ln\left(\frac{Tt}{1.78r^2S}\right) \quad (31)$$

or

$$s(r, t) \cong \frac{Q}{4\pi T} 2.30 \log\left(2.25 \frac{Tt}{r^2S}\right) \quad (32)$$

where:

$s(r, t)$ = drawdown at distance r and time t (L)

Q = constant pumping rate (L^3T^{-1})

T = transmissivity (L^2T^{-1})

t = time (T)

- r = radial distance of observation well (L)
- S = storativity (dimensionless)
- \log = logarithm base 10
- \ln = natural logarithm

Because the infinite series is truncated, the solution is only appropriate for values of $u < 0.01$ or $1/u > 100$. When assessing the applicability of the Cooper-Jacob approximation it is useful to keep in mind that since $u = r^2S/(4Tt)$, larger values of T and t and smaller the values of r and S produce smaller values of u . Practically then, drawdown data from observation wells closer to the pumped well and from longer test periods will more likely fit the assumptions of the Jacob method.

Equations (31) and (32) reveal that the drawdown as a function of time in a totally confined aquifer is logarithmic as shown in Figure 30. When field data of drawdown versus time data are plotted as a semi-logarithmic graph with the drawdown on the arithmetic scale and time on the logarithmic scale, a portion of the curve forms a straight line (Figure 32). The early time and drawdown data are asymptotic to the time axis as the logarithmic scale has no zero point. Cooper and Jacob developed a method that uses the straight-line portion of the time-drawdown semi-logarithmic plot to compute values of T and S .

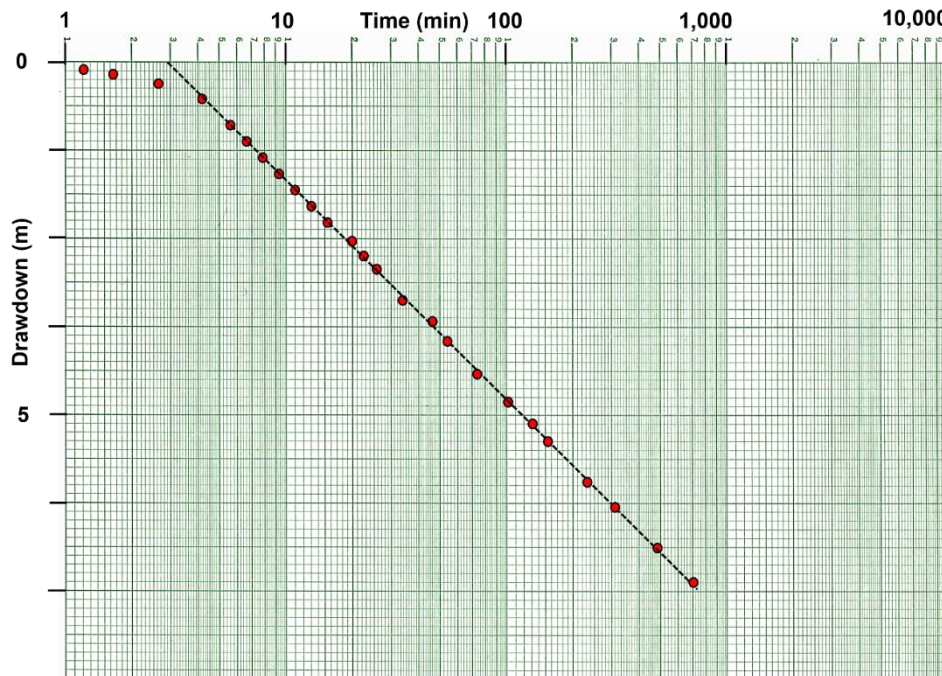


Figure 32 - Example of a semi-log plot of drawdown and time data (red dots) for an observation well. A straight line (dashed black line) is fitted to the data ignoring the early time data that is asymptotic to the time axis because the log axis has no zero value.

The data presented in Figure 32 can also be plotted with the zero drawdown at the lower left corner. This reverses the slope of the line. The orientation of the y axis (drawdown progression) has no effect on the Cooper-Jacob methodology.

The T and S values are based on the slope of the straight-line portion of the curve. Using Equation (32) the slope of the interpreted straight-line portion of the data is given by Equation (33).

$$s_2 - s_1 = \frac{2.3 Q}{4\pi T} \ln\left(\frac{t_2}{t_1}\right) \quad (33)$$

where:

s_2 = drawdown associated with the later time, t_2 (L)

s_1 = drawdown associated with the early time, t_1 (L)

Q = constant pumping rate (L^3T^{-1})

t_2 = late time (T)

t_1 = early time (T)

T = transmissivity (L^2T^{-1})

When the time interval equals one log cycle (e.g., log 10 to log 100) then the log of $t_2/t_1 = 1$. The change in drawdown for this time interval, $s_2 - s_1$ is defined as $\Delta s_{\log-t}$ (Figure 33). T is then calculated using Equation (34).

$$T = 2.3 \frac{Q}{4\pi \Delta s_{\log-t}} \quad (34)$$

where:

T = transmissivity (L^2T^{-1})

Q = constant pumping rate (L^3T^{-1})

$\Delta s_{\log-t}$ = change in drawdown over one log cycle of time (L)

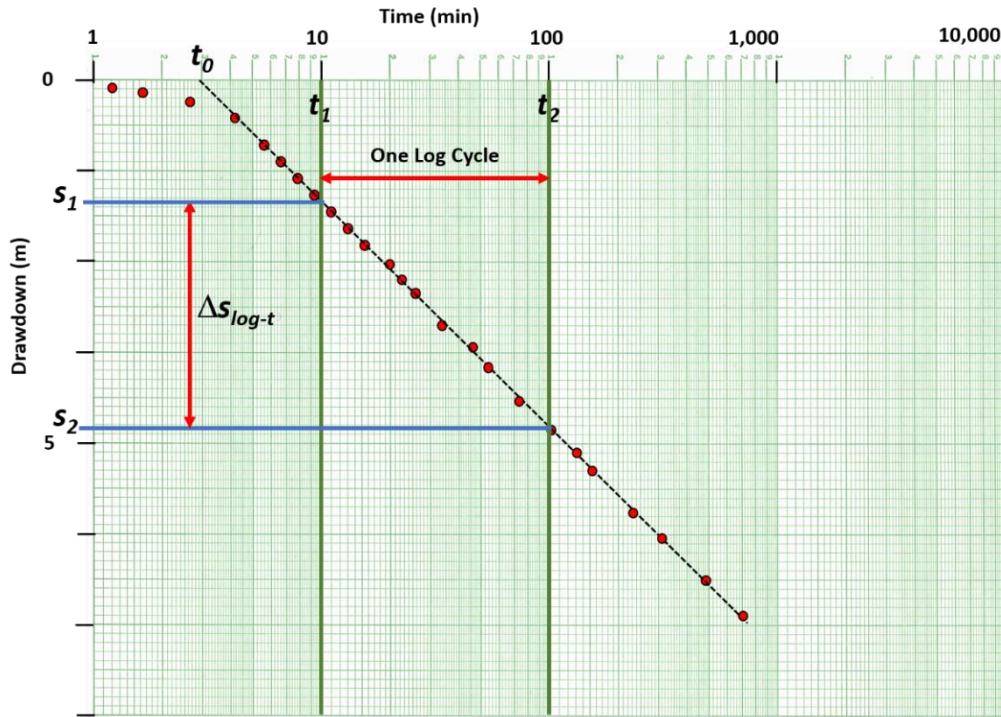


Figure 33 - Semi-log plot of drawdown (red dots) on an arithmetic scale and time on a log scale collected at an observation well in a confined aquifer. A value of $\Delta s_{\log-t}$ is derived as the difference in drawdown (s_2-s_1) over one log cycle of time (t_1 to t_2). The fitted line (dashed black line) is projected to the time axis to obtain a value of t_0 where the projected fitted straight line intersects the value of drawdown equal to zero.

The storativity can be estimated using Equation (35) with t_0 being the point where the projected fitted straight line intersects the value of drawdown equal to zero (Figure 33).

$$S = 2.25 \frac{Tt_0}{r^2} \tag{35}$$

where:

- S = storativity (dimensionless)
- T = transmissivity (L^2T^{-1})
- t_0 = time when $s = 0$ for the fitted straight line (T)
- r = radial distance to the observation point (L)

The estimate of T using this method is well supported by the mathematical approach. As the slope of the line of field data is smaller (less drawdown measured over time) the value of T is larger. The determination of S using this approach is less robust because small differences in the interpreted slope may result in significant differences in t_0 which is based on a logarithmic scale. The use of this method to estimate S is also not recommended when only the pumping well drawdown and time data are available. This is because when the assumptions are not met, for example, the pumping well is not 100 percent efficient and/or is affected by partial penetration effects such that the recorded

drawdown is greater than in the adjacent aquifer material. The corresponding interpolated t_0 value is then incorrect, yielding incorrect estimates of S . The good news is that when time-drawdown data are only available from the pumping well, a Cooper-Jacob plot can be used to approximate T because the slope of the semi-log plot remains the same whether the well is 100 percent efficient or affected by partial penetration affects (specifics about this are presented in Section 12). It is suggested that the Cooper-Jacob approximation should only be applied when a semi-log straight line portion of the drawdown curve dominates the time-drawdown data, u is small based on estimates of T and S for the unit being pumped, and the Theis model is an appropriate conceptual model for the unit being investigated.

Example

Values of T and S are computed in this example using the data presented in Figure 33. Assuming that the data presented in Figure 33 represent the time-drawdown data collected 600 m from a well pumping at a constant rate of 2,610 L/min (3,758 m³/d) in a totally confined sand aquifer that is 10 m thick. The change in drawdown over one log cycle of time (10 to 100 min) is: 4.85 m (s_2) - 1.32 m (s_1) = 3.53 m ($\Delta s_{\log-t}$). T is calculated using Equation (34).

$$T = 2.3 \frac{3758 \frac{\text{m}^3}{\text{d}}}{4 (3.14) 3.53 \text{ m}} = 194.9 \frac{\text{m}^2}{\text{d}}$$

Using the projection of the straight line to the time axis, $t_0 = 2.8$ min (0.0019 d). S is approximated using Equation (35).

$$S = 2.25 \frac{194.9 \frac{\text{m}^2}{\text{d}} 0.0019 \text{ d}}{(600 \text{ m})^2} = 0.000002 \text{ or } 2 \times 10^{-6}$$

8.3.3 Cooper-Jacob Distance-Drawdown Method

When multiple observation wells are monitored during a pumping test of a confined system, the drawdown data collected at a common time (i.e., t constant) can be used to estimate T and S using the Cooper-Jacob distance-drawdown approximation. The idea is that the drawdown data collected simultaneously from at least two wells (three or more is better) located at different radial distances from the pumping well define the character (slope) of the cone of depression (Figure 34). The pumping-well water level and corresponding radius is not used as a data point because measured drawdown is influenced by well loss and, in some cases, partial penetration (Section 12).

It is logical that when keeping the discharge constant, the steepness and extent of the cone of depression measured in a water-bearing formation is directly related to the values of T and S (e.g., Figure 29). Shallower cones of depression would be associated with higher values of T and S , whereas lower values would create deeper drawdown cones (pumping rate and other factors held constant). The drawdown collected at two or more

observation wells located at different radial distances from the pumping well, $s(r_1,t)$, $s(r_2,t)$, $s(r_3,t)$ and so on (Figure 34) are related to T and S as shown in Equation (36).

$$s(r_1, t) - s(r_2, t) = \frac{2.3 Q}{2 \pi T} \log\left(\frac{r_2}{r_1}\right) \tag{36}$$

where:

- $s(r_1,t)$ = the drawdown at distance r_1 from the pumping well at time t (L)
- $s(r_2,t)$ = the drawdown at distance r_2 from the pumping well at time t (L)
- Q = constant pumping rate at the production well (L^3T^{-1})
- r_2 = radial distance of observation well 2 (L)
- r_1 = radial distance of observation well 1 (L)
- T = transmissivity (L^2T^{-1})

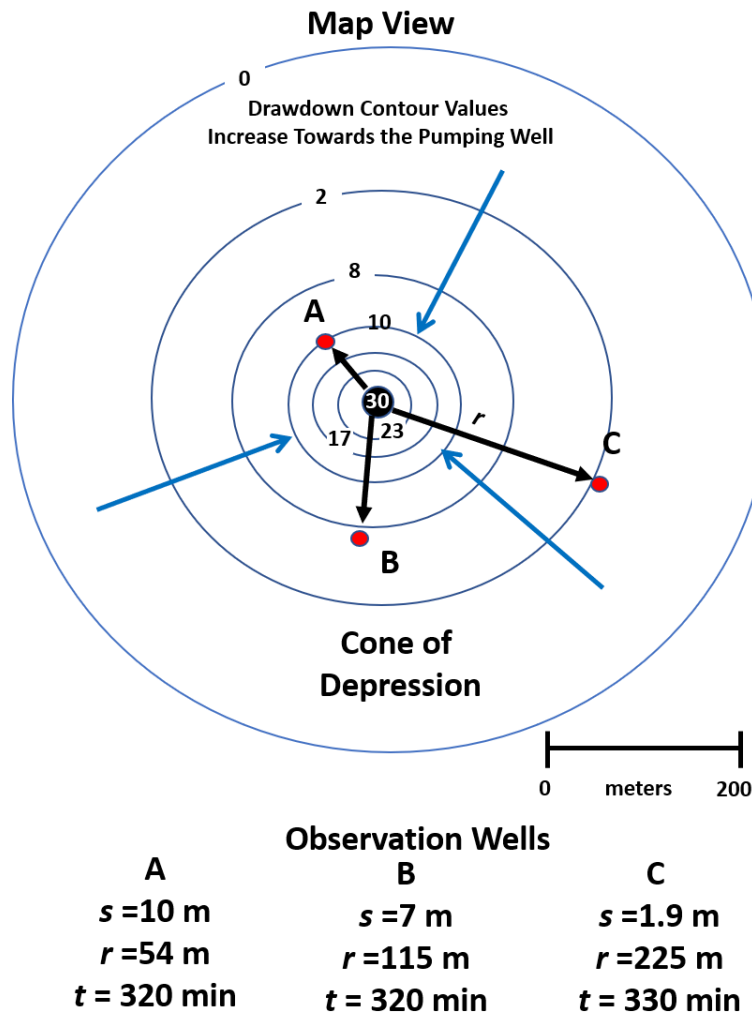


Figure 34 - Schematic map view of the cone of depression in a totally confined aquifer at 320 min after a constant rate of pumping was initiated. Three observations wells (red dots) are located at different radial distances from the pumping well. Blue arrows indicate radial flow to the well. The symbols s , r , and t , indicate drawdown, radial distance, and time since pumping began, respectively.

The transmissivity is determined graphically by computing $\Delta s_{\log-r}$ over one log cycle of distance as shown in Figure 35 and applying Equation (37). As was done for the time-drawdown data, a plot of drawdown at a specified time since pumping started on the arithmetic axis and the observation well radial distances on the log axis is constructed (Figure 35) and estimates of T and S are computed using Equation (37) and Equation (38), respectively. The value for r_0 is derived from the location where the fitted straight line crosses the zero-drawdown axis.

$$T = \frac{2.3 Q}{2 \pi \Delta s_{\log-r}} \quad (37)$$

where:

- T = transmissivity (L^2T^{-1})
 Q = constant discharge rate of the pumping well (L^3T^{-1})
 $\Delta s_{\log-r}$ = difference in drawdown over one log cycle of radial distance (dimensionless)

$$S = 2.25 \frac{Tt}{r_0^2} \quad (38)$$

where:

- S = storativity (dimensionless)
 T = transmissivity (L^2T^{-1})
 r_0 = radial distance where the fitted straight line crosses $s=0$ (L)
 t = time (T)

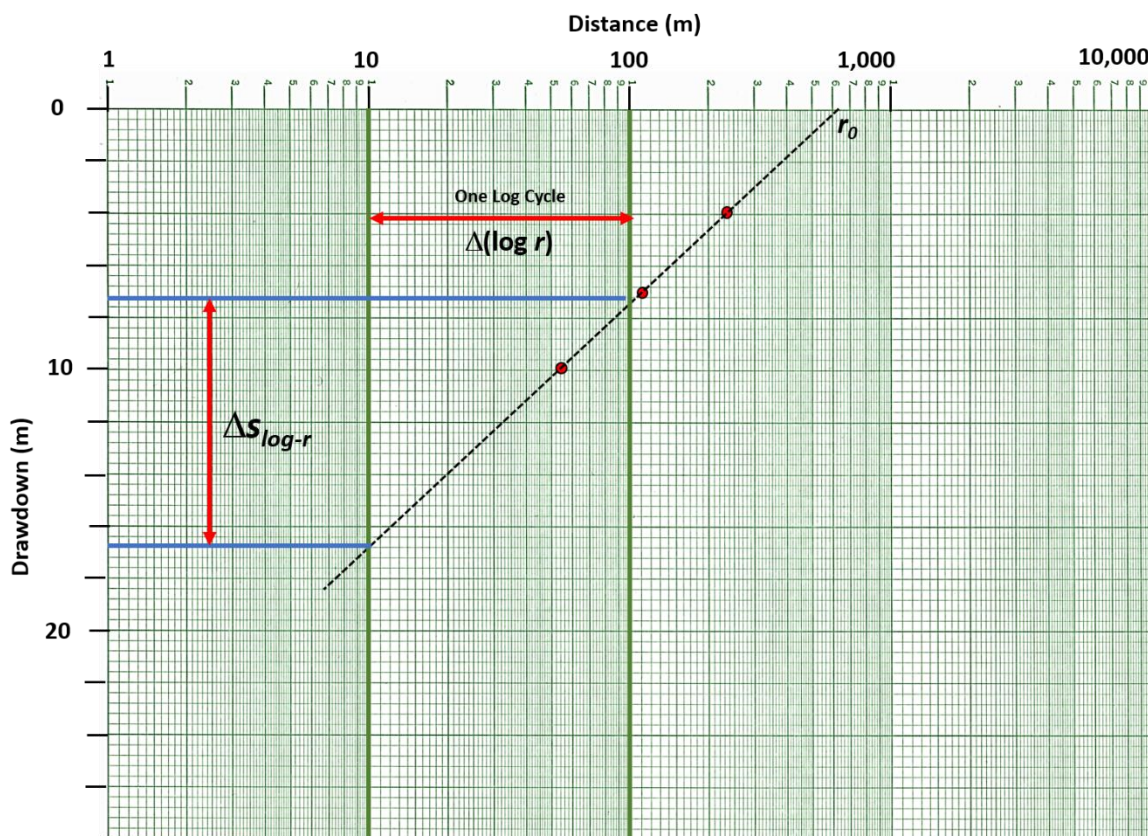


Figure 35 - Plot of the drawdown at a fixed time in the three observation wells shown in Figure 34. The drawdown is plotted on the arithmetic axis and the radial distance from the pumping well to the observation wells on the log axis. A value of $\Delta s_{\log-r}$ is derived over a log cycle of r ($\log(100 \text{ m}/10 \text{ m})$). Values of T and S are computed using Equations (37) and (38).

Example

Calculating T and S using Equations (37) and (38) is illustrated with the data presented in Figure 34 and Figure 35. Three observation wells provide drawdown data collected 320 min after the production well had been pumping at a constant rate of 3,758 m^3/d . The sandstone aquifer is 40 m thick and is totally confined. From the semi-log plot shown in Figure 35 $\Delta s_{\log-r}$ is computed over one log cycle of r .

$$\Delta s_{\log-r} = 16.7 \text{ m} - 7.4 \text{ m} = 9.3 \text{ m}$$

$$T = \frac{2.3 \left(3758 \frac{\text{m}^3}{\text{d}} \right)}{2 (3.14) 9.3 \text{ m}} \log \left(\frac{100 \text{ m}}{10 \text{ m}} \right) = 148 \frac{\text{m}^2}{\text{d}}$$

Then, S is approximated using $r_0 = 640 \text{ m}$.

$$S = 2.25 \frac{148 \frac{\text{m}^2}{\text{d}} 320 \text{ min} \frac{1 \text{ d}}{1440 \text{ min}}}{(640 \text{ m})^2} = 0.00018 \text{ or } 1.8 \times 10^{-4}$$

8.3.4 Analyzing Recovery Data

When a pumping well is turned off water levels begin to recover. As shown in Figure 4 the rate of recovery mirrors the drawdown rate. Water levels rise rapidly at first then more slowly at later times. Theis (1935) found that, mathematically, the recovery curve responds as if at the time pumping ceases, the production well continues to pump, but an injection well starts injecting water at the location of the pumping well at the pumping rate. With time the water level fully recovers to near the pre-pumping level. The final recovery level would theoretically be slightly less than the original static level. This is because a volume of water was removed from storage during the test with no mechanism to replace it. Given an aquifer of infinite extent, this volume is an insignificant portion of the total volume of water in the confined groundwater system, so for practical purposes, the system fully recovers.

The recovery process creates a second set of data for the same test that can be analyzed to estimate T and S . Often observation well recovery data are analyzed and then results compared to the T and S values computed from pumping data. Ideally, they should be identical, but this rarely occurs as differences in curve matching or straight-line analysis of the data sets introduces some error. Usually, all the hydrogeologic property values derived from drawdown and recovery of observation wells will be averaged to generate values assigned to the water-bearing unit being tested. Recovery data at the pumping well are often valuable if the pumping well water levels are difficult to monitor because of turbulence in the well casing during pumping or well efficiency effects measured water levels causing them to be lower than theoretical values. When the pumping well is shut off, at early times the water level recovers rapidly, and the frequency of water level data collection should be adjusted to match the drawdown measurement schedule implemented at the beginning of the pumping phase.

When drawdown versus time data from an observation well is plotted on arithmetic scales the difference in water levels during recovery can be described using two terms, residual drawdown, and calculated recovery (Figure 36). The residual drawdown, s' , is obtained by subtracting the observed recovered water level from the corrected-static water level. The calculated recovery ($s-s'$) is obtained by extending the trend of the drawdown curve as if pumping had continued to obtain a projected value of s and subtracting the residual drawdown from that value. Calculated recovery data may include errors because it relies on an accurate estimate of T from the pumping phase of the test which may be in error due to extraneous influences such as variable discharge rate during the pumping phase. In this case the Theis semi-log method of estimating T is applied.

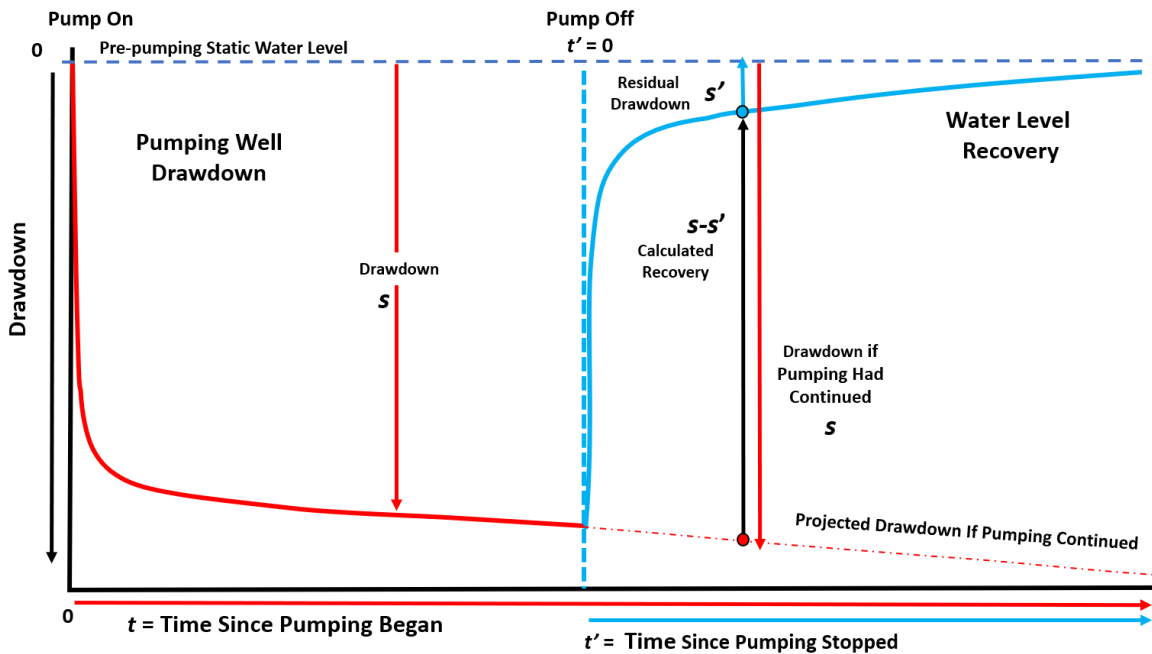


Figure 36 - Schematic of drawdown and recovery data for an observation well is plotted on arithmetic scales. Once the well is shut off the drawdown curve begins to recover at a rate that decreases with time. The remaining drawdown, measured from the corrected-static water level during recovery, is referred to as residual drawdown, s' . A second description of recovery is provided by the computed calculated recovery, $s-s'$. The calculated recovery requires a projection of the drawdown (s) that would occur if the production well was still pumping after the pumping well is shut off. This is represented by the red dash-dot line that can be projected from the drawdown rates observed at the time the pump was shut off or calculated once the aquifer parameters have been estimated from the drawdown portion of the data set.

Theis Semi-log Method for Estimating T from Residual Recovery Data

Theis (1935) presented a procedure to estimate T that eliminates the complications of estimating residual recovery from a projected drawdown curve by using the residual drawdown data directly. In this case, the residual drawdown s' is plotted versus t/t' on a semi-log plot as shown in Figure 37. $\Delta s'_{log-t}$ is derived over one log cycle of t/t' where t is the time since the pumping started and t' is the time since the pump was shut off. T is calculated using Equation (39).

$$T = 2.3 \frac{Q}{4\pi \Delta s'_{log-t}} \tag{39}$$

where:

- T = transmissivity (L^2T^{-1})
- Q = constant pumping rate (L^3T^{-1})
- $\Delta s'_{log-t}$ = the change in residual drawdown over one log cycle change t/t' (L)

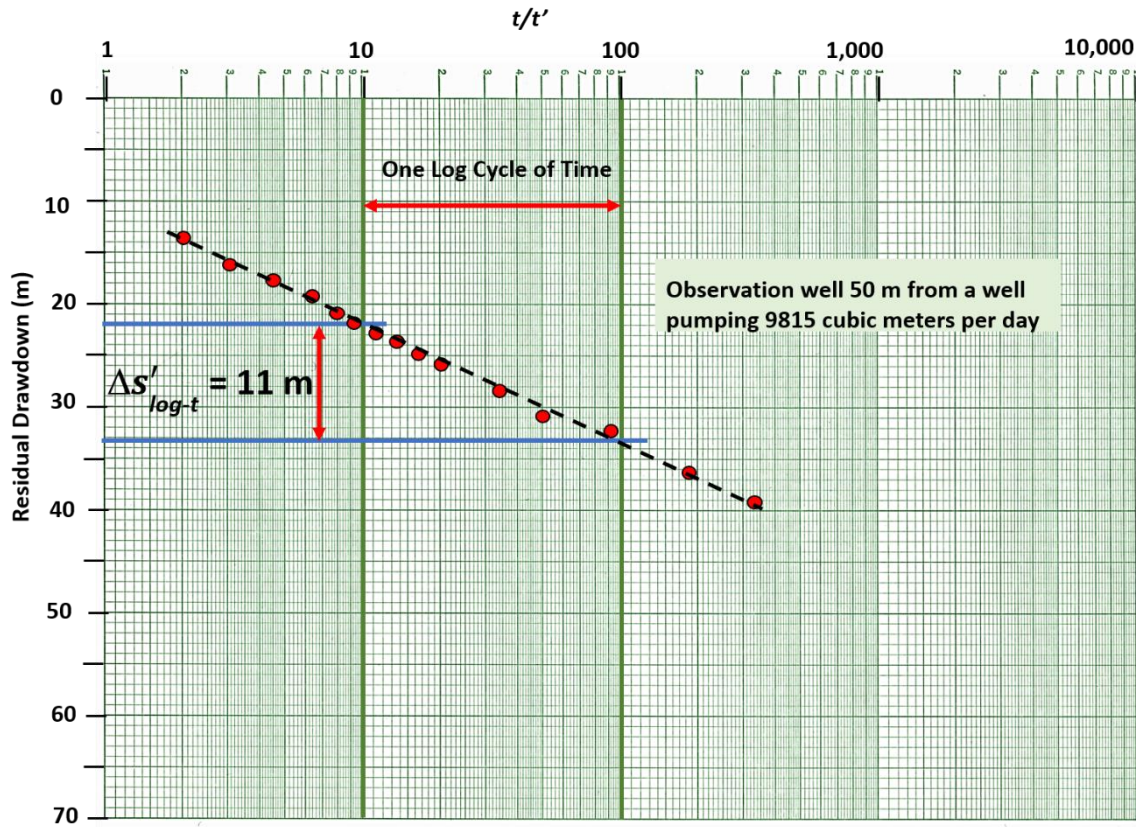


Figure 37 - Semi-log plot of residual drawdown versus t/t' in an observation well 50 m from the pumping well, The time since the pumping started is t and the time since the pumping stopped is t' . The slope of the projected straight line (dashed black line) is determined to be 11 m over one log cycle of t/t' .

This methodology is not used to derive a value of S . Kruseman and de Ridder (2000) provide further explanation of how residual drawdown data are used. Their textbook is supplied without cost on the gw-project.org website.

Example

Using the data presented in Figure 37 along with the information that the well was pumped at a constant rate of 9,815 m³/d for 100 min. The graph reveals that $\Delta s'_{log-t}$ is 11 m.

$$T = 2.3 \frac{Q}{4\pi\Delta s'_{log-t}} = 2.3 \frac{9815 \frac{\text{m}^3}{\text{d}}}{4 (3.14) 11 \text{ m}} = 163 \frac{\text{m}^2}{\text{d}}$$

Theis Curve Matching Method for Estimating T using Calculated Recovery Data

Calculated recovery data can be used to estimate T and S but provides less certain results because variation in pumping rate may lead to an inaccurate projected drawdown curve that us used to calculate recovery. For this analysis, calculated recovery is plotted versus time since pumping stopped—setting time zero at the time the pump was turned off—as illustrated in Figure 36. Calculation of T and S is described by Sterrett (2007). The calculated recovery $s-s'$ versus t' is plotted on a log-log scale (Figure 38) and matched to the

This type curve plotted at the same scale to derive the four match point values: $s-s'$, t' , $W(u)$ and $1/u$. These are used in Equations (40) and (41)—which are modifications of Equations (28) and (29)—to calculate T and S , respectively. The match point is shown in Figure 39. The projected drawdown after pumping ceases can be in error because it is estimated, and this may cause error in the estimated T and S values.

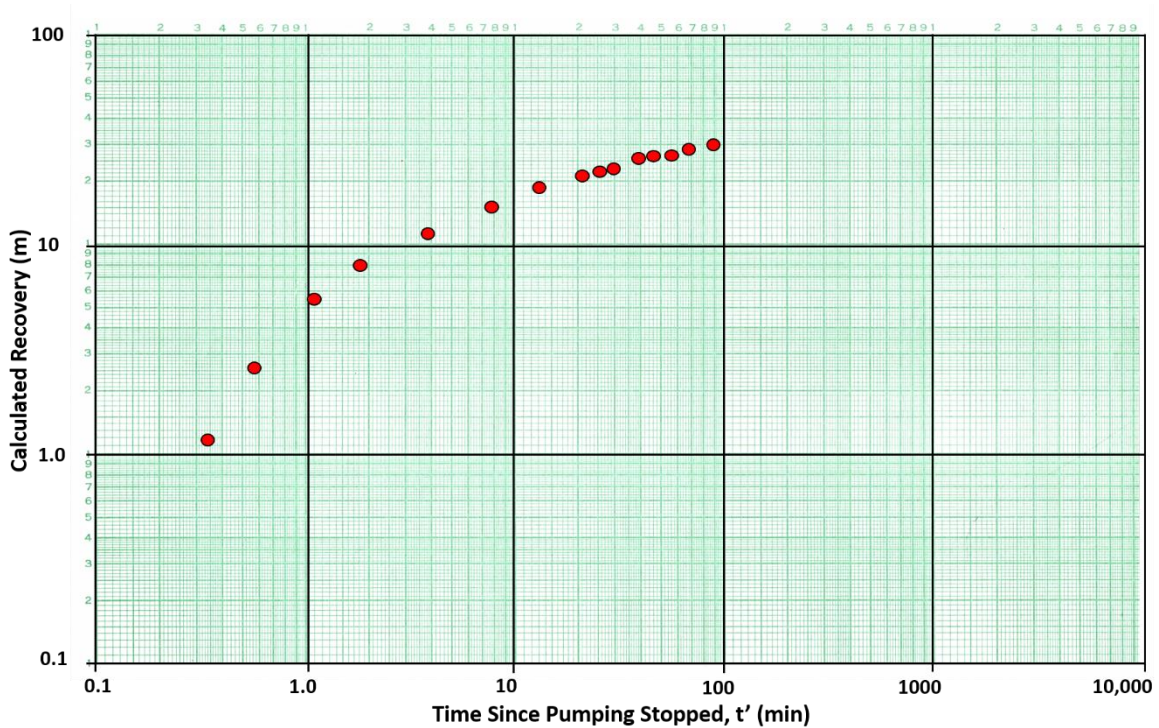


Figure 38 - Plot of calculated recovery versus time since the pumping stopped on log-log scales for water levels in an observation well that is 65 m from the pumping well. Red dots are calculated recovery values.

$$T = \frac{Q}{4\pi(s - s')} W(u) \tag{40}$$

$$S = \frac{u4Tt'}{r^2} \tag{41}$$

where:

- T = transmissivity (L^2T^{-1})
- Q = constant pumping rate (L^3T^{-1})
- $s-s'$ = calculated recovery (L)
- $W(u)$ = Theis well function (dimensionless)
- S = storativity (dimensionless)
- u = integral argument (dimensionless)
- t' = time since the pumping stopped (T)
- r = radial distance to pumping well (L)

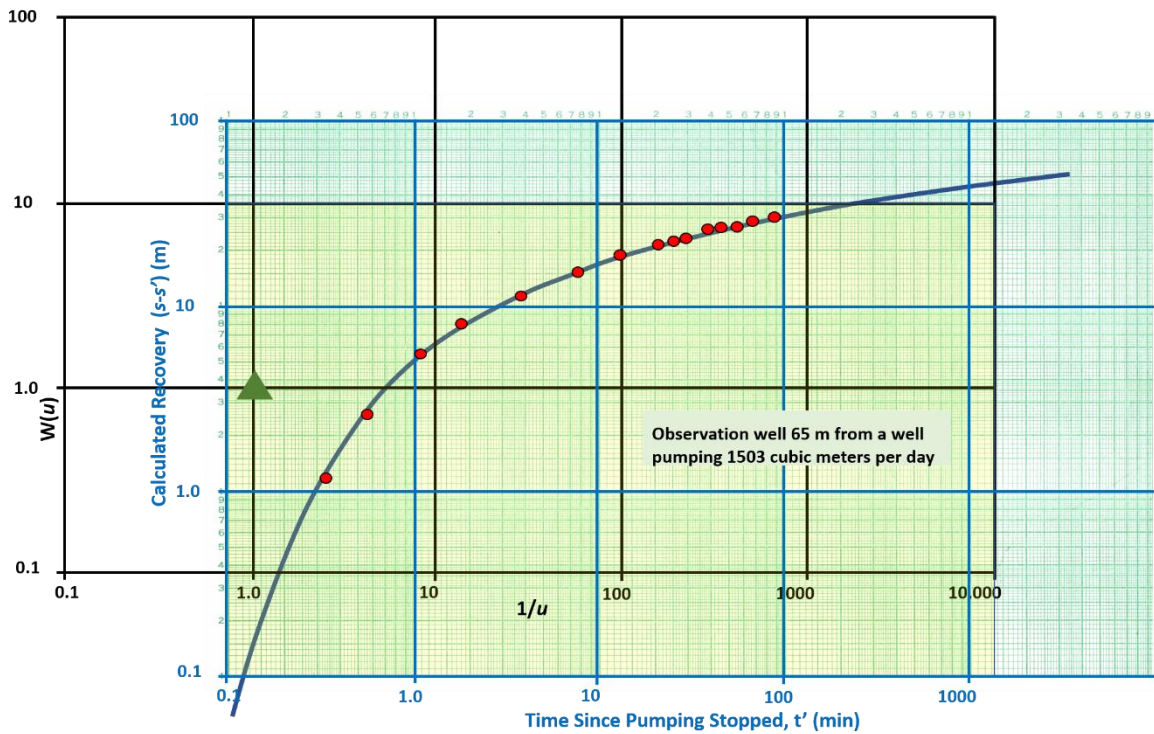


Figure 39 - Curve match for calculated recovery versus time and the Theis curve. Match point is $W(u)=1$, $1/u=1$, calculated recovery $(s-s')=3.6$ m, and $t'=1.3$ minutes.

Example

Using Equation (40) and information that the pumping well yielded $1,503 \text{ m}^3/\text{d}$ and the observation well was 65 m from the pumping well; along with the data in Figure 38, values of T and S can be calculated using recovery data. From Figure 38, $W(u) = 1$, $1/u = 1$, calculated recovery $(s-s') = 3.6$ m, and $t' = 1.3$ min.

$$T = \frac{Q}{4\pi(s - s')} W(u) = \frac{1503 \frac{\text{m}^3}{\text{d}}}{4 (3.14) (3.6 \text{ m})} (1) = 33.2 \frac{\text{m}^2}{\text{d}}$$

Using Equation (41), an estimate of S can be derived as shown here.

$$S = \frac{u^2 T t'}{r^2} = \frac{(1) (4) 33.2 \frac{\text{m}^2}{\text{d}} 1.3 \text{ min} \frac{1 \text{ d}}{1440 \text{ min}}}{(65 \text{ m})^2} = 0.000028 \text{ or } 3 \times 10^{-5}$$

8.3.5 Variable Discharge Pumping Test

The application of most analytical solutions to pumping test data require the pumping discharge be held at a constant rate during the test. If the rate varies significantly during a test, typically a weighted average pumping rate is computed. This is accomplished by assigning a pumping time interval for each measured discharge, multiplying each discharge variation by the interval time, adding these time-weighted discharge intervals

together and dividing by the total pumping time. An example is provided in Section 5.4.2. Ideally, when a constant discharge test is planned, variations in discharge will be small.

Evaluation of tests with significant variability in discharge rates is beyond the scope of this book. The US Department of Energy provides an open-source software package that can be used for such advanced analyses called [nSIGHTS](#) (n-dimensional Statistical Inverse Graphical Hydraulic Test Simulator). The department provides an [overview of the software application](#) in the form of a PowerPoint presentation.

Lohman (1972) presents an additional straight-line solution for a fully confined aquifer where the drawdown is constant and the pumping-well discharge is allowed to vary over time. All other Theis assumptions are applicable. This condition is most commonly associated with conducting a pumping test using a flowing well that is fully opened from its static state at the beginning of the test. Jacob and Lohman (1952) derived equations and solution methods for this condition. The reader is referred to Lohman (1972) for details of the mathematical derivation and application of the methodology.

8.3.6 Applicability Of Methods Presented in this Section

Each of the methods used to process and analyze pumping test data described in this section apply to totally confined systems. However, Theis's curve-matching methodology is not restricted to analyzing test results from a fully confined system. This technique is used to analyze the response of leaky, and unconfined systems by using early-time drawdown data. In the early portion of the pumping test, the drawdown closely matches the Theis function as shown in Figure 40, so aquifer properties can be estimated by matching that portion of the data to the Theis well function. The log-log plots of drawdown are also used to assess whether boundaries may be influencing observed drawdown (Figure 40). Experienced hydrogeologists review the shape of a log-log plot of test data and use that information to assist them in selecting an appropriate analytical approach.

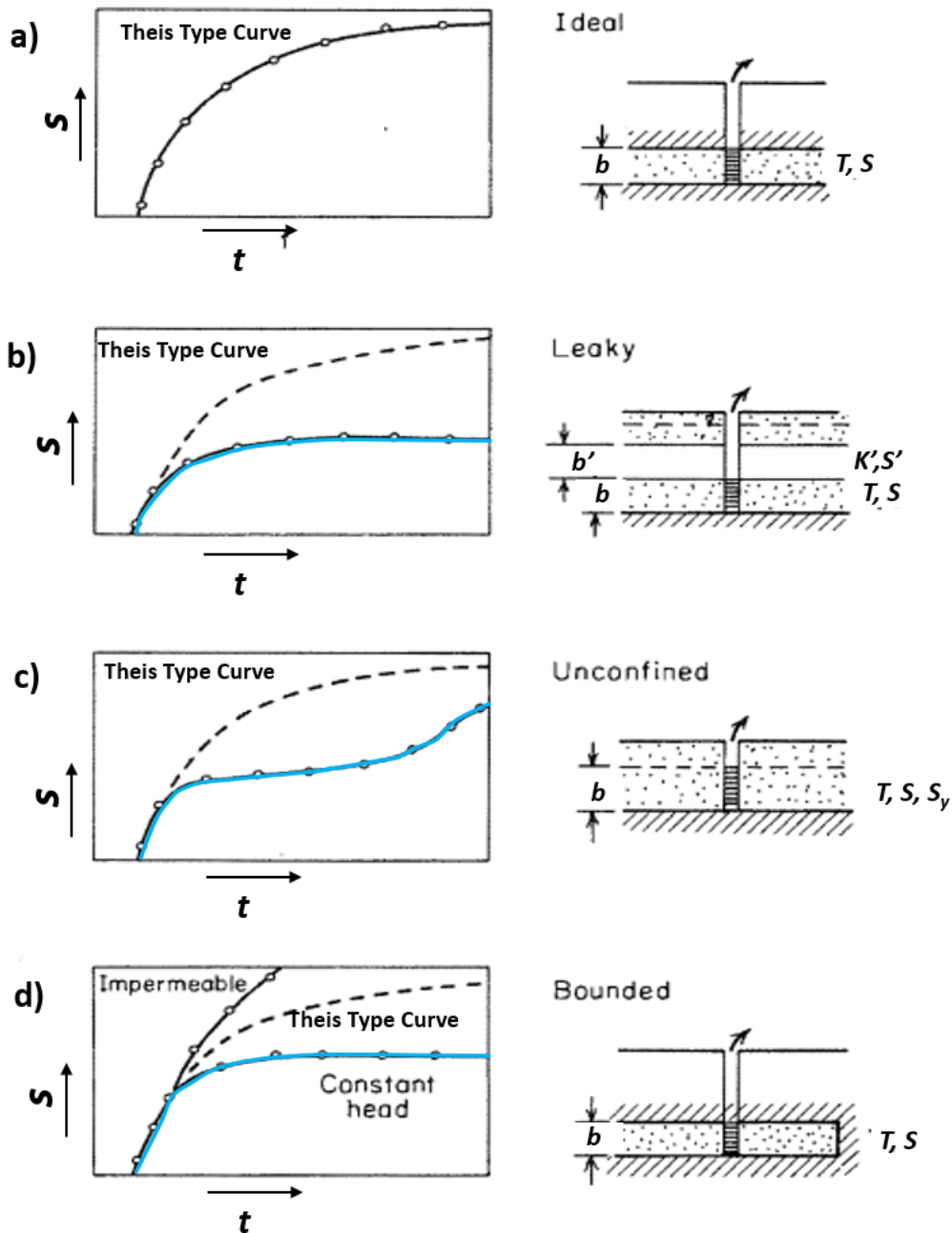


Figure 40 - Schematics of log-log plots of time (x axis) and drawdown in an observation well (y axis) showing ideal drawdown behavior in response to a constant discharge pumping test of an isotropic and homogeneous groundwater unit (speckled unit). T is transmissivity, S is storativity, S_y is specific yield, b is the initial saturated thickness of the unit, b' is the thickness of a leaky confining unit, K' is the vertical hydraulic conductivity of the leaky confining unit, and S' is the storativity of the confining unit (modified from Freeze & Cherry, 1979).

- a) Pumping response to ideal Theis conditions. Pumping test data (open circles) fall on the curve. The dashed line in illustrations b-d is the ideal Theis response (a totally confined system) that is used for comparison.
- b) Pumping response to leakage through the leaky confining unit (blue line open circles). In this setting, data fall below the Theis curve and reach equilibrium.
- c) Pumping response to unconfined conditions (open circles). The data match the Theis response at early times then drawdown slows (blue line) due to drainage of water from pores at the water table. Drawdown may reach an equilibrium and then increase to join the Theis curve trend at later times.
- d) Pumping response when lateral boundaries are encountered, a lateral recharge boundary (blue line) where drawdown is constant after inflow equals well discharge and a lateral impermeable boundary (solid black line) where drawdown is larger than the Theis curve.

Section 9 discusses how pumping-test time-drawdown data for a confined system are affected by the addition of water from overlying or underling confining units and aquifers during testing.

8.4 An Opportunity to Work with Pumping Test Data from a Confined Aquifer

Section 8 discussed well hydraulics in totally confined aquifer units. [Exercise 2](#) ↓ provides a hands-on opportunity to work with data collected at multiple observation wells during a pumping test.

9 Transient Analytical Models for Pumping in a Leaky Confined Aquifer

Productive hydrogeologic units that are confined by overlying semipermeable confining units or aquitards (e.g., Woessner & Poeter, 2020) are often referred to as “leaky confined” aquifers. Gradients created by pumping can cause groundwater to leak into the confined system through the confining beds from overlying or underlying hydrogeologic units. This leakage becomes a source of some of the groundwater pumped by the well. The leakage causes the rate of drawdown in the pumping well to slow down (relative to rates predicted by the Theis equation) and potentially reach steady-state conditions (if leakage rates are high enough). In addition, water released from storage in a confining bed can leak into a confined system causing the rate of drawdown in the confined unit to be less than predicted by the Theis equation. One or both conditions can occur when confining beds are permeable. Though the term leaky confined aquifer is used to describe the drawdown time response, it is the confining beds that are leaky not the principal unit being pumped.

9.1 Formulation of Equations to Address Leaky Confined Conditions

Cooper (1963), Jacob (1946), Hantush and Jacob (1954), and Hantush (1960) all contributed to developing analytical solutions that describe hydraulic responses to pumping in confined systems with leaky confining beds. As the confined unit is being pumped it is receiving water from leakage, thus not all Theis assumptions (Section 6.3) apply. Leaky confined conditions assume one or both of two settings.

1. Water enters the pumped confined unit from overlying or underlying units and release of water from storage in the confining beds is negligible. Overlying and underlying water-bearing units separated by the confining units are sufficiently permeable and extensive such that heads in the unpumped overlying and underlying aquifers remain constant when pumping the principal aquifer.
2. Water enters the pumped confined unit from water released from storage within the confining units.

Figure 41 and Figure 42 present conceptual models of leaky confined settings with and without aquitard storage, respectively. The mathematics of these two settings are developed separately in Sections 9.2 and 9.3.

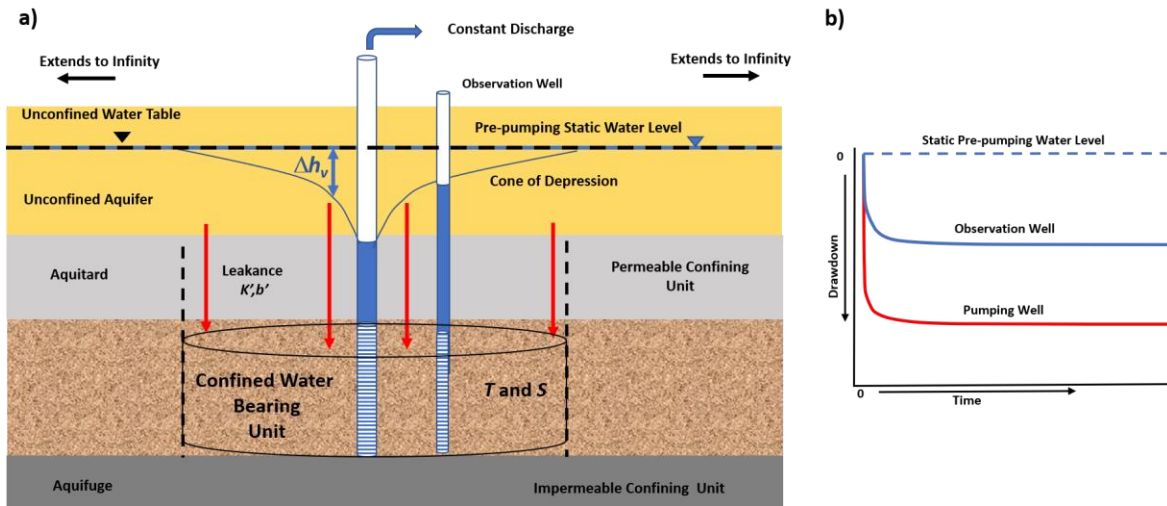


Figure 41 - Conceptual model of a Hantush-Jacob leaky confined system. a) As the production well is pumped, water starts to leak through the overlying aquitard. A difference in head, Δh_v (vertical blue double arrow) induces flow between the overlying unconfined system and the pumped confined aquifer. The overlying aquifer supplying water is extensive and permeable such that the static water level in that aquifer (water table in this example) does not change during pumping of the confined aquifer. The red arrows represent leakage from the overlying aquifer that flows through the confining unit. Leakage is defined by Darcy's Law (i.e., the product of the difference in head between the aquifers (Δh_v) and the vertical hydraulic conductivity (K') of the confining unit divided by the confining unit thickness (b'). The dashed vertical lines and cylinder outline the zone at a specified time where leakage enters the confined aquifer. b) Example of drawdown versus time at the pumping well and observation well. The water level changes begin to level out (stop declining) in this example.

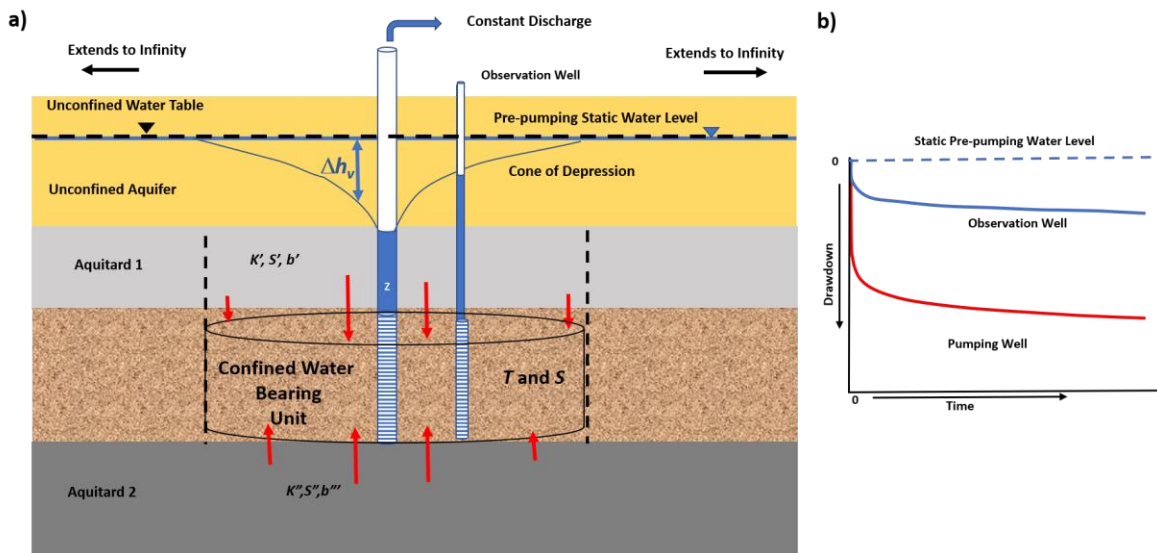


Figure 42 - Conceptual model of the modified Hantush (1960) solution setting. A well is pumped in a confined unit where water is being derived from the release of storage in both the aquifer and the confining beds. a) In addition to water being released from storage in the confined water-bearing unit, water from overlying aquitard 1 and/or underlying aquitard 2 are flowing into the confined aquifer. The properties of aquitard 1 are vertical hydraulic conductivity, K' , storativity, S' , and thickness, b' . The properties of aquitard 2 are the vertical hydraulic conductivity, K'' , storativity, S'' and thickness b'' . b) The drawdown in the pumping well and observation well are less than those observed if the pumped unit is totally confined. When leakage rates do not equal the test pumping rate, water levels will not stabilize, instead they will continue to decline.

9.2 Hantush-Jacob Solution (Leaky Confined-No Water Released from Aquitard Storage)

Hantush and Jacob (1954) developed an equation that describes conditions in a leaky confined system without the effects of release of additional water from storage within a confining aquitard (Figure 41). The following subsections present the mathematical development of the Hantush-Jacob equation and application of the method.

9.2.1 Formulation of the Hantush-Jacob Equation

Equation (42) is the Hantush-Jacob solution describing flow in leaky confined aquifer without the effects of release from aquitard storage.

$$s(r, t) = \frac{Q}{4\pi T} \int_{\frac{r^2 S}{4Tt}}^{\infty} \frac{1}{y} \exp \left\{ -y - \frac{r^2}{4B^2 y} \right\} dy \quad (42)$$

where:

- $s(r, t)$ = drawdown at distance r , at time t (L)
- Q = discharge ($L^3 T^{-1}$)
- T = transmissivity ($L^2 T^{-1}$)
- r = radial distance to an observation well (L)
- S = storativity of the confined aquifer (dimensionless)
- t = time (T)
- r = radial distance (L)
- $u = r^2 S / (4Tt)$
- y = variable of integration (dimensionless)
- $B = (Tb'/K')^{0.5}$
- b' = saturated thickness of the confining unit (L)
- K' = vertical hydraulic conductivity of the confining unit (LT^{-1})
- $r/B = r / (Tb'/K')^{0.5}$ (dimensionless)

The Hantush-Jacob equation is written using the Hantush-Jacob well function, $W(u, r/B)$ as shown in Equation (43).

$$s(r, t) = \frac{Q}{4\pi T} W \left(u, \frac{r}{B} \right) \quad (43)$$

where:

- $s(r, t)$ = drawdown at a radial distance r at a time t (L)
- Q = constant pumping rate ($L^3 T^{-1}$)
- T = confined aquifer transmissivity ($L^2 T^{-1}$)
- $W(u, r/B)$ = Hantush-Jacob well function (integral) (dimensionless)

The well function incorporates two variables, u and r/B as shown in Equation (44).

$$u = \frac{r^2 S}{4Tt} \quad , \quad \frac{r}{B} = \frac{r}{\sqrt{\frac{Tb'}{K'}}} \tag{44}$$

where:

- r = radial distance to an observation well (L)
- S = storativity of the confined aquifer (dimensionless)
- T = confined aquifer transmissivity (L^2T^{-1})
- t = time since the pumping started (T)
- $B = (Tb'/K')^{0.5}$
- K' = vertical hydraulic conductivity of a confining unit (LT^{-1})
- b' = thickness of confining bed (L)

The vertical hydraulic conductivity of the confining unit (K') divided by the confining unit thickness, b' , is referred to as vertical leakance (Anderson et al., 2015). Values for $W(u,r/B)$ have been tabulated by Hantush (1956) and are presented in Figure 43.

u	r/B	12	0.004	0.006	0.008	0.01	0.02	0.04	0.06	0.08	0.1	0.2	0.4	0.6	0.8	1	2	4	6	8
0		12.7	11.3	10.5	9.89	9.44	8.06	6.67	5.87	5.29	4.85	3.51	2.23	1.55	1.13	0.842	0.228	0.0223	0.0025	0.0003
0.000002		12.1	11.2	10.5	9.89	9.44														
0.000004		11.6	11.1	10.4	9.88	9.44														
0.000006		11.3	10.9	10.4	9.87	9.44														
0.000008		11.0	10.7	10.3	9.84	9.43														
0.00001		10.8	10.6	10.2	9.80	9.42	8.06													
0.00002		10.2	10.1	9.84	9.58	9.30	8.06													
0.00004		9.52	9.45	9.34	9.19	9.01	8.03	6.67												
0.00006		9.13	9.08	9.00	8.89	8.77	7.98	6.67												
0.00008		8.84	8.81	8.75	8.67	8.57	7.91	6.67												
0.0001		8.62	8.59	8.55	8.48	8.40	7.84	6.67	5.87	5.29										
0.0002		7.94	7.92	7.90	7.86	7.82	7.50	6.62	5.86	5.29										
0.0004		7.24	7.24	7.22	7.21	7.19	7.01	6.45	5.83	5.29	4.85									
0.0006		6.84	6.84	6.83	6.82	6.80	6.68	6.27	5.77	5.27	4.85									
0.0008		6.55	6.55	6.54	6.53	6.52	6.43	6.11	5.69	5.25	4.84									
0.001		6.33	6.33	6.32	6.32	6.31	6.23	5.97	5.61	5.21	4.83	3.51								
0.002		5.64	5.64	5.63	5.63	5.63	5.59	5.45	5.24	4.98	4.71	3.50								
0.004		4.95	4.95	4.95	4.94	4.94	4.92	4.85	4.74	4.59	4.42	3.48	2.23							
0.006		4.54				4.54	4.53	4.48	4.41	4.30	4.18	3.43	2.23							
0.008		4.26				4.26	4.25	4.21	4.15	4.08	3.98	3.36	2.23							
0.01		4.04				4.04	4.03	4.00	3.95	3.89	3.81	3.29	2.23	1.55	1.13					
0.02		3.35				3.35	3.35	3.34	3.31	3.28	3.24	2.95	2.18	1.55	1.13					
0.04		2.68				2.68	2.68	2.67	2.66	2.65	2.63	2.48	2.02	1.52	1.13	0.842				
0.06		2.30				2.30	2.29	2.29	2.28	2.27	2.26	2.17	1.85	1.46	1.11	0.839				
0.08		2.03				2.03	2.02	2.02	2.01	2.00	1.94	1.69	1.39	1.08	0.832					
0.1		1.82				1.82	1.82	1.82	1.81	1.80	1.75	1.56	1.31	1.05	0.819	0.228				
0.2		1.22				1.22	1.22	1.22	1.22	1.22	1.19	1.11	0.996	0.857	0.715	0.227				
0.4		0.702				0.702	0.702	0.701	0.700	0.693	0.665	0.621	0.565	0.502	0.210					
0.6		0.454				0.454	0.454	0.454	0.453	0.450	0.436	0.415	0.387	0.354	0.177	0.0222				
0.8		0.311				0.311	0.310	0.310	0.310	0.308	0.301	0.289	0.273	0.254	0.144	0.0218				
1		0.219							0.219	0.218	0.213	0.206	0.197	0.185	0.114	0.0207	0.0025			
2		0.049									0.049	0.048	0.047	0.046	0.044	0.034	0.011	0.0021	0.0003	
4		0.0038										0.0038	0.0037	0.0037	0.0036	0.0031	0.0016	0.0006	0.0002	
6		0.0004													0.0004	0.0003	0.0002	0.0001	0	
8		0																		0

Figure 43 - Table of selected $W(u,r/B)$, u and r/B values (modified from Fetter (2001) and Hantush (1956)).

The relationship between u , r/B and $W(u,r/B)$ is illustrated in Figure 43. As u and r/B become smaller, values of $W(u,r/B)$ become larger. Figure 44 displays type curves created by plotting selected values of $W(u,r/B)$ versus $1/u$ for different values of r/B . Figure 44

illustrates that as values of $1/u$ increase, values of $W(u,r/B)$ for a given r/B begin to approach constants. The smaller the r/B value, the longer values of $W(u,r/B)$ mirror the Theis type curve ($W(u)$). If r/B is very small, the leaky confined equation becomes the Theis equation where confining beds are assumed to be impermeable.

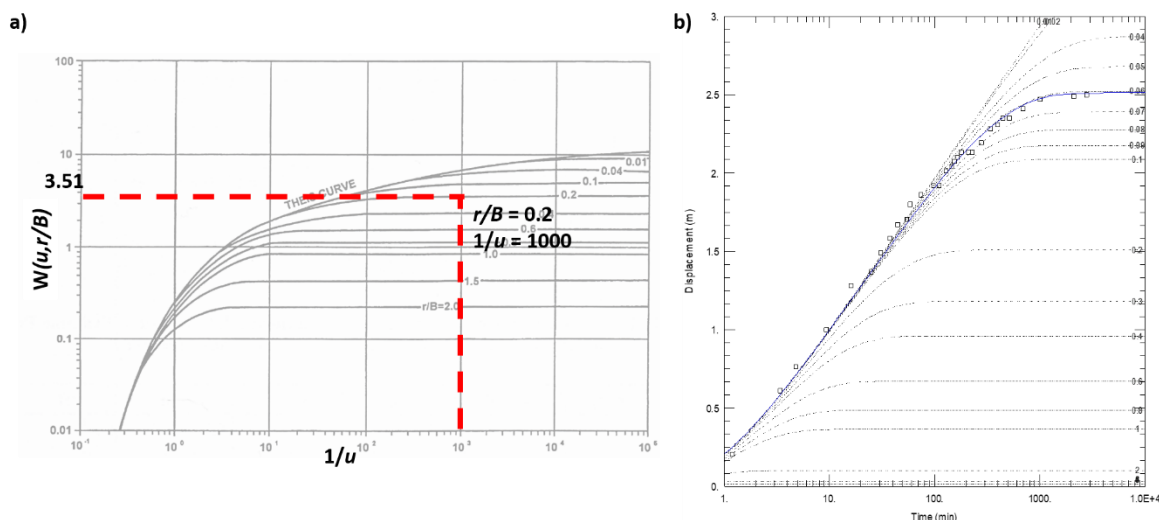


Figure 44 - Hantush-Jacob type curves for the leaky confined aquifer with vertical flow through the confining bed without the release of water from confining bed storage. a) The Theis curve is plotted for a reference (fully confined). The dashed red lines illustrate the relationship between $1/u$, r/B and $W(u,r/B)$. b) Generation of type curves for $r/B = 0.01-2.00$. Y axis displacement is drawdown. Open circles and blue line are test data match to $r/B = 0.06$ (modified from Lohman (1972), Kasenow (2003), and AQTESOLV v4.5, www.aqtesolv.com).

The table of values (Figure 43) and the plotted type curves (Figure 44) represent a subset of values that are generated by substituting combinations of u and r/B into the analytical solution to produce values of $W(u,r/B)$. If type curves with other values of r/B than shown in Figure 44 are required, they can be generated using the available analytical solution (e.g., Hantush & Jacob, 1954). When an analytical solution is not available, most often table or type curve data sets are linearly interpolated using data tables or figures like Figure 44.

9.2.2 Predicting Drawdown in Leaky Confined System with the Hantush-Jacob Equation

The drawdown in a production well or observation wells at any radial distance at any time can be computed for the Hantush-Jacob leaky confined setting. Solution inputs include a constant pumping rate (Q), the radial distance to the observation point (r), the confined unit transmissivity and storativity (T and S), and the vertical hydraulic conductivity and thickness (K' and b') of the aquitard. Again, the general simplifying assumptions are applicable (Section 6.3), such as the aquifer is isotropic and homogeneous, and flow in the confined aquifer is essentially horizontal. Values used in the equations must have compatible units so that drawdown is reported in length units.

Example

We forecast the drawdown at a distance of 17.9 m from a well pumping a constant rate of 500 L/min (720 m³/d) for 0.1 day in a 30 m thick sand and gravel aquifer. The confined aquifer has a transmissivity of 200 m²/d and a storativity of 0.0003. The confined aquifer is overlain by a sequence of aquitards and aquifers. The overlying aquitard is 40 m thick and has a vertical hydraulic conductivity of 1.0 m/d. The underlying confining unit is considered impermeable and has a very low hydraulic conductivity (on the order of 0.01 m/d). Using Equations (43) and (44) the value of r/B can be computed as follows.

$$\frac{r}{B} = \frac{17.9 \text{ m}}{\sqrt{\frac{200 \frac{\text{m}^2}{\text{d}} 40 \text{ m}}{1.0 \frac{\text{m}}{\text{d}}}}} = 0.2$$

Next u is computed as shown here.

$$u = \frac{(17.9 \text{ m})^2 0.0003}{4 \left(200 \frac{\text{m}^2}{\text{d}}\right) 0.1 \text{ d}} = 0.001$$

Then, using Figure 43, the $W(u, r/B)$ corresponding to these values is about 3.51. Now using Equation (43), drawdown is calculated at a distance of 17.9 m after 0.1 d of pumping at a constant rate of 720 m³/d as follows.

$$s(17.9 \text{ m}, 0.1 \text{ d}) = \frac{720 \frac{\text{m}^3}{\text{d}}}{4 (3.14) 200 \frac{\text{m}^2}{\text{d}}} 3.51 = 1.0 \text{ m}$$

The values presented in Figure 43 provide a limited data set. A plot of the table and additional values are provided as the Hantush-Jacob type curves in Figure 44. These can also be used to obtain a value of $W(u, r/B)$ when values of $1/u$ and r/B are known. For the example above when the point corresponding to $1/u = 1000$ and $r/B = 0.2$ is plotted on the set of type curves in Figure 44, the well function is read from the y axis as $W(u, r/B) = 3.51$.

9.2.3 Pumping Test Data from a Confined Aquifer with a Leaky Confining Bed Without Additional Water Released from Aquitard Storage

Early-time drawdown data from a pumping test in a leaky confined system will initially mirror the Theis curve, as nearly all water being pumped is initially derived from release of water from storage within the pumped unit. However, as leakage from adjacent lower hydraulic conductivity units begins to make up a portion of the pumping well discharge, the rate of drawdown will begin to decline such that the time-drawdown data will no longer mirror the Theis type curve. If the total leakage rate through the confining layer becomes equal to the pump discharge rate, the drawdown in the leaky confined

aquifer will cease declining and stabilize (plateau). An example of test data from a leaky confined aquifer with vertical flow through the confining bed is presented in Figure 45.

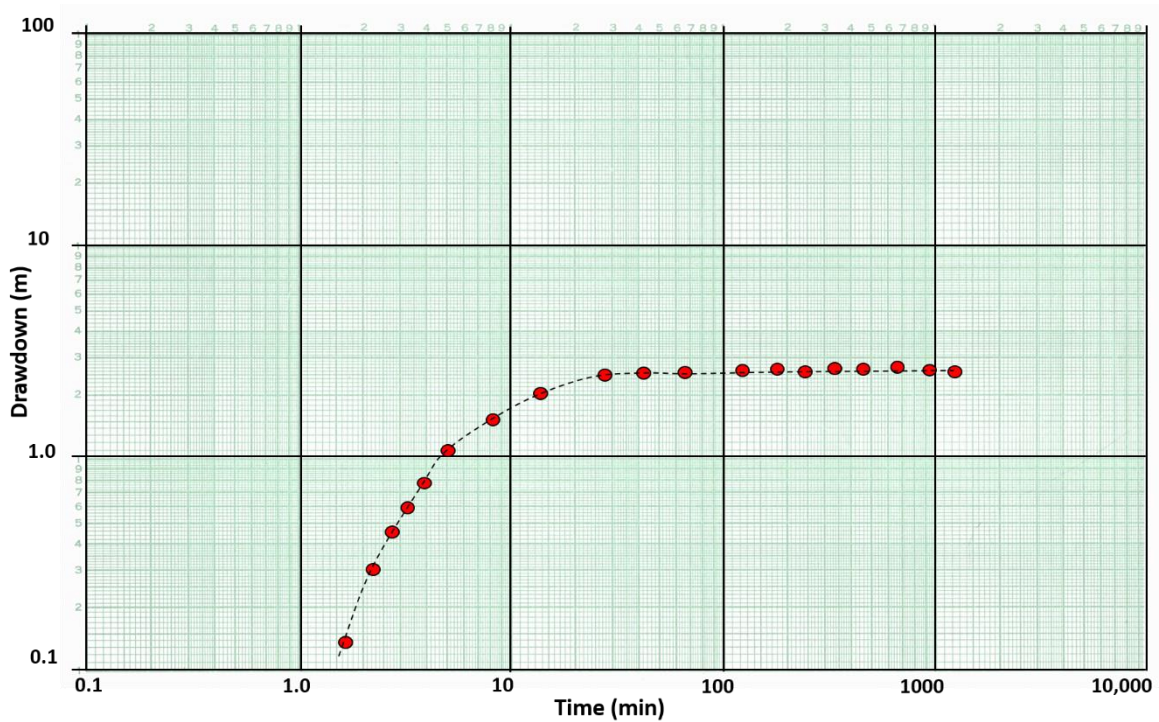


Figure 45 - A schematic of time-drawdown data for an observation well located 100 m from a well pumping at a constant rate of 2,500 m³/d for 1 day. The confined unit being pumped is a 50 m thick sand and gravel that is overlain by a 25 m thick confining unit. Data from the pumping test is plotted on log-log scales. The red dots are measured drawdown and the dashed black line is hand fitted to the curve.

9.2.4 Hantush-Jacob Curve Matching Method for a Pumping Test in a Confined Aquifer with a Leaky Confining Bed Without Water Released from Aquitard Storage

A process similar to the Theis curve matching method described in Section 8.3 is applied here. A set of leaky confined aquifer log-log type curves are used (Figure 46). A plot of the drawdown and time data for an observation well is created using the same log-log scale. While keeping the axes parallel, the field data are matched to a type curve as described for the Theis method previously (Figure 46).

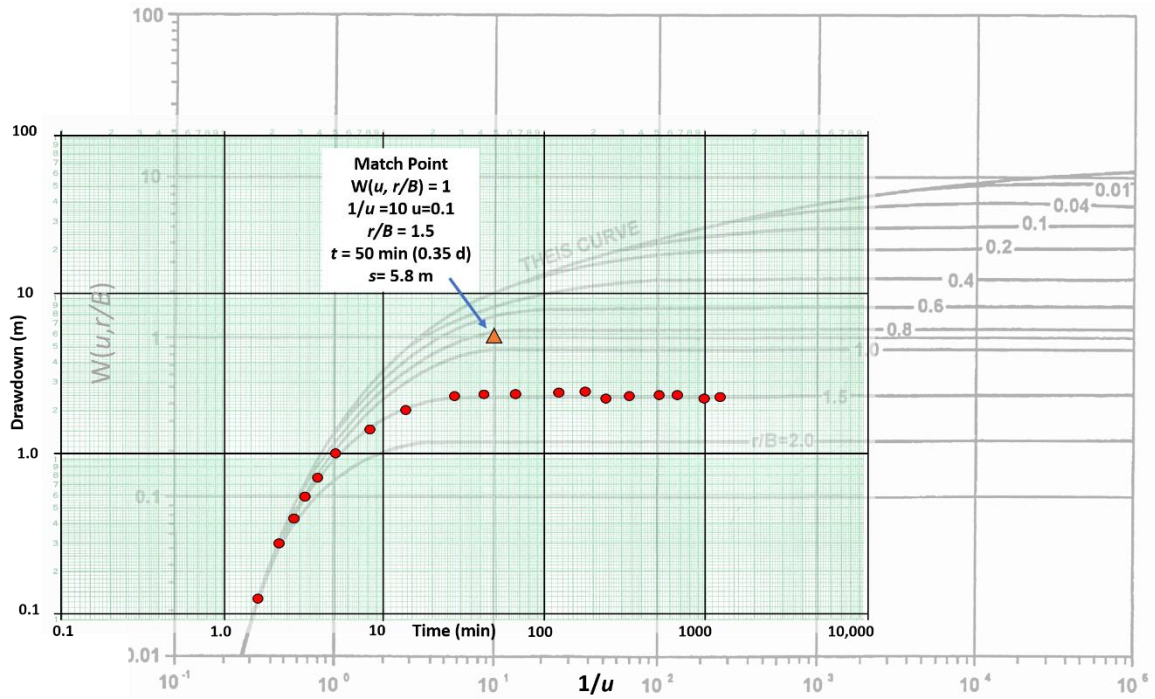


Figure 46 - Curve match method for an aquifer test of a leaky confined aquifer with vertical flow in the confining bed. The data are shown in red dots and the match point is an orange triangle.

If values fall between plotted r/B values, a value is linearly interpolated between the two adjacent values or computed from the analytical solution. A match point is selected in the overlapping fields and values of r/B , $1/u$, $W(u,r/B)$, s , and t are determined.

Estimates of T and S for the leaky confined unit can be derived using the five match point values. T is computed using Equation (45) and the storativity, S , using Equation (46) (S). The vertical hydraulic conductivity, K' , of the aquitard is derived using Equation (46).

$$T = \frac{Q}{4\pi s} W\left(u, \frac{r}{B}\right) \tag{45}$$

where:

- T = transmissivity (L^2T^{-1})
- Q = constant pumping rate (L^3T^{-1})
- s = drawdown (L)

$W(u,r/B)$ = Hantush-Jacob well function (dimensionless)

$$S = \frac{u4Tt}{r^2} \quad , \quad K' = \frac{Tb'\left(\frac{r}{B}\right)^2}{r^2} \tag{46}$$

where:

- r = radial distance to observation point (L)
- S = storativity of the confined aquifer (dimensionless)

- T = confined aquifer transmissivity (L^2T^{-1})
 t = time since the pumping started (T)
 u = variable of integration derived from the curve match (dimensionless)
 r/B = $r/(Tb'/K')^{0.5}$
 K' = vertical hydraulic conductivity of confining bed (LT^{-1})
 b' = thickness of confining bed (L)

Example

The data for this example are listed in Figure 45. Assume drawdown is measured at an observation well located 100 m from a well pumping at a constant rate of 2,500 m³/d. The confined water-bearing unit is overlain by a semi-permeable aquitard that is 25 m thick and underlain by a low permeability confining unit. The match point values are listed on Figure 45. Calculate T , S , and K' .

$$T = \frac{2500 \frac{\text{m}^3}{\text{d}}}{4 (3.14) 5.8 \text{ m}} (1) = 34.3 \frac{\text{m}^2}{\text{d}}$$

$$S = \frac{(0.1) (4) 34.3 \frac{\text{m}^2}{\text{d}} 0.35 \text{ d}}{(100 \text{ m})^2} = 0.00048$$

$$K' = \frac{34.3 \frac{\text{m}^2}{\text{d}} 25 \text{ m} (1.5)^2}{(100 \text{ m})^2} = 0.19 \frac{\text{m}}{\text{d}}$$

9.2.5 Hantush Inflection-Point Method for a Pumping Test in a Confined Aquifer with a Leaky Confining Bed Without Water Released from Aquitard Storage

Hantush (1956) developed a method to determine the hydraulic properties of a leaky confined water-bearing unit receiving water from vertical flow through the confining bed using a semi-log plot of the time-drawdown data from an observation well. If the thickness of the confining unit is known, the vertical hydraulic conductivity of the confining units can also be computed. Though this sounds like an easier approach, it involves additional mathematical tools. An example time-drawdown plot for an observation well is presented in Figure 47.

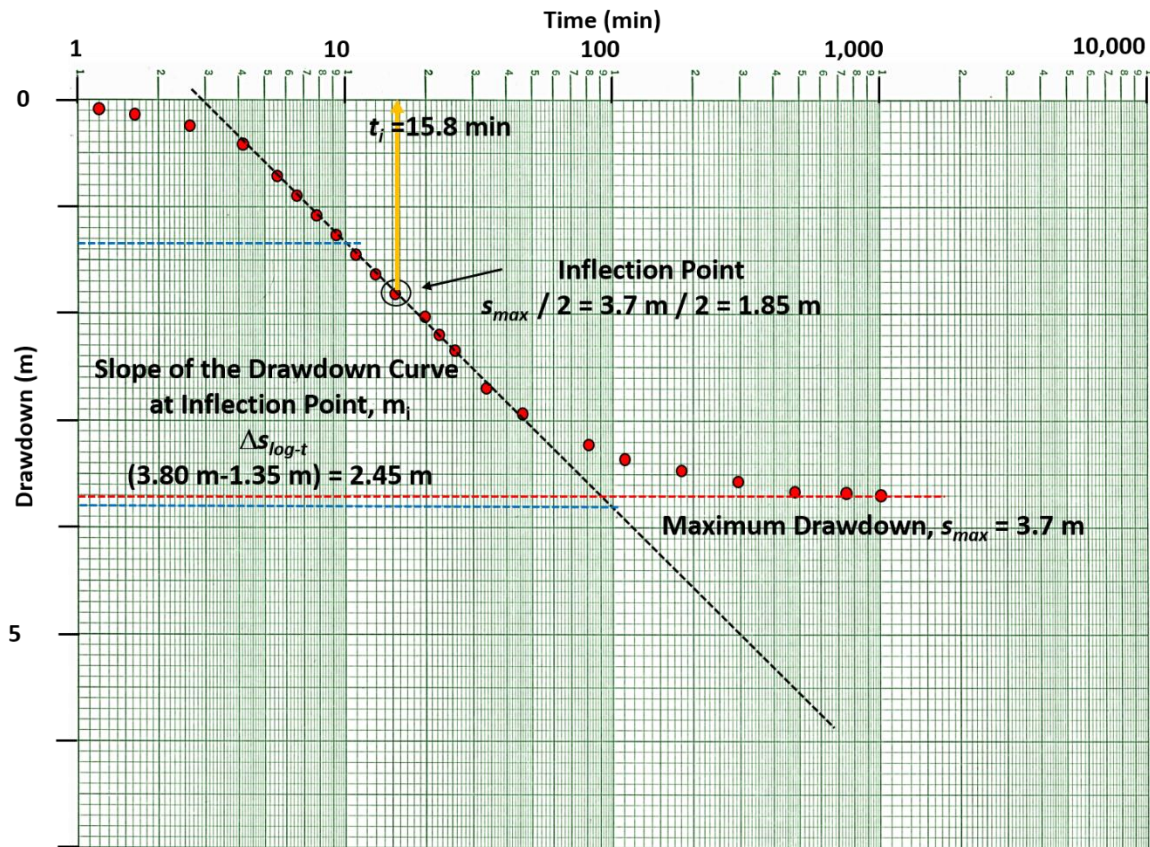


Figure 47 - A schematic semi-log plot of observation well data for a leaky confined formation. A straight-line plot is created, and the maximum drawdown is identified. The inflection point (drawdown value) is defined as $\frac{1}{2}$ the maximum drawdown. The time associated with the inflection point is noted as is the difference in drawdown over one log cycle of time, $\Delta s_{\log-t}$ (defined by the blue dashed lines). Equations presented in this section are used to estimate T and S.

The Hantush (1956) inflection-point method has several steps. Fetter (2001) summarized them as follows.

1. Produce a semi-log plot of time-drawdown data for an observation well as shown in Figure 47. Select a value for the maximum drawdown. If the data has not stabilized (i.e., reached equilibrium), project the drawdown curve to estimate a maximum drawdown.
2. The inflection point is defined as $\frac{1}{2}$ of the maximum drawdown.
3. Determine the time associated with the inflection point and the slope of the straight-line portion of the curve over one log cycle of time. Hantush (1956) presents several useful relationships to define the inflection point as shown in Equations (47), (48), (49), (50), and (51).

$$u_i = \frac{r^2 S}{4Tt_i} = \frac{r}{2B} \tag{47}$$

$$m_i = \frac{2.3Q}{4\pi T} \exp\left(\frac{-r}{B}\right) \quad (48)$$

$$s_i = 0.5 (s_{max}) = \frac{Q}{4\pi T} K_0\left(\frac{r}{B}\right) \quad (49)$$

$$B = \left(\frac{T}{\frac{K'}{b'}}\right)^{0.5} \quad (50)$$

$$f\left(\frac{r}{B}\right) = \frac{2.3 s_i}{m_i} = \exp\left(\frac{r}{B}\right) K_0\left(\frac{r}{B}\right) \quad (51)$$

where:

- u_i = value of u at the inflection point (dimensionless)
- r = radial distance from the pumping well to the observation well (L)
- S = storativity of the confined aquifer (dimensionless)
- T = transmissivity of the confined aquifer (L^2T^{-1})
- t_i = time at the inflection point m_i (T)
- B = defined in Equation (50) (L)
- m_i = slope of drawdown over one log cycle of time at the inflection point (dimensionless)
- Q = constant discharge rate (L^3T^{-1})
- s_i = drawdown at the inflection point (L)
- s_{max} = maximum drawdown (plateaued or projected to plateau) (L)
- K_0 = Bessel function zero-order of the second kind (dimensionless)
- K' = vertical hydraulic conductivity of the confining unit (LT^{-1})
- b' = thickness of the confining unit (L)
- $f(r/B)$ = function of r/B (dimensionless)

As the values of s_i and m_i can be derived as discussed earlier, and as shown on Figure 47, the value of $f(r/b)$ is computed. With a value for $f(r/b)$, r/b can be found by solving the second part of Equation (51). Function tables for $f(x) = \exp(x)K_0(x)$ are shown in Figure 48.

x	$K_0(x)$	$\exp(x)K_0(x)$	x	$K_0(x)$	$\exp(x)K_0(x)$
0.001	7.02	7.03	0.25	1.54	1.98
0.005	5.41	5.44	0.30	1.37	1.85
0.01	4.72	4.77	0.35	1.23	1.75
0.015	4.32	4.38	0.40	1.11	1.66
0.02	4.03	4.11	0.45	1.01	1.59
0.025	3.81	3.91	0.50	0.92	1.52
0.03	3.62	3.73	0.55	0.85	1.47
0.035	3.47	3.59	0.60	0.78	1.42
0.04	3.34	3.47	0.65	0.72	1.37
0.045	3.22	3.37	0.70	0.66	1.33
0.05	3.11	3.27	0.75	0.61	1.29
0.055	3.02	3.19	0.80	0.57	1.26
0.06	2.93	3.11	0.85	0.52	1.23
0.065	2.85	3.05	0.90	0.49	1.20
0.07	2.78	2.98	0.95	0.45	1.17
0.075	2.71	2.92	1.0	0.42	1.14
0.08	2.65	2.87	1.5	0.21	0.96
0.085	2.59	2.82	2.0	0.11	0.84
0.09	2.53	2.77	2.5	0.062	0.760
0.095	2.48	2.72	3.0	0.035	0.698
0.10	2.43	2.68	3.5	0.020	0.649
0.15	2.03	2.36	4.0	0.011	0.609
0.20	1.75	2.14	4.5	0.006	0.576
			5.0	0.004	0.548

Figure 48 - Values for $f(x) = \exp(x)K_0(x)$ where x in the Hantush inflection method is equal to r/B (Hantush, 1956).

The inflection method then derives hydraulic properties of the leaky confined aquifer using Equations (52) and (53).

$$T = \frac{QK_0\left(\frac{r}{b}\right)}{2\pi s_{max}} \tag{52}$$

$$S = \frac{4Tt_i}{2rB} \tag{53}$$

Where the parameters are defined above for Equations (50) and (51).

Example

The example shown in Figure 47 is used here to compute T and S for the leaky confined aquifer with vertical flow through the confining bed. Assume the observation well is located 75 m from the pumping well ($Q = 4,250 \text{ m}^3/\text{d}$) and the leaky confining unit is 15 m thick; then the following approach is used:

$$s_{max} = 3.7 \text{ m}$$

$$s_i = 1.8 \text{ m}$$

$$t_i = 15.8 \text{ min (0.011 d)}$$

$$m_i = 2.45 \frac{\text{m}}{\text{min}}$$

then

$$f\left(\frac{r}{B}\right) = \frac{2.3 (1.8 \text{ m})}{2.45 \frac{\text{m}}{\text{min}}} = 1.7$$

Using the relationship $f(r/B) = 1.7 = \exp(r/B)K_0(r/B)$, then from Figure 48, the value is between $\exp(x)K_0(x) = 1.66$ and $\exp(x)K_0(x) = 1.75$. The interpolation is shown below.

x	$K_0(x)$	$\exp(x) K_0(x)$
0.40	1.11	1.66
0.37 (interpolated)	1.16 (interpolated)	1.7
0.35	1.23	1.75

Given that $x = 0.37 \text{ m}$, with the observation well located 75 m from the pumping well, then $B = 75 \text{ m} / 0.37 = 203 \text{ m}$. Now using Equation (52).

$$T = \frac{4250 \frac{\text{m}^3}{\text{d}} 1.16}{2 (3.14) 3.7 \text{ m}} = 212 \frac{\text{m}^2}{\text{d}}$$

S is then computed from Equation (53).

$$S = \frac{4 \left(212 \frac{\text{m}^2}{\text{d}} \right) 0.011 \text{d}}{2 (75 \text{ m}) (203 \text{ m})} = 0.0003 = 3 \times 10^{-4}$$

Now since the thickness of the confining unit is known, 15 m, an estimate of the vertical hydraulic conductivity, K' , can be made using Equation (54).

$$K' = \frac{Tb'}{B^2} \quad (54)$$

where:

K' = vertical hydraulic conductivity of the confining bed (LT^{-1})

T = transmissivity of the confined aquifer (L^2T^{-1})

b' = thickness of the confining unit (L)

B = defined in Equation (50)

$$K' = \frac{212 \frac{\text{m}^2}{\text{d}} 15 \text{ m}}{(203 \text{ m})^2} = 0.08 \frac{\text{m}}{\text{d}}$$

9.3 Hantush Equation for a Leaky Confined System with Water Released from Confining Bed Storage

When pumping a confined aquifer with a permeable confining bed contributing water to the pumped aquifer, the reduction in head in the aquifer creates a hydraulic gradient in the confining bed toward the aquifer. As heads in the confining bed are lowered, water is released from storage and flows to the confined aquifer. If the confining bed is relatively thin, the gradient change reaches the top of the bed relatively quickly and then stabilizes such that release of water from storage within the confining bed ceases. If there is an aquifer on the other side of the discharge confining bed, it provides a source of water that flows through the confining bed to the pumped aquifer. Hantush (1960) developed a set of analytical solutions that account for leakage of water from aquitard storage into a confined aquifer as it is pumped. His work also addresses leakage into a confined system from vertical flow through confining beds as described by Hantush-Jacob and illustrated in Figure 41. Conceptual models of such leakage are illustrated in Figure 49.

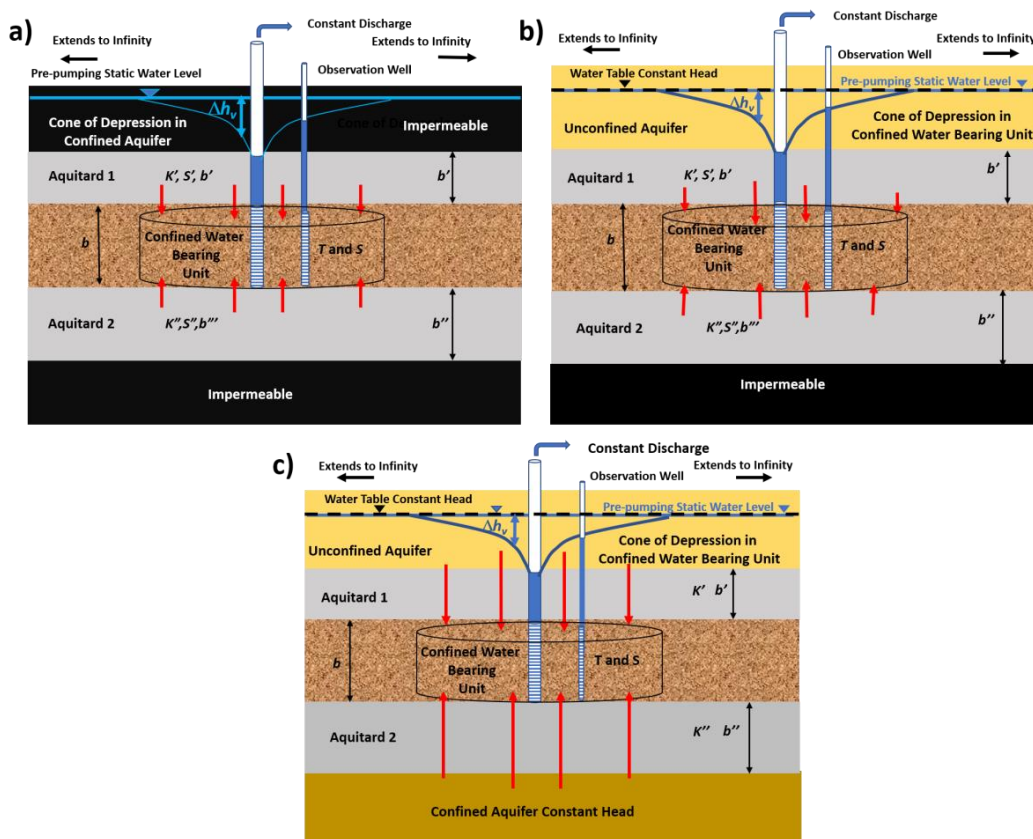


Figure 49 - Conceptual models that can be represented by the Hantush equation (1960).

- a) Drawdown in a confined aquifer that receives water from storage in one or two confining beds when the beds overlying and underlying the confining beds are not permeable.
- b) Drawdown in a confined aquifer that receives water from storage in overlying and/or underlying confining beds, as well as leakage of water through the confining bed from a highly transmissive unit such as an unconfined water table aquifer.
- c) Drawdown in a confined aquifer receiving water via direct flow through a confining bed that has negligible storage from a highly transmissive aquifer above and/or below the confining bed.

The general analytical solution for leaky conditions given by Hantush (1960) is presented in Equation (55). The different conditions shown in Figure 49 can be represented using variations of this equation. Similar to the Theis well function for drawdown when pumping a fully confined water bearing unit, the Hantush integral includes an infinite series and can be represented using an approximation as shown in Equation (56). The Hantush well function uses the parameter b to account for the relative properties of the aquifer and its overlying and underlying layers. Drawdown in a confined unit with one or two adjacent confining unit(s) that release(s) water from storage that is overlain or underlain by an impermeable unit is calculated as shown in Equation (57).

$$s(r, t) = \frac{Q}{4\pi T} \int_u^\infty \frac{1}{y} \exp\{-y\} \operatorname{erfc}\left(\frac{\frac{\beta}{\sqrt{u}}}{\sqrt{y(y-u)}}\right) dy \quad (55)$$

$$H(u, \beta) = W(u) - \frac{4\beta}{(\pi u)^{0.5}} \left[0.2577 + 0.6631 \exp\left(\frac{-u}{2}\right) \right] \quad (56)$$

$$s(r, t) = \frac{Q}{4\pi T} H(u, \beta) \quad (57)$$

where:

- $s(r, t)$ = drawdown at a radial distance r and time t (L)
- r = radial distance to the observation well (L)
- t = time (T)
- Q = constant well discharge rate (L^3T^{-1})
- T = transmissivity of the confined pumped unit (L^2T^{-1})
- y = variable of integration
- erfc = complementary error function (dimensionless)
- β = represents the relative transmissibility and storage of the pumped unit and the contributing overlying and/or underlying units as shown in Equations (58) and (59) (dimensionless)
- u = $r^2S/(4Tt)$
- $H(u, \beta)$ = Hantush well function integral (dimensionless)
- $W(u)$ = Theis well function (dimensionless)

When storage comes from only one confining bed, b is described by Equation (58). This represents the case illustrated in Figure 49a with one aquitard—which can be above or below the pumped unit. In this case the other aquitard shown in Figure 49a is impermeable. For the setting with two confining beds, b includes terms for both aquitards and is described by Equation (59).

$$\beta = \frac{r}{4} \sqrt{\frac{K'S'}{b'TS}} \tag{58}$$

$$\beta = \frac{r}{4} \left(\sqrt{\frac{K'S'}{b'TS}} + \sqrt{\frac{K''S''}{b''TS}} \right) \tag{59}$$

where:

- r = radial distance to the pumping well (L)
- K' = vertical hydraulic conductivity of the first confining unit (LT^{-1})
- K'' = vertical hydraulic conductivity of the second confining unit (LT^{-1})
- S' = storativity of the first confining unit (dimensionless)
- S'' = storativity of the second confining unit (dimensionless)
- b' = thickness of the first confining unit (L)
- b'' = thickness of the second confining unit (L)
- T = transmissivity of the confined unit being pumped (L^2T^{-1})
- S = storativity of the confined unit being pumped (dimensionless)

Drawdown in the confined aquifer can be calculated with Equation (57) by using Equation (56) to calculate the Hantush well function ($H(u,\beta)$) or reading/interpolating the value from a table (Figure 50) or type curves (Figure 51).

$\mu \backslash \beta$	0.001	0.005	0.01	0.05	0.10	0.20	0.50	1.0	2.0	5.0	10.0	20.0
0.000001	11.9842	10.5908	9.9259	8.3395	7.6497	6.9590	6.0463	5.3575	4.6721	3.7756	3.1110	2.4671
0.000005	10.8958	9.7174	9.0866	7.5284	6.8427	6.1548	5.2459	4.5617	3.8836	3.0055	2.3661	1.7633
0.00001	10.3739	9.3203	8.7142	7.1771	6.4944	5.8085	4.9024	4.2212	3.5481	2.6822	2.0590	1.4816
0.00005	9.0422	8.3171	7.8031	6.3523	5.6821	5.0045	4.1090	3.4394	2.7848	1.9622	1.3943	0.8994
0.0001	8.4258	7.8386	7.3803	5.9906	5.3297	4.6581	3.7700	3.1082	2.4658	1.6704	1.1359	0.6878
0.0005	6.9273	6.6024	6.2934	5.1223	4.4996	3.8527	2.9933	2.3601	1.7604	1.0564	0.6252	0.3089
0.001	6.2624	6.0193	5.7727	4.7290	4.1337	3.5045	2.6650	2.0506	1.4776	0.8271	0.4513	0.1976
0.005	4.6951	4.5786	4.4474	3.7415	3.2483	2.6891	1.9250	1.3767	0.8915	0.4001	0.1677	0.0493
0.01	4.0163	3.9334	3.8374	3.2752	2.8443	2.3325	1.6193	1.1122	0.6775	0.2670	0.0955	0.0221
0.05	2.4590	2.4243	2.3826	2.1007	1.8401	1.4872	0.9540	0.5812	0.2923	0.0755	0.0160	0.00164
0.1	1.8172	1.7949	1.7677	1.5768	1.3893	1.1207	0.6947	0.3970	0.1789	0.0359	0.00552	0.00034
0.5	0.5584	0.5530	0.5463	0.4969	0.4436	0.3591	0.2083	0.1006	0.0325	0.00288	0.00015	
1.0	0.2189	0.2169	0.2144	0.1961	0.1758	0.1427	0.0812	0.0365	0.00993	0.00055	0.00002	
5.0	0.00115	0.00114	0.00112	0.00104	0.00093	0.00076	0.00042	0.00017	0.00003			

Figure 50 - Tables of the Hantush well function for variables u and β (from Fetter (2001)). Type curves of $H(u,\beta)$ versus $1/u$ are illustrated in Figure 51.

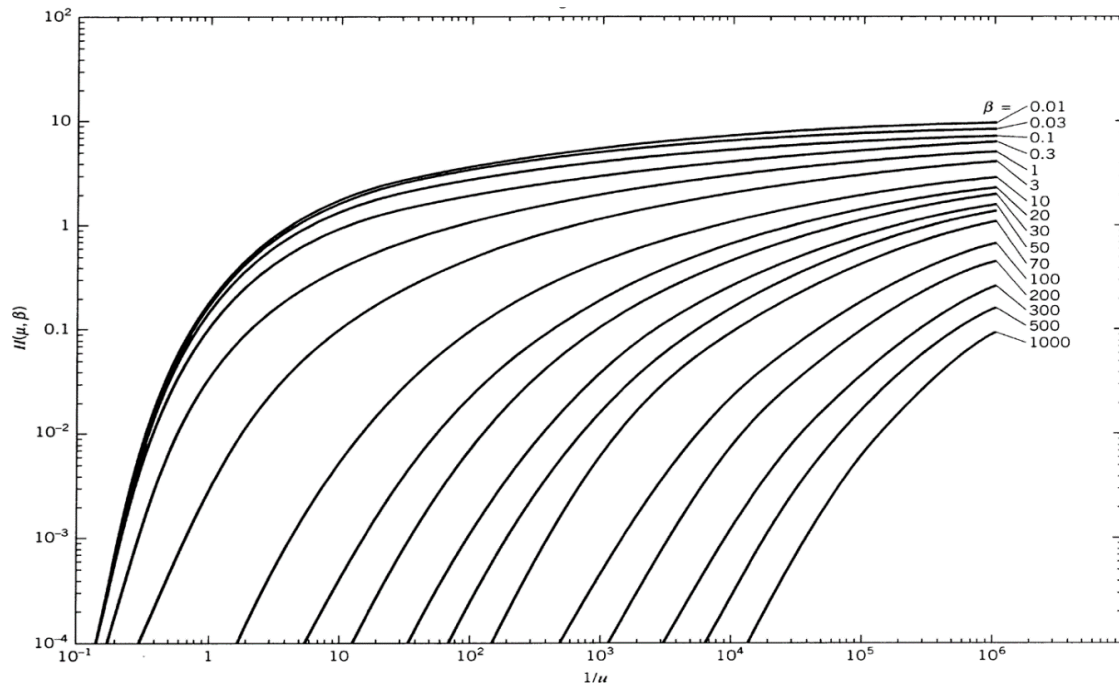


Figure 51 - Type curves of $H(u, \beta)$ versus $1/u$ plotted on log-log axes (modified from Reed (1980); Kruseman & de Ridder (2000); Kasenow (2001)).

The table of values (Figure 50) and plotted type curves (Figure 51) represent a subset of $H(u, \beta)$ values that can be generated by substituting combinations of u and β into Equation (56) or by using mathematical software packages to solve the integral portion of Equation (55). The required values are commonly interpolated from the table or curves presented in Figure 50 and Figure 51 respectively.

9.3.1 Using the Hantush Equation to Predict Drawdown in Leaky Confined Units with Water Released from Confining Bed Storage

When the hydraulic properties of the sequence of geologic units as illustrated in Figure 49a are known, the Hantush equation can be used to approximate drawdown at an observation point at any time t after the pumping commenced.

Example

A fully penetrating well pumps at $500 \text{ m}^3/\text{d}$ for 0.2 d from a 30 m thick leaky confined sand rich aquifer that is overlain by a silt rich aquitard that is 20 m thick. The confining units are overlain and underlain by impermeable units (Figure 49a). The observation well is located 53 m from the pumping well. The transmissivity of the confined aquifer is $300 \text{ m}^2/\text{d}$ and the storativity is 0.00003 . The vertical hydraulic conductivity of the confining bed is 0.3 m/d and the storativity of the confining bed is 0.00001 . Calculate the drawdown in the observation well after 0.2 d of pumping.

Using the definition of u ($u=r^2S/(4Tt)$) along with Equations (58) and (60), and the information listed above, $H(u, b)$ is obtained by first computing u and b , and then using Figure 50 to obtain the Hantush well function.

$$u = \frac{r^2 S}{4 T t} = \frac{(53 \text{ m})^2 0.00003}{4 \left(300 \frac{\text{m}^2}{\text{d}}\right) 0.2 \text{ d}} = 0.0004$$

$$\beta = \frac{r}{4} \sqrt{\frac{K' S'}{b' T S}} = \frac{53 \text{ m}}{4} \sqrt{\frac{0.3 \frac{\text{m}}{\text{d}} (0.00001)}{20 \text{ m} \left(300 \frac{\text{m}^2}{\text{d}}\right) 0.00003}} = 0.05$$

With $u = 0.0004$ and $b = 0.05$, $H(u,b)$ is obtained by interpolation from Figure 50 or Figure 51. With $u = 0.0004$, $b = 0.05$ then $H(u,b)$ is about 6.52.

u	β	$H(u,\beta)$
0.0001	0.05	7.1771
0.0004	0.05	6.52 (interpolated)
0.0005	0.05	6.3523

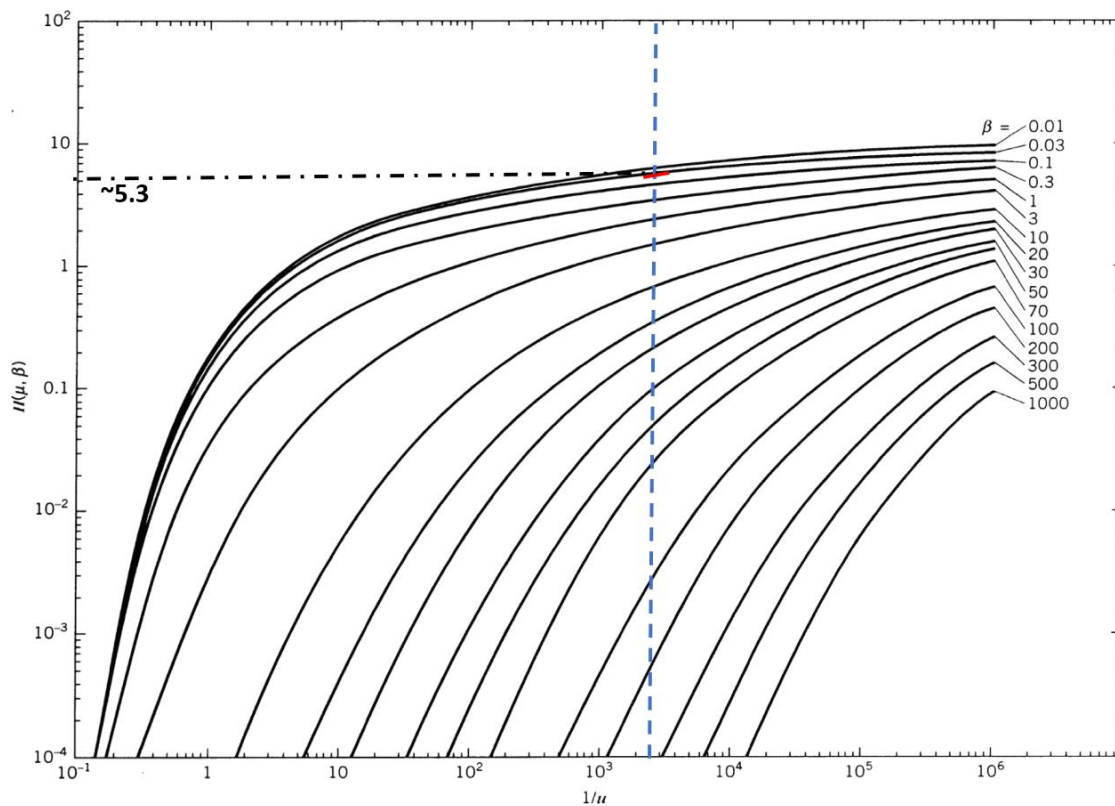


Figure 52 - Hantush type curves plotted on log-log scales. The dashed vertical blue line is the computed value of $1/u$ (2,500) for the example problem. The red line is the interpolated value of β , about 0.05, and the black dot dashed line is the interpolated value of $H(u,\beta)$, about 5.3. This value is lower than derived from the tables. The close plotting of the type curves made interpretation difficult for the designated β value (modified from Kruseman & de Ridder, 2000; Kasenow, 2001).

Then Equation (57) provides the value of drawdown.

$$s(r, t) = \frac{500 \frac{\text{m}^3}{\text{d}}}{4 (3.14) 300 \frac{\text{m}^2}{\text{d}}} 6.52 = 0.87 \text{ m}$$

9.3.2 Hantush Curve Matching Method to Compute T and S from a Pumping Test in Leaky Confined Unit with Aquitard Storage

The Hantush equation can be used to determine T and S from time-drawdown data collected in an observation well when a leaky confined aquifer is pumped and water is released from aquitard storage. The hydraulic conductivity and storage properties of adjacent confining units can also be derived. Standard curve-matching techniques described in Section 8.3.1 can be used.

After data from a pumping test has been collected, T and S for a leaky confined aquifer with the release of water from confining bed storage is estimated by first plotting drawdown versus time on a log-log graph at the same scale as the type curves as shown in (Figure 53).

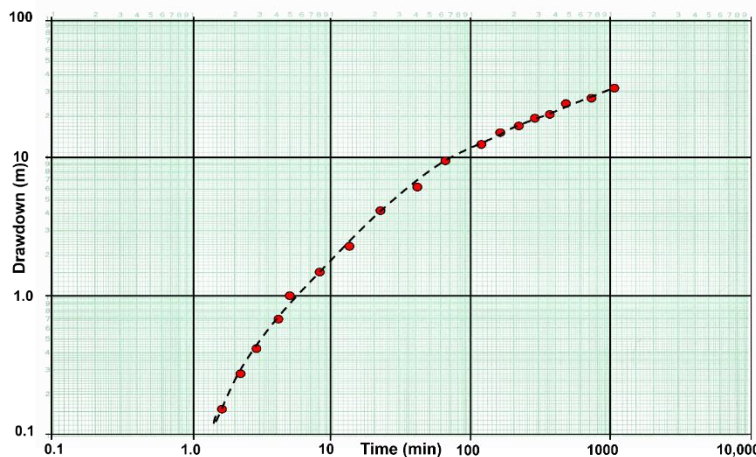


Figure 53 - Log-log plot of the response of an observation well to the pumping of a well in a leaky confined aquifer with water being released from confining bed storage.

The data graph (Figure 53) is overlain on the type curves (Figure 51). Keeping the axes parallel, the field data graph and type curve graph are overlain and shifted until the curves match (Figure 54). A match point is selected from the overlapping portion of the two plots and values of $H(u, \beta)$, $1/u$, s , t and β are obtained. Estimates of T and S for the leaky confined unit as well as its hydraulic conductivity, and, at early times, storativity values of the confining beds can be estimated using Equations (60) and (61) which are obtained from rearranging Equation (57) and the definition of u ($u=r^2S/(4Tt)$), respectively. Early time refers to the period after pumping begins when the confining unit is releasing water from storage. Early time is less than $b'S'/10K'$.

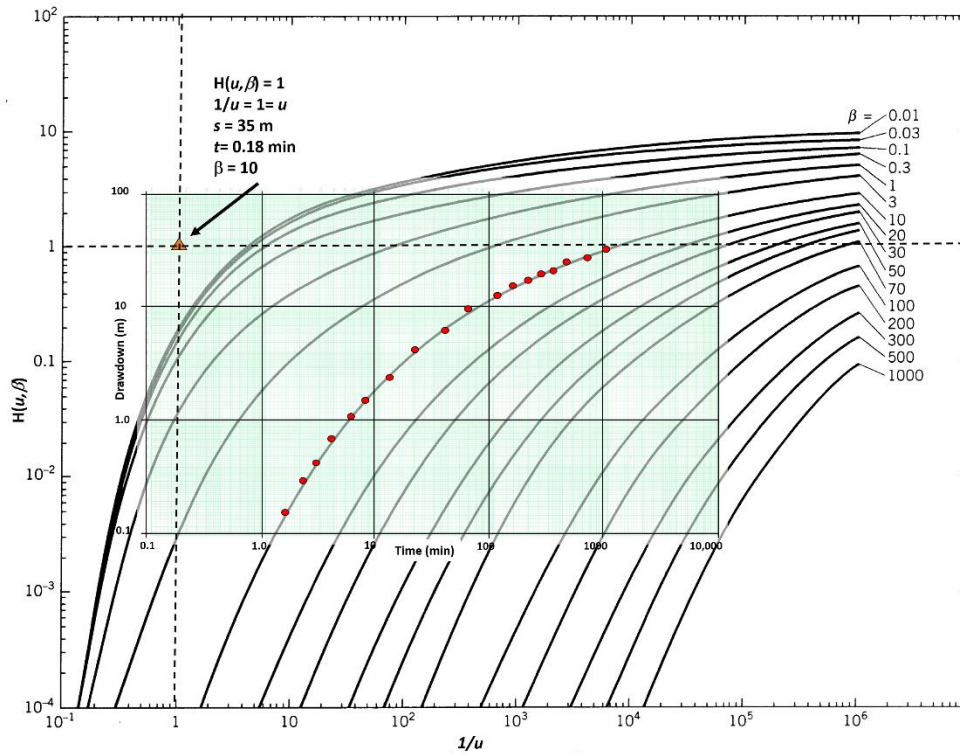


Figure 54 - Curve matching of the data from an observation well with the Hantush type curves. The scales of both graphs are equal and their axes are kept parallel. The value of β is obtained from the corresponding curve and the match point values are obtained at the location of the orange triangle (modified from Reed, 1980; Kruseman & de Ridder, 2000).

$$T = \frac{Q}{4\pi s} H(u, \beta) \tag{60}$$

$$S = \frac{u(4Tt)}{r^2} \tag{61}$$

where:

- T = transmissivity (L^2T^{-1})
- s = drawdown (L)
- Q = constant pumping rate (L^3T^{-1})
- $H(u, \beta)$ = Hantush Well Function (dimensionless)
- u = $r^2S/(4Tt)$ (dimensionless)
- r = radial distance to the observation well (L)
- t = time since pumping started (T)
- S = storativity of the confined aquifer (dimensionless)

Once T and S are computed for the pumped confined aquifer, estimates of the vertical hydraulic conductivity and storage properties of the confining unit can be derived as described by Schwartz and Zhang (2003). For conditions shown in Figure 49a, when

$K''b''S'' = 0$ then $K'S'$ is calculated using Equation (62) which is a rearrangement of Equation (58). When $K''S''=K'S'$ (Figure 49a) then $K'S'$ is calculated using Equation (63) which is a rearrangement of Equation (59) .

$$K'S' = \frac{16 b'TS\beta^2}{r^2} \quad (62)$$

$$K'S' = \frac{16 TS\beta^2}{r^2} \left(\frac{b'b''}{b'+b''+2(b'b'')^{0.5}} \right) \quad (63)$$

where:

β = defined by Equation (58) for Equation (62), and Equation (59) for Equation (63)

r = radial distance to the pumping well (L)

S' = storativity of the first confining unit (dimensionless)

S'' = storativity of the second confining unit (dimensionless)

S = storativity of the confined unit being pumped (dimensionless)

T = transmissivity of the confined unit being pumped (L^2T^{-1})

K' = vertical hydraulic conductivity of the first confining unit (LT^{-1})

b' = thickness of the first confining unit (L)

K'' = vertical hydraulic conductivity of the second confining unit (LT^{-1})

b'' = thickness of the second confining unit (L)

Example

The data presented in Figure 54 represent drawdown in a fully-penetrating observation well responding to a fully-penetrating well in a confined aquifer that is pumped continuously for 1 day at 1,000 m³/d. The production well and observation well are completed in a 20 m thick sandstone unit. The observation well is 100 m from the pumping well. The confining unit overlying the leaky confined unit is a sandy shale that is 10 m thick. Based on this information and the curve matching results, the T and S of the confined sandstone unit can be computed as follows using Equations (60) and (61).

$$T = \frac{1000 \frac{m^3}{d}}{4 (3.14) 35 m} (1) = 2.3 \frac{m^2}{d}$$

$$S = \frac{1 (4) 2.3 \frac{m^2}{d} 0.000125}{(100 m)^2} = 0.0000001 \text{ or } 1 \times 10^{-7}$$

A rearrangement of Equation (58) is used to solve for hydraulic conductivity of the confining bed using either a known or estimated value for storativity of the confining bed. Methods to estimate the confined storativity are provided in [Box 2](#). When the confining

unit is fractured rock, Lohman (1972) suggests confining unit storativity can be estimated by multiplying the thickness of the unit in meters by 0.0000003/m. In this example the confining bed storativity is estimated as 10 m times 0.0000003/m and equals 0.000003. β from the curve match is 10. Then Equation (62) is rearranged to solve for K' .

$$K' = \frac{16 b' T S \beta^2}{S' r^2} = \frac{16 (10 \text{ m}) 2.3 \frac{\text{m}^2}{\text{d}} (0.0000001) (10)^2}{(0.000003) (100 \text{ m})^2} = 0.12 \frac{\text{m}}{\text{d}}$$

9.4 An Opportunity to Work with Pumping Test Data from a Leaky Confined Aquifer

Section 9 discussed well hydraulics in leaky confined aquifer units. [Exercise 3](#)  provides a hands-on opportunity to work with data collected at an observation well during a pumping test.

10 Transient Analytical Models for Pumping an Unconfined Aquifer

Unlike a confined aquifer, when an unconfined system is pumped, a portion of the unit is physically dewatered as water levels decline. If aquifer materials are isotropic and homogeneous, coarse-grained, and the release of water from storage is more or less instantaneous, the response of the aquifer to pumping will mirror the Theis type curve. In this setting, the Theis equation with a storativity of S_y is used to represent the unconfined response to pumping (Figure 55a).

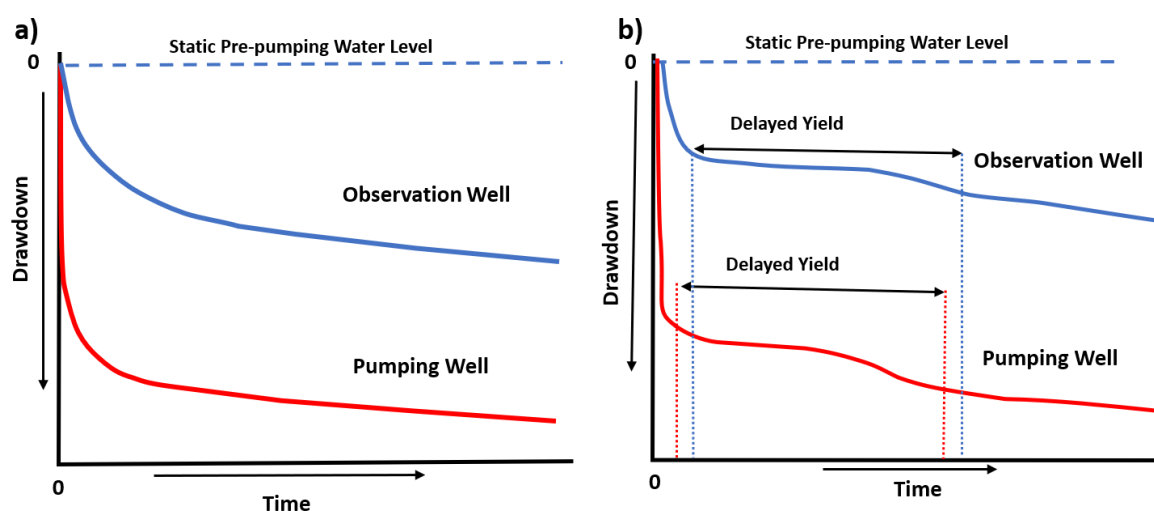


Figure 55 - Schematics of the arithmetic time-drawdown response of a pumping well and observation well finished in an unconfined aquifer that is pumped at a constant rate. A) Aquifer behaves as an isotropic homogeneous system with water instantaneously released from storage (S_y). b) Aquifer drawdown is affected by a delay in the release of water from storage. The period of delayed yield for the pumping well and the observation well is indicated by double black arrows and vertical dashed red and blue lines, respectively.

However, more often drawdown exhibits a time delay. This is generally attributed to the vertical flow of gravity drainage from pores above the water table that occurs as the water table is lowered. The resulting drawdown data often show an intermediate time reduction of slope and then a continued steeper decline (Figure 55b). The temporary reduction in drawdown is caused by what is referred to as delayed yield. Analysis of both these responses to pumping is discussed in this section.

10.1 Approximating the Response of Pumping Unconfined Aquifers Using Theis Approach

As illustrated in Figure 56, time-drawdown data in unconfined units will sometimes mirror the Theis type curve response. For example, in an isotropic and homogeneous high hydraulic conductivity system with large pore spaces being pumped at a rate that results in a small reduction in saturated thickness, drawdown is likely to mirror a Theis-like response.

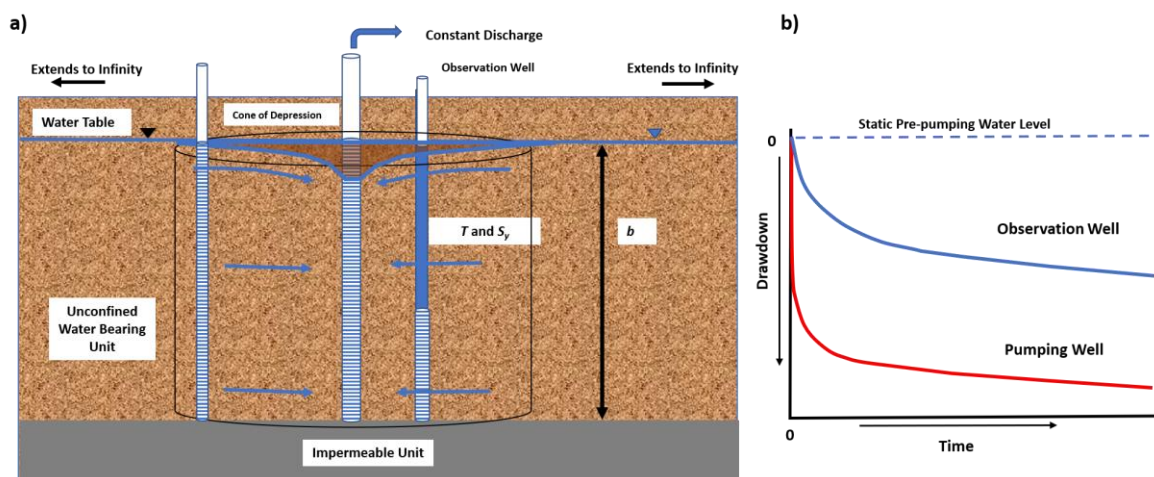


Figure 56 - Conceptual model of the response of an isotropic and homogeneous coarse-grained unconfined water-bearing unit to constant pumping. The volume of the cone of depression affected at a specific time is represented by the cylinder. The initial saturated thickness is b . The volume dewatered is shown in brown. A) In this setting the coarse nature of the material is such that the capillary fringe is small, and the release of gravity-drained water added to the declining water table is instantaneous. B) The arithmetic drawdown response mirrors the Theis logarithmic decline.

The analytical equation describing the resulting drawdown behavior is the Theis equation (Theis, 1935) shown here as (64). If the formational properties (T and S_y) are known, drawdown at any location and time can be computed using Equation (64). To compute u the confined storativity is replaced with the unconfined storativity (Equation (65), S_y (discussed in detail in Box 2).

$$s(r, t) = \frac{Q}{4\pi T} W(u) \tag{64}$$

$$u = \frac{r^2 S_y}{4Tt} \tag{65}$$

where:

$s(r,t)$ = drawdown at a radial distance r and time t (L)

Q = constant well discharge rate (L^3T^{-1})

T = transmissivity (L^2T^{-1})

t = time (T)

$W(u)$ = Theis well function (dimensionless)

S_y = unconfined storativity (specific yield) (dimensionless)

The predicted drawdown is considered representative if the degree of aquifer dewatering at the prescribed radial distance from the pumping well is small, less than 10 percent (Kasenow, 2001; USDI, 1981).

Example

If an unconfined aquifer with $T= 300 \text{ m}^2/\text{d}$ and $S_y = 0.08$ is pumped at $1,000 \text{ m}^3/\text{d}$ for 0.5 days, compute the drawdown at 100 m from the pumping well. The pre-pumping

saturated thickness of the unconfined aquifer is 25 m. Equation (65) is used to compute u and then the Theis well function is determined from the table shown in Figure 26.

$$u = \frac{(100 \text{ m})^2 0.08}{4 \left(300 \frac{\text{m}^2}{\text{d}}\right) 0.5 \text{ d}} = 1.33$$

This value of u falls outside of the range of the table in Figure 26, however the value is readily obtained using the [WolframAlpha.com equation solver](http://WolframAlpha.com) on the Internet as shown in Figure 27 where $W(1.33)$ is found to be 0.13 and s can be calculated as follows.

$$s = \frac{1000 \frac{\text{m}^3}{\text{d}}}{4 (3.14) 300 \frac{\text{m}^2}{\text{d}}} 0.13 = 0.035 \text{ m}$$

Next, we check whether the predicted drawdown values need to be corrected. If they are less than 10 percent of the initial aquifer thickness, then correction is not needed.

$$\text{percent thickness} = \frac{0.035 \text{ m}}{25 \text{ m}} (100) = 0.14 \text{ percent}$$

Less than 10 percent of the aquifer is dewatered at this location, so no drawdown correction is needed.

In some cases, drawdown due to pumping in an unconfined unit measurably reduces the saturated thickness, yet no delayed yield is observed. In these settings T varies spatially and temporally due to the substantial differences in thickness, $b=h$, and $T=Kb$. Drawdown predicted by the unconfined Theis equation is less (drawdown values are smaller) than what would occur in the field for an unconfined system experiencing significant reduction of saturated thickness. Jacob (1950) suggested that the predicted drawdowns should be corrected to represent the actual drawdown that would occur with significant dewatering. He recommended that a correction was needed if the ratio of drawdown to the initial saturated thickness was greater than 0.02. This value is more conservative than the 10 percent guidance by the UDSI (1981). Schwartz and Zhang (2003) present a method to correct the computed drawdown. The resulting corrected drawdown value will be greater than the Theis equation computed value.

$$s = b - (b^2 - 2s'b)^{0.5} \quad (66)$$

where:

- s = corrected drawdown for the unconfined aquifer (L)
- s' = drawdown computed using the standard Theis method (L)
- b = pre-pumping saturated thickness of the unconfined aquifer (L)

Example

The Theis equation is used to estimate the drawdown, 5.6 m, at an observation well located 150 m from a well pumping at $600 \text{ m}^3/\text{d}$. The pre-pumping saturated thickness was

110

30 m. Because some dewatering occurs, $5.6 \text{ m}/30 \text{ m} = 0.19$, the resulting final water table drawdown would be derived using Equation (66).

$$s = 30 \text{ m} - ((30 \text{ m})^2 - (2 (5.6 \text{ m}) (30 \text{ m}))^{0.5}) = 6.25 \text{ m}$$

10.1.1 Pumping Test Analysis

When a pumping test of this type of unconfined system is conducted, curve matching methods as described in Section 8 are applied. If dewatering is less than 10 percent during a pumping test—or, using Jacob's (1950) recommendation, is less than $s/b = 0.02$ —then standard curve matching methods using the Theis type curve can be performed using Equations (67) and (68).

$$T = \frac{Q}{4\pi s} W(u) \quad (67)$$

$$S_y = \frac{u4Tt}{r^2} \quad (68)$$

where:

- T = transmissivity (L^2T^{-1})
- Q = constant pumping rate (L^3T^{-1})
- s = drawdown (L)
- $W(u)$ = Theis well function (dimensionless)
- S_y = specific yield unconfined storage coefficient (dimensionless)
- u = integral argument (dimensionless)
- t = time (T)
- r = radial distance to pumping well (L)

However, if during a pumping test significant dewatering occurs at observation points drawdowns need to be corrected before a Theis curve matching approach is applied. Again, this is because with a reduction in saturated thickness more drawdown occurs than if the aquifer remained fully saturated during the test (constant T) because the reduced thickness reduces T . This correction was described by Jacob (1963) and in Section 7 of this book. It is shown here as Equation (69). The correction is valid for conditions where 10 to 25 percent of saturated thickness dewatered during the test (Kasenow, 2001). Once the data set is corrected it can be used to generate a drawdown time curve, after which a Theis curve matching analysis is performed.

$$s_c = s - \frac{s^2}{2b} \quad (69)$$

where:

- s_c = corrected unconfined drawdown (L)

- s = measured drawdown during the unconfined pumping tests (L)
- b = initial saturated thickness (L)

Example

An example of unconfined pumping test results that mirrors the Theis model is shown in Figure 57.

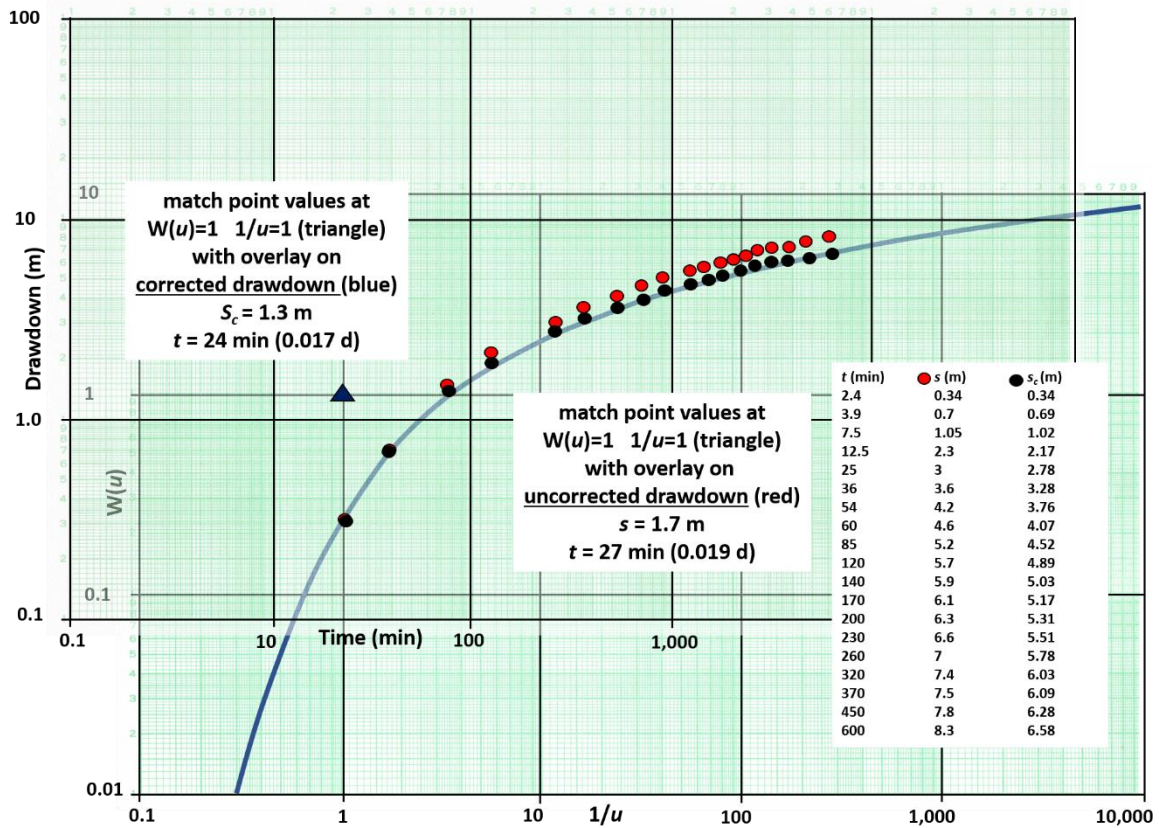


Figure 57 - Unconfined aquifer pumping test data without delayed yield for an observation well located 10 m from a well pumping at a constant rate of 3,000 m³/d. The red dots represent the observed drawdown data. The pre-pumping saturated thickness was 20 m. The black dots are the corrected data to be used in a Theis curve matching analysis. The black triangle is the match point for the corrected drawdown. The match point location for the uncorrected data is not shown and was derived from a separate curve match (not shown). A table of time-drawdown data is shown where s is the original field drawdown and s_c is the corrected data.

T and S_y are calculated for both the corrected and uncorrected curve matches, so results can be compared. The uncorrected data was matched (not shown) and a match point with values of $W(u) = 1$, $1/u = 1$ ($u=1/1=1$), $s=1.7$ m and time = 27 min (0.019 d) was obtained. Using Equations (67) and (68), T and S_y are computed.

$$T = \frac{3000 \frac{\text{m}^3}{\text{d}}}{4 (3.14) 1.7 \text{ m}} (1) = 140.5 \frac{\text{m}^2}{\text{d}}$$

$$S_y = \frac{1 (4) 140.5 \frac{\text{m}^2}{\text{d}} 0.019 \text{ d}}{(10 \text{ m})^2} = 0.11$$

Using the match point for the corrected data T and S_y are computed.

$$T = \frac{3000 \frac{\text{m}^3}{\text{d}}}{4 (3.14) 1.3 \text{ m}} (1) = 183.7 \frac{\text{m}^2}{\text{d}}$$

$$S_y = \frac{1 (4) 183.7 \frac{\text{m}^2}{\text{d}} 0.019 \text{ d}}{(10 \text{ m})^2} = 0.14$$

The use of the corrected unconfined drawdown results in the hydrogeologic properties of the unconfined aquifer being represented by higher values (not influenced by the effects of dewatering).

This section explains that the Theis solution can be used to represent conditions observed in an unconfined aquifer. When an unconfined system is pumped and little change in saturated thickness occurs, the Theis equation and curve-matching method can be directly applied. However, when the unconfined system becomes significantly dewatered during pumping T is variable, thus using predicting future drawdown conditions by the Theis method without drawdown correction will overestimate the magnitude of the forecasted drawdowns. The next section presents analytical models used to forecast drawdowns and analyze pumping data sets for unconfined systems that experience delayed yield.

10.2 Formulating Equations to Represent the Delayed Yield Response

As shown in Figure 58, when some water table aquifers are pumped, the drawdown response begins by rapidly declining then slows, and may exhibit a temporary hiatus before continuing to decline. This response is attributed to three conditions: 1) at early times instantaneous release of stored water throughout the aquifer thickness occurs as water pressure declines, so the elastic storativity of the unit controls the rate of drawdown ($S=bS_s$); 2) at intermediate times the decreased pressure throughout the aquifer causes a vertical gradient that results in water draining from pores above the water table which has an affect similar to leakage from an overlying unit and thus slows the progression of water level decline; 3) at later times drawdown in the depressurized aquifer is controlled by the release of water stored in pores at the water table so specific yield controls the rate of drawdown ($S=S_y$). The delayed yield response has been generally attributed to gravity-drained water from the capillary fringe and the vadose zone reaching the water table after drawdown has

started. The duration of the delayed yield phenomenon is thought to be controlled by vertical gradients created in the zone above the water table as the water table is lowered and the transmissivity of the aquifer (e.g., Domenico & Schwartz, 1998).

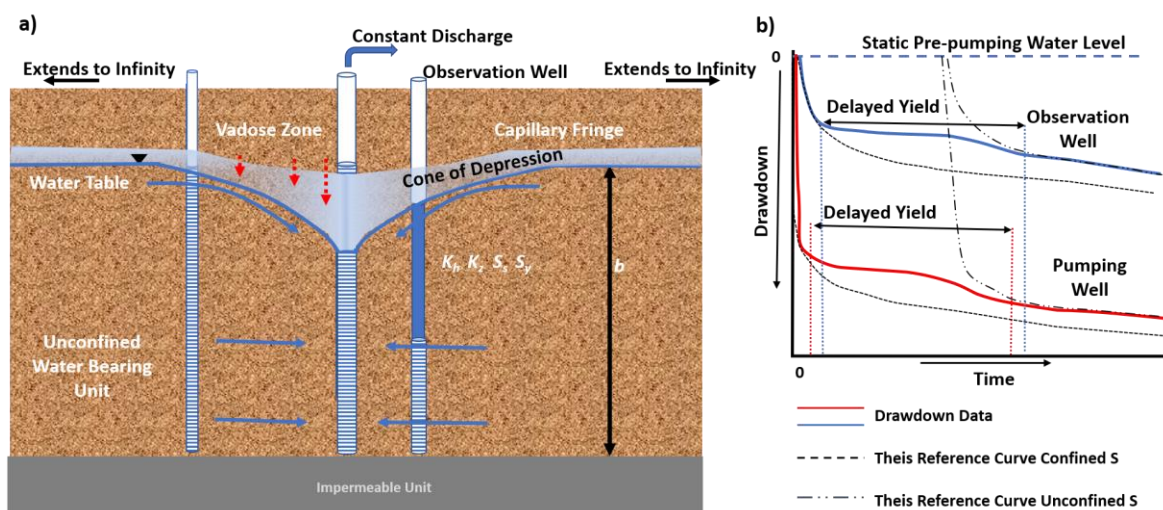


Figure 58 - Conceptual model of an unconfined aquifer with delayed yield. As the water table begins to decline, water is released from storage in the saturated portion of the aquifer ($S=S_y b$). A reduction in the rate of drawdown occurs as downward gradients near and above the water table increase and water moves downward from pores draining near the water table, within the migrating capillary fringe, and in the partially saturated pores of the vadose zone (e.g., Nwankwor et al., 1992). As time progresses, the cone of depression expands and the rate of drainage from the capillary fringe and vadose zone declines until drawdown follows that of the Theis model with storativity equal to specific yield ($S=S_y$).

- A cross-sectional representation of an infinite unconfined aquifer that is pumped at a constant rate. The blue arrows represent groundwater flow paths. b is the initial saturated thickness, while K_h and K_v are the horizontal and vertical hydraulic conductivities. In the initial stages of pumping the water table declines and a vertical gradient occurs in the zone above the water table. The capillary fringe water and associated vadose zone water (light blue and purple shaded regions above the water table) move vertically (dashed red arrows) recharging the water table. As pumping continues the rate of gravity drainage slows and drawdown becomes directly controlled by the S_y of the unconfined aquifer.
- Conceptual arithmetic plots of the observed water level response to pumping when delayed yield occurs. The drawdown increases rapidly at first, then slows as the volume of water draining from the zone above the water table temporarily increases. As the availability of drainable water in the zone above the water table decreases, the rate of drawdown increases because it is controlled solely by drainage of pores at the water table. The double arrows indicate the period of delayed yield starting when drawdown data depart from the theoretical Theis curve defined by elastic storage, S (black dashed curves) and ending when the data rejoin the Theis curve defined by drainage of pores at the water table, S_y (black dot-dashed lines).

Conceptually, as pumping begins most of the discharge is composed of stored water being released by compression of the aquifer matrix and expansion of the water, analogous to the response of a confined aquifer, $S=bS_s$ (Figure 58 and Box 2). Work by Nwankwor and others (1992) shows that the contribution of gravity drainage from the vadose zone also occurs as pumping is initiated, however the volume reaching the water table is small. As the water table declines, vertical gradients above the water table increase with time over an expanding zone around the well, inducing more vertical flow from pores in the downwardly migrating capillary fringe and in the vadose zone above the fringe. Nwankwor and others (1992) refer to water in these pores as excess storage. The period of reduced drawdown is referred to as delayed yield. It is observed at intermediate times of

the pumping test when the volume of inflow from above is sufficient to supplement the volume of water flowing from the formation to the well by temporally providing a second source of water to the aquifer. The initiation and duration of the delay are controlled by the volume and rate of drainage (excess storage) as well as the properties of the saturated portion of the aquifer (T).

Historically, some researchers attributed the mechanisms controlling delayed yield solely to processes occurring in the saturated portion of the aquifer (e.g., Neuman, 1975). Today it is known that processes in both the saturated and vadose zone are involved (Nwankwor et al., 1992; Lin et al., 2019).

The period of delayed yield can last from seconds to tens of hours (Todd & Mays, 2003). As pumping continues, the contribution of water from the zone above the water table decreases and release of water from storage is dominated by drainage of water from pores at the water table ($S=S_y$), thus heads begin to decline again after plateauing. Both the initial drawdown and the post-delayed-yield drawdown response mirror the Theis model in which pumped water is derived only from water released from aquifer storage (Figure 59).

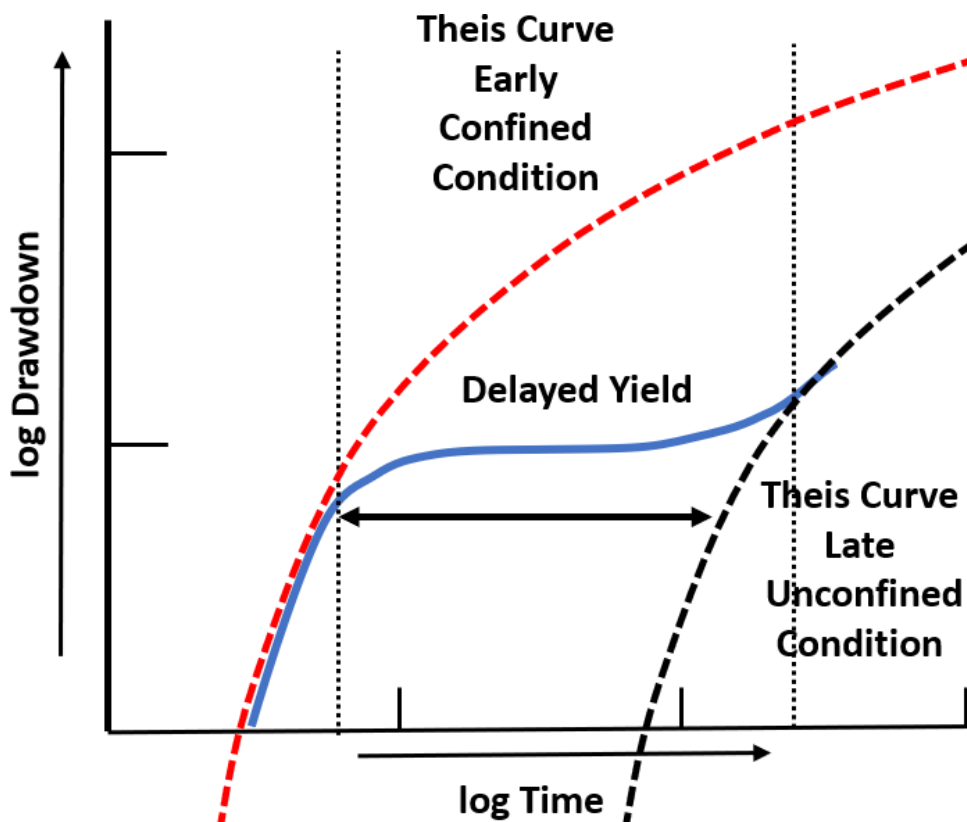


Figure 59 - Schematic of a log-log plot of the response of an observation well during pumping of an unconfined aquifer. Early time data matches a Theis curve (red dashed curve) reflecting elastic storage (S) before drainage is significant. The delayed yield portion of the curve departs from the Theis conditions during intermediate time as indicated by a double black arrow and vertical dotted black lines. As the test progresses drawdown increases and matches a late time Theis curve (black dashed curve) based on drainage of pores at the water table as controlled by specific yield (S_y).

10.3 Formulating Delayed Yield Analysis

Section 6 stated that differential equations describing the response of drawdown to pumping in unconfined settings are non-linear and cannot be solved directly because the independent variables (e.g., thickness and transmissivity) are a function of the dependent variable (i.e., head). Analytical approaches describing the response of unconfined groundwater systems have been developed assuming transient drawdown behavior can be approximated by combinations of linear differential equations. Analytical equations developed to represent the delayed yield process are mathematically complex and different representations of the delayed yield analytical solutions yield slightly different values of aquifer properties (e.g., Lin et al., 2019; Nwankwor et al., 1992).

As described in Lohman (1972), Boulton (1954a, 1954b, 1963) along with Boulton and others (1964) developed a set of analytical equations and type curves to analyze hydraulic testing data exhibiting delayed yield. These approaches were modified by Neuman (1972, 1974, 1975). He generated a linear differential equation that assumed a line sink for the pumping well and instantaneous drainage from the capillary fringe and unsaturated zone above the water table (Moench et al., 2001).

Strictly speaking, it is not correct to assume “instantaneous release of stored water from pores at the water table”. Drainage occurs from pores within the capillary fringe and unsaturated pores above the capillary fringe but this drainage is not instantaneous. As the water table declines, a vertical hydraulic gradient occurs within the zone above the water table including the capillary fringe, especially near the pumped well (Nwankor et al, 1992). Drawdown of the capillary fringe is slower than drawdown of the water table. For this reason, it is best to use drawdown data from observation wells that are several aquifer thicknesses distant from the pumped well where vertical gradients within the saturated zone are very small.

Since Neuman’s work a number of authors have attempted to incorporate the effect of the release and movement of water in the capillary fringe and unsaturated zone within the cone of depression into delayed yield analytical solutions (e.g., Moench et al, 2001; Nwankwor et al., 1992). Lin and others (2019) provide a good summary of previous efforts and a modified method to assess unconfined hydraulic tests with delayed yield. The equations they derived are solved and linked with field test data using sophisticated numerical methods. Methods developed by Tartakovsky & Neuman (2007) and Moench (1997) are available most commercial software packages (Section 13).

Neuman’s curve matching methods are presented here to be consistent with other sections of this book. Moench and others (2001) state that for the conditions they evaluated, Neuman curve matching with late time data provided reasonable estimates of T , K_h , K_z , and S_y (where K_z is the vertical hydraulic conductivity of the aquifer). However, their work and the work of others revealed that Neuman’s approach missed the effects of storage-release processes at early times. They argue that other methods to estimate storage properties

should be used when relying on early and intermediate drawdowns. Such methods account for the addition of stored water to the water table by unsaturated flow processes (Moench et al., 2001).

Recognizing these issues, this book presents the curve-matching method described by Neuman (1975) which is found in many groundwater textbooks. It provides tables of variables and plotted families of curves. Readers interested in a more detailed discussion of delayed yield representations will find it in Moench and others (2001) and Lin and others (2019). Commercial software packages typically include the Neuman method as well as other methods that can be used to analyze unconfined pumping test results. Lists of software and the methods they employ are provided in Section 13 of this book.

10.3.1 Mathematical Development of a Delayed Yield Analysis Method

The Neuman (1974, 1975) solution involves an integral with three variables, u_a , u_y , and η as shown in Equation (70). $W(u_a, u_y, \eta)$ is the Neuman well function. Schwartz and Zhang, (2003) note that evaluation of Neuman's analytical solution takes "...a large amount of time". Strengthening his original work, numerical methods have been applied to increase accuracy and efficiency of computations (Moench & Qgata, 1984; Moench 1993, 1995, 1996). The resulting general equation is described by Equations (70), (71), (72), and (73).

$$s(r, t) = \frac{Q}{4\pi T} W(u_a, u_y, \eta) \quad (70)$$

$$u_a = \frac{r^2 S}{4Tt} \quad (71)$$

$$u_y = \frac{r^2 S_y}{4Tt} \quad (72)$$

$$\eta = \frac{r^2 K_z}{b^2 K_h} \quad (73)$$

where:

- $s(r, t)$ = drawdown at a radial distance r and time t (L)
- Q = constant well discharge rate ($L^3 T^{-1}$)
- T = transmissivity ($L^2 T^{-1}$)
- S = storativity under early time confined conditions (bS_s) (dimensionless)
- b = pre-pumping saturated thickness (L)
- S_s = specific storage (L^{-1})
- S_y = storativity at late times, specific yield (dimensionless)
- t = time (T)
- r = radial distance to the observation well (L)
- $W(u_a, u_y, \eta)$ = Neuman unconfined well function (dimensionless)

- u_a = early time values of u (dimensionless)
- u_y = late time values of u (dimensionless)
- K_z = unconfined vertical hydraulic conductivity (LT⁻¹)
- K_h = unconfined horizontal hydraulic conductivity (LT⁻¹)

Computation of drawdown at an observation well located some distance r from the pumping well requires values of T , S , and S_y , the initial saturated thickness of the aquifer b , and the horizontal and vertical hydraulic conductivity values of the unconfined aquifer as indicated in Equations (70) through (73). These parameters are used to generate a value of the well function, $W(u_a, u_y, \eta)$, from compiled tables (Figure 60 and Figure 61). Computations to predict drawdown using Equation (70) can then be made for any value or r and t . Early time drawdown prediction uses u_a of Equation (71) and late time drawdown prediction uses u_y of Equation (72).

$1/u_A$	$\beta = 0.001$	$\beta = 0.004$	$\beta = 0.01$	$\beta = 0.03$	$\beta = 0.06$	$\beta = 0.1$	$\beta = 0.2$	$\beta = 0.4$	$\beta = 0.6$
4×10^{-1}	2.48×10^{-2}	2.43×10^{-2}	2.41×10^{-2}	2.35×10^{-2}	2.30×10^{-2}	2.24×10^{-2}	2.14×10^{-2}	1.99×10^{-2}	1.88×10^{-2}
8×10^{-1}	1.45×10^{-1}	1.42×10^{-1}	1.40×10^{-1}	1.36×10^{-1}	1.31×10^{-1}	1.27×10^{-1}	1.19×10^{-1}	1.08×10^{-1}	9.88×10^{-2}
1.4×10^0	3.58×10^{-1}	3.52×10^{-1}	3.45×10^{-1}	3.31×10^{-1}	3.18×10^{-1}	3.04×10^{-1}	2.79×10^{-1}	2.44×10^{-1}	2.17×10^{-1}
2.4×10^0	6.62×10^{-1}	6.48×10^{-1}	6.33×10^{-1}	6.01×10^{-1}	5.70×10^{-1}	5.40×10^{-1}	4.83×10^{-1}	4.03×10^{-1}	3.43×10^{-1}
4×10^0	1.02×10^0	9.92×10^{-1}	9.63×10^{-1}	9.05×10^{-1}	8.49×10^{-1}	7.92×10^{-1}	6.88×10^{-1}	5.42×10^{-1}	4.38×10^{-1}
8×10^0	1.57×10^0	1.52×10^0	1.46×10^0	1.35×10^0	1.23×10^0	1.12×10^0	9.18×10^{-1}	6.59×10^{-1}	4.97×10^{-1}
1.4×10^1	2.05×10^0	1.97×10^0	1.88×10^0	1.70×10^0	1.51×10^0	1.34×10^0	1.03×10^0	6.90×10^{-1}	5.07×10^{-1}
2.4×10^1	2.52×10^0	2.41×10^0	2.27×10^0	1.99×10^0	1.73×10^0	1.47×10^0	1.07×10^0	6.96×10^{-1}	
4×10^1	2.97×10^0	2.80×10^0	2.61×10^0	2.22×10^0	1.85×10^0	1.53×10^0	1.08×10^0		
8×10^1	3.56×10^0	3.30×10^0	3.00×10^0	2.41×10^0	1.92×10^0	1.55×10^0			
1.4×10^2	4.01×10^0	3.65×10^0	3.23×10^0	2.48×10^0	1.93×10^0				
2.4×10^2	4.42×10^0	3.93×10^0	3.37×10^0	2.49×10^0	1.94×10^0				
4×10^2	4.77×10^0	4.12×10^0	3.43×10^0	2.50×10^0					
8×10^2	5.16×10^0	4.26×10^0	3.45×10^0						
1.4×10^3	5.40×10^0	4.29×10^0	3.46×10^0						
2.4×10^3	5.54×10^0	4.30×10^0							
4×10^3	5.59×10^0								
8×10^3	5.62×10^0								
1.4×10^4	5.62×10^0	4.30×10^0	3.46×10^0	2.50×10^0	1.94×10^0	1.55×10^0	1.08×10^0	6.96×10^{-1}	5.07×10^{-1}

$1/u_A$	$\beta = 0.8$	$\beta = 1.0$	$\beta = 1.5$	$\beta = 2.0$	$\beta = 2.5$	$\beta = 3.0$	$\beta = 4.0$	$\beta = 5.0$	$\beta = 6.0$	$\beta = 7.0$
4×10^{-1}	1.79×10^{-2}	1.70×10^{-2}	1.53×10^{-2}	1.38×10^{-2}	1.25×10^{-2}	1.13×10^{-2}	9.33×10^{-3}	7.72×10^{-3}	6.39×10^{-3}	5.30×10^{-3}
8×10^{-1}	9.15×10^{-2}	8.49×10^{-2}	7.13×10^{-2}	6.03×10^{-2}	5.11×10^{-2}	4.35×10^{-2}	3.17×10^{-2}	2.34×10^{-2}	1.74×10^{-2}	1.31×10^{-2}
1.4×10^0	1.94×10^{-1}	1.75×10^{-1}	1.36×10^{-1}	1.07×10^{-1}	8.46×10^{-2}	6.78×10^{-2}	4.45×10^{-2}	3.02×10^{-2}	2.10×10^{-2}	1.51×10^{-2}
2.4×10^0	2.96×10^{-1}	2.56×10^{-1}	1.82×10^{-1}	1.33×10^{-1}	1.01×10^{-1}	7.67×10^{-2}	4.76×10^{-2}	3.13×10^{-2}	2.14×10^{-2}	1.52×10^{-2}
4×10^0	3.60×10^{-1}	3.00×10^{-1}	1.99×10^{-1}	1.40×10^{-1}	1.03×10^{-1}	7.79×10^{-2}	4.78×10^{-2}			
8×10^0	3.91×10^{-1}	3.17×10^{-1}	2.03×10^{-1}	1.41×10^{-1}						
1.4×10^1	3.94×10^{-1}									
2.4×10^1										
4×10^1										
8×10^1										
1.4×10^2										
2.4×10^2										
4×10^2										
8×10^2										
1.4×10^3										
2.4×10^3										
4×10^3										
8×10^3										
1.4×10^4	3.94×10^{-1}	3.17×10^{-1}	2.03×10^{-1}	1.41×10^{-1}	1.03×10^{-1}	7.79×10^{-2}	4.78×10^{-2}	3.13×10^{-2}	2.15×10^{-2}	1.52×10^{-2}

Figure 60 - Table of well function values for early times presented by Kruseman and de Ridder (2000) for the Neuman well function for unconfined aquifers with delayed yield. They used a slightly different notation than presented in this book, using u_A as equivalent to u_a and β in the place of η . That is, values of β in this table are equivalent to η in this book (after Kruseman & de Ridder, 2000).

l/u_B	$\beta = 0.001$	$\beta = 0.004$	$\beta = 0.01$	$\beta = 0.03$	$\beta = 0.06$	$\beta = 0.1$	$\beta = 0.2$	$\beta = 0.4$	$\beta = 0.6$
4×10^{-4}	5.62×10^0	4.30×10^0	3.46×10^0	2.50×10^0	1.94×10^0	1.56×10^0	1.09×10^0	6.97×10^{-1}	5.08×10^{-1}
8×10^{-4}									
1.4×10^{-3}									
2.4×10^{-3}									
4×10^{-3}								6.97×10^{-1}	5.08×10^{-1}
8×10^{-3}								6.97×10^{-1}	5.09×10^{-1}
1.4×10^{-2}								6.98×10^{-1}	5.10×10^{-1}
2.4×10^{-2}								7.00×10^{-1}	5.12×10^{-1}
4×10^{-2}								7.03×10^{-1}	5.16×10^{-1}
8×10^{-2}						1.56×10^0	1.09×10^0	7.10×10^{-1}	5.24×10^{-1}
1.4×10^{-1}						1.56×10^0	1.10×10^0	7.20×10^{-1}	5.37×10^{-1}
2.4×10^{-1}				2.50×10^0	1.95×10^0	1.57×10^0	1.11×10^0	7.37×10^{-1}	5.57×10^{-1}
4×10^{-1}				2.51×10^0	1.96×10^0	1.58×10^0	1.13×10^0	7.63×10^{-1}	5.89×10^{-1}
8×10^{-1}	5.62×10^0	4.30×10^0	3.46×10^0	2.52×10^0	1.98×10^0	1.61×10^0	1.18×10^0	8.29×10^{-1}	6.67×10^{-1}
1.4×10^0	5.63×10^0	4.31×10^0	3.47×10^0	2.54×10^0	2.01×10^0	1.66×10^0	1.24×10^0	9.22×10^{-1}	7.80×10^{-1}
2.4×10^0	5.63×10^0	4.31×10^0	3.49×10^0	2.57×10^0	2.06×10^0	1.73×10^0	1.35×10^0	1.07×10^0	9.54×10^{-1}
4×10^0	5.63×10^0	4.32×10^0	3.51×10^0	2.62×10^0	2.13×10^0	1.83×10^0	1.50×10^0	1.29×10^0	1.20×10^0
8×10^0	5.64×10^0	4.35×10^0	3.56×10^0	2.73×10^0	2.31×10^0	2.07×10^0	1.85×10^0	1.72×10^0	1.68×10^0
1.4×10^1	5.65×10^0	4.38×10^0	3.63×10^0	2.88×10^0	2.55×10^0	2.37×10^0	2.23×10^0	2.17×10^0	2.15×10^0
2.4×10^1	5.67×10^0	4.44×10^0	3.74×10^0	3.11×10^0	2.86×10^0	2.75×10^0	2.68×10^0	2.66×10^0	2.65×10^0
4×10^1	5.70×10^0	4.52×10^0	3.90×10^0	3.40×10^0	3.24×10^0	3.18×10^0	3.15×10^0	3.14×10^0	3.14×10^0
8×10^1	5.76×10^0	4.71×10^0	4.22×10^0	3.92×10^0	3.85×10^0	3.83×10^0	3.82×10^0	3.82×10^0	3.82×10^0
1.4×10^2	5.85×10^0	4.94×10^0	4.58×10^0	4.40×10^0	4.38×10^0	4.38×10^0	4.37×10^0	4.37×10^0	4.37×10^0
2.4×10^2	5.99×10^0	5.23×10^0	5.00×10^0	4.92×10^0	4.91×10^0	4.91×10^0	4.91×10^0	4.91×10^0	4.91×10^0
4×10^2	6.16×10^0	5.59×10^0	5.46×10^0	5.42×10^0	5.42×10^0	5.42×10^0	5.42×10^0	5.42×10^0	5.42×10^0

l/u_B	$\beta = 0.8$	$\beta = 1.0$	$\beta = 1.5$	$\beta = 2.0$	$\beta = 2.5$	$\beta = 3.0$	$\beta = 4.0$	$\beta = 5.0$	$\beta = 6.0$	$\beta = 7.0$
4×10^{-4}	3.95×10^{-1}	3.18×10^{-1}	2.04×10^{-1}	1.42×10^{-1}	1.03×10^{-1}	7.80×10^{-2}	4.79×10^{-2}	3.14×10^{-2}	2.15×10^{-2}	1.53×10^{-2}
8×10^{-4}						7.81×10^{-2}	4.80×10^{-2}	3.15×10^{-2}	2.16×10^{-2}	1.53×10^{-2}
1.4×10^{-3}					1.03×10^{-1}	7.83×10^{-2}	4.81×10^{-2}	3.16×10^{-2}	2.17×10^{-2}	1.54×10^{-2}
2.4×10^{-3}					1.04×10^{-1}	7.85×10^{-2}	4.84×10^{-2}	3.18×10^{-2}	2.19×10^{-2}	1.56×10^{-2}
4×10^{-3}	3.95×10^{-1}	3.18×10^{-1}	2.04×10^{-1}	1.42×10^{-1}	1.04×10^{-1}	7.89×10^{-2}	4.87×10^{-2}	3.21×10^{-2}	2.21×10^{-2}	1.58×10^{-2}
8×10^{-3}	3.96×10^{-1}	3.19×10^{-1}	2.05×10^{-1}	1.43×10^{-1}	1.05×10^{-1}	7.99×10^{-2}	4.96×10^{-2}	3.29×10^{-2}	2.28×10^{-2}	1.64×10^{-2}
1.4×10^{-2}	3.97×10^{-1}	3.21×10^{-1}	2.07×10^{-1}	1.45×10^{-1}	1.07×10^{-1}	8.14×10^{-2}	5.09×10^{-2}	3.41×10^{-2}	2.39×10^{-2}	1.73×10^{-2}
2.4×10^{-2}	3.99×10^{-1}	3.23×10^{-1}	2.09×10^{-1}	1.47×10^{-1}	1.09×10^{-1}	8.38×10^{-2}	5.32×10^{-2}	3.61×10^{-2}	2.57×10^{-2}	1.89×10^{-2}
4×10^{-2}	4.03×10^{-1}	3.27×10^{-1}	2.13×10^{-1}	1.52×10^{-1}	1.13×10^{-1}	8.79×10^{-2}	5.68×10^{-2}	3.93×10^{-2}	2.86×10^{-2}	2.15×10^{-2}
8×10^{-2}	4.12×10^{-1}	3.37×10^{-1}	2.24×10^{-1}	1.62×10^{-1}	1.24×10^{-1}	9.80×10^{-2}	6.61×10^{-2}	4.78×10^{-2}	3.62×10^{-2}	2.84×10^{-2}
1.4×10^{-1}	4.25×10^{-1}	3.50×10^{-1}	2.39×10^{-1}	1.78×10^{-1}	1.39×10^{-1}	1.13×10^{-1}	8.06×10^{-2}	6.12×10^{-2}	4.86×10^{-2}	3.98×10^{-2}
2.4×10^{-1}	4.47×10^{-1}	3.74×10^{-1}	2.65×10^{-1}	2.05×10^{-1}	1.66×10^{-1}	1.40×10^{-1}	1.06×10^{-1}	8.53×10^{-2}	7.14×10^{-2}	6.14×10^{-2}
4×10^{-1}	4.83×10^{-1}	4.12×10^{-1}	3.07×10^{-1}	2.48×10^{-1}	2.10×10^{-1}	1.84×10^{-1}	1.49×10^{-1}	1.28×10^{-1}	1.13×10^{-1}	1.02×10^{-1}
8×10^{-1}	5.71×10^{-1}	5.06×10^{-1}	4.10×10^{-1}	3.57×10^{-1}	3.23×10^{-1}	2.98×10^{-1}	2.66×10^{-1}	2.45×10^{-1}	2.31×10^{-1}	2.20×10^{-1}
1.4×10^0	6.97×10^{-1}	6.42×10^{-1}	5.62×10^{-1}	5.17×10^{-1}	4.89×10^{-1}	4.70×10^{-1}	4.45×10^{-1}	4.30×10^{-1}	4.19×10^{-1}	4.11×10^{-1}
2.4×10^0	8.89×10^{-1}	8.50×10^{-1}	7.92×10^{-1}	7.63×10^{-1}	7.45×10^{-1}	7.33×10^{-1}	7.18×10^{-1}	7.09×10^{-1}	7.03×10^{-1}	6.99×10^{-1}
4×10^0	1.16×10^0	1.13×10^0	1.10×10^0	1.08×10^0	1.07×10^0	1.07×10^0	1.06×10^0	1.06×10^0	1.05×10^0	1.05×10^0
8×10^0	1.66×10^0	1.65×10^0	1.64×10^0	1.63×10^0	1.63×10^0	1.63×10^0	1.63×10^0	1.63×10^0	1.63×10^0	1.63×10^0
1.4×10^1	2.15×10^0	2.14×10^0	2.14×10^0	2.14×10^0	2.14×10^0	2.14×10^0	2.14×10^0	2.14×10^0	2.14×10^0	2.14×10^0
2.4×10^1	2.65×10^0	2.65×10^0	2.65×10^0	2.64×10^0	2.64×10^0	2.64×10^0	2.64×10^0	2.64×10^0	2.64×10^0	2.64×10^0
4×10^1	3.14×10^0	3.14×10^0	3.14×10^0	3.14×10^0	3.14×10^0	3.14×10^0	3.14×10^0	3.14×10^0	3.14×10^0	3.14×10^0
8×10^1	3.82×10^0	3.82×10^0	3.82×10^0	3.82×10^0	3.82×10^0	3.82×10^0	3.82×10^0	3.82×10^0	3.82×10^0	3.82×10^0
1.4×10^2	4.37×10^0	4.37×10^0	4.37×10^0	4.37×10^0	4.37×10^0	4.37×10^0	4.37×10^0	4.37×10^0	4.37×10^0	4.37×10^0
2.4×10^2	4.91×10^0	4.91×10^0	4.91×10^0	4.91×10^0	4.91×10^0	4.91×10^0	4.91×10^0	4.91×10^0	4.91×10^0	4.91×10^0
4×10^2	5.42×10^0	5.42×10^0	5.42×10^0	5.42×10^0	5.42×10^0	5.42×10^0	5.42×10^0	5.42×10^0	5.42×10^0	5.42×10^0

Figure 61 - Table of well function values for late time presented by Kruseman and de Ridder (2000) for the Neuman well function for unconfined aquifers with delayed yield. They used a slightly different notation than presented in this book, using u_B as equivalent to u_y and β in the place of η . That is, values of β in this table are equivalent to η in this book (after Kruseman & de Ridder, 2000).

As stated previously, the table of values (Figure 60 and Figure 61) represent a subset of values that are generated by substituting combinations of u_a , u_y , and η into the analytical solution to produce values of $W(u_a, u_y, \eta)$. The values in the tables can be plotted to create type curves. If type curves with other values of η are required they can be generated using an available analytical solution (e.g., Neuman, 1972, 1974, 1975). Most often other values of η are interpolated from the tables shown in Figure 60 and Figure 61.

Example

In this example the drawdown at an observation well located 200 m from the pumping well in an unconfined aquifer is computed. The pre-pumping saturated thickness is 30 m, $T = 3,000 \text{ m}^2/\text{d}$, $S_y = 0.15$, $K_z = 10 \text{ m/d}$ and $K_h = 100 \text{ m/d}$. Assume the well has been

pumping at a constant rate of 2,505 m³/d for 1 day and that delayed yield is likely to have ceased. The late time u_y value is used to estimate storativity.

$$u_y = \frac{(200 \text{ m})^2 0.15}{4 \left(3000 \frac{\text{m}^2}{\text{d}} \right) (1 \text{ d})} = 0.5, \text{ then } \frac{1}{u_y} = 2 = \frac{1}{u_B} \text{ of Figure 61}$$

$$\eta = \frac{(200 \text{ m})^2 10 \frac{\text{m}}{\text{d}}}{(30 \text{ m})^2 100 \frac{\text{m}}{\text{d}}} = 4.4 = \beta \text{ of Figure 61}$$

The following values are from Figure 61.

1/u_B equivalent to 1/u_y of this book	β equivalent to η of this book	W(u_A,u_B,β) equivalent to W(u_a,u_y,η) of this book
1.4	4.0	0.455
2.4	4.0	0.718
1.4	5.0	0.430
2.4	5.0	0.709

Using the values from Figure 61 and linear interpolation, first estimate the value of the well function associated with $\beta=4$ and $1/u_B=2$, which is $W(u_A, u_B, \beta)=0.6128$. Next determine the well function value associated with $\beta=5$ and $1/u_B=2$, which is $W(u_A, u_B, \beta)=0.5974$. Finally, interpolate between those values for the well function associated with $1/u_B=2$ and $\beta=4.4$, which is $W(u_A, u_B, \beta)=0.6066$. Then, substituting these values into Equation (70), knowing that for $u_y=0.5$, $1/u_B=2$, $\eta=4.4$, and $W(u_a, u_y, \eta)=0.6066$, $s=0.04$ m as show here.

$$s = \frac{2505 \frac{\text{m}^3}{\text{d}}}{4 (3.14) 3000 \frac{\text{m}^2}{\text{d}}} (0.6066) = 0.04 \text{ m}$$

10.4 Computing T and S from Aquifer Test Data

Curve matching and numerical methods are used to match field time-drawdown data with analytical solutions that use u_a , u_y , η and $W(u_a, u_y, \eta)$. Curve matching techniques described in Section 8.3.1 are applicable here. Neuman's representation of the instantaneous release of water from storage assumptions result in poor values of S that are usually higher than the field value of the early-time confined storage, and lower than the field value for the late-time specific yield. The transmissivity values obtained using Neuman's techniques are considered representative of field properties. Nwankwor and others (1992) recommend S_y should only be computed from late time test data citing the need for at least a three-day pumping test.

Again, to build a basic understanding of the methods used to analyze field data, a description of the manual approach is presented in this section. When the values in Figure 60 and Figure 61 are plotted on log-log scales a family of curves is created. These type curves are a bit complicated, as values of $W(u_a, u_y, \eta)$ are plotted on the vertical axis, values of $1/u_a$ are plotted on the top x axis, values of $1/u_y$ are plotted on the lower x axis, and a family of curves are derived for values of η . In addition, the Theis curves for confined conditions (S) and unconfined conditions (S_y) are also plotted (Figure 62).

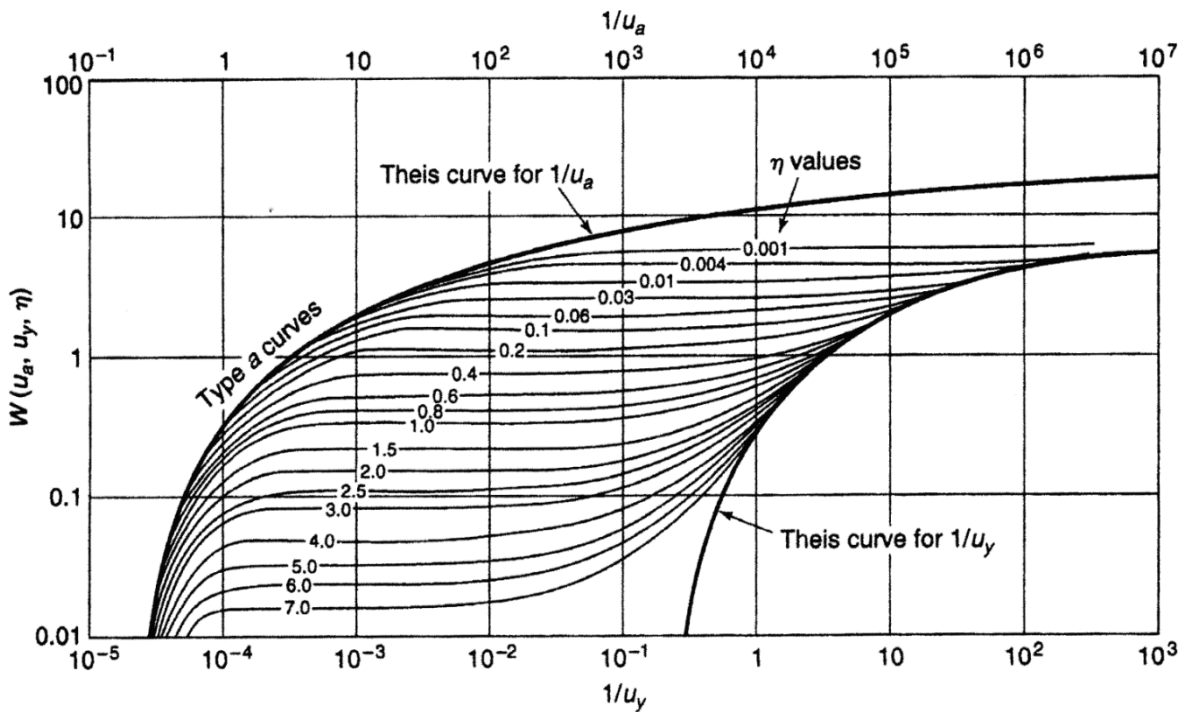


Figure 62 - Neuman type curves for unconfined systems with delayed yield (Todd and Mays, 2005).

When a delayed yield is observed in drawdown data from an unconfined pumping test (Figure 63), curve matching is a two-step process (Figure 64 and Figure 65).

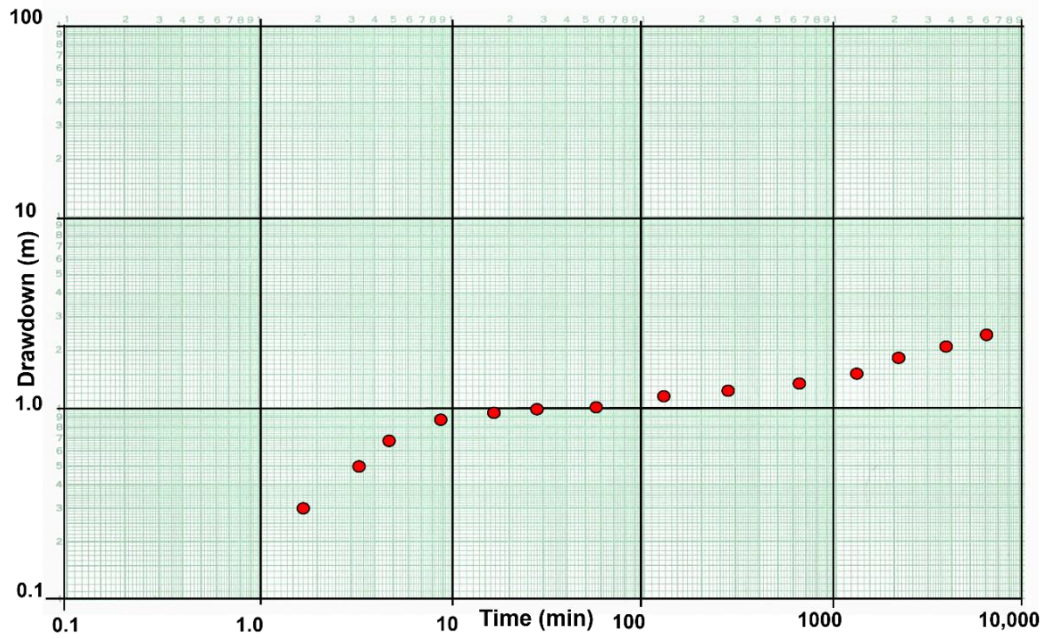


Figure 63 - An example of a log-log time-drawdown plot of field data (solid red dots) collected at an observation well in an unconfined aquifer being pumped at a constant rate.

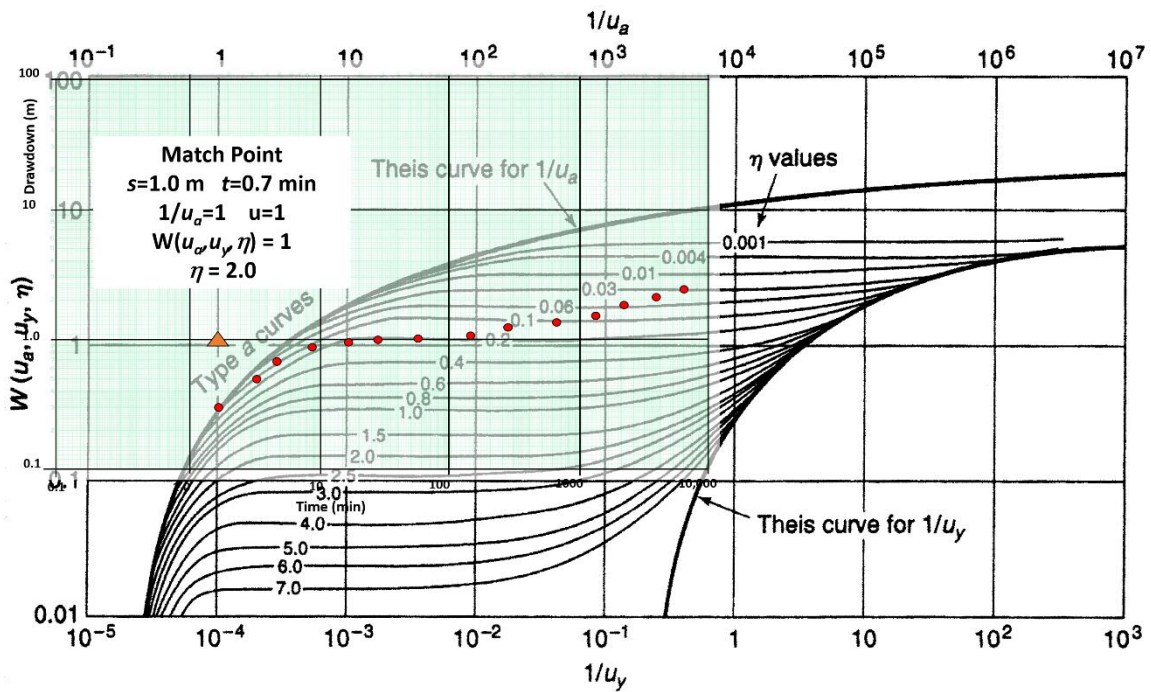


Figure 64 - Matching early time-drawdown data with Neuman's (1975) unconfined delayed yield type curves.

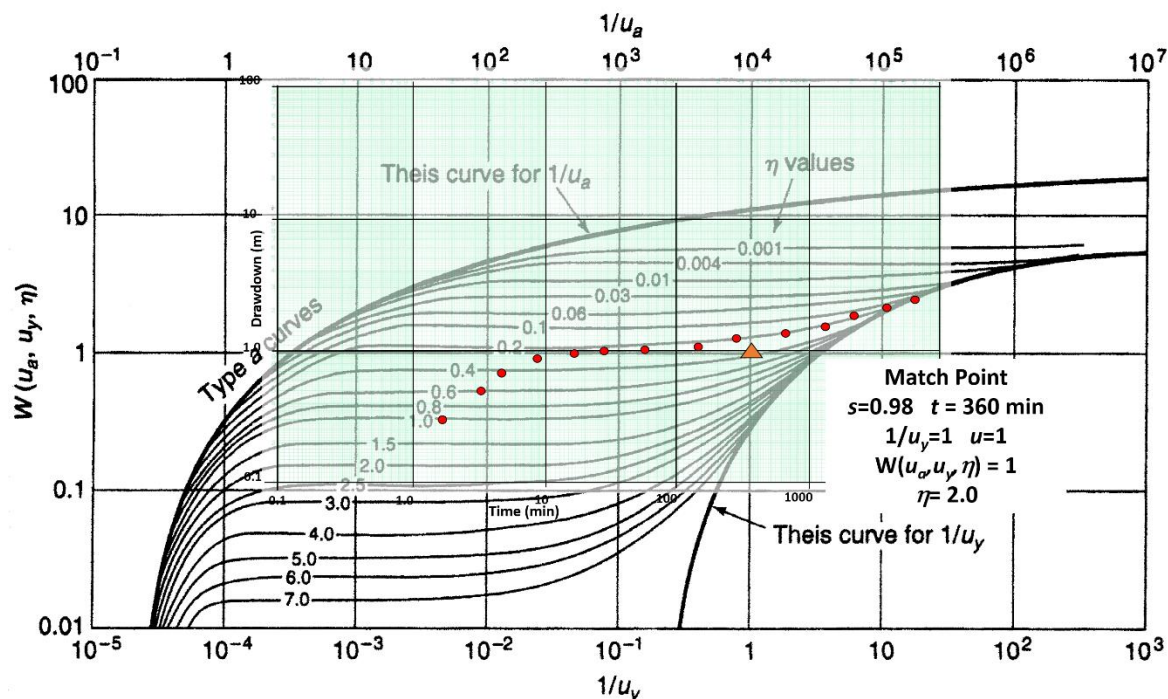


Figure 65 - Matching late time-drawdown data with Neuman's (1975) unconfined delayed yield type curves.

Standard curve matching procedures are applied. Plots are prepared using identical log-log scales and axes are kept parallel. The first step is to match the early-time data with the left-hand portion of Figure 62. A match point is selected using the top x-axis ($1/u_a$) and the left vertical scale ($W(u_a, u_y, \eta)$). Then s and t values are obtained from the drawdown plot, and the η curve value is noted (Figure 64). When delayed yield is affecting the drawdown data, the complete type curve plot (Figure 64) is not treated as continuous because the periods of delayed yield are variable and aquifer specific. The second step is to slide the data plot to the right along the η curve used to match the early data and determine the best match to the late time data (Figure 65). The data matches should be on the same η curve. The late-time data are matched, and a second match point is selected. The late-time match point includes $1/u_y$ taken from the lower x-axis, $W(u_a, u_y, \eta)$ from the vertical axis, s and t from the time-drawdown curve, and the value of the η curve.

When T is calculated for both the early- and late-time data, values are usually very similar. Values are averaged to determine a representative value. As stated earlier, S values are often poorly represented (as shown in the example below). Thus, storage values obtained by curve matching are often replaced with lab or literature-derived values are used to represent the unconfined aquifer instead of computed values (e.g., Box 2 of this book, as well as Woessner & Poeter, 2020). Analyzing time drawdown data for an extended period after the delayed-yield portion of the response dissipates is recommended to generate more representative specific yield values from late-time data.

Transmissivity is computed by rearranging Equation (70) to Equation (74). Storativity values are calculated by solving for S and S_y in Equations (71) and (72). The

horizontal hydraulic conductivity can be estimated as T/b and the vertical hydraulic conductivity can be obtained by rearranging Equation (73) to Equation (78).

$$T = \frac{Q}{4\pi S} W(u_a, u_y, \eta) \quad (74)$$

$$\frac{u_a 4Tt}{r^2} = S \quad (75)$$

$$\frac{u_y 4Tt}{r^2} = S_y \quad (76)$$

$$\frac{T}{b} = K \quad (77)$$

$$\frac{\eta b^2 K_h}{r^2} = K_z \quad (78)$$

where:

- $s(r,t)$ = drawdown at a radial distance r and time t (L)
- Q = constant well discharge rate (L^3T^{-1})
- T = transmissivity (L^2T^{-1})
- S = storativity under early time confined conditions (dimensionless)
- S_y = storativity at late times, specific yield (dimensionless)
- t = time (T)
- r = radial distance to the observation well (L)
- u_a = early time values of u (dimensionless)
- u_y = late time values of u (dimensionless)
- $W(u_a, u_y, \eta)$ = unconfined well function (dimensionless)
- K_z = unconfined vertical hydraulic conductivity (LT^{-1})
- K_h = unconfined horizontal hydraulic conductivity (LT^{-1})
- b = pre-pumping saturated thickness (L)
- η = variable defined by Equation (73) (dimensionless)

Example

T , S , and S_y can be estimated using the match points (Figure 64 and Figure 65) if it is assumed that the data represented in Figure 63 were collected at an observation well located 120 m from the pumping well during a 4-day hydraulic test with a well pumping at 4,000 m³/d. The aquifer has a pre-pumping saturated thickness of 28 m and is sand and gravel. Match point data in Figure 64 are used to compute the transmissivity from early-time data using Equation (74) and storativity using Equation (75).

$$T = \frac{4000 \frac{m^3}{d}}{4 (3.14) 1 m} (1) = 318 \frac{m^2}{d}$$

$$S = \frac{(1) 4 \left(318 \frac{\text{m}^2}{\text{d}} \right) 0.0005 \text{ d}}{(120 \text{ m})^2} = 0.000044 \text{ or } 4.4 \times 10^{-5}$$

Using the late time match point of Figure 65 and Equations (74) and (76), transmissivity and specific yield are calculated.

$$T = \frac{4000 \frac{\text{m}^3}{\text{d}}}{4 (3.14) 0.98 \text{ m}} (1) = 325 \frac{\text{m}^2}{\text{d}}$$

$$S_y = \frac{(1) 4 \left(325 \frac{\text{m}^2}{\text{d}} \right) 0.25 \text{ d}}{(120 \text{ m})^2} = 0.02$$

Averaging the T values yields a value of $322 \text{ m}^2/\text{d}$. In this example the confined storage coefficient seems reasonable, but the specific yield is quite small and most likely not representative of field conditions. This suggests that analytical formulations may not fully capture the release of water as the aquifer dewateres.

The horizontal hydraulic conductivity is computed using Equation (77)

$$\frac{322 \frac{\text{m}^2}{\text{d}}}{28 \text{ m}} = 11.5 \frac{\text{m}}{\text{d}}$$

Next using Equation (78) and match point value of $\eta = 2.0$, vertical hydraulic conductivity is calculated.

$$K_z = \frac{(1) 2.0 (28 \text{ m})^2 11.5 \frac{\text{m}}{\text{d}}}{(120 \text{ m})^2} = 1.3 \frac{\text{m}}{\text{d}}$$

Analytical approaches to describing the response of wells when pumping an unconfined system were outlined in this section. Numerical methods can also be used to approximate the response of unconfined aquifers to pumping. However, representation of delayed yield processes requires additional model complexity (e.g., Anderson et al., 2015; Diersch, 2014).

Section 11 presents methods to assess how boundaries, well interference, and anisotropy affect efforts to forecast drawdowns and estimate hydrogeologic properties.

11 Effects of Well Interference, Boundaries, and Aquifer Anisotropy on Drawdown

Estimates of T , S , and other aquifer parameters can be used to predict the spatial distribution of combined drawdown when multiple wells are pumping. The presence of recharge and impermeable boundaries also influences time-drawdown responses when a cone of depression reaches the boundary. When aquifer conditions are not isotropic and homogeneous cones of depression are distorted. The effect of each of these conditions on drawdown during pumping tests is examined in this section.

11.1 Well Interference

Well interference occurs when the cone of depression of two or more pumping wells overlap (Figure 66). As a well is pumped its cone of depression expands over time. If a second well in the same aquifer is also pumping its cone of depression also expands. In the regions of the aquifer where the cones of depression overlap, the drawdown in the zone of overlap is the composite drawdown from both pumping wells. Drawdown at a location affected by multiple pumping wells is additive in linear systems (e.g., fully confined aquifers with laminar flow). Additive means that the solutions can be calculated separately and superposed (i.e., added together). Where the linearity is not applicable (e.g., unconfined aquifers with more than about 10 percent drawdown, dewatering of confined aquifers, turbulent flow in open fractures) then superposition may not be valid and should be used with caution. The more nonlinear the conditions the greater the error in the superposed solution.

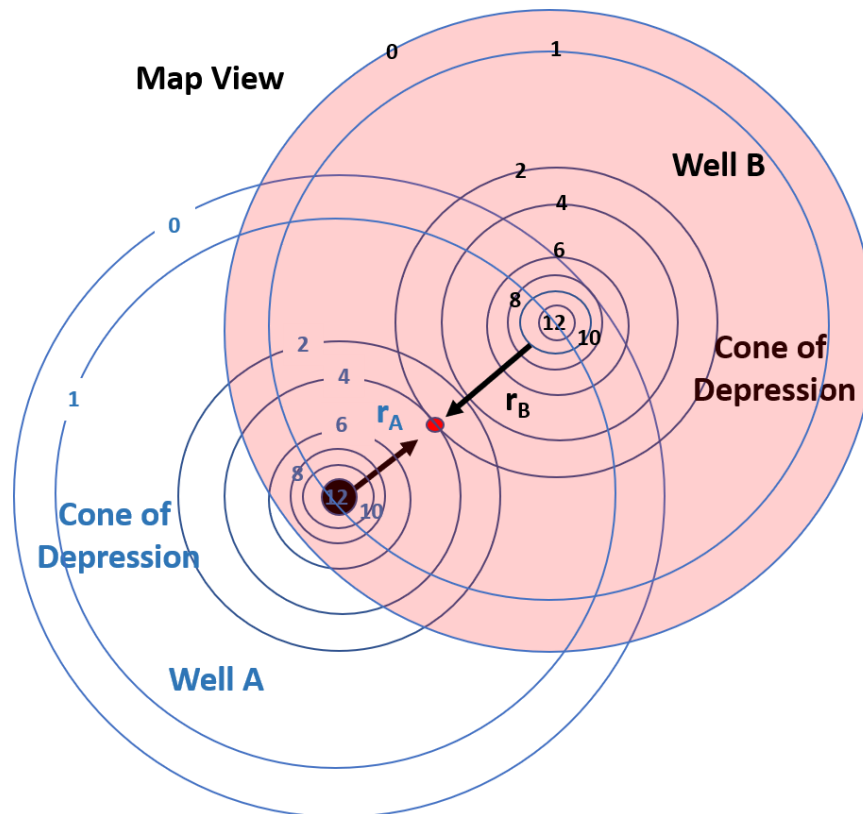


Figure 66 - Illustration of well interference created by pumping two wells at the same rate for an equal length of time. The wells penetrate a totally confined aquifer that is isotropic and homogeneous. Both wells A and B are constructed similarly, and their pumping rate and schedule is the same in this example. The pumping wells could each operate at any rate for any length of time and the approach to generating a composite cone of depression is the same. The red dot represents the location of an observation well that is not pumping. The schematic shows drawdown for each well as contours in units of length. r_A and r_B are the radial distances to the unpumped observation well from wells A and B.

The term well interference is used when a pumping well is influenced by drawdown from one or more nearby pumping wells. At the observation well location (red dot, Figure 66) the overlapping cones of depression show that at this time the observation well is experiencing a drawdown of 4 units from pumping of Well A and 2 units from pumping of Well B. The total drawdown at the observation well under the confined conditions is 6 units. The pumping of both wells also affects the drawdown in the pumping wells. Both pumping wells create a drawdown of 12 units at the pumping well location and experience an additional drawdown of 1 unit from the other pumping well for a total of 13 units of drawdown in both pumping wells. A sketch of the composite cone of depression is shown in Figure 67.

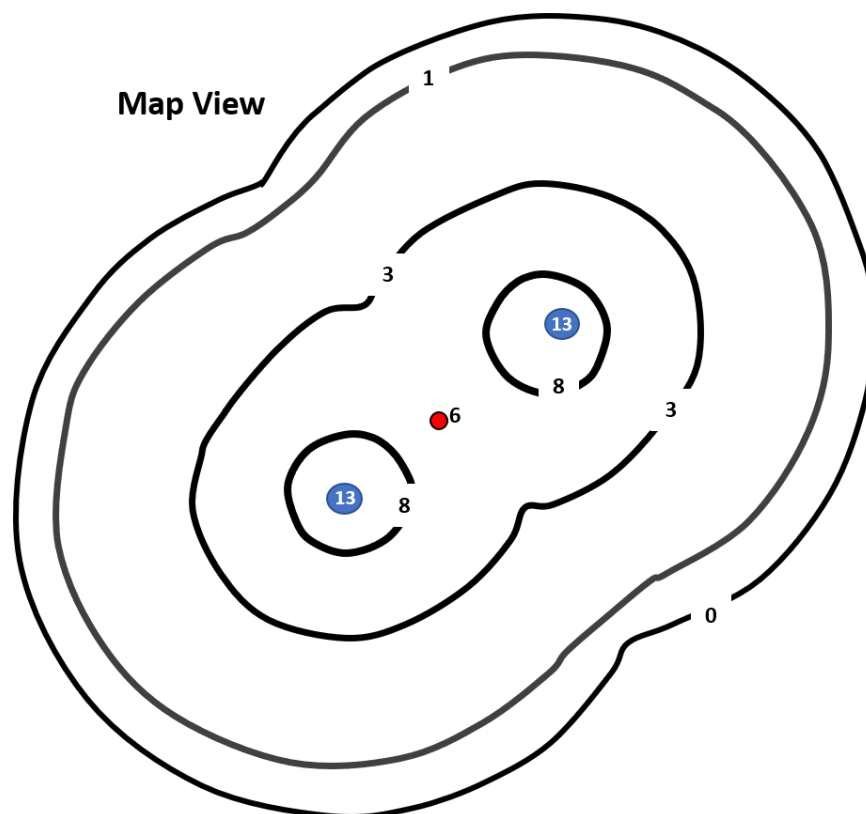


Figure 67 - Sketch of the composite cone of depression created from conditions illustrated in Figure 66. This diagram was created by assigning combined drawdowns to locations where the drawdown contours overlapped and then hand contouring the resulting drawdown values. The blue dots are the pumping wells where the composite drawdown is 13 units of length. The red dot represents an observation well drawdown of 6 units of length. The black lines represent contours of drawdown in units of length.

Figure 67 shows the resulting cone of depression due to well interference in map view. Well interference can also be viewed in cross section (Figure 68). The same approach can be used to determine the interference effect of multiple wells pumping at different rates and for different lengths of time on any pumping or observation well located in the zone of interference. Combining the drawdowns by adding the effects at a location is referred to as superposing the cones of depression and the method is referred to as superposition. In well fields where multiple wells are pumping on different schedules and at different rates the resulting potentiometric surface reflects well interference (composite water levels) as shown in Figure 69.

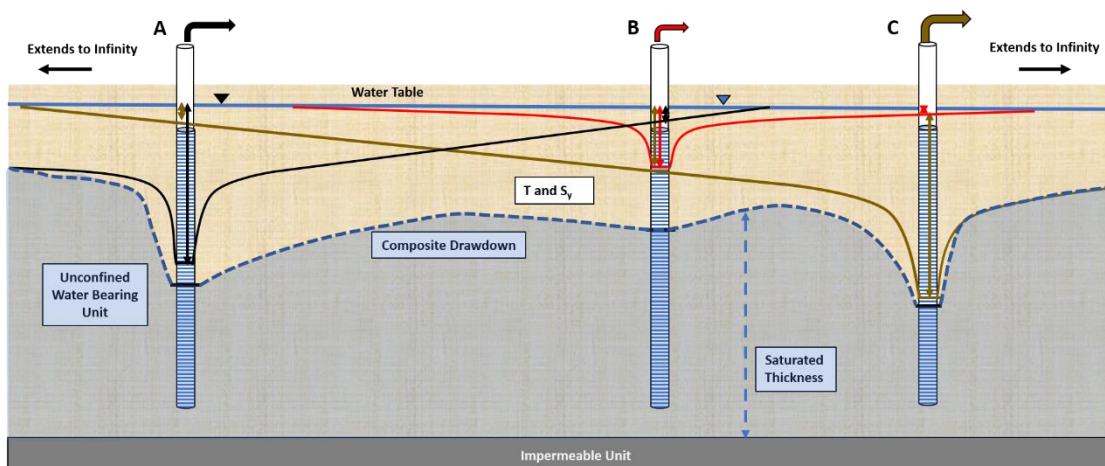


Figure 68 - Schematic cross section showing well interference and the resulting drawdown profile for an isotropic and homogeneous unconfined aquifer effected by pumping of three wells. The drawdown at each well is shown by arrows keyed to the color of the well discharge (Well A black, Well B red, Well C brown). When the well drawdown profiles are superimposed, the drawdowns are added, and the composite drawdown profile is obtained (dashed blue line). Determining well interference in an unconfined aquifer is more difficult than in a confined aquifer because transmissivity decreases as drawdown increases increasing the drawdown relative to that in an aquifer of constant saturated thickness.

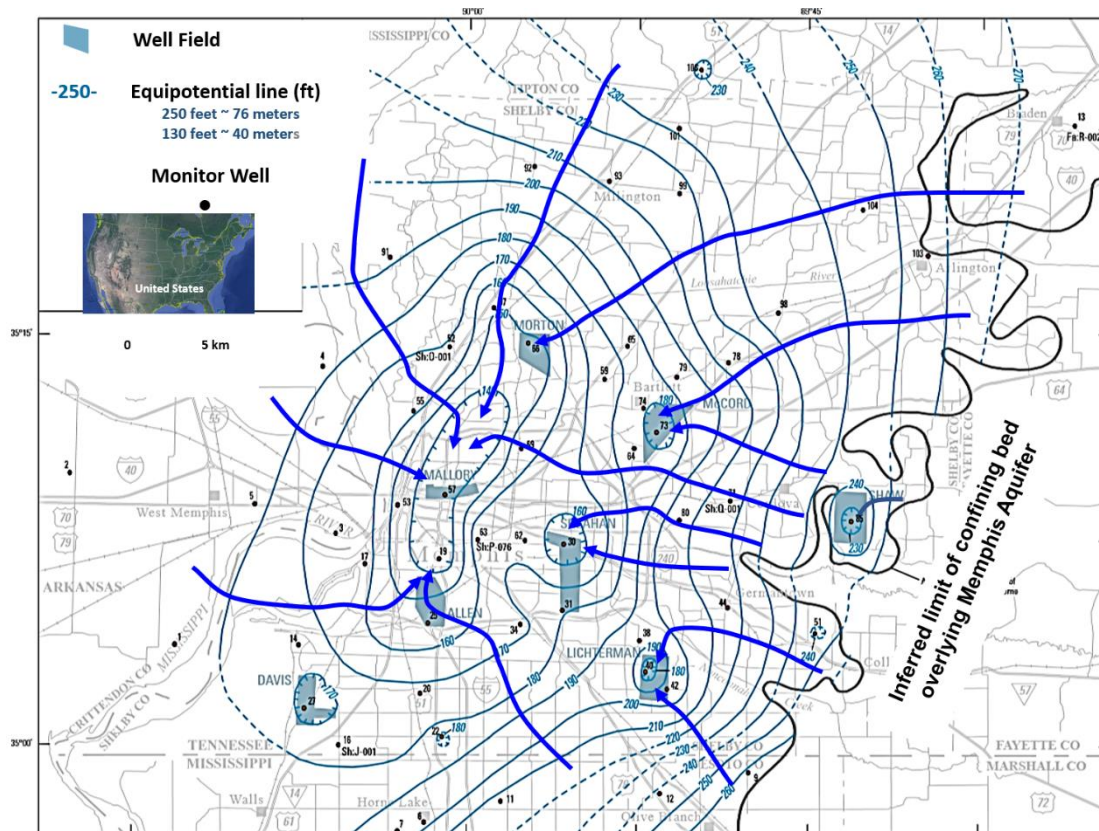


Figure 69 - Potentiometric surface based on September to November 2010 water level data for the confined Memphis Sand Aquifer located beneath Memphis, Tennessee, USA. Equipotential lines are solid green and dashed where inferred. All units are in feet. Hatched contours indicate depressed areas of the potentiometric surface associated with pumping centers (well fields) that have operated for an extended period of time. The curved black solid line in the eastern portion of the area represents the location of the transition from unconfined conditions in the east to confined conditions in the west. Flow lines are blue arrows. Pumping has captured groundwater flowing throughout the area as flow lines converge at well field locations where multiple wells are pumping. Initial groundwater flow was from southeast to the west, now production wells have altered the flow paths with groundwater principally moving to the pumping centers (lowest potentiometric contours) (modified from Kingsbury, 2018; Woessner & Poeter, 2020).

This superposition methodology is straightforward and can be used to remove unwanted interference that occurs during a hydraulic test (a single well pumping at a constant rate) affected by unplanned starts and shutdowns of other nearby pumping wells. This is shown in Figure 70 where startup and shut down of two adjacent pumping wells effect drawdown at a pumping test observation well. Such effects need to be removed before analyzing the data to estimate values of T and S .

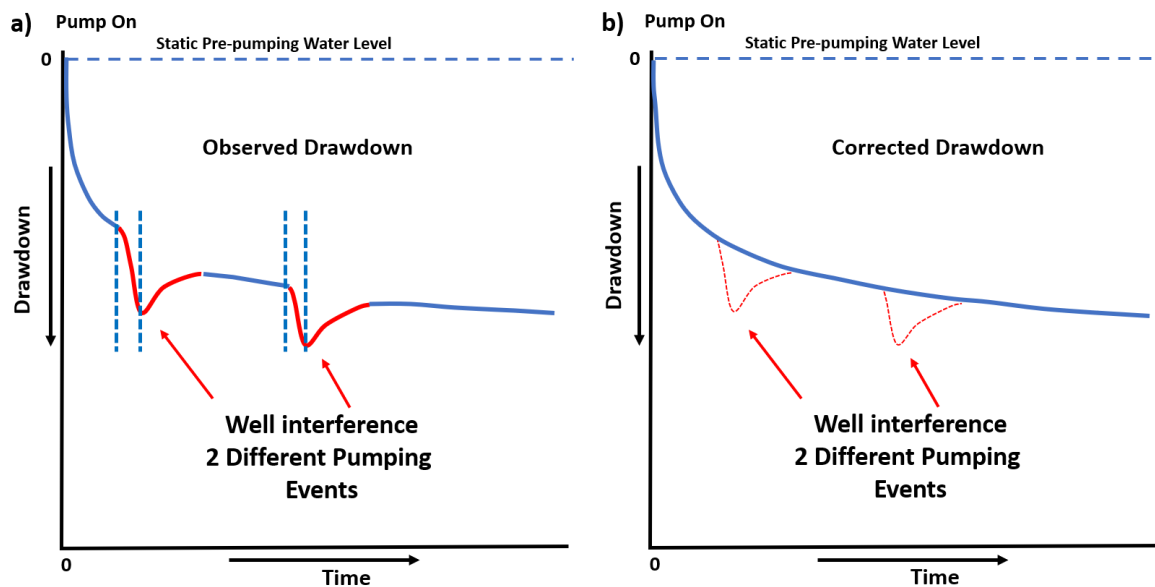


Figure 70 - Arithmetic plots of observed drawdown in a pumping test observation well. a) Drawdown where nearby wells start up and shut down (vertical dashed blue lines) during the test. The red portions of the drawdown curve represent the composite drawdown at the observation well and interference from the adjacent pumping wells. b) Pumping drawdown data are corrected for the well interference by removing the additional drawdown from the adjacent pumping wells and reproducing the drawdown trend (solid blue line).

In some settings, the startup and shut down of additional pumping wells may not affect pumping or observation well drawdown because they are located too far from the test well or pumping rates and durations are too small to cause identifiable interference. When estimates of the tested formation T and S are known, the degree of interference from other pumping wells can be computed from standard well hydraulic equations before initiation of a pumping test (e.g., Theis equation; Hantush-Jacob equation, etc.).

11.2 Using Superposition to Represent Simple Boundary Conditions

One of the basic assumptions used to develop analytical solutions to predict drawdown in wells penetrating unconfined, confined, leaky confined, and unconfined units, and associated confining beds is that the set of geologic units being represented are infinite in lateral extent and no boundaries are present in the portion of the aquifer being stressed. In an extensive groundwater system, where boundaries are located tens of kilometers from the test site and the cone of depression of the hydraulic test may only extend a few kilometers, the assumption of an infinite water-bearing unit is reasonable (Figure 71, Well A).

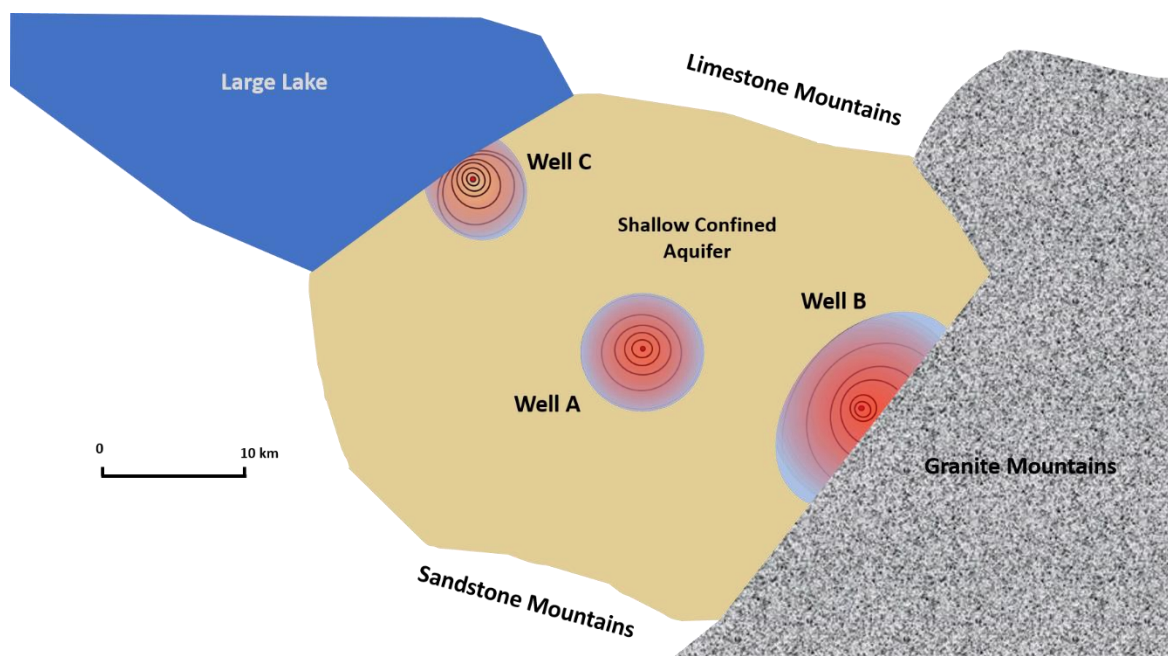


Figure 71 - Schematic map view of a shallow isotropic and homogeneous confined aquifer (tan) that is bordered by impermeable granite bed rock, a well-connected large lake, and mountain ranges that allow some flow into the aquifer. Cones of depression are plotted for three wells that are pumping at similar rates. Red represents more drawdown and blue less drawdown. Black lines represent drawdown contours that have larger magnitude near the center of the cone of depression. At Well A, the cone of depression is symmetrical, as pumping has not encountered boundaries that limit the expansion of the cone. At this site, for analytical purposes, the aquifer can be assumed to represent a system that is infinite in extent. At Well B, the cone of depression encountered the impermeable bedrock and began to expand along the boundary and deepen. The equipotential lines indicate flow is parallel to the boundary converging toward the position of the well where flow lines turn to flow to the well. Well C, is near a large lake that is in communication with the aquifer. The lake provides water to the pumping well through lateral aquifer recharge so drawdown slows and eventually the cone no longer grows when inflow from the lake equals the pumping rate. The equipotential lines indicate flow across the boundary.

Hydraulic testing can identify boundary conditions that alter drawdown at observation wells or production wells. When boundaries are encountered the trend in drawdown will change as pumping continues. The rate of drawdown will decrease if a recharge boundary (Figure 71, Well C) is encountered, and the rate of drawdown will increase if an impermeable boundary (Figure 71, Well B) is contacted. The effect of boundaries on drawdown trends for pumping or observation wells in an aquifer behaving as a Theis system (i.e., totally confined) are shown in Figure 72. Figure 73 illustrates the effect of boundaries on the shape of Cooper-Jacob semi-log time-drawdown plots.

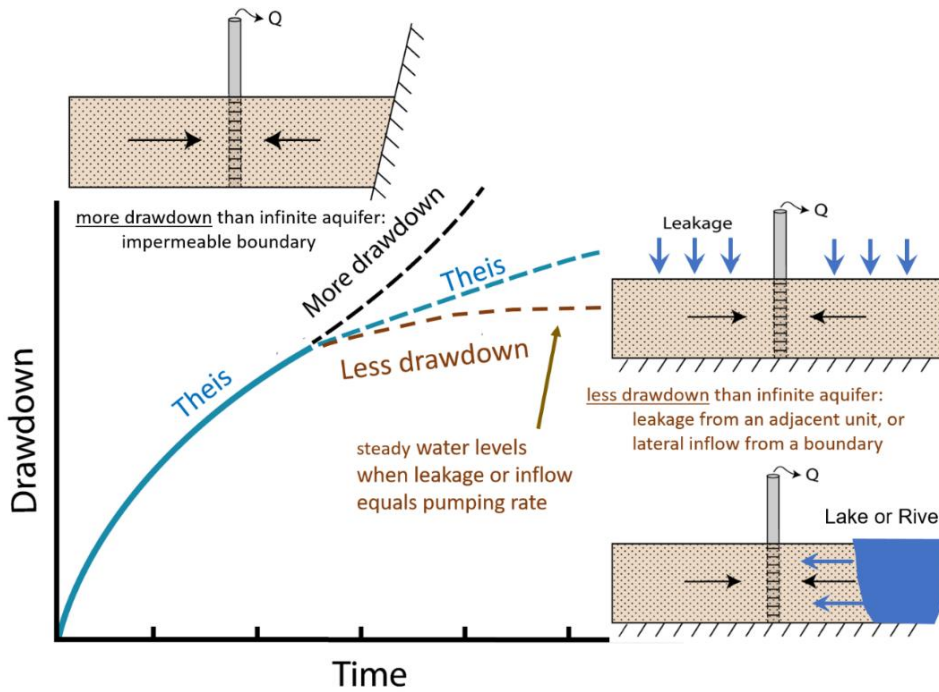


Figure 72 - A log-log plot of drawdown versus time for a pumping well penetrating a confined aquifer. The blue line represents the drawdown expected if the aquifer behaves as a Theis system and is unbounded. The time-drawdown curve also shows the response of the theoretical Theis conditions if the cone of depression encounters a no-flow boundary (upper black dashed line). The lower dashed curve indicates that the drawdown would be less if recharge or leakage from a boundary is encountered (Cherry, 2022).

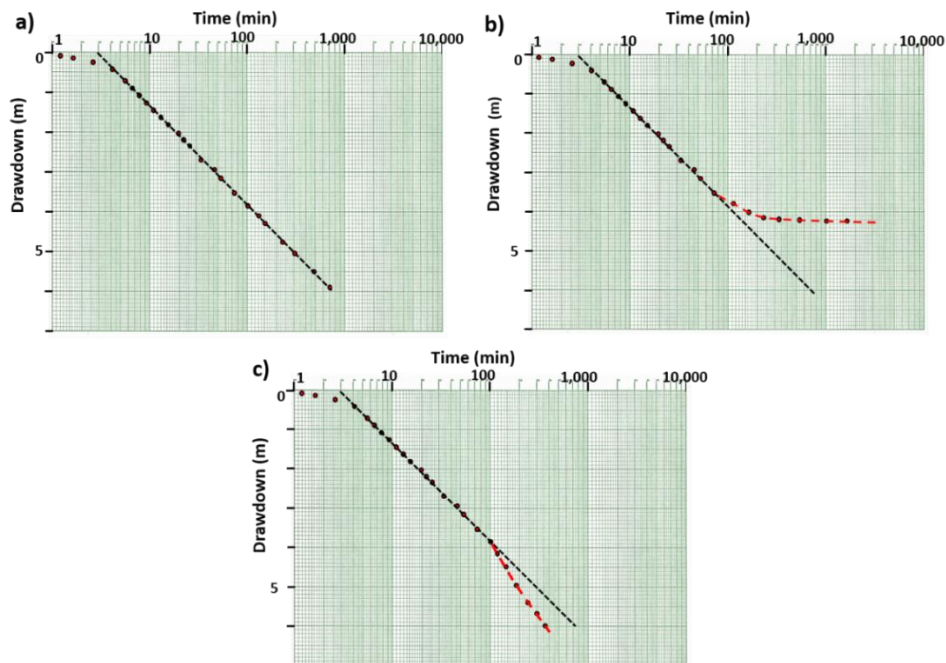


Figure 73 - Examples of boundary condition influences on time-drawdown data collected during a constant-discharge pumping test of a confined unit. Plots are semi-log graphs. Drawdown changes occur in both pumping and observation wells. a) The theoretical response of a totally confined aquifer that is not affected by boundary conditions, the aquifer is infinite in extent. b) The deviation in the time-drawdown data (red dashed line) that shows the slope of the drawdown trend is decreasing and reaching equilibrium as a recharge boundary is encountered. c) The deviation in the time-drawdown data when an impermeable boundary is encountered as shown by the red dashed line. Drawdown increases with time.

Care must be taken to determine the likely source of the observed drawdown response when assessing the presence or absence of aquifer boundaries. In this section, we discuss lateral recharge boundaries in contrast to recharge from local confining beds and overlying aquifers as discussed in Section 9 (i.e., Hantush-Jacob and Hantush Equations). Leaky aquifer settings will cause drawdown curve slopes to decrease without the cone of depression encountering an adjacent physical boundary. Unconfined aquifers with delayed yield also exhibit a period of decreased slope and a period of increasing drawdown that are not related to a lateral recharge boundary.

As stated, at some test sites physical boundaries adjacent to the groundwater system may be close enough to affect hydraulic testing and/or planned production rates. When the configurations of boundaries are relatively simple, e.g., a linear boundary, the effect of the boundary on the predicted drawdown can be addressed using image well theory based on superposition of analytical solutions. As boundary conditions become less geometrically linear and more complex, other techniques such as numerical modeling are more appropriate because analytical models cannot easily address complex boundaries (e.g., Anderson et al., 2015).

11.2.1 Image Well Methodology

Image well methodology generates the drawdown distribution that would result when pumping near a boundary. It applies standard analytical models developed in previous sections. The method involves first replacing the bounded confined or unconfined system with an infinite aquifer, then placing one or more image wells on the other side of the boundary at the same distance the pumping well is located from the identified boundary. Depending on the boundary being simulated, image wells are either pumped or water is injected at the same rate as the actual pumping well. The resulting image-well and operating-well drawdown cones are superimposed to generate a distribution of drawdown in the portion of the aquifer in which the pumping well is located.

The image well methodology is described by Ferris and others (1962). Their work is featured in numerous textbooks (e.g., Freeze & Cherry, 1979; Fetter, 2001; Schwartz & Zhang, 2003), state and federal agency documents (e.g., Lohman, 1972), and professional handbooks (e.g., Sterrett, 2007). Basically, image well methodology uses superposition to represent a boundary by either creating a condition where head does not change along the boundary by using an image well with Q of opposite sign as the pumping well, or a condition where the gradient across the boundary is zero using an image well with a Q having the same sign as the pumping well.

11.2.2 Linear Impermeable and Recharge Boundaries

Ferris and others (1962) present the image well method to determine the water table map and profile for a pumping well in an unconfined groundwater system near an impermeable linear boundary that is infinite in extent (Figure 74). The methodology can also be used to represent confined and leaky confined systems.

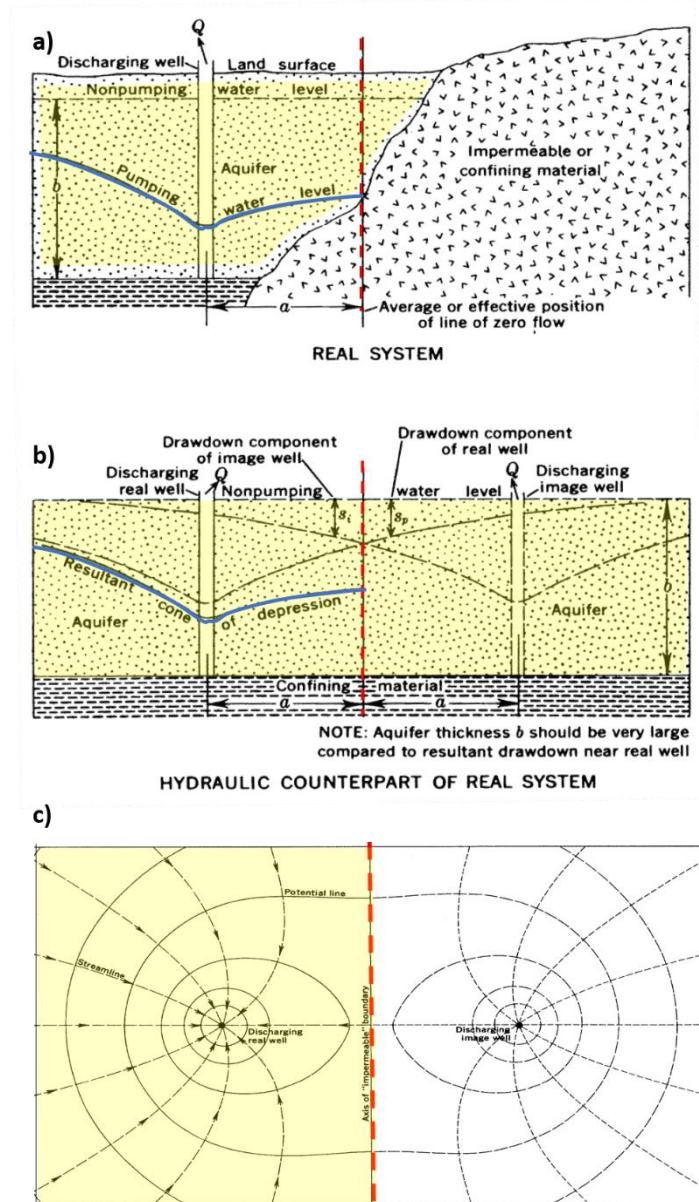


Figure 74 - Illustration of the application of image well methodology to generate the cone of depression for a well in an unconfined system that is pumping next to an impermeable boundary (from Ferris, et al., 1962.

- a) Cross section of the unconfined unit and impermeable boundary material. The dashed red line represents the boundary which approximates the position of the field feature that is of irregular shape. The final resultant drawdown profile is plotted in blue.
- b) The application of image well methodology (hydraulic counterpart of the real system). The boundary is created mathematically by placing a continuous infinite aquifer with properties equal to the field aquifer (yellow) in the white area with a pumping well (image well) positioned an equal distance from the boundary as the original well. To generate the drawdown profile and cone of depression resulting from the presence of the impermeable boundary, both wells are started at the same time at the original pumping well rate. This results in the mathematical water level being the same at the boundary and decreasing away from the boundary on both sides such that the gradient is zero, thus there is no flow and an impermeable boundary is created. The composite drawdown profile and cone of depression are derived for a specified time by superposing the original pumping well drawdown, s_p , and the image well drawdown, s_i , as shown by the blue drawdown profile.
- c) A map view of the composite cone of depression. Only the yellow shaded portion of the diagram is used to represent conditions at the site because the image well is not physically present at the site. The area shaded in yellow shows dashed black streamlines (groundwater flow directions) and solid black composite contour lines of hydraulic head that mirror drawdown. Water levels decline and drawdown increases toward the well.

Figure 74 explains the application of image well theory to represent a linear impermeable boundary. The cone of depression in the aquifer is not symmetrical because no water is available to flow from the impermeable bedrock on the right into the aquifer. As a result, the cone of depression needs to expand to the top and bottom and left side of the map view to capture water from storage in order to supply the volume of water pumped from the well. As the water level contours are at right angles to the boundary, groundwater flow is parallel to the impermeable boundary (e.g., Woessner & Poeter, 2020).

A constant flux or recharge boundary is simulated by using the same process with the opposite sign on Q to simulate a linear boundary that is infinite in extent as shown in Figure 75 (Ferris et al., 1962).

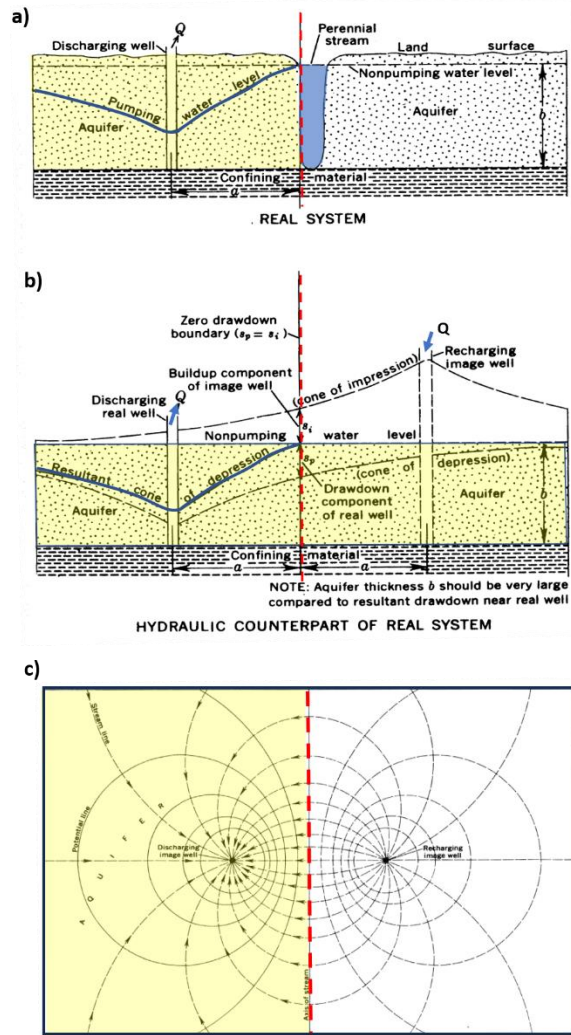


Figure 75 - Illustration of the application of image well methodology to generate the cone of depression of a well in an unconfined system with a well pumping next to a connected recharge boundary (Ferris, et al., 1962). The recharge boundary is represented by a fully penetrating stream. This condition could also be thought of as a boundary where any amount of pumping near the boundary would not alter the head at the boundary (constant head boundary).

- a) Cross section of the unconfined aquifer and recharge boundary. The dashed red line represents the boundary which approximates the position of the field feature that is of irregular shape. The final resultant drawdown profile is plotted in blue.
- b) The application of image well methodology (hydraulic counterpart of the real system). The boundary is created mathematically by placing a continuous infinite system with properties equal to the field setting (yellow area) in the white area with an injection well (image well) positioned an equal distance from the boundary as the original well. The image well injects water at the same rate that water is pumped from the original well. The injection well creates a cone of impression (water levels rise above the background water level, negative drawdown). This results in the mathematical water level being the same at the boundary and decreasing away from the boundary on the field side of the boundary and increasing on the image side creating a flow across the boundary. To generate the drawdown profile both wells are started at the same time with equal pumping and injection rates. The composite drawdown profile and cone of depression at a specified time are derived by superposing the pumping well drawdown, s_p , and the image well water level rise (negative drawdown), s_i , as shown by the blue drawdown profile. It represents the pumping of the original well with a recharge boundary present.
- c) A map view of the composite cone of depression. Only the yellow shaded portion of the diagram is used to represent conditions at the site because the image well is not physically present. The area shaded in yellow shows dashed black streamlines (groundwater flow directions) and solid black composite contour lines of hydraulic head that mirrors drawdown. Water levels do not change at the boundary and drawdown increases toward the pumping well.

Figure 75 explains how to apply image well theory in the presence of a linear recharge boundary. The cone of depression in the aquifer is not symmetrical because water is contributed by flow from the recharge boundary. Drawdown is less to the right of the pumping well and greater to the left of the well. The groundwater elevation contours are parallel to the recharge boundary and decrease towards the well. Water is flowing at right angles from the boundary to the well (e.g., Woessner & Poeter, 2022).

If the drawdown at an observation well located near an impermeable linear boundary needs to be predicted, the composite drawdown from both the pumping well and image well are computed at the observation well location (Figure 76). When a recharge boundary is present, the drawdown at an observation well is derived by combining the effect of the pumping well and the drawup (negative drawdown) from the image well. Again, both pumping and image well values are added to generate the total drawdown at the observation well.

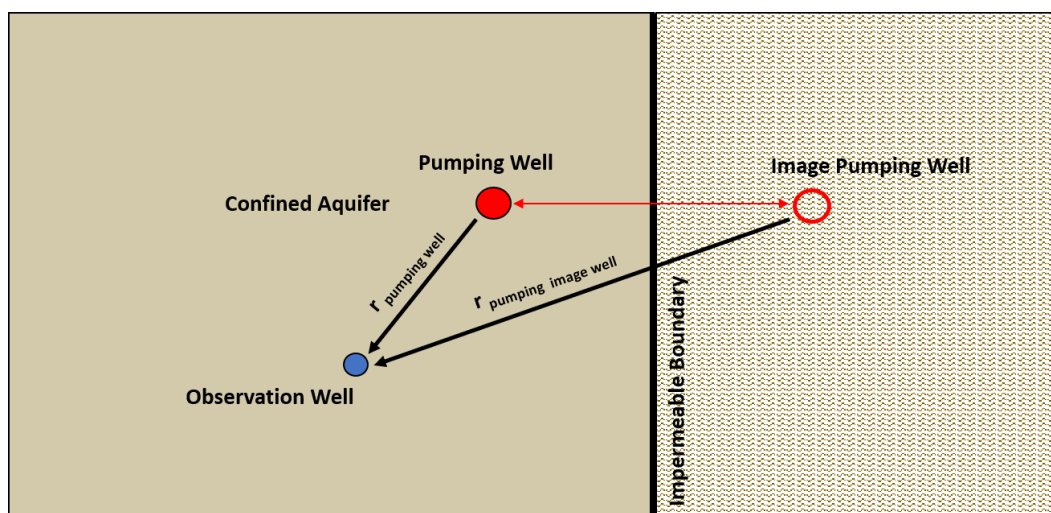


Figure 76 - Map view of a pumping well (red dot) and corresponding image well (open red dot) in a setting with a single linear impermeable boundary. To compute the drawdown in an observation well the radial distances are determined from both the pumping well and image well, then the resulting drawdowns at that location are calculated and added together.

Ferris and others (1962) also presented how image well methods could be used to simulate systems with dual linear boundaries of infinite extent and more complex boundary configurations using image well theory. An example of using image well theory to represent the presence of both a linear impermeable boundary and recharge boundary near a pumping well is presented in [Box 3](#).

Image well methods are easily applied to simple single linear boundaries. Image well theory uses superposition and is based on computing drawdown and drawup by solving analytical equations (e.g., Theis, Jacob, Hantush). As boundaries become more complex, image well methods are not adequate to represent conditions. Typically, numerical groundwater modeling techniques are used to represent complex boundaries (e.g., Anderson et al., 2015; Woessner & Poeter, 2020).

11.3 Development of Cones of Depression in Anisotropic Heterogeneous Material

The simplifying assumptions needed to develop analytical solutions to forecast drawdown and analyze hydraulic testing data state that the unit being pumped is isotropic and homogeneous. This allows for radial flow and the development of mathematics to produce analytical solutions. However, uniform aquifer parameters within the cone of depression may not be present in many settings. Instead, the geologic setting and depositional and structural history often result in anisotropic and heterogeneous conditions. In such cases, the cone of depression is not symmetrical when the aquifer is pumped (Figure 77).

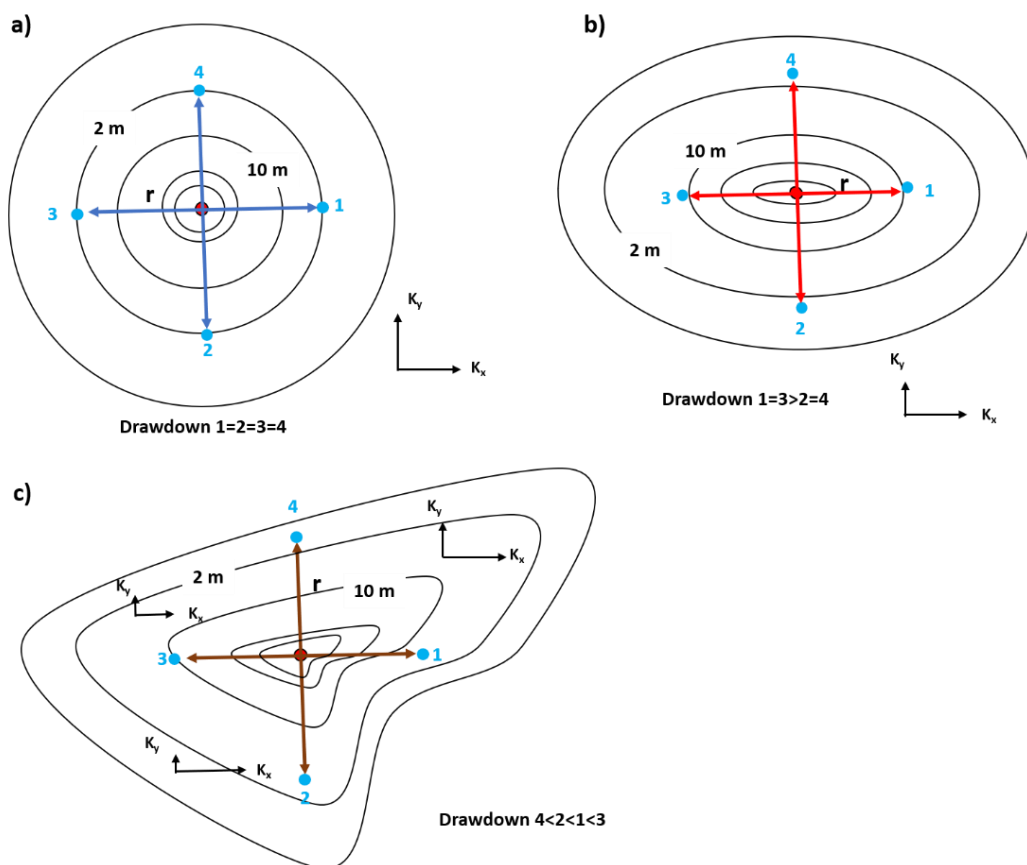


Figure 77 - Schematic map views of cones of depression (two-dimensional) associated with a pumping well in a water-bearing unit with a) isotropic homogeneous, b) anisotropic homogeneous, and c) anisotropic heterogeneous conditions. The red solid dot represents a pumping well. Solid blue dots represent observation wells numbered 1, 2, 3, and 4, located at equal radial distances (r) from the pumping well. Maps represent drawdown at a specified time. The cone of depression associated with pumping in isotropic and homogeneous conditions shown in (a) has equal drawdown at observation wells located at equal distances from the pumping well. The cone of depression associated with pumping in anisotropic homogeneous conditions (b), where $K_x > K_y$ has an elongated shape in the direction of the x axis (higher hydraulic conductivity) and the drawdown cone is narrower and steeper in the y direction which is the direction of lower hydraulic conductivity. The cone of depression associated with a pumping well in anisotropic heterogeneous conditions (c) has different drawdown at each well even though they are located at the same radial distance from the pumping well.

The cone of depression becomes less symmetrical and drawdown at equal distances from the pumping well varies more as hydraulic properties of the pumped unit are more

anisotropic and heterogeneous (Figure 77). When conditions are heterogeneous and anisotropic, T and S computed from observation well time-drawdown data collected at equal distances from the pumping well will be higher or lower than the isotropic, homogeneous case. This is illustrated in a conceptual semi-log plot of time-drawdown data from observation wells located at equal radial distances (r) for a pumping well in Figure 78.

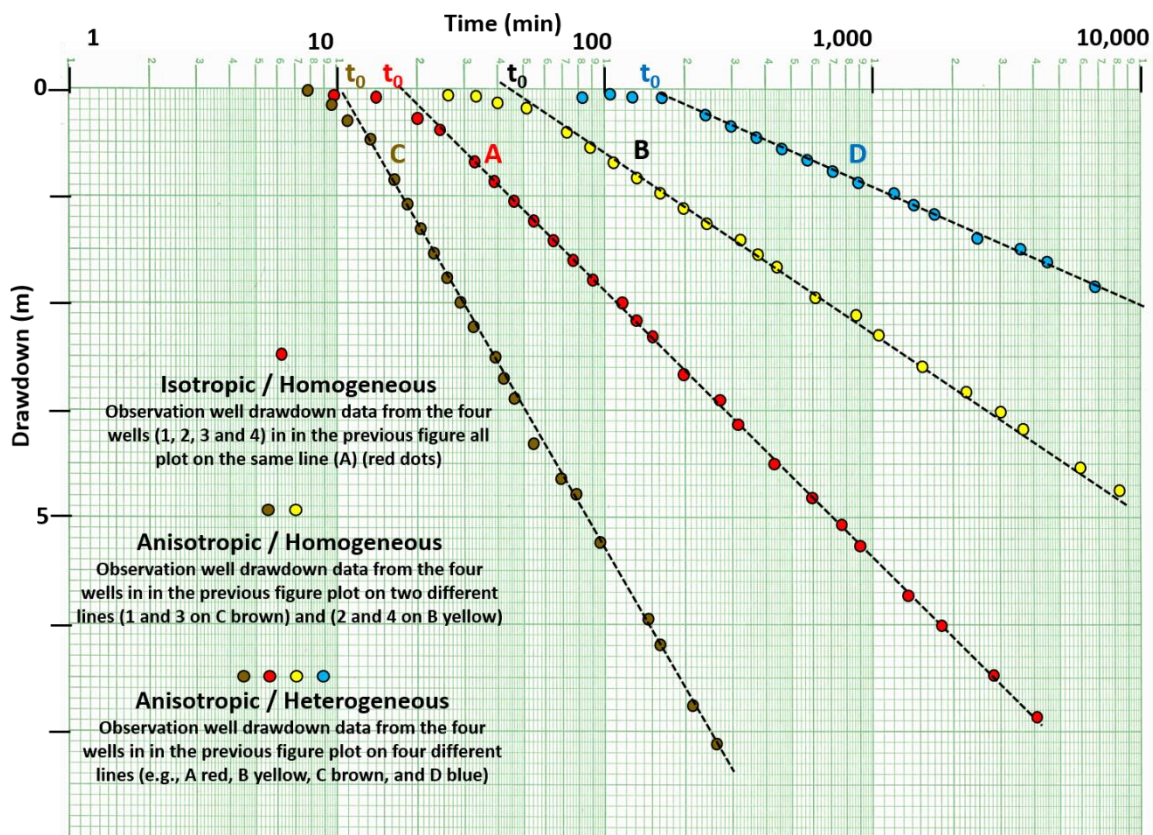


Figure 78 - Conceptual semi-log plot of time-drawdown data for equally spaced observation wells (Figure 77) collected for hydraulic tests conducted in a totally confined groundwater system. The straight-line portion of the curves from different observation wells equidistant from the pumping well have different slopes and t_0 intercepts as T and S are more variable. Plot A represents drawdown data collected under isotropic and homogeneous conditions. Drawdown data from each of the four observation wells plot along the line passing through the red dots. Under simple anisotropic conditions drawdown data from two observation-wells located along the axis of lower hydraulic conductivity plot on one line (e.g., B, yellow dots) and the other two observation-well data sets plot on a different line (e.g., C, brown dots). In an anisotropic and heterogeneous case, data from each observation well plot on a separate line (e.g., A, B, C, and D).

As most field conditions are not isotropic and homogeneous, T and S values derived from multiple observation wells will not be equal. Most often, for a test with multiple observation wells, the resulting values are averaged or high, low, and average values of parameters are used to forecast groundwater conditions. Use of the high and low values indicates the degree of uncertainty in the forecasted conditions.

In some settings, observation wells are not available when conducting pumping tests. The next section addresses how estimates of hydrogeologic properties of groundwater systems can be derived using only a single pumping well.

11.4 An Opportunity to Use Well Hydraulics to Evaluate well Interference in the Presence of a Recharge Boundary

Section 11 discussed well interference and the influence of boundaries on drawdown cones. [Exercise 4](#) provides a hands-on opportunity to apply well-hydraulics concepts to evaluate these effects.

12 Estimating Hydrogeologic Properties Using a Single Pumping Well

Transient or steady-state time-drawdown and recovery data generated from a single well pumping test can be used to estimate hydraulic properties of confined and unconfined aquifers. Standard curve-matching methods can be applied using corrected drawdown data. In addition, variable-rate pumping methods and well-performance test analyses can be used to generate aquifer properties using data collected in a pumping well.

12.1 Special Considerations When Using Drawdown Data from a Pumping Well

Under ideal conditions, analytical solutions (Sections 7 through 10) and their simplifying assumptions can be applied to single-well pumping-test data to determine corresponding values of T and S . However, wells need to be fully penetrating and 100 % efficient. When using drawdown in the pumping well for the analysis, the pumping well radius is often substituted in the equations that require a radial distance to an observation well. The screen or perforated-casing radius is used unless the well construction includes an envelope of gravel pack. When this occurs, the well radius is defined as the effective well radius and includes the radius of the perforated interval and gravel pack.

However, when a single pumping well is the only source of drawdown data, it must be recognized that the recorded drawdown data are often influenced by partial penetration, well-bore storage, and well loss, which are functions of the well design. Partial-penetration and well-loss effects result in lower water levels in the pumping well as compared to the adjacent aquifer. Well-bore-storage effects temporarily reduce the rate of early water level decline when large diameter wells are pumping at low rates. Each of these conditions are usually present to some degree and directly affect the predicted or reported drawdown at the pumping well. As with observation well test records, pumping-well drawdowns can be impacted by well interference, barometric, tidal, and, in unconfined cases, recharge events and direct evapotranspiration.

Most often partial penetration and well-loss conditions result in greater drawdown measured in the pumping well than if they were not present. As a result, computed T and S values are lower than properties of the formation. Ideally, pumping-well drawdown would be corrected before analyses were undertaken.

During the early-time period of some pumping tests—especially in large-diameter wells—pumped water is derived not only from the aquifer but also from water stored in the well casing or annular space (and filter pack) surrounding the screened or perforated interval. This results in a reduction in the observed drawdown in the pumping well and is referred to as a wellbore storage effect. As time progresses, formational water makes up an increasing portion of the well discharge until wellbore storage effects are sufficiently small,

and flow is supplied by the aquifer. The influence of wellbore storage on drawdown data is most easily observed using log-log plots of time-drawdown data. The early-time data will appear as a straight line diverging from the Theis curve. Papadopulos and Cooper (1967) developed an analytical method and a set of type curves that can be used to analyze confined-aquifer-test data affected by wellbore storage. Moench (1997) generated an analytical solution for pumping unconfined aquifers that accounts for well bore storage. He also provides a set of type curves.

The total observed pumping-well drawdown can be visualized as having several components as shown in Figure 79 and explained by Equation (79).

$$s_T = s_F + s_{pp} + s_{WL} + s_I + s_O \quad (79)$$

where:

- s_T = total observed drawdown in the pumping well (L)
- s_F = component of drawdown based solely on the formational properties (T, S) (L)
- s_{pp} = component of drawdown resulting from partial penetration of the perforated interval (L)
- s_{WL} = component of drawdown from linear and non-linear well loss (L)
- s_I = component of drawdown from well interference (L)
- s_O = component of drawdown from other factors with a positive or negative sign (e.g., wellbore storage, barometric effects, tides, recharge) (L)

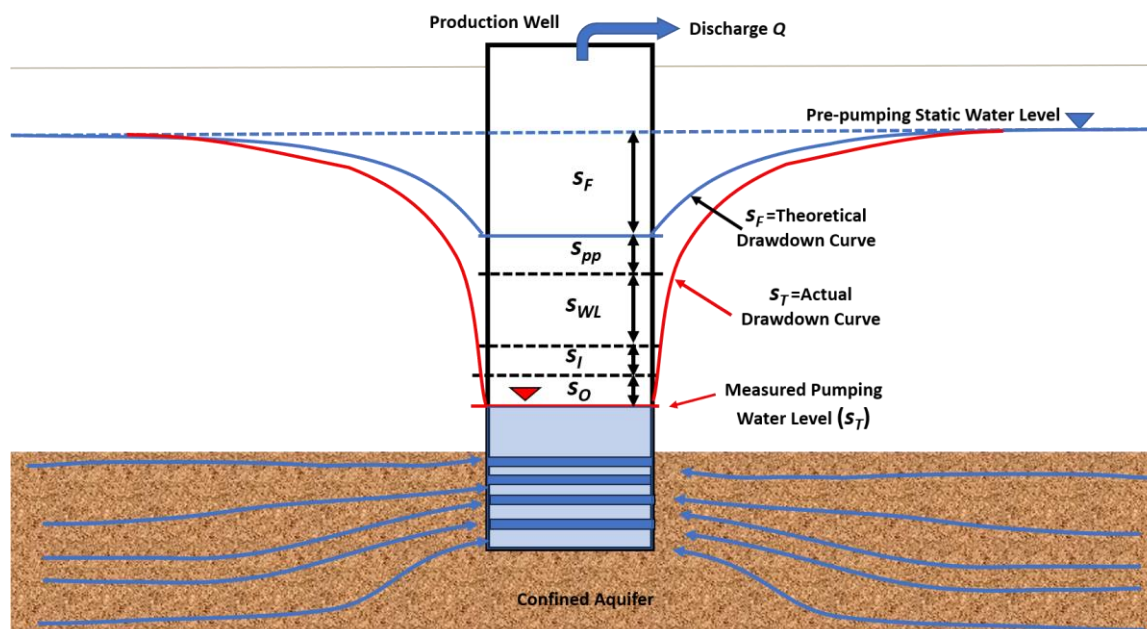


Figure 79 - Schematic of a partially penetrating pumping well in a confined aquifer (sand pattern) showing components of the total drawdown (s_T) as represented by the red profile. The formational drawdown (s_F) is shown in the blue drawdown profile and is the drawdown if the well is 100 percent efficient and fully penetrating. Additional components contributing to the total drawdown observed in the pumping well may include the effects of partial penetration which results in longer flow paths to the well as indicated by the blue flow lines (s_{PP}), well loss resulting from the well construction, design, and pumping rate (s_{WL}), drawdown from wells pumping nearby which is called well interference (s_I), and other factors causing the water levels to rise or fall such as wellbore storage and barometric effects (s_O).

The measured water levels in the pumping well will be similar to the theoretical drawdown shown in blue on Figure 79 if:

- the pumping well is fully penetrating and 100 percent efficient,
- wellbore storage has been depleted
- there are no head losses due to turbulent flow caused by high flow rates and/or obstructions in the well, and
- there is no interference from nearby pumping wells or other hydraulic stresses on the unit being tested.

The following sections describe how the factors that require special consideration influence drawdown data in the pumping well and present methods used to quantify the magnitude of their effect and to correct the drawdown data.

12.1.1 Partial Penetration

A partially penetrating pumping well produces vertical components of flow near the well in both confined and unconfined aquifers. The vertical flow component creates longer flow paths that result in the flow system expending more energy to deliver water to the well than if all flow is horizontal. Partial-penetration effects can occur in an unconfined aquifer as pumping begins even if a well is fully penetrating when the saturated thickness adjacent to the pumping well is reduced significantly during the test.

Todd and Mays (2005) provide methods to compute the increase in drawdown attributed to the head loss during groundwater flow to a partially penetrating well. They report that if the perforated interval of the well penetrates 85 percent or more of the aquifer then correction is not necessary, but it is generally accepted that correction is not necessary if the screened portion of a well penetrates 80 percent or more of the aquifer thickness.

When considering the effects of partial penetration only, the total drawdown is composed of the formational drawdown, s_F , and the additional drawdown Δs_{pp} caused by partial penetration as shown in Equation (80) and Figure 80.

$$s_T = s_F + \Delta s_{pp} \quad (80)$$

where:

- s_T = total drawdown in pumping well including effects of partial penetration and formational drawdown (L)
- s_F = formational drawdown (L)
- Δs_{pp} = drawdown due to partial penetration (L)

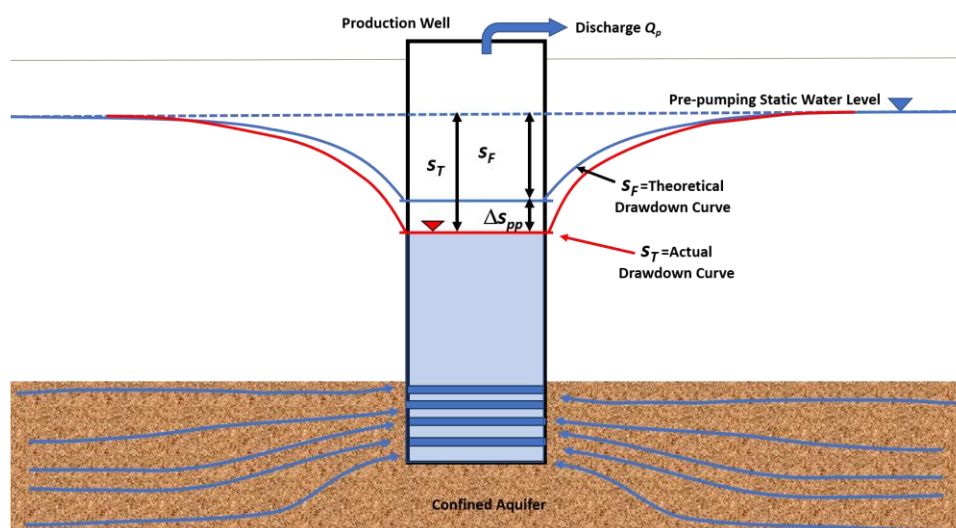


Figure 80 - Total drawdown, s_T , associated with a partially penetrating pumping well when both formational drawdown, s_F , and drawdown related to the effects of partial penetration, Δs_{pp} occur.

Huisman (1972) and Todd and Mays (2005) present methods to compute the effects of partial penetration using steady-state formulations, the variables shown in Figure 80 and Figure 81, and a penetration factor $p = h_s/b$, screen length (h_s) divided by the saturated aquifer thickness (b).

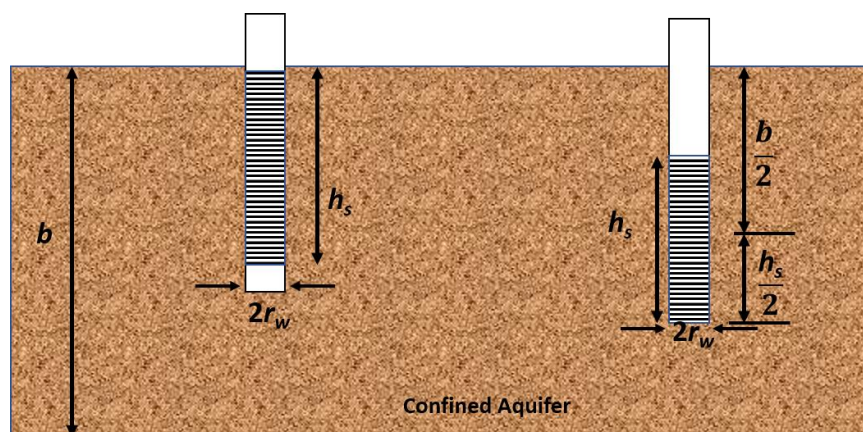


Figure 81 - Schematic of a confined aquifer (sand pattern) and the perforated interval (horizontal black lines) for two production wells. b represents the initial saturated thickness of the aquifer. h_s is the length of the perforated interval and r_w is the radius of the well (after Todd & Mays, 2005).

The additional drawdown associated with partial penetration under steady-state conditions in a confined aquifer as represented on the left-hand side of Figure 80 is defined for $p > 0.2$ by Todd & Mays (2003) in Equation (81). When the well screen is centered in the formation as shown in the right-hand portion of Figure 81, then $p = (h_s/2)/(b/2)$ and this ratio is substituted into Equation (81) that becomes Equation (82).

$$\Delta s_{pp} = \frac{Q_p}{(2\pi T)} \left(\frac{1-p}{p} \right) \ln \left(\frac{(1-p)h_s}{r_w} \right) \quad (81)$$

where:

- Δs_{pp} = additional drawdown resulting from partial penetration (L)
- Q_p = partially penetrating well pumping rate (L^3T^{-1})
- T = transmissivity (L^2T^{-1})
- p = penetration factor, h_s/b (dimensionless)
- h_s = length of well screen (L)
- b = saturated thickness of aquifer (L)
- r_w = radius of the pumping well (L)

$$\Delta s_{pp} = \frac{Q_p}{(2\pi T)} \left(\frac{1-p}{p} \right) \ln \left(\frac{(1-p)h_s}{2r_w} \right) \quad (82)$$

where:

- Δs_{pp} = additional drawdown resulting from partial penetration (L)
- Q_p = partially penetrating well pumping rate (L^3T^{-1})
- T = transmissivity (L^2T^{-1})
- p = penetration factor, h_s/b (dimensionless)
- h_s = length of well screen (L)
- b = saturated thickness of aquifer (L)

r_w = radius of the pumping well (L)

Based on the Thiem equation for unconfined aquifers, the drawdown resulting from partial penetration is defined by Todd and Mays (2005) as shown in Equation (85).

$$\Delta s_{pp} 2h_w = \frac{Q_p}{(\pi K)} \left(\frac{1-p}{p} \right) \ln \frac{((1-p)h_s)}{r_w} \quad (83)$$

where:

Δs_{pp} = drawdown resulting from partial penetration (L)

h_w = saturated thickness of the unconfined aquifer at pre-pumping conditions (L)

Q_p = partially penetrating well pumping rate (L^3T^{-1})

K = hydraulic conductivity (LT^{-1})

p = penetration factor $p = h_s/b$ (dimensionless)

h_s = length of well screen (L)

r_w = radius of the pumping well (L)

The total drawdown in an unconfined aquifer is defined as shown in Equation (84).

$$s_T = \sqrt{s_F^2 + \Delta s_{pp} 2h_w} \quad (84)$$

where:

s_T = total drawdown in pumping well including effects of partial penetration and formational drawdown (L)

s_F = formational drawdown (L)

Δs_{pp} = drawdown from partial penetration (L)

h_w = saturated thickness of the unconfined aquifer at a fully penetrating well (L)

The partial-penetration conditions that cause the additional drawdown are conceptualized as being constant once pumping begins. The partial-penetration correction can be applied to transient or steady-state drawdown data.

Example

A well with a radius of 0.15 m finished in a confined unit is pumped at a continuous rate of 4000 m³/d to near steady state and the total drawdown is 34 m. The screened interval is 10 m in length, and it is located just below the upper boundary of a 45 m thick aquifer. If the aquifer transmissivity is 940 m²/d, how much of the drawdown is due to partial penetration?

The penetration factor is 10 m/45 m = 0.22. Using Equation (81), Δs_{pp} is computed as shown here.

$$\Delta s_{pp} = \frac{Q_p}{(2\pi T)} \left(\frac{1-p}{p} \right) \ln \frac{((1-p)h_s)}{r_w}$$

$$\Delta s_{pp} = \frac{4000 \frac{\text{m}^3}{\text{d}}}{2 (3.14) 940 \frac{\text{m}^2}{\text{d}}} \frac{1 - (0.22)}{(0.22)} \ln \frac{((1 - 0.22)10 \text{ m})}{0.15 \text{ m}} = 9.5 \text{ m}$$

If a total observed drawdown in the partially penetrating well bore is 26.01 m, then rearranging Equation (80) the formational drawdown would be defined as $s_F = s_T - \Delta s_{pp}$, so $s_F = 26.01 \text{ m} - 9.5 \text{ m} = 16.51 \text{ m}$. If time-drawdown data were collected during a transient test, drawdown would be corrected by -9.5m.

In addition to the equations presented above, other authors have addressed methods to assess partial penetration effects with analytical solutions for steady-state and transient conditions (e.g., Sternberg, 1973; Brons & Marting, 1961; Bradbury & Rothschild (1985); Hantush, 1966; Neuman, 1975; Kipp 1973). Most commercial hydraulic-test-analysis software packages incorporate methods to correct data for partial penetration once well construction data are entered.

12.1.2 Well Loss and Using Step-Drawdown Tests to Assess Loss

Well loss is the component of the total drawdown in a production well due to the loss of energy resulting from turbulent flow of water through the screened or slotted interval (or the damaged borehole wall), as well as flow inside the casing to the pump intake as shown in Figure 82 and expressed by Equation (85).

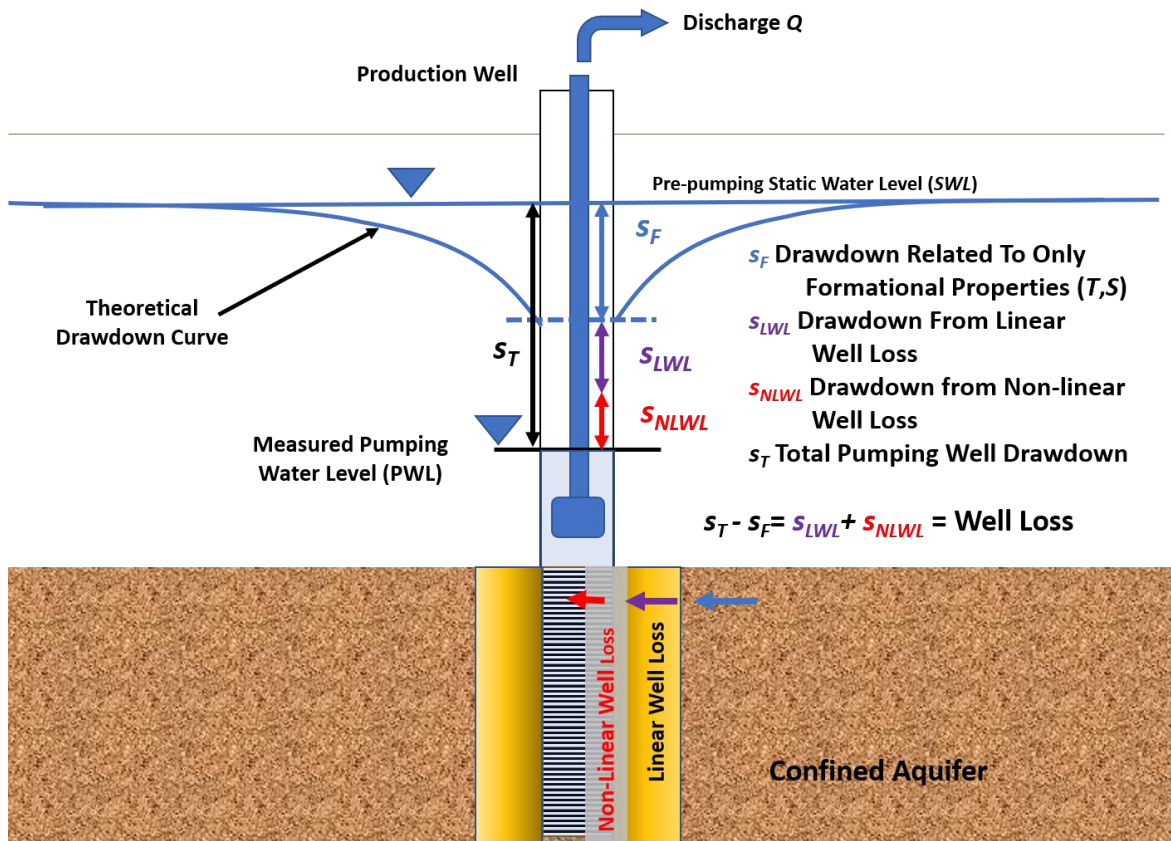


Figure 82 - Schematic showing the components of well loss in a fully penetrating pumping well finished in an isotropic and homogeneous confined aquifer. The measured drawdown is greater than if the well was 100 percent efficient and only the formational drawdown occurred as shown with the theoretical drawdown curve (s_F). The well loss is conceptualized as having two drawdown components, linear well loss (s_{LWL}), and non-linear well loss (s_{NLWL}). As water in the vicinity of the wellbore converges to the perforated interval, head loss occurs as it passes through the area around the well that was impacted by well construction (linear well loss). Head loss also occurs as water moves through the perforations and up the well bore to the pump (non-linear well loss).

$$s_{WL} = s_{LWL} + s_{NLWL} \tag{85}$$

where:

- s_{WL} = total well loss (L)
- s_{LWL} = linear well loss (L)
- s_{NLWL} = non-linear well loss (L)

When additional drawdown in a pumping well occurs from well loss, the total drawdown in the pumping well is the drawdown occurring due to the transmission and storage properties of the formation, s_F , and the total well loss (s_{WL}) as expressed in Equation (86).

$$s_T = s_F + s_{WL} \tag{86}$$

where:

- s_T = total drawdown (L)

- s_F = formational drawdown (L)
- s_{WL} = total well loss drawdown (L)

Hydraulic gradients near the well bore are often affected by formational damage caused by well construction. These include zones of lower hydraulic conductivity (introduction of well cuttings and drilling fluids) that are present adjacent to the well borehole called skin effects (e.g., Sterrett, 2007). As the converging flow enters this area, gradients increase and additional head loss (linear well loss [s_{LWL}]) occurs. These are termed linear losses because their magnitude is directly proportional to the well-discharge rate. Sometimes the damage zone has less resistance to flow because of performed well development and/or pumping that mobilize fines in the formation, drawing them into the well and enhancing formation conductivity near the well such that s_{LWL} can be negative (Sterrett, 2007). The second component of head loss occurs as flow passes through the perforated interval (screen openings or cut slots) and moves up the well bore to the pump. This reduction in the total head is referred to as non-linear well loss (s_{NLWL}). These are termed non-linear losses because their magnitude increases nonlinearly as well discharge increases. Figure 83 illustrates the impact of these losses on drawdown.

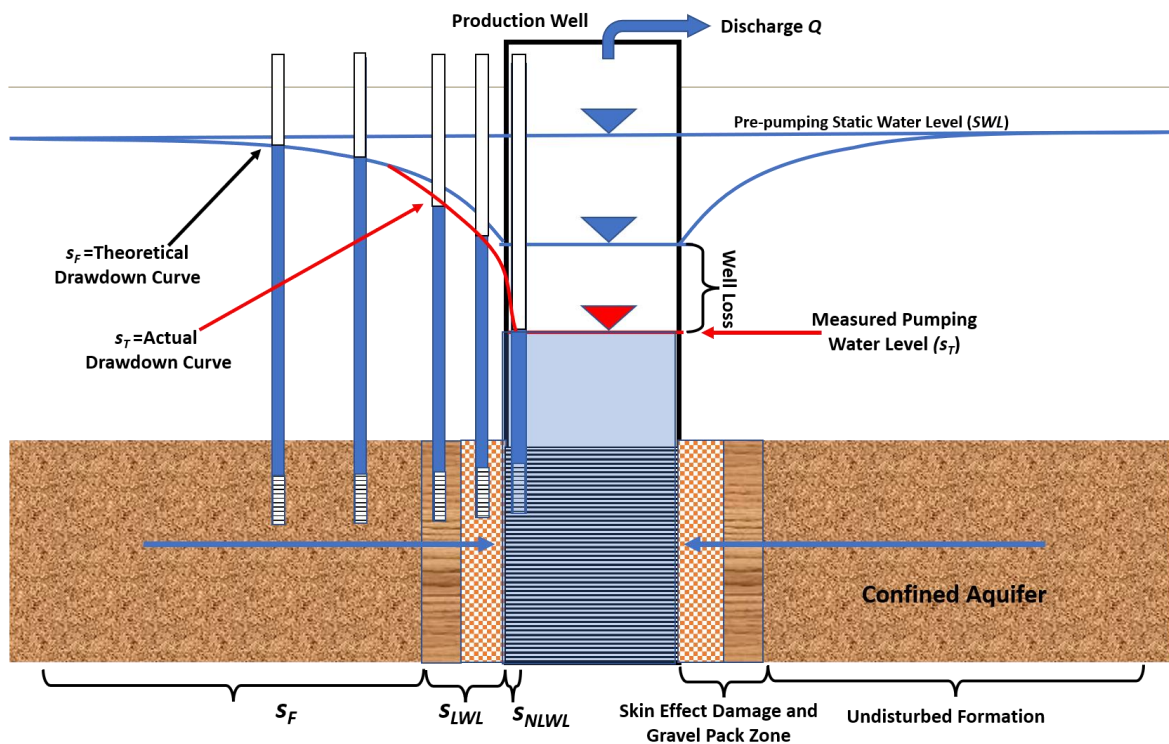


Figure 83 – Schematic of the change in water levels as water flows to the fully penetrating well bore completed in an isotropic and homogeneous confined aquifer being pumped at a constant rate (sand pattern). The small diameter wells (imaginary) are included in the diagram to illustrate the effect of well loss. The blue profile shows the theoretical drawdown (s_F) derived when the well has zero well loss (100 percent efficient). The red profile is created by adding the effects of well loss ($s_{LWL} + s_{NLWL}$) (red line). Zones of formational, linear, and non-linear well loss are illustrated at the base of the diagram.

Well loss is a function of the flow rate, being larger at higher pumping rates as shown in Equation (87).

$$s_T = B_1Q + B_2Q + CQ^2 \quad (87)$$

where:

- s_T = total drawdown (L)
- B_1 = formational aquifer properties (TL^{-2})
- Q = well discharge (L^3T^{-1})
- B_2 = formational conditions for linear well loss (TL^{-2})
- C = coefficient representing a non-linear well loss coefficient (T^2L^{-5})

In Equation (87), $B_1Q=s_F$, $B_2Q=s_{LWL}$, and $CQ^2=s_{NLWL}$. The values of B_1 and B_2 are not separable when time-drawdown data are available for only the pumping well. Jacob (1947) developed a relationship between the value BQ representing the formational drawdown and the non-linear or turbulent well loss component, CQ^2 (Equation (88)). B in this relationship can be conceptualized as B_1+B_2 . For a confined aquifer, B can be calculated using the Cooper-Jacob transient approximation in which the linear well loss component is formally included. That is, B equals $\frac{1}{4\pi T} \ln \left\{ \frac{Tt}{1.78r^2S} \right\}$, as shown in Equation (31) of Section 8.3.2. Rorabaugh (1953) suggests that the commonly used squared term on C in the non-linear well loss term can be replaced with a variable that is near two but can be less or greater than two. Rorabaugh (1953) provides additional information. Traditionally, a value of two is assumed.

$$s_T = BQ + CQ^2 \quad (88)$$

where:

- s_T = total drawdown in the pumping well (L)
- B = represents formational aquifer properties (TL^{-2})
- Q = well discharge (L^3T^{-1})
- C = coefficient representing non-linear well loss (T^2L^{-5})

When T and S are known, Equation (88) is used to correct pumping well drawdown for non-linear well loss by computing CQ^2 and subtracting it from the observed drawdown, $s_F = s_T - CQ^2$. Step-drawdown tests are used to estimate the well loss coefficient C .

Step-Drawdown Test and Methods to Compute Well Loss Coefficient and Estimate T

A step-drawdown test (often referred to as a step test) is conducted by pumping a well at various rates and recording time-drawdown data in the well. These tests can be used to investigate the drawdown response to pumping when flow rates increase and

decrease. Step-drawdown testing is used to characterize the well loss that occurs at various pumping rates. This methodology is most often used to quantify the well-loss coefficient, C . The coefficient is used to compute well-loss components of the total drawdown at a prescribed pumping rate and to correct drawdown versus time data to reflect drawdown attributed only to formational properties and conditions.

During a step-drawdown test, the pumping rate is increased from an initially low constant rate through a series of sequentially higher constant pumping rates (steps). Typically, each step is of equal duration, lasting from approximately 30 minutes to 2 hours (Kruseman & de Ridder, 2000). Each step should be of sufficient duration to allow the dissipation of wellbore storage effects. Any number of steps can be conducted; however, at least three are recommended. The steps are usually increased sequentially but can be started and stopped allowing full recovery (Figure 84). The step test is usually designed so that the stepped pumping rates include or bracket the desired pumping rate for a production well. This allows computation of the well-loss coefficient at that planned pumping rate. Step tests are also used to evaluate well performance including selecting pumping rates with lower well loss and identifying whether well conditions have changed over time (Sterrett, 2007).

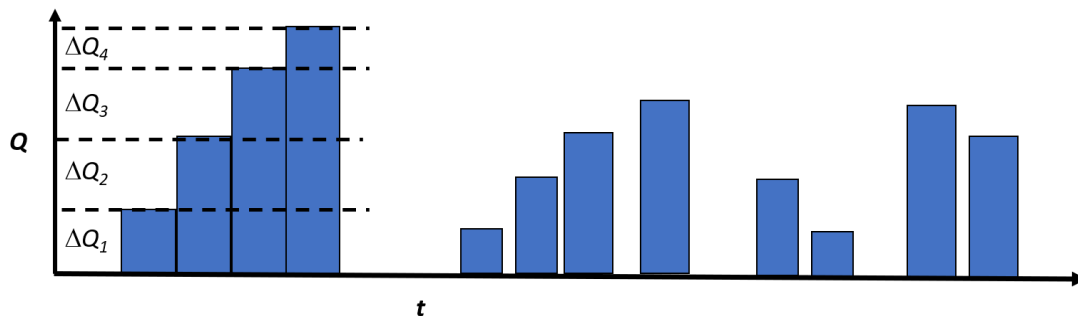


Figure 84 - Step-drawdown tests are most often conducted as one continuous test where the pumping rate is held constant for a period and then increased by a value of ΔQ as shown in the left-hand portion of the graph. The length of time each step is pumped, and the ΔQ can vary. Time-drawdown data are collected for each step. A second approach, shown in the middle and right-hand side of the diagram, illustrates that step test data sets can also be derived when a well is pumped at a constant rate, then the pumping is stopped, and the well is allowed to recover. Repeating this method for various pumping rates creates a step test data set.

Step-drawdown test results are plotted on a semi-log scale as drawdown versus time. The change in drawdown between each step is designated as Δs_{step} and the change in discharge between each step is defined as ΔQ . Figure 85 shows data from a continuous step test where each step reached steady-state drawdown or near steady-state. Figure 86 shows a transient step test where each step lasted 30 minutes or more and drawdown was still declining as the next step started. In this case, Δs_{step} is the difference between the straight-line projection of the drawdown of the previous step and the drawdown after 30 minutes of pumping at the new rate.

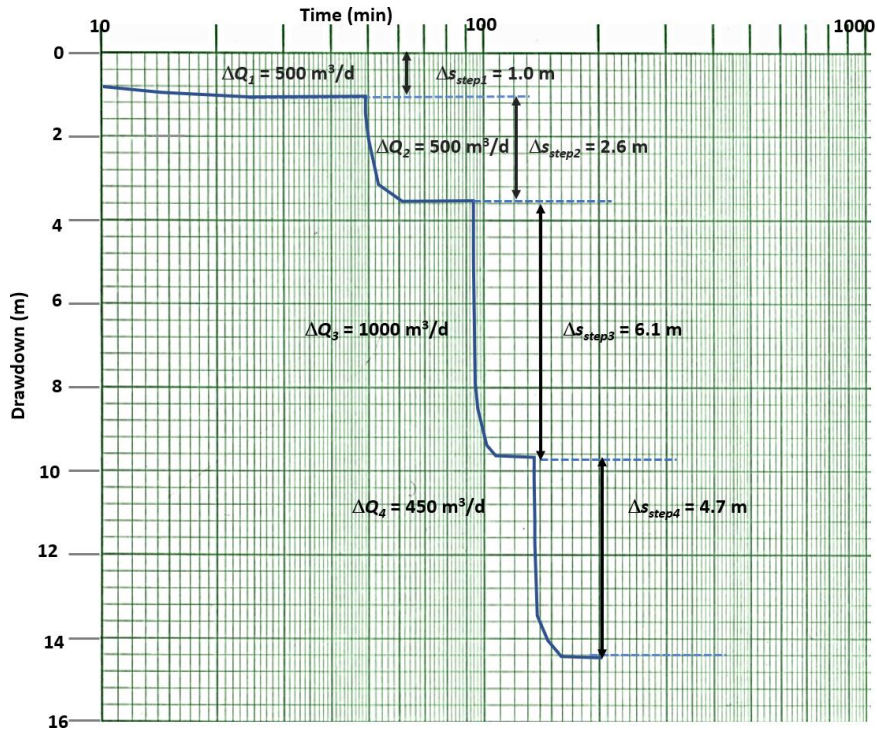


Figure 85 - Step-drawdown test where sequential constant pumping rates were used, and the drawdown reached steady-state at each step. Dashed lines represent an extension of the observed drawdown trend. Values of ΔQ and Δs_{step} are shown. Total pumping rates and drawdown for an individual step are obtained by adding the change in pumping rate and additional drawdown to those of the previous steps.

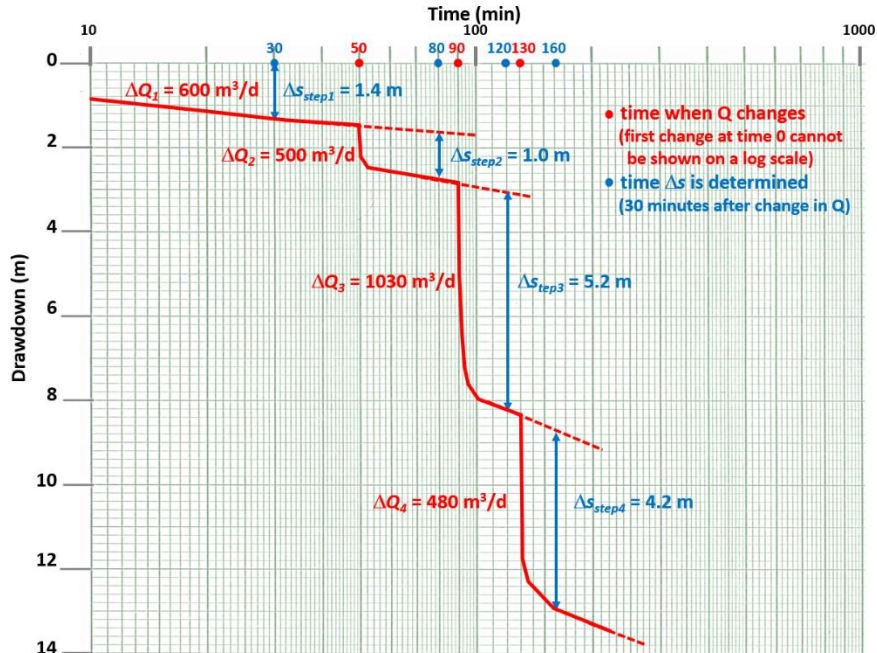


Figure 86 - Transient step-drawdown test with sequential constant rates. Pumping of each step equaled or exceeded 30 minutes. Dashed lines represent extensions of the observed drawdown trends. Using a 30-minute interval from the start of each step, values of ΔQ and Δs_{step} are shown. Total pumping rates and drawdown for each step (after 30 minutes of pumping) are obtained by adding the changes in pumping rates and drawdown up to that point (i.e., $\Sigma \Delta Q$ and $\Sigma \Delta s_{step}$).

Analysis of the steady-state step-drawdown test shown in Figure 85 is described next. To estimate the turbulent flow coefficient, C , and the formational coefficient, B , of Equation (88), an arithmetic plot of the total discharge for each step and the total drawdown divided by the total step discharge for each step (s/Q_T) is plotted (Figure 87). Q_T is the cumulative pumping rate for a step, e.g., Q_T for step 2 is $\Delta Q_1 + \Delta Q_2$, and for step 3 $Q_T = \Delta Q_1 + \Delta Q_2 + \Delta Q_3$. This approach is referred to as the Hantush-Bierschenk method (Hantush, 1964; Bierschenk, 1963).

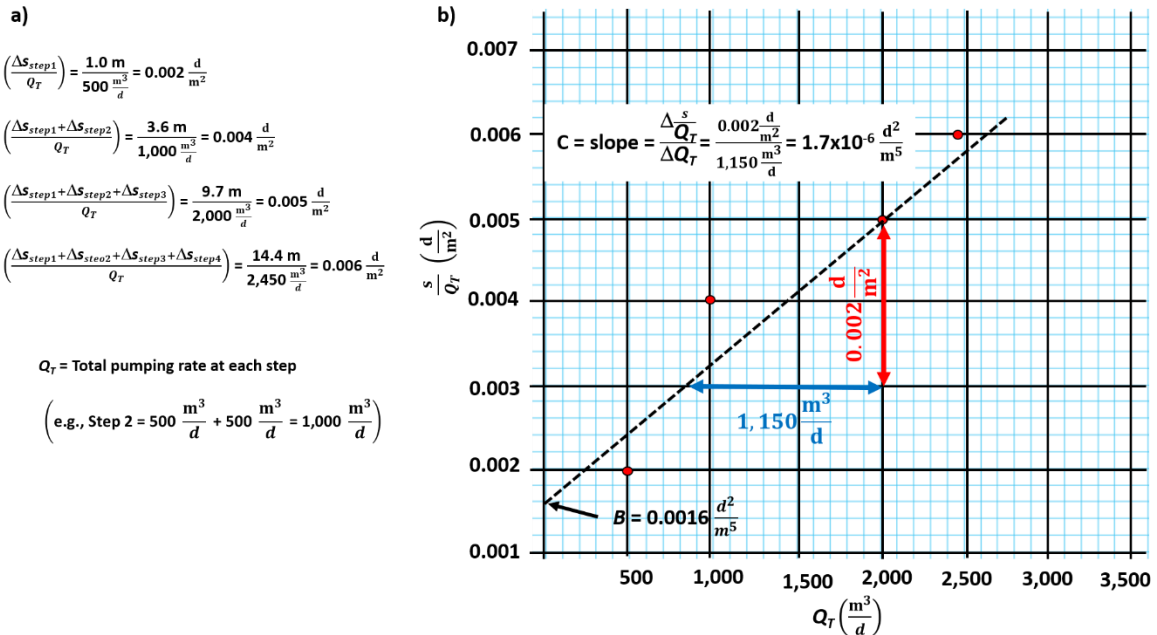


Figure 87 - Example of a Hantush-Bierschenk plot used to analyze steady-state step-drawdown data to determine the turbulent well loss coefficient, C , and the value of B . a) Calculations of values of Q_T , s , and s/Q_T for each step. b) Plot of s/Q_T for each step versus the total pumping rate (Q_T) at the step. The slope of a fitted straight line (dashed line) is the value C and the intercept of the fitted line on the y-axis is the value B .

The well-loss coefficient is derived from the slope of the fitted line shown in Figure 87. Given the scatter of the data in this example, C values will vary depending on the location of the fitted line. The well loss, s_{WL} , from turbulent conditions is then calculated at a specified discharge as CQ^2 . The turbulent well-loss coefficient described by Jacob (1950) is assumed to be a constant. For example, if the well producing the data shown in Figure 87 was being pumped at $2,500 \text{ m}^3/\text{d}$, the turbulent well loss would be $(0.0000017 \text{ d}^2/\text{m}^5) (2,500 \text{ m}^3/\text{d})^2 = 10.6 \text{ m}$.

The coefficient B of Equation (87) is related to the formational properties and represents some linear well loss as discussed in previous sections. It is derived from the y-axis intercept of the fitted straight line. If other time-drawdown data collected from an observation well during a constant discharge pumping test are available, an estimate of B_1 of Equation (87) can be derived using standard curve-matching methods because the observation well is not pumped so it is 100 percent efficient.

Without an independent method to estimate B_1 , the value B derived from step test analyses is assumed to represent an estimate of the formational drawdown, $s_F = BQ$. In that case, aquifer properties will be underestimated because the drawdown used to estimate B contains some undefined well loss, and thus is greater than the drawdown for only formational conditions, B_1 . When steady-state conditions occur, the Thiem Equation can be applied to estimate T for confined conditions (Equations (89), (90), (91), and (92)).

$$s_T = \frac{Q}{2\pi T} \ln\left(\frac{r_0}{r_w}\right) + CQ^2 \quad (89)$$

$$s_F = s_T - CQ^2 \quad (90)$$

$$s_F = BQ = \frac{1}{2\pi T} \ln\left(\frac{r_0}{r_w}\right) Q \quad (91)$$

$$B = \frac{1}{2\pi T} \ln\left(\frac{r_0}{r_w}\right) \quad (92)$$

where:

- B = coefficient for a confined aquifer under steady-state conditions (TL^{-2})
- T = transmissivity (Kb) (L^2T^{-1})
- Q = constant pumping rate (L^3T^{-1})
- s_T = static water level minus the head in the pumping well (L)
- s_F = drawdown attributed to formational properties (L)
- r_w = radius of the pumping well (L)
- r_0 = radial distance where drawdown equals 0 (estimated) (L)

The pumping-well radius is derived from the well-construction information. However, when a gravel pack is present the well radius is often replaced by the effective well radius; that includes the screen radius and radius of the surrounding gravel pack. The effective radius is then used as r_w in the Thiem and Theis single-well pumping equations.

When steady-state unconfined conditions are present, the total and formational drawdowns are usually approximated assuming the saturated thickness only changes a small amount during pumping. This allows application of the equations for confined aquifers, Equations (89) through (92).

In Equation (92), the value of B is derived from the plot shown in Figure 87. The radius of the well is obtained from field measurements and well construction records. Once the value of B is graphically determined, values of T and $K=T/b$ can be computed using Equation (92). However, the solutions depend on an estimate of the radial distance from the pumping well where drawdown is zero, r_0 . An arbitrary value of 500 m is often assumed for steady-state confined conditions because it is sufficiently large and using another

sufficiently large value makes little difference in the result. When pumping rates are high, assumed distances can be increased by 1.5 to 2 times. Estimates of T change with different radial-distance values (zero drawdown). However, because the radial distance is divided by the well radius and the natural logarithm is applied to the ratio, final estimates vary slightly when larger or smaller distances are used.

Results of a transient step-drawdown test such as the one shown in Figure 86 can be analyzed using the same approach as described in Figure 87. Figure 88 is a plot of s/Q_T versus Q_T for the transient test. Values of s/Q_T for each step are computed using drawdown values measured at the end of the designated constant time, in this case the first 30 minutes.

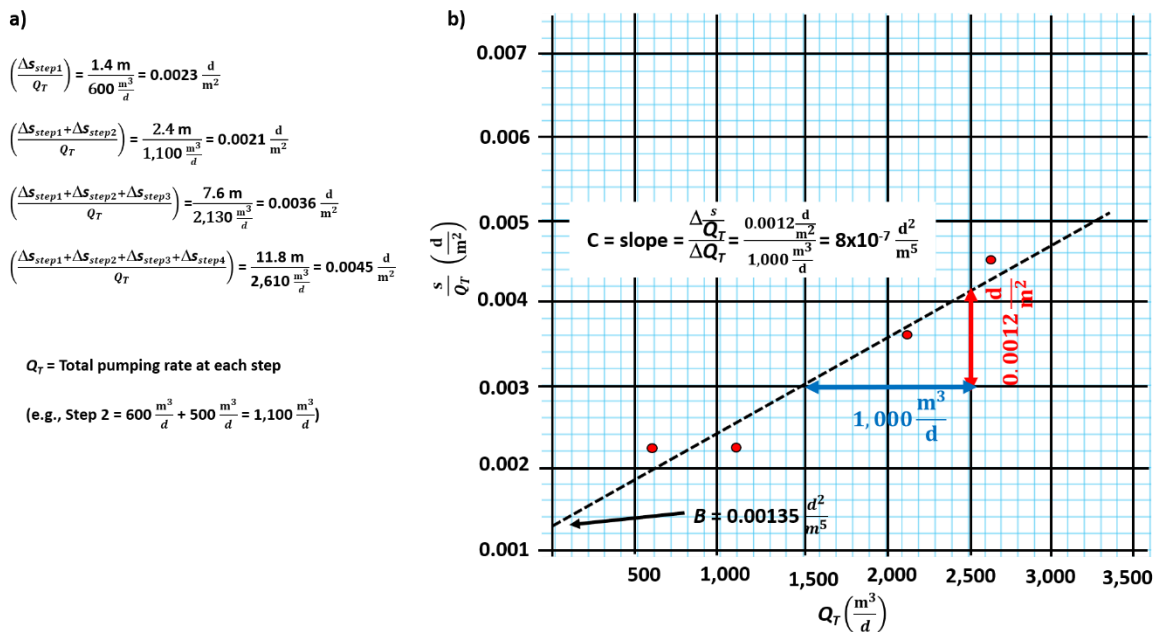


Figure 88 - A Hantush-Biershenk plot used to analyze transient step-drawdown data to determine the turbulent well loss coefficient, C , and the value of B in a confined system. a) Calculations of values of Q_T , s and s/Q_T for each step using drawdown at the end of the 30-minute interval since the step began. b) Plot of s/Q_T for each step versus the total pumping rate (Q_T) at the step. The slope of a fitted straight line (dashed line) is the value C and the intercept of the fitted line on the y -axis is the value B .

Again, using the relationship shown in Equation (88) shows $BQ = s_f$. Estimates of T will be higher if only B_1 is used. Defining B using the Cooper-Jacob approximation for a confined aquifer for $u < 0.01$ yields Equation (93).

$$B = \frac{1}{4\pi T} 2.30 \log \left(2.25 \frac{Tt}{r_w^2 S} \right) \tag{93}$$

where:

- B = formational coefficient for transient conditions (TL^{-2})
- T = transmissivity (L^2T^{-1})
- t = constant time step length corresponding to the reported drawdown value (T)

r_w = radius of the pumping well (L)

S = storativity (dimensionless)

Transient estimates of B require an estimate of S . This is often derived by estimating the specific storage (S_s) of the aquifer material and computing a value of $S = S_s$ (as discussed in Box 2). In addition, the estimate of B is time dependent. Thus, it is not used to estimate formational drawdown at other than early times (length of a step). The computed T values and estimates of S can be used to compute drawdowns at other times using appropriate analytical solutions (confined aquifer). If sufficient time-drawdown data are collected in the first step of the step test these data can be corrected for non-linear well loss and then used to curve match and compute additional estimates of T and S .

Jacob (1950) developed another method to estimate C using at least three consecutive steps from a step-drawdown test. Most often this method is used for confined transient conditions and the change in drawdown is compared for equal time intervals since the step began, drawdown after 30 minutes or 1 hour for example (Figure 86). The turbulent well-loss coefficients bracketed by two pumping rates are computed as shown in Equations (94), (95), and (96).

$$C_1 = \frac{\left(\frac{\Delta S_{step2}}{\Delta Q_2}\right) - \left(\frac{\Delta S_{step1}}{\Delta Q_1}\right)}{\Delta Q_1 + \Delta Q_2} \quad (94)$$

$$C_2 = \frac{\left(\frac{\Delta S_{step3}}{\Delta Q_3}\right) - \left(\frac{\Delta S_{step2}}{\Delta Q_2}\right)}{\Delta Q_2 + \Delta Q_3} \quad (95)$$

$$C_3 = \frac{\left(\frac{\Delta S_{step4}}{\Delta Q_4}\right) - \left(\frac{\Delta S_{step3}}{\Delta Q_3}\right)}{\Delta Q_3 + \Delta Q_4} \quad (96)$$

where:

C_1, C_2, C_3 = well loss turbulence coefficient for steps 1-2, 2-3 and 3-4
(T^2L^{-5})

$\Delta S_{step1}, \Delta S_{step2}, \Delta S_{step3}, \Delta S_{step4}$ = drawdown for each step after a constant pumping
period (L)

$\Delta Q_1, \Delta Q_2, \Delta Q_3, \Delta Q_4$ = changes in pumping rates between steps (L^3T^{-1})

C can be computed based on the response of two sequential steps using the transient step-drawdown data shown in Figure 86. Some researchers discourage using this approach because in the original formulation of C it is assumed to be constant (Jacob, 1950). However, often when this method is used most C values show variability. When values of C are similar, they can be averaged or a value more representative of the pumping rate selected is used to compute well loss.

Example

Using Jacob's method (1950) compute C from the transient data set shown in Figure 86, the time interval for analysis of each step is 30 minutes from the beginning of the step.

$$C_1 = \frac{\left(\frac{1 \text{ m}}{500 \frac{\text{m}^3}{\text{d}}}\right) - \left(\frac{1.4 \text{ m}}{600 \frac{\text{m}^3}{\text{d}}}\right)}{600 \frac{\text{m}^3}{\text{d}} + 500 \frac{\text{m}^3}{\text{d}}} = -3.0 \times 10^{-7} \frac{\text{m}^5}{\text{d}^2}$$

$$C_2 = \frac{\left(\frac{5.2 \text{ m}}{1030 \frac{\text{m}^3}{\text{d}}}\right) - \left(\frac{1.0 \text{ m}}{500 \frac{\text{m}^3}{\text{d}}}\right)}{500 \frac{\text{m}^3}{\text{d}} + 1030 \frac{\text{m}^3}{\text{d}}} = 2.0 \times 10^{-6} \frac{\text{m}^5}{\text{d}^2}$$

$$C_2 = \frac{\left(\frac{4.2 \text{ m}}{480 \frac{\text{m}^3}{\text{d}}}\right) - \left(\frac{5.2 \text{ m}}{1030 \frac{\text{m}^3}{\text{d}}}\right)}{1030 \frac{\text{m}^3}{\text{d}} + 480 \frac{\text{m}^3}{\text{d}}} = 2.4 \times 10^{-6} \frac{\text{m}^5}{\text{d}^2}$$

The coefficients are used to compute the additional drawdown caused by non-linear well loss. The negative value computed between the first two steps suggests the well was developing when pumped at 1,100 m³/d in the second step. If a step-drawdown test is completed and then followed by a constant discharge pumping test using the single well, the computed well loss (additional drawdown) for that pumping rate would be subtracted from the observed drawdown data before time-drawdown data were analyzed to estimate T and S .

12.1.3 Well Interference

It is best if other nearby wells are not operating during a single pumping test. However, if the operating schedules of surrounding wells in the area are known, well interference can be computed using standard analytical solutions or they can be observed during non-pumping test periods. This involves monitoring water levels prior to and after pumping to see if adjacent pumping wells are impacting the water levels at the test well. If the effects of pumping in the surrounding wells are observed in the time-drawdown data of the test well, they can be removed as described in Section 11.1. Observed drawdown may be affected during both drawdown and recovery.

12.1.4 Other Conditions that Effect Pumping Well Drawdown

Other factors may influence water levels during a single-well test

- wellbore storage effects can occur, and are more pronounced for larger-diameter wells and lower pumping rates;

- confined systems can be affected by barometric pressure changes, tidal loading, and direct loading; and
- unconfined systems may be impacted by tidal loading, evapotranspiration cycles, river-stage changes, and short- or long-term recharge events.

Wellbore-storage effects were discussed in Section 12.1. Additional details on the effects of changing barometric pressure as well as both tidal and direct loading on observed water levels are discussed in Section 5. Water-level changes in the pumping well due to these factors will be small in most cases. These factors will have a greater effect on late-time data when drawdown changes due to formational conditions are also small. If time-drawdown data need to be corrected for these perturbations, Kruseman and de Ridder (2000) and Sterrett (2007) provide a list of corrections. Procedures for determining production-well efficiency are described in [Box 4](#).

12.2 Drawdown and Recovery Curve-Matching Methods for a Single Pumping Well

Time-drawdown and recovery data for a single pumping well can be analyzed using the appropriate analytical solutions and standard curve-matching methods discussed in previous sections. Automated software analysis can also be applied (Section 13). Data need to be corrected for partial-penetration and well-loss effects before curve matching as described in Section 12.1.

12.2.1 Analyzing Time-Drawdown Data

Drawdown corrections discussed in Section 5 and Sections 12.3 through 12.5 will produce drawdown data sets that represent formational aquifer properties. The Theis, Cooper-Jacob, Hantush, Neuman, and other methods can be applied to estimate T and S . Log-log data plots can be matched with type curves or by using numerical methods, and as appropriate, semi-log plots analyzed to yield aquifer properties and properties of confining units (e.g., leaky confining units). Specific examples are not provided here because they are discussed in Sections 8 through 10.

If single-well time-drawdown data are not corrected for well loss or partial penetration, curve-matching and straight-line analytical methods will still provide reasonable estimates of T , but poor estimates of S . This is because the effects of well loss at a constant pumping rate and partial penetration are constant. These conditions increase the drawdown by fixed quantities. This results in maintaining the shape of data plotted on log-log scales and the slope of data plotted on semi-log scales. Thus, curve-matching techniques result in match points with reasonable values of the well function and drawdown, and poor values for integration variables like u and time as illustrated in Figure 89.

This is an important conclusion. It means that a carefully conducted pumping test without observation wells may be well worth the cost. Together with the step drawdown

tests such a pumping test can provide robust estimate of field-scale transmissivity near the pumped well in addition to information on the efficiency of the well.

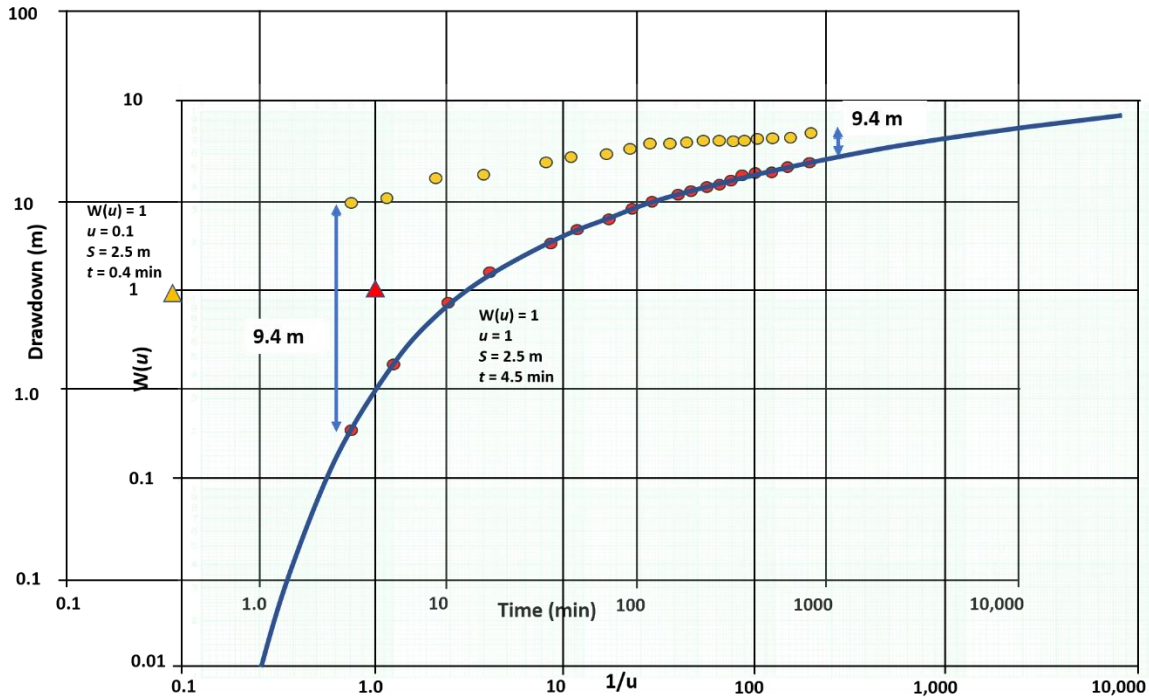


Figure 89 - Time-drawdown data for a pumping well completed in a confined water-bearing unit. Orange solid dots represent field-collected data at the pumping well and red solid dots show corrected drawdown at the pumping well if partial penetration and/or well loss is occurring. This example shows an offset (lower water levels) of 9.4 m. Curve matching methods conducted on both data sets yield match point values shown as orange (uncorrected, curve matching not shown) and red (corrected) triangles. $W(u)$ and s are equal at both of the selected match points while u and t are different. Calculations of T from uncorrected time-drawdown data (orange dots) yield good estimates of T (compared with the corrected computed T), but poor estimates of S . Once again, S can be approximated using methods presented in Box 2.

An example of another set of corrected and uncorrected single-well drawdown data analyzed using the Cooper-Jacob straight-line method is shown in Figure 90. The slope of the lines is the same, so the calculation of T yields the same values for both curves. This is because the Cooper-Jacob method does not rely on the absolute magnitude of the drawdown as the Theis method does. It depends on the rate of change of drawdown. However, the straight-line intercept, t_0 , is smaller for the uncorrected field data set impacted by the 6 m offset (Figure 89). The storativity calculation is dependent on the magnitude of the drawdown. Analyzing uncorrected drawdown data will yield a poor estimate of S .

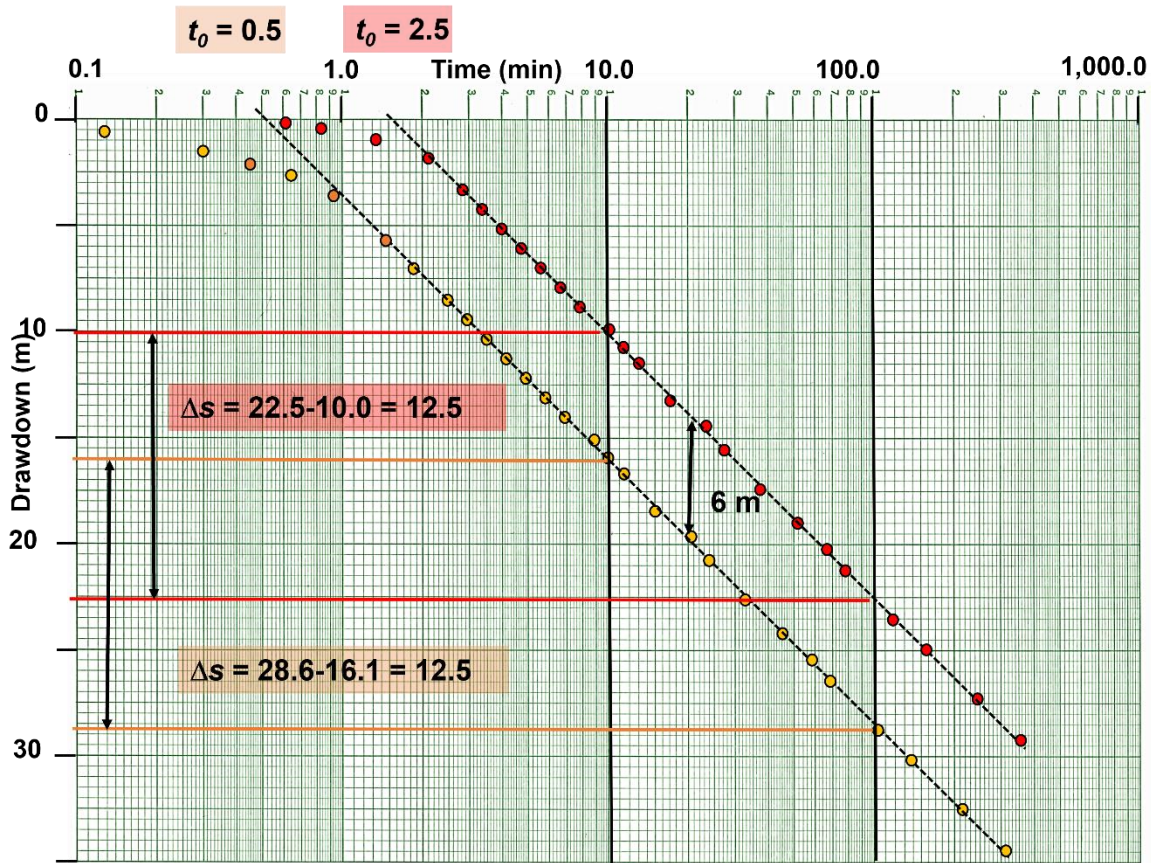


Figure 90 - Time-drawdown data for a pumping well finished in an isotropic and homogeneous confined aquifer. Orange solid dots represent field data collected at the pumping well and red solid dots show the formational drawdown at the pumping well if the effects of partial penetration and/or well loss are not occurring (corrected data). This example shows an offset (lower water levels) of 6 m. The slope of the two lines is the same. Calculations of T from uncorrected time-drawdown data (orange dots) yield the same T value as that derived from the corrected data (red dots). Since the lines are offset by additional drawdown the t_0 intercept used to calculate S is smaller for the field-measured drawdown than the corrected data set. As a result, the uncorrected data set represented by the orange dots will yield a poor estimate of S . Once again, if only uncorrected drawdown data are available, S can be approximated using methods described in Box 2.

12.2.2 Analyzing Recovery Data

Plots of calculated-recovery or residual-recovery (Section 8, Figure 36) data collected after shutdown of a single-well pumping test can be used to compute estimates of T and S . Partial-penetration effects are present during recovery and require correction of recovery data before analysis as described above.

The effect of well loss on recovery data is different than on drawdown data. Once the pump is shut off, the well-loss-impacted water level in the borehole is lower than the head directly outside the casing as shown in Figure 91. This results in rapid flow of water into the well bore until water levels inside and outside the casing are equal. Once this occurs water-level recovery is based on formational properties and no well-loss correction is required (Figure 91).

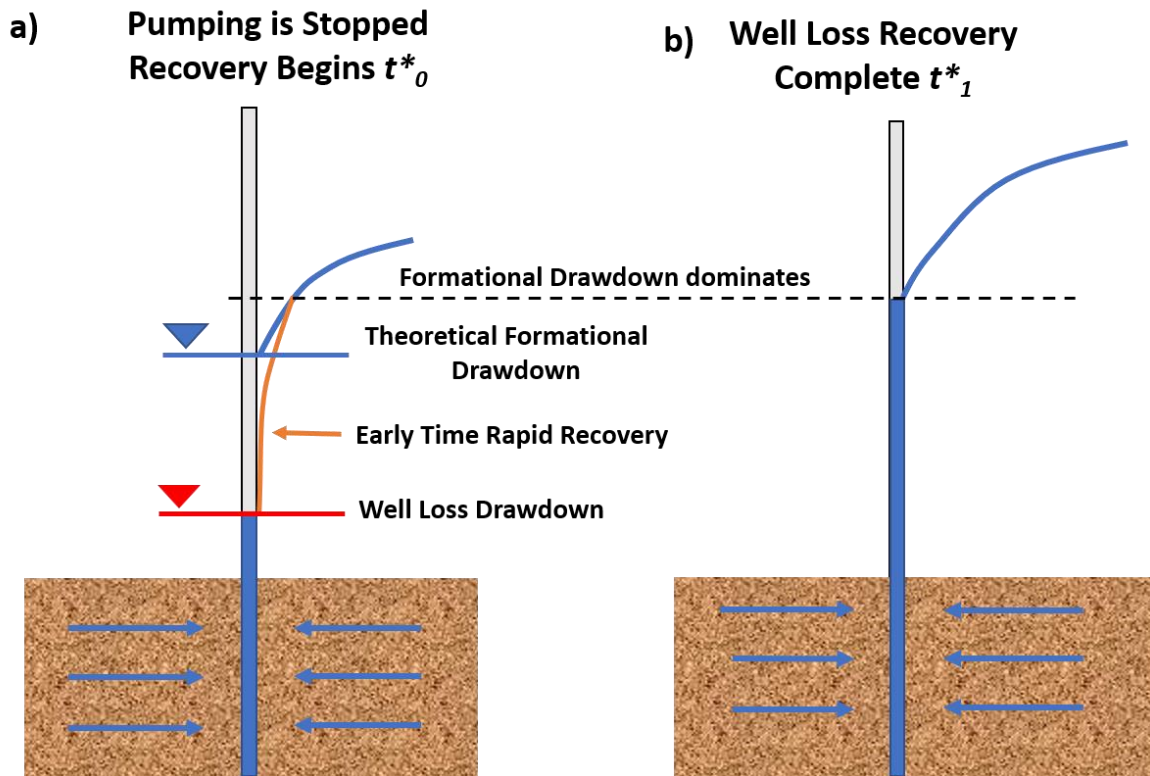


Figure 91 - Schematic of the effect of well loss on the pumping level during recovery for an isotropic and homogeneous confined aquifer. The blue line represents the theoretical formational drawdown level at the end of pumping if well loss is not present. The red line represents the effect of well loss at the end of pumping. a) Well loss causes the water level in the pumping well to be lower than if the well loss was zero. The sketch shows the position of the water level (red) when the pumping is complete and the pump is shut off, t^*_0 . The orange line represents the borehole water-level response once recovery begins. After the pumping stops water continues to move to the well under the field gradients. The steep gradient near the well between the water level in the wellbore (well loss level) and the head immediately outside of the wellbore (formational head) results in rapid flow of water into the well bore and rapid recovery of the water level in the pumping well so that it soon reflects the formational water level at the well radius (often within minutes of shutting off the well). b) After this, water level recovery in the pumping well follows the formational response. This later time-recovery data can be used to estimate T and S .

Hargis (1979) reported an example of the water level in a 40 percent efficient well that recovered to formational drawdown levels within four minutes after one day of pumping. Well-loss effects are negated once this resetting of the recovery water level has occurred. By ignoring early-time recovery data, the remaining water-level data will produce representative aquifer properties if the well is fully penetrating, and no other influences are affecting recovery water levels. Examples of the effect of well loss on early recovery data are illustrated in Figure 92.

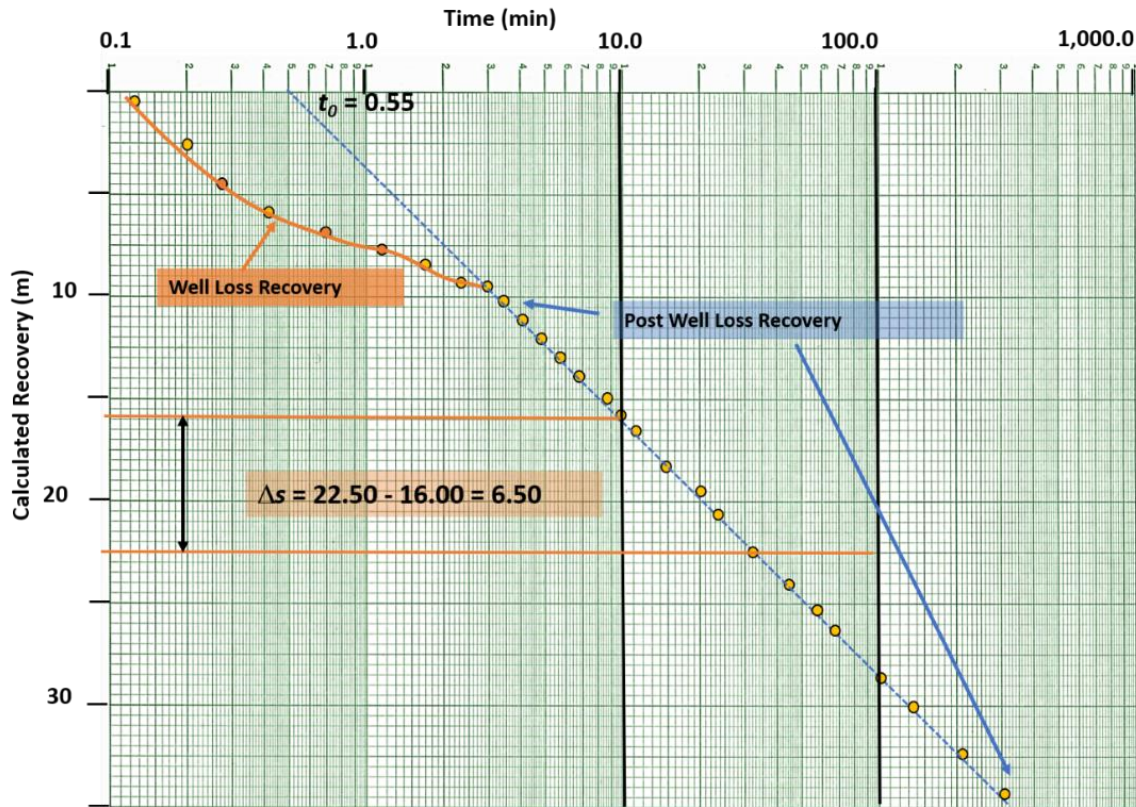


Figure 92 - Schematic of a log-log plot of calculated recovery data impacted by well loss for single-well pumping in an isotropic and homogeneous confined aquifer. The early-time data are impacted by the rapid rise in water levels caused by well loss recovery. The later time data, in this example after 10 minutes, are unaffected by the early-time change in water levels caused by well-loss recovery. A dashed blue line is fitted to the late-time data. If other additional conditions are not impacting the calculated recovery data (e.g., partial penetration) the calculated recovery data requires no further correction to estimate T and S .

If the well is partially penetrating, either the recovery data will need to be corrected to compute T and S , or as described in the drawdown section, log-log plots and semi-log plots can be used to compute T ; however, S will be poorly estimated.

12.3 Steady-State Approximation of Transmissivity

Pumping a well until steady-state conditions are generated allows for application of steady-state equations to solve for T . The pumping rate, the radius of the pumping well, and an estimate of the radial distance where drawdown is zero are needed to estimate T . The steady-state drawdown in the pumping well needs to be corrected for partial penetration and well losses so that it more closely represents formational drawdown. If this is not done T and K estimates will be underestimated as the observed drawdown at the well is lower than if only formational properties were controlling the pumping water level as shown in Figure 93.

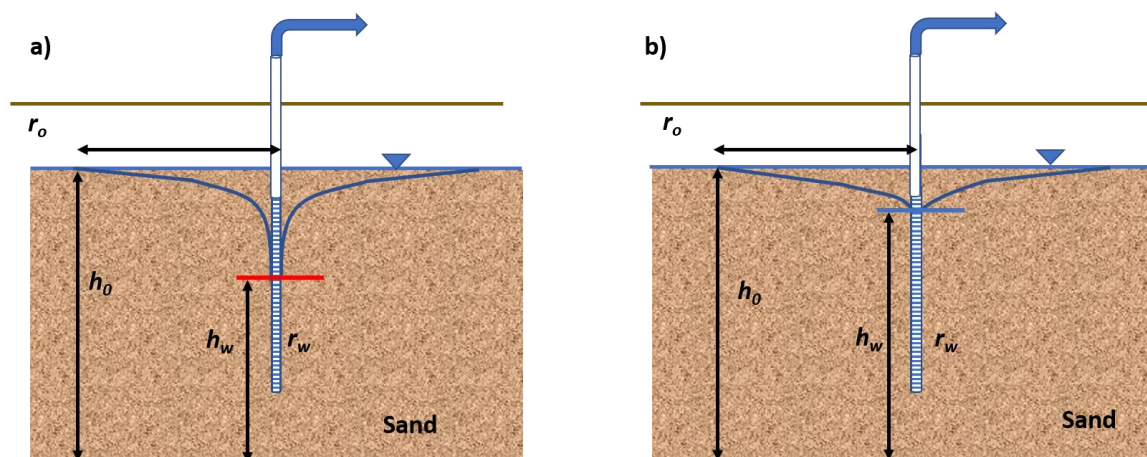


Figure 93 - Unconfined sand aquifer with a single pumping well. The saturated thickness of the aquifer at the well of radius r_w is h_w and the saturated thickness at the radial distance r_0 where drawdown is zero is h_0 . Values of h are measured from the aquifer base. a) The pumping level is impacted by well loss and partial penetration. b) Pumping-well drawdown is corrected for the effects of partial penetration and well loss.

The Thiem equation describing the relationship of the steady-state drawdown at two radial distances for unconfined and confined conditions is presented in Equation (97) and Equation (98), respectively, with Figure 94 presenting the parameters for confined aquifer systems. The corrected drawdown is paired with the well radius. For unconfined conditions, an arbitrary radial distance of 250 m is often used for the zero-drawdown distance and for confined aquifers an arbitrary value of 500 m is used.

$$K = \frac{Q}{\pi(h_0^2 - h_w^2)} \ln\left(\frac{r_0}{r_w}\right) \quad (97)$$

where:

- K = unconfined aquifer hydraulic conductivity (LT^{-1})
- Q = constant pumping rate (L^3T^{-1})
- h_0 = saturated thickness at the radius of zero drawdown (L)
- h_w = saturated thickness at the pumping well (L)
- r_0 = radial distance where drawdown is zero (L)
- r_w = radius of the pumping well (L)

$$T = \frac{Q}{2\pi(h_0 - h_w)} \ln\left(\frac{r_0}{r_w}\right) \quad (98)$$

where:

- T = confined aquifer transmissivity (Kb) (L^2T^{-1})
- Q = constant pumping rate (L^3T^{-1})
- h_0 = head at the radial distance where drawdown is zero (L)
- h_w = head at the pumping well (L)
- r_0 = radial distance at which drawdown is zero (L)

r_w = radius of the pumping well (L)

The well radius is represented by the effective radius (screen radius + gravel pack radius) when a gravel pack is present.

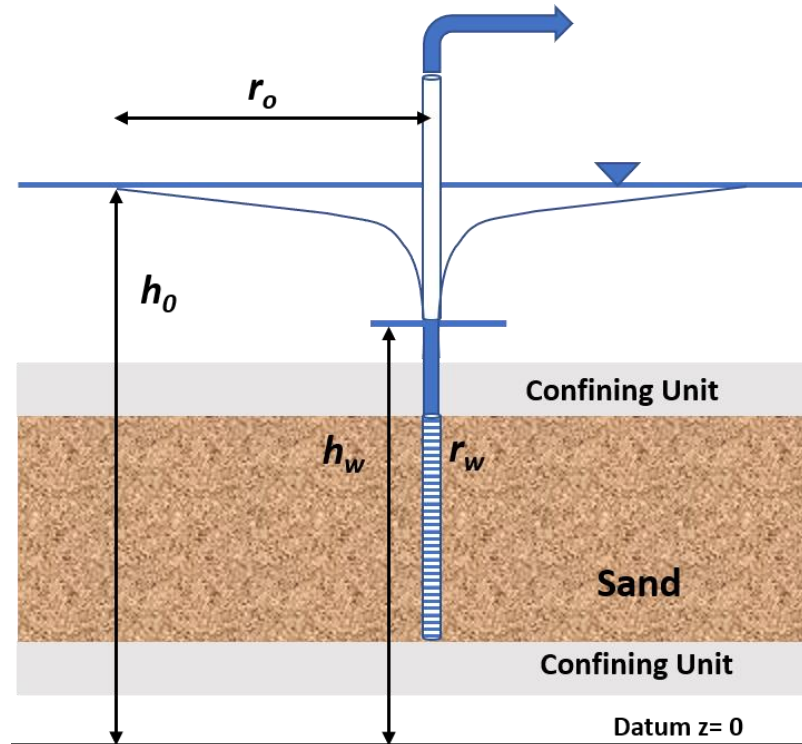


Figure 94 - Defining parameters for a steady-state single well pumping test in a confined aquifer. The head value, h_w , is assigned to the radius of the pumping well, r_w , and the head value, h_o , assigned to the radial distance, r_o , where no drawdown occurs, are measured from a horizontal datum. The pumping well drawdown requires correction for partial penetration and well loss.

Example

A single well penetrating a confined aquifer is pumped for 8 hours at a rate of 1000 m^3/d . The head at the pumping well with a radius of 0.05 m seems to have stabilized at 856.8 m. The static head at the beginning of the test is 879.1 m. Analysis of the partial penetration and well loss effects suggest they contribute an additional 8.4 m to the measured head. Compute T for the aquifer.

The head at r_w equals $856.8 \text{ m} + 8.4 \text{ m} = 865.2 \text{ m}$. The value is added because the measured head value (not drawdown) is lower than if only formational properties affected the response. At an estimated radial distance of 500 m (r_o) the head is equal to the static water level, 879.1 m. Then T is calculated using Equation (98).

$$T = \frac{1000 \frac{\text{m}^3}{\text{d}}}{2 (3.14) (879.1 \text{ m} - 865.2 \text{ m})} \ln \left(\frac{500 \text{ m}}{0.05 \text{ m}} \right) = 105.5 \frac{\text{m}^2}{\text{d}}$$

12.4 Performance Tests, Specific Capacity Data, and Estimating T

A performance test is typically conducted when a new production well is completed. Tests are primarily performed to estimate well yields and can also be used to estimate values of T .

The performance test involves measuring the starting water level, pumping a well at a constant rate for a period of time, and measuring the ending water level (at the time the pump is shut down). Transmissivity of the geologic material in which the well is completed is estimated by coupling this test with well-construction data that identifies the perforated interval and the degree of screen penetration, and geologic well logs to classify the water-bearing unit as confined or unconfined. Often performance-test data are provided on existing driller's logs. When such records are available, analysis costs are reduced because fieldwork is not required. Certainly, a hydrogeologist can conduct a performance test on an existing well using its pump or by installing a test pump in an unused well. However, if a hydrogeologist is going to pump a well it would be better to measure drawdown over time and then use single-well pumping-test analysis techniques to estimate properties as described in Section 12.2.

12.4.1 Cautions when Using Performance Test Results

Analysis of performance-test data often relies on the information a drilling contractor reports after completing a well. Data are most useful when a pump is used to produce the well yield. When new wells are completed, testing is often performed when the drill rig is still on the site before installing a pump. In these settings, static water levels are measured, and then water is either bailed or air-lifted from the well by setting the drill stem below the static water level and lifting the water out of the well with compressed air (Sterrett, 2007). The reported pumping rates are usually estimated. When a bailer is used discharge is determined by knowing the approximate volume of the bailer used and the number of bails per minute. If water is airlifted the discharge is estimated by periodically noting the time required to collect a known volume (e.g., a 5-gallon or 20-liter bucket) or measured with a flow meter on the outlet. Discharge may not be constant; thus, the reported value contains uncertainty. Further uncertainty is introduced because the final pumping water level is difficult to measure when these methods are used to extract water. Once bailing is stopped some recovery may occur in the pumping well before the water level is measured. Some recovery may also occur after airlifting is completed. Unfortunately, often the depth of the suspended drill rod (airlifting) and not the actual measured water level is reported as the final pumping level. When a pump is set and used to conduct the test, pumping rates and water levels are usually more reliable. Performance-test records should be used with caution and the realization that there is uncertainty in the reported flow rate and water levels. Professional judgment is needed to interpret the reported data.

The performance-test drawdown cannot be corrected for well loss because a step-drawdown test is not performed. If a step-drawdown test was performed it should be used to estimate aquifer properties instead of the performance test and the component of drawdown attributed to well loss would be defined as discussed in Section 12.1. Depending on the well construction, partial penetration may also impact reported drawdowns. The pumping level would need to be corrected (Equation (80)). If drawdown data are not corrected for well loss and/or partial penetration, drawdowns will be greater than drawdown in a fully penetrating and 100 percent efficient well. As a result, computed values of T will be underestimated and should be considered to provide only an order-of-magnitude estimate.

Storativity is not computed from performance-test data sets. Rather, it is estimated by the groundwater professional when transient conditions are assumed (Box 2). The selected value of S will result in only small changes to the estimated values of T .

12.4.2 Methods to Estimate Transmissivity from Performance Tests

First, it must be determined whether the well is completed in a confined or unconfined unit by assessing the reported geological sequence of materials, the static water level in the well, the driller's reported first encounter of water (water table), and the location and extent of the perforated interval. Not all drillers' logs have complete information on the first water encountered, so professional judgment, the geological literature, and nearby well logs are often required to assign the well to a confined or unconfined aquifer.

Using performance test data, T can be estimated by calculating the specific capacity of a well. Specific capacity is the well yield divided by the drawdown reported for the length of pumping time as in Equation (99). Generally, if multiple performance tests are examined and pumping durations are similar, the larger the specific capacity of a well the greater the T of the formation.

$$\text{Specific Capacity} = \frac{Q}{s_F} \quad (99)$$

where:

Q = constant pumping rate (L^3T^{-1})

s_F = drawdown corrected for partial penetration and well loss at some time
(L)

However, specific capacity varies with time, becoming smaller as time and drawdown increase (Figure 95). Ideally, a representative specific capacity would only be reported once steady-state conditions had been reached. However, this is rarely the case, as performance tests often only last one-half hour to two hours. Methods used to estimate T from specific-capacity data include interpreting data as representing steady-state and transient conditions as discussed in Sections 12.4.3 through 12.4.5. However, aquifer-property

estimates computed using specific-capacity data should be considered as reconnaissance level, rough estimates, or order of magnitude values. In many cases well and testing data may be incomplete, or several assumptions are required to apply equations making results more uncertain. However, when used with an appreciation for their limitations, methods to characterize aquifer properties can be useful.

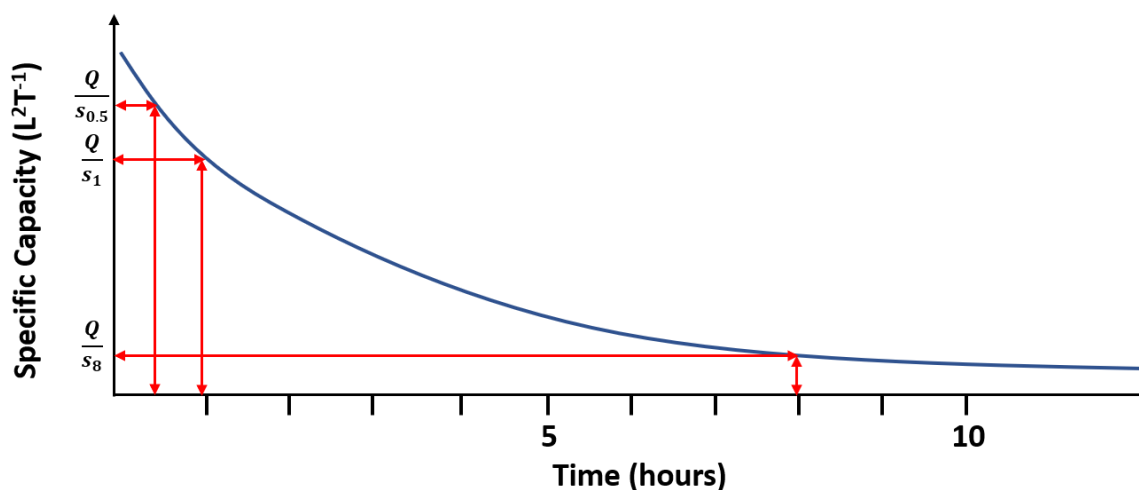


Figure 95 - Schematic arithmetic plot of the transient change in specific capacity during pumping at a constant rate. The shape of the curve illustrates that head response to pumping is logarithmic. Computed specific capacities are higher at early times and smaller at later times. $Q/s_{0.5}$ corresponds to the specific capacity computed after 0.5 h of pumping. In this illustration, the time scale suggests that changes in drawdown become small after 5 to 10 hours of pumping and thus changes in the computed values of specific capacity are also small. If drawdown reaches a steady state, the specific capacity becomes constant.

12.4.3 Using Specific Capacity to Estimate Transmissivity Assuming Steady-State Conditions

As discussed in Section 12.3, when performance-test data are assumed to represent drawdown at steady state, the corrected well drawdown (for partial penetration) can be used in the Thiem Equations (Equations (97) and (98)). For confined systems T is a function of the head at the pumping well (assigned to r_w , the radius of the pumping well) and the head at the radial distance at which drawdown is zero, r_0 . Values of r_0 are assumed to be 250 m and 500 m for unconfined or confined systems respectively. Again, as a caution, performance tests may not represent steady-state conditions because pumping durations are often too short. Near steady-state conditions can occur when pumping rates are low and water-bearing materials are highly transmissive, and/or when recharge boundaries are encountered after short pumping times.

12.4.4 Using Specific Capacity Data to Estimate Transmissivity Assuming Transient Conditions

Well-performance data can be used to estimate T when pumping duration is short and conditions are assumed to be transient. For example, if the test is run for only 30 min to an hour, it is likely that the recorded drawdown does not represent steady-state conditions. Assuming the confined Cooper-Jacob approximation can be used to represent

transient conditions where S is estimated (for confined or unconfined conditions, Box 2) and the time used in the analyses is the duration of pumping recorded for the test, then the Theis assumptions are applied as shown in Equations (100) and (101).

$$\frac{s}{Q} = \frac{1}{4\pi T} 2.30 \log \left(2.25 \frac{Tt}{r_w^2 S} \right) \quad (100)$$

$$\frac{Q}{s} = \frac{1}{\frac{1}{4\pi T} 2.30 \log \left(2.25 \frac{Tt}{r_w^2 S} \right)} \quad (101)$$

where:

- s = corrected final drawdown (L)
- Q = constant well discharge (L^3T^{-1})
- T = transmissivity (L^2T^{-1})
- \log = logarithm base 10
- t = duration of the performance test (T)
- r_w = radius of the pumping well (L)
- S = storativity (estimated) (dimensionless)

The well radius is represented by the effective radius (screen radius + gravel pack radius) when a gravel pack is present.

A log-log graphical solution to Equation (101) is obtained by plotting the Q/s versus T with values of $T = 100, 1,000, \text{ and } 10,000 \text{ m}^2/\text{d}$ substituted into Equation (101) along with the radius of the pumping well, the pumping rate, the length of time the well was pumped, and an estimate of S as discussed in Box 2 as shown in Figure 96.

Example

If a 0.15-m-radius well penetrating a confined aquifer with $S = 0.0001$ (estimated) is pumped for 30 minutes (0.02 d) and has a specific capacity of $4,000 \text{ m}^3/\text{d} / 9 \text{ m} = 444.4 \text{ m}^2/\text{d}$, then the corresponding Q/s for the values of $T = 100, 1,000 \text{ and } 10,000 \text{ m}^2/\text{d}$ are $86 \text{ m}^2/\text{d}$, $743 \text{ m}^2/\text{d}$, and $6,538 \text{ m}^2/\text{d}$. A log-log plot of the relationship is produced, and a straight line is fitted to the data. Then the specific capacity value derived from the performance test, $444.4 \text{ m}^2/\text{d}$ is used to determine the corresponding value of T , $600 \text{ m}^2/\text{d}$ as shown in Figure 96.

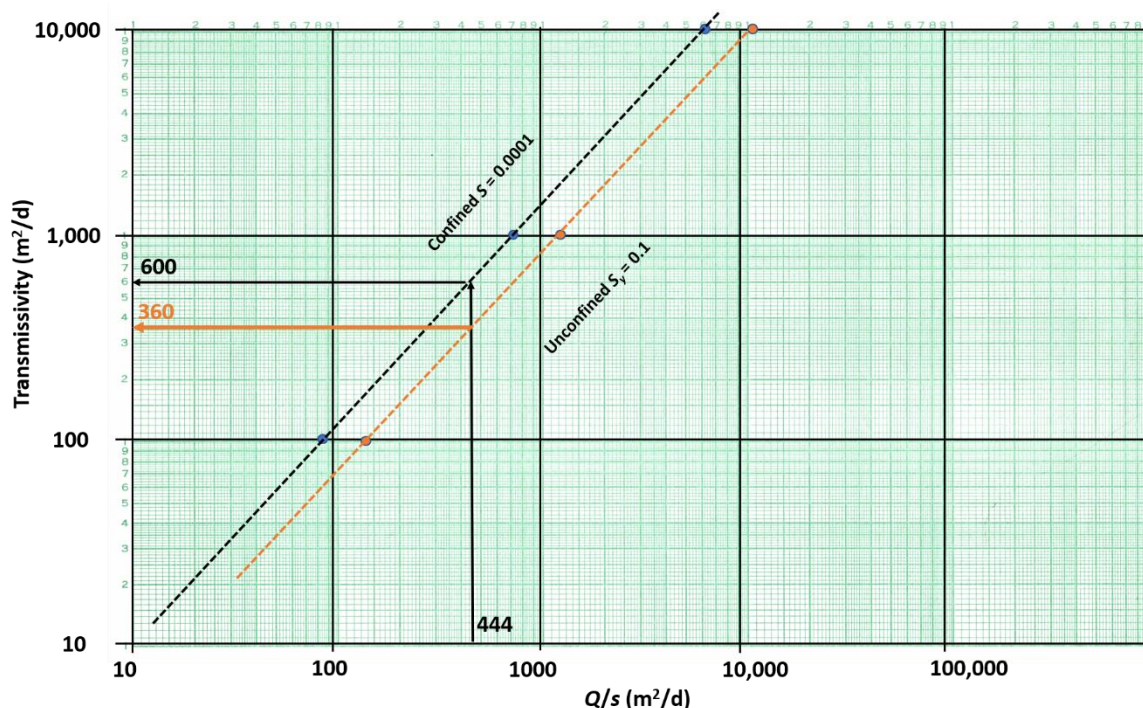


Figure 96 - Log-log plot of specific capacity and transmissivity for a 0.15 m radius well pumping at 4,000 m³/d for 30 minutes, and fully penetrating a confined aquifer with a storativity of 0.0001 (blue dots and black dashed fitted line). The specific capacity of the pumping well after 30 min (0.02 d) of pumping was 444 m²/d. The corresponding *T* value for a confined water-bearing unit with the stated properties is 600 m²/d. If the penetrated material was unconfined with a storativity of 0.1, the values would be the orange dots which are fitted with the orange dashed line, and the result is shown with solid orange arrows. The corresponding transmissivity value is 360 m²/d.

The Cooper-Jacob approximation can also be used to describe the general behavior of an unconfined unit without much change in saturated thickness near the pumping well.

Walton (1970) evaluated the positions and slopes of plots like those shown in Figure 96. He showed that at longer pumping times (>8 hours) fitted lines for the confined aquifer and unconfined aquifer changed little in position and had a constant slope. Todd and Mays (2005) show transient results of changes in specific capacity, storativity, and transmissivity for confined aquifers after 1 day of pumping at a constant rate (Figure 97).

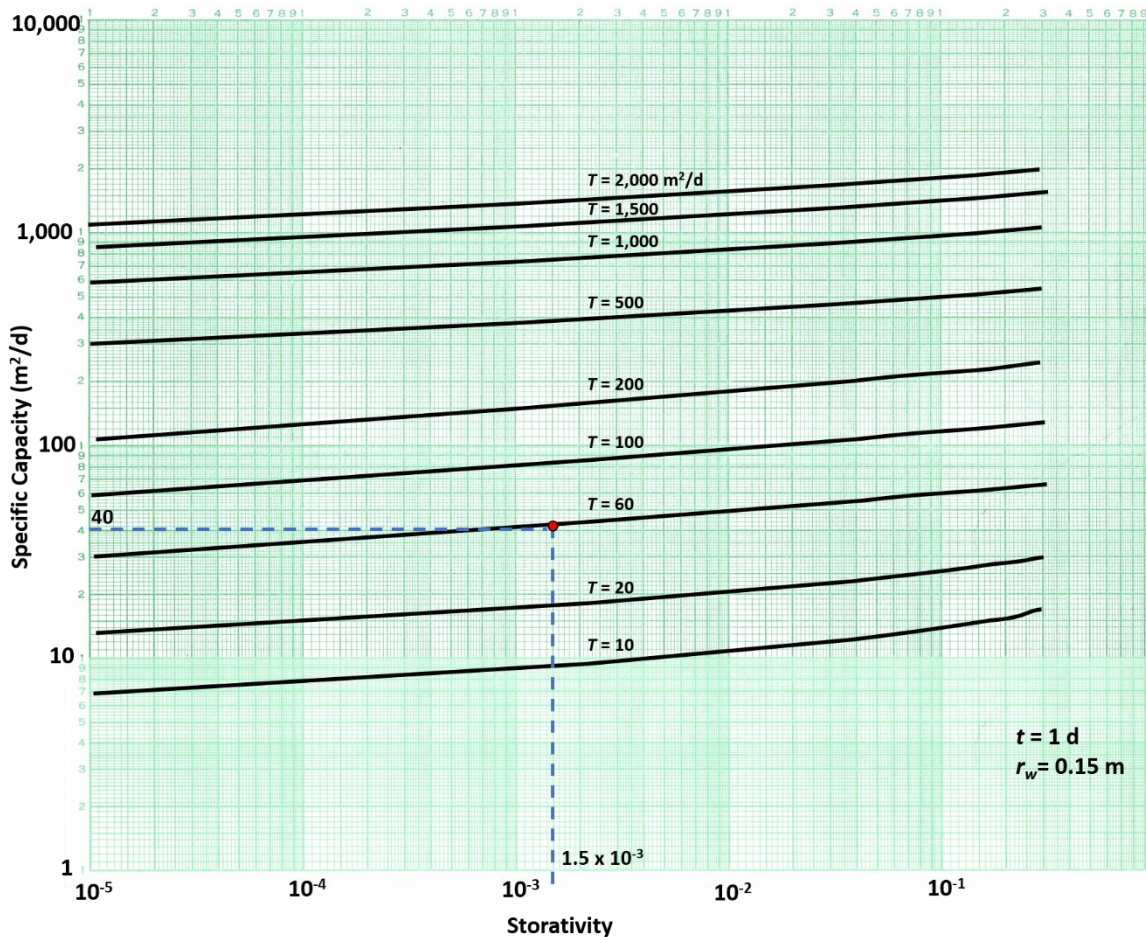


Figure 97 - Relationship of specific capacity, storativity, and transmissivity for a single, 100 percent efficient, pumping well that fully penetrates a confined aquifer. The well has a radius of 0.15 m and is pumped for 1 day. *T* values are derived by selecting the specific capacity value and the storativity value (dashed blue lines) and then interpreting the value of *T*. In this example, the tested well has a specific capacity of 40 m²/d and a storativity of 1.5 X 10⁻³, thus the estimated *T* value is 60 m²/d (modified from Todd & Mays, 2005; Bentall, 1963).

The transmissivity relationship for a fully penetrating, 100-percent efficient well shown in Figure 97 is not very sensitive to the value of storativity (i.e., the lines are almost horizontal). The use of such plots assumes that *Q/s* is near steady state (declining very slowly) which may be a reasonable assumption after 1 full day of pumping a well at a constant rate. However, such long-term pumping rates are rarely used when well performance tests are conducted (e.g., they are typically 30 minutes to 2 hours).

12.4.5 Basic Equations Relating Specific Capacity to Transmissivity

Kasenow (2001) thoroughly discusses how specific-capacity data can be used to estimate transmissivity. Other authors have suggested simplified relationships between specific capacity and transmissivity like the graphical data presented in Figure 97. Driscoll (1986) and others suggested a general estimate of *T* from the specific capacity for a pumping well that penetrates a confined or unconfined

aquifer could be obtained using Equations (102) and (103). These equations assume general properties of the formations. The duration of pumping is not considered, yet Q/s changes with time. These equations should be used cautiously as they assume Q/s is a representative value of groundwater conditions.

Transmissivity for confined conditions is estimated using Equation (102) as presented by Driscoll (1986).

$$T = 1.39 \left(\frac{Q}{s} \right) \quad (102)$$

Transmissivity for unconfined conditions is estimated using Equation (103) Driscoll (1986).

$$T = 1.04 \left(\frac{Q}{s} \right) \quad (103)$$

where:

- T = transmissivity (L^2T^{-1})
- Q = constant discharge (L^3T^{-1})
- s = drawdown in a fully penetrating and 100 percent efficient well (L)

Studies of areas with both performance tests and pumping tests with observation wells have been used to develop empirical relationships between specific capacity and T . Razack and Huntley (1991) looked at over 200 pairs of performance and pumping tests for wells in an alluvial basin. They found that pumping test-derived T values were underestimated by the specific-capacity data. These differences were attributed to the presence of turbulent well loss in the specific-capacity data. They generated the relationship for T shown in Equation (104).

$$T = 15.3 (Q/s)^{0.67} \quad (104)$$

where (in units of meters and days):

- T = transmissivity in m^2d^{-1}
- Q = constant discharge in m^3d^{-1}
- s = drawdown in a fully penetrating and 100 percent efficient well in m

Using equations developed for specific study areas may not be appropriate as conditions for a particular well and hydrogeologic setting may be different than those from which a relationship was derived.

This section introduced several methods to estimate T using pumping and drawdown data from a single well. When possible, drawdown should be corrected for factors impacting the total drawdown such as partial penetration, well loss, well interference, and other factors described in this section. Well loss is best addressed by

conducting a step-drawdown test. However, when only performance-test results are available, T can still be estimated, but the computed value is likely to be lower than the field value.

The best approach to using single-pumping-well data is to perform constant-rate discharge tests where drawdown is measured over time. Analyses of such data allow the use of traditional curve-matching and semi-log plotting methods which produce more representative values of T .

The following section addresses how software tools are used to generate estimates of T and S . In most cases such programs apply analytical models with methods similar to curve matching to generate aquifer properties.

12.5 An Opportunity to Evaluate Hydrogeologic Properties Using Data from a Pumping Well

Section 12 discussed estimating hydraulic properties using single-well test data. [Exercise 5](#) and [Exercise 6](#) provide hands-on opportunities to use some of these techniques.

13 Using Software to Analyze Hydraulic Test Data with a Pumping Well

This section describes the use of software to analyze pumping-test data using analytical models, manual curve matching (as described in previous Sections), and automated-analysis methods. It focuses on three commercially available software packages, AQTESOLV (aqtesolv.com), AquiferTest V12 (waterloohydrogeologic.com), and Aquifer^{win32} Version 6 (groundwatermodels.com). Each allows the user to select from a dozen or more analytical models (i.e., equations).

These software packages use graphical user interfaces that produce computer-generated plots and type curves and apply sophisticated numerical methods to automate the analysis of hydraulic-testing data. In addition to standard conditions (e.g., confined, leaky confined and unconfined) these programs often incorporate analyses of the effects of partial penetration, anisotropic conditions, the presence of significant well-bore storage, effects of variable pumping rates, and the analysis of constant-head tests, as well as the response of fractured and dual-porosity systems to pumping (e.g., Moench, 1984). The programs also include methods to determine pumping-well efficiency, aquifer properties from single-pumping-well tests and step-drawdown tests. Some of the programs have predictive modeling capabilities that given hydraulic properties and conditions generate a head distribution resulting from pumping at a specified rate and schedule.

This section is intended to broadly describe the function and capabilities of the three most widely used commercially available software programs, but not include specifics on the operation of each program. Some additional detail regarding individual tools is provided in referenced boxes. The extensive documentation included with the individual software packages provide information on features that are not discussed here.

Each software system includes a demonstration or trial version that can be accessed without cost to explore program features. In addition to these commercially available tools, programs developed by researchers that include numerical methods or spreadsheets are often described in the groundwater literature. Some options for freeware that can be used to analyze pumping-test data are listed here.

- PyTheis-A python tool for analyzing pump test data, doi.org/10.3390/w13162180 (Chang et al., 2021)
- Wells-A multi-well, variable-rate, pumping-test analysis tool from Los Alamos National Laboratory in the USA, <https://wells.lanl.gov/>, (originally developed at the University of Mining and Geology, Sofia, Bulgaria, in 1992 by Velimir V. Vesselinov)

- Spreadsheets for the Analysis of Aquifer-Test and Slug-Test Data, <https://pubs.usgs.gov/of/2002/ofr02197/spreadsheets.html> (Halford & Kuniansky, 2002)
- Simple Procedures for Analysis of Slug Tests in Formations of High Hydraulic Conductivity using Spreadsheet and Scientific Graphics Software kgs.ku.edu/Hydro/Publications/OFR00_40/ (Butler & Garnett, 2000)
- Automated Estimation of Aquifer Parameters from Arbitrary-Rate Pumping Tests in Python and MATLAB that can solve for aquifer-parameter using values from multiple wells <https://ngwa.onlinelibrary.wiley.com/doi/abs/10.1111/gwat.13338> (Benson, 2023)
- DISOLV: A Python package for the interpretation of borehole dilution tests https://nora.nerc.ac.uk/id/eprint/527089/1/Collins_et_al-2020-Groundwater.pdf (Collins & Bianchi, 2020)

A literature search may provide other applicable non-commercial tools that can be used to assess specific conditions.

13.1 Pumping Test Analysis Software Packages

The three software packages described this section include AQTESOLV (<http://www.aqtesolv.com>), AquiferTest V12 (waterloohydrogeologic.com), and Aquifer^{win32} Version 6 (groundwatermodels.com). Each includes a number of analytical models that can be used to analyze pumping tests of confined, leaky confined, unconfined, and fractured-rock or dual-porosity conditions. They also provide analysis of step-drawdown tests and slug tests. Both drawdown and recovery data can be assessed.

Each program provides the user with a number of methods to assess pumping tests. For example, AQTESOLV software addresses application of 13 solution techniques for confined-aquifer conditions, seven for leaky aquifers, five for unconfined systems, five for fractured aquifers, and nine solutions for constant-head tests (Figure 98).

Aqtesolv Methods for Hydraulic Test Analysis

Confined Aquifers

Theis (1935)/Hantush (1961) Solution for a Pumping Test in a Confined Aquifer
 Theis (1935) Solution for a Recovery Test in a Confined Aquifer
 Theis (1935) Solution for a Step-Drawdown Test in a Confined Aquifer
 Cooper-Jacob (1946) Solution for a Pumping Test in a Confined Aquifer
 Moench-Prickett (1972) Solution for a Pumping Test in a Confined/Unconfined Aquifer
 Butler (1988) Solution for a Pumping Test in a Confined Aquifer
 Papadopulos-Cooper (1967) Solution for a Pumping Test in a Confined Aquifer
 Dougherty-Babu (1984) Solution for a Pumping Test in a Confined Aquifer
 Dougherty-Babu (1984) Solution for a Step-Drawdown Test in a Confined Aquifer
 Hantush (1962) Solution for a Pumping Test in a Wedge-Shaped Confined Aquifer
 Murdoch (1994) Solution for a Pumping Test in a Confined Aquifer
 Daviau et al. (1985) Solution for a Pumping Test in a Confined Aquifer
 Barker (1988) Solution for a Pumping Test in a Confined Aquifer

Leaky Aquifers

Hantush-Jacob (1955)/Hantush (1964) Solution for a Pumping Test in a Leaky Aquifer
 Hantush-Jacob (1955) Solution for a Step-Drawdown Test in a Leaky Aquifer
 Hantush (1960) Solution for a Pumping Test in a Leaky Aquifer
 Cooley-Case (1973) Solution for a Pumping Test in a Confined Aquifer Overlain by a Water-Table
 Aquitard
 Neuman-Witherspoon (1969) Solution for a Pumping Test in a Leaky Aquifer
 Moench (1985) Solution for a Pumping Test in a Leaky Aquifer

Unconfined Aquifers

Theis (1935) Solution for a Pumping Test in an Unconfined Aquifer
 Cooper-Jacob (1946) Solution for a Pumping Test in an Unconfined Aquifer
 Neuman (1974) Solution for a Pumping Test in an Unconfined Aquifer
 Moench (1997) Solution for a Pumping Test in an Unconfined Aquifer
 Tartakovsky-Neuman (2007) Solution for a Pumping Test in an Unconfined Aquifer

Fractured Aquifers

Moench (1984) Solution for a Pumping Test in a Fractured Aquifer
 Gringarten-Witherspoon (1972) Solution for a Pumping Test in a Fractured Aquifer
 Gringarten-Ramey-Raghavan (1974) Solution for a Pumping Test in a Fractured Aquifer
 Gringarten-Ramey (1974) Solution for a Pumping Test in a Fractured Aquifer
 Barker (1988) Solution for a Pumping Test in a Fractured Aquifer

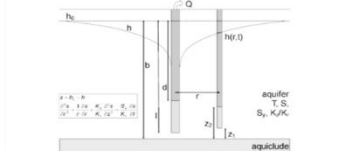
Figure 98 - Example of analytical solutions describing conditions in confined, leaky confined, unconfined, and fractured aquifers provided by the standard and professional versions of AQTESOLV. The solutions are organized by pumping tests of confined, leaky confined, unconfined, and fractured aquifers. References for each supported analysis method are listed. Full references are provided in the reference section of this book. Professional judgment is used to appropriately match the model to the field conditions prior to applying one of these models (modified from <http://www.aqtesolv.com>).

These software packages provide complete references for incorporated analytical solutions and include detailed information on the related simplifying assumptions, limitations, and application of each solution. Many of the methods are also described in the work of Kruseman and de Ridder (2000), *Analysis and Evaluation of Pumping Test Data*⁷, a

book that is available free-of-charge on the gw-project.org website. Users should become familiar with the specific analytical model before applying it to analyze hydraulic-test data. The appropriate conceptual model and corresponding limitations must be recognized to avoid misuse of a selected solution.

An example of the type of documentation provided by the software AQTESOLV to address unconfined pumping-test results is presented in Figure 99.

AQTESOLVE Explanation of the Neuman Method to Analyze Unconfined Conditions with Delayed Yield



Shlomo P. Neuman (b. 1938), Regents Professor Emeritus of Hydrology and Water Resources at the University of Arizona, derived an analytical solution for unsteady flow to a fully or partially penetrating well in an anisotropic unconfined aquifer with delayed gravity response. The solution assumes a line source for the pumped well and therefore neglects wellbore storage.

The **Neuman (1974)** solution may be used to determine the hydraulic properties (**transmissivity**, **elastic storage coefficient**, **specific yield**) and vertical hydraulic conductivity of **unconfined** (water-table or phreatic) **aquifers**. Analysis involves matching type curves to drawdown data collected during a pumping test.

The **delayed yield response** described by the Neuman model assumes instantaneous drainage at the water table and exhibits **three distinct drawdown segments**. Early-time response is controlled by the transmissivity and elastic storage coefficient and is analogous to the response of a confined aquifer. Late-time response is a function of transmissivity and specific yield (drainable porosity). At intermediate time, response is controlled by the aquifer's vertical hydraulic conductivity.

Traditionally, one matches **Type A curves** to early-time drawdown data and **Type B curves** to late-time response (**Neuman 1975**). **AQTESOLV** provides tools for Type A and Type B visual curve matching plus **specialized curves** for the interpretation of delayed yield in a water-table aquifer.

AQTESOLV uses computational enhancements by Moech (**1993, 1996**) to calculate type curves for the Neuman solution.

You are not restricted to constant-rate tests with the Neuman solution. **AQTESOLV** incorporates the principle of superposition in time to simulate variable-rate and recovery tests with this method.

Assumptions

- ✓ aquifer has infinite areal extent
- ✓ aquifer is homogeneous, anisotropic and of uniform thickness
- ✓ control well is fully or partially penetrating
- ✓ aquifer is unconfined with delayed gravity response
- ✓ flow is unsteady
- ✓ diameter of a pumping well well is very small so that storage in the well can be neglected

Equations

The **Neuman (1974)** equations for unsteady flow to a partially penetrating well in an unconfined aquifer with delayed gravity response are as follows:

$$s = \frac{Q}{4\pi T} \int_0^\infty 4\mu J_0(\mu\sqrt{\beta}) \left[u_0(y) + \sum_{n=1}^\infty u_n(y) \right] d\mu \quad (1)$$

$$\beta = \frac{r^2 K_z}{b^2 K_r} \quad (2)$$

$$\sigma = \frac{S}{S_y} \quad (3)$$

$$t_s = \frac{Tt}{S_y r^2} \quad (4)$$

$$s_D = \frac{4\pi T}{Q} s \quad (5)$$

Drawdown in a piezometer is found using the following equations:

$$u_0(y) = \frac{[1 - \exp(-t_s \beta (y^2 - \gamma_n^2))] \cosh(\gamma_n z_D)}{[y^2 + (1 + \sigma)\gamma_n^2 - (y^2 - \gamma_n^2)^2 / \sigma] \cosh(\gamma_n)} \cdot \frac{\sinh(\gamma_n(1 - d_D)) - \sinh(\gamma_n(1 - l_D))}{(l_D - d_D) \sinh(\gamma_n)} \quad (6)$$

$$u_n(y) = \frac{[1 - \exp(-t_s \beta (y^2 + \gamma_n^2))] \cos(\gamma_n z_D)}{[y^2 + (1 + \sigma)\gamma_n^2 - (y^2 + \gamma_n^2)^2 / \sigma] \cos(\gamma_n)} \cdot \frac{\sin(\gamma_n(1 - d_D)) - \sin(\gamma_n(1 - l_D))}{(l_D - d_D) \sin(\gamma_n)} \quad (7)$$

The following equations are used to evaluate drawdown in a partially penetrating observation well:

$$u_0(y) = \frac{[1 - \exp(-t_s \beta (y^2 - \gamma_n^2))] [\sinh(\gamma_n z_{2D}) - \sinh(\gamma_n z_{1D})]}{[y^2 + (1 + \sigma)\gamma_n^2 - (y^2 - \gamma_n^2)^2 / \sigma] \cosh(\gamma_n)} \cdot \frac{\sinh(\gamma_n(1 - d_D)) - \sinh(\gamma_n(1 - l_D))}{(z_{2D} - z_{1D})(l_D - d_D) \sinh(\gamma_n)} \quad (8)$$

$$u_n(y) = \frac{[1 - \exp(-t_s \beta (y^2 + \gamma_n^2))] [\sin(\gamma_n z_{2D}) - \sin(\gamma_n z_{1D})]}{[y^2 + (1 + \sigma)\gamma_n^2 - (y^2 + \gamma_n^2)^2 / \sigma] \cos(\gamma_n)} \cdot \frac{\sin(\gamma_n(1 - d_D)) - \sin(\gamma_n(1 - l_D))}{(z_{2D} - z_{1D})(l_D - d_D) \sin(\gamma_n)} \quad (9)$$

The gamma terms in (6)-(9) are the roots of the following equations:

$$\sigma \gamma_n \sinh(\gamma_n) - (y^2 - \gamma_n^2) \cosh(\gamma_n) = 0, \quad \gamma_n^2 < y^2 \quad (10)$$

$$\sigma \gamma_n \sin(\gamma_n) + (y^2 + \gamma_n^2) \cos(\gamma_n) = 0 \quad (11)$$

$$(2n - 1)(\pi/2) < \gamma_n < n\pi, \quad n \geq 1$$

where

- b is aquifer thickness [L]
- d_D is dimensionless depth to top of pumping well screen (d/b)
- J_0 is Bessel function of first kind, zero order
- K_r is the radial (horizontal) hydraulic conductivity [L/T]
- K_z is the vertical hydraulic conductivity [L/T]
- l_D is dimensionless depth to bottom of pumping well screen (l/b)
- Q is pumping rate [L³/T]
- r is radial distance from pumping well to observation well [L]
- s is drawdown [L]
- S is elastic storage coefficient [dimensionless]
- S_y is specific yield [dimensionless]
- t_s is dimensionless time with respect to S
- t is elapsed time since start of pumping [T]
- T is transmissivity [L²/T]
- y is a variable of integration
- z_D is dimensionless elevation of piezometer opening above base of aquifer (z/b)
- z_{1D} is dimensionless elevation of bottom of observation well screen above base of aquifer (z_1/b)
- z_{2D} is dimensionless elevation of top of observation well screen above base of aquifer (z_2/b)

The foregoing equations developed by Neuman (1974) can be difficult to evaluate in practice; therefore, **AQTESOLV** incorporates more efficient numerical methods developed by Moech (**1993, 1996**) for the computation of the Neuman solution.

Data Requirements

- ✓ pumping and observation well locations
- ✓ pumping rate(s)
- ✓ observation well measurements (time and displacement)
- ✓ aquifer saturated thickness
- ✓ partial penetration depths (optional)

Solution Options

- ✓ variable pumping rates
- ✓ multiple pumping wells
- ✓ multiple observation wells
- ✓ partially penetrating pumping and observation wells
- ✓ boundaries

Estimated Parameters

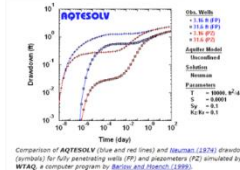
- ✓ T (transmissivity)
- ✓ S (elastic storage coefficient)
- ✓ S_y (specific yield)
- ✓ β or K_z/K_r (hydraulic conductivity anisotropy ratio)

AQTESOLV displays β for tests with a single observation well or K_z/K_r for multiple observation wells.

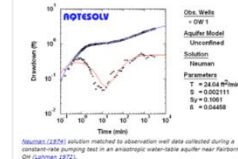
Curve Matching Tips

- Use the **Cooper and Jacob (1946)** solution to obtain preliminary estimates of aquifer properties. Determine T by matching a straight line to late-time data. If the wells are fully penetrating, you also may estimate S from the late-time match. Obtain an approximate estimate S from early-time data.
- Choose **Match-Visual** to perform visual curve matching using the procedure for type curve solutions.
- Use active type curves for more effective visual matching with variable-rate pumping tests.
- Select values of β and K_z/K_r from the Family and Curve drop-down lists on the toolbar.
- Use parameter tweaking to perform visual curve matching and sensitivity analysis.
- Perform visual curve matching prior to automatic estimation to obtain reasonable starting values for the aquifer properties.

Benchmark



Example



Neuman (2006) solution matched to observation well data collected during a constant-rate pumping test in an anisotropic water-table aquifer near a fault. (See caption 2.2.2.2)

References

Neuman, S.P., 1974. Effect of partial penetration on flow in unconfined aquifers considering delayed gravity response. Water Resources Research, vol. 10, no. 2, pp. 303-312.

Figure 99 - Explanation of the Neuman solution for unconfined aquifers as presented in AQTESOLV. A general description, assumptions, the analytical equation, data requirements, solution options, estimated parameters, curve matching tips, benchmark, example, and the reference are provided (from the aqtesolv.com web site).

All too often, some software users try to fit all the models available in a software package to the test data until they find a fit. However, a selected analytical model must match the appropriate site conceptual model and hydrologic conditions. A confined fractured-rock solution (Baker, 1988; Figure 98) does not appropriately represent the behavior of an unconfined sand and gravel aquifer! Additional concerns are expressed by experienced users. Van der Kamp & Neville (personal communication, 2023) make three important points:

1. Computer-assisted interpretation packages are frequently applied with separate analyses for the pumping well and the individual observation wells. This practice should be avoided. The user is responsible for obtaining internally consistent parameter estimates and for identifying those wells for which the responses are not representative of the bulk formation. Obtaining varying parameter estimates by fitting a model that assumes constant parameters only demonstrates that the data are being matched with the wrong model.
2. The software may obtain non-physical parameter estimates. It is up to the user to identify when a parameter estimate is unrealistic, and to understand why.
3. Although the software may report parameter estimates with many significant figures, hydrogeologists should never do so.

Available software packages are powerful and extremely useful when properly applied.

13.2 Data Plotting and Curve-Matching Methods

Software packages accommodate importing time-drawdown data from spreadsheets or data recorders. Plot choices include linear, semi-log or log-log plots. In addition, a plot of the slope of the drawdown curve can be selected as an option. This plot of $\Delta s/\Delta \log(t)$ is called a derivative plot (Figure 100). A derivative plot of the appropriate type curve and field data can be used to further support the automatically-derived, or visually-aided, curve match. Typically, the software generates the drawdown derivative over specified time intervals calculated as shown in Figure 101. If the size of the time interval is small then the derivative plot can be noisy, making it difficult to identify trends. Typically, methods to reduce noise and smooth the data are implemented. AQTESOLV provides three methods to smooth the derivative data including methods by Bourdet and others (1989) as well as by Spane and Wurstner (1993).

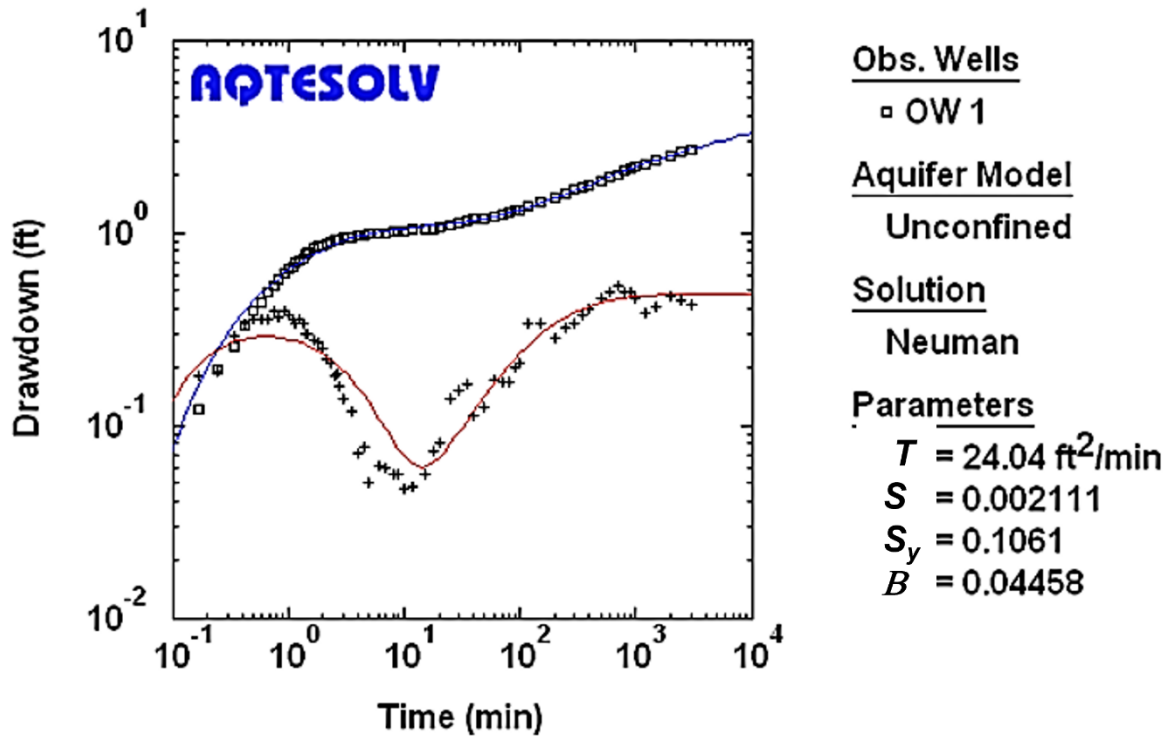


Figure 100 - Log-log plot of observation well time-drawdown (squares) and computed time derivative data (plus signs) for a hydraulic test of an unconfined aquifer produced in AQTESOLV (Neuman, 1972). Parameters are in units of gallons, feet, and days. Type-curve solutions derived by using the Neuman analytical representation were selected for curve matching (blue line is the type curve and red line is the computed derivative of the selected type curve) (from the aqtesolv.com web site).

The following simple formula is used to compute the derivative:

$$\left(\frac{\partial s}{\partial \ln T}\right)_i = \frac{(\Delta S_{i-1} / \Delta \ln T_{i-1}) \Delta \ln T_{i+1} + (\Delta S_{i+1} / \Delta \ln T_{i+1}) \Delta \ln T_{i-1}}{\Delta \ln T_{i-1} + \Delta \ln T_{i+1}}$$

where T is an appropriate time function (e.g., elapsed time or Agarwal equivalent time). Essentially, this formula is a weighted average of slopes computed from data points on either side of data point i . In the above formula, the two slopes are

$$\Delta S_{i-1} / \Delta \ln T_{i-1}$$

and

$$\Delta S_{i+1} / \Delta \ln T_{i+1}$$

Figure 101 - Explanation of the method used to compute the derivative of the drawdown-time data and type curves as presented in AQTESOLV V4.5 User's Guide (2004-2007).

These software programs can also help the user understand the nature of the groundwater system because the characteristic shape of the drawdown versus time curve in the different plotting domains (i.e., arithmetic, semi-log, log-log, and particularly the derivative graph) provides insight into the most appropriate conceptual model of the aquifer and the behavior of the pumping well.

Popular aquifer-test analysis software programs are commercial products using proprietary software and must be purchased (although demo or student versions are available). Boxes describing the specific software packages are included in this book to provide a general description of the individual software capabilities and functions and provide examples of program results. They are not intended to be comprehensive. Each program has a downloadable demonstration, trial, or student version that can be used to get a free introduction to the software. As previously stated, these three software packages are considered the industry standards. AQTESOLV V4.5 is described in [Box 5](#)↓, AquiferTest V12 is described in [Box 6](#)↓, and Aquifer^{win32} V6 is described in [Box 7](#)↓.

Most agencies and consultants use one or more of these three software packages to analyze hydraulic-testing results. When analyses of hydraulic-test data sets are routinely required, one of the commercially available programs can be a useful part of a hydrogeologic toolbox.

The next section describes performing and analyzing slug tests.

PART 2: SLUG TESTS

Hydraulic testing of unpumped wells is most often accomplished by using slug-test methods. Slug tests rapidly change the standing water level in a well and then record the rate of recovery as the perturbed water level returns to static. An advantage of this test is that it is easy to perform and is often completed within seconds or minutes.



This photograph shows a solid weighted slug (capped white PVC pipe), pressure transducer recording box, and an electric tape used to conduct slug tests at the Naval Air Warfare Center in New Jersey, USA (USGS, 2014).

14 Estimating Hydrogeologic Properties Using a Single Unpumped Well

This section focuses on gathering hydraulic-property information using a single unpumped well. Hydraulic tests referred to as slug tests are conducted by perturbing the water level in a well bore then recording water-level recovery with time. The rate of recovery is interpreted to estimate hydrogeologic properties.

14.1 The Slug Test

Slug tests are used to obtain estimates of horizontal hydraulic conductivity by observing the rate of recovery of induced water-level change in a well bore. Storage properties are usually not computed; however, some methods can provide estimates of storativity (e.g., Butler, 1998; Cooper et al., 1967).

A slug test can be conducted by causing the head in the well to rapidly rise by adding a slug (volume) to a well bore, or rapidly decline by removing a slug (volume) from the well bore. Once the initial change in water level occurs, the rate of water level recovery is recorded. When the static water level in a well is rapidly raised or lowered the rate of water-level recovery is proportional to the horizontal (radial) hydraulic conductivity of material adjacent to the perforated portion of the well (Figure 102). Slug tests can be conducted in low- to high-permeability formations of confined and unconfined systems.

Slug-test types are referred to as either a slug-in test (or falling-head test), or a slug-out test (or rising-head slug test). When conducting a slug-in test the head is initially increased and declines (falls) back to the static water level. When water level is rapidly lowered, a slug-out test, the water level increases (rises) returning to the equilibrium position (Figure 102).

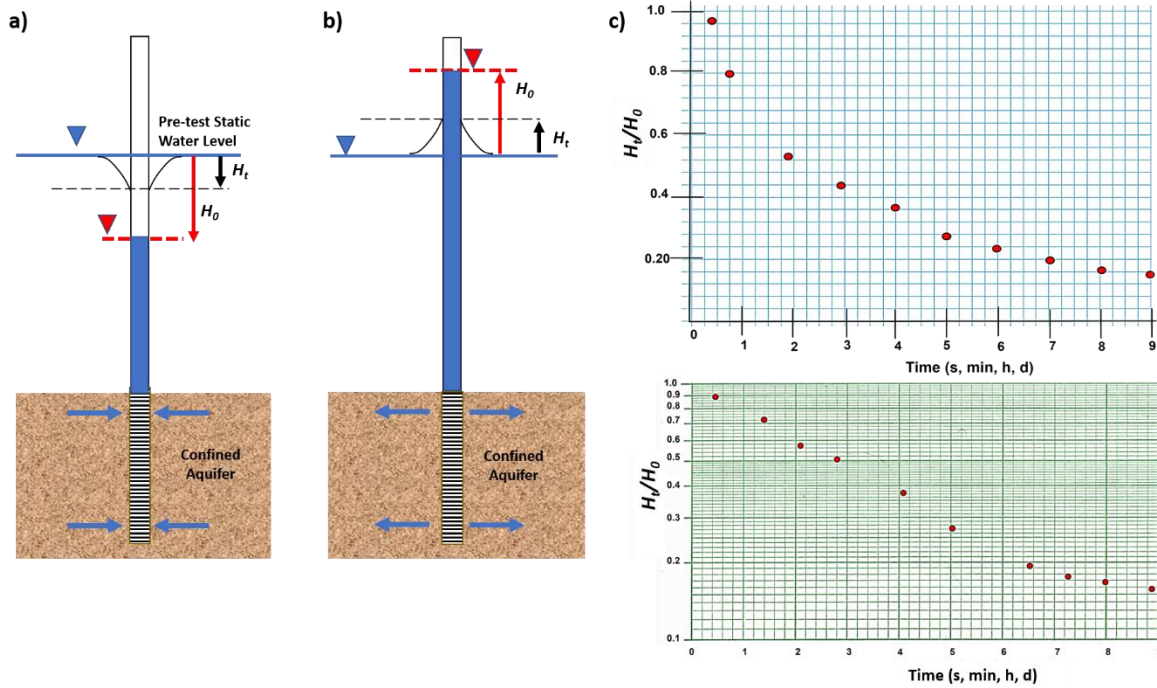


Figure 102 - Schematic of slug tests where the water level is instantaneously lowered or raised in a well penetrating a confined aquifer. The horizontal black lines show the perforated interval in communication with the aquifer. Red items show initial conditions at the time the slug is withdrawn or inserted when the abrupt change of the water level in the well bore creates a steep gradient between the head in the well bore and the formation. a) A rising head slug test or slug-out test. b) A falling head slug test or slug-in test. c) Plots of the ratio of the normalized head, H_t/H_0 and time for a test with an overdamped water level response. H_0 is the initial maximum rise or fall of the water level and H_t is the unrecovered head at some time t . The upper plot is arithmetic, and the lower plot is a semi-log plot. The recovery rate is generally logarithmic as shown in this example.

A slug test is used to characterize the hydrogeologic conditions in the immediate vicinity of the perforated interval of an unpumped well. The test samples a much smaller volume of hydrogeologic material than a pumping test. Care in interpreting results is needed as results are often dominated by conditions related to the well drilling and design, the degree of well development and hydrogeologic properties of materials immediately adjacent to the borehole (e.g., Vonhof, 1975). Slug-test results are therefore more representative of local conditions and less representative of overall aquifer conditions.

When several slug tests are conducted from similarly constructed and developed wells at a study site, overall aquifer conditions can be estimated by combining slug-test results. Slug tests are easy to execute, inexpensive, and can be applied to existing wells including small-diameter monitoring wells and piezometers. Consequently, slug tests are the test of choice at sites where pumping wells are not available or, in some cases, the groundwater system is contaminated.

The type of water-level response during a slug test is referred to as either overdamped, underdamped, or critically damped (Figure 103).

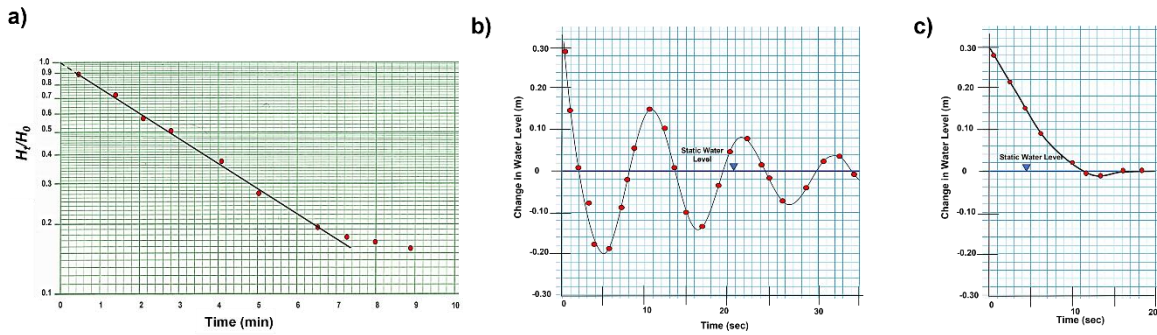


Figure 103 - Examples of overdamped, underdamped, and critically damped slug test results. a) An overdamped response plotted as the log of H_t/H_0 versus time (Figure 102). The black straight line is fitted to the straight-line portion of the data. b) An underdamped slug test response plotted on arithmetic scales as the change in water level versus time. The response is oscillatory. c) Plot of a critically damped response. This response shows the change in water level versus time plotted on arithmetic scales. The critically damped response is considered transitional, between the overdamped and underdamped response.

Overdamped recovery occurs when the unrecovered water level H_t divided by the initial maximum water level at the start of the test, H_0 , logarithmically declines as represented in Figure 103. The uncovered ratio of H_t/H_0 is plotted on a log scale. The resulting straight-line portion of the data set is fitted with a straight line. The slope of the straight-line is proportional to the formational hydraulic conductivity. Overdamped responses are observed for tests conducted in low to moderate hydraulic conductivity settings. Schematics of the overdamped responses of slug tests conducted in sand, silt and clay rich formations are shown in Figure 104.

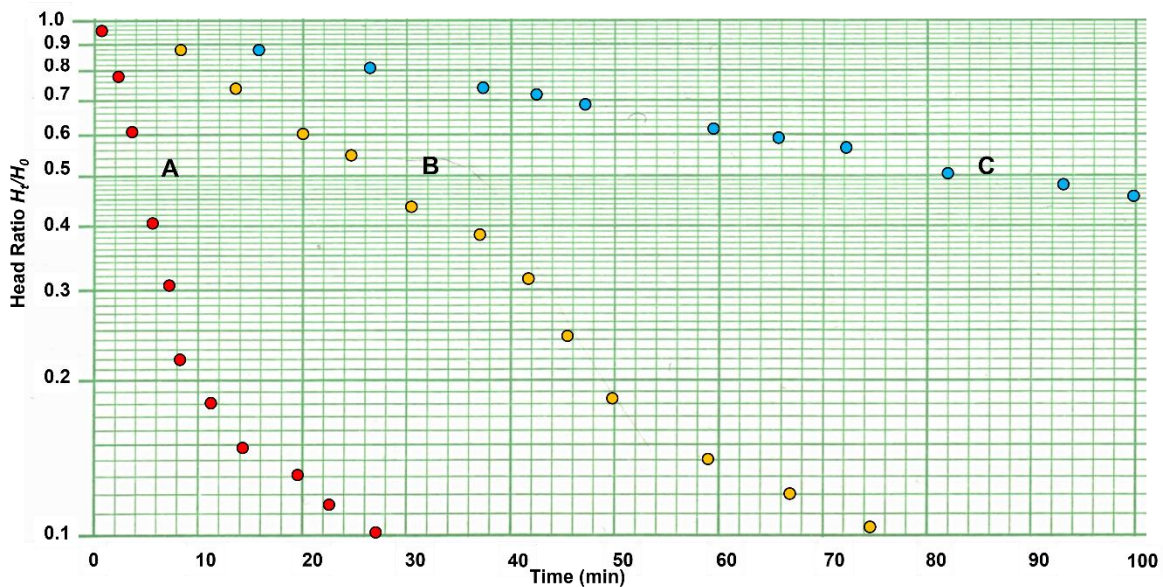


Figure 104 - Hypothetical example of the overdamped response (head ratio or normalized head) of slug tests performed in a sand rich formation (A), a silt rich formation (B) and a clay rich formation (C). The slope of the curve is smaller for lower horizontal hydraulic conductivity, $K_A > K_B > K_C$.

The underdamped oscillatory water-level changes are observed when high-hydraulic-conductivity formations are slug tested (Figure 103). The hydraulic

conductivity in these settings is related to the degree of dampening, as well as the period and timing of the oscillations (Butler et al., 2003). The critically damped response is seen when hydraulic conductivities are between moderate and high (Figure 103). Critically damped response data are often analyzed using methods developed for both overdamped and underdamped responses.

Slug tests can be completed in small-diameter observation wells and unpumped water-supply wells. In settings with small-diameter wells that penetrate highly permeable materials, an individual test may be completed in a few seconds. In the opposite setting where permeabilities are low, hours to days to months may be required to reach full recovery of test water levels. Slug tests are not restricted to use in aquifer systems (permeable systems that yield water to wells for a specific use). They are also used to characterize low-permeability units such as aquitards and fractured rocks as discussed in Section 16.

14.2 Performing a Slug Test

Slug tests are almost always conducted using a single well. The test method requires the water level in the borehole to rapidly rise or fall (Figure 102). It is assumed for most slug tests that the water level in the well instantaneously reaches a new position (no time is lost) at time = 0. However, some testing methods allow the change in water level to occur over a period, when a brief pumping interval is followed by a long water-level recovery time. These tests can be analyzed if initiation of the head data collection is started immediately after the maximum head change is obtained. An initial static water-level measurement is needed to establish the pretest condition for all tests. When extensive pumping precedes data collection, time-drawdown data should be collected and a recovery-analysis method applied.

Conducting a slug test requires careful planning including obtaining information on well construction and site conditions. The Kansas Geological Survey, U.S.A., is known for its research on the application of slug-test methods (Butler, 1998). Their recommendations for conducting a successful slug test are incorporated in the following material.

14.2.1 Assessing the Hydrogeologic Setting and Well Construction

A site conceptual model is needed to assess the nature of the formations being tested. Are the formations aquifers or aquitards (Woessner & Poeter, 2020)? Are they confined or unconfined? Do the wells fully penetrate the formations? Could boundary conditions impact the results? Each of these questions requires resolution prior to conducting tests and analyzing results.

Water supply wells, observation wells, or open boreholes can be used to conduct slug tests. Designing a slug test requires knowledge of the length and location of the borehole and perforated interval or length of well screen penetrating the formation, the

presence of a gravel pack, and the diameter and lengths of the blank well casings (Figure 105).

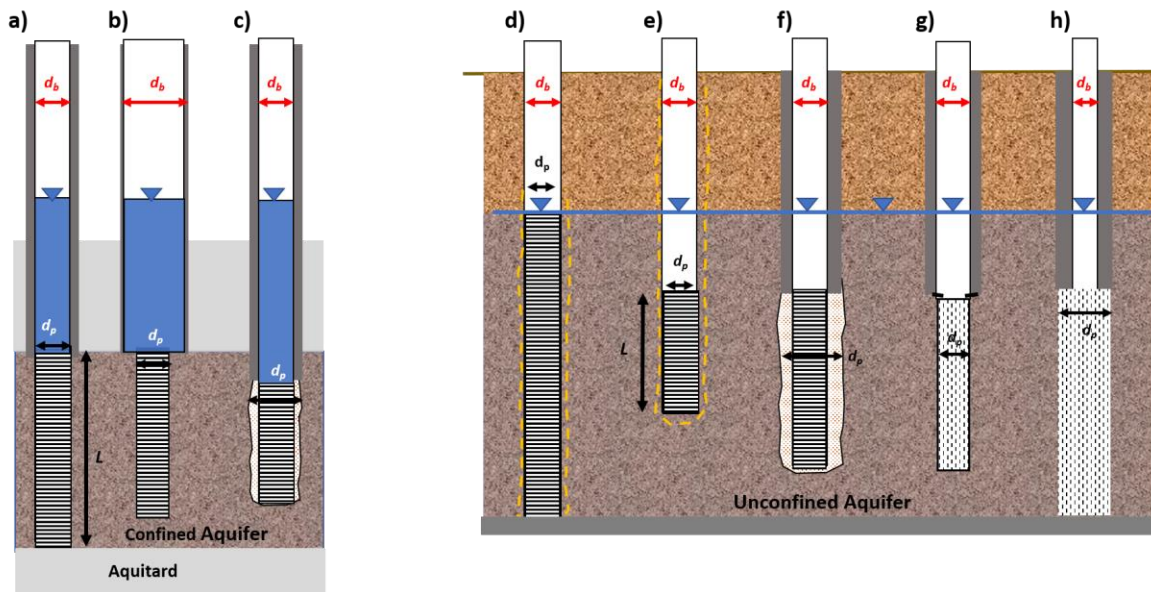


Figure 105 - General well configurations used for slug testing in confined and unconfined aquifers. The horizontal lines and vertical dashes represent perforated casing intervals (screens). d_b is the diameter of the cased well bore and d_p is the diameter of the perforated casing. When a gravel pack is included, the effective diameter includes the combined perforated interval and the gravel-pack diameters. The length of the perforated interval (L) and its position in the aquifer can vary. Wells can be fully or partially penetrating (as shown). The dark gray shading represents grout placed around the blank well casing (e.g., cement or bentonite).

- A fully penetrating well in a confined aquifer. The casing diameter and screen diameter are the same.
- A partially penetrating confined aquifer well with a larger well casing diameter than the screen diameter.
- A partially penetrating confined aquifer well with a gravel pack around the screened interval. The effective perforated interval diameter includes the screen and surrounding gravel pack.
- A fully penetrating well in an unconfined aquifer where the dashed yellow line indicates the well installation is completed in a borehole or driven to depth without fill around the screen or casing and the formation is allowed to collapse around the well.
- A partially penetrating well in an unconfined aquifer where the dashed yellow line indicates the well installation is completed in a borehole or driven to depth without fill around the screen or casing and the formation is allowed to collapse around the well.
- A partially penetrating well in an unconfined aquifer where a larger borehole is drilled and then an assembled casing and screen are placed in the borehole. The bore hole outside of the screen is filled with a filter pack (gravel pack) of coarse material (Sterrett, 2007) then the casing interval is grouted. When analyzing the test data, the perforated casing diameter typically includes the gravel pack, effective diameter.
- A partially penetrating well in an unconfined aquifer where the screened interval is a smaller diameter than the well casing. After the borehole was drilled to the screen depth the casing was set and grouted, then a slightly smaller diameter borehole is advanced, and a screen installed.
- A partially penetrating well in an unconfined aquifer with a smaller casing diameter than the well screen. The large borehole is drilled to depth and then the casing and screen were set; then the borehole is grouted.

14.2.2 Special Considerations for Water Table Systems

Slug tests can easily be conducted in water-bearing units that are confined. They can also be conducted when a water table is present, and the perforated interval is below the water table (Figure 105). However, if the perforated interval extends above the water table, only slug-out or rising-head slug tests should be performed (Figure 106). In this setting, falling-head tests are avoided because the water level at the start of the test after

the introduction of the slug would be higher than the static water level extending into the vadose zone. When this occurs the water level falls more rapidly than it would in the saturated portion of the aquifer because it flows into the partially saturated zone above the water table. Analysis of the resulting data produces a hydraulic conductivity value that is higher than the value representative of the saturated unit (Todd & Mays, 2005).

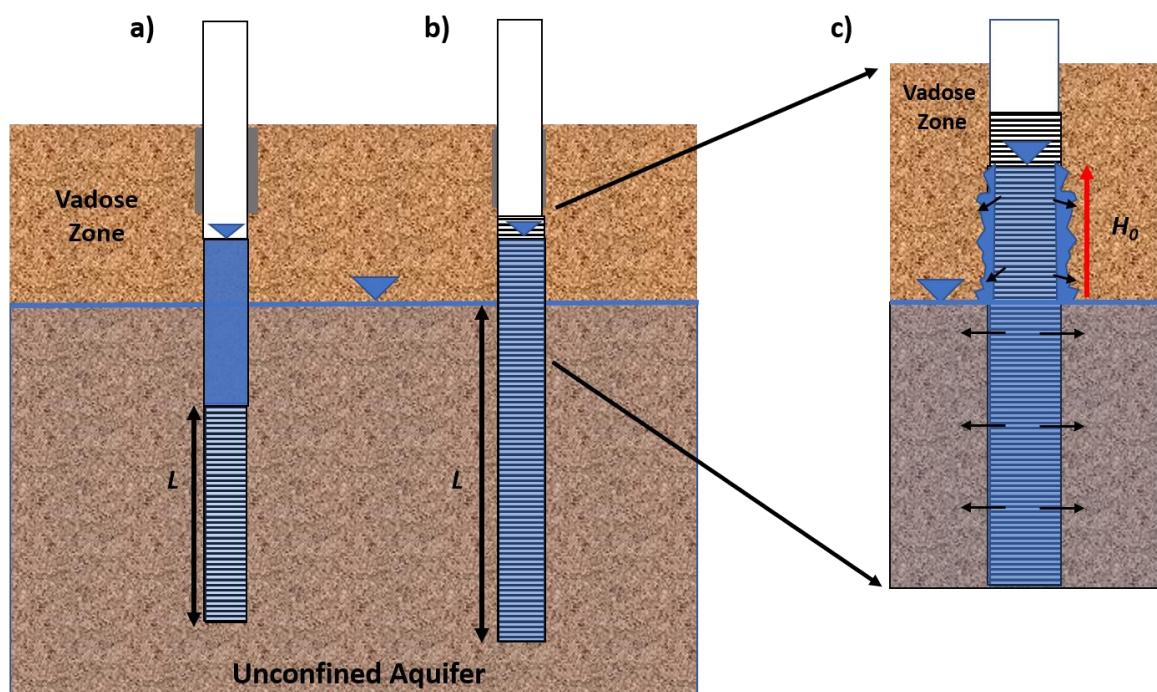


Figure 106 - Water-level in a well in an unconfined aquifer after introduction of a solid slug at the start of a slug-in test in a well with the screen completely below the water table and a well with a screen that extends above the water table. a) When the perforated interval is completed below the water table, slug-in or slug-out tests can be successfully completed. b) If the screened interval extends above the water table only slug-out tests should be conducted because a slug-in test will overestimate the saturated horizontal hydraulic conductivity due to some of the water flowing into the unsaturated zone. c) Enlargement of (b) showing the factors affecting the rate of the head decline when a slug-in test is performed in a well with a screen extending above the water table. During the water level decline a portion of the water enters the unsaturated zone and the resulting rate of water level decline is greater than it would be if only the saturated portion of the aquifer was controlling the rate of decline.

14.2.3 Free Exchange of Water with the Formation

Another criterion for conducting a successful slug test is that the perforated or screened interval is hydrologically well connected to the formation being tested. This means the number, size, and configuration of the perforations should not inhibit the exchange of water between the formation and the well. If the configuration of perforations (too small or too few) inhibits the movement of water to and from the formation, the test may reflect the "hydraulic conductivity" of the well hardware instead of the geologic material (Figure 107).

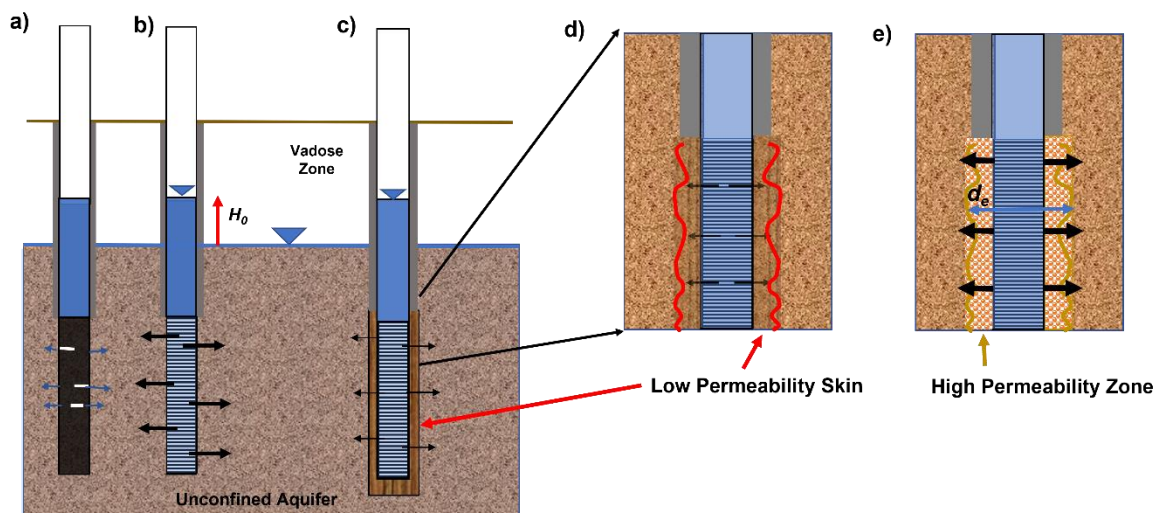


Figure 107 - Schematic of a falling-head slug test in an unpumped well penetrating an unconfined aquifer.

- Well design with a perforated interval (black portion of the casing with white perforations) that is not well connected to the formation. Head recovery will be controlled by the poorly designed perforated interval not the formational properties.
- Perforated interval that is fully connected to the formation. Water in the well bore freely communicates with the formation.
- Perforated interval adjacent to a portion of the borehole damaged during drilling such that finer material has been left behind. The damaged area will control the rate of change of the borehole water level, this is called a skin effect.
- Insert showing drilling damage to the formation producing a low permeability zone. The smaller arrows indicate the connection to the surrounding aquifer is poor.
- An example of a zone around the perforated interval of a well where the permeability has been enhanced. This can occur by the addition of a gravel pack (coarse material placed outside of the perforated casing) or the removal of natural fines in the formation by well development. When a gravel pack is present the effective radius, d_e , of the perforated interval includes the gravel pack.

Often the formational material opposite the perforated interval becomes less permeable during the drilling process (Figure 107), especially in fine-grained material or when drilling fluids are used in well construction. In some cases, the process of drilling and installing the well results in finer material entering the formation or the clays present are smeared to the borehole wall. This is referred to as forming a skin of lower-permeability material. This skin effect or borehole skin (Fetter, 2001) restricts the exchange of water between the well bore and formation. Therefore, hydraulic-conductivity values computed from slug-test results will underestimate the properties of the formation. Well-development procedures like surging, bailing, and over-pumping can increase the permeability of the skin and should be implemented during well construction (e.g., Sterrett, 2007). In some settings, too much development may not only remove the fines that entered a formational material during drilling but also remove additional natural fines in the formation. This creates a zone of higher-than-normal hydraulic conductivity adjacent to the screen and if it extends a significant distance into the formation may impact test data. In this case the well may recover more rapidly because of the presence of this high hydraulic conductivity zone. As a result, hydraulic-conductivity values will be higher than the formational value. Finally, in many observation or water-supply wells, gravel pack is

added to enhance the permeability around the perforated interval to assure perforations are not plugged with formational fines. When this design is used, the effective diameter of the perforated interval needs to include the gravel pack (Figure 107e).

14.2.4 Raising and Lowering the Water Level

Typically, instantaneously inducing a change in water level in the well being tested is accomplished by submerging or removing a solid slug from the water-filled well bore. These actions result in a rise or fall of the borehole water level. The degree of change is a function of the volume of the slug and volume of water per length of the well bore (Figure 108).

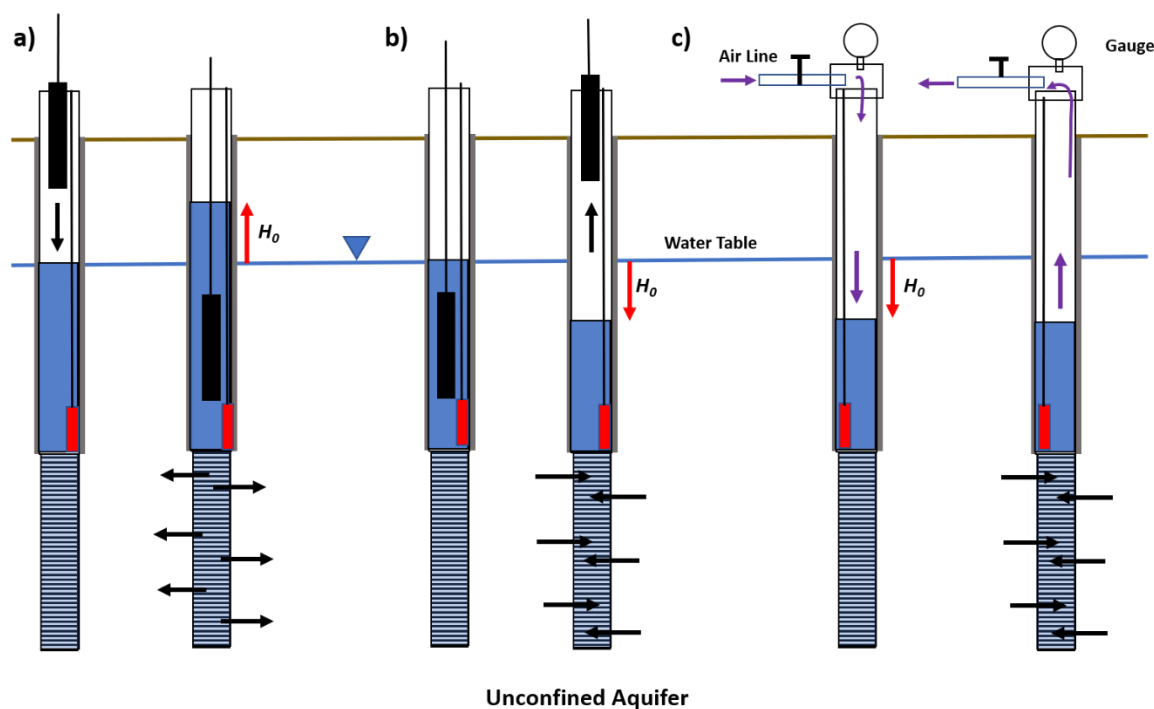


Figure 108 - Slug-test methods used to raise and lower the water level in an unpumped well. This example shows an unconfined aquifer, however, the methods applied to a confined aquifer would be the same. The black rectangles represent solid slugs of a known volume. The red rectangles are transducers suspended in the well. H_0 is the maximum change in water level measured from the static at the initiation of the test.

- A slug-in or falling-head slug test. The solid cylinder is dropped into the well water so that it is totally submerged (second image). The water level instantly rises.
- A slug out or rising-head slug test. The solid slug is placed in the well and the water level comes back to equilibrium (static water level). The slug is then rapidly removed from the well and water level data collected.
- A pneumatic rising-head slug test where the water level is initially depressed by an increase in air pressure in the closed well bore. Air is pumped into the well until the water level is depressed to the desired level. At that time a valve to the air-tight cap is closed. The air pressure in the casing is read by a pressure gauge or a second transducer installed at the location of the pressure gauge. The test is initiated when the airline is detached, and the valve is opened allowing the air to escape.

If a falling-head slug test is desired, the slug is suspended on a cord and dropped into the well until it is totally submerged. This displaces a known volume of water resulting in a water-level rise. Based on the volume of water displaced, the maximum height to which the water will rise can be computed and checked against the observed maximum level. The

decline in water level over time is then recorded. Using a solid slug, a rising-head test can be accomplished by lowering a solid slug on a cord into the well, allowing it to totally submerge, and waiting for the water level to stabilize. Once the water level in the well has returned to equilibrium (static conditions) the slug can be yanked either totally out of the well or high enough that the entire slug is above the static water level. This results in a rapid lowering of the water level, a slug-out test. The rising water level is recorded over time.

If the water level in the well bore is close to the surface, a continuous solid rod can be used as a slug when inserted into the well a known distance. The volume of solid rod that is submerged then removed, or the volume the solid rod inserted below the water level is required to compute H_0 values as the test is initiated.

A bailer can be used to lower the water level in a test well. One method uses the bailer to remove a single volume of water. The bailer is lowered into the well until it is totally submerged. Water levels in the well are allowed to return to equilibrium. Then at the start of the test, the bailer full of water is yanked from the well. This removes a volume of water causing a rapid fall in the water level. The rising water levels over time are monitored. It is best to totally remove the bailer from the well to prevent water from leaking back into the well. A second method is referred to as a bail-down method, where the bailer is used to extract water multiple times to lower the water level. Once the water level has reached the desired depth, bailing ceases and water level recovery is recorded. The bail-down method is only useful in lower hydraulic conductivity material. This method is appropriate when storage properties are not being estimated as it assumes the non-instantaneous water level decline allows estimates for K assuming a semi steady-state condition. Neither of the bailer methods are likely to be used when the water in the well bore is contaminated, as special precautions are often required to dispose of the contaminated bailed water. To prevent water-quality impacts, when a solid slug is used to conduct a test in a contaminated well the slug needs to be decontaminated before it is used to conduct tests in other wells.

A third method involves the use of compressed air to create a rising-head slug test (Figure 108c). An increase in the well-bore air pressure is used to lower the water level in the well and hold it at a given depth below the static water level. The well is fitted with an airtight cap, a pressure gauge, and an air line with a valve. The pressure gauge can also be replaced by a second transducer that senses air pressure in the well bore. A small compressor or hand pump is used to increase the air pressure between the water surface and the well cap. The pressure gauge records the pressure in the well bore relative to atmospheric pressure. The pressure readings can be converted to feet (or meters) of water level change. Once the increased pressure level is established in the well bore the valve is closed and the compressed air line removed. When the test starts the airline valve is opened allowing the over-pressurized well-bore air to escape. The depressed water level begins to

recover because the well bore is at atmospheric pressure. The submerged transducer measures the change in the overlying water level during recovery.

Finally, a volume of water can be dumped into the well bore as quickly as possible to create a rise in the water level. This is challenging if large volumes of water are needed to make a measurable change in the water level (large casing diameters or high hydraulic conductivities). In some settings the addition of water for the test may negatively influence other site conditions, including changing the local water chemistry. This method may be appropriate in a river study where small-diameter piezometers (a centimeter in diameter) are driven into the riverbed and slug tests are performed by adding a volume of river water to the wells (e.g., Woessner, 2020). The physical addition of water to the well may not be acceptable if wells are in a contaminated groundwater system as the addition of a different quality water may impact future water-quality-analysis results.

14.2.5 Recording Water-Level Change

Methods for measuring water levels in wells are presented in Section 4 of this book. As with hydraulic testing using pumping wells, it is important to record early-time water-level changes. When tests are conducted by putting in or extracting slugs or bailers, measuring devices like float recorders are not appropriate because cables often get tangled. In addition, when wells recover quickly (seconds or a few minutes), steel tapes and even electric tapes often cannot be deployed rapidly enough to obtain enough early-time data points for a robust analysis. The best method for obtaining water-level data is a pressure transducer/data recorder installed at a sufficient depth that the use of a solid slug will not disturb the instrument. If test water levels recover slowly, electric or steel tapes can be used to record levels.

When beginning a test, the static water level must be recorded with a steel or electric tape to establish a reference point for the test measurements. Transducer records are linked with the static water level to convert pressure readings to water-level changes. A micro barometer should be used during the test if closed transducers (i.e., absolute rather than relative transducers) are used in order to determine if atmospheric-pressure adjustments to the test data are necessary. However, the test is typically completed within a short time interval (e.g., 10s of minutes) thus correction for barometric changes may not be necessary.

When solid slugs are used, the initial maximum rise or fall of the head can also be computed based on the volume of the well casing per unit of length and the known volume of the slug. For example, if the water in a 10 cm diameter PVC well casing is perturbed by submerging a 5 cm diameter solid slug that is 30 cm long, the volume of water displaced by the slug would be given by the volume of a cylinder with the dimensions of the slug: $\text{volume} = \pi(\text{square of the radius of the slug})(\text{height of the slug}) = 3.14 (2.5 \text{ cm})^2 (30 \text{ cm}) = 589 \text{ cm}^3$. A well bore that is 10 cm in diameter contains 78.5 cm^3 of water in each centimeter of its length, i.e., $(3.14(5 \text{ cm})^2(1\text{cm})=78.5 \text{ cm}^3)$. Thus, the water level will rise 1 cm for every

78.5 cm³ added. So, the addition of the 589 cm³ slug would result in a maximum rise of 589 cm³/78.5 cm³/1 cm = 7.5 cm. Thus, the initial measurement (H_0) should be about 7.5 cm.

14.2.6 Test Repeatability

Slug tests are relatively easy to perform. Butler (1998) suggests that multiple slug tests should be conducted at a well. He recommends a well should be slug tested at least three times and then the values averaged to produce a representative horizontal hydraulic conductivity value. In some cases, the process of performing the slug test may also result in some well development (surging the fines from the perforated interval) or formation plugging (moving more fines to the perforated interval). If test values during multiple testing are changing consistently (sequentially increasing or decreasing), additional well development may be needed before values are considered reliable and reproduceable. This issue can be checked by computing the maximum measured head change for each test; the normalized head change should be ≥ 0.9 for each test, indicating that formational changes are not occurring during the test (Butler, 1998).

14.3 Field Data: Overdamped, Underdamped and Critically Damped Water-Level Responses to Slug Tests

The water-level response (displacement) from a slug test can be classified as overdamped, underdamped, or critically damped (Figure 103).

Overdamped recovery occurs when the ratio of the normalized head (i.e., the unrecovered water level H_t divided by the initial maximum water level at the start of the test, H_0) declines logarithmically as shown in Figure 109. When overdamped slug-test data are plotted as the logarithm of the ratio H_t/H_0 versus time, a portion of the data form a straight line that can be used to extract information for the appropriate equation to calculate K (e.g., Hvorslev, 1951) as discussed in Section 14.4.1). However, Butler (1996, 1998) notes that the selection of the straight-line portion can be complicated when the plot has more than one straight section. Some plots have two straight sections, a very early straight portion and a second at later times (Figure 109).

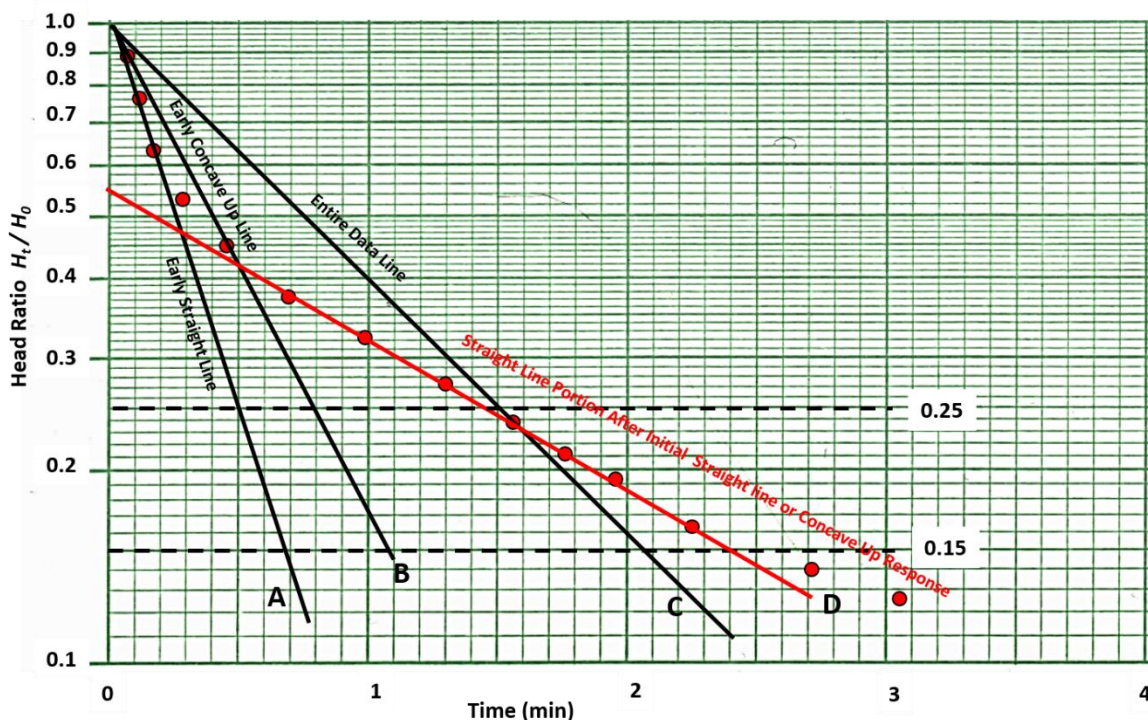


Figure 109 - Schematic of an overdamped slug-test data set that exhibits an early straight-line and a concave upward trend. In this example, fitted lines A, B and C have greater slopes than the red line D, which is considered to be representative of the formation properties (Butler, 1996). Early time data fitted with line A most likely reflects the release of water from a gravel pack or leakage of water down a poorly sealed well bore. The concave upward portion of the curve shows elastic storage is an early component of the observed water level change. The fitted line B incorporates this trend. When the entire data set is fit to a straight line, C, the calculated hydraulic conductivity will be higher than the formational value because the effect of the gravel pack and storage are included in the response. Line D is fit to the straight-line portion of the plot that occurs after the effects of leakage or gravel pack effects no longer dominate the data. Butler (1996) recommends that when early data trends occur, the straight-line portion should be selected using the second straight-line section of the data. He suggests that the data between head ratio values of 0.25 and 0.15 (dashed black lines) should be used to represent the formational properties, line D.

Very early time data that form an initial straight-line section is often related to the release of water from a gravel-packed well or from water leaking down an unsealed well bore (Figure 107). Butler (1996, 1998) recommends not misinterpreting an early-time trend as representative of formational response. Butler (1996) suggests that when the early straight-line portion or a concave-upward trend is present, a line should be fit to the remaining straight-line portion of the data set. He suggests this portion should be encompassed by the 0.25 to 0.15 values of the head ratio (Figure 109). Butler’s (1996) analyses of a data set showed when the Hvorslev method (Hvorslev, 1951) was applied using the straight-line portion between 0.25 and 0.15 values of K were within 5 percent of values obtained using another type-curve slug-test method (Cooper et al., 1967).

Early-time data can also exhibit a concave-upward trend (Figure 109). This trend often reflects the effects of formation storativity (elastic storage) on the early recovery data. This section of data should be ignored when fitting a line to the data, and the second straight-line portion of the data should be used to represent formation water-level response. For some data sets, a second approach can be applied that does not rely on

straight-line interpretations and accounts for storage (i.e., Cooper et al., 1967; Hyder et al., 1994).

When slug-test responses are overdamped, depending on the hydrogeologic properties of the material, the length of the test can vary. For higher hydraulic conductivity, smaller maximum head change, and longer perforated intervals, water-level recovery will be more rapid. In extremely low-permeability material, full recovery may require weeks or longer.

Overdamped slug-test data for confined aquifers can also be plotted as the ratio of H_t/H_0 versus the log of time and matched to type curves developed by Cooper and others (1967) as shown in Figure 110. An early curved slope is interpreted as a response to formation storativity. Methods to analyze these data are presented in Section 14.4.

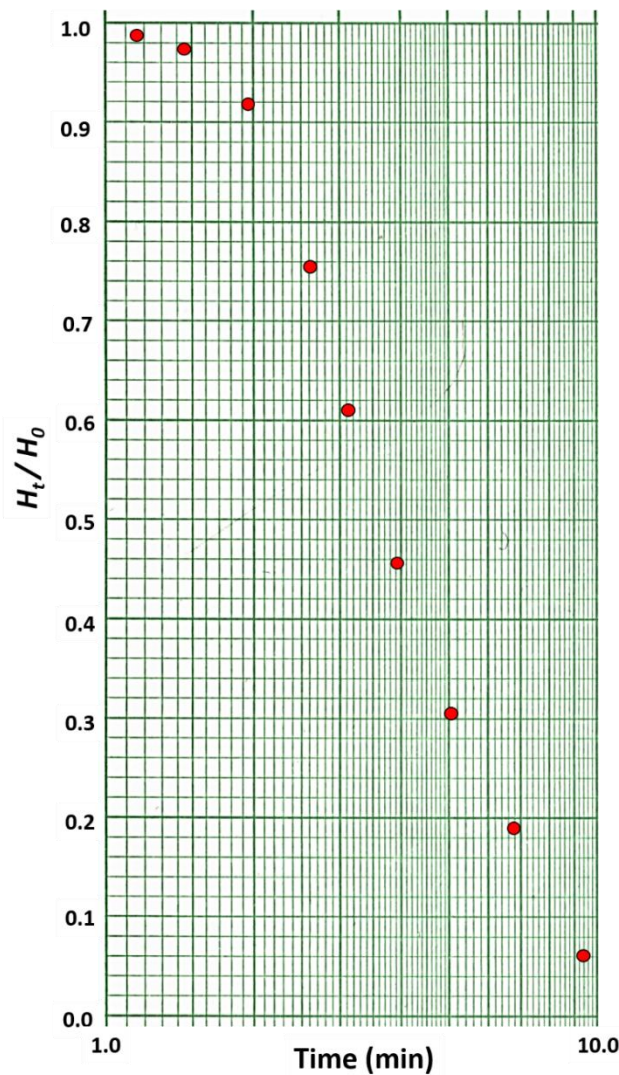


Figure 110 - Example of slug test data for a confined aquifer plotted as H_t/H_0 versus the log of time. Analysis of the data is completed by curve matching as described by Cooper and others (1967).

Underdamped water-level responses yield an oscillatory response (Figure 103b). The water-level changes decay exponentially until the initial static condition is realized. This response is most often observed when wells penetrate high hydraulic conductivity groundwater systems. Tests often are completed within 10s of seconds. Section 14.5 describes methods developed to analyze test data displaying an underdamped response.

Butler (1998) notes that slug-test responses sometimes show a transitional response between the overdamped and underdamped conditions (Figure 103c). This state is referred to as critically damped. The curve shows a concave-downward curvature at later times especially when plotted as the log of head versus time. Analysis techniques applied to this transitional data can be addressed using overdamped or underdamped analytical approaches. Butler (1998) and Butler and others (2003) discuss analysis of critically damped data sets.

14.4 Methods to Interpret Overdamped Slug Tests

This section presents the development, basic assumptions, and applications of the most common methods used to analyze overdamped slug-test data. These methods include those developed by Hvorslev (1951), Bouwer and Rice (1976), Bouwer (1989), Cooper and others (1967), and Hyder and others (1994).

14.4.1 Hvorslev Slug Test Method

Hvorslev (1951) prepared a report for the Waterways Experiment Station Corps of Engineers, U.S. Army that addressed his experiments and observations examining how water levels in boreholes, piezometers, and monitoring wells responded when borehole water levels were purposefully raised or lowered. The report describes how formational hydraulic properties and the well design (shape factors) influence the water level recovery as a function of time.

Hvorslev (1951) developed a semi-analytical solution applying a quasi-steady-state approach that assumes elastic storage can be neglected. Other simplifying assumptions include the formation being tested is isotropic, homogeneous, and uniform in thickness. The solution can be applied to partially or fully penetrating wells. The formulation is based on confined conditions. Analyses are applied to unconfined and confined systems. Falling-head or rising-head test data are analyzed using a semi-log plot and an interpolated straight line (Figure 109).

Hvorslev (1951) developed several empirical equations to represent well designs in formations. There is no consideration of the water table as a fixed or moving boundary. His method allows for screens of varying diameters and lengths. In some settings well bores are only open at the bottom or can be partially filled with sediment. Notation used by Hvorslev (1951) is shown in Figure 111.

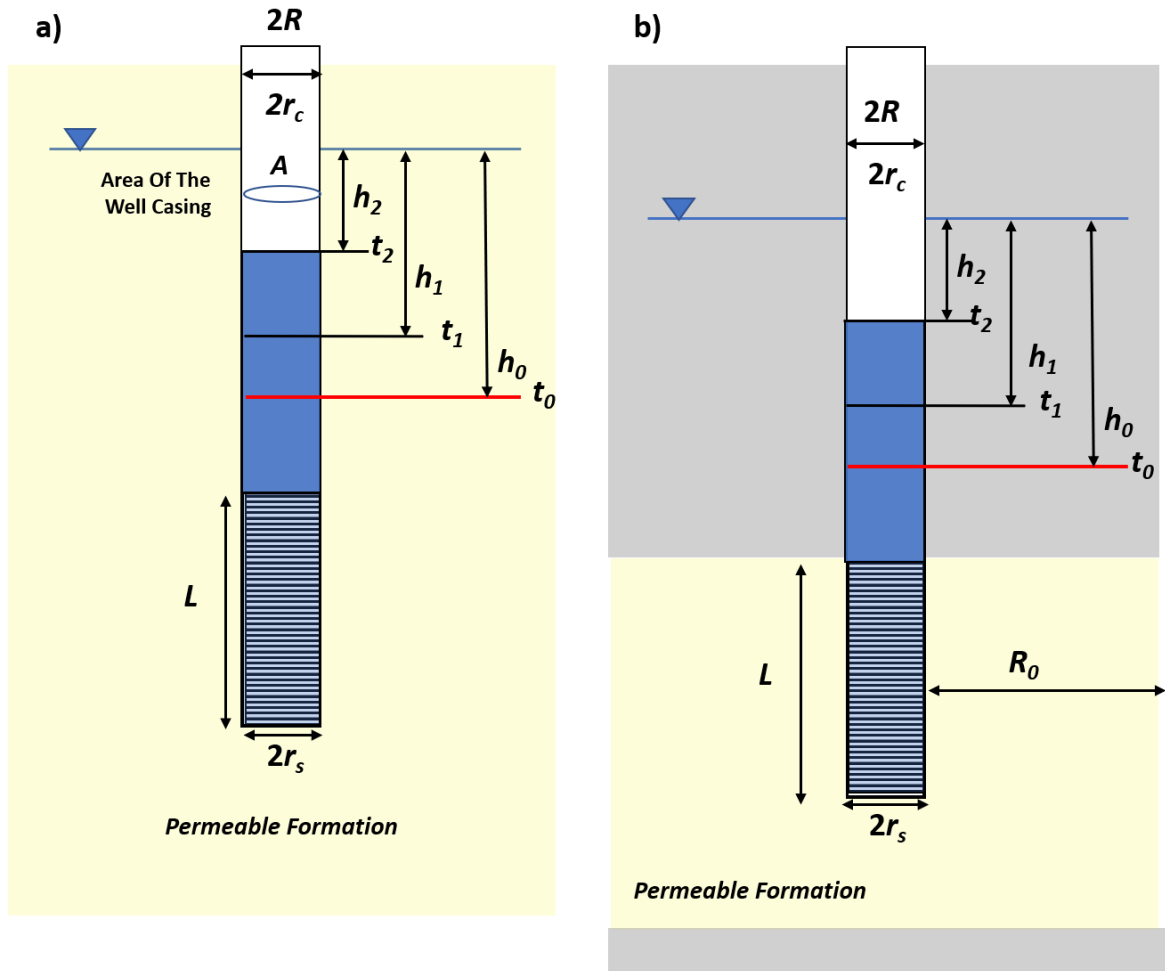


Figure 111 - General notation for parameters used in the Hvorslev slug test method as defined for Equations (105) and (106). a) An example of a well completed in an unconfined system. b) An example of a well completed in a confined system (gray units are impermeable). R_0 is the distance to the location where h does not change.

General equations describing the relationship between hydraulic conductivity, cross sectional area of the well, a shape factor representing the well configuration, and the slope of the of the normalized head, $1/(t_2-t_1) \ln (h_1/h_2)$, were formulated. Equation (105) shows the hydraulic conductivity is directly proportional to the area of the well casing and the slope of the slug test data, and inversely proportional to the well shape factor. The slope of the data plot is determined using the difference in two values of the normalized head at different times (h_1 and h_2) and difference in the two corresponding times (t_1 and t_2) (Figure 112). Hvorslev defines the normalized head H_t/H_0 as H in his work. Equation (106) uses what is referred to as the basic time-lag method to determine the slope of the slug-test data. This approach represents the slope using the relationship that when the value of the normalized head equals 0.37 (log of 0.368 = -1) the corresponding time value can be read from the graph, $T_{0.37}$ (Figure 112).

$$K = \frac{A}{F} \left(\frac{1}{t_2 - t_1} \right) \ln \frac{h_1}{h_2} \tag{105}$$

$$K = \frac{A}{F} \frac{1}{T_{0.37}} \tag{106}$$

where:

K = hydraulic conductivity (LT^{-1})

A = cross-sectional area of the well casing, πr_c^2 (L^2)

F = shape factor that for some configurations is dependent on one or more of L, R, r_c, r_s (dimensionless)

h_1 = normalized head at time t_1 (L)

h_2 = normalized head at time t_2 (L)

t_1 = time at head h_1 (T)

t_2 = time at head h_2 (T)

$T_{0.37}$ = basic time lag (T)

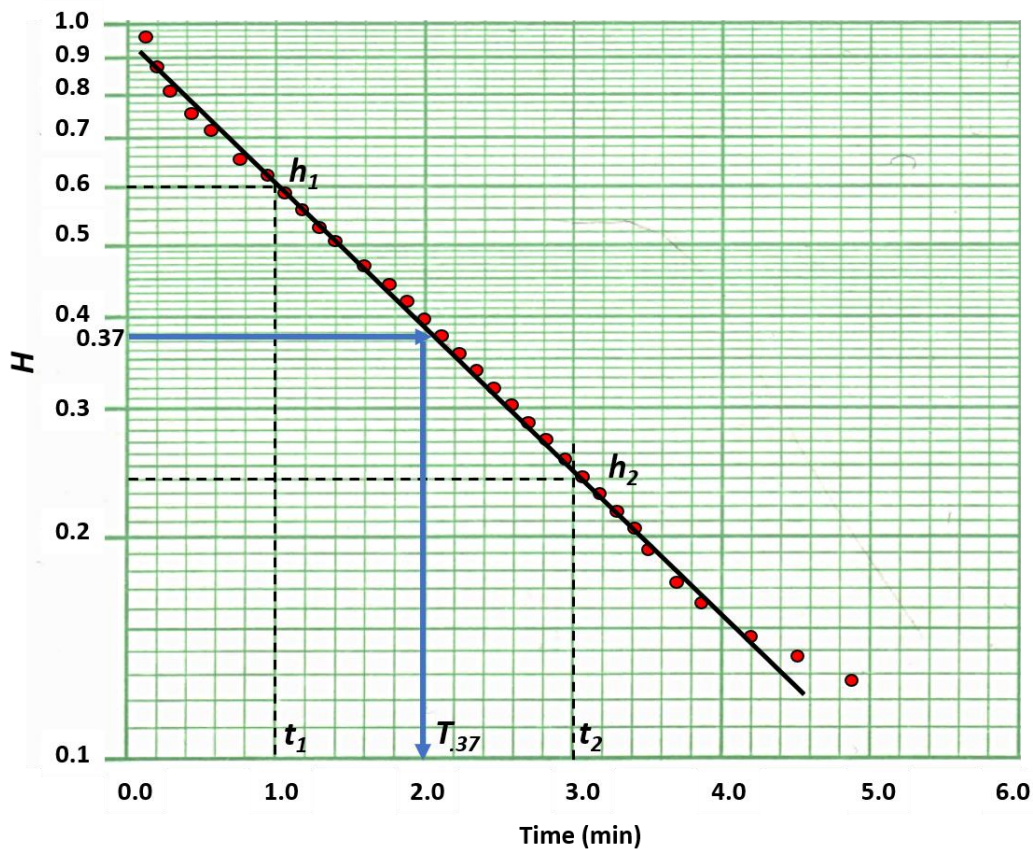


Figure 112 - Semi-log plot of slug test results (red dots) and a fitted straight line. The slope of the line is determined by two points of normalized head values (H), h_1 and h_2 and time values t_1 and t_2 . The normalized head on the graph (H) is the unrecovered head measured from the static water level divided by the depth or height to which the water level drops or rises at the beginning of the test (measured from the static water level), which is H/H_0 as shown in Figure 111. Also shown is the procedure for reading $T_{0.37}$ from the graph for use in the time lag method where the H/H_0 value is 0.37.

The shape factor in Equations (105) and (106) is empirically derived for the well configuration and position in the formation being tested using analytical solutions for steady-state flow. General well notations are presented in Figure 111. Four shape factors and equations to compute K for unconfined settings and two sets of conditions for confined settings are included in Figure 113. Figure 114 provides graphs of empirical constants and an equation for determining K in an unconfined anisotropic setting.

Condition		Diagram	Shape factor, F	Permeability, k by variable head test	Applicability
Observation well or piezometer in saturated isotropic stratum of infinite depth	(a) Uncased hole		$F = 16\pi DSR$	$k = \frac{R}{16DS} \times \frac{(h_2 - h_1)}{(t_2 - t_1)}$ for $\frac{D}{R} < 50$	Simplest method for permeability determination; not applicable in stratified soils; for values of S see Fig. 2.17
	(b) Cased hole, soil flush with bottom		$F = \frac{11R}{2}$	$k = \frac{2\pi R}{11(t_2 - t_1)} \ln\left(\frac{h_1}{h_2}\right)$ for 6 in. $\leq D \leq 60$ in.	Used for permeability determination at shallow depths below the water table; may yield unreliable results in falling head test with silting of bottom of hole
	(c) Cased hole, uncased or perforated extension of length L		$F = \frac{2\pi L}{\ln(L/R)}$	$k = \frac{R^2}{2L(t_2 - t_1)} \ln\left(\frac{L}{R}\right) \ln\left(\frac{h_1}{h_2}\right)$ for $\frac{L}{R} > 8$	Used for permeability determinations at greater depths below water table
	(d) Cased hole, column of soil inside casing to height L		$F = \frac{11\pi R^2}{2\pi R + 11L}$	$k = \frac{2\pi R + 11L}{11(t_2 - t_1)} \ln\left(\frac{h_1}{h_2}\right)$	Principal use is for permeability in vertical direction in anisotropic soils
Observation well or piezometer in aquifer with impervious upper layer	(e) Cased hole, opening flush with upper boundary of aquifer of infinite depth		$F = 4R$	$k = \frac{\pi R}{4(t_2 - t_1)} \ln\left(\frac{h_1}{h_2}\right)$	Used for permeability determination when surface impervious layer is relatively thin; may yield unreliable results in falling head test with silting of bottom of hole
	(f) Cased hole, uncased or perforated extension into aquifer of finite thickness: (1) $\frac{L_1}{T} \leq 0.20$ (2) $0.2 < \frac{L_2}{T} < 0.85$ (3) $\frac{L_3}{T} = 1.00$ <i>Note.</i> R_0 equals effective radius to source at constant head		(1) $F = C_s R$ (2) $F = \frac{2\pi L_2}{\ln(L_2/R)}$ (3) $F = \frac{2\pi L_3}{\ln(R_0/R)}$	$k = \frac{\pi R}{C_s(t_2 - t_1)} \ln\left(\frac{h_1}{h_2}\right)$ $k = \frac{R^2 \ln(L_2/R)}{2L_2(t_2 - t_1)} \ln\left(\frac{h_1}{h_2}\right)$ for $\frac{L_2}{R} > 8$ $k = \frac{R^2 \ln(R_0/R)}{2L_3(t_2 - t_1)} \ln\left(\frac{h_1}{h_2}\right)$	Used for permeability determinations at depths greater than about 5 ft, for values of C_s , see Fig. 2.17 Used for permeability determinations at greater depths and for fine grained soils using porous intake point of piezometer Assume value of $\frac{R_0}{R} = 200$ for estimates unless observation wells are made to determine actual value of R_0

[From U.S. Department of the Navy, Naval Facilities Engineering Command (1982)].

Figure 113 - Well conditions, shape factors, and equations to compute hydraulic conductivity ($K =$ permeability, k , on the table). Figure 114 is the figure referred to as 2.17 in the text in the left-hand column. Values of C_s and S are also defined on Figure 114 (US Department of the Navy, 1982).

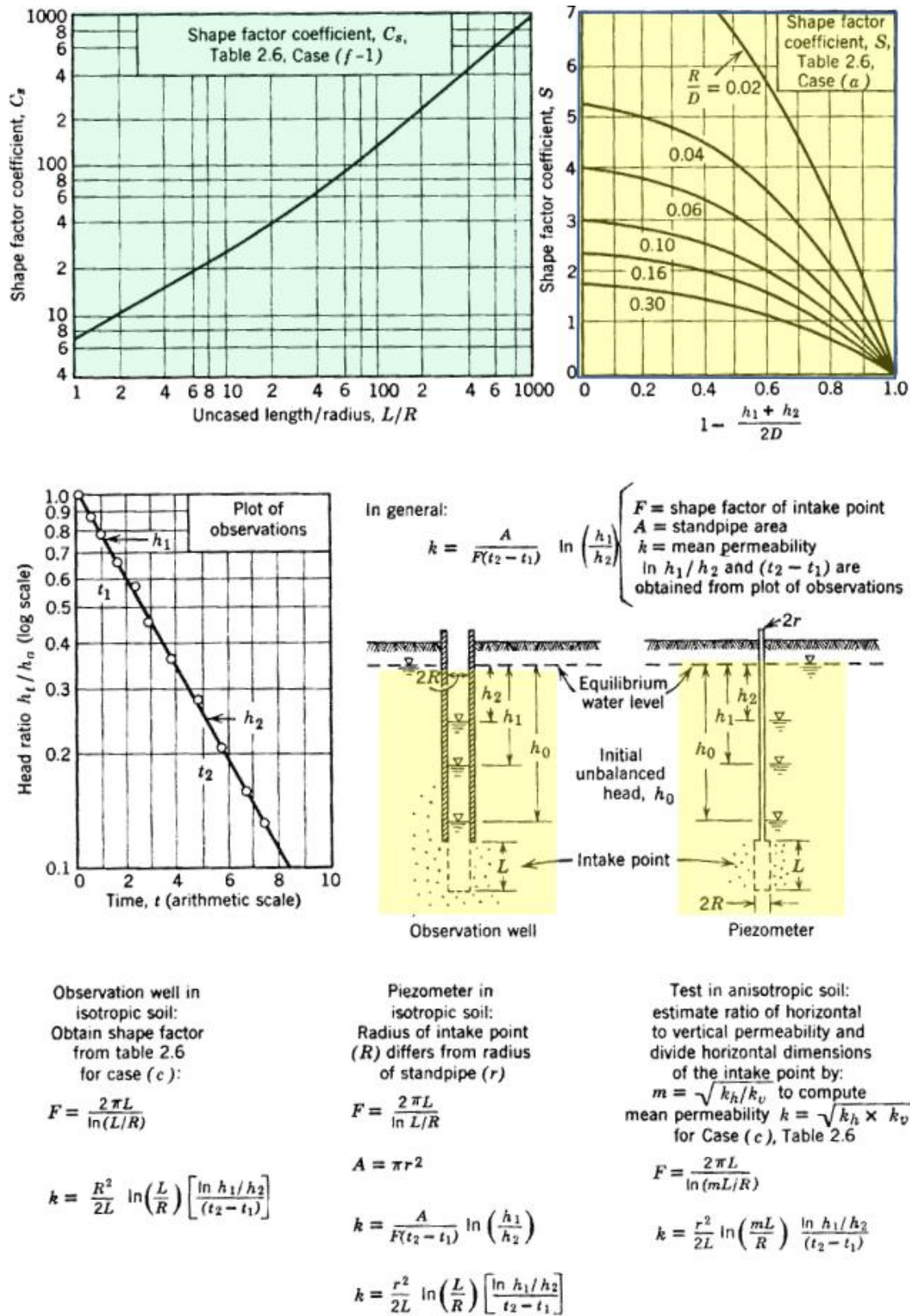


Figure 114 - The empirical constant, C_s in relation to L/R (US Department of the Navy, 1982). This is the figure referred to as 2.17 in the text of Figure 113. The shape factor chart for S in the upper right-hand corner is modified from Spangler (1963). Permeability is equivalent to hydraulic conductivity. F is the shape factor. Other parameters are defined in the text and in Figure 111 and Figure 113. The lower right hand corner diagram and text present a shape factor for an anisotropic formation in an unconfined setting.

Hydrogeology textbooks often include only a single equation for the Hvorslev method that is identical to condition (c) in Figure 113 and the equations in the lower left-hand portion of Figure 114. The equation has the criteria that the ratio of $L/R > 8$ which is the case in most small-diameter monitoring wells or piezometers where the screen length (L) is much greater than the radius of the casing (R). The equation includes the shape factor shown in Figure 113c. Condition (c) of Figure 113 is associated with Equations (107) and (108). These equations account for a difference in the well casing (r_c) and screen radius (r_s). The screen length is defined as the effective screen length and the screen radius also includes the gravel pack if present as shown in Figure 115b. Either Equation (107) or (108) can be used to compute K (Figure 113c). Figure 115 is a schematic of the properties used to develop Equations (107) and (108).

$$K = \frac{r_c^2 \ln\left(\frac{L_e}{r_s}\right)}{2 L_e (t_2 - t_1)} \ln\left(\frac{h_1}{h_2}\right) \quad (107)$$

$$K = \frac{r_c^2 \ln\left(\frac{L_e}{r_s}\right)}{2 L_e T_{0.37}} \quad (108)$$

where:

- h_1/h_2 = ratio of values used to define the slope (dimensionless)
- t_2-t_1 = times corresponding to the change in the normalized head, h_2 and h_1 (T)
- L_e = effective length of well screen (L)
- r_c = radius of the casing (L)
- r_s = radius of the screen interval (L)
- $T_{0.37}$ = time associated with the value of $H_i/H_0 = 0.368$ (T)
- K = hydraulic conductivity (LT^{-1})

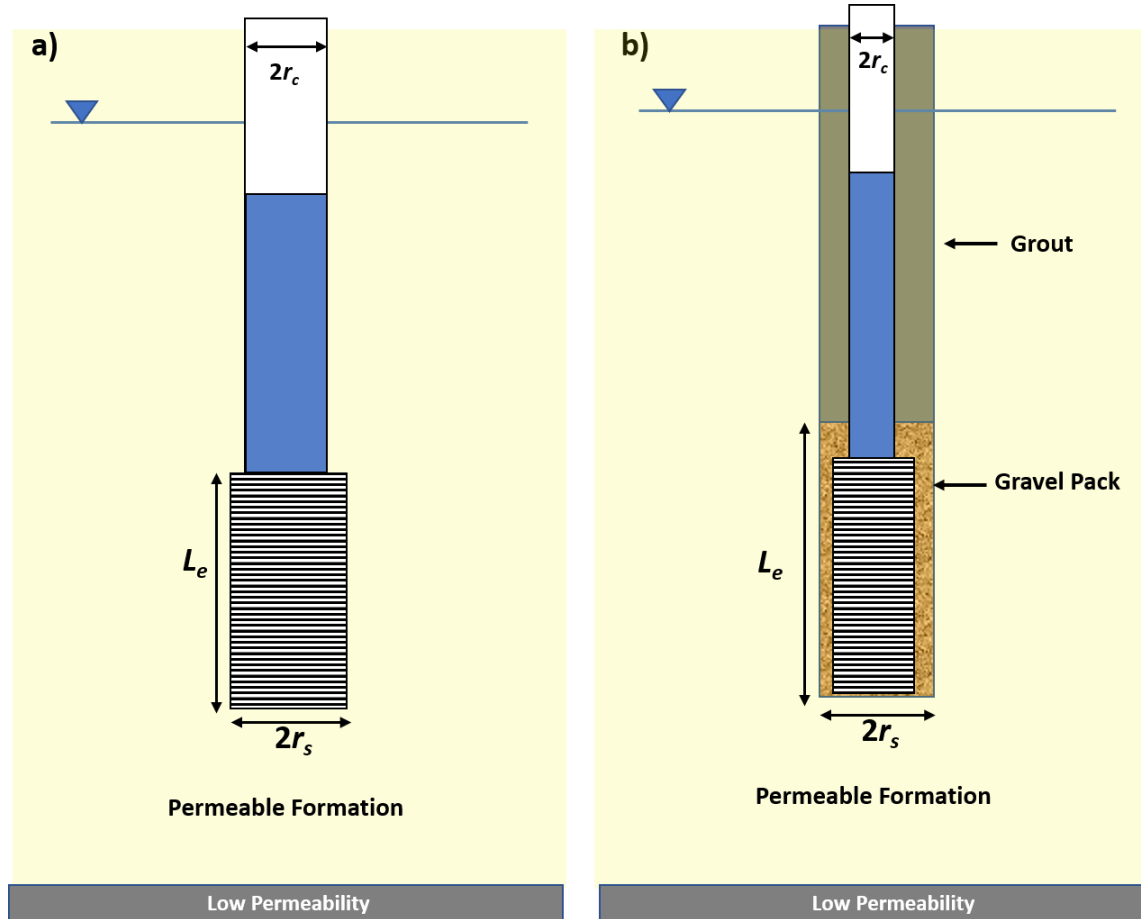


Figure 115 - The parameters used to solve for the hydraulic conductivity as defined in Equations (107) and (108). L_e is the effective length of the well screen. a) A well design where the radius of the well screen is larger than the radius of the well casing. b) A gravel packed well where the effective well screen radius and effective length of the well screen include well screen and gravel pack.

The effective well screen length, L_e is the length of screen or the length of the gravel pack surrounding the screen. The screen radius also includes the gravel pack dimensions when present. In some shape functions (e.g., the $f(3)$ of Figure 113) a value referred to as the effective radius of the slug test (R_o) is specified. This represents the distance the casing water flows from a falling-head test into the formation or the distance formational water travels to the well in a rising-head test. The value is empirical and generally assumed to be either the length of the well screen (L_e) or 200 times the effective radius of the well screen (including the gravel pack when present) (US Department of Navy, 1982; Butler, 1996). R_o is used as the effective radius of influence in other slug-test methods (e.g., Bouwer & Rice, 1976).

Example

Assume a slug test was completed in a screened well penetrating an unconfined formation designed as shown in Figure 116.

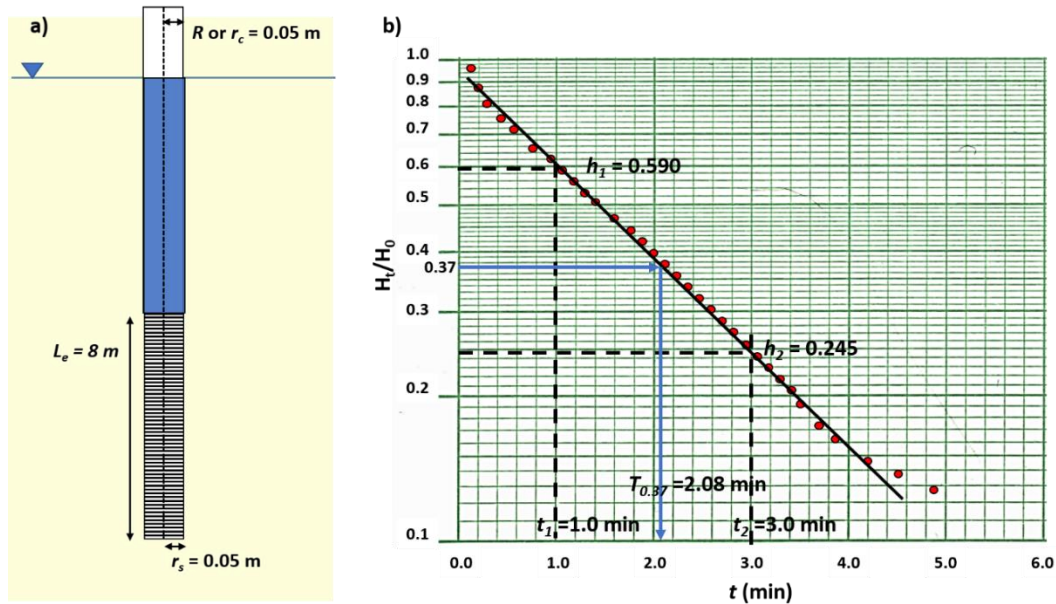


Figure 116 - Well design and slug-test data collected during the testing of an unpumped well. a) Well parameters. b) Semi-log plot of slug-test results. Values of h_1 , t_1 , h_2 , t_2 and the time lag $T_{0.37}$ are shown.

Examining the well design and recognizing it is constructed in an unconfined aquifer the method presented in Figure 113c is appropriate if the constraint that $L_e/R > 8$ is met; that factor is checked, $8 \text{ m} / 0.05 \text{ m} = 160$, so the criteria is met. Thus, Equation (107) is applied.

$$K = \frac{r_c^2 \ln\left(\frac{L_e}{r_s}\right)}{2 L_e (t_2 - t_1)} \ln\left(\frac{h_1}{h_2}\right)$$

$$K = \frac{(0.05 \text{ m})^2 \ln\left(\frac{8 \text{ m}}{0.05 \text{ m}}\right)}{2 (8 \text{ m}) (3 \text{ minutes} - 1 \text{ minute})} \ln\left(\frac{0.59 \text{ m}}{0.245 \text{ m}}\right) = 0.00035 \frac{\text{m}}{\text{minute}}$$

$$K = 0.0003 \frac{\text{m}}{\text{minute}} \frac{1440 \text{ minute}}{1 \text{ day}} = 0.50 \frac{\text{m}}{\text{day}}$$

The hydraulic conductivity can also be computed using the time-lag equation, Equation (108).

$$K = \frac{r_c^2 \ln\left(\frac{L_e}{r_s}\right)}{2 L_e T_{0.37}} = \frac{(0.05 \text{ m})^2 \ln\left(\frac{8 \text{ m}}{0.05 \text{ m}}\right)}{2 (8 \text{ m}) (2.08 \text{ minutes})} = 0.00038 \left(\frac{\text{m}}{\text{minute}}\right)$$

$$K = 0.00038 \frac{\text{m}}{\text{minute}} \frac{1440 \text{ minute}}{1 \text{ day}} = 0.54 \frac{\text{m}}{\text{day}}$$

Though the values are not identical, this is expected as readings of parameter values from the graph will contain some degree of error.

14.4.2 Bouwer and Rice Slug-Test Method

The Bouwer and Rice method is based on the work of Bouwer and Rice (1976) and Bouwer (1989). The underlying conceptual model is identical to the Hvorslev analysis. The Bouwer and Rice method uses a different representation for the shape factor.

The test methodology is applicable to open boreholes and wells fully or partially penetrating unconfined formations. The water table is a fixed boundary rather than a boundary that may be affected by testing. It can be used in confined conditions if the upper confining unit is leaky with an aquiclude as the lower boundary. Formations are assumed to be of constant thickness and infinite in lateral extent; the water table is near horizontal and does not change during the test, and formation-storage effects are negligible. It is assumed conditions are isotropic and homogeneous and the saturated thickness of the formation being tested does not change. Also, water-level changes induced by slug testing are assumed to be instantaneous (Kruseman & de Ritter, 2000).

The method is based on a mathematical model founded on the steady-state governing equation for radial flow. The parameter definitions are shown in Figure 117. Field data are plotted as the log of the remaining drawdown with time (Figure 118).

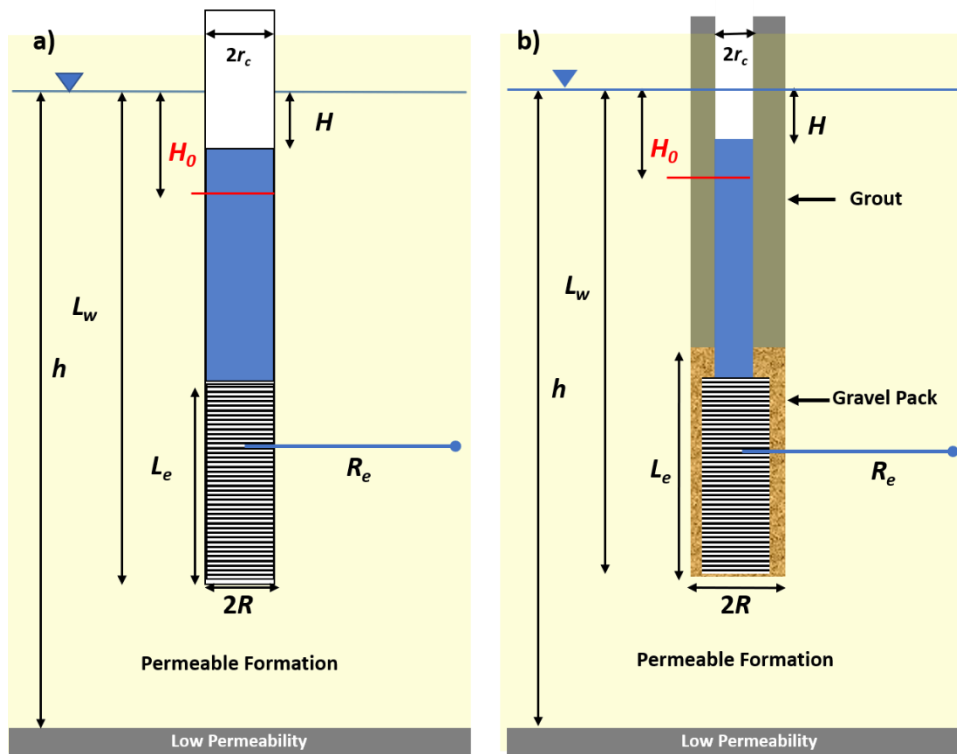


Figure 117 - Definitions of parameters used in the Bouwer and Rice method. This example shows the response to a rising head test where H_0 is the drawdown at t_0 and H is the remaining drawdown at time t . R_e is the effective radius of the slug test. a) A well where the radius of the well casing and well screen are the same. b) A setting where the well casing radius is smaller than the well screen radius. The screen length, L_e , includes the gravel-pack length. The screen radius, R , also includes the radius of the gravel pack when present.

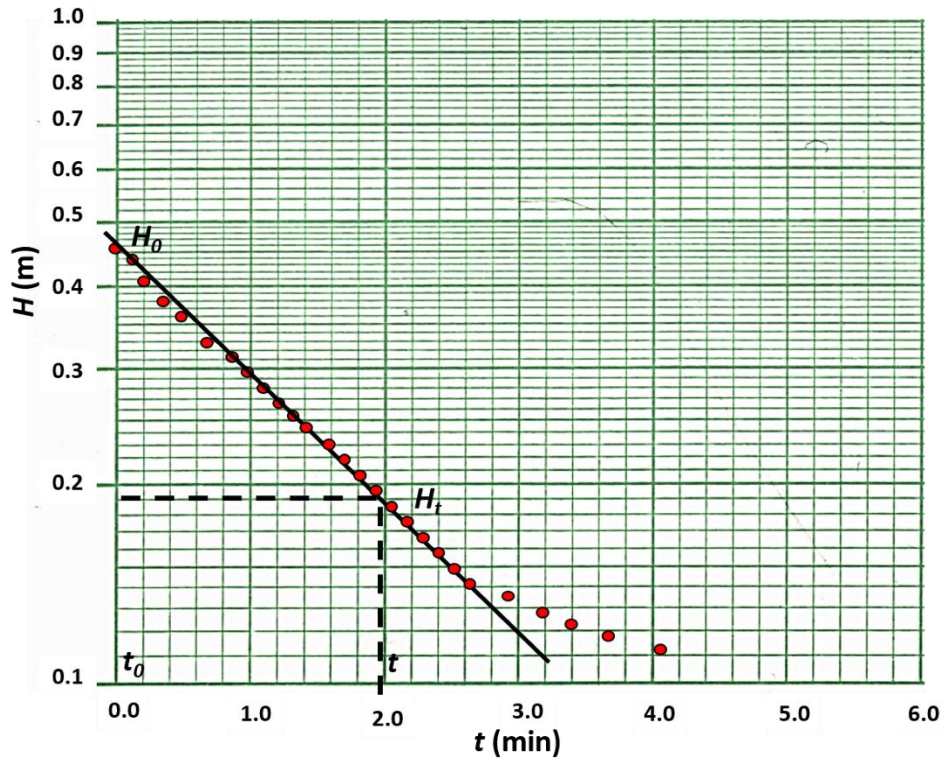


Figure 118 - Semi-log data plot of a rising head slug test. The log of the value H (remaining drawdown) is plotted over time. The initial value of H is H_0 .

A straight-line is fitted to the early time data (Figure 118). Issues discussed in the section on overdamped responses should be considered (Figure 109) when fitting a straight line to the semi-log plots.

Bouwer and Rice (1976) developed an analytical solution with several empirical parameters as shown in Equation (109) (Butler, 1998). Parameters are illustrated in Figure 117.

$$K = \frac{r_c^2 \ln\left(\frac{R_e}{R}\right)}{2 L_e t} \ln \frac{H_0}{H_t} \tag{109}$$

where:

- H_0 = maximum water level change (drawdown in a rising head test at time t_0) (L)
- H or H_t = remaining drawdown in a rising head test at time t (L)
- t = the time associated with H_t (T)
- r_c = radius of the casing (L)
- R = radius of the screened interval including the gravel pack if present (L)
- L_e = effective length of the screen including the gravel pack if appropriate (L)
- R_e = the effective radius of the slug test influence (L)

$$K = \text{hydraulic conductivity (LT}^{-1}\text{)}$$

The parameter R_e represents the radius of influence of the slug test in the formation. This is defined as an empirical value. It is computed as a constant, $\ln(R_e/R)$. Bouwer and Rice (1976) and Bouwer (1989) estimate the dimensionless ratio of $\ln(R_e/R)$ in Equation (109). Considering Figure 117, they used two approaches for this estimate based on the position of the well in the unconfined formation. The estimation process includes additional non-linear empirical constants that are derived from Figure 119 or computed from the equations defining the curves which are provided by (Butler, 1998, p. 109).

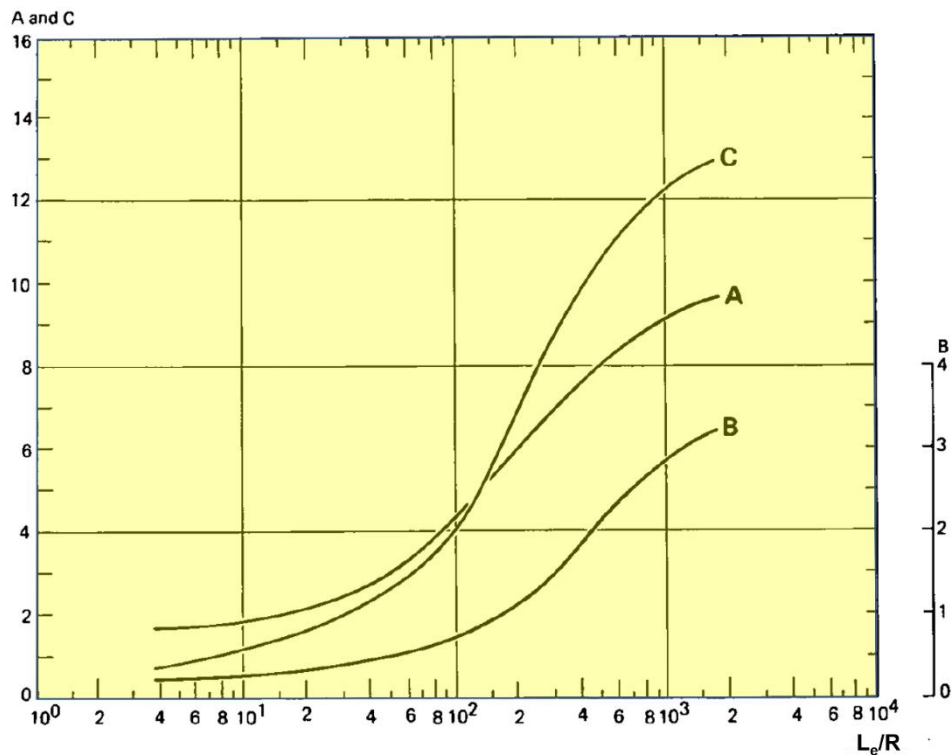


Figure 119 - Empirical constants used in the Bouwer and Rice method estimate of $\ln(R_e/R)$ (Kruseman & de Ritter, 2000).

If conditions are such that L_w , the distance of the bottom of the well from the water table, is less than h , the saturated thickness of the aquifer (Figure 117), then Equation (111) is applied to estimate $\ln(R_e/R)$. Parameters for Equation (110) and Equation (111) are defined in Figure 117. Empirical parameters A, B and C are derived from Figure 119. If L_w equals h , then Equation (111) is used.

$$\ln\left(\frac{R_e}{R}\right) = \left(\frac{1.1}{\ln\left(\frac{L_w}{R}\right)} + \left(\frac{(A + B) \ln\left[\frac{h - L_w}{R}\right]}{\frac{L_e}{R}} \right) \right)^{-1} \tag{110}$$

$$\ln\left(\frac{R_e}{R}\right) = \left[\frac{1.1}{\ln\left(\frac{L_w}{R}\right)} + \frac{C}{\frac{L_e}{R}} \right]^{-1} \tag{111}$$

Zlotnik (1994) developed a method to account for anisotropic conditions in the formation being slug tested. He defined R , the radius of the well screen, as $R^* = R(K_z/K_r)^{0.5}$, where K_z is the vertical hydraulic conductivity and K_r is the radial or horizontal hydraulic conductivity. The value R^* is substituted for R in Equations (109) through (111) when conditions are anisotropic. Slug testing does not provide direct measurement of the vertical hydraulic conductivity. Estimates of vertical hydraulic conductivity are often assumed to be an order of magnitude smaller than horizontal values in stratified rock or sediments. However, in some settings horizontal to vertical hydraulic conductivity ratios can be 1000:1 (Anderson et al., 2015).

Example

If the data plotted in Figure 118 represent a rising-head slug test (slug out of a well), and the formation tested is isotropic, homogenous, and unconfined as shown in Figure 120, then the hydraulic conductivity can be computed using Equation (109).

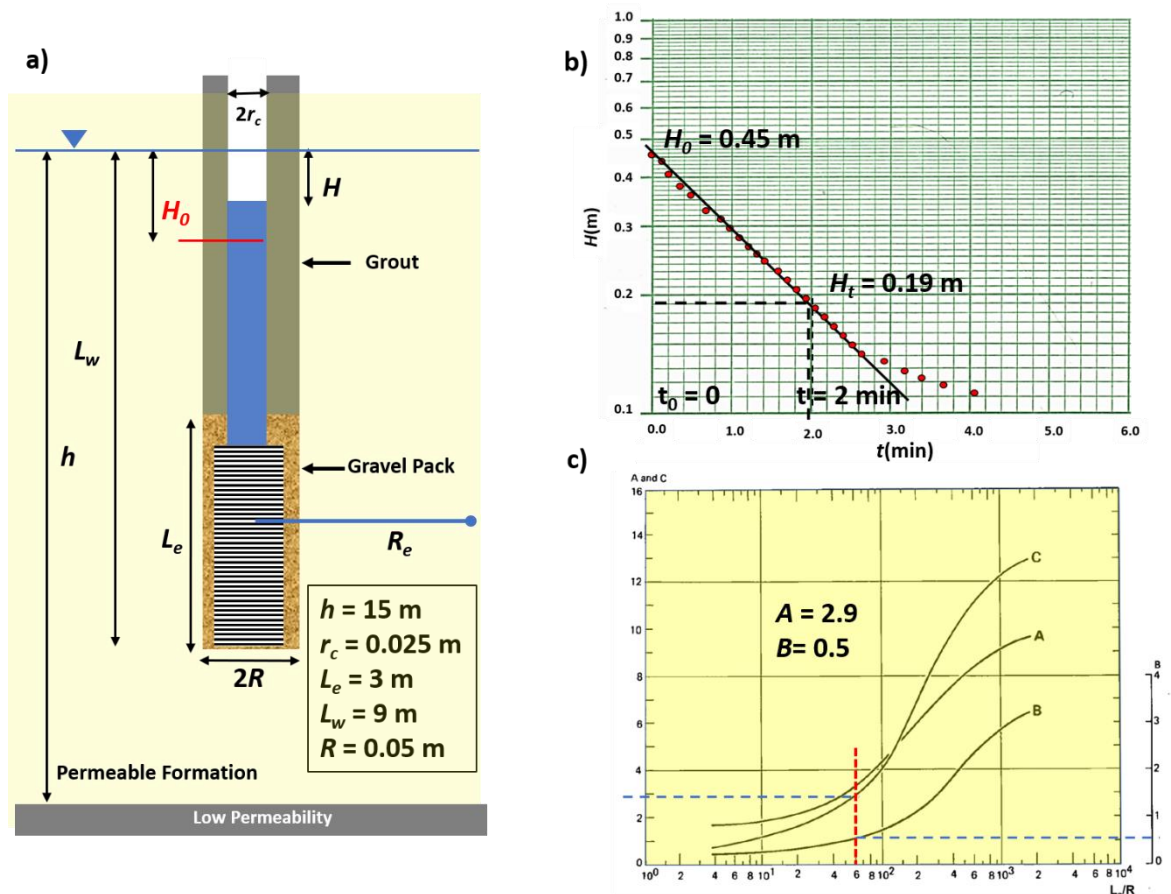


Figure 120 - Conditions under which a slug-out, rising-head test, was conducted. a) Parameters of the test well. b) Semi-log plot of the field data for the log of H versus time. c) Empirical relationships of A , B and C versus L_e/R (modified from Kruseman & de Ritter, 2000).

The first step is to estimate $\ln(R_e/R)$ using Equation (110). As L_w , 9 m, is less than h , 15 m, the constants from Figure 120 are $A=2.9$ and $B=0.5$.

$$\begin{aligned}\ln\left(\frac{R_e}{R}\right) &= \left(\frac{1.1}{\ln\left(\frac{R}{L_w}\right)} + (A+B) \ln\left(\frac{h-L_w}{\frac{R}{L_e}}\right) \right)^{-1} \\ &= \left(\frac{1.1}{\ln\left(\frac{0.05 \text{ m}}{9 \text{ m}}\right)} + (2.9+0.5) \ln\left(\frac{15 \text{ m} - 9 \text{ m}}{\frac{0.05 \text{ m}}{\frac{3 \text{ m}}{0.05 \text{ m}}}}\right) \right)^{-1} = 2.14\end{aligned}$$

The K is calculated using Equation (109).

$$\begin{aligned}K &= \frac{r_c^2 \ln\left(\frac{R_e}{R}\right)}{2 L_e t} \ln \frac{H_0}{H_t} = \frac{(0.025 \text{ m})^2 2.14}{2 (3 \text{ m}) 2 \text{ minutes}} \ln \frac{0.45 \text{ m}}{0.19 \text{ m}} = 0.000096 \frac{\text{m}}{\text{minute}} \\ K &= 0.000096 \frac{\text{m}}{\text{minute}} \frac{1440 \text{ minute}}{1 \text{ day}} = 0.14 \frac{\text{m}}{\text{day}}\end{aligned}$$

14.4.3 Cooper-Bredehoeft-Papadopoulos Slug-Test Method

The method developed by Cooper and others (1967) is used to assess slug-test results in wells that fully penetrate a confined aquifer. The method is commonly referred to as the Cooper-Bredehoeft-Papadopoulos method.

The method requires that the perforated interval of the test well fully penetrates the fully confined geologic unit being tested. It assumes the unit being tested is infinite in lateral extent, isotropic, and homogeneous. Values of T and S are computed. The test configuration and nomenclature are presented in Figure 121.

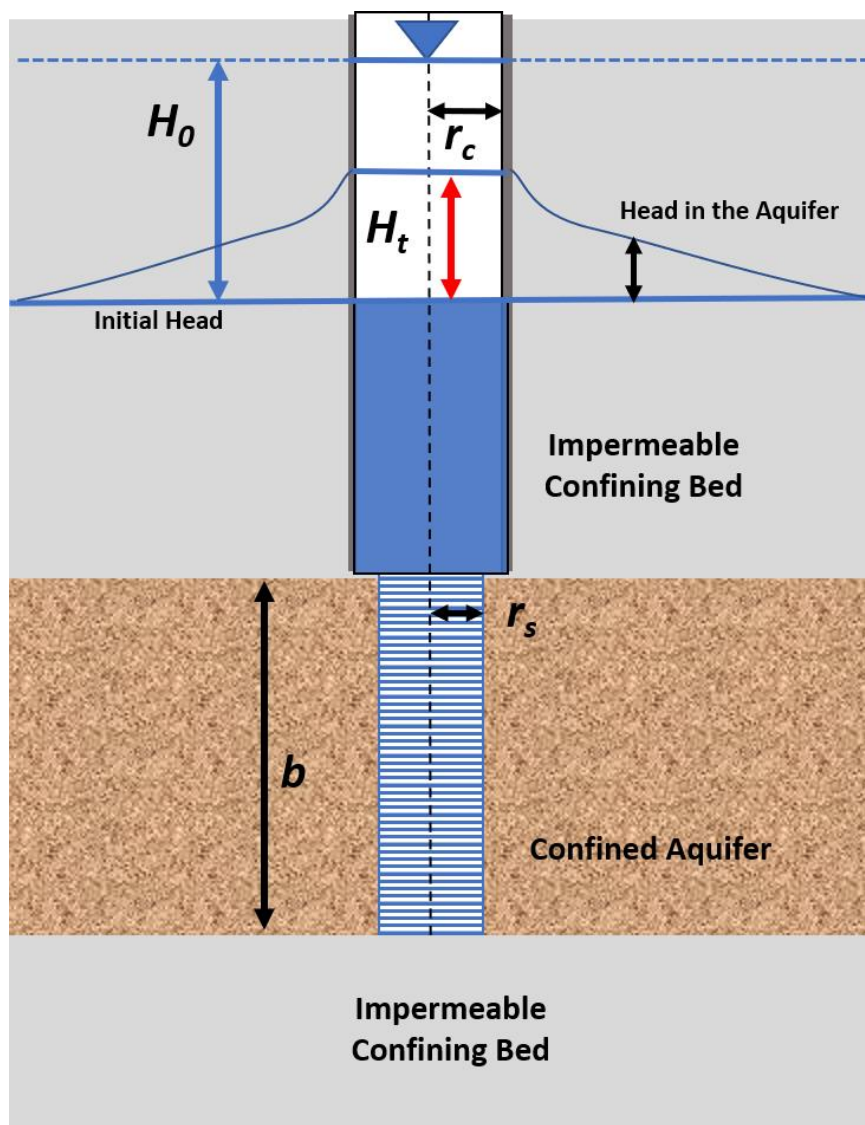


Figure 121 - Slug-in test configuration and parameters used for the Cooper-Bredehoeft-Papadopoulos Method. The tightly confined system of thickness b is fully penetrated by the screened interval of radius r_s . The casing radius is r_c . At the start of the test the water level in the well instantaneously rises to a position H_0 above the static water level. The decline of the water level over time is measured as H_t (after Cooper et al., 1967).

Cooper and others (1967) developed a slug-test analytical solution for the rise or fall of head in a fully penetrating well completed in a totally confined aquifer. Their method includes the general assumptions for the development of analytical solutions for confined aquifers discussed in Sections 6 and 8. Additional assumptions include that the head in the well is static at the beginning of the test and changes instantaneously at $t_0 = 0$; the well diameter is finite, meaning the water stored in the well bore must be considered; in response to an instantaneous head change in the well the rate at which the water flows from or to the well bore (falling-head or rising-head test) equals the rate of change of water volume in the well casing; and well loss is negligible (Kruseman & de Ridder, 2000).

The resulting solution is a function $F(\alpha, \beta)$ with two variables of integration, α and β (Kruseman & de Ridder, 2000) as shown in Equations (112) and (113).

$$\frac{H_t}{H_0} = F(\alpha, \beta) = \frac{8\alpha}{\pi^2} \int_0^\infty \frac{\exp\left(-\frac{\beta u^2}{\alpha}\right)}{u f(u, \alpha)} du \quad (112)$$

and

$$f(u, \alpha) = [uJ_0(u) - 2\alpha J_1]^2 + [uY_0(u) - 2\alpha Y_1(u)]^2 \quad (113)$$

where:

H_t = head at time t after the maximum head change occurs (L)

H_0 = instantaneous change of head at time t_0 (L)

$F(\alpha, \beta)$ = a function including an integral with variables α and β (dimensionless)

J_0 and J_1 = Bessel functions of the first kind, orders 1 and 2

Y_0 and Y_1 = Bessel functions of the second kind, orders 1 and 2

The complete definition of the well function is given in Kruseman and de Ridder (2000, p. 239). The variables of integration are defined by Equations (114) and (115).

$$\alpha = \frac{r_s^2 S}{r_c^2} \quad (114)$$

$$\beta = \frac{Tt}{r_c^2} \quad (115)$$

where:

α = parameter abbreviation (dimensionless)

β = parameter abbreviation (dimensionless)

r_s = radius of the screen (L)

r_c = radius of the casing (L)

S = storativity (dimensionless)

T = transmissivity (L^2T^{-1})

t = time (T)

The type curves are plotted from tables generated by using various values of α and β (Figure 122 and Figure 123). Additional table values and type curves can be plotted by using the analytical solutions and inputting additional values of β and α . Most often curves are computed using computer-assisted methods (Section 14.6).

a) Table 1. $10^{-10} \leq \alpha \leq 10^{-6}$

β	$\alpha = 10^{-6}$	$\alpha = 10^{-7}$	$\alpha = 10^{-8}$	$\alpha = 10^{-9}$	$\alpha = 10^{-10}$
0.001	0.9994	0.9996	0.9996	0.9997	0.9997
0.002	0.9989	0.9992	0.9993	0.9994	0.9995
0.004	0.9980	0.9985	0.9987	0.9989	0.9991
0.006	0.9972	0.9978	0.9982	0.9984	0.9986
0.008	0.9964	0.9971	0.9976	0.9980	0.9982
0.01	0.9956	0.9965	0.9971	0.9975	0.9978
0.02	0.9919	0.9934	0.9944	0.9952	0.9958
0.04	0.9848	0.9875	0.9894	0.9908	0.9919
0.06	0.9782	0.9819	0.9846	0.9866	0.9881
0.08	0.9718	0.9765	0.9799	0.9824	0.9844
0.1	0.9655	0.9712	0.9753	0.9784	0.9807
0.2	0.9361	0.9459	0.9532	0.9587	0.9631
0.4	0.8828	0.8995	0.9122	0.9220	0.9298
0.6	0.8345	0.8569	0.8741	0.8875	0.8984
0.8	0.7901	0.8173	0.8383	0.8550	0.8686
1.0	0.7489	0.7801	0.8045	0.8240	0.8401
2.0	0.5800	0.6235	0.6591	0.6889	0.7139
3.0	0.4554	0.5033	0.5442	0.5792	0.6096
4.0	0.3613	0.4093	0.4517	0.4891	0.5222
5.0	0.2893	0.3351	0.3768	0.4146	0.4487
6.0	0.2337	0.2759	0.3157	0.3525	0.3865
7.0	0.1903	0.2285	0.2655	0.3007	0.3337
8.0	0.1562	0.1903	0.2243	0.2573	0.2888
9.0	0.1292	0.1594	0.1902	0.2208	0.2505
10.0	0.1078	0.1343	0.1620	0.1900	0.2178
20.0	0.02720	0.03343	0.04129	0.05071	0.06149
30.0	0.01286	0.01448	0.01667	0.01956	0.02320
40.0	0.008337	0.008898	0.009637	0.01062	0.01190
50.0	0.006209	0.006470	0.006789	0.007192	0.007709
60.0	0.004961	0.005111	0.005283	0.005487	0.005735
80.0	0.003547	0.003617	0.003691	0.003773	0.003863
100.0	0.002763	0.002803	0.002845	0.002890	0.002938
200.0	0.001313	0.001322	0.001330	0.001339	0.001348

c) Table 3. $10^{-1} \leq \alpha \leq 10$

β	$\alpha = 0.1$	$\alpha = 0.2$	$\alpha = 0.5$	$\alpha = 1$	$\alpha = 2$	$\alpha = 5$	$\alpha = 10$
0.000001	0.9993	0.9990	0.9984	0.9977	0.9968	0.9948	0.9923
0.000002	0.9990	0.9986	0.9977	0.9968	0.9955	0.9927	0.9894
0.000004	0.9986	0.9980	0.9968	0.9955	0.9936	0.9898	0.9853
0.000006	0.9982	0.9975	0.9961	0.9945	0.9922	0.9876	0.9822
0.000008	0.9980	0.9971	0.9955	0.9936	0.9910	0.9857	0.9796
0.00001	0.9977	0.9968	0.9949	0.9929	0.9900	0.9841	0.9773
0.00002	0.9968	0.9955	0.9929	0.9900	0.9858	0.9776	0.9683
0.00004	0.9955	0.9936	0.9899	0.9858	0.9801	0.9687	0.9558
0.00006	0.9944	0.9922	0.9877	0.9827	0.9757	0.9619	0.9464
0.00008	0.9936	0.9909	0.9858	0.9800	0.9720	0.9562	0.9387
0.0001	0.9928	0.9899	0.9841	0.9777	0.9688	0.9512	0.9318
0.0002	0.9898	0.9857	0.9776	0.9687	0.9562	0.9321	0.9059
0.0004	0.9855	0.9797	0.9685	0.9560	0.9389	0.9061	0.8711
0.0006	0.9822	0.9752	0.9615	0.9465	0.9258	0.8869	0.8458
0.0008	0.9794	0.9713	0.9557	0.9385	0.9151	0.8711	0.8253
0.001	0.9769	0.9679	0.9505	0.9315	0.9057	0.8576	0.8079
0.002	0.9670	0.9546	0.9307	0.9048	0.8702	0.8075	0.7450
0.004	0.9528	0.9357	0.9031	0.8686	0.8232	0.7439	0.6684
0.006	0.9417	0.9211	0.8825	0.8419	0.7896	0.7001	0.6178
0.008	0.9322	0.9089	0.8654	0.8202	0.7626	0.6662	0.5797
0.01	0.9238	0.8982	0.8505	0.8017	0.7400	0.6384	0.5492
0.02	0.8904	0.8562	0.7947	0.7336	0.6595	0.5450	0.4517
0.04	0.8421	0.7980	0.7214	0.6489	0.5654	0.4454	0.3556
0.06	0.8048	0.7546	0.6697	0.5919	0.5055	0.3872	0.3030
0.08	0.7734	0.7190	0.6289	0.5486	0.4618	0.3469	0.2682
0.1	0.7459	0.6885	0.5951	0.5137	0.4276	0.3168	0.2428
0.2	0.6418	0.5774	0.4799	0.4010	0.3234	0.2313	0.1740
0.4	0.5095	0.4458	0.3566	0.2902	0.2292	0.1612	0.1207
0.6	0.4227	0.3642	0.2864	0.2311	0.1817	0.1280	0.09616
0.8	0.3598	0.3072	0.2397	0.1931	0.1521	0.1077	0.08134
1	0.3117	0.2648	0.2061	0.1663	0.1315	0.09375	0.07120
2	0.1786	0.1519	0.1202	0.09912	0.08044	0.05940	0.04620
4	0.08761	0.07698	0.06420	0.05521	0.04668	0.03621	0.02908
6	0.05527	0.04999	0.04331	0.03830	0.03326	0.02663	0.02185
8	0.03963	0.03658	0.03254	0.02933	0.02594	0.02125	0.01771
10	0.03065	0.02870	0.02600	0.02376	0.02130	0.01776	0.01499
20	0.01408	0.01361	0.01288	0.01219	0.01133	0.009943	0.008716
40	0.006680	0.006568	0.006374	0.006171	0.005897	0.005395	0.004898
60	0.004367	0.004318	0.004229	0.004132	0.003994	0.003726	0.003445
80	0.003247	0.003214	0.003163	0.003105	0.003022	0.002853	0.002668
100	0.002577	0.002559	0.002526	0.002487	0.002431	0.002313	0.002181
200	0.001271	0.001266	0.001258	0.001247	0.001230	0.001194	0.001149
400	0.0006307	0.0006295	0.0006272	0.0006242	0.0006195	0.0006085	0.0005944
600	0.0004193	0.0004188	0.0004177	0.0004163	0.0004141	0.0004087	0.0004016
800	0.0003140	0.0003137	0.0003131	0.0003123	0.0003110	0.0003078	0.0003035
1000	0.0002510	0.0002508	0.0002504	0.0002499	0.0002490	0.0002469	0.0002440

b) Table 2. $10^{-7} \leq \alpha \leq 10^{-1}$

β	$\alpha = 10^{-1}$	$\alpha = 10^{-2}$	$\alpha = 10^{-3}$	$\alpha = 10^{-4}$	$\alpha = 10^{-5}$
1.00×10^{-3}	0.9771	0.9920	0.9969	0.9985	0.9992
2.15×10^{-3}	0.9658	0.9876	0.9949	0.9974	0.9985
4.64×10^{-3}	0.9490	0.9807	0.9914	0.9954	0.9970
1.00×10^{-2}	0.9238	0.9693	0.9853	0.9915	0.9942
2.15×10^{-2}	0.8860	0.9505	0.9744	0.9841	0.9888
4.64×10^{-2}	0.8293	0.9187	0.9545	0.9701	0.9781
1.00×10^{-1}	0.7460	0.8655	0.9183	0.9434	0.9572
2.15×10^{-1}	0.6289	0.7782	0.8538	0.8935	0.9167
4.64×10^{-1}	0.4782	0.6436	0.7436	0.8031	0.8410
1.00×10^0	0.3117	0.4598	0.5729	0.6520	0.7080
2.15×10^0	0.1665	0.2597	0.3543	0.4364	0.5038
4.64×10^0	0.07415	0.1086	0.1554	0.2082	0.2620
7.00×10^0	0.04625	0.06204	0.08519	0.1161	0.1521
1.00×10^1	0.03065	0.03780	0.04821	0.06355	0.08378
1.40×10^1	0.02092	0.02414	0.02844	0.03492	0.04426
2.15×10^1	0.01297	0.01414	0.01545	0.01723	0.01999
3.00×10^1	0.009070	0.009615	0.01016	0.01083	0.01169
4.64×10^1	0.005711	0.005919	0.006111	0.006319	0.006554
7.00×10^1	0.003722	0.003809	0.003884	0.003962	0.004046
1.00×10^2	0.002577	0.002618	0.002653	0.002688	0.002725
2.15×10^2	0.001179	0.001187	0.001194	0.001201	0.001208

Figure 122 - Tables of the well function $F(\alpha, \beta)$ values computed for the Cooper-Bredehoeft-Papadopoulos method analytical solution of slug tests in a totally confined aquifer with a fully penetrating well. a) α from 1×10^{-10} to 1×10^{-6} and β from 0.001 to 200; b) α from 1×10^{-5} to 1×10^{-1} and β from 0.001 to 215; c) α from 0.1 to 10 and β from 1×10^{-6} to 1000 (Kruseman & de Ritter, 2000).

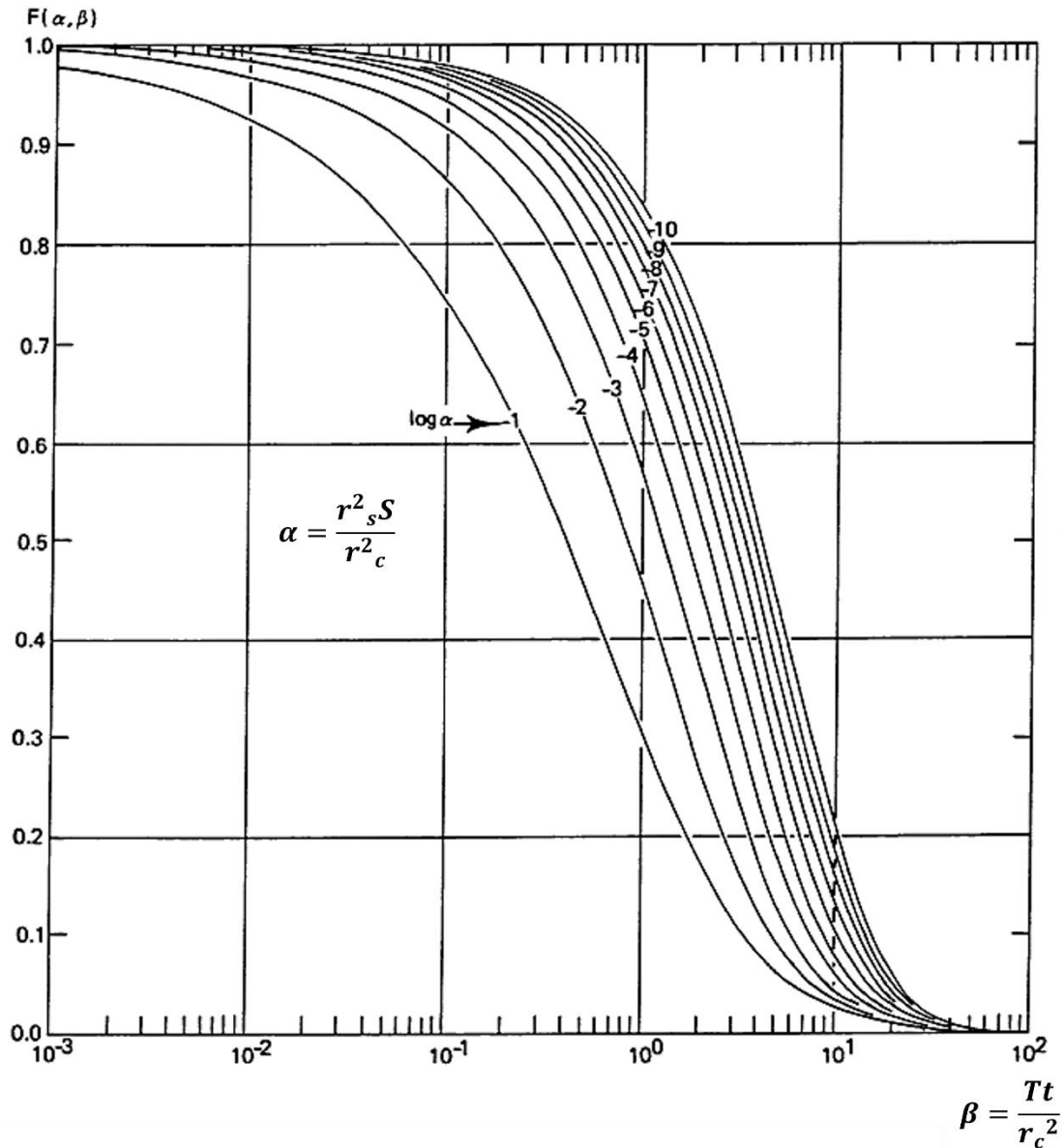


Figure 123 - Type curves for analyzing slug test data for a confined aquifer with a fully penetrating well using the Cooper-Bredehoeft-Papadopoulos Method. Values of $F(\alpha, \beta)$ are plotted on the arithmetic vertical scale and β on the horizontal logarithmic scale (modified from Kruseman & de Ritter, 2000).

To analyze slug-test data for the described confined-aquifer conditions the field data are plotted as H_t/H_0 on the arithmetic vertical axis and the log of t on the horizontal axis. Both the type curves and field data are plotted on the same semi-log scales, the horizontal axes are kept parallel, and the curves are matched by sliding them horizontally. The plots are not moved vertically. The match point yields values of $F(\alpha, \beta)$, α , β , H_t/H_0 , and t (Figure 124). The matched value of α and β are then used to solve for T and S .

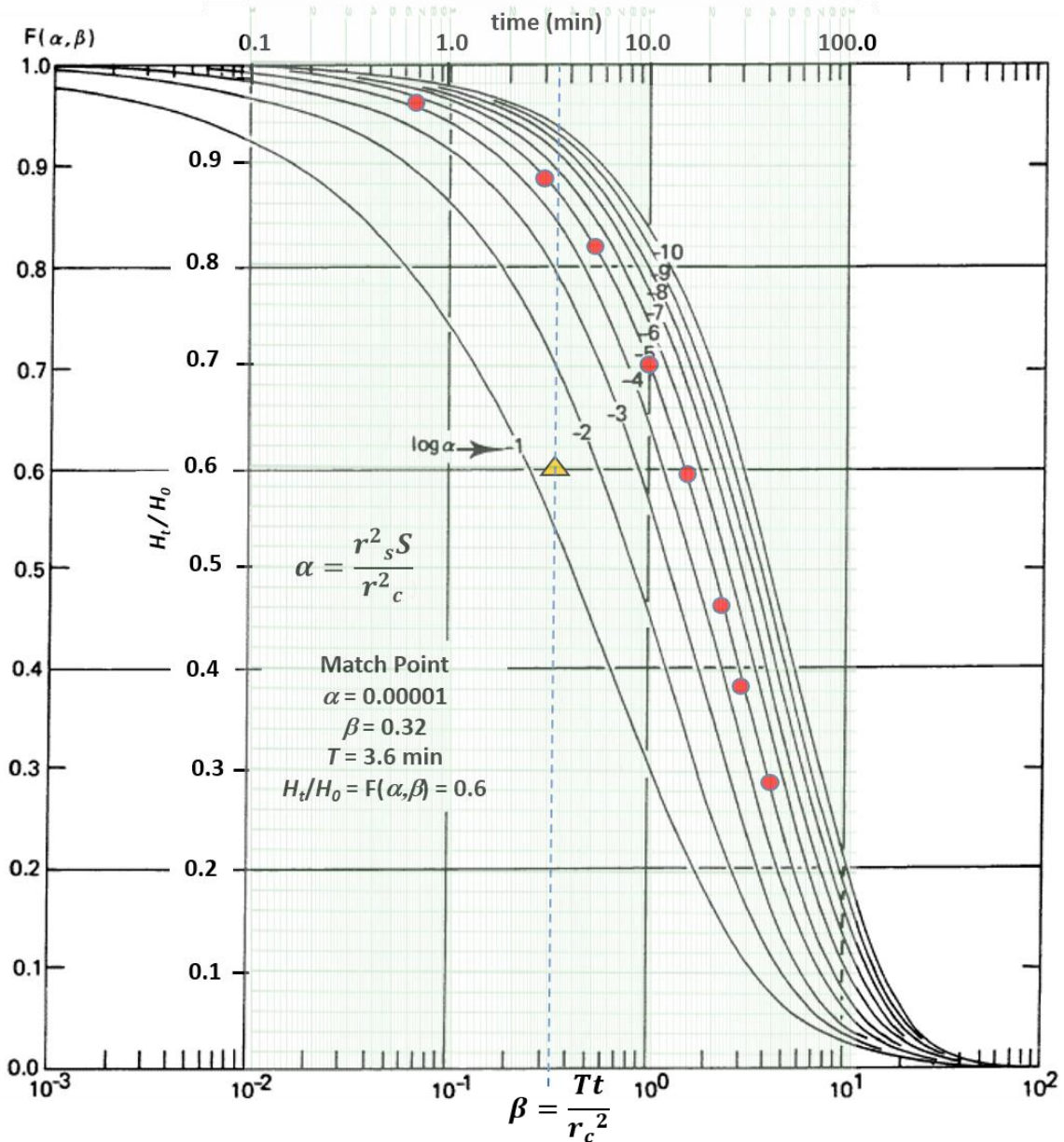


Figure 124 - Cooper-Bredehoeft-Papadopoulos Method of curve matching. Semi-log plots of the test data and the type curves are prepared on the same scales. The test data are then moved horizontally keeping the vertical axes values for both plots coincident until the observation data matches one of the curves. A match point is then chosen in the overlapping fields from which values of β and t are derived. α is the value of the curve matched with the field data. For this method the values of H_t/H_0 and $F(\alpha, \beta)$ are equal and not used in the calculation of T and S .

Example

Assume the data presented in Figure 124 represents a falling-head slug test of a totally confined aquifer that is 30 m thick (b). The well is fully penetrating, and the well radius and screen radius are the same, $r_s = r_c = 10 \text{ cm}$.

The match point yields $\beta = 0.7$ at $t = 3.6 \text{ min}$ and $\alpha = 0.00001$. Using Equation (115), rearranged to solve for T , yields $2.8 \text{ m}^2/\text{d}$.

$$\beta = \frac{Tt}{r_c^2}$$

$$T = \frac{\beta r_c^2}{t} = \frac{0.7 \left(10 \text{ cm} \frac{1 \text{ m}}{100 \text{ cm}}\right)^2}{\left(3.6 \text{ minute} \frac{1 \text{ d}}{1440 \text{ minute}}\right)} = \frac{2.8 \text{ m}^2}{\text{d}}$$

$$K = \frac{T}{b} = \frac{\frac{2.8 \text{ m}^2}{\text{d}}}{30 \text{ m}} = \frac{0.09 \text{ m}}{\text{d}}$$

S is computed using Equation (114).

$$\alpha = \frac{r_s^2 S}{r_c^2}$$

$$S = \frac{\alpha r_c^2}{r_s^2} = \frac{0.00001 (10 \text{ cm})^2}{(10 \text{ cm})^2} = 0.00001$$

14.4.4 KGS Slug Test Method

The Cooper and others (1960) model used to analyze a slug test in a confined aquifer was generalized more recently by Hyder and others (1994). As the principal authors were associated with the Kansas Geological Survey the model is referred to as the KGS model (1994). The KGS method is included here because it is a more general method supported by the software packages.

The KGS method uses a curve-matching method that is similar to the approach of Cooper and others (1960). It accounts for partial penetration, anisotropy, skin effects and can be used to analyze both confined and unconfined conditions. The model parameters are represented in Figure 125.

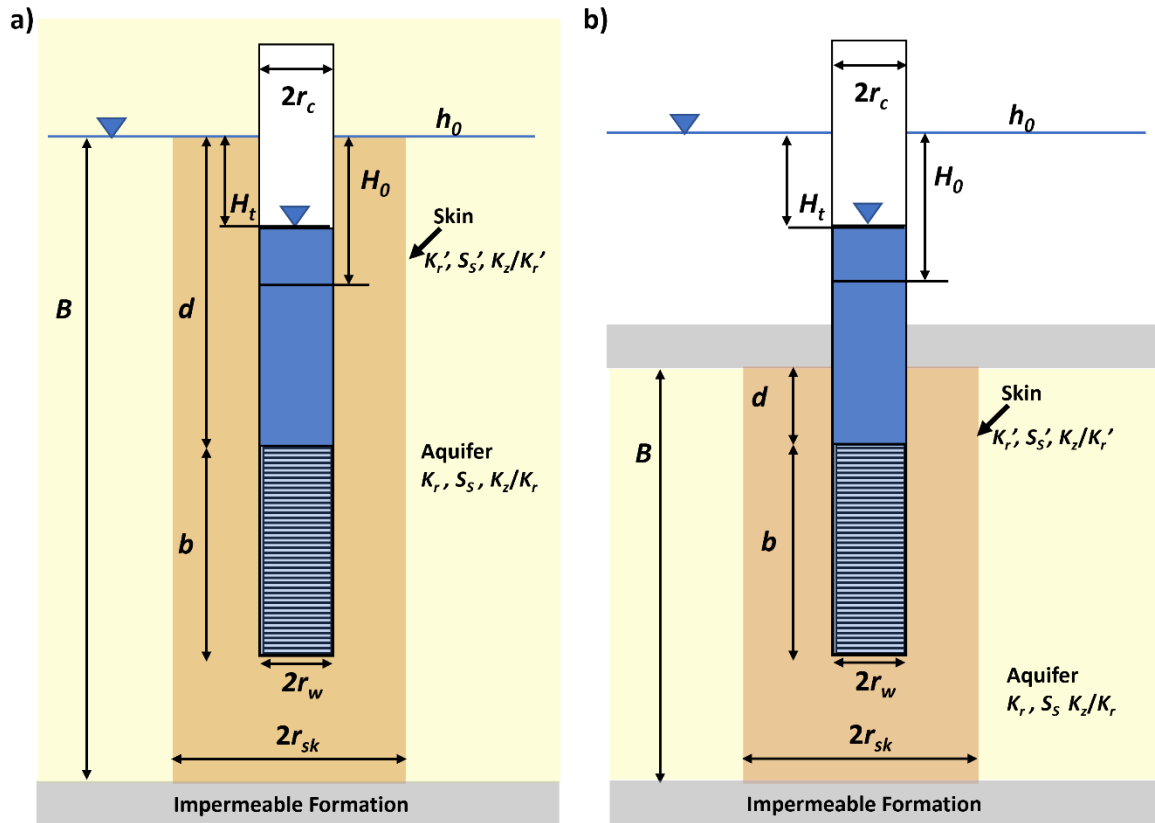


Figure 125 - Schematic of the parameters used in the KGS slug-test method (Hyder et al., 1994). Gray shading represents impermeable material, yellow shading is the aquifer ($K_r, S_s, K_z/K_r$), and light orange shading represents a skin effect zone with different hydraulic properties ($K_r', S_s', K_z/K_r'$). H_0 is the instantaneous head change from the static (h_0) at the beginning of the test and H_t is the head measured from the static at some time during the test. B is the aquifer thickness. d is the length of the blank casing in the aquifer and b is the length of screen. r_w is screen radius, r_c is the casing radius and r_{sk} is the radius of the skin zone. a) A representation of unconfined conditions. b) A representation of confined conditions.

The analytical solution developed by Hyder and others (1994) is based on the conditions that the aquifer is infinite in extent, homogeneous, and of uniform thickness; the potentiometric surface is initially horizontal; the well is fully or partial penetrating; water-level change is instantaneous; conditions can be confined or unconfined; and flow is unsteady. Hydraulic anisotropy and skin effects can be accounted for. However, the authors stress that although accounting for specific storage, anisotropy, and skin effect is theoretically possible, the model is rather insensitive to these parameters. The analytical solution is written as shown in Equation (116).

$$\frac{H_t}{H_0} = F\left(\beta, \alpha, \varphi, \frac{d}{b}, \frac{b}{B}\right) \quad (116)$$

where:

- H_t = water level in the well at time t (L)
- H_0 = water level at in the well at the start of the test, at time t_0 (L)
- β = $K_r B t / r^2$ (dimensionless)

- $\alpha = (r_w^2 S_s B) / r_c^2$ (dimensionless)
 $\psi = (K_z / K_r)^{0.5} / (b / r_w)$ (dimensionless)
 $B =$ saturated thickness of the aquifer (L)
 $t =$ time (T)
 $K_r =$ radial hydraulic conductivity (LT^{-1})
 $r_c =$ well-casing radius (L)
 $r_w =$ screen or perforated interval radius (L)
 $S_s =$ aquifer specific storage (L^{-1})
 $K_z =$ vertical aquifer hydraulic conductivity (LT^{-1})
 $b =$ length of screen or perforated interval (L)

Type curves are generated by plotting the normalized head (H_t/H_0) versus the logarithm of β for field well configuration parameters ($\psi, d/b, b/B$). An example is presented in Figure 126.

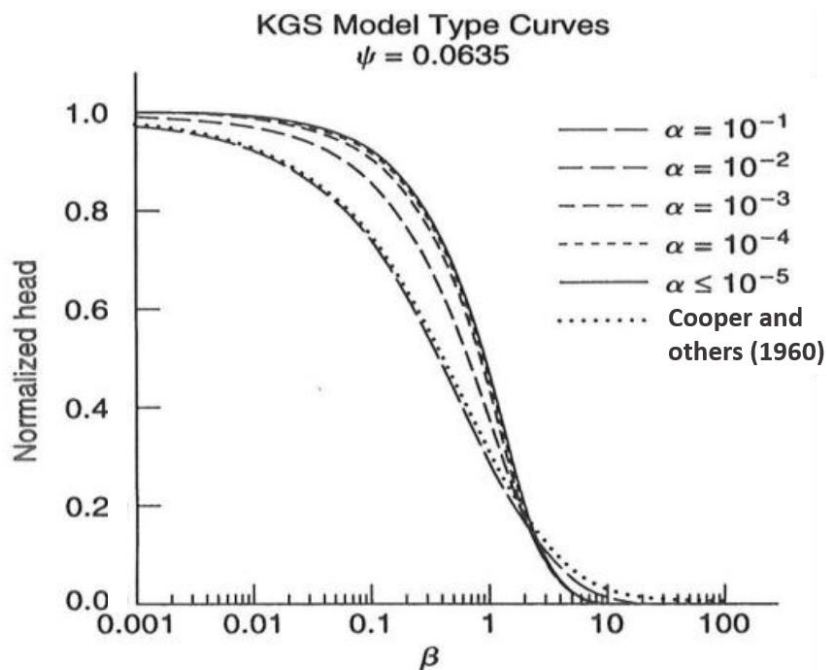


Figure 126 - Type curves for the KGS slug-test method where $\psi = 0.0635$. Normalized head values are plotted on the y axis and the logarithm of β on the x axis. Type curves for various values of α are shown. For comparison with the method of Cooper and others (1960), the dotted line equivalent to $\alpha=0.1$ is presented (Hyder et al., 1994; Butler, 1998).

The field data are plotted as H_t/H_0 versus time since the test began and the recovering head at time t is divided by the head at the beginning of the test (Figure 127).

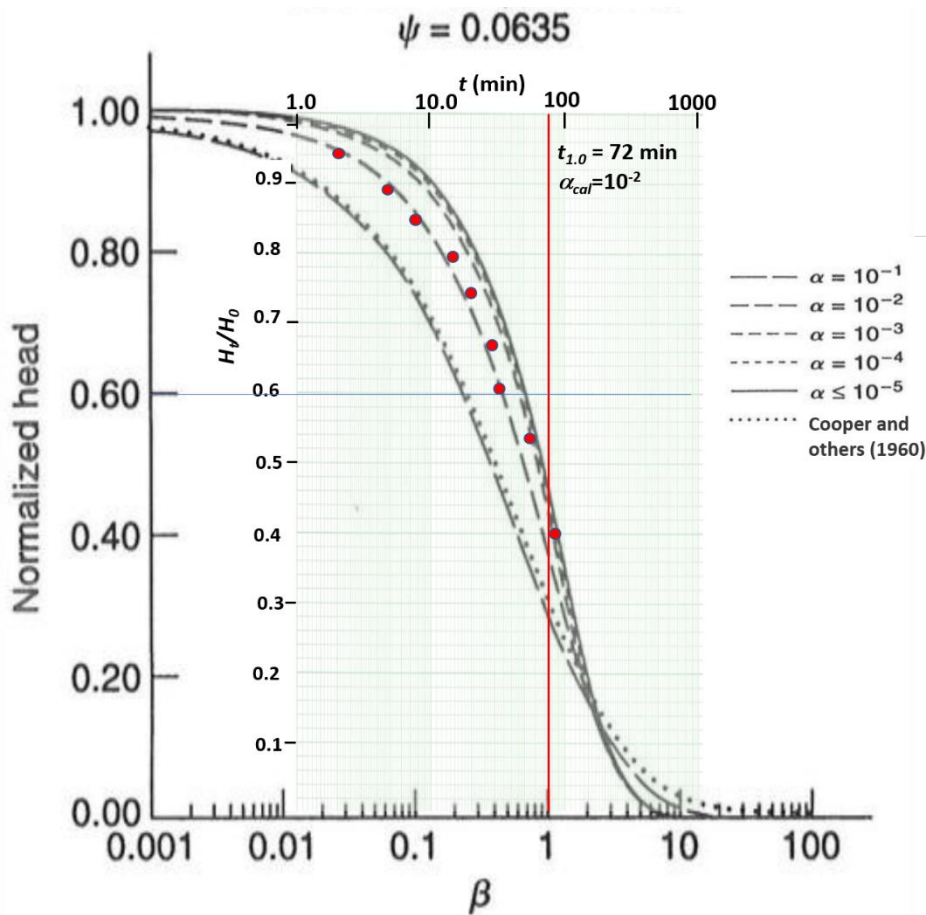


Figure 127 - Example of KGS curve matching. The field data are plotted at the same scale as the type curves as is done when using the method of Cooper and others (1960). The type curve is overlain on the field data and matched to an α curve by sliding the type curve along the x axis. No vertical movement of either graph occurs. Once a curve match is achieved, the field time value ($t_{1.0}$) corresponding to $\beta=1$ is read from the x axis and α is estimated from the matching point (α_{cal}). With these data, the radial hydraulic conductivity is derived from the definition of β .

$$K_r = \frac{r_c^2}{bt_{1.0}} \tag{117}$$

where:

- K_r = radial hydraulic conductivity (LT^{-1})
- r_c = well casing radius (L)
- b = length of screen or perforated interval (L)
- $t_{1.0}$ = time corresponding to $\beta=1.0$ for curve match to field data as shown in Figure 127 (T)

Specific storage is computed accounting for partial penetration.

$$S_s = \alpha_{cal} \frac{r_c^2}{r_w^2 b} \tag{118}$$

where:

- S_s = specific storage (L^{-1})

- α_{cal} = α match value
 r_c = well casing radius (L)
 r_w = screen or perforated interval radius (L)
 b = length of screen or perforated interval (L)
 $t_{1.0}$ = time corresponding to $\beta=1.0$ for curve match to field data as shown in Figure 127 (T)

Example

A slug-out test is performed on a partially penetrating well in a fine-grained unconfined system. The well screen and casing radius are 0.0248 m. The well screen is 0.39 m long and partially penetrates the 4 m thick aquifer. No skin effect is identified, and the aquifer is assumed to be isotropic ($K_r=K_z$). The ψ value is 0.0635 for this well configuration. The radial hydraulic conductivity is calculated from the curve match shown in Figure 127.

Using the curve match and well parameters K_r is calculated assuming $K_z/K_r = 1$.

$$K_r = \frac{r_c^2}{bt_{1.0}}$$

$$K_r = \frac{(0.0248 \text{ m})^2}{0.39 \text{ m} \cdot 72 \text{ min} \cdot \frac{1 \text{ d}}{1440 \text{ min}}} = \frac{0.032 \text{ m}}{\text{d}}$$

$$S_s = \alpha_{cal} \frac{r_c^2}{r_w^2 b}$$

$$S_s = 0.01 \frac{(0.0248 \text{ m})^2}{(0.0248 \text{ m})^2 \cdot 0.39 \text{ m}} = 0.26 \text{ m}$$

Limitations of the KGS Method

A comparison study by Ismael (2016) showed that the KGS model (Hyder et al., 1994) provided similar estimates of K to the Hvorslev (1951) method when applied to two unconfined-aquifer settings. Butler (1998) states that when using the KGS method with a fully penetrating well S_s estimates may not be reliable especially when $\psi > 0.005$. He notes that when using the KGS model, it is "...virtually impossible to estimate the anisotropy ratio in field applications". He states that a shift in the field data suggesting a decrease in the anisotropy ratio cannot be separated from one caused by a decrease in radial hydraulic conductivity. Butler (1998) suggests anisotropic conditions are better distinguished using multiple-well slug-test methods presented in his book and the literature.

As with other curve-matching methods, software can provide calculations using appropriate well-configuration type curves and apply automated-matching methodologies. However, the user needs to specify an initial value for anisotropy, which is often assigned a value of one because it is not known, even though the vertical hydraulic

conductivity is typically lower in most materials—a notable exception is loess which often has a higher vertical hydraulic conductivity due to its wind-blown deposition. Manual fine tuning of the automated computed match improves the parameter estimates as discussed in Section 14.6.

14.5 Method to Interpret Underdamped Slug Tests

An underdamped-response of a groundwater system to slug testing is commonly encountered when formational hydraulic conductivity is high. The response to a slug-in or slug-out test is oscillatory as shown in Figure 103. The oscillatory behavior of the water level is like that of a damped spring as described in physics books where the force of gravity on a mass hung from a spring and the energy stored in the spring counteract and the motion gradually dissipates as the kinetic energy is converted to thermal energy (e.g., Kreyszig, 1979).

Several authors have developed methods to analyze an underdamped slug test response including van der Kamp (1976), Kipp (1985), Springer and Gelhar, 1991), Wylie and Magnuson (1995), McElwee and Zenner (1998), Zurbuchen and others (2002), Butler (1998), and Butler and others (2003). Butler and Garnett (2000) produced a Kansas Geologic Survey open file report and Butler and others (2003) published a journal article that presents a type-curve methodology for assessing test results from unconfined and confined formations based on descriptions by Springer and Gelhar (1991) and Butler (1998). They developed two high-hydraulic conductivity models based on the Bouwer and Rice (1976) and Hvorslev (1951) slug-test formulations, the high-K Bouwer and Rice, and the high-K Hvorslev models (Butler & Garnett, 2000; Butler et al., 2003). Their work utilized spreadsheet models to develop type curves and generate estimates of K . They provide free access to the spreadsheet models on the [KGS website](#)⁷. The methods are described in the paper by Butler and Garnett (2000) published by the KGS and the journal article by Butler and others (2003). A description of this methodology follows.

Slug testing of high hydraulic conductivity formations (like sand and gravels, and gravels) requires attention to detail as the oscillatory response often occurs over the first few seconds to 10s of seconds of the test. In cases where slug-displacement volumes are small, and screened intervals long, observable water-level responses may only last a few seconds. A successful test requires an instantaneous water-level change and a transducer set to record water-level variations with a time interval of a fraction of a second if possible. Butler and others (2003) report that the pneumatic air-displacement method is recommended for head displacement as the release of air pressure at the initiation of the test results is a near-instantaneous head change (Figure 109, Figure 128). Solid slugs are used when pneumatic test methods are unavailable.

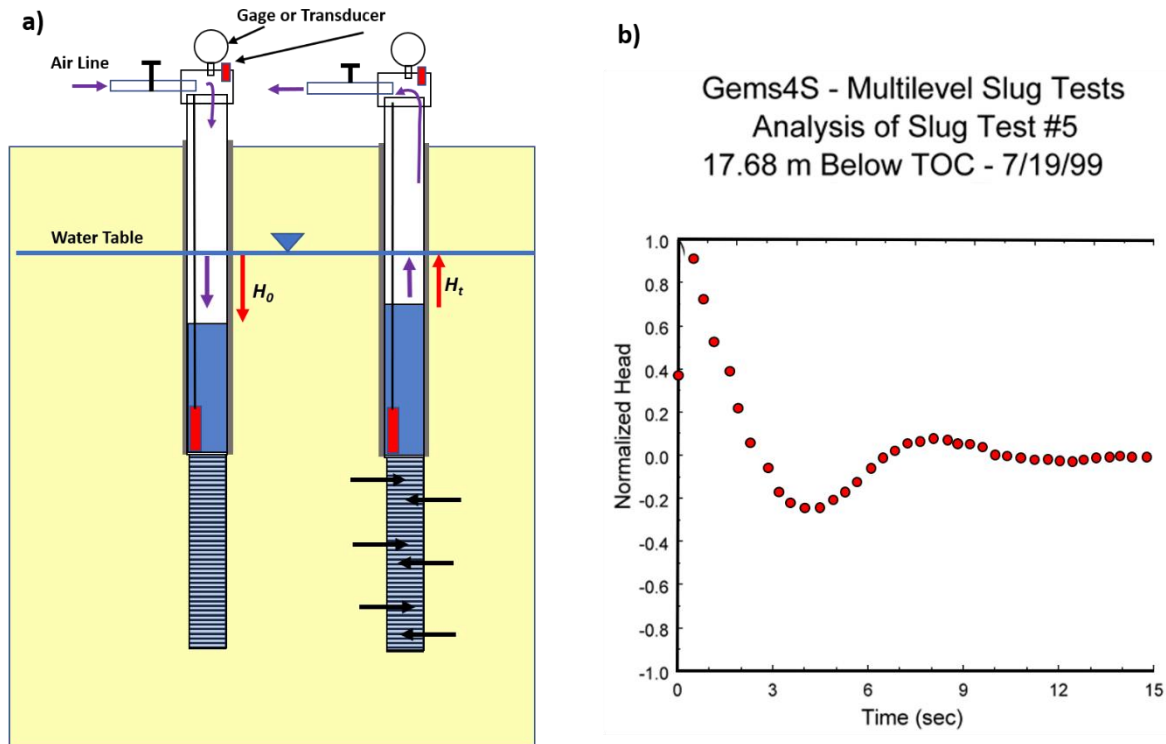


Figure 128 - Pneumatic slug test set up and plot of normalized head change data. An initial static head measurement is taken before the test is initiated. a) Pneumatic slug-test set up as described in Figure 108. The casing is capped and fitted with a valve, airline, and gauge and/or pressure transducer. A second transducer is placed below the maximum water level, H_0 . The water table is depressed by pressurizing the water column in the sealed casing. The valve is closed and H_0 computed from the pressure gage reading or a cap mounted pressure transducer (small red rectangle). At time zero the valve is opened, and the water level is allowed to recover. A transducer (large vertical red rectangle) in the well records the water level response. b) Plot of normalized slug test head data (red dots), H_t/H_0 . The normalized head data are plotted on an arithmetic scale with a zero value (static-fully recovered water level), and positive and negative values centered on the static water level.

Prior to beginning the slug test a static water level is measured using steel or electronic water-level tape. At the initiation of the test the well is capped, and the casing pressurized. The displacement value H_0 is estimated from the pressure gage or cap transducer reading (air pressure depressing the water level). It is recommended that multiple tests be conducted using different displacements, H_0 . Values of K should not be dependent on H_0 . Butler and Garnett (2000) and Butler and others (2003) report that the depth of the transducer below the static level is important. They found that when the well transducer was located within 0.5 m of the static water level the resulting measured maximum value of H_t/H_0 was 0.9 or higher. They suggest that if the test is run and the recorded maximum normalized head is less than 0.9, the test should be repeated with the transducer raised to a new position closer to the static water level. Of course, the transducer must be below the water level (H_0) measured at the beginning of the test. It is also important that the transducer sensitivity range, accuracy, and recording interval meet the slug-test design.

14.5.1 Development of Type-Curve Equations

Butler (1996), Butler and Garnett (2000), and Butler and others (2003) provide the theory and equations used to develop type curves for analysis of oscillatory data. The methodology is applicable to unconfined and confined systems. An example of data analysis by this method follows.

Type curves based on C_D , a dimensionless damping factor, t_d dimensionless time, and the normalized water-level deviation, w_d , are generated using the overdamped type-curve equations based on the damped-spring solution (Kreyszig, 1979) as shown in Equations (119), (120), and (121). The equations express the relationship between the dimensionless normalized head w_d at dimensionless time t_d (i.e., $w(t_d)$) for various values of the dimensionless damping parameter C_D . The L_e term is calculated as part of the curve matching process (i.e., $L_e = (t^*/t_d^*)^2 g$, where $*$ denotes a curve match value and g is the acceleration due to gravity (modified from Butler and Garnett, 2000; Butler et al., 2003).

$$w_d(t_d) = e^{-\frac{C_D}{2}t_d} \left[\cos(\omega_d t_d) + \frac{C_D}{2\omega_d} \sin(\omega_d t_d) \right], C_D < 2 \quad (119)$$

$$w_d(t_d) = e^{-t_d} [1 + t_d], C_D = 2 \quad (120)$$

$$w_d(t_d) = \left(\frac{1}{\beta_1 - \beta_2} \right) (\beta_1 e^{\beta_2 t_d} - \beta_2 e^{\beta_1 t_d}), C_D > 2 \quad (121)$$

where:

- C_D = damping parameter (dimensionless)
- g = acceleration of gravity (LT^{-2})
- H_0 = change in water level initiating a slug test (initial displacement (L))
- L_e = effective length of water column in well calculated as part of the curve matching process (i.e., $L_e = (t^*/t_d^*)^2 g$, where $*$ denotes a curve match value and g is the acceleration due to gravity (L))
- t_d = time parameter ($(g/L_e)^{0.5}t$) where t = time (dimensionless)
- w = deviation of water level from static level in well (L)
- w_d = normalized water-level deviation (T)
- ω_d = frequency parameter ($|1 - (C_D/2)^2|^{0.5}$) (dimensionless)
- β_1 = $-(C_D/2) - \omega_d$ (dimensionless)
- β_2 = $-(C_D/2) + \omega_d$ (dimensionless)

For values of w_d , t_d , and C_D type curves are generated and plotted on an arithmetic scale with $w_d = 0$ representing the static normalized water level (Figure 129). The slug-test data are plotted on the same vertical scale as the type curves being utilized (Figure 130).

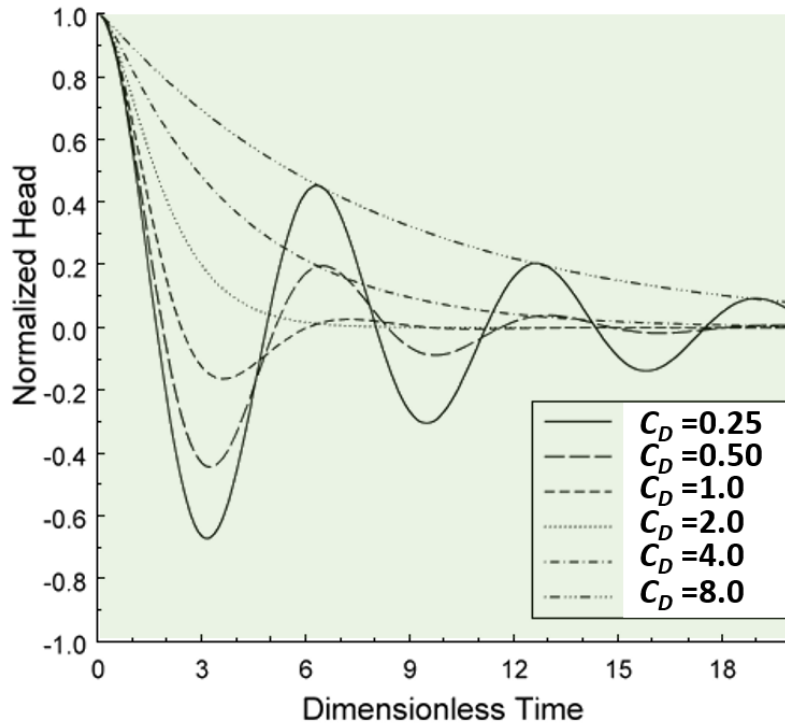


Figure 129 - Type curves used to analyze overdamped slug test responses. The arithmetic plot of normalized head (w_d) versus dimensionless time (t_d) for various dampening parameter values C_D (Butler & Garnett, 2000).

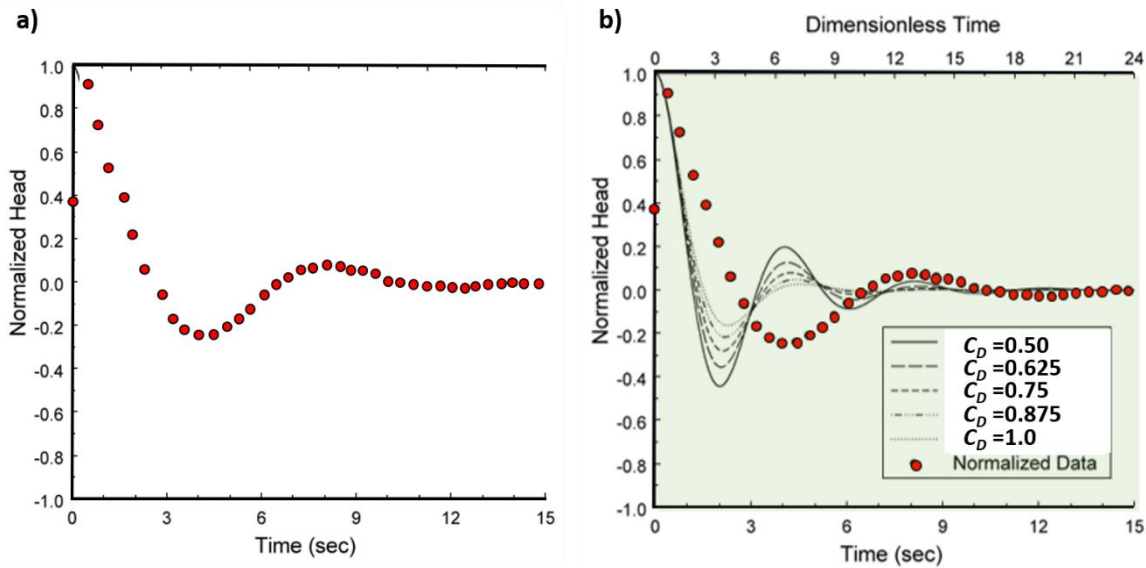


Figure 130 - Example from Butler and Garnett (2000) of slug test GEMS4S conducted at the Geohydrological Experimental and Monitoring Site (GEMS) in Douglas County Kansas, USA. a) Slug-test results shown in red dots plotted as normalized head versus time at the same vertical scale as the type curves. b) Slug-test data superposed on the type curves representing curves generated for the dimensional damping parameter C_D between 0.50 and 1.0. This superposition is shown to illustrate the process. Field data and type curves are adjusted to obtain a match. The base x axis is the slug-test time, and the upper x axis is the type-curve dimensionless time. The illustrated type curves and data do not match in this figure (Butler & Garnett (2000)).

The slug-test data are superposed on the type-curve plot. The normalized head and dimensionless time scales are identical. The test time scale (x axis on Figure 130) is the slug-test time data, and the upper x axis is the type-curve dimensionless time axis. To obtain

the best match between the field data and type curve, the field-data plot remains unchanged as the type-curve plot is stretched and contracted horizontally, attempting to generate the best match with the C_D values. The scale of the vertical axes is not changed. Once a match is determined, values of C_D^* , t_d^* , and t^* (* is used to designate match values) are generated and used to solve for K . The Excel® spreadsheet software provided by Butler and Garnett (2000) kgs.ku.edu/Hydro/Publications/OFR00_40/ generates a family of type curves that most closely match the slug-test data and facilitates the fitting process. Iterative adjustment by the user is relied upon to generate visual matches between the data and type curves. Butler and others (2003) describe the use of the type-curve generator spreadsheet and high- K estimator spreadsheets. The Butler and Garnett (2000) fitting process and results for their example problem are shown in Figure 131.

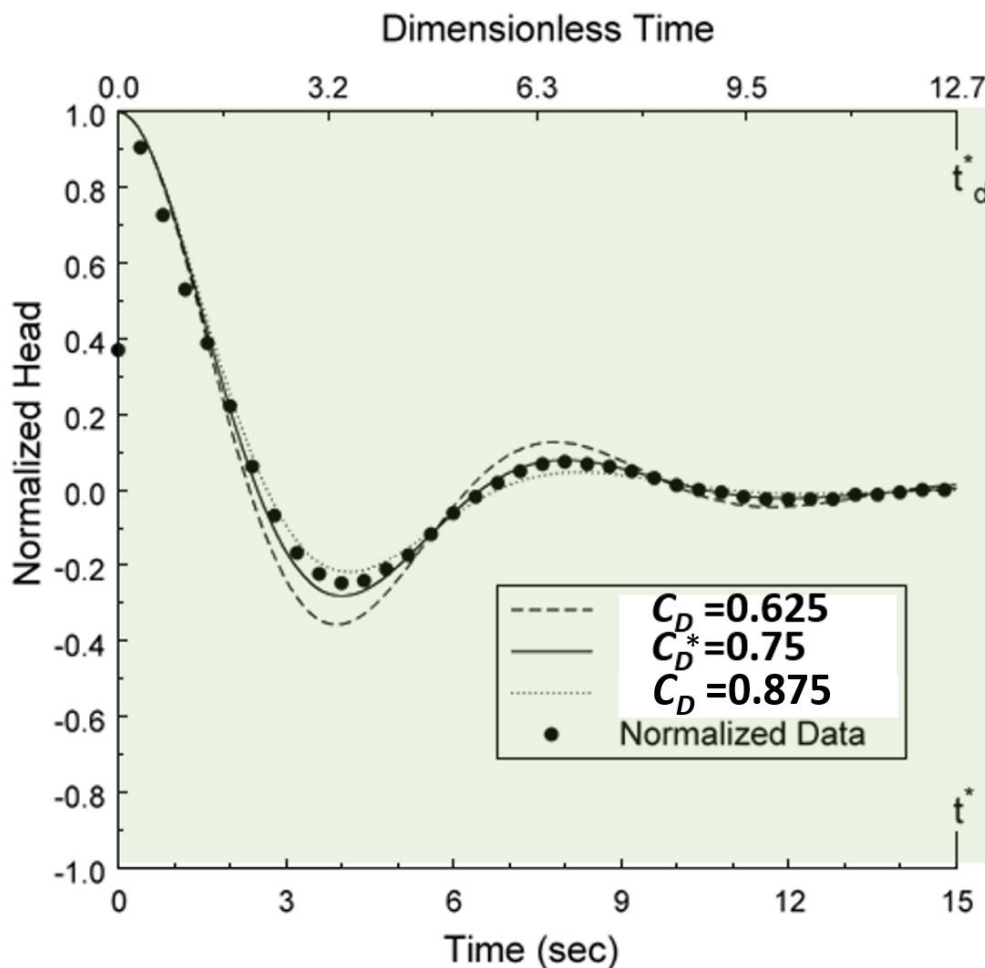


Figure 131 - Final match of slug-test data (black dots) presented by Butler and Garnett (2000). Only the C_D values that most closely match the field data are shown with a best match of $C_D^*=0.75$ in this example. The additional match values are $t_d^* = 12.7$, and the corresponding slug-test data time $t^* = 15$ sec (Butler & Garnett, 2000).

Butler and others (2003) note that matches can be achieved because the value t_d controls the period (duration), and C_D controls the degree of curvature or oscillatory behavior. The curve match for the example shown in Figure 130 provides values of $C_D^* =$

0.75, $t_d^* = 12.7$ and $t^* = 15$ sec (* denotes these as match values). These values are used to solve for K using the Unconfined-High- K Bouwer and Rice model (Springer & Gelhar, 1991) or the Confined-High- K Hvorslev model (Butler, 1998). The High- K models are contained in the High- K Estimator spreadsheet that also requires well construction data, and an estimate of the effective length of the water column (L_e).

14.5.2 Unconfined-High- K Bouwer and Rice Model

The Unconfined-high- K Bouwer and Rice Model is based on the work of Springer and Gelhar (1991) as presented by Butler and others (2003) and shown here as Equation (122).

$$K_r = \frac{t_d^* r_c^2 \ln\left(\frac{R_e}{r_s}\right)}{t^* 2 b C_D^*} \quad (122)$$

where:

- t_d^* = curve match time (dimensionless)
- t^* = slug-test curve match time (T)
- r_c = well-casing radius corrected for the radius of the transducer cable (L)
- r_s = radius of the well screen or borehole in isotropic aquifer, $r_s (K_z/K_r)^{0.5}$ for anisotropic systems (L)
- K_r = radial hydraulic conductivity (LT^{-1})
- R_e = effective radius of the slug test is computed as $\ln(R_e/r_s)$ from Equation (110) or (111) where h is the aquifer thickness (units of L) and L_w is the distance from the bottom of the well screen to the water table (units of L), and L_e is the effective length of the well screen (b as defined here) (units of L). Figure 121 provides definitions of these parameters. (dimensionless)
- b = screen length (L)
- C_D^* = match of dampening parameter (dimensionless)

The High- K Bouwer and Rice model can be used when the base of the well screen is in contact with an impermeable boundary (lower boundary). The L_e parameter used to compute R_e is defined in Figure 116 as the effective length of the well screen. It is not the same L_e factor used in the type-curve calculations of Equations (119), (120), and (121) as defined in the list of parameters below Equation (121). The High- K -Estimator spreadsheet assists in computing the K_r value.

14.5.3 Confined – High- K Hvorslev Model

The High- K Hvorslev model was developed by Butler and others (2003). It is defined by Equation (123).

$$K_r = \left(\frac{t_d^*}{t^*}\right) \frac{r_c^2 \ln\left(\frac{b}{2r_s} + \left(1 + \left(\frac{b}{2r_s}\right)^2\right)^{0.5}\right)}{2 b C_D^*} \tag{123}$$

where:

- t_d^* = curve match time (dimensionless)
- t^* = slug-test curve match time (T)
- r_c = well-casing radius corrected for the radius of the transducer cable (L)
- r_s = radius of the well screen or borehole in isotropic aquifer, $r_s (K_z/K_r)^{0.5}$ for anisotropic systems (L)
- K_r = radial hydraulic conductivity (LT⁻¹)
- b = screen length (L)
- C_D^* = match of dampening parameter (dimensionless)

The High-K Hvorslev model does not represent conditions where the bottom of the casing is adjacent to an impermeable bottom boundary. Butler and others (2003) state that if this condition occurs the term $2r_s$ in the numerator of Equation (123) should be replaced with r_s . They state that corrections for small-diameter wells can also be incorporated.

Example

A pneumatic slug test was performed in a high hydraulic conductivity, isotropic, confined aquifer as shown in Figure 132.

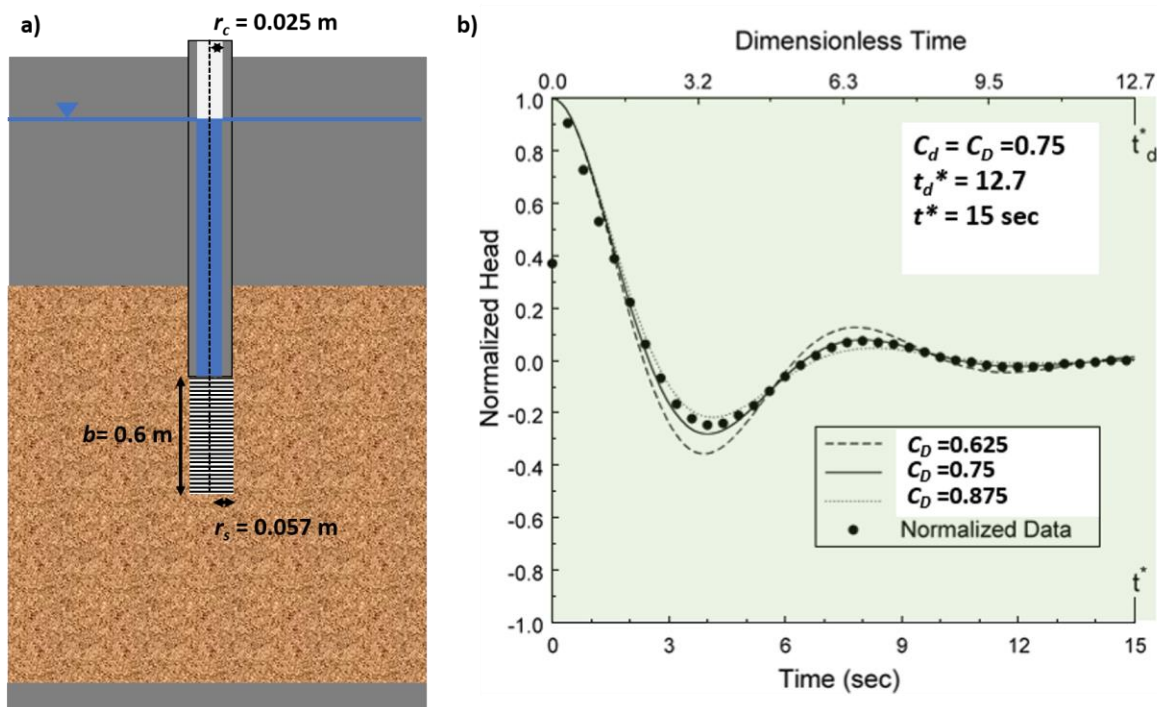


Figure 132 - Set up for a slug test of an isotropic and homogenous sand and gravel confined aquifer and a hypothetical plot of the slug-test results. a) Well configuration. b) Normalized slug-test results and curve-match parameters.

The slug-test results were normalized and curve matched to the type curves shown in Figure 128. Parameters derived from the type-curve match are $C_D = 0.75$, $t_d^* = 12.7$ and $t^* = 15$ sec. The formation is confined so the High-K Hvorslev Model is applied.

$$K_r = \left(\frac{t_d^*}{t^*}\right) \frac{r_c^2 \ln\left(\frac{b}{2r_s} + \left(1 + \left(\frac{b}{2r_s}\right)^2\right)^{0.5}\right)}{2 b C_D^*}$$

$$= \left(\frac{12.7 \text{ s}}{15 \text{ s}}\right) \frac{(0.025 \text{ m})^2 \ln\left(\frac{0.6 \text{ m}}{2(0.057 \text{ m})} + \left(1 + \left(\frac{0.6 \text{ m}}{2(0.057 \text{ m})}\right)^2\right)^{0.5}\right)}{2 (0.6 \text{ m}) (0.75)} = 0.0014 \frac{\text{m}}{\text{s}}$$

$$K_r = 0.0014 \frac{\text{m}}{\text{s}} \frac{86400 \text{ s}}{\text{d}} = 121 \frac{\text{m}}{\text{d}}$$

14.5.4 Transitional Slug-Test Responses

The curve matching methods described above have also been applied to non-oscillatory slug test responses in highly conductive settings. Results may show a mix of responses. These are referred to as transitional slug test data sets because conditions show a system is acting partly as overdamp and partly as undamped (Figure 103). Butler and others (2003) provide an example of a set of curves derived from the packer test of an interval of a highly conductive aquifer. The data are plotted and then the curve-matching methodology and K_r calculations are performed. The authors conclude that the underdamped curve-matching methods and equations provided good estimates of formational properties when hydraulic conductivity values are high. When curve-matching results were compared to values computed using the conventional overdamped Hvorslev equation method (straight-line approach) the conventional method produced values that were 13 percent higher than those derived from underdamped curve matching. The authors concluded that when the values of C_D were greater than three, conventional underdamped methods provided reasonable values.

14.6 Software Available to Analyze Slug Tests

The same commercially available software packages used to analyze pumping tests include modules to analyze slug-test data. As with pumping-test software analyses, slug-test analytical methods are constrained by the hydrogeological setting and well configuration. The most widely used commercial software packages are AQTESOLV (aqtesolv.com↗), AquiferTest V12 (waterloohydrogeologic.com↗), and Aquifer^{win32} Version 6 (groundwatermodels.com↗). General information regarding slug-test analysis capabilities of each program is found in [Box 8](#)↕. The individual software web-sites provide additional details.

Free software packages are also available to analyze underdamped and overdamped data. One [software package available on the Kansas Geological Survey Site](#)[↗] has been addressed in this section (Butler & Garnett, 2000). A search of the internet will find additional software to analyze overdamped responses, e.g., Wylie and Magnuson (1995) present spreadsheet modeling of a slug test using the van der Kamp method; Matos-Rosillo and others (2018) provide *SlugIn 1.0: A Free tool for automated Slug Test Analysis*; Halford and Kuniansky (2002) offer an open-file report titled *Documentation of Spreadsheets for the Analysis of Aquifer-Test and Slug-Test Data*. This [USGS publication](#)[↗] includes spreadsheets for the Bouwer and Rice Method, van der Kamp Method and the Cooper, Bredehoeft, and Papadopulos Method. Geoprobe Drilling Rig and Tool Manufacturer developed a pneumatic slug-test system and provides Slug Test Analysis Software (Geoprobe, 2016) for pneumatic slug testing that can be downloaded from [Geoprobe](#)[↗].

Part 3 addresses methods used to perform hydraulic tests of open boreholes, called packer tests. Packer tests are most often applied to characterize an isolated portion of an uncased borehole.

14.7 An Opportunity to Evaluate Hydrogeologic Properties Using Slug-Test Data

Section 14 discussed estimating hydraulic properties using slug test data. [Exercise 7](#)[↘] provides hands-on opportunities to evaluate slug-test data.

PART 3: PACKER TESTS

Packer tests are conducted to determine the hydraulic properties of sections of an uncased or open borehole. Packers are installed to seal off a test interval. Constant-discharge or constant-head tests are conducted to characterize hydraulic properties. Section 15 briefly describes packer-test methods.



This photograph shows the installation of two packers used to isolate a section of open borehole (<http://www.usgs.gov/media/images/photograph-usgs-hydrologists-and-packers-well-testing>).

15 Basic Hydraulic Testing with Packers

This section addresses how the hydrogeologic properties of sections of boreholes can be characterized. In some settings it is desirable to determine the hydraulic properties of one or more sections of a borehole penetrating semi-consolidated or consolidated materials. In others, a portion of a screened interval penetrating an unconsolidated formation that has collapsed around the screened interval during well completion can be characterized using packers set inside the screen.

Bradbury and others (2006) provide a good summary of borehole characterization methods in "[Contaminant Transport through Aquitards: Technical Guidance for Aquitard Assessment](#)", which is available for download on the gw-project.org site. It provides information on the application of geophysical tools, instrumentation, and methods to estimate hydraulic properties. It is recommended that the reader review this document to broaden the discussion presented here that focuses mainly on the use of packers to isolate intervals of the borehole and characterize hydrogeologic properties of these isolated sections.

15.1 The Packer Test

Hydraulic testing of isolated portions of a borehole is usually accomplished using inflatable packers to seal off the interval of interest (Figure 133). Single-packer systems can be used to test the entire interval of borehole/well below the packer, or a double-packer (also called straddle-packer) system can be installed to test the zone located between the packers.

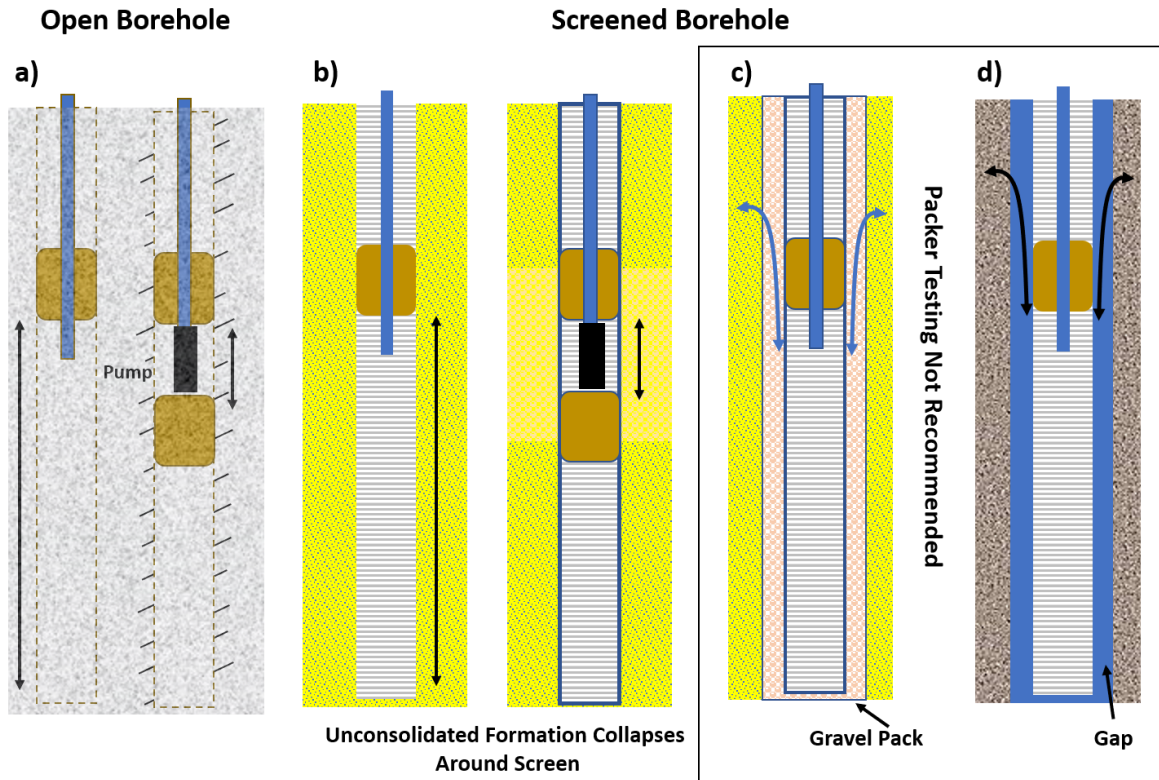


Figure 133 - Packers (brown rectangles) are used to isolate a portion of a borehole or perforated zone of a well to allow characterization of the zone below (single) or in between the packers (double). Black rectangles represent pumps. a) Packer systems in an open borehole in unfractured and fractured rock (angled lines) in which slug tests, pumping tests, or injection tests can be performed. b) Packer systems in a screened borehole in which pumping, or injection tests can be performed. The formation is well connected to the screen. c) Single packer inside a well screen surrounded by a gravel pack that allows leakage of water from a portion of the borehole above the packer. Packer testing is not recommended under this condition. d) Packer in a well screen that is not seated in the formation and has a gap between the screen and formation. Packer testing is not recommended in this condition.

Packers are typically constructed of thick rubber or other flexible material and are inflated with nitrogen, compressed air, or water to form a tight seal against the borehole wall. The packers (single or double) are designed with an open-center portion that allows for testing tools and the installation of pressure transducers (Figure 134).

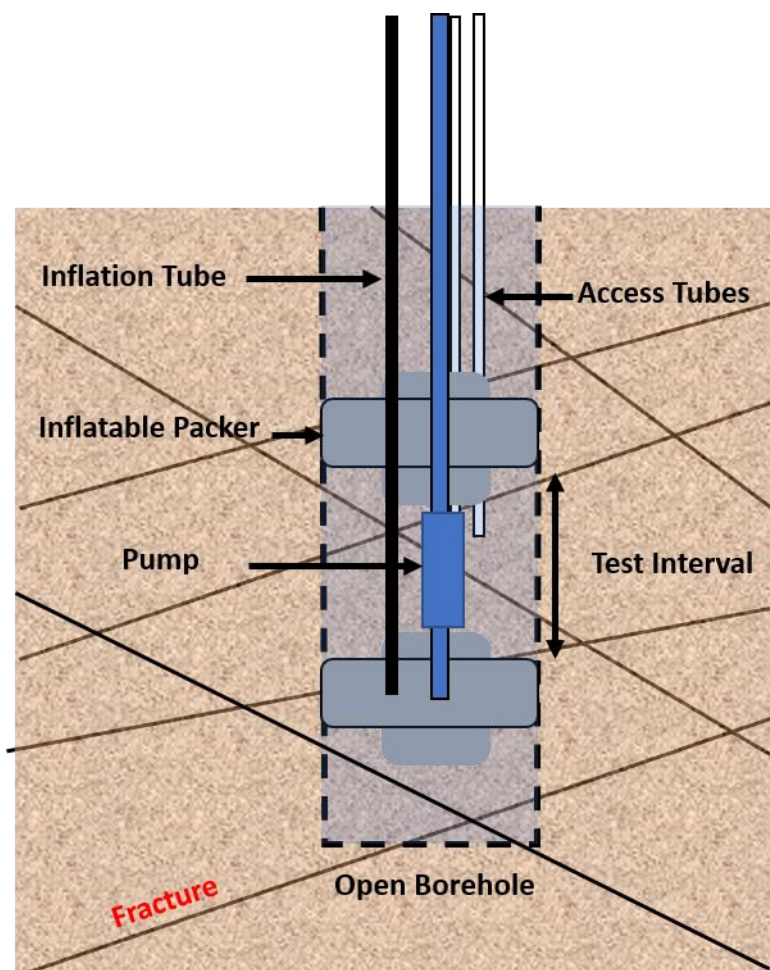


Figure 134 - Schematic of inflatable packer set up in a fractured rock (angled lines) uncased (open) borehole (dashed lines). Double-packer systems are also called straddle packers. The packer assemblage shown is suspended by a pipe (blue). The pipe can be left as an open pipe, or a pump installed in the test region (blue rectangle). The packers are inflated using an airline in this diagram (black). The assembly also includes one or more access ports (open pipes) which can be outfitted with transducers or water samplers.

15.1.1 Selecting the Test Interval

It is important to have a clear purpose for the packer test. A goal could be to select only the most productive zones for screening when casing a new water-supply well, to identify the overall generalized hydrogeologic properties of the formation, or to determine the characteristics of fractures or fault zones.

The test design and test method(s) will depend upon the stated goals and the hydrogeological conceptual model of the setting. This includes the local hydrostratigraphy, groundwater-flow directions, anticipated magnitudes of hydrogeologic properties, and a general water budget. When fractured systems are being evaluated the likely density and connectedness of secondary permeability features is also valuable information.

Site information is derived from the literature, drillers logs and investigative tools such as coring and borehole geophysical investigations. When traditional water-well

drilling methods are used to construct an open borehole, drillers' logs and samples of the cuttings are reviewed. In addition, reviewing the driller's notes on observed changes in water production is valuable.

In some geologic settings boreholes may be constructed by coring. This method can provide continuous samples of the geologic material that greatly aids in the selection of test zones. The drill crew can monitor changes in injection pressure at the rig control panel to estimate relative differences in permeability throughout the borehole. Depth to water measured at the beginning of each drilling shift can also be useful for estimating heads in different portions of the borehole.

In addition to observations made during well drilling, most often further investigations of the borehole are completed before a selection of a packer-testing intervals. Once the borehole is completed, a suite of borehole geophysical tools can be deployed to identify precise locations of lithologic changes, as well as zones of higher permeability and increased fracturing. Methods include a caliper log to assess borehole diameter and condition and an acoustic televiewer log to identify fractures. Additional logs may be needed depending on the formational properties and testing purpose. Shapiro (2007) recommends that a flow-meter log be conducted under static conditions and pumped conditions prior to determining test intervals. Detailed temperature profiles are often useful to characterize fractured systems (e.g., Pehme et al., 2014).

When selecting a test interval, it should be recognized that the borehole construction process may have altered the borehole wall creating a "skin" of lower-permeability material that coats or plugs portions of the formation. An appropriate well-development technique is recommended prior to testing, such as surging, jetting, or over pumping to reduce the influence of the skin (Sterrett, 2007).

15.1.2 Setting up the Packer System

Shapiro (2007) described the components and setup of a packer system referred to as the Multifunction Bedrock-Aquifer Transportable Testing Tool (BAT). His publication provides a good framework for understanding how a packer system is designed and installed and is used here to describe general packer-system installation and operation.

A packer system is set up for a given interval of the borehole. It is often attached to a rigid pipe that is lowered into the borehole or, in some settings, a cable and winch. If attached to a steel pipe, rigid-pipe extensions are added to the testing equipment to reach deeper locations. Because of the size and weight of the equipment and the need to raise and lower it in the borehole, a service truck with a boom, winch, and cable is often required to secure the tools while the packer system is lowered, operated, and raised.

Electricity is required to operate recording devices such as electronic valves and computers. Often an electric submersible pump is placed in the test interval. An onsite generator is used when power is not available.

Additional tubing and connectors are attached to allow inflation and deflation of the packers, and to house transducers and other equipment. If water is to be injected into the test zone from the surface, a reservoir to hold the water is required.

It is recommended to follow the manufacturer's instructions when installing, inflating, and deflating the packers. Shapiro (2007) provides further details on the setup and installation of packer equipment. Refer to inflation/deflation tables by depth and borehole size to determine the inflation pressure. Too much inflation pressure can fracture/damage the borehole wall and too little pressure can result in leakage between the packer and the borehole wall.

Shallow, small-diameter borehole intervals are sometimes isolated using flexible packers made of closed-cell foam attached to the outside of a rigid rod or tube. At locations with shallow wells these can be pushed into place and removed by hand. Small-diameter inflatable packers can be constructed using available hardware or purchased commercially.

15.2 Testing Methods and Analyses

Packer testing is most frequently applied to boreholes in rock. Testing methods can also examine bulk properties and properties of individual fractures. The work of Quinn and others (2012) is comprehensive reference on borehole testing in fractured rock and provides details on a versatile straddle-packer system they developed to provide transmissivity estimates. They list four types of hydraulic tests used in porous media that are commonly applied to fractured-rock boreholes. These are also applicable to some screened boreholes in good communication with the undisturbed formation (Figure 133). Tests include constant-head step test, instantaneous slug, constant-rate pumping, and recovery after constant-rate pumping. In some settings where groundwater-velocity data are desired, borehole-dilution methods that circulate a tracer in the packed-off section of the borehole are used (e.g., Maldaner et al., 2018). Slug, constant-rate pumping, and constant-head injection/withdrawal tests are discussed here. Refer to Quinn and others (2012) for application of other methods.

The packer-test records should include a drillers log, borehole configuration, the dimensions of the test interval, top and bottom elevations of the packers, time and water-level change data, and the start and stop times. A transducer system is usually used to monitor heads in the test zone. When data loggers are connected to an onsite recording and visualization system, real-time head changes and flow rates can be observed.

Packer-isolated sections of a borehole can be tested using standard slug-test methods described in Section 14, pumping tests for single wells presented in Section 12, and constant-head injection/withdrawal, step-rate injection, and drill-stem tests described in this section.

15.2.1 Slug Tests

A single- or dual-packer system can be used to isolate a zone of interest such that a rising- or falling-head slug test can be executed. A transducer located in the packed-off zone is installed and records water-level changes with time. As described in Section 14, the head is instantaneously raised or lowered, and the response of the recovering head is observed. Standard slug-test analysis methods for a given formation type (unconfined or confined) can be used to analyze the data as described in Section 14.

15.2.2 Constant-Rate Pumping Tests

When a pump is installed between a double packer or below a single packer, a constant-discharge aquifer test can be conducted, and T values can be approximated. As observation wells are rarely used, estimates of S are usually poor as explained in Section 12. Transient or steady-state testing can be performed. Most often the test will be conducted and analyzed as a single-well test. Analyses methods have been described previously in Sections 7 through 10 and Section 12.

15.2.3 Constant-Head Injection/Withdrawal Test

This section describes how a constant-head injection test is performed using a dual-packer system. Lapcevic and others (1999) provide a complete discussion of constant-head testing methods.

A constant-head injection/withdrawal test (also referred to as a Lugeon test or constant-pressure test) injects or withdraws water under a constant head to or from a packed-off test interval until a constant-flow rate is achieved. This simulates steady-state conditions (Ziegler, 1976). To achieve a constant-flow rate at a constant head, water could be pumped into the test interval, however, when permeabilities are low, flow rates may be difficult to maintain. Lapcevic and others (1999) report that more commonly a series of water-filled tanks of varying diameters pressurized with nitrogen are used to maintain constant- (and sometimes very-low) flow rates (Figure 135). Manometers are attached to each tank to measure the tank's level and the constant head is maintained by a control panel. The flow rate is measured by monitoring the rate of change of the manometer level in each tank with the pressure held constant as the tanks empty. Lapcevic and others (1999) report that this set up generates a wide range of flow rates such that zone transmissivities ranging from 1×10^{-10} to 1×10^{-3} m²/s can be measured. They recommend that multiple tests should be conducted by increasing the pressure used during each test.

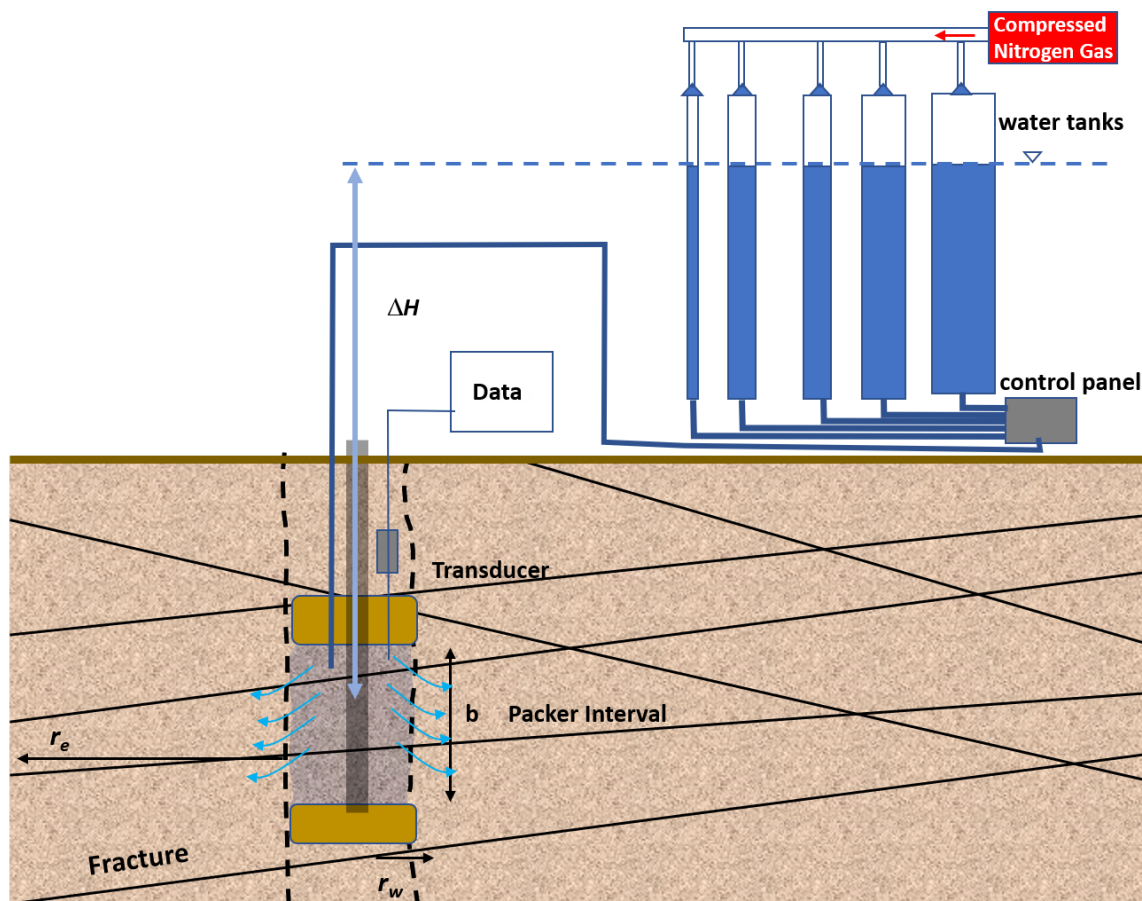


Figure 135 - Set-up of a constant-head injection test using multiple tanks to maintain a constant head and flow rate. A constant head is maintained between the packer interval and the pressurized water tanks (ΔH). The dashed cross section of a borehole is displayed with two packers isolating a test zone (b). Pressurized nitrogen gas is used to empty the tanks at a constant rate. r_w is the radius of the borehole and r_e is the radius of influence of the test (modified from Lapcevic et al., 1999).

Analyzing Injection/Withdrawal Test Results

The constant-head injection/withdrawal test is run until the flow rate is no longer changing. The interval transmissivity can be estimated using the Thiem equation for a confined system as shown in Equation (124). It is assumed that purely radial flow is occurring from the packed off interval.

$$T = \frac{Q}{2 \pi \Delta H} \ln \left(\frac{r_e}{r_w} \right) \quad (124)$$

where:

- T = transmissivity (Kb where b is the interval thickness) (L^2T^{-1})
- Q = constant discharge (L^3T^{-1})
- ΔH = difference in hydraulic head (L)
- r_e = radius of influence (L)
- r_w = radius of the borehole (L)

The radius of influence is the extent that injection test affects conditions in the material surrounding the test zone. Lapcevic and others (1999) note that r_e is often assumed to be 10 to 15 m (Bliss & Ruston, 1984). The T calculation is not very sensitive to r_e as shown by Equation (124) where r_e is divided by r_w and then the natural log of this ratio is computed (Doe & Remer, 1980).

Example

A 4-m section (b) of a 0.1-m diameter borehole in a fractured sandstone is isolated by a straddle-packer system (two packers). An injection test is conducted where the head difference is 5 m, and the steady-state flow rate is $1 \text{ m}^3/\text{d}$. The transmissivity (Kb) of the test zone is computed using Equation (124). The radius of influence (r_e) is assumed to be 12 m.

$$T = \frac{Q}{2 \pi \Delta H} \ln \left(\frac{r_e}{r_w} \right) = \frac{1 \frac{\text{m}^3}{\text{d}}}{2 (3.14) 5 \text{ m}} \ln \left(\frac{12 \text{ m}}{0.05 \text{ m}} \right) = 0.174 \frac{\text{m}^2}{\text{d}}$$

The horizontal hydraulic conductivity is then equal to $T/b = 0.174 \text{ m}^2/\text{d}/4\text{m} = 0.044 \text{ m/d}$. Zones with individual or several fractures can be represented as an equivalent single fracture using an equivalent individual fracture aperture, $2b_{eq}$. This can be computed from the zone T value (Equation (124)) by applying the cubic law (e.g., Lapcevic et al., 1999) as shown in Equation (125).

$$2b_{eq} = \left(\frac{T12\mu}{\gamma} \right)^{0.33} \quad (125)$$

where:

$2b_{eq}$ = equivalent fracture aperture (L)

T = transmissivity (L^2T^{-1})

μ = viscosity of water (MTL^{-1})

γ = specific weight of water (MT^2L^{-2})

15.2.4 Step-Rate Injection Test (Lugeon Test)

Lugeon tests are commonly performed in geotechnical or underground-mining applications to estimate the hydraulic conductivity and flow regime of a specific test interval. The test method was pioneered by Maurice Lugeon (1933) and later described by Houlsby (1976). It is based on observing the response of the test zone to inflow rate of injected water as the water pressure in the zone increases and decreases. The test set up is presented in Figure 136.

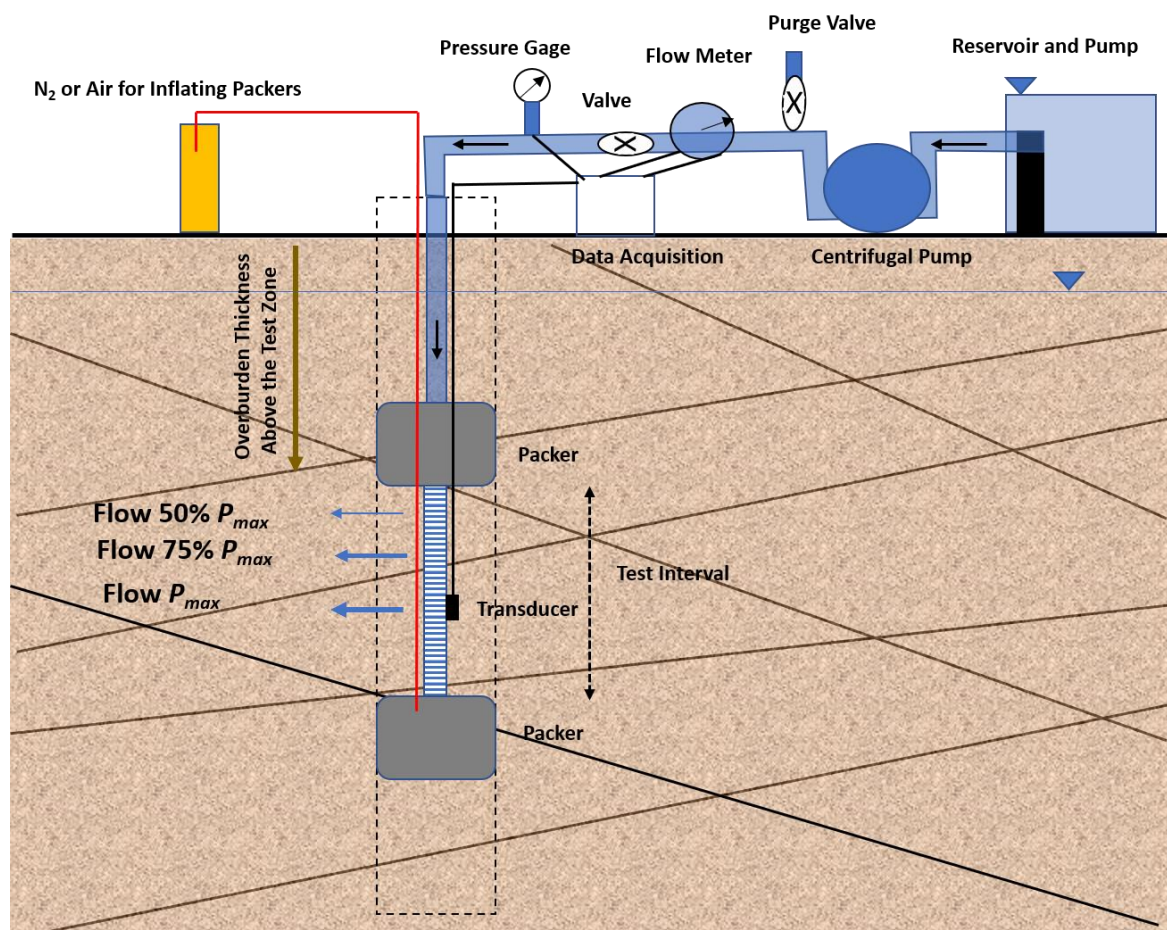


Figure 136 - Schematic set up of a Lugeon test. A dual-packer system inflated with gas isolates the test zone. The injection test uses water from a reservoir and a pump to pressurize the system and inject water into the test zone. The data collected are the inflow rate at a given pressure over time after rate stabilization. The maximum pressure, P_{max} , is computed based on the thickness of overburden overlying the test interval multiplied by 1 pound per square inch per foot (2.26×10^4 pascals/m). Flow rates at pressures of 50, 75 and 100 percent of P_{max} are determined and applied during the test; then the pressures are sequentially lowered back to 50 percent and flow rates recorded again for each interval.

The test is conducted using five stages of water pressure injection. Steps 1 through 3 increase pressure while steps 4 and 5 duplicate the pressure of steps 2 and 1, respectively. The five-step pressure 'loop' allows for interpretation of the flow regime and aids in selection of the most representative hydraulic conductivity value (Quiñones-Rozo, 2010).

The maximum injection pressure (P_{max}) is determined prior to starting the test. P_{max} must not exceed the confinement stress in the test interval to avoid hydraulic fracturing. P_{max} is typically estimated at 1 pound per square inch (psi) per foot of overburden above the test interval ($6,895$ Pascal = 1 psi). For example, a P_{max} of 200 psi (1.38 MPa) would be appropriate for a test interval located from 61 to 67 m (200 to 220 ft) below ground surface. The vertical thickness of overburden above the test interval is used to calculate P_{max} in an angled borehole or for a test conducted beneath a sloping terrain. P_{max} represents the highest injection pressure (step 3) and steps 1, 2, 4, and 5 represent multiples of P_{max} as shown in Figure 137 (Quiñones-Rozo, 2010).






Step	Description	Pressure Range	Relative Pressure
1	Low	50% (P_{max})	
2	Medium	75% (P_{max})	
3	High (P_{max})	(P_{max})	
4	Medium	75% (P_{max})	
5	Low	50% (P_{max})	

Figure 137 - Five pressure steps used in a Lugeon test. P_{max} is the maximum pressure computed as 1 psi per foot of overburden above the test zone (2.26×10^4 pascals per meter of overburden above the test zone). After step rates have stabilized, the total flow rate is measured every minute over a 10 min interval and the flow rate is determined by averaging the values (Quiñones-Rozo, 2010).

Water pressure and flow rate are recorded during each step of the test using a totalizing flowmeter, pressure gage/sensor, and timer. A purge valve on the injection system is used to vent excess pressure from the injection pump which controls the injection pressure into the test interval (Figure 135). After establishing a constant-flow rate, each stage is typically run for 10 minutes. Pressure and totalizing flowmeter readings are recorded each minute, and the total 'take' (inflow volume) of the test interval is calculated in liters for each step. The average flow rate is computed from the step data. A hydraulic conductivity value is calculated for each step, expressed as an empirical Lugeon value, which is defined as the hydraulic conductivity required to achieve a flow rate of 1 liter per minute per meter of test interval under a reference water pressure equal to 1 MPa.

Lugeon tests are analyzed based on the total injection pressure and flow during a given step. One Lugeon is equivalent to 1.3×10^{-5} centimeters per second under homogenous and isotropic conditions (Quiñones-Rozo, 2010). Separate Lugeon values are calculated for each step using Equation (126).

$$Lugeon\ Value = \alpha \frac{q}{L} \frac{P_0}{P} \tag{126}$$

where:

$Lugeon$ = reflects hydraulic conductivity of 1.3×10^{-5} centimeters per second when determined under homogenous, isotropic conditions

α = dimensionless unit-conversion factor (1 for SI units which would be in liters per minute, meters, and megapascals)

q = average flow rate from a single step (in liters per minute)

L = length of test interval (in meters)

P_0 = reference pressure, which is defined as 1 megapascal

P = total pressure head above static pressure (i.e., injection pressure + pressure head + frictional losses)

Houlsby (1976) developed a method to select a representative Lugeon value or equivalent hydraulic conductivity to represent the test interval using the observed patterns of Lugeon values. His method uses a bar graph of Lugeon values calculated for each step. The test values are matched to a pattern, and a method to generate a representative hydraulic conductivity value is selected. The patterns are labeled as representing flow regimes that include (1) laminar flow, (2) turbulent flow, (3) dilation, (4) wash-out, or (5) void filling. Each regime is described in the caption of Figure 138.

	Step	Pressure Stages	Lugeon Pattern	Representative Lugeon Value
Laminar	1			Average of all values
	2			
	3			
	4			
	5			
Turbulent	1			Highest Pressure Step
	2			
	3			
	4			
	5			
Dilation	1			Lowest value from low or medium pressure steps
	2			
	3			
	4			
	5			
Wash-Out	1			Highest Lugeon Value Recorded
	2			
	3			
	4			
	5			
Void Filling	1			Final Lugeon Value (Step 5)
	2			
	3			
	4			
	5			

Figure 138 - Lugeon-test patterns and flow-regime interpretation (Houlsby, 1976). The pressure stages are the same for each Lugeon pattern. However, the calculation of a representative hydraulic conductivity value is dependent on the pattern of test Lugeon values. (1) Laminar Flow – All Lugeon values for each step are similar, therefore laminar flow is occurring. The representative value is the average of all five steps. (2) Turbulent flow – The lowest Lugeon value occurs at the highest pressure, therefore turbulent flow is occurring. The representative value is the Lugeon value for the highest pressure. (3) Dilation – The highest Lugeon value occurs at the highest pressure, therefore fracture dilation is occurring at high pressure. The representative value is the average of the low pressure (1,5) or medium pressure (2,4) steps. (4) Wash-Out – Lugeon values increase with each step regardless of pressure, therefore gouge or weathered minerals are washing out of fractures. The representative Lugeon value is the highest observed value unless special conditions dictate otherwise. (5) Void Filling – Lugeon Values decrease with each step regardless of pressure, therefore gouge or weathered minerals are filling in small aperture fractures. The representative value is the Lugeon value for the lowest pressure.

Example

A 11.6-m long test section of borehole in a fractured sandstone is isolated by a straddle-packer system (two packers). The first Lugeon test step is conducted for 10 minutes, has an average total head pressure above static of 0.084 megapascals (MPa) and the formation takes a total of 390 liters throughout the step. Using Equation (126) with an SI unit conversion factor of one, a total head of 0.084 MPa, and an average flow rate of 39 liters per minute yields 40 Lugeons.

$$\text{Lugeon Value} = \alpha \frac{q}{L} \frac{P_0}{P} = 1 \frac{39 \frac{\text{L}}{\text{min}}}{11.6 \text{ m}} \frac{1 \text{ MPa}}{0.084 \text{ MPa}} = 40 \text{ Lugeons}$$

A Lugeon value of 40 is approximately 5.2×10^{-4} cm/s. As indicated in the parameter definitions for Equation (126), one Lugeon value is equivalent to 1.3×10^{-5} centimeters per second under homogenous and isotropic conditions (Quiñones-Rozo 2010).

The software program AquiferTest V12 provides methods to interpret Lugeon-test results. The user's manual provides details on methods and data requirements (Waterloo Hydrogeologic, 2021).

15.2.5 Drill-Stem Test

Estimates of horizontal hydraulic conductivity using a packed-off interval of a borehole have been of interest to the petroleum industry for many years (e.g., Mathews & Russel, 1967; Earlougher, 1977). The drill-stem test procedure is also applicable to the characterization of some confined hydrogeologic settings.

Conceptually, a drill-stem test involves outfitting the drill stem with a test apparatus within the interval of interest that has packers, valves, and pressure-monitoring systems. The packer system is used to isolate a section of borehole. Valves are opened at the start of the test and fluid from the packer zone flows into the drill stem for a period of time. Then the valve is closed. The pressure system monitors the starting formational pressures and the recovery pressures after the valve is closed. A discharge rate is computed from the rate that the volume of water fills the drill stem once the test is initiated. Analyses of the data are achieved by using recovery theory once the valve system is closed. Domenico and Schwartz (1998) have a brief discussion of the method and data analysis. Additional, detail and methods are found on sites like [wiki.aapg.org/Drill stem testing](http://wiki.aapg.org/Drill_stem_testing)[↗] and in the literature.

Section 16 addresses hydraulic testing to characterize low-permeability units such as confining units or aquitards.

16 Special Considerations for Characterizing Low-Permeability Systems, Aquitards

Saturated geologic materials that do not yield enough water to be used as a reliable water supply are generally referred to as low-permeability units and, when they confine an aquifer, aquitards (Woessner & Poeter, 2020). Characterization of these systems can be more difficult because in situ pumping tests require low yields and have small zones of influence.

All low-permeability units that would not be considered aquifers or aquifuges are referred to using the general term aquitards in this section. Aquitards retard the flow of groundwater. Units that almost totally preclude water movement can be referred to as aquicludes, and if totally impermeable, aquifuges (Woessner & Poeter, 2020). Though these terms imply sequentially decreasing permeability, the terms are only qualitative. Generally, characterization of low-permeability units is difficult, and in some cases, standard pumping or slug tests is impractical because water does not flow to or from the unit at a high enough rate to conduct such tests.

Two publications provided on the gw-project.org web-site specifically relate to hydrogeologic characterization of aquitards. These include [*Contaminant Transport Through Aquitards: Technical Guidance for Aquitard Assessment*](#) by Bradbury and others (2006) and [*Contaminant Transport Through Aquitards: A State-of-the-Science Review*](#) by Cherry and others (2006). Though these reports focus on contaminant transport they include detailed information about the character of aquitards and the tools used to characterize hydrogeologic properties of these units. These publications are noted because they can broaden the reader's understanding of aquitard characterization beyond that provided in this book. This section provides a general overview of methods to determine transmission and storage properties of aquitards.

16.1 Properties of Aquitards

Aquitards can be found at or near the surface (e.g., saturated, clay-rich tills) and at depth (e.g., shale and mudstone units). When aquitards are extensive and overlay deeper confined aquifers, they are commonly referred to as confining units (Figure 139). In some settings these units contain zones of higher-permeability materials and may be discontinuous.

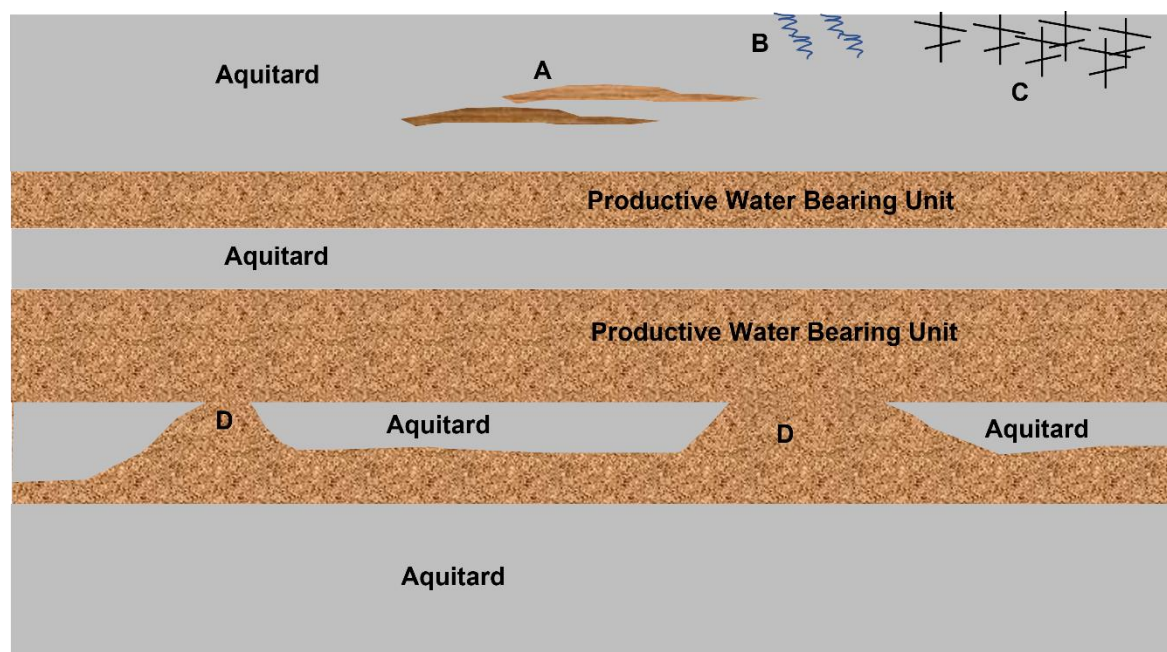


Figure 139 - Schematic of a sequence of aquitards and productive water-bearing units. Aquitards can be homogeneous, heterogeneous, contain macropores, fractures, and erosional or depositional windows that limit the local extent of aquitards. The gray shading represents a uniform homogeneous aquitard. "A" represents a heterogeneous setting where lenses of material with differing permeability are present. "B" shows macropores created by roots near land surface. "C" shows fractures that can be near the surface or at depth depending on the geologic history of the region. "D" shows windows within an aquitard that allow movement of water between productive water-bearing units.

Aquitards are often composed of non-indurated silts and clays, mudstones, shales, or other low-permeability rocks. Clay- and silt-rich systems are typically unlithified and are deposited in lacustrine, glacial, or marine environments. Lithified aquitards include mudstones, shales, some well cemented sedimentary rocks including chemical precipitates, and fractured igneous and metamorphic rocks (Cherry et al., 2004). In some settings, secondary porosity and permeability are present, most often as macro-pores or fractures in near-surface deposits and fractures in deeper formations, features that usually enhance permeability.

Cherry and others (2006) and Bradbury and others (2006) provide good reviews of the role of aquitards in influencing the movement of groundwater and contaminants, as well as extensive discussions of aquitard types, depositional histories, and the post-depositional processes affecting aquitards. The authors state that non-indurated aquitards with 10 to 15 percent clay are classified as clayey aquitards that effectively limit flow and contaminant migration when they do not contain preferential flow paths such as root holes (near-surface deposits with macro-pores) or fractures. Hydraulic studies that measure vertical gradients within aquitards have shown that, in some cases, the conditions restricting groundwater flow are not uniform but occur over a limited vertical portion of the aquitard as shown in Figure 140 (e.g., Cherry et al., 2006; Meyer et al., 2008; Meyer et al., 2014; Meyer et al., 2016). Most characterization methods assume the distribution of

hydraulic conductivity in an aquitard is isotropic and homogeneous, although most aquitards are heterogeneous.

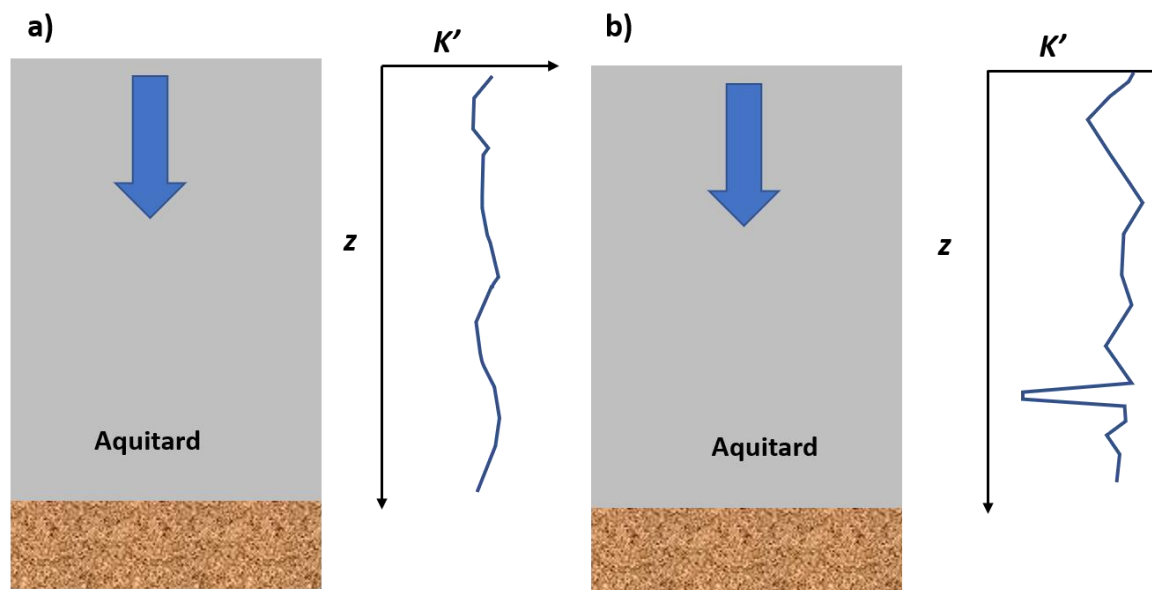


Figure 140 - A schematic of the distribution of vertical hydraulic conductivity, K' , in two aquitards. The blue arrow represents water flowing downward. a) The K' in this example is relatively uniform with depth, z . b) This aquitard has a zone about 75 percent of the distance from the top where a low K' is indicated. This zone will control the rate of vertical movement in this system.

16.2 Test Methods Used to Estimate Aquitard Properties

This section focuses on the physical characterization of hydrogeologic properties of aquitards. In this book, we purposefully use the terms pumping test and hydraulic test instead of aquifer test. Conceptually, the pumping-test techniques described in previous sections are applicable to both highly conductive and, in some settings, lower-permeability units that may be considered aquitards. This section addresses some of the specific methods used to characterize the hydrogeologic properties of aquitards. Cherry and others (2006) and Bradbury and others (2006) also describe methods used to evaluate the integrity of aquitards as this condition relates to the potential for migration of contaminants from an impacted source through an aquitard.

Cherry and others (2006) suggest that characterization of aquitard hydraulic properties can be grouped into the application of external and internal methods. Internal methods include laboratory methods applied to samples and cores of the aquitard, performing hydraulic tests within a borehole penetrating the aquitard, and observing head responses to recharge or loading. External methods involve pumping a productive water-bearing unit above or below an aquitard and then interpreting time-drawdown data from observation wells in the principal water-bearing unit and, in some cases, in the adjacent aquifer and/or aquitard.

16.2.1 Internal Methods

Direct internal investigation of an aquitard includes collecting and testing sample cores as well as installing wells and conducting pumping and/or slug tests. Indirect internal methods include monitoring the response of the near surface unconsolidated aquitard material to recharge events and monitoring the aquitard's response to external loading.

Laboratory Methods

Researchers have observed that hydraulic-property values estimated from laboratory investigations of samples of uniform aquitards without significant secondary affects (developed macropores and/or fracturing) may be equivalent to those derived from field-scale methods (Cherry et al., 2006). However, laboratory-scale samples of heterogeneous materials may poorly represent field-scale properties, as the density and general interconnectedness of zones of different lithologies and secondary permeability features may be missing, overrepresented, or underrepresented at the laboratory scale. In some cases, laboratory samples are repacked and yield unrepresentative results. When any of these conditions occur, laboratory-derived hydraulic conductivity values often underestimate field-scale permeability (Haefner, 2000; Neuzil, 1986; van der Kamp, 2001).

[Box 9](#) illustrates some of the laboratory methods such as the falling-head permeameter, triaxial cell, and consolidometer that are used to derive hydraulic conductivities of low-permeability material.

Field Methods

The following subsections describe internal field methods for characterizing hydrogeologic properties of aquitards.

Pumping tests

Conceptually, a pumping well and observation wells could be constructed in an aquitard. In most settings, the low yield potential and permeability of the unit would limit the pumping rate and the distance at which observation wells would respond to pumping. In addition, if more permeable units underlie or overlie the aquitard, they must be accounted for in the analysis. In some settings, pumping a single well at a low constant rate with measurements of drawdown and time may be most useful. This is discussed in Section 12. If a successful pumping test is conducted, drawdown responses in the aquitard would be analyzed using methods described in Sections 7 through 10.

Slug Tests

Slug tests, as described in Section 14, determine internal horizontal hydraulic conductivities of screened portions of aquitards. Hydraulic-conductivity values reflect the nature of the material within a few meters of the test interval. The local nature of the test may not capture conditions where secondary permeability or material heterogeneity dominate the formation. Slug testing does not provide direct measurement of the vertical

hydraulic conductivity. Estimates of vertical hydraulic conductivity are often assumed to be an order of magnitude smaller than horizontal values in stratified rock or sediments. However, in some settings horizontal to vertical hydraulic conductivity ratios can be 1000:1 (Anderson et al., 2015). In contrast, aquitard vertical hydraulic conductivity may be greater than horizontal values in laterite or saprolite materials where remnant structures such as weathered quartz veins may be present (Cherry et al., 2004).

Changes in the near-well hydraulic conductivity can occur when wells and piezometers are installed in unlithified aquitards (e.g., Cherry et al., 2006). Drilling can smear silt and clay along the borehole wall, reducing permeability. This skin effect artificially slows the rate of the head response causing hydraulic conductivity values to be underestimated. If the boring, well-completion, and development processes enhance the permeability, values of hydraulic conductivity at the well will be overestimated. Perforated intervals should be developed prior to testing (e.g., Sterrett, 2007).

Slug-test responses in aquitards are overdamped as discussed in Section 12. In aquitards, head changes during a slug test occur slowly and can take hours to days or months to fully recover. In some low-permeability settings, the static water level after the drilling and completion of a piezometer or monitoring well may be below the fully recovered head. Often, collection of water-level data as recovery occurs can be used as a slug-out test and analyzed accordingly as explained in Section 14. Often in low-permeability materials, monitoring wells with small diameters (smaller volumes to be filled) are used to observe head change. Aquitard well design must accommodate slugs or pneumatic methods, and water-level monitoring tools.

Constant-Drawdown Tests

Characterization of a low-permeable unit can also be evaluated using a constant-drawdown method. This method usually involves the head in the well to rise or fall and then at some point during the recovery water is continuously injected or extracted at varying flow rates to keep the head constant. Data collected are the well-design factors and the inflow or outflow rate, Q , needed to keep the unrecovered head (H) constant (e.g., Mieussens & Ducasse, 1977; Tavenas et al., 1990; Neville & Markle, 2000) as illustrated in Figure 141.

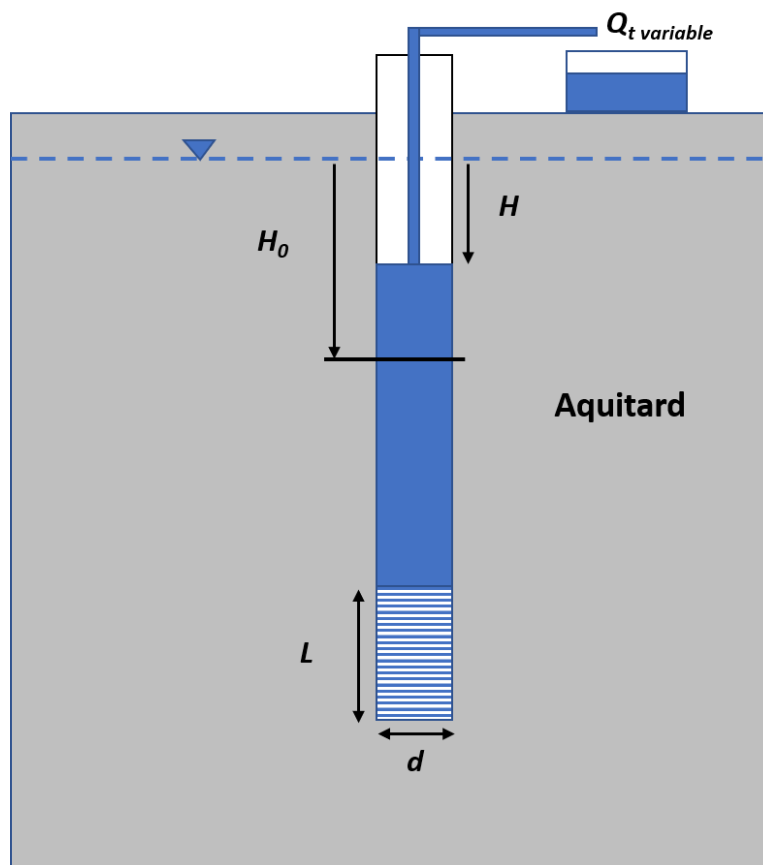


Figure 141 - Slug-out constant drawdown test set up for a monitoring well. The dashed blue line is the static water level. A slug of water is removed from the well (H_0) and at some time during the recovery the unrecovered head, H , in the well is stabilized by extracting volumes of water over time. The test time, t , starts when the variable discharge begins. L is the length of the perforated interval and d is the diameter.

Tavenas and others (1990) developed a method to analyze the data using plots of $Q(t)$ versus $1/t^{0.5}$. This relationship should be linear after 5 to 10 minutes from the test initiation. Using an arithmetic plot, a line is fitted to the linear portion of the data and then extrapolated to $1/t^{0.5} = 0$. The steady-state flow, $Q_{infinity}$, is determined by the intersection with the y axis. Using the steady-state flow rate, K_h is computed as shown in Equation (127).

$$K_h = \frac{Q_{infinity}}{F H} \quad (127)$$

where:

- K_h = horizontal hydraulic conductivity (LT^{-1})
- $Q_{infinity}$ = Steady-state flow rate from graph (L^3T^{-1})
- F = shape factor for the monitoring well (function of radius, screen length and other factors) (L)
- H = unrecovered head as illustrated in Figure 141 (L)

The shape factor can be approximated as suggested by Hvorslev (1951) and shown in Equation (128).

$$F = \frac{2 \pi L}{\ln\left(\frac{L}{d} + \left(1 + \left(\frac{L}{d}\right)^2\right)^{.5}\right)} \quad (128)$$

where:

L = perforated length (L)

d = diameter of the perforated interval (L)

Tavenas and others (1990) provide additional discussion of parameters. The Jacob-Lohman (1952) solution as outlined by Lohman (1972) may also be applicable for analyzing constant-head tests. This method assumes a constant head from a flowing well where the change in discharge over time is recorded.

When aquitard material lies at or near the surface, permeability has been investigated using other methods referenced by Cherry and others (2006). These include monitoring and analyzing head changes within the aquitard induced by

- Natural, precipitation-induced recharge (e.g., Davis, 1972; Keller et al., 1989; Boldt-Leppin & Hendry, 2003),
- flow into a large, augured cavity (Keller et al., 1989), and
- construction loading and unloading (van der Kamp & Maathuis, 1985).

Aquitard properties can also be estimated based on the calibration of one-dimensional and three-dimensional numerical models given hydraulic test data from a site (e.g., Pavelko, 2004; Hart et al., 2005; Anderson et al., 2015).

16.2.2 External Methods

External methods include pumping adjacent water-bearing units and observing the changes in water levels in the aquitard or in monitoring wells in the pumped aquifer. Examples of these methods are presented in the following subsections.

Pumping Test with An Observation Well in the Aquitard

Neuman and Witherspoon (1972) develop a method to determine the diffusivity, K'/S_s' (aquitard horizontal hydraulic conductivity and specific storage), when a pumping test is conducted in the underlying or overlying aquifer and a monitoring well or piezometer is installed in the aquitard in concert with a monitoring well in the aquifer as shown in Figure 142. The aquitard well and aquifer-observation well are at the same radial distance from the pumping well. When an aquifer monitoring well is not present, the drawdown in the pumped aquifer can be projected for the specified radial distance using a Theis analysis of the test data (Neuman & Witherspoon, 1972).

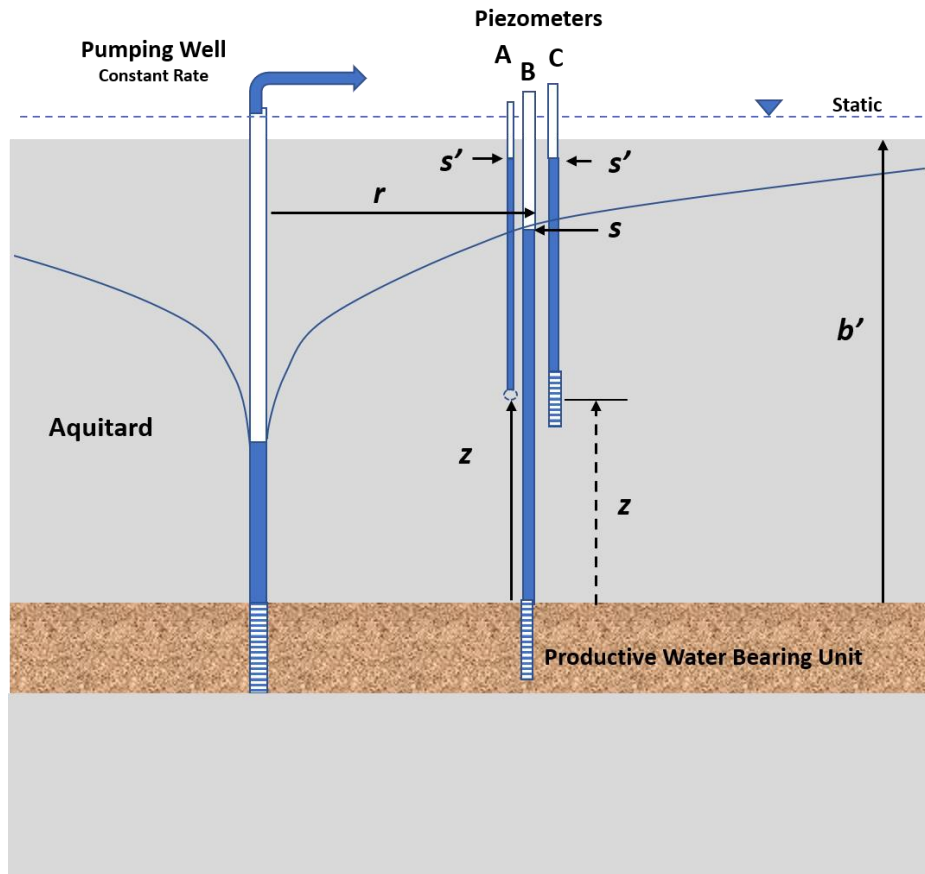


Figure 142 - Schematic of a pumping test conducted in an aquifer and observation wells in that unit (well B) as well as the overlying aquitard (well C). z is the distance from the top of the water bearing unit to the open interval of the observation well in the aquitard. Neuman and Witherspoon (1972) assumed the observation well opening was represented by a point (indicated by A). Rowe and Nadarajah (1993) accounted for the length of well screen where z is the distance from the boundary to the center of the well screen (dashed) (C). The radial distance to the observation well is r . b' is the thickness of the aquitard unit. At a time after the pumping starts and when drawdown in the aquitard is observed, values of drawdown s' in the aquitard and s in the unit being pumped (measured from the initial static water level elevation) are recorded.

The method assumes units being pumped and aquitards are infinite in lateral extent and the monitoring wells are located within about 60 m of the pumping well. Detailed observations of drawdown should be collected at early test times. The usable early-time response of drawdown in the main pumped water-bearing unit and aquitard are conservatively constrained as indicated by Equation (129).

$$t \leq 0.1 \frac{S_s' b'^2}{K'} \quad (129)$$

where:

- t = the time since the beginning of the pumping (T)
- S_s' = specific storage of the aquitard (L^{-1})
- b' = thickness of the aquitard (L)
- K' = hydraulic conductivity of the aquitard (isotropic) (LT^{-1})

The time computed by Equation (129) is considered overly conservative (Neuman & Witherspoon, 1969). They suggest that the early-time limit can be determined by observing when the straight-line portion of a log-log time-drawdown plot for an observation well in the aquitard begins to depart from a linear slope.

At a radial distance (r) and a selected time (t), drawdown (s) is measured in a monitoring well in the water-bearing unit and drawdown (s') is measured in a monitoring well or piezometer located in the aquitard. Both wells are located at the same radial distance from the pumping well. Neuman and Witherspoon (1972) assumed that the piezometer in the aquitard is represented as a point (the midpoint of the open interval) and head changes are instantaneous. They developed several curves that relate the drawdown ratio to parameters, t_D and t_D' (Figure 142). As stated previously, additional curves for matching can be generated from the appropriate analytical solution.

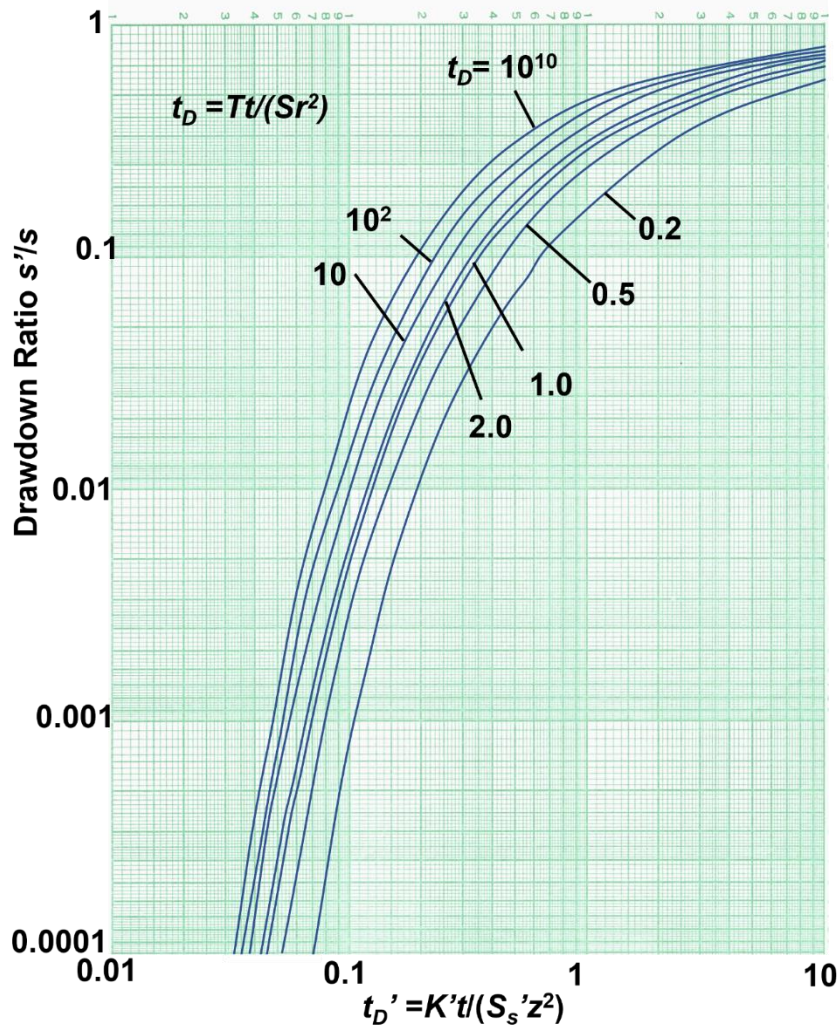


Figure 143 - Neuman and Witherspoon (1972) ratio-method plots showing the relationship between the drawdown in the pumped unit and an observation well (point source) in an aquitard (s'/s), and factors t_D and t_D' . t_D values between 10^2 and 10^{10} are very close together and can be interpolated (modified from Neuman & Witherspoon, 1972; Rowe & Nadarajah, 1993).

Parameters are defined as shown in Equations (130) and (131).

$$t_D = \frac{Tt}{Sr^2} \quad (130)$$

where:

- T = pumped unit transmissivity (L^2T^{-1})
- t = time since the pumping began (T)
- S = storativity of the pumped unit (dimensionless)
- r = radial distance to the aquitard piezometer (L)

and

$$t_D' = \frac{K't}{S_s z^2} \quad (131)$$

where:

- K' = aquitard vertical hydraulic conductivity (LT^{-1})
- t = time since pumping began (T)
- S_s' = specific storage of aquitard (L^{-1})
- z = vertical distance from the top of the aquifer to the aquitard piezometer (L)

When t_D is less than 100, estimates of t_D' should use the relationships shown in Figure 143. If t_D is greater than 100, multiple curves plot close together and estimated values of t_D' are often determined by using the curve labeled 10^2 . This will yield acceptable results with a small error (e.g., Neuman & Witherspoon, 1972; Rowe & Nadarajah, 1993).

The ratio method requires that the estimates of T and S be computed for the water-bearing unit being pumped using early-time data when leakage rates and volumes are low. Often a Theis analysis can be applied.

Ideally, a standard monitoring well is installed in the pumping unit at the same radial distance from the pumping well as the monitoring well in the confining unit. Again, at early-time, the ratio of drawdown in the aquitard well and aquifer-monitoring well, s'/s , is computed. The relationships of s'/s and the computed t_D value are used to determine a value of t_D' by reading from the x axis of Figure 143. The unknown variable is K'/S_s' . A value of S_s' is derived from consolidation testing as described in Box 9.3 or the literature as explained in Box 2. Once S_s' is estimated, a value of K' is calculated. Neuman and Witherspoon (1972) reported values of K'/S_s' as representing the portion of the aquitard defined by the distance z (e.g., the portion of the aquitard within the distance z from the aquifer unit which may overlie or underlie the aquitard).

Rowe and Nadarajah (1993) modified Neuman and Witherspoon's (1972) ratio method by accounting for the perforated length of an aquitard-monitoring well. This contrasts with the point-location assumption of Neuman and Witherspoon (1972) as shown

in Figure 142. They note that the ratio method used the assumption that the piezometer had an immediate response to pressure change in the aquifer. Rowe and Nadarajah (1993) addressed the effects of using finite-length perforated intervals in aquitard wells and presented graphics with correction factors for aquitard-monitoring well-drawdown data. The measurement location is represented as the midpoint of the screened interval. They also examined the effect of aquitard-monitoring wells located near the top of the pumping-unit boundary as expressed in Equation (132). Rowe and Nadarajah (1993) provide more details in their publication.

$$K' = \frac{t_D' S_s' z^2 B_2^2}{t B_1} \quad (132)$$

where:

- $t_D' = K't/(S_s'z^2)$ from Figure 1 in Rowe and Nadarajah (1993), which is the same as Figure 142 in this book (L^2)
- $S_s' =$ specific storage of aquitard (L^{-1})
- $z =$ distance from the aquifer to the midpoint of the piezometer screen in the aquitard (L)
- $t =$ elapsed time since pumping began (T)
- $B_1 =$ correction factor for time (Figure 5 in Rowe and Nadarajah, 1993) (dimensionless)
- $B_2 =$ correction factors for time (Figure 8 in Rowe and Nadarajah, 1993) (dimensionless)

Figures for Rowe and Nadarajah (1993) correction factors are reproduced in [Box 10](#) for Groundwater Project readers who do not have access to commercial journals.

In some settings, a number of monitoring wells are placed in an aquitard and the underlying or overlying aquifer is pumped to qualitatively determine if the aquitard is homogeneous or contains heterogeneities such as high-permeability zones or fractures. Grisak and Cherry (1975) conducted a sequence of pumping tests with wells in an aquifer overlain by a surficial clay-rich aquitard. Multi-level monitoring wells were placed in the aquitard. By comparing the rates and magnitudes of responses they interpreted that some wells were finished in blocks of unfractured matrix and others intersected fractures in the aquitard. They then used Hantush analyses of the pumping tests to derive broad-scale K' values for the aquitards and finite-element modeling to adjust estimates of K' so model results matched observed observation-well water levels.

Pumping Tests with Observation Wells in Adjacent Productive Units

Pumping tests conducted in productive water-bearing units confined by aquitards yield information on the hydraulic properties of aquitards. If water-level responses to pumping mirror the Theis solution, then the aquitards are acting as impermeable units. In

these settings, leakage rates through the aquitard and water released from aquitard storage are sufficiently small and the aquitard is considered impermeable (aquiclude).

In contrast, if aquifer drawdowns reflect the addition of water via the aquitard, then pumping-test analyses can provide information on the vertical hydraulic conductivity of the aquitard and, in some cases, the storage properties of the adjacent confining unit.

When pumping-test results match the Hantush-Jacob or Hantush models for leaky aquifers the general properties of the associated aquitards can be determined as illustrated in Figure 144, which repeats the images of Figure 49 for the readers' convenience in recalling the groundwater-system settings. Analysis methods are discussed in Section 9 and are not restated here.

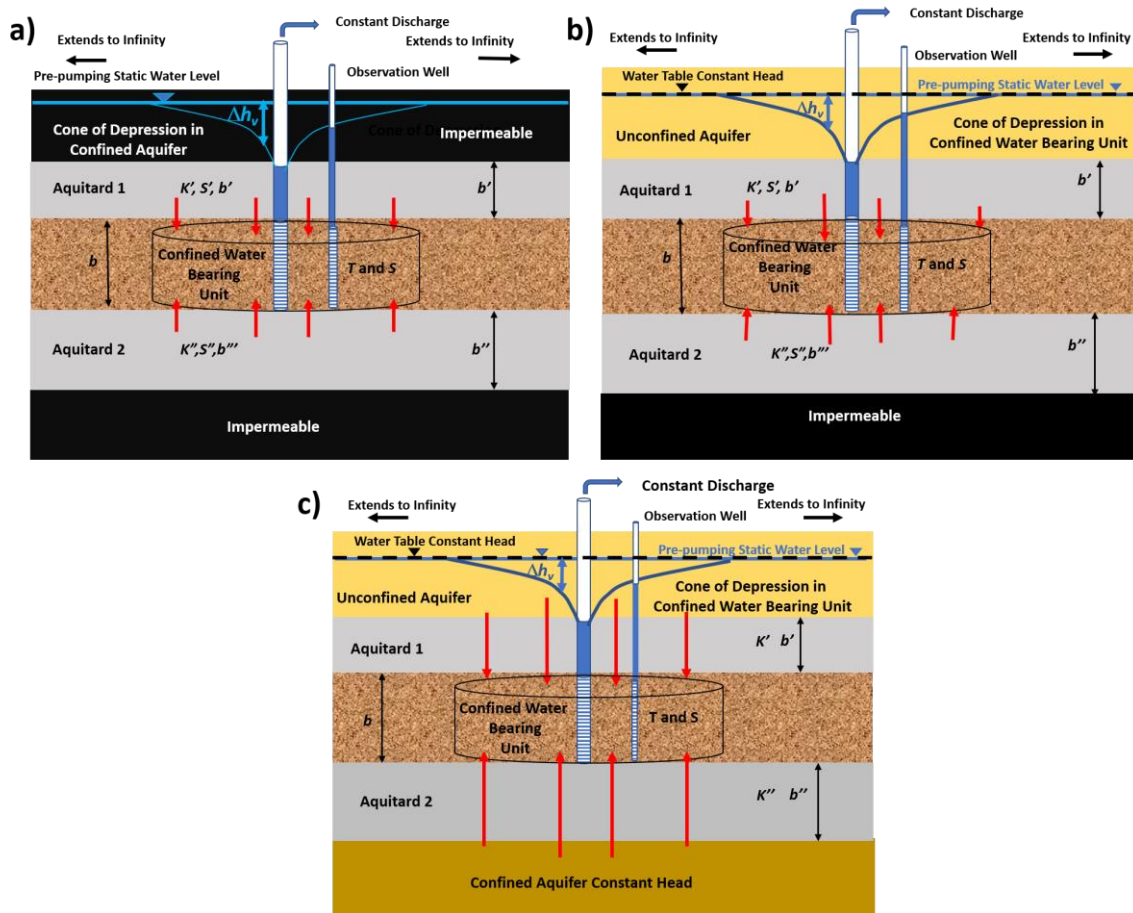


Figure 144 - Standard pumping-test methods that yield hydrogeologic properties of the confining units that are associated with a confined water-bearing unit.

- Drawdown in a confined aquifer that receives water from storage in one or two confining beds when the beds overlying and underlying the confining beds are not permeable.
- Drawdown in a confined aquifer that receives water from storage in overlying and/or underlying confining beds, as well as leakage of water through the confining bed from a highly transmissive unit such as an unconfined water-table aquifer.
- Drawdown in a confined aquifer receiving water via direct flow through a confining bed that has negligible storage from a highly transmissive aquifer above and/or below the confining bed.

Aquitards generally restrict the movement of groundwater and contaminants. When building conceptual models, developing water budgets, mapping flow paths, assessing resident times, and constructing three-dimensional numerical models, it is as important to establish the properties of aquitards as well as those of aquifers. This section provides basic methods used to characterize aquitards. Additional methods can be found in the literature and the reader is directed to these when assessing more complex settings (e.g., Cherry et al., 2006; Bradbury et al., 2006).

17 Wrap-up

This book is intended to provide the reader with the conceptual, mathematical, and practical foundation of hydraulic testing and how it is used to obtain hydrogeologic properties of groundwater systems. It provides basic concepts and methods to conduct and analyze hydraulic tests. Field-scale values of hydraulic conductivity, transmissivity, and storativity derived from hydraulic testing underpin all site- and regional-scale hydrogeological investigations.

This book presents methods used to analyze test data in addition to laying out the mechanics of conducting pumping, slug, and packer tests. We emphasized the constraints of applying analytical models (analytical equations) to forecast future aquifer responses to pumping and to fit observed hydraulic-test responses to existing basic models. Explaining and illustrating manual curve-matching methods was purposefully presented so that the reader clearly understands the processes used to derive hydrogeologic properties when applying automated analysis tools.

Responsible application of basic analytical models is a goal of this book. Available pumping- and slug-test-analysis software applies these same models. When preparing to analyze pumping tests it is easy to open a commercial software program with 20 available analytical methods describing a wide variety of settings, and then without properly accounting for aquifer type, well design, or test conditions, “magically” generate estimates of hydrogeologic parameters using best-fit approaches. We contend that without knowing the constraints under which the individual models were developed (assumptions and limits) and understanding nuances of the curve-matching process (fitting of the type curves and observed data set), the easy-to-use software can be easily misused. Such actions occur even though the software developers go to extensive lengths to provide users with detailed information, including describing assumptions and limitations of each analytical tool provided. The hydrogeological context of each test site determines the possible appropriate conceptual models, not the other way around (i.e., getting a good fit in automated software does not mean that the analysis is appropriate for a site). The selected conceptual model must be carefully evaluated to determine if it appropriately describes the field setting that is being evaluated. In many cases, field conditions do not result in data that fit well with analytical models. This is because assumptions such as the tested unit being homogeneous, isotropic, and infinite in lateral extent may not accurately represent conditions at the test site.

As with pumping test approaches, slug- and packer-testing methods must also fit the hydrogeologic setting. When conducting these types of tests it is important that the formational properties are being tested instead of perforated-interval conditions and skin effects. The formation should be freely connected to the screened/open interval. Data

collection in some cases requires recording head changes in fractions of a second, while others require months.

The section on analyzing results of single-well pumping tests is presented because groundwater investigations are costly. Allocated project funds may not allow drilling of new wells specifically for pumping and slug testing. Pumping a single well and recording time-drawdown data during a step test and constant-discharge test provide well-loss information and reasonable estimates of transmissivity. Evaluation of a number of performance test results as reported on driller's logs is often adequate to estimate order of magnitude transmissivity values of a system without conducting new well tests.

Many authors have formulated additional analytical models for a wide variety of hydrogeologic conditions since Theis (1935) initially developed his analytical solution and curve-matching method. Analytical solutions are still the primary tools used to analyze pumping-test data. When conditions are more complex, fewer analytical models are available. This can sometimes be addressed by combining analytical solutions (e.g., superposition to include well interference and hydraulic boundaries; or analytic element methods as described by Haitjema (1995)). In other settings, numerical groundwater-flow modeling tools calibrated to hydraulic-test data are used to evaluate hydraulic-parameter magnitudes and distributions, as well as the effect of boundary conditions in complex hydrogeological settings (e.g., Anderson et al., 2015). Such tools are more flexible in representing anisotropic and heterogeneous settings with complex boundary conditions and multiple layers. However, relatively simple analytical models are most often used to analyze hydraulic-test results for estimation of K , T , S and S_s . When applied with care, the analytical results provide hydrogeologists with aquifer and aquitard characteristics needed to quantify groundwater flows, and to forecast responses to pumping and naturally occurring perturbations of the groundwater system.

18 Exercises

These problems focus on analyzing pumping-test and slug-test data. Curve-matching or straight-line interpretations can be used as appropriate to analyze time-drawdown data. Data can be plotted by hand on graph paper supplied in Box 1, using spreadsheet programs (e.g., Excel®), open-source solution methods, or commercially available software packages. In some cases, it may be helpful to copy figures of type curves presented in this book into a program (e.g., PowerPoint®; Excel®) that allows the user to stretch axes to match plots of time-drawdown data you have prepared. Remember when manually inspecting type curves and data sets, the graph scales must match.

Free demo versions of the three most popular hydraulic testing software may also be applied as appropriate to complete these problems, including

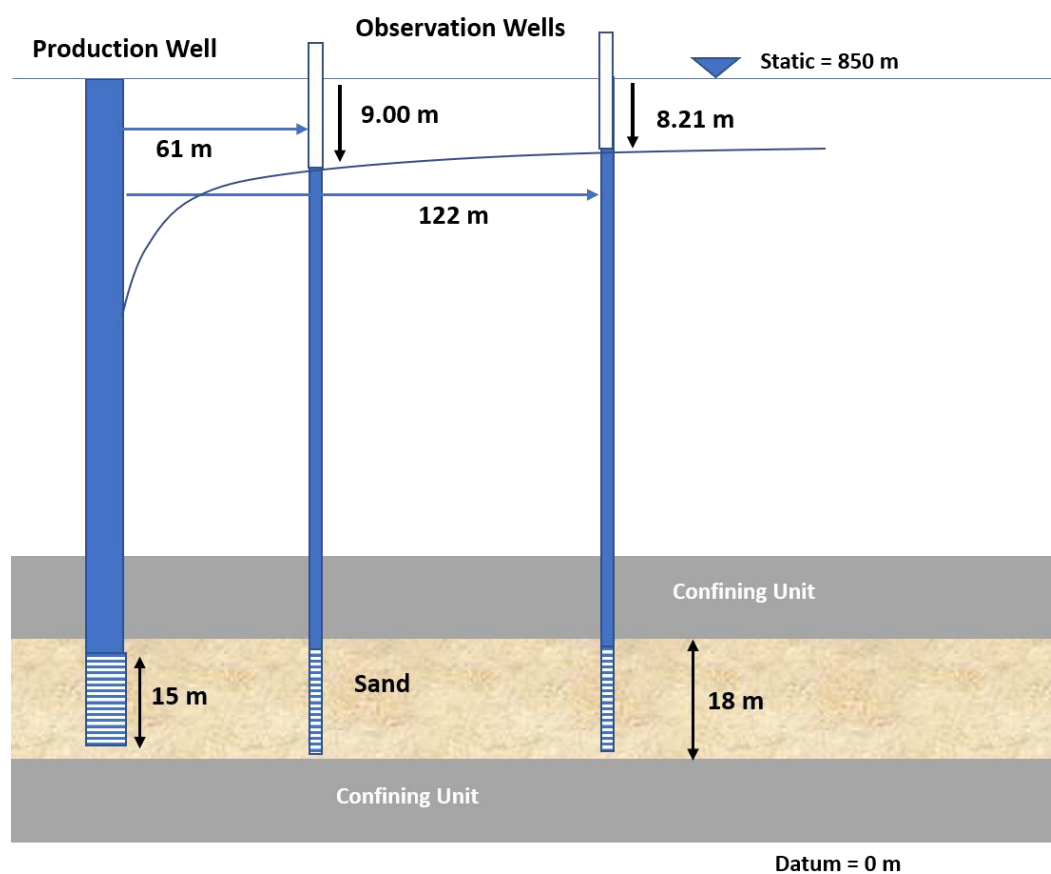
- AQTESLOV (aqtesolv.com↗),
- AquiferTest (waterloohydrogeologic.com↗) with a 15-day trial version available at this [link](#)↗, and
- Aquifer^{win32} Version 6 (groundwatermodels.com↗) with a demo version available in the zip file that [will download when this link is clicked](#)↗.

Mastering the use of one or more of these programs takes time. Help files and documentation are available on the websites.

We recommend that the reader first use a manual curve-matching method as described in the previous sections before numerical modeling. This aligns with our goal of having the hydrogeologist understand the foundational principles used in hydraulic-test analyses. After completing a standard curve-matching solution, a software-generated match can be derived. When both methods are executed, the results should be compared and contrasted. [Box 11](#)↘ provides AQTESOLV solutions for Problems 1, 2, 3 and 5 and compares them to hand-matched results.

Exercise 1

A 0.2 m diameter production well finished in a confined sand aquifer was pumped continuously at 300 L/minute for 10 hours. The water levels in the pumping well and two observation wells appeared to stabilize at about 6 hours as shown in this image.



Cross section of a confined sand water bearing unit. The production well is pumped at a constant rate of 300 L/min for 10 hours and the drawdown in two observation wells is observed under what appear to be steady state conditions. Drawdowns from the static pre-pumping water levels are shown along with the radial distances of wells from the production well.

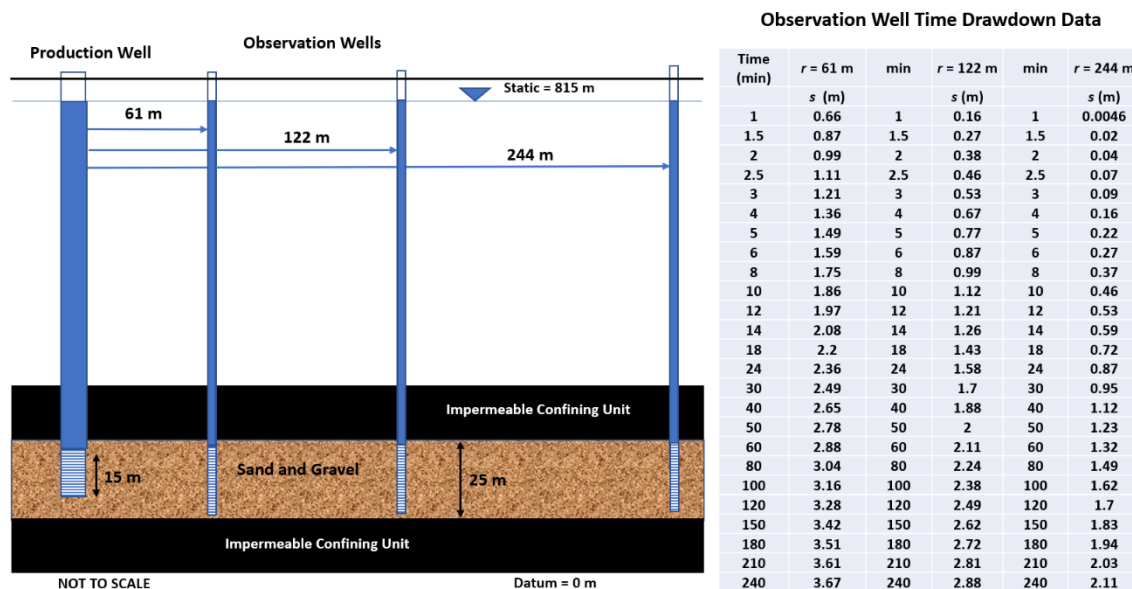
- Assuming the pumping test reached steady state or pseudo steady state by 10 hours compute T and K .
- Do you need to account for the effects of partial penetration on the observation well data? Why or why not?
- Assuming the production well radius is 0.1 m and the measured drawdown in the pumping well is 24 m, calculate the production well efficiency (i.e., measured drawdown divided by theoretical drawdown). A semi-log plot of drawdown (arithmetic scale) versus distance (log scale) using the observation well data will be helpful.

[Solution to Exercise 1 ↴](#)

[Return to where text linked to Exercise 1 ↴](#)

Exercise 2

A pumping test is conducted on a production well located in an extensive, isotropic, homogeneous, 25-m thick, totally confined, sand and gravel aquifer. The production well has a 15 m screened interval. The well is pumped at a constant rate of 1,200 m³/d for 240 minutes. Time-drawdown data are collected at three observation wells located 61 m, 122 m, and 244 m from the pumping well as shown in the image below. An Excel® data base of the time-drawdown data is available on the [web page for this book](#).



Information related to Exercise 2. A production well is pumped at a constant rate in a totally confined isotropic and homogeneous aquifer that is infinite in lateral extent. Time-drawdown data are collected from three observation wells. Configuration of the pumping well location, screen length and location of the observation wells are shown in cross section. Time-drawdown data sets for the three observation wells are presented (modified from Lohman, 1972).

- Prepare log-log pots of the time-drawdown data for each of the observation wells. Using manual or automated curve matching, determine values of transmissivity and storativity for each data set.
- Compare and contrast the values computed. Should they all be the same? If not, how would you present the results to the well owner?
- Analysis of pumping a confined aquifer can also be accomplished using the Cooper-Jacob straight line method. Plot the time-drawdown data for the observation well located at 122 m from the pumping well as a semi-log plot and determine T and S . Compare these results to the results from the part (a) type curve analyses, and comment on their similarity or differences.
- The confined time-drawdown data can also be interpreted using the distance-drawdown method. Make a semi-log plot of the distance-drawdown data at 100 minutes and calculate T and S . Compare these results to those derived from type curve and time-drawdown straight line analyses. Discuss why the values are similar or different.

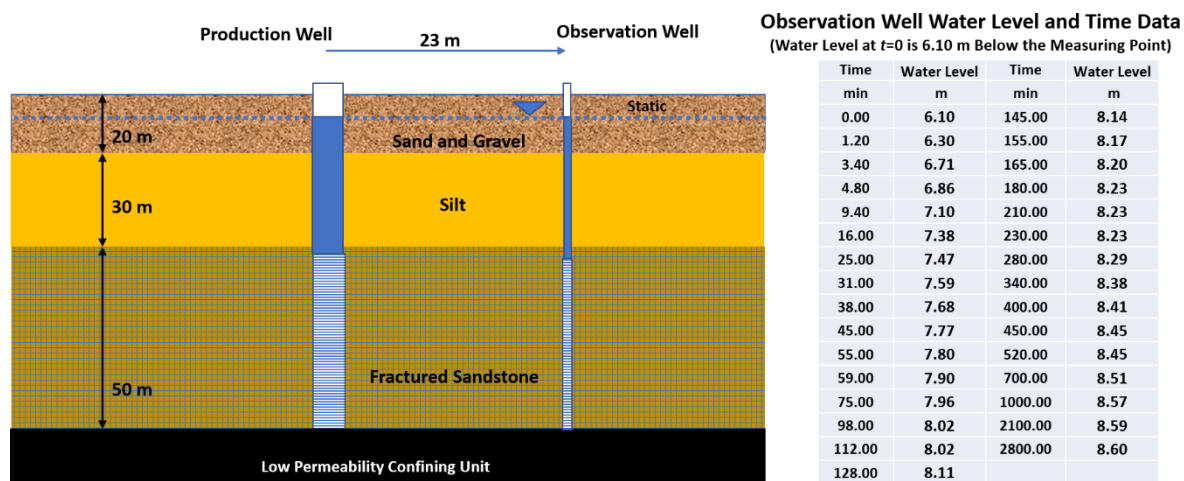
- e) Using the distance-drawdown plot examine the efficiency (i.e., measured drawdown divided by theoretical drawdown) of the production well. If the production well diameter is 0.20 m and the drawdown at 100 minutes in the pumping well is 12.34 m, what is the efficiency of the pumping well?
- f) The well is planned to be used to supplement the city water system. After a seasonal supply evaluation, it was decided to pump the well for 200 days at a constant rate of 1,000 m³/d. There are other wells in the area and a regulatory agency wants to know if other wells would be affected when this well is pumped. Ignoring the effects of pumping in the other wells, what is the predicted drawdown 1000 m from this well at the end of the pumping period?

[Solution to Exercise 2](#) ↓

[Return to where text linked to Exercise 2](#) ↑

Exercise 3

An irrigation well is designed and installed in a 50 m thick highly fractured sandstone that is overlain by 30 m of silt which is in turn overlain by 20 m of sand and gravel. The static water levels in the three units are similar, about 6 m below and surface. The production well is fully penetrating the water producing zone. A 6-cm diameter, fully penetrating, observation well was constructed in the highly fractured sandstone 23 m from the production well. A 1.9-day constant rate pumping test was conducted at a rate of $196 \text{ m}^3/\text{d}$ and the observation well water levels were monitored with an electric water level sensor. The test conditions are illustrated in the image shown here.



Cross section of hydrogeologic conditions associated with a pumping test. A fractured sandstone is the principal water bearing unit. Static water levels in each unit are about 6 m below land surface. The water level time data collected during the test are shown in the table.

An Excel® data base of the time-drawdown data is available on the [web page for this book](#).

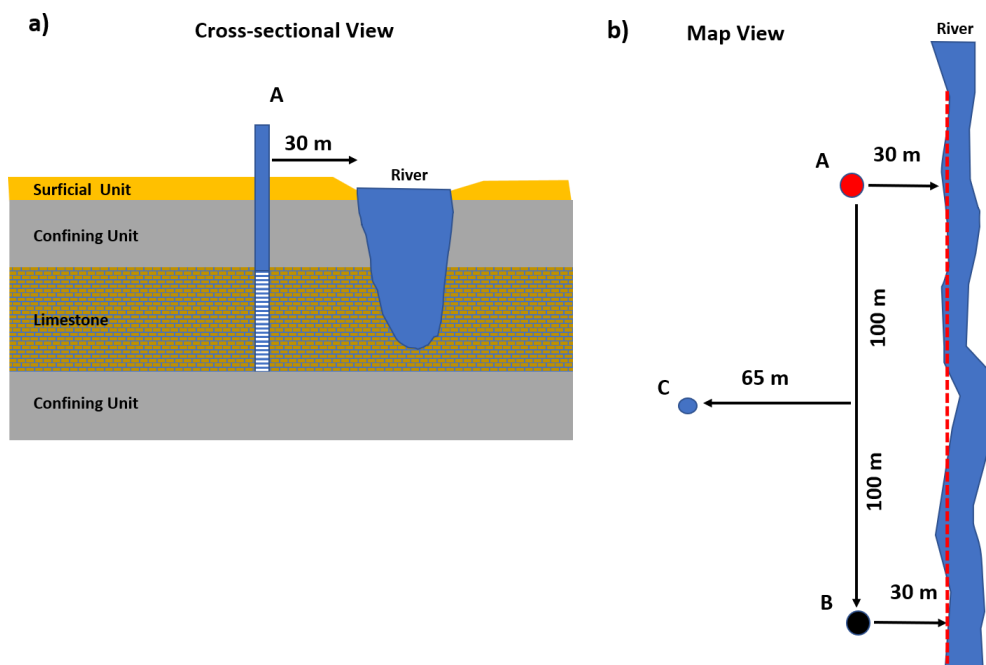
- Convert the water level data to drawdown and plot the data.
- After reviewing the site data, select an analytical approach. Explain why you choose the analytical model used. Treat the highly fractured sandstone as an equivalent porous medium (Woessner & Poeter, 2020). Compute T and S for the highly fractured sandstone aquifer.
- Based on your analysis, estimate the vertical hydraulic conductivity of the confining silt layer.

[Solution to Exercise 3](#)

[Return to where text linked to Exercise 3](#)

Exercise 4

A well (A) pumping at $900 \text{ m}^3/\text{d}$ is located near a river as shown in the image below. The river penetrates a fractured, permeable, confined limestone. A second production well (B) is located 200 m from the first well. A previous pumping test of the formation at well A yielded a T of $75 \text{ m}^2/\text{d}$ and an S of 0.00003.



Production wells located near a fully penetrating river. On average, the distance to the river in the confined aquifer is 30 m from the pumping well as shown by the red dashed line. a) Cross section showing production well A and the lithology. b) Map view of the well locations relative to the river.

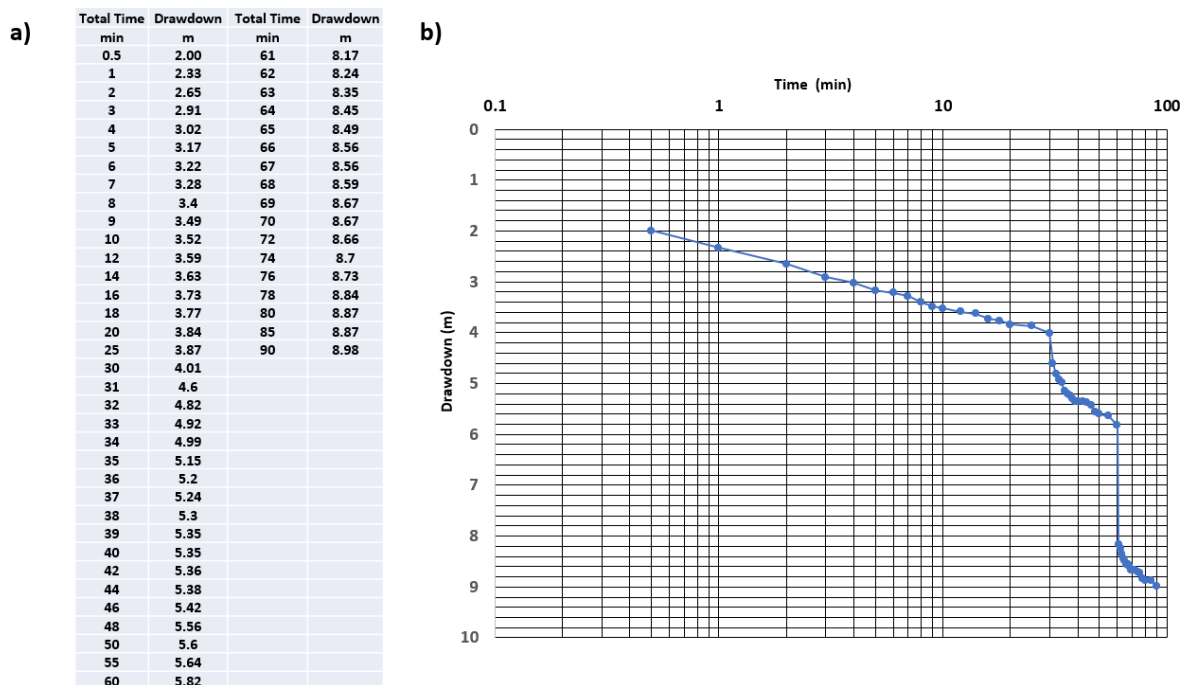
- Compute the well interference (drawdown) that would occur at B when well A is pumped at $900 \text{ m}^3/\text{d}$ for 50 days.
- If during the same 50 days of pumping well A, the well at location B is pumped at $450 \text{ m}^3/\text{d}$, what would be the drawdown at unpumped observation well C at the end of the 50 days of pumping?

[Solution to Exercise 4](#) ↴

[Return to where text linked to Exercise 4](#) ↲

Exercise 5

A production well was designed to yield 2,000 m³/d from a 40 m thick confined gravel-rich aquifer. The well was 40 cm in diameter and screened over 35 m. Once the well was completed, a step test was conducted by pumping the well at 1,400 m³/d, 1,790 m³/d and then 2,520 m³/d for a total of 90 minutes with each step lasting 30 min. The time-drawdown data and a semi-log plot of the time-drawdown data are presented here.



Step-drawdown test data for a production well. a) Time-drawdown data for three steps. b) Plot of the log of time versus drawdown.

An Excel® data base of the time-drawdown data is available on the [web page for this book](#).

- Calculate the value of C and B for this system. Compute the well loss expected when pumping the well at 2,000 m³/d.
- Estimate the total drawdown after pumping the well for 30 min at 2,000 m³/d.
- Estimate transmissivity using the first 30 minutes of time-drawdown data (step 1) (use the Cooper-Jacob method).

[Solution to Exercise 5](#)

[Return to where text linked to Exercise 5](#)

Using this driller's log answer the following questions:

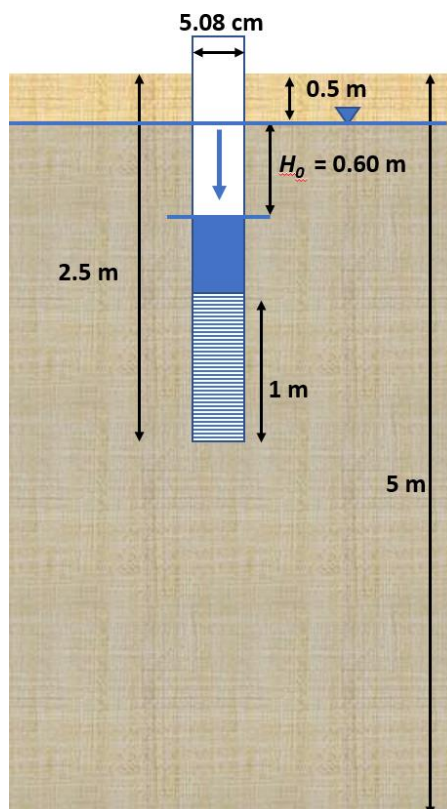
- a) What depth interval and geologic material did the driller perforate to produce water to the well?
- b) Is this water producing unit likely confined or unconfined? Support your answer.
- c) Examine the static water level and performance test information, compute the specific capacity of the well.
- d) Based on the pumping data recorded by the driller, estimate the transmissivity of the aquifer using two methods. When applying each method justify your approach
 - 1) Method 1: Assume the pumping has not proceeded to a steady state.
 - 2) Method 2: Assume the pumping has resulted in near steady state conditions (simple equation approximation).
- e) When you only have performance data for a single pumping well do you anticipate the formational values of T will be greater or less than the values you computed? Why?

[Solution to Exercise 6](#) ↓

[Return to where text linked to Exercise 6](#) ↑

Exercise 7

A monitoring well that is 5.08 cm in diameter was installed in an unconfined silt-rich formation that is 5 m thick. The base of the well screen is located 2.5 m below the land surface and is 1 m long. The water table is 0.5 m below land surface. A slug out test was performed on this well as illustrated in the image below.



Time	Lowered Water Level
s	m
0	0.6
27	0.55
48	0.51
70	0.48
97	0.44
139	0.39
172	0.34
230	0.3
268	0.26
303	0.23
355	0.19
420	0.16
477	0.13
547	0.1
633	0.08

Slug out test conducted in a silt-rich unconfined formation. a) Unpumped well design and location of screened interval. The slug test was conducted by lowering the water level by 0.6 m. This is the water level at the start of the test (H_0). b) After 10.5 minutes (633 s) the water level had recovered within 0.08 m of the static water elevation (modified from Todd and Mays, 2005).

An Excel® data base of the time-drawdown data is available on the [web page for this book](#).

- Select an appropriate method to analyze the slug test data. Explain your choice.
- Use this method to calculate K.

[Solution to Exercise 7](#)

[Return to where text linked to Exercise 7](#)

19 References

- Agarwal, R. G. (1970). An investigation of wellbore storage and skin effects in unsteady liquid flow: 1. Analytical treatment. *Society of Petroleum Engineers Journal*, 10, 279–289.
- Alley, W. M., Reilly, T. E., & Franke, O. L. (1999). *Sustainability of ground-water resources* (Circular 1186). US Geological Survey. <http://pubs.usgs.gov/circ/circ1186/>.
- Anderson, M. P., Woessner, W. W., & Hunt, R. J. (2015). *Applied groundwater modeling: Simulation of flow and advective transport* (2nd ed.). Elsevier.
- AQTESOLV. (2023). *Software for the design and interpretation of aquifer tests* [Computer software]. <http://www.aqtesolv.com/>.
- AQTESOLV. (2004–2007). *User guide* (Version 4.5) [Computer software]. HydroSOLVE, Inc.
- AquiferTest. (2023). *Software for analyzing, interpreting and visualizing pumping and slug test data* (Version 12) [Computer software]. <https://www.waterloohydrogeologic.com/help/aquifertest/>.
- Aquifer^{Win32}. (2023). *Groundwater modeling software supporting analysis of aquifer slug and step tests* (Version 5) [Computer software]. <https://www.groundwatermodels.com>.
- Standards Australia. (1990). *Australia standard: Committee on test pumping water wells* (Committee CE/28 AS 2368-1990). Standards Australia. <https://www.saiglobal.com/PDFTemp/Previews/OSH/As/as2000/2300/2368.PDF>.
- Barker, J. A., (1988). A generalized radial flow model for hydraulic tests in fractured rock. *Water Resources Research*, 24(10), 1796–1804.
- Barker, J. A., & Black, J. H. (1983). Slug tests in fissured aquifers. *Water Resources Research*, 19(6), 1558–1564.
- Benson, D. (2023). Automated estimation of aquifer parameters from arbitrary-rate pumping tests in python and MATLAB. *Groundwater Online*. <https://doi.org/10.1111/gwat.13338>.
- Bentall, R. (1963). *Methods for determining permeability, transmissibility and drawdown* (Water-Supply Paper 1536) (pp. 243–341). US Geological Survey.
- Binkhorst, G., & Robbins, G. (1998). Conducting and interpreting slug tests in monitoring wells with partially submerged screens. *Ground Water*, 36(2), 225–229.
- Black, J. H. (1978). The use of the slug test in groundwater investigations. *Water Services, March*, 174–178.
- Boldt-Leppin, B. E. J., & Hendry, M. J. (2003). Application of harmonic analysis of water levels to determine vertical hydraulic conductivities in clay-rich aquitards. *Ground Water*, 41, 514–522.
- Boulton, N. S. (1954a). Unsteady radial flow to a pumped well allowing for delayed yield from storage. *International Association of the Science of Hydrology Publication*, 37, 472–477.

- Boulton, N. S. (1954b). The drawdown of the water table under nonsteady conditions near a pumped well in an unconfined formation. In *Proceedings [London], part 3* (pp. 564–579). Institute of Civil Engineers.
- Boulton, N. S. (1963). Analysis of data from non-equilibrium pumping tests allowing for delayed yield from storage. In *Proceedings [London], 26* (pp. 469–482). Institute of Civil Engineers.
- Boulton, N.S., Stallman, R. W, Walton, W. C., & Ineson, J. (1964). Analysis of data from non-equilibrium pumping tests allowing for delayed yield from storage. In *Proceedings of the Institute of Civil Engineers [London], 28*, 603–610.
<https://doi.org/10.1680/iicep.1964.10023>.
- Bouwer, H. (1989). The Bouwer and Rice slug test - An update. *Ground Water*, 27(3), 304–309.
- Bouwer, H., & Rice, R. C. (1976). A slug test for determining hydraulic conductivity of unconfined aquifers with completely or partially penetrating wells. *Water Resources Research*, 12, 3040309.
- Bradbury, K. R., Gotkowitz, M. B., Hart, D. J., Eaton, T. T., Cherry, J. A., Parker, B. L., & Borchardt, M. A. (2006). *Contaminant transport through aquitards: A state-of-the-science review and technical guidance for aquitard assessment*. American Water Works Association (AWWA) Research Foundation.
- British Standard. (2003). *Hydrometric determinations - Pumping tests for water wells - Considerations and guidelines for design, performance and use* (British Standard ISO 14686:2003). BSI. http://ansdimat.com/ru/normative/BS_ISO_14686_2003.pdf.
- Bourdet, D., Ayoub, J. A., & Pirard, Y. M. (1989). Use of pressure derivative in well test Interpretation. *SPE Formation Evaluation*, June, 293–302.
- Butler, J. J., Jr. (1988). Pumping tests in nonuniform aquifers - The radially symmetric case. *Journal of Hydrology*, 101, 15–30.
- Butler, J. J., Jr. (1996). Slug tests in site characterization - Some practical considerations. *Environmental Geosciences*, 3(3), 154–63.
- Butler, J. J., Jr. (1998). *The design, performance and analysis of slug tests*. CRC Press.
- Butler, J. J., Jr., & Garnett, E. J. (2000). *Simple procedures for analysis of slug tests in formations of high hydraulic conductivity using spreadsheet and scientific graphics software* (Open-File Report 2000-40). Kansas Geological Survey.
https://www.kgs.ku.edu/Hydro/Publications/OFR00_40/.
- Butler, J. J., Jr., Garnett, E. J., & Healey, J. M. (2003). Analysis of slug tests in formations of high hydraulic conductivity. *Groundwater*, 41(5), 620-631.
- Butler, J. J., Jr., & Zhan, X. (2004). Hydraulic tests in highly permeable aquifers. *Water Resources Research*, 40, W12402. <https://doi.org/10.1029/2003WR002998>.
- Carpenter, G. W., & Stephenson, R. W. (1986). Permeability testing in the triaxial cell. *Journal of ASTM International*, 9(1), GTH10605J. <https://doi.org/10.1520/GTJ10605J>.
- Chang, S. W., Memari, S. S., & Clement, T. P. (2021). PyTheis - A Python tool for analyzing pump test data. *Water*, 13(16), 2180. <https://doi.org/10.3390/w13162180>.

- Cherry, J. A., Parker, B. L., Bradbury, K. R., Eaton, T. T., Gotkowitz, M. G., & Hart, D. J. (2006). *Contaminant transport through aquitards: A state-of-the-science review*. American Water Works Association (AWWA) Research Foundation.
- Clark, W. E. (1967). Computing the barometric efficiency of a well. *Journal of Hydraulics*, 93(HY4), 93–98.
- Clonts, M. D., & Ramey, H. J. (1986). *Pressure transient analysis for wells with horizontal drainholes* (Paper SPE 15116). Society of Petroleum Engineers.
- Cohen, A. J. B., & Cherry, J. A. (2020). *Conceptual and visual understanding of hydraulic head and groundwater flow*. The Groundwater Project. <https://gw-project.org/books/conceptual-and-visual-understanding-of-hydraulic-head-and-groundwater-flow/>.
- Collins, S. L., & Bianchi, M. (2020). DISOLV: A Python package for the interpretation of borehole dilution tests. *Groundwater*, 58(5), 805–812. [https://nora.nerc.ac.uk/id/eprint/527089/1/Collins et al-2020-Groundwater.pdf](https://nora.nerc.ac.uk/id/eprint/527089/1/Collins_et_al-2020-Groundwater.pdf).
- Cooley, R. L., & Case, C. M. (1973). Effect of a water table aquitard on drawdown in an underlying pumped aquifer. *Water Resources Research*, 9(2), 434–447.
- Cooper, H. H., Jr. (1963). Type curves for nonsteady radial flow in an infinite leaky artesian aquifer. In R. Bentall (Compiler), *Shortcuts and special problems in aquifer tests* (Water-Supply Paper 1545-C, C48-C55). US Geological Survey.
- Cooper, H. H., Jr., Bredehoeft, J. D., & Papadopoulos, I. S. (1967). Response of finite-diameter well to an instantaneous change in water. *Water Resources Research*, 3, 63–269.
- Cooper, H. H., Jr., & Jacob, C. E. (1946). A generalized graphical method for evaluating formation constants and summarizing well-field history. *American Geophysical Union Transactions*, 27(4), 526–534.
- Dagan, G. (1978). A note on packer, slug, and recovery tests in unconfined aquifers. *Water Resources Research*, 14(5), 929–934.
- Das, B. M. (1983). *Advanced soil mechanics* (pp. 5–11). Hemisphere.
- Daviau, F., Mouronval, G., Bourdarot, G., & Curutchet, P. (1985, September 22–25). *Pressure analysis for horizontal wells* [Paper presentation, SPE Paper 14251]. 60th Annual Technical Conference and Exhibition, Las Vegas, Nevada, USA.
- Davis, S. N. (1972). Use of naturally occurring phenomena to study hydraulic diffusivities of aquitards. *Water Resources Research*, 8, 500–507.
- Diersch, H. J. G. (2014). *FEFLOW: Finite element modeling of flow, mass and heat transport in porous and fractured media*. Springer.
- Domenico, P. A., & Mifflin, M. D. (1965). Water from low permeability sediments and land subsidence. *Water Resources Research*, 4, 563–576.
- Domenico, P. A., & Schwartz, F. W. (1997). *Physical and chemical hydrogeology* (2nd ed.). Wiley.
- Dougherty, D. E., & Babu, D. K. (1984). Flow to a partially penetrating well in a double-porosity reservoir. *Water Resources Research*, 20(8), 1116–1122.
- Drage, J. (2022). *Domestic wells - Introduction and overview*. The Groundwater Project. <https://gw-project.org/books/domestic-wells-introduction-and-overview/>.

- Driscoll, F. G. (1986). *Groundwater and wells* (2nd ed.). Johnson Division.
- Duffield, G. M. (2022). *Aqtesolv manual* [Computer software].
<http://www.aqtesolv.com/manual.asp>.
- Dunn, D. (2023). *Aquifer storativity*. Hydrogeology and geology website.
<https://www.dunnhydrogeo.com/home/aquifer-storativity-t>.
- Dupuit, J. (1863). *Études théoriques et pratiques sur le mouvement des eaux dans les canaux découverts et à travers les terrains perméables* [Theoretical and practical studies of the movement of water in open channels and across permeable terrains] (2nd ed.). Paris: Dunod.
- Earlougher, R. C., Jr. (1977). *Advances in well test analysis* (Monograph Series 5). Society of Petroleum Engineers.
- Environmental Simulations, Inc. (2019). *Guide to using Aquifer^{Win32}* (Version 6) [Computer software]. Environmental Simulations, Inc.
- Ferris, J. G., Knowles, D. B., Brown, R. H., & Stallman, R. W. (1962). *Theory of aquifer tests* (Water-Supply Paper 1536-E) (pp. 69–174). US Geological Survey.
- Fetter, C. W. (2001). *Applied hydrogeology* (4th ed.). Prentice Hall.
- Freeze, R. A., & Cherry, J. A. (1979). *Groundwater*. The Groundwater Project. <https://gw-project.org/books/groundwater/>.
- Geoprobe. (2016). *Slug test ST analysis software* [Computer software].
<https://geoprobe.com/direct-image/software/slug-test-analysis-software>.
- Gringarten, A. C., & Ramey, H. J. (1974). Unsteady state pressure distributions created by a well with a single horizontal fracture, partial penetration or restricted entry. *Journal of the Society of Petroleum Engineers*, 14, 413–426.
[https://www.scirp.org/\(S\(351jmbntvnsjt1aadkozje\)\)/reference/referencespapers.aspx?referenceid=1161592](https://www.scirp.org/(S(351jmbntvnsjt1aadkozje))/reference/referencespapers.aspx?referenceid=1161592).
- Gringarten, A. C., & Witherspoon, P. A. (1972). A method of analyzing pump test data from fractured aquifers. In *Rock Mechanics, 3-B* (pp. 1–9) [Symposium]. International Society of Rock Mechanics and International Association of Engineering Geology, Stuttgart, Germany.
- Grisak, G. E., & Cherry, J. A. (1975). Hydrologic characteristics and response of fractured till and clay confining a shallow aquifer. *Canadian Geotechnical Journal*, 12, 23–43.
- Grover, R. E. (1874). *Transient groundwater hydraulics*. Water Resources Publications.
- Haefner, R. J. (2000). Characterization methods for fractured glacial tills. *Ohio Journal of Science*, 100, 73–87.
- Haitjema, H. M. (1995). *Analytic element modeling of groundwater flow*. Academic Press.
- Halford, K., & Kuniansky, E. L. (2002). *Documentation of spreadsheets for the analysis of aquifer-test and slug-test data* (Open-File Report 02-197). US Geological Survey.
- Haneberg, W., Allred, B., Swearingen, P., & Gibson, A. (1998). *Consolidation test results, Triaxial permeability values, and particle size distributions, 98th Street ground water*

- monitoring well, Albuquerque, New Mexico (Open File Report #436). New Mexico Bureau of Mines and Mineral Resources.
- Hantush, M. S. (1956). Analysis of data from pumping tests in leaky aquifers. *American Geophysical Union Transactions*, 37(6), 702–714.
- Hantush, M. S. (1959). Nonsteady flow to flow wells in leaky aquifers. *Journal of Geophysical Research*, 64(5), 1043–1052.
- Hantush, M. S. (1960). Modification of the theory of leaky aquifers. *Journal of Geophysical Research*, 65(11), 3713–3725.
- Hantush, M. S., & Jacob, C. E. (1954). Plane potential flow of ground water with linear leakage. *American Geophysical Union Transactions*, 35(6), 917–936.
- Hantush, M. S., & Jacob, C. E. (1955). Non-steady radial flow in an infinite leaky aquifer. *American Geophysical Union Transactions*, 36(1), 95–100.
- Hargis, D. R. (1979). *Analysis of factors affecting water level recovery data* [Doctoral dissertation, University of Arizona]. University of Arizona Digital Archive. <http://hdl.handle.net/10150/191053>.
- Hart, D. J., Bradbury, K. R., & Feinstein, D. T. (2004). The vertical hydraulic conductivity of an aquitard at two spatial scales. *Groundwater*, 44(2), 201–211. <https://doi.org/10.1111/j.1745-6584.2005.00125.x>.
- Hemker, C. J., & Maas, C. (1987). Unsteady flow to wells in layered and fissured aquifer systems. *Journal of Hydrology*, 10(3–4), 231–249.
- Houlsby, A. (1976). Routine interpretation of the Lugeon water-test. *Quarterly Journal of Engineering Geology*, 9, 303–313.
- Hurst, W., Clark, J. D., & Brauer, E. B. (1969). The skin effect in producing wells. *Journal of Petroleum Technology*, November, 1483–1489.
- Hvorslev, M. J. (1951). *Time lag and soil permeability in groundwater observations* (Bulletin 36). US Army Corps of Engineers Waterway Experimentation Station.
- Hyder, Z., Butler, J. J., Jr., McElwee, C. D., & Liu, W. (1994). Slug tests in partially penetrating wells. *Water Resources Research*, 30(11), 2945–2957.
- Ismael, R. (2016). *Slug tests in unconfined aquifers* [Unpublished master's thesis]. Western Michigan University.
- Jacob, C. E. (1946). Radial flow in a leaky artesian aquifer. *American Geophysical Union Transactions*, 27(2), 198–205.
- Jacob, C. E. (1963). Determining the permeability of water-table aquifers. In R. Bentall, (Compiler), *Methods of determining permeability, transmissibility, and drawdown* (Water-Supply Paper 1536-1) (pp. 245–271). US Geological Survey.
- Jacob, C. E. (1940). On the flow of water in an elastic artesian aquifer. *Transactions of the American Geophysical Union*, 21(2), 574–588.
- Jacob, C. E. (1950). *Flow of groundwater in engineering hydraulics* (pp. 3321–3386). John Wiley & Sons.

- Jacob, C. E., & Lohman, S. W. (1952). Nonsteady flow to a well of constant drawdown in an extensive aquifer. *American Geophysical Union Transactions*, 33, 559–569.
- Kingsbury, J. A. (2018). Altitude of the potentiometric surface, 2000–15, and historical water-level changes in the Memphis aquifer in the Memphis area, Tennessee (Scientific Investigations Map 3415). US Geological Survey.
<https://doi.org/10.3133/sim3415>.
- Kasenow, M. (1997). *Introduction to aquifer analysis* (4th ed.). Water Resources Publications.
- Kasenow, M. (1996). *Production well analysis: New methods and computer program in well hydraulics*. Water Resources Publications.
- Kasenow, M. (2001). *Applied ground-water hydrology and well hydraulics* (2nd ed.). Water Resources Publications.
- Keller, C. K., van der Kamp, G., & Cherry, J. A. (1989). Multiscale study of the permeability of a thick clayey till. *Water Resources Research*, 25, 2299–2317.
- Kipp, K. L., Jr. (1973). Unsteady flow to a partially penetrating, finite radius well in an unconfined aquifer. *Water Resources Research*, 9(2), 448–462.
<https://doi.org/10.1029/WR009i002p00448>.
- Kipp, K. L., Jr. (1985). Type curve analysis of inertial effects in the response of a well to a slug test. *Water Resources Research*, 21(9), 1397–1408.
- Kreyszig, E. (1979). *Advanced engineering mathematics* (4th ed.). John Wiley & Sons.
- Kruseman, G. P., & de Ritter, N. A. (2000). *Analysis and evaluation of pumping test data* (2nd ed.) International Institute for Land Reclamation and Improvement Publication 47.
<https://gw-project.org/books/analysis-and-evaluation-of-pumping-test-data/>.
- Lapcevic, P. A., Novakowski, K. S., & Sudicky, E. A. (1999). Groundwater flow and solute transport in fractured media. In J. W. Delleur (Ed.), *The handbook of groundwater engineering* (pp. 17–39). CRC Press.
- Lin, Y.-C., Huang, C.-S., & Yeh, H.-D. (2019). Analysis of unconfined flow induced by constant rate pumping based on the lagging theory. *Water Resources Research*, 55(5), 3925–3040.
- Loaiciga, H. A. (2009). Derivation approaches for the Theis (1935) equation. *Groundwater*, 48(1), 2–5.
- Lohman, S. W. (1972). *Ground-water hydraulics* (Professional Paper 708). US Geological Survey.
- Lugeon, M. (1933). Barrages et géologie: méthodes de recherches, terrassement et imperméabilisation [Dams and geology: Research methods, earthworks and waterproofing]. Librairie de l'Université, F. Rouge & Cie.
- Maldaner, C. H., Quinn, P. M., Cherry, J. A., & Parker, B. L. (2018). Improving estimates of groundwater velocity in a fractured rock borehole using hydraulic and tracer dilutions methods. *Journal of Contaminant Hydrology*, 214, 75–86.
- Matthews, C. S., & Russell, D. G. (1967). *Pressure buildup and flow tests in wells*. Society of Petroleum Engineers Monograph Series 1.

- Martos-Rosillo, S., Guardiola-Albert, C., Bentiez, A., Pastor, J., Gozalez, A., & Valsero, J. (2018). SlugIn 1.0: A free tool for automated slug test analysis [Computer software]. *Groundwater*, 56(3), 362–365.
- McElwee, C. D., & Zenner, M. A. (1998). A nonlinear model for analysis of slug-test data. *Water Resources Research*, 34(1), 55–66.
- McWhorter, E. B., & Sunada, D. K. (1977). *Groundwater hydrology and hydraulics*. Water Resources Publications.
- Meyer, J. R., Parker, B. L., Arnaud, E., & Runkel, A. C. (2016). Combining high resolution vertical gradients and sequence stratigraphy to delineate hydrogeologic units for a contaminated sedimentary rock aquifer system. *Journal of Hydrology*, 534, 505–523. <https://doi.org/10.1016/j.jhydrol.2016.01.015>↗.
- Meyer, J. R., Parker, B. L., & Cherry, J. A. (2014). Characteristics of high-resolution hydraulic head profiles and vertical gradients in fractured sedimentary rocks. *Journal of Hydrology*, 517, 493–507. <https://doi.org/10.1016/j.jhydrol.2014.05.050>↗.
- Meyer, J. R., Parker, B. L., & Cherry, J. A. (2008). Detailed hydraulic head profiles as essential data for defining hydrogeologic units in layered fractured sedimentary rock. *Environmental Geology*, 56(1), 27–44. <https://link.springer.com/article/10.1007/s00254-007-1137-4>↗.
- Mieussens, C., & Ducasse, P. (1977). Mesure en place des coefficients de permeabilite et des coefficients de consolidation horizontaux et verticaux [Measurement in place of permeability coefficients and horizontal and vertical consolidation coefficients]. *Canadian Geotechnical Journal*, 14, 76–90.
- Moench, A. F. (1984). Double-porosity models for a fissured groundwater reservoir with fracture skin. *Water Resources Research*, 20(7), 831–846.
- Moench, A. F. (1985). Transient flow to a large diameter well in an aquifer with storative semiconfining layers. *Water Resources Research*, 21(8), 1121–1131.
- Moench, A. F. (1993). Computation of type curves or flow to partially penetrating wells in water-table aquifers. *Ground Water*, 31, 966–971.
- Moench, A. F. (1995). Combining the Neuman and Boulton models for flow to a well in an unconfined aquifer. *Ground Water*, 33, 378–384.
- Moench, A. F. (1966). Flow to a well in a water-aquifer: An improved Laplace transform solution. *Ground Water*, 34, 593–596.
- Moench, A. F., & Ogata, A. (1984). Analysis of constant discharge wells by numerical inversion of Laplace transform solutions. In J. S. Rosenshein & G. D. Bennet (Eds.), *Groundwater hydraulics: Water resources monographs 9* (pp. 146–170). American Geophysical Union.
- Moench, A. F. (1997). Flow to a well of finite diameter in a homogeneous, anisotropic water table aquifer. *Water Resources Research*, 33(6), 1397–1407.

- Moench, A. F., & Prickett, T. A. (1972). Radial flow in an infinite aquifer undergoing conversion from artesian to water-table conditions. *Water Resources Research*, 8(2), 494–499.
- Moench, A. R., Garabedian, S. P., & LeBlanc, D. R. (2001). *Estimate of the hydraulic parameters from an unconfined aquifer test conducted in a glacial outwash deposit, Cape Cod, Massachusetts* (Professional Paper 1629). US Geological Survey.
- Morris, D. A., & Johnson, A. I. (1967). *Summary of hydrologic and physical properties of rock and soil materials, as analyzed by the Hydrologic Laboratory of the United States Geological Survey, 1948–60* (Water-supply paper 1839-D). US Geological Survey.
- Murdoch, L. C. (1994). Transient analyses of an interceptor trench. *Water Resources Research*, 30(11), 3023–3031.
- Neuman, S. P. (1972). Theory of flow in unconfined aquifers considering delayed response of the water table. *Water Resources Research*, 8, 1031–1045.
- Neuman, S. P. (1974). Effect of partial penetration on flow in unconfined aquifers considering delayed gravity response. *Water Resources Research*, 10(2), 303–312.
- Neuman, S. P. (1975). Analysis of pumping test data from anisotropic unconfined aquifers considering delayed gravity response. *Water Resources Research*, 11, 329–342.
- Neuman, S. P., & Witherspoon, P. A. (1969). Theory of flow in a confined two aquifer system. *Water Resources Research*, 5(4), 803–816.
- Neuman, S. P., & Witherspoon, P. A. (1972). Field determination of the hydraulic parameters of leaky multiple aquifer systems. *Water Resources Research*, 8, 1284–1298.
- Neuzil, C. E. (1986). Groundwater flow in low-permeability environments. *Water Resources Research*, 22, 1163–1195.
- Neville, C. J., & Markle, J. M. (2000). *Interpretation of t constant-head tests: Rigorous and approximate analyses* [Conference session]. First Joint IAH - CNC/CGS Groundwater Specially Conference, Montreal, Quebec, Canada. S. S. Papadopulos and Associates.
- Nwankwor, G., Gillham, R., van der Kamp, G., & Akindunni, F. (1992). Unsaturated and saturated flow in response to pumping of an unconfined aquifer: Field evidence of delayed drainage. *Groundwater*, 30(5), 690–700.
- Ohio Environmental Protection Agency. (2006). *Technical guidance manual for groundwater investigations: Pumping and slug tests* (pp. 4–40). Ohio Environmental Protection Agency, Division of Drinking and Ground Waters.
<https://epa.ohio.gov/static/Portals/30/remedial/docs/groundwater/TGM%20Chap4%200Rev1%20Final,%202012-2006Arch.pdf>.
- Olsen, H. W., Gill, J. D., Arthur, A. T., & Nelson, K. R. (1991). Innovations in hydraulic-conductivity measurements. *Transportation Research Record, Transportation Research Board*, 1309, 9–17.
- Osborne, P. S. (1993). *Suggested operating procedures for aquifer pumping tests* (EPA/540/s-93/403). US Environmental Protection Agency.

- Ozkan, E., & Raghavan, R. (1991). New solutions for well-test analysis problems: Part I-Analytical considerations. *Society of Petroleum Engineers Formation Evaluation*, September, 359–368.
- Papadopoulos, I. S., & Cooper, H. H. (1967). Drawdown in a well of large diameter. *Water Resources Research*, 3(1), 241–244.
- Pehme, P., Parker, B. L., Cherry, J. A., & Blohm, D. (2014). Detailed measurement of the magnitude of orientation of thermal gradient in lined boreholes for characterizing groundwater flow in fractured rock. *Journal of Hydrology*, 26, 101–114.
- Peres, A. M., Onur, M., & Reynolds, A. C. (1989). A new analysis procedure for determining aquifer properties from slug test data. *Water Resources Research*, 25(7), 1591–1602.
- Petersen, J. H. (1956). *An analysis of the consolidation-permeability characteristics of clay soils* [Master 's thesis]. Rensselaer Polytechnic Institute.
- Poeter, E., & Hsieh, P. (2020). Graphical construction of groundwater flow nets. The Groundwater Project Guelph, Ontario, Canada, <https://gw-project.org/books/graphical-construction-of-groundwater-flow-nets/>.
- Poeter, E., Fan, Y., Cherry, J., Wood, W., & Mackay, D. (2020). Groundwater in our water cycle. The Groundwater Project Guelph, Ontario, Canada, <https://gw-project.org/books/groundwater-in-our-water-cycle/https://gw-project.org/books/graphical-construction-of-groundwater-flow-nets/>.
- Quiñones-Rozo, C. (2010). Lugeon test interpretation, revisited. In *Collaborative management of integrated watersheds* (pp. 405–414). United States Society of Dams 30th Annual Conference.
- Quinn, P., Cherry, J. A., & Parker, B. L. (2012). Hydraulic testing using a versatile straddle packer system for improved transmissivity estimation in fractured-rock boreholes. *Hydrogeology Journal*, 20, 1529–1547.
- Razack, M., & Huntley, D. (1991). Assessing transmissivity from specific capacity data in a large and heterogeneous alluvial aquifer. *Ground Water*, 29(6), 856–861.
- Reed, J. E. (1980). *Type curves for select problems of flow to wells in confined aquifers* (Techniques of Water-Resources Investigations, Chapter B3). US Geological Survey.
- Rivera, A. (2014). Groundwater basics in Canada's groundwater resources. In A. Rivera (Ed.), *Canada's groundwater resources* (pp. 24–61). Fitzhenry and Whiteside.
- Rorabaugh, M. I. (1953, September). Graphical and theoretical analysis of step-drawdown test of artesian well. In *Proceedings of the American Society of Civil Engineers*, 79 (12), 1–23. ASCE.
- Rowe, R. K., & Nadarajah, P. (1993). Evaluation of the hydraulic conductivity of aquitards. *Canadian Geotechnical Journal*, 30, 781–800.
- Schwartz, F. W., & Zhang, H. (2003). *Fundamentals of ground water*. John Wiley & Sons.
- Shapiro, A. M. (2007). *Characterizing hydraulic properties and ground-water chemistry in fractured-rock aquifers: A user's manual for the multifunctional Bedrock*

- Aquifer Transportable Testing Tool (BAT³)* [Computer software] (Open-File Report 2007-1134). US Geological Survey.
- Spane, F. A., Jr., & Wurstner, S. K. (1993). DERIV: A computer program for calculating pressure derivatives for use in hydraulic test analysis. *Ground Water*, 31(5), 814–822.
- Spangler, M. G. (1963). *Soil engineering* (2nd ed.). International Textbook Company.
- Springer R. K., & Gelhar, L. W. (1991). *Characterization of large-scale aquifer heterogeneity in glacial outwash by analysis of slug tests with oscillatory responses, Cape Cod, Massachusetts* (Water Resources Investigations Report 91-4034) (pp. 36–40). US Geological Survey.
- Sterrett, R. J. (2007). *Groundwater and wells* (3rd ed.). Johnson Screens.
<https://johnsonscreens.com/books/>.
- Tartakovsky, G. D., & Neuman, S. P. (2007). Three-dimensional saturated-unsaturated flow with axial symmetry to a partially penetrating well in a compressible unconfined aquifer. *Water Resources Research*, 43(1), W01410.
<https://doi.org/10.1029/2006WR005153>.
- Tavenas, F., Diene, M., & Leroueil, S. (1990). Analysis of the in situ constant-head permeability test in clays. *Canadian Geotechnical Journal*, 27, 305–314.
- Taylor, C. J., & Alley, W. M. (2001). *Ground-water-level monitoring and the importance of long-term water-level data* (Circular 1217). US Geological Survey.
<https://doi.org/10.3133/cir1217>.
- Thiem, G. (1906). *Hydrologische methoden* [Hydrological methods]. Gebhart.
- Theis, C. V. (1935). The relation between the lowering of the piezometric surface and the rate and duration of discharge of a well using ground-water storage. *American Geophysical Union Transactions*, 15, 519–524.
- Thompson, P. L., & Kilgore, R. T. (2006). *Hydraulic design of energy dissipators for culverts and channels* (3rd ed.) (FHWA-NHI-06-086, Hydraulic Engineering Circular Number 14). US National Highway Institute.
- Todd, D. K., & Mays, L. W. (2005). *Groundwater hydrology* (3rd ed.). John Wiley & Sons.
- US Department of the Interior, Water and Power Resources Service (USDI). (1981). *Ground water manual - A water resources technical publication*. US Government Printing Office.
- US Department of the Navy. (1982). *Soil mechanics* (NAVFACX Design Manual 7.1). Naval Facilities Engineering Command.
- US Nuclear Regulatory Commission. (2015). *List of ASTM standards for the analysis of hydraulic characteristic of aquifer by aquifer pumping tests* (NRC-080 6/8/15).
<https://www.nrc.gov/docs/ML1515/ML15159B191.pdf>.
- van der Kamp, G. (1976). Determining aquifer transmissivity by means of well response tests - The underdamped case. *Water Resources Research*, 12(1), 7-1–7-7.
- van der Kamp, G. (2001). Methods for determining the in situ hydraulic conductivity of shallow aquitards - An overview. *Hydrogeology Journal*, 9, 5–16.
- van der Kamp, G., & Maathuis, H. (1985). Excess hydraulic head in aquitards under solid waste emplacements. In S. P. Neuman & E. S. Simpson (Eds.), *Hydrogeology of rocks of*

low permeability. Association Internationale des Hydrogeologues, Committee of USA Members.

- Walton, W. C. (1970). *Groundwater resources evaluation*. McGraw Hill.
- Warren, J. E., & Root, P. J. (1963). The behavior of naturally fractured reservoirs. *Society of Petroleum Engineers Journal*, 3, 245–255.
- Washington State Department of Ecology. (2020). *Aquifer test procedures* (Water Resources Program Guidance Publication 20-11-93). Water Resources Program, Washington State Department of Ecology.
<https://fortress.wa.gov/ecy/publications/summarypages/2011093.html>↗.
- Waterloo Hydrogeologic. (2021). *User's manual AquiferTest 11: Pumping and slug test analysis, interpretation and visualization software* [Computer software]. Waterloo Hydrogeologic.
- Weight, W. D. (2019). *Practical hydrogeology* (3rd ed.). McGraw Hill Education.
- Woessner, W. W. (2020). *Groundwater - surface water exchange*. The Groundwater Project.
<https://gw-project.org/books/groundwater-surface-water-exchange/>↗.
- Woessner, W. W., & Poeter, E. P. (2020). *Hydrogeologic properties of earth materials and principles of groundwater flow*. The Groundwater Project. <https://gw-project.org/books/hydrogeologic-properties-of-earth-materials-and-principles-of-groundwater-flow/>↗.
- Wylie, A., & Magnuson, S. (1995). Spreadsheet modeling of slug tests using the van der Kamp method. *Ground Water*, 33(2), 326–329.
- Ziegler, T. W. (1976). *Determination of rock permeability* (Technical Report S-76-2). US Army Waterways Experiment Station.
- Zlotnik, V. (1994). Interpretation of slug and packer tests in anisotropic aquifers. *Ground Water*, 32(5), 761–766. <https://doi.org/10.1111/j.1745-6584.1994.tb00917.x>↗.
- Zurbuchen, B. R., Zlotnik, V. A., & Butler, J. J., Jr. (2002). Dynamic interpretation of slug tests in highly permeable aquifers. *Water Resources Research*, 38(3), 7-1– 7-18.
<https://doi.org/10.1029/2001WR000354>↗.

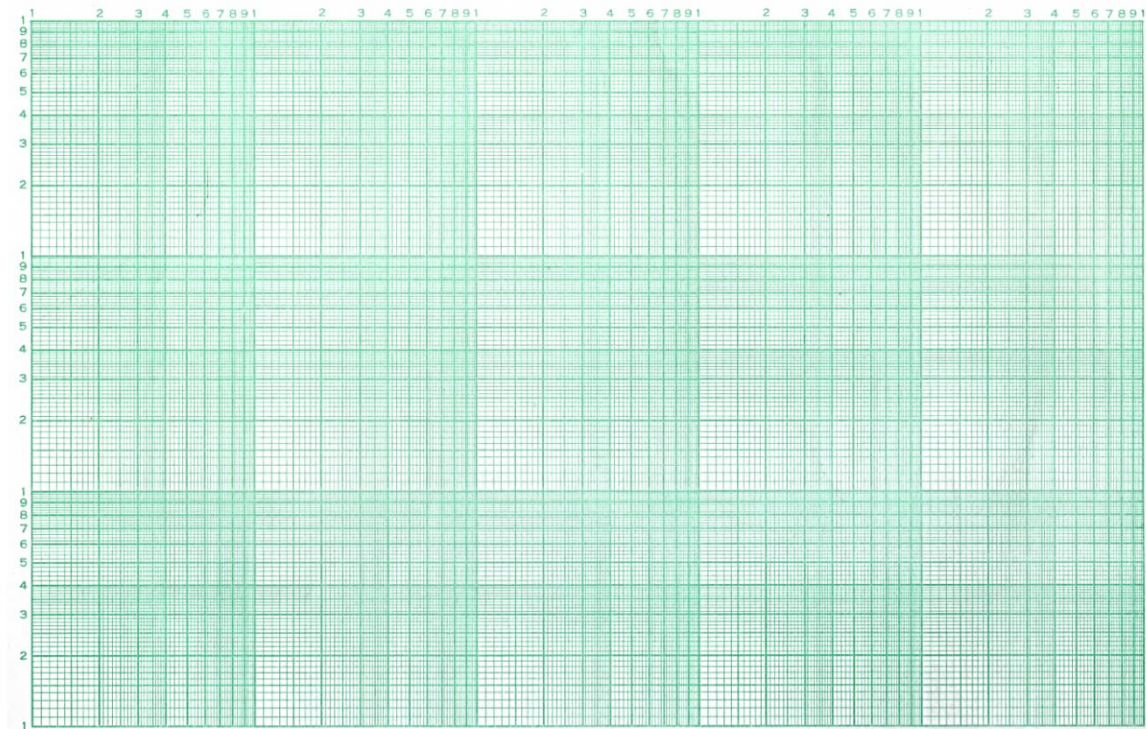
20 Boxes

Box 1 Samples of Graph Paper for Curve Matching Methods

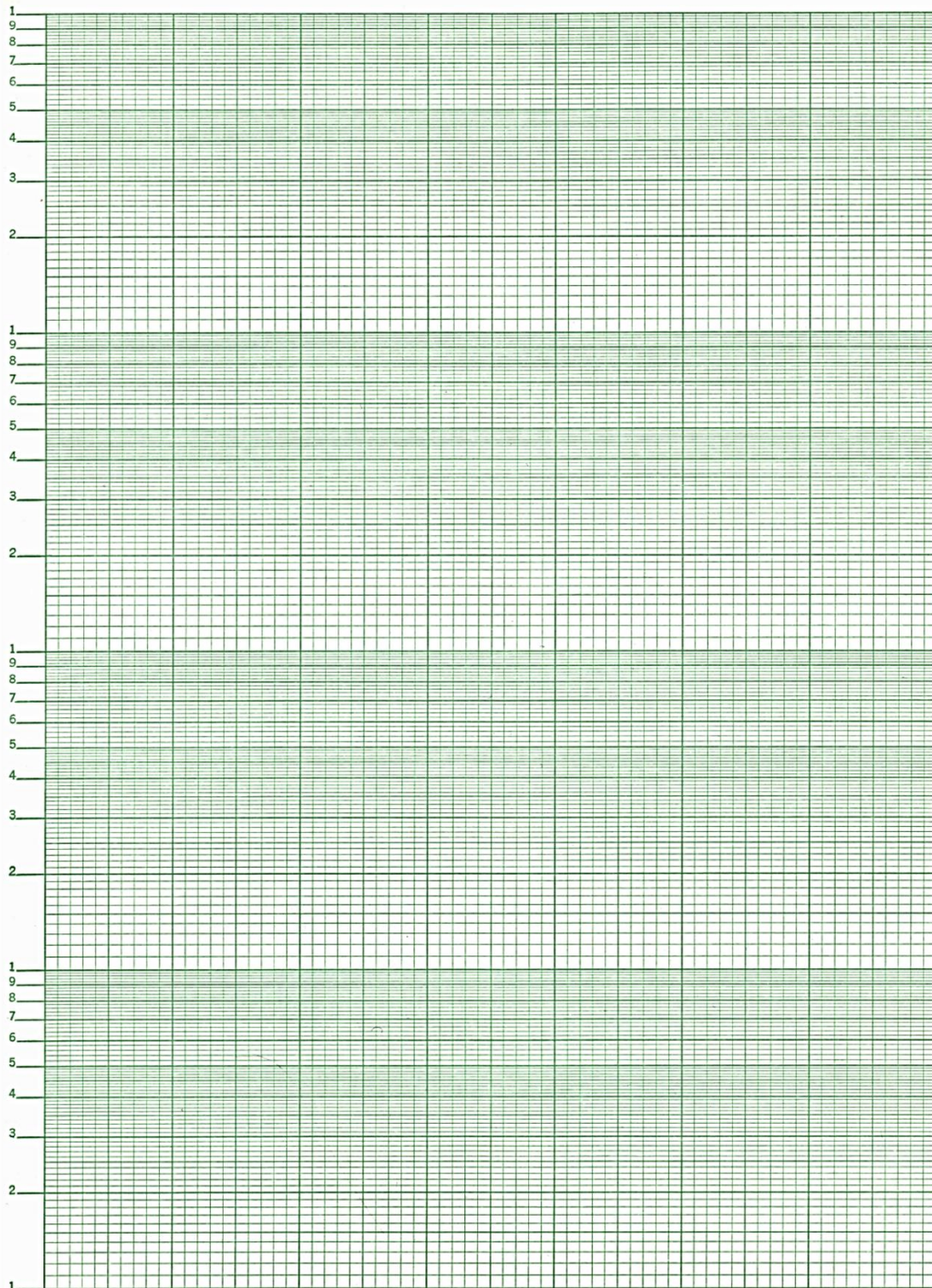
Free printable graph paper can be found at the following link:

<https://www.thoughtco.com/free-printable-graph-paper-608952>.

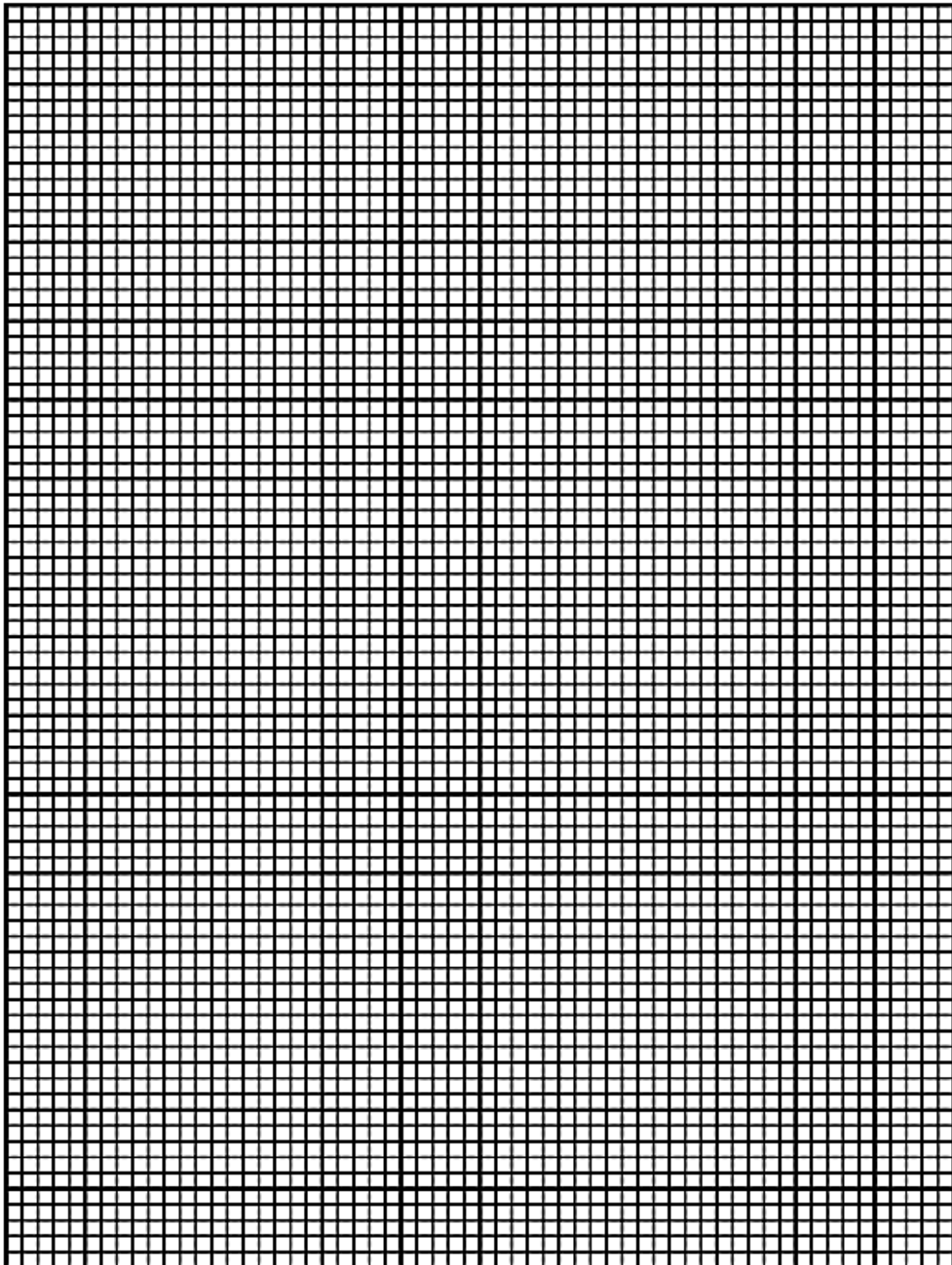
Log-log Graph paper



Semi-log paper



Arithmetic graph paper



[Return to where text linked to Box 1](#) ↗

Box 2 Estimating Storativity and Specific Storage (S_s)

Saturated geologic materials both transmit and store water. The storage capacity is defined by storativity. Excerpts from Woessner and Poeter (2020) that pertain to defining storativity and specific storage for unconfined and confined water bearing units are reproduced here for the reader’s convenience. Tables of values are also provided in this Box.

Unconfined Aquifer Storativity

The storativity for an unconfined aquifer is dominated by the gravity drainage term, specific yield (S_y). Specific yield reflects the volume of water that drains by gravity when the water table is lowered or fills with water when the water table is raised (Figure Box 2-1). The storativity (S) of an unconfined aquifer is composed of two components as shown in Equation Box 2-1.

$$S_{unconfined} = S_y + S_s b_{average} \tag{Box 2-1}$$

where:

$S_{unconfined}$ = storativity of an unconfined aquifer (dimensionless)

S_y = specific yield (dimensionless)

S_s = specific storage (L^{-1})

$b_{average}$ = average thickness before and after a water level change (L)

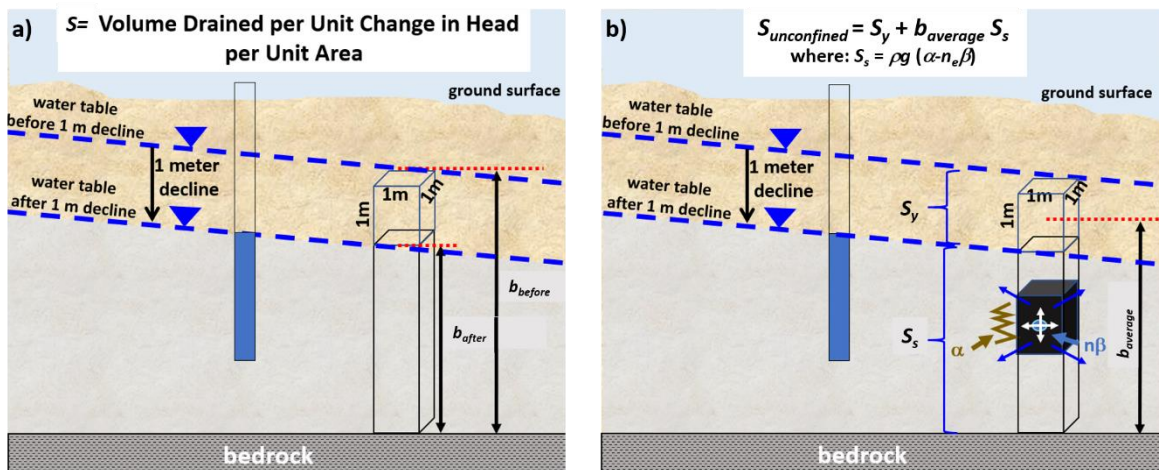


Figure Box 2-1 - Schematic of components of storativity (S) of an unconfined aquifer. a) Illustration of the definition of the storage coefficient, which is the volume of water released or added to storage per unit change in head normal to the earth’s surface per unit area. b) As the water table is lowered 1 meter, the volume of water released per cubic meter of unconfined aquifer is almost entirely accounted for by water that drains from pores as described by specific yield, S_y . The portion of the aquifer that underlies the drained portion also yields a small quantity of water (small blue arrows in black volume) in response to the reduced weight (water drained) of overlying water. The structure of the solids (black volume) compresses (reducing the volume of pore space) as indicated by the compressibility of the aquifer skeleton, α , (jagged vertical line). In addition, there is a small expansion of the slightly compressible water, $n\beta$, (blue dot and white arrows). This property of the aquifer is called specific storage, S_s . The volume of water released from gravity drainage is orders of magnitude larger than the volume squeezed from the saturated portion of the aquifer, $S_s b_{average}$. As a result, S_y is used to represent unconfined aquifer storativity (Woessner & Poeter, 2020; gw-project.org).

The specific yield is the volume of water that can drain by gravity from a saturated volume of material divided by the total volume of that material. The fractional volume of water that remains in the sample is called specific retention (S_r). It is assumed that, when water is added to storage and the water table rises, the pore spaces that fill already contain only the volume of water indicated by the value of specific retention.

The second term of Equation Box 2-1 is the product of the specific storage (S_s) and the average of saturated thickness before and after drainage ($b_{average}$). The specific storage is defined as the volume of water that is released from (or added to) storage per unit volume of saturated material. When multiplied by the saturated thickness it accounts for a small amount of water that is released from a unit area of aquifer in response to the relief of stress on the material below the drained pores. It is usually orders of magnitude smaller than the specific yield and is ignored when characterizing storage properties of unconfined systems (Woessner & Poeter, 2020). Table 3 in Woessner and Poeter (2020) is reproduced here to provide estimates of S_y for range of earth materials (Table Box 2-1).

Table Box 2-1 - Summary of specific yield values of common earth materials compiled by Morris and Johnson (1967) with additional data from Rivera (2014), Freeze and Cherry (1979), and Domenico and Schwartz (1998) (from Woessner & Poeter, 2020). "NA" represents not available.

Measurements of Specific Yield for Some Common Earth Materials (Percent)		
Material	Number of Samples	Range of Specific Yield Percent
Unconsolidated Sediments		
Clay	27	1 - 18
Silt	299	1 - 40
Loess	5	14 - 22
Eolian sand	14	32 - 47
Sand (fine)	287	1 - 46
Sand (medium)	297	16 - 46
Sand (coarse)	143	18 - 43
Gravel (fine)	33	13 - 40
Gravel (medium)	13	17 - 44
Gravel (coarse)	9	13 - 25
Consolidated Sediments		
Shale	NA	0.5 - 5
Siltstone	13	1 - 33
Sandstone (fine-grained)	47	2 - 40
Sandstone (medium-grained)	10	12 - 41
Limestone and dolomite	32	0 - 36
Karstic limestone	NA	2 - 15
Igneous and Metamorphic Rocks		
Fresh granite and gneiss	NA	<0.1
Weathered granite/gneiss	NA	0.5 - 5
Fractured basalt	NA	2 - 10
Vesicular basalt	NA	5 - 15
Tuff	90	2 - 47

Confined Storativity and Specific Storage

Confined systems remain saturated as the potentiometric surface rises and falls. No gravity drainage occurs. Storativity of a confined system is composed of the water released by the compression and expansion of the unit framework and stored water (Figure Box 2-2). The following material is reproduced from Woessner and Poeter (2020).

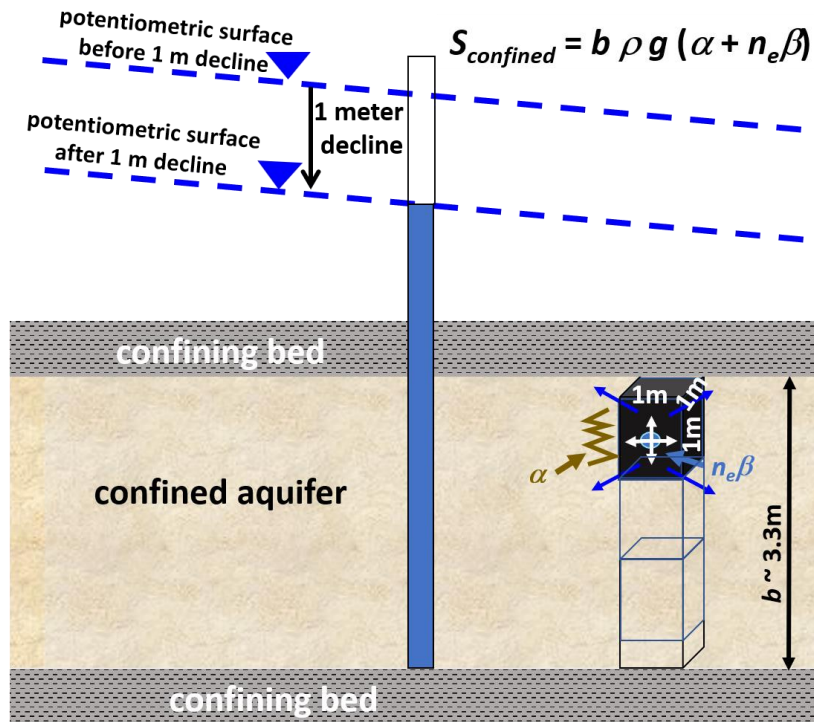


Figure Box 2-2 - Schematic of the parameters controlling storativity, S , of a confined aquifer. The aquifer remains fully saturated as a unit change in the potentiometric surface occurs. Water is released from the entire saturated thickness, b , of the aquifer by compression of the skeleton, α (jagged line) and expansion of the pore water (blue arrows), $n_e\beta$ (Woessner & Poeter, 2020; gw-project.org).

When water is released from or added to storage the saturated geologic material either expands or contracts (changes in the effective stress (grain to grain) and/or the water expands or contracts (changes in the pore water pressure). The storativity is defined as representing the volume of water released from or entered storage per unit change in head normal to the surface, per unit area. As the aquifer remains saturated no water gravity drains from the formation.

The confined storativity is defined as the specific storage multiplied by the unit’s saturated thickness (Equation Box 2-2).

$$S_{confined} = S_s b = b \rho g (\alpha + n_e \beta) \tag{Box 2-2}$$

where:

- $S_{confined}$ = storativity of an unconfined aquifer (dimensionless)
- S_s = specific storage (L^{-1})
- b = unit saturated thickness (L)
- d = density of water (ML^{-3})
- g = acceleration due to gravity (LT^{-2})

- a = compressibility of solid matrix (LT^2M^{-1})
 n_e = effective porosity (dimensionless)
 β = compressibility of water (LT^2M^{-1})

The specific storage, S_s , is defined as the volume of water released from or entered storage per unit change in head normal to the surface, per unit volume of material. The difference in the storativity and specific storage term is that storativity includes the storage properties of the entire thickness of the unit and the specific storage describes the properties of a unit volume of the material.

Computing Specific Storage

Equation Box 2-3 is used to compute specific storage when values of the compressibility of the materials making up confined system are measured or estimated from literature values.

$$S_s = \rho g (\alpha + n_e \beta) \quad (\text{Box 2-3})$$

where:

- S_s = specific storage (L^{-1})
 α = compressibility of the material solid structure (LT^2M^{-1})
 n_e = effective porosity (dimensionless)
 β = compressibility of water (LT^2M^{-1})
 ρ = density of water (ML^{-3})
 g = acceleration due to gravity (LT^{-2})

Domenico and Mifflin (1965) presented a table of vertical compressibility, α , for geologic materials. This information can be used with Equation Box 2-3 to compute specific storage for various confined materials. Dunn (2023) reports that the specific storage values can also be computed assuming water is incompressible ($\beta=0$).

Domenico and Mifflin (1965) noted that the specific storage can be approximated by Equations Box 2-4 through Box 2-6. Parameters such as vertical compressibility, the bulk modulus of compression, and coefficient of consolidation are derived from laboratory tests or the literature. Box 9 briefly describes laboratory triaxial and consolidation testing methods used to obtain these parameters.

$$S_s = (a_v \gamma_w) / (1 + e) \quad (\text{Box 2-4})$$

where:

S_s = specific storage (L^{-1})

α = compressibility of the material solid structure (LT^2M^{-1})

γ_w = specific weight of water ($ML^{-2}T^{-2}$)

e = void ratio (dimensionless)

$$S_s = \gamma_w / E_c \quad (\text{Box 2-5})$$

where:

S_s = specific storage (L^{-1})

γ_w = specific weight of water ($ML^{-2}T^{-2}$)

E_c = bulk modulus of compression ($ML^{-1}T^{-2}$)

$$S_s = K_v / c_v \quad (\text{Box 2-6})$$

where:

S_s = specific storage (L^{-1})

K_v = vertical permeability (LT^{-1})

c_v = coefficient of vertical consolidation (L^2T^{-1})

We modified Table 1 of Domenico and Mifflin (1965) to report values of specific storage in units of m^{-1} (Table Box 2-2). Two values of specific storage are shown, one computed assuming water is incompressible and the last column accounting for the compressibility of water, $m_e B$, given an assumed porosity value (Woessner & Poeter, 2020). Table Box 2-2 shows that including the compressibility of water in the calculation of S_s has minimal influence on specific storage values (i.e., differences occur in the 3rd significant figure and beyond). Dunn (2023) also provides a good discussion of specific storage (<https://www.dunnhydrogeo.com/home/aquifer-storativity-t>).

Table Box 2-2 Material properties including, geologic unit skeletal compressibility (α), assumed values of effective porosity (n_e), an assumed value for the specific weight of water γ as $9,810 \text{ kgm}^{-2}\text{s}^{-2}$, and calculated values of S_s with and without consideration of the compressibility of water ($\beta = 4.3 \times 10^{-10} \text{ ms}^2\text{kg}^{-1}$). Porosity values are based on material type and have little effect on the calculation of S_s due to the low compressibility of water (modified from Domenico & Mifflin (1965) and Dunn (2023) at the website: <https://www.dunnhydrogeo.com/home/aquifer-storativity-t>).

Material	α range $\text{ms}^2\text{kg}^{-1}$	$S_s = \gamma\alpha$ m^{-1}	Assumed n_e dimensionless	$S_s = \gamma(\alpha+n_e\beta)$ m^{-1}
Plastic Clay	2.0×10^{-6}	1.96×10^{-2}	0.6	1.96×10^{-2}
	2.5×10^{-7}	2.45×10^{-3}	0.6	2.46×10^{-3}
Stiff Clay	2.5×10^{-7}	2.45×10^{-3}	0.5	2.45×10^{-3}
	1.3×10^{-7}	1.28×10^{-3}	0.5	1.28×10^{-3}
Medium Hard Clay	1.3×10^{-7}	1.28×10^{-3}	0.4	1.28×10^{-3}
	6.8×10^{-8}	6.67×10^{-4}	0.4	6.69×10^{-4}
Loose Sand	1.0×10^{-7}	9.81×10^{-4}	0.35	9.82×10^{-4}
	5.1×10^{-8}	5.00×10^{-4}	0.35	5.02×10^{-4}
Dense Sand	2.0×10^{-8}	1.96×10^{-4}	0.3	1.97×10^{-4}
	1.3×10^{-8}	1.28×10^{-4}	0.3	1.29×10^{-4}
Dense Sandy Gravel	1.0×10^{-8}	9.81×10^{-5}	0.15	9.87×10^{-5}
	5.1×10^{-9}	5.00×10^{-5}	0.15	5.07×10^{-5}
Rock fissured/jointed	6.8×10^{-9}	6.67×10^{-5}	0.01	6.68×10^{-5}
	3.3×10^{-10}	3.24×10^{-6}	0.01	3.28×10^{-6}
Rock sound	3.3×10^{-10}	3.24×10^{-6}	0.0001	3.24×10^{-6}

Another common method used to estimate S for confined aquifers was proposed by Lohman (1972). He noted that storativity of confined aquifers typically range from 0.00001 to 0.001 (1×10^{-5} to 1×10^{-3}). He suggests the storativity for a confined aquifer can be approximated as $0.000003/\text{m}$ times the aquifer thickness in meters. This approximation basically results in using $0.000003/\text{m}$ as an estimate of the specific storage for all confined earth materials. Using his approach, estimated storativity values are in the 10^{-5} to 10^{-4} range when the thickness of rock based confined systems are 10's to 100's of meters. Lohman's (1972) approach provides a poor estimate of specific storage when aquifer or aquitard materials are something other than hard rock. Thus, specific storage estimates based on Table Box 2-2 should be used with aquifer thicknesses to estimate storativity values for confined systems when pumping test computed values are not available.

[Return to where text first links to Box 2](#) ↑

Box 3 Image Well Theory Application when Two Linear Boundaries are Present.

Ferris and others (1962) present an example that shows how a single image well is not adequate to represent a setting with more than one linear boundary. The authors illustrate that an unconfined system bounded by a linear impermeable boundary and recharge boundary (fully penetrating perennial stream) requires a complex set of image wells to represent the cone of depression that would result from pumping a single well (Figure Box 3-1).

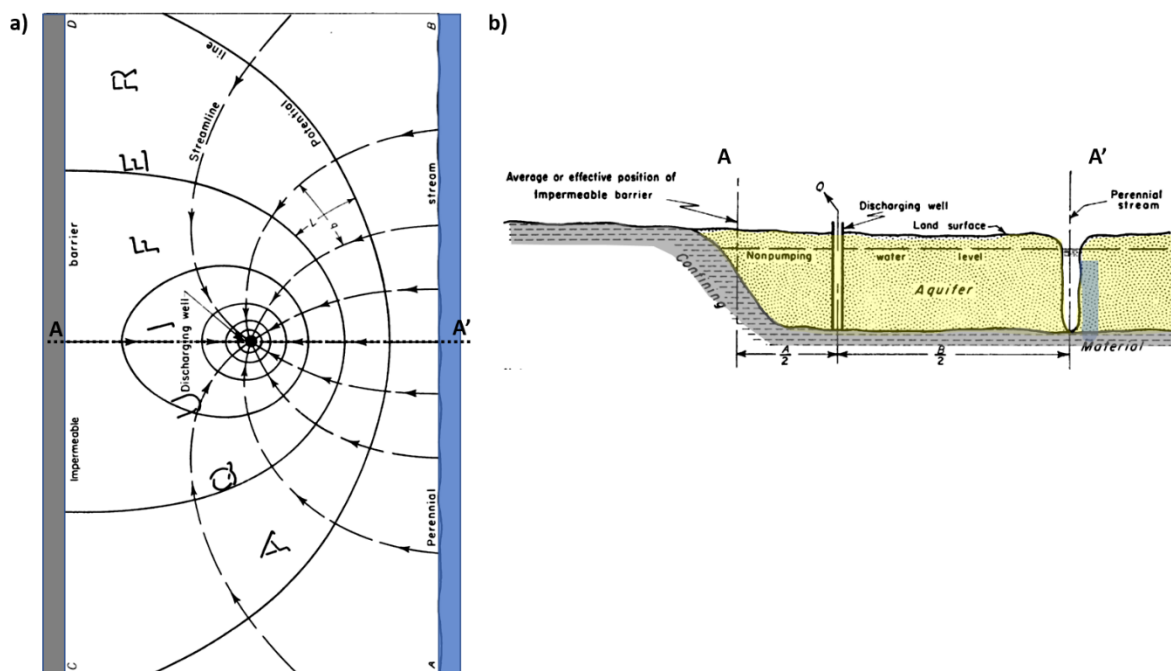


Figure Box 3-1 - Schematic showing a map view and a cross-sectional view of an unconfined system bounded by a linear impermeable boundary and a parallel recharge boundary. a) A map view with groundwater flow lines and contours of water levels resulting from pumping a single well at a constant rate. Dashed arrows show groundwater flow and solid lines are water table elevation contours decreasing towards the well. b) Schematic cross section (A-A') of site conditions showing the location of a pumping well and the relation of the boundary conditions (modified from Ferris et al., 1962).

The setting depicted in Figure Box 3-1 would seem to be straightforward as illustrated in the image well discussion in Section 11. However, the placement of initial image wells on each side of the two boundaries creates a more complex analysis. The image wells do not just interact with one boundary but affect both boundaries. For example, the pumping image well to the left of the impermeable boundary will affect the representation of the recharge boundary to the right. As one might guess, the presence of the injection image well to the right of the recharge boundary will also influence the impermeable boundary representation. Ferris and others (1962) explain that multiple appropriately spaced image wells are required to properly represent the final cone of depression for this two-boundary setting. Ferris and others (1962) discuss this condition and other multiple-boundary systems in their publication. Figure Box 3-2a is from their publication

and explains how the image wells were placed. This is illustrated in more detail in Figure Box 3-2b. When an impermeable barrier is present, image wells representing the effect of the barrier must have the same sign for Q as the Q of the field well it reflects. When a recharge boundary is being represented by an image well it must have the opposite sign as Q for the field well. Thus, to represent a recharge boundary for a pumping well, the image well is an injection well which, mathematically, provides water that flows across the boundary. To represent a recharge boundary for an injection well, the image well is a pumping well which, mathematically, receives water that flows across the boundary representing the injected fluid flowing out to the feature that the boundary represented. This sounds complicated but is illustrated in Figure Box 3-2. Ferris and others (1962) point out that, in theory, these combinations of image wells would extend to infinity. However, as the distance of the image wells from the boundaries increases the magnitude of their influence decreases and is less and less significant to the composite drawdown/drawup. For each image well the influence on the bounded water-bearing unit and drawdown caused by the field well is additive, and the resulting cone of depression is a composite of all the calculated drawdowns within the cone.

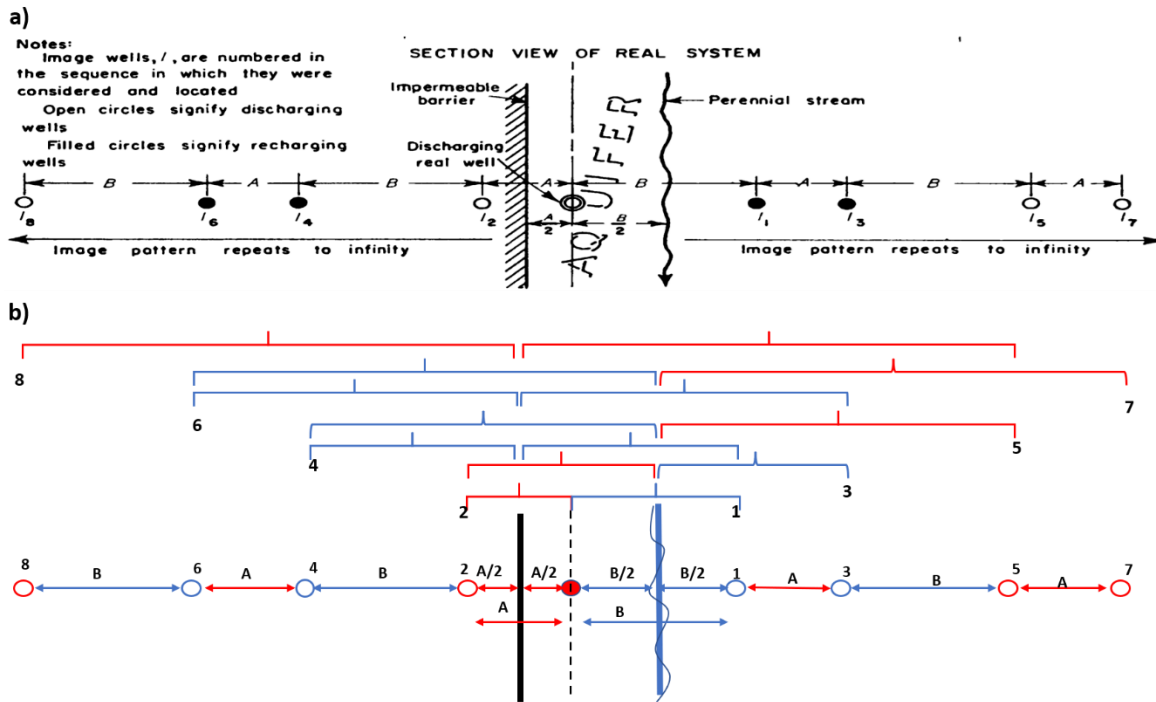


Figure Box 3-2 - Schematic of a map view of a pumping well bounded by both an extensive linear impermeable boundary and an extensive linear recharge boundary (Figure Box 3-1). a) Ferris and others (1962) representation of the location and type of image wells needed to generate a composite data set to construct a cone of depression for a specified time. They note that for this geometry the pattern of image wells repeats from what is shown and theoretically extends to infinity. b) An interpretation of how the image wells were located. A and B are the spacing of the initial image wells from the boundaries. Blue arrows, brackets and open circles are representative of recharge (injection) image wells. Red arrows, brackets and red open circles are representative of impermeable boundary image wells (pumping). Image well 1 is an injection well that has a reverse sign on Q from the pumping well to represent the recharge boundary. Image well 2 is a pumping well that has the same sign as Q of the pumping well to represent the impermeable boundary. Image well 3 represents the reflection of image well 2 across the recharge boundary thus it has the opposite sign on Q as compared to image well 2. Image well 4 represents the reflection of image well 1 across the impermeable boundary thus it has the same sign on Q as compared to image well 1. Image well 5 represents the effect of the recharge boundary on image well 4 so it has opposite sign on Q as image well 4. Image well 6 represents the effect of the impermeable boundary on image well 5 so it has the same Q as image well 5. Image well 7 represents the reflection of image well 6 across the recharge boundary so it has the opposite sign. Image well 8 represents the reflection of image well 7 across the impermeable boundary so it has the same sign. The addition of image wells continues to infinity but soon they are far enough from the physical area between the impermeable and recharge boundaries that the additional drawdown is insignificant (modified from Ferris et al., 1962).

[Return to where text linked to Box 3](#) ↑

Box 4 Production Well Efficiency

Forecasting drawdown at the pumping well assumes no additional head loss occurs as the water enters the well. This is usually not the case, so drawdown measured in the pumping well is usually greater than the theoretical values computed from the well hydraulics analytical equations. One factor effecting the pumping water well could be partial penetration of the screen and the resulting longer vertical flow paths. When there is head loss due to partial penetration (i.e., the well penetrates less than 80 percent of the aquifer) the difference between the theoretical pumping level and the observed level is referred to as well loss (Figure Box 4-1). Additional head loss occurs when groundwater flows through the damaged formation near the well and through the perforated or screened casing at high velocity causing turbulent flow.

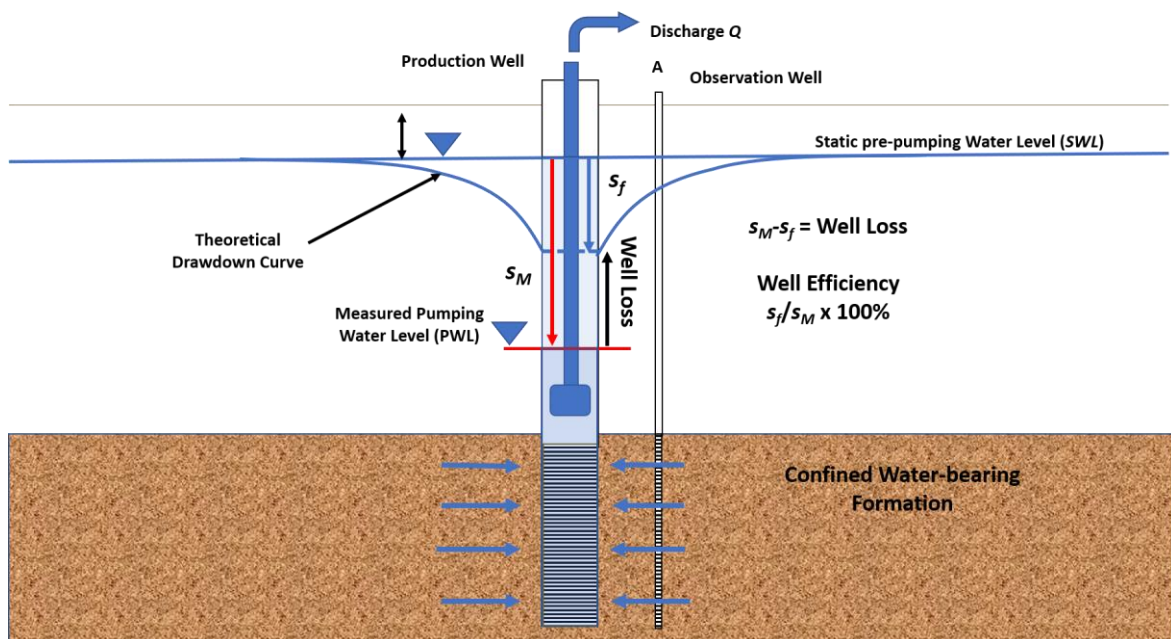


Figure Box 4-1 - Comparison of the measured pumping well drawdown (s_M) and the computed theoretical formational drawdown (s_f) for a fully penetrating well. The difference between the measured drawdown and the theoretical drawdown is the well loss. The production well efficiency is computed by multiplying the ratio of s_f/s_M by 100 percent. Most production wells are less than 100 percent efficient because high velocities and turbulent flow in the area associated with the screened or perforated casing cause additional head loss during pumping.

The ratio of the theoretical drawdown to the actual measured drawdown is a measure of the pumping well efficiency (E) as shown in Equation Box 4-1.

$$E = \frac{s_{theoretical\ formational}}{s_{measured}} 100\ percent \quad (\text{Box 4-1})$$

The theoretical drawdown in the pumping well can be computed using analytical well hydraulics equations where the radial distance is set equal to the well radius. The computed head does not account for well loss, so the computed theoretical drawdown represents a 100 percent efficient well.

When aquifers behave as totally confined, a second method can be used to determine the theoretical drawdown in the pumping well. This distance-drawdown method projects the cone of depression represented by a semi-log plot of observation well drawdowns—which are not pumped so are 100 percent efficient—for a fixed time at various distances from the pumping well to the radius of the production well (Figure Box 4-2). The projected theoretical drawdown is then compared to the actual measured pumping well drawdown to compute the well efficiency (Equation Box 4-1). Once the well efficiency is determined, the pumping well drawdown data can be corrected for the well loss (Figure Box 4-1) and the corrected drawdown obtained can be used for analysis because it meets the simplifying assumptions.

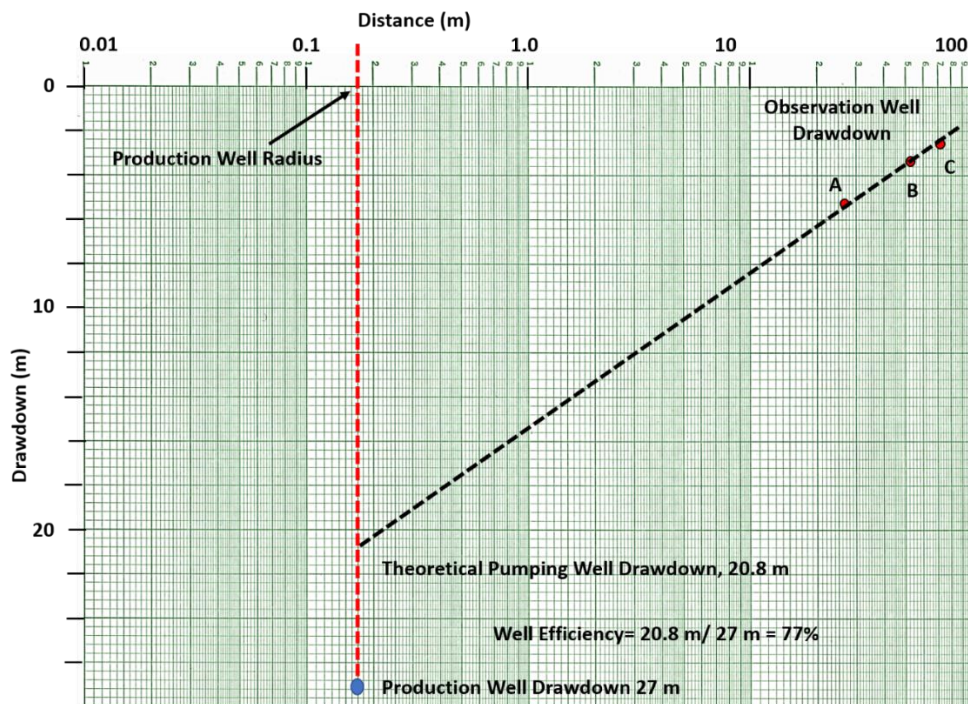


Figure Box 4-2 - A distance-drawdown method used to determine well efficiency and the theoretical pumping well drawdown when hydraulic testing a totally confined aquifer that is consistent with the Theis model. A semi-log distance-drawdown plot where A, B and C are observation well measurements of drawdown at various radial distances collected at the same time (e.g., 100 min). The dashed black line represents a projection of the logarithmic cone of depression to the radius of the pumping well which is indicated by the red dashed line at 0.17 m. The intersection of the two dashed lines is the theoretical pumping well drawdown caused by formational properties at the specified time. The difference between the actual pumping well drawdown at 100 min (blue dot) and the theoretical drawdown is used to determine the production well efficiency reported here as 0.77 multiplied by 100 percent = 77 %.

A third method to determine well efficiency is to analyze the time-drawdown results of a step-drawdown test of the production well as discussed in Section 12. The step test compares drawdown in the production well at various pumping rates maintained for specified periods of time and the data are used to compute production well loss (Sterrett, 2007).

[Return to where text linked to Box 4 ↑](#)

Box 5 AQTESOLV

AQTESOLV V4.5 (aqtesolv.com) provides multiple methods to analyze hydraulic tests for confined, leaky confined, unconfined, and fractured aquifers as described in Figure 99 of Section 13.1 of this book. Automatic curve matching executes a nonlinear weighted least-squares parameter estimation method that includes singular value decomposition. Statistical analyses of the fit between the data and the theoretical curve are provided (e.g., residual plots and standard error analysis).

When curve matching, the author recommends getting close to the parameter values by initially matching the field data with a Cooper-Jacob straight-line analysis. Once approximate values of T and S are generated, a more appropriate model that represents the actual aquifer conditions is selected. An example of automatic curve matching is presented in Figure Box 5-1 showing both the type curve and derivative curve.

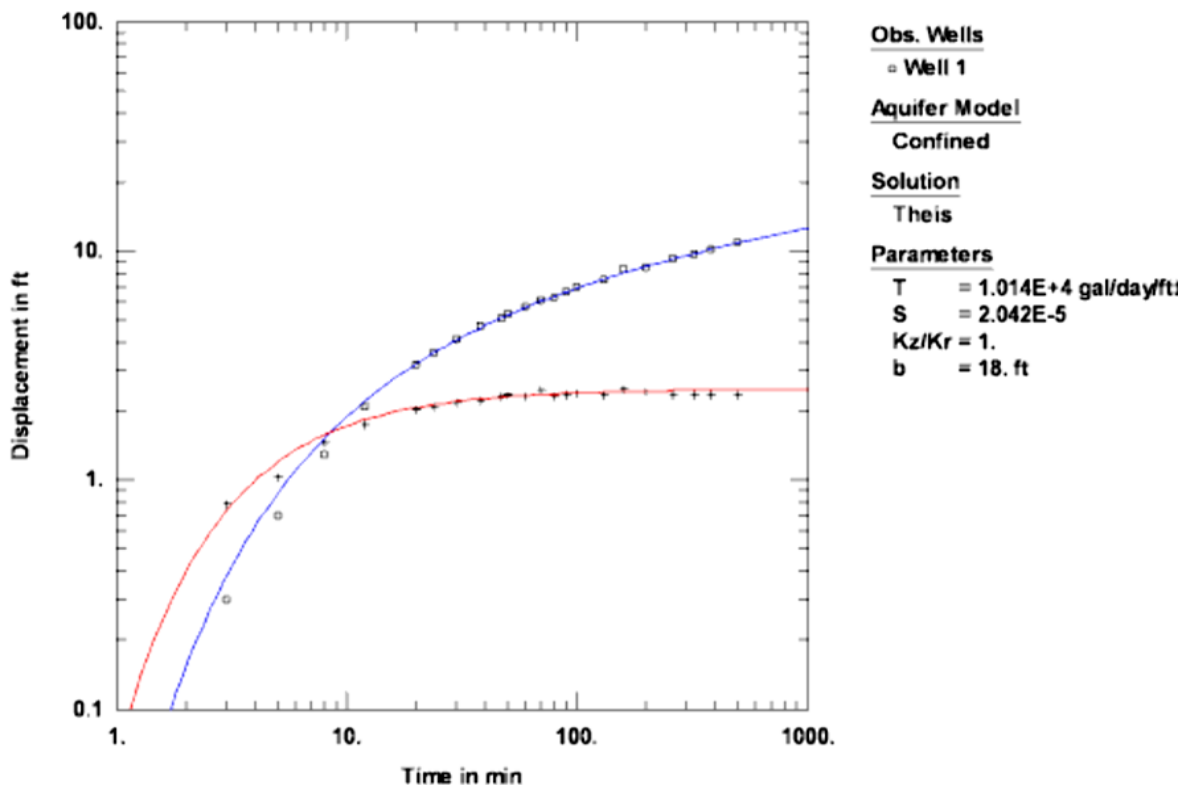


Figure Box 5-1 - Example of the match of a drawdown (displacement on the y axis) versus time curve (open squares) for observation well 1 with the Theis type curve (blue line). The derivative curve for the field data (plus signs) and type curve for the derivative (red curve) are also shown. T is in units of gallons/day/foot, the anisotropy ratio is 1 and the thickness of the pumped aquifer (b) is 18 ft (from the AQTESOLV V4.5 User's Guide, 2004–2007; aqtesolve.com).

A second example of matching field data is illustrated for a leaky confined aquifer using the Hantush-Jacob equation that considers water leakage to the confined unit by vertical flow through a confining bed from an overlying groundwater source (Figure Box 5-2).

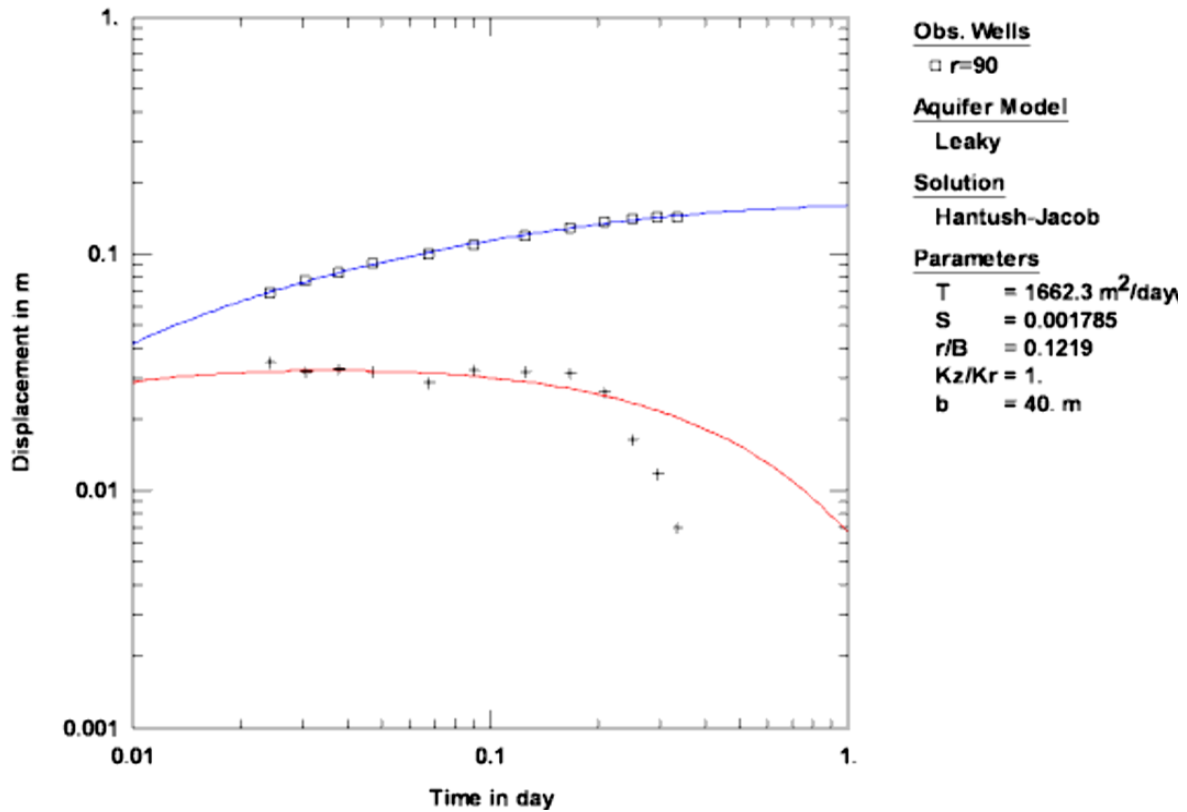


Figure Box 5-2 - Example of an automatic curve match of observation well data finished in a leaky confined aquifer to a theoretical Hantush-Jacob curve. The blue line is the type curve match, and the red line is the time-drawdown derivative match to the type curve derivative data. The Hantush-Jacob model was used to determine *T* and *S* values. A second fit was attempted using the Hantush model, however, an analysis of the standard error suggested the Hantush model fit had greater uncertainty. Values of *T* in m²/d, *S*, and *r/B* are derived. *r/B* is $r/(T(K'b)^{0.5})$ where *K'* is the vertical hydraulic conductivity of the confining bed and *b'* is the confining bed thickness. The pumped aquifer has an anisotropy ratio of 1 and the aquifer thickness (*b*) is 40 m (from the AQTESOLV V4.5 User's Guide, 2004–2007; aqtesolv.com↗).

The AQTESOLV V4.5 User's Guide (2004–2007) provides an additional source of information and examples. Videos produced to demonstrate how the program can be used are available on the internet and some are referenced on the 2023 website (aqtesolv.com↗). The software developer recommends going directly to the website for information on the capabilities and applications (aqtesolv.com↗).

[Return to where text linked to Box 5](#)↑

Box 6 AquiferTest V12

AquiferTest V12 is a hydraulic test analysis tool developed by Waterloo Hydrogeologic. Details on its capabilities and limitations are explained on the website (waterloohydrogeologic.com) and in the accompanying user's manual (<https://www.waterloohydrogeologic.com/help/aquifertest/>).

AquiferTest V12 provides multiple methods to analyze hydraulic tests for confined, leaky confined, unconfined, dual porosity, and bounded aquifers (recharge boundary and barrier boundary) as delineated in Figure Box 6-1. It can also account for aquifer anisotropy, well effects such as partial penetration, well bore storage, and variable pumping rates. It includes the capability to set up a pumping well and forecast the resulting response at observation wells located in the same hydrogeologic formation. It breaks analysis into two groups:

- the fixed analysis assumption applies methods as originally published without the option to adjust standard assumptions, and
- customized analyses that allow modification of initial conditions as shown in Figure Box 6-1.

Fixed Analysis Without Adjustment of Model Assumptions

- Theis Recovery (1935)
- Cooper-Jacob Type I (Time Drawdown) (1946)
- Cooper-Jacob Type II (Distance-Drawdown) (1946)
- Cooper-Jacob Type III (Time-Distance-Drawdown) (1946)

Allow Adjustment of Model Assumptions

- Theis (1935)
- Hantush-Jacob (Walton) (1955)
- Neuman (1975)
- Theis with Jacob Correction (1944)
- Warren-Root Double Porosity (Fracture Flow) (1963)
- Papadopulos-Cooper (1967)
- Agarwal Recovery (1970)
- Moench Fracture Flow (1984)
- Hantush with storage (1960)
- Neuman-Witherspoon (1969)
- Agarwal Skin Effects (1970)^{PRO}
- Multi-Layer-Aquifer (Hemker & Maas, 1999)^{PRO}
- Horizontal Wells (Clonts and Ramey, 1986)^{PRO}

Figure Box 6-1 - List of type curve analytical methods that are provided in the AquiferTest V12 software. The analysis techniques that are termed fixed do not allow the user to modify assumptions, thus are standard Theis Curve Matching and Cooper-Jacob straight-line methods. The list of methods that allow model assumption adjustments use formulations that include conditions like well bore storage, partial penetration, well loss effects, variable pumping rates and schedules, and boundaries. The PRO in the last three models indicate they are included in an upgraded version of the software referred to as AquiferTest 12 Pro. Complete references are found in the reference section of this book. Details of these methods are found in the user's manual/help file <https://www.waterloohydrogeologic.com/help/aquifertest/>.

To assist the user in identifying the aquifer conditions that are represented by the observed drawdown data, AquiferTest V12 uses diagnostic plots as shown in Figure Box 6-2.

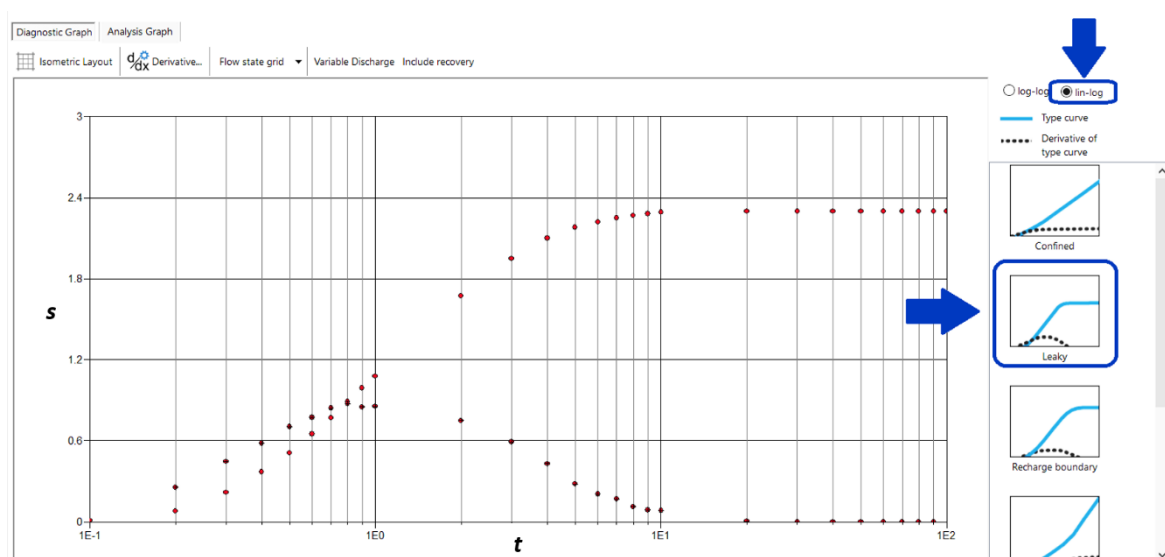


Figure Box 6-2 - A diagnostic plot of observation well or pumping well drawdown versus time data (red diamonds) on a log-log scale presented in Aquifer Test V12. A second plot is the derivative data (lower curve) ($\Delta s/\Delta \log(t)$). On the right-hand side of the diagram are type curves (blue lines) and derivative plots (black dots) used to compare with the plotted observed data. This analysis is intended to suggest if the observed data are representative of conceptualized hydrogeologic conditions or reflect additional factors affecting the data. This data plot looks similar to the data plot expected for a leaky confined aquifer (from <https://www.waterloohydrogeologic.com/help/aquifertest/>).

The diagnostic plots are used as a visual aid to compare the observed drawdown time data with theoretical type curves. In addition to the standard type curve plots, the derivative of the type curve is plotted. AquiferTest V12 notes that the derivative curves provide an additional set of data to use when curve matching (Figure Box 6-2).

Once the user has selected an appropriate analytical model, automatic curve fitting and manual curve fitting methods can be applied. Fitting methods use the “downhill simplex method” to automatically match the drawdown data with the designated aquifer type (e.g., confined, leaky, unconfined, and dual porosity). The automatic curve matching methodology applies a minimizing algorithm to non-linear functions. User curve matching of drawdown time data and derivative data can be performed using a computer mouse by moving the data curve over the type curve until a visual match is determined. Parameter values are then automatically computed using the appropriate analytical equations.

The curve matching methodology described in this book is the same process that is used in AquiferTest V12. Superposition methods and image wells are used when boundaries, multiple pumping wells, or variable pumping rates occur. Partially penetrating wells are handled using corrections to observed data (Reed, 1980). Step tests can also be analyzed. Examples of the software output are shown in Figures Box 6-3 and Box 6-4.

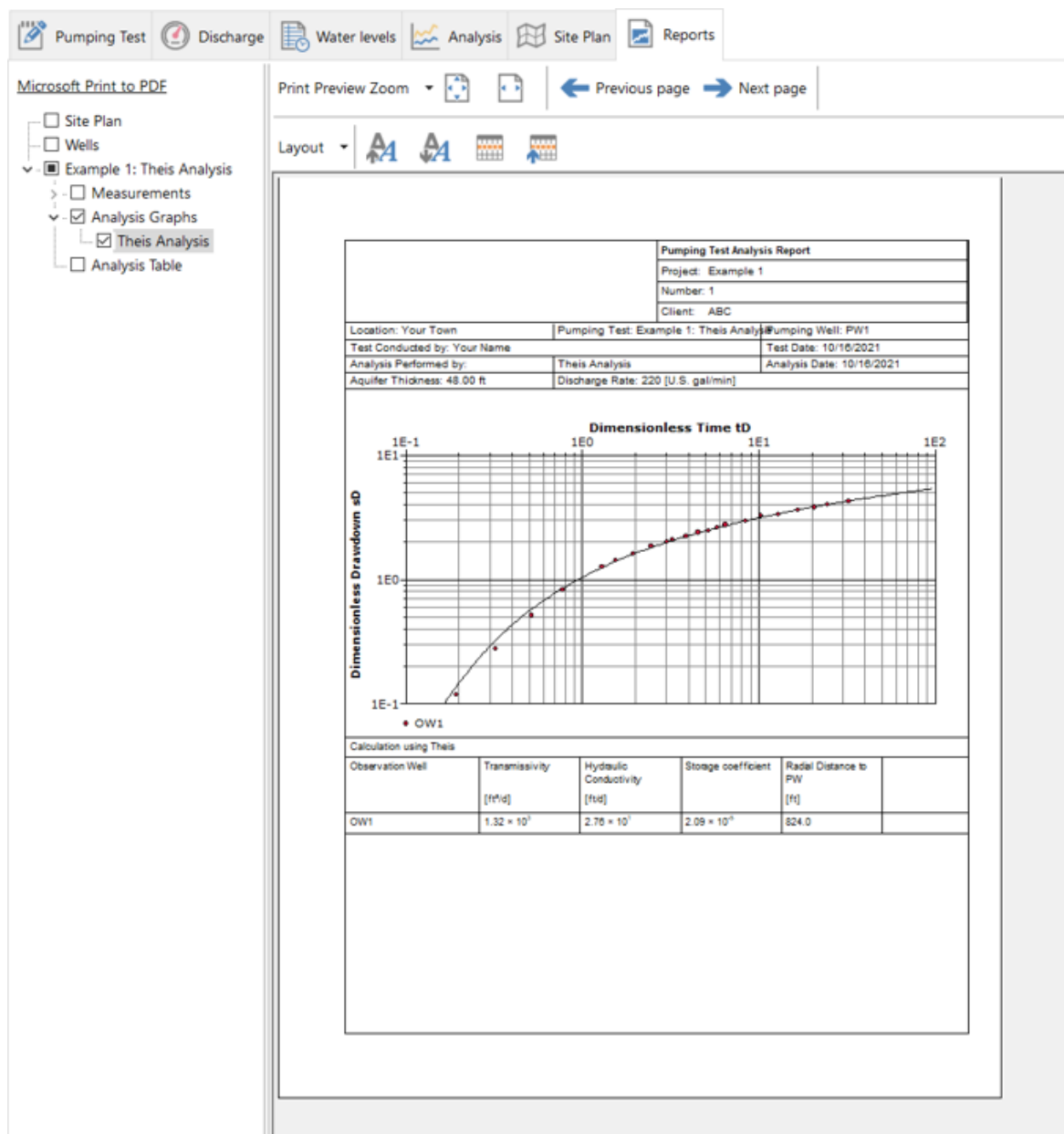


Figure Box 6-3 - Example of test data (red dots) curve match to the Theis solution (black line) using Aquifer Test V12. When the curve match is shown as a single graph the field data axes are referred to as dimensionless. A value of T in ft^2/d , K in ft/d and S are computed.

(from <https://www.waterloohydrogeologic.com/help/aquifertest/>).

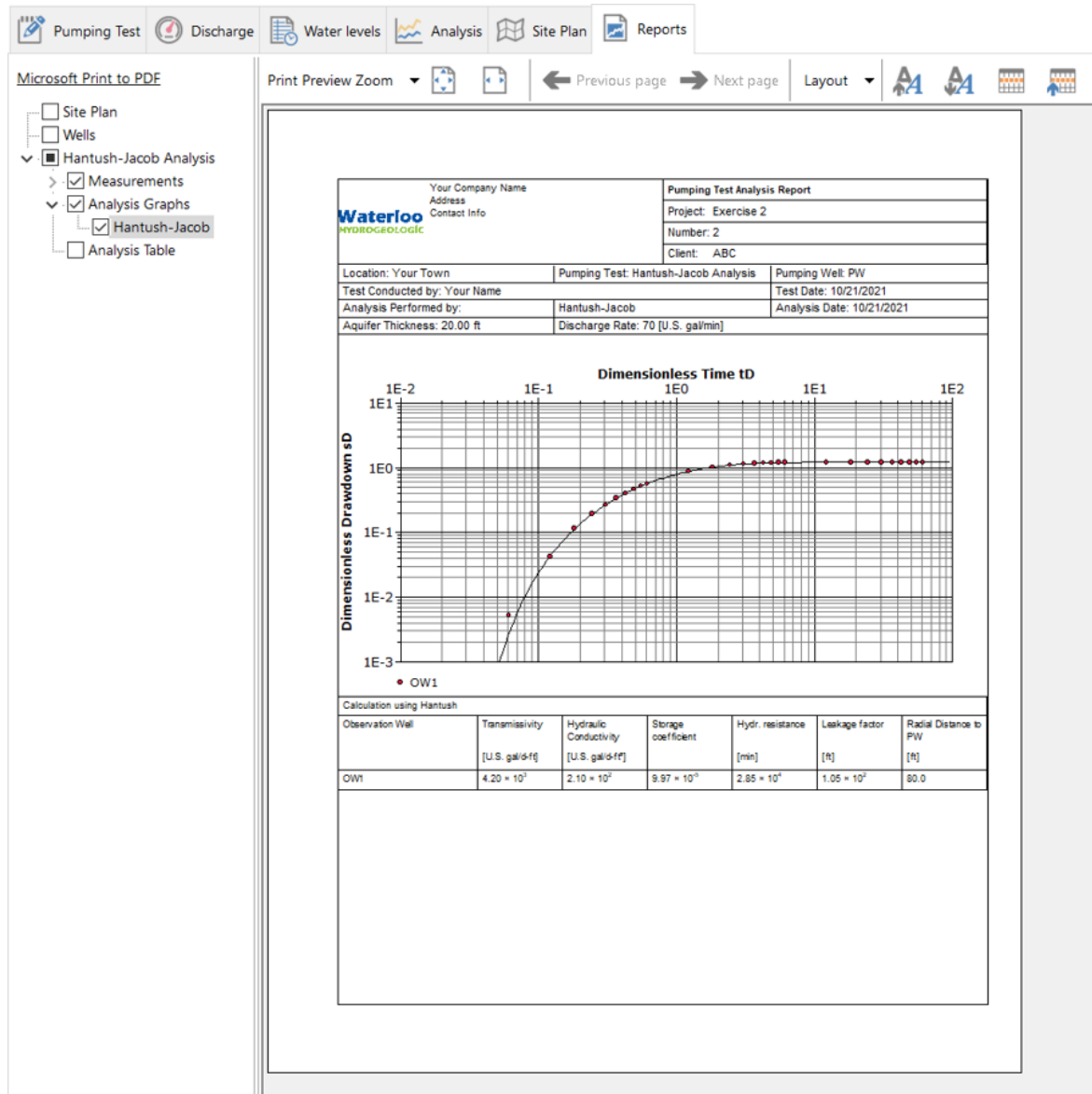


Figure Box 6-4 - Example of test data (red dots) curve match to the Hantush-Jacob solutions solution (black line) using Aquifer Test V12. These are the same data as shown in Figure Box 6-2. When the curve match is shown as a single graph the field data axes are referred to as dimensionless. A value of T in gallons/(ft d), hydraulic conductivity (gallons/ft² d), S , hydraulic resistance ($c = D'/K'$ where D' is the confining bed thickness and K' is the confining bed vertical hydraulic conductivity) in ft/min., and leakage factor ($L = (Tc)^{0.5}$) in feet are computed (from <https://www.waterloohydrogeologic.com/wp-content/uploads/2021/11/AQTHelp.pdf>).

The software also includes methods to analyze well performance including specific capacity data, well loss and well efficiency. AquiferTest V12 allows analyses of drawdown in unpumped aquifers over or underlying the aquifer being pumped using a multi-layer-aquifer-analysis.

The user’s manual is well written (waterloohydrogeologic.com/help/aquifertest/). In addition, videos are available on the internet to assist a user in getting started.

[Return to where text linked to Box 6](#) ↑

Box 7 Aquifer^{Win32} V6

The aquifer test software created by Environmental Simulations, Inc. is Aquifer^{Win32} V6 (www.groundwatermodels.com). This software includes components used to analyze pumping, slug test, and well performance data, and it provides analytic element models to produce theoretical aquifer tests results including contour maps and hydrographs. Aquifer^{Win32} V6 provides analyses using solutions for confined, leaky confined, unconfined, and fractured rock aquifers. It also includes methods to represent partial penetration, variable pumping rates, well bore storage and delayed yield. The analytical equations represented in Aquifer^{Win32} V6 are shown in Figure Box 7-1.

Pumping Test Analyses

Cooper & Jacob, 1946	A generalized graphical method for evaluating formation constants and summarizing well field history. (Cooper Jacob Straight Line Method)
Theis, 1935	Constant discharge from a fully penetrating well in a nonleaky aquifer*
Theis, 1935 (Unconfined)	Constant discharge from a fully penetrating well in a nonleaky aquifer*
Theis, 1946 (Recovery)	Recovery test after constant discharge from a fully penetrating well in a nonleaky aquifer
Hantush, 1961	Constant discharge from a partially penetrating well in a nonleaky aquifer*
Papadopoulos & Cooper, 1967	Constant discharge from a fully penetrating well of finite diameter in a nonleaky aquifer*
Hantush, 1960	Constant discharge from a well in a leaky aquifer with storage of water in the confining beds*
Hantush & Jacob, 1955	Constant discharge from a fully penetrating well in a leaky aquifer*
Hantush, 1964	Constant discharge from a partially penetrating well in a leaky aquifer*
Neuman, 1972	Theory of flow in unconfined aquifers considering delayed response of the water table*
Neuman, 1974	Effects of partial penetration on flow in unconfined aquifers considering delayed aquifer response*
Moench, 1984	Double-Porosity Models for a Fissured Groundwater Reservoir with Fracture Skin*
Moench, 1985	Transient Flow to a Large-Diameter Well in an Aquifer With Storative Semiconfining Layers*
Moench, 1997	Flow to a well of finite diameter in a homogeneous, anisotropic water table aquifer

* Analysis available for use in pump test simulator

Figure Box 7-1 - Analytical models supported in the Aquifer^{Win32} V6 software. Full references are provided in the reference section of this book. The pumping test simulator allows the user to mathematically pump a well in a user determined aquifer type and generate the drawdown at monitoring wells located at various radial distances from the pumping well under transient conditions (from <https://www.groundwatermodels.com>; Environmental Simulations, Inc., 2019).

The aquifer test analyses use both automatic computation and manual curve matching methods. The automatic approach uses the Marquardt (modified Gauss-Newton) nonlinear least-squares technique to generate the best statistical match between a selected type curve (e.g., Theis Equation, Hantush Equation) and the hydraulic test drawdown versus time data. The user’s manual states that the Aquifer^{Win32} V6 approach to analyzing hydraulic testing data is designed to be like the visual curve matching techniques described in typical hydrogeology texts and in this book. It encourages visual adjustment of automatically matched curves using up and down arrows in the program or the computer mouse. Derivative analyses can also be performed. The user’s manual describes the methods to calculate the derivative. Automatic and visual curve matching of the derivative curves are available.

Examples of hydraulic test data matching the Theis (1935) and Hantush (1960) analytical models are presented in Figures Box 7-2 and Box 7-3.

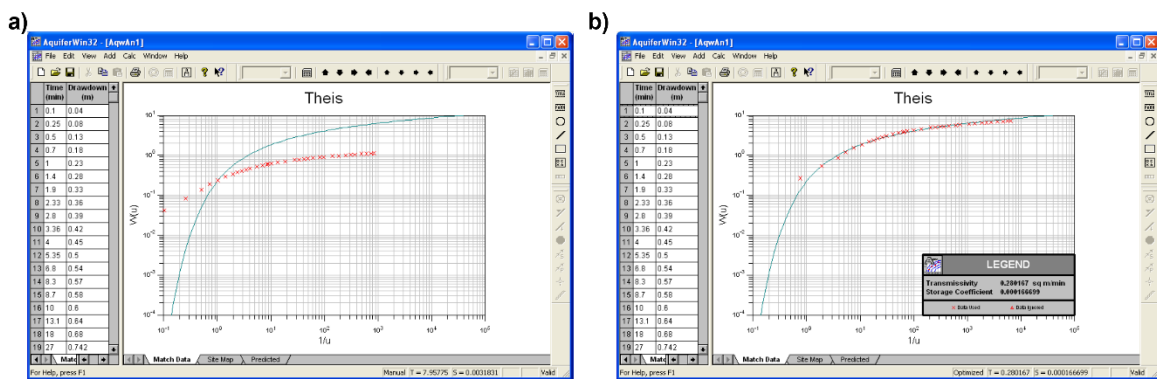


Figure Box 7-2 - Example of drawdown time data (red x) partially shown in the left-hand column with the Theis type curve (blue line) in the Aquifer^{Win32} V6 software. a) The data plotted on the type curve graph before curve matching. b) Data matched by automatic methods and manual adjustment (from Environmental Simulations, Inc., 2019).

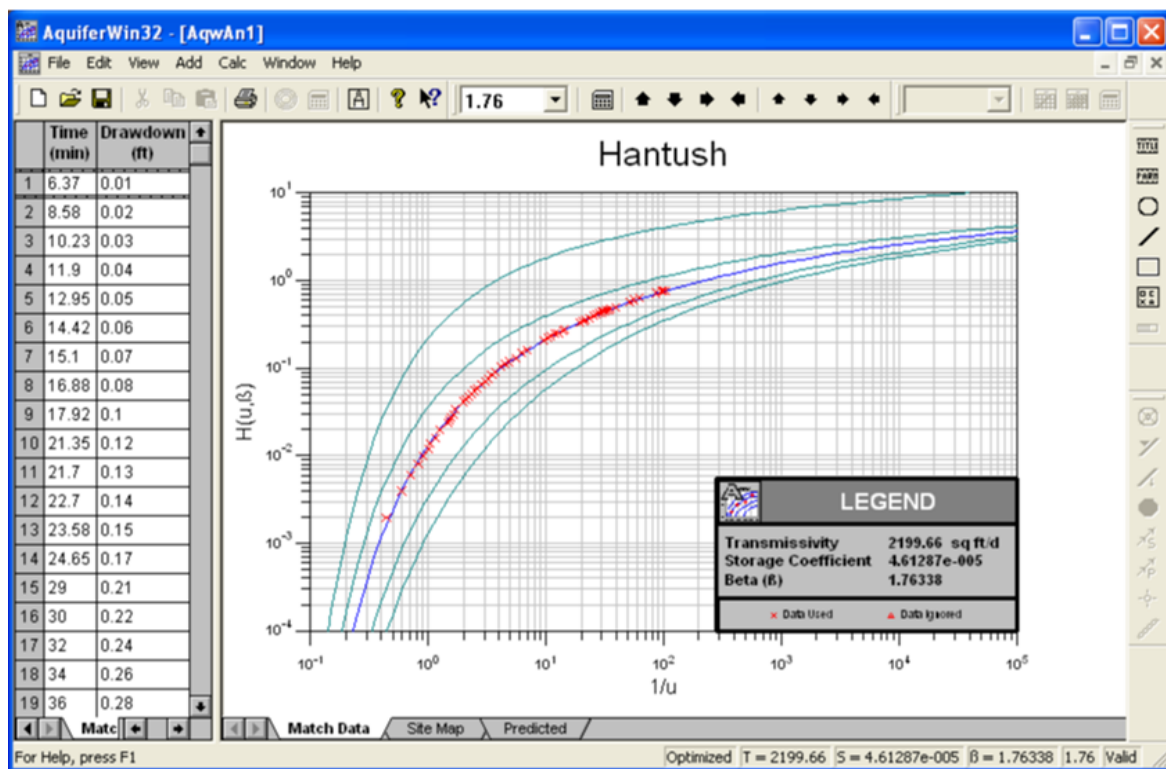


Figure Box 7-3 - Example of time-drawdown data (red x) partially shown in the left-hand column matched to Hantush (1960) type curves using the Aquifer^{Win32} V6 software. Values of *T*, *S* and β are derived. (Environmental Simulations, Inc., 2019).

Another feature of Aquifer^{Win32} V6 is simulation of aquifer tests results. This requires values of *T* and *S* and other related parameters (e.g., *K'*, β), as well as pumping and observation well construction information including the degree of penetration. The program produces a contour map of drawdown for a given pumping rate and time. The time-drawdown curves for an observation well placed at any radial distance from the pumping well can be generated.

The software also includes groundwater modeling capabilities using an analytical element flow model in which analytical equations and image wells can be used to model steady-state groundwater flow. Analytical element modeling is discussed by Haitjema (1995).

[Return to where text linked to Box 7.1](#)

Box 8 Software Used to Analyze Slug Tests

AQTESOLV 4.5 software has the most extensive set of solutions applied to slug test data sets (<http://www.aqtesolv.com/>) as listed in Figure Box 8-1. The reader is referred to the AQTESOLV web site for details of the individual methods and their application.

Slug Tests in Confined Aquifers	Std	Pro
Bouwer-Rice (1976)	✓	✓
Cooper-Bredehoeft-Papadopulos (1967)	✓	✓
Dougherty-Babu (1984)		✓
Hvorslev (1951)	✓	✓
Hyder et al. (1994)/KGS Model		✓
Butler (1998)		✓
Butler-Zhan (2004)		✓
Peres et al. (1989) deconvolution		✓
McElwee-Zenner (1998) nonlinear slug test		✓
Slug Tests in Unconfined Aquifers	Std	Pro
Bouwer-Rice (1976)	✓	✓
Hvorslev (1951)	✓	✓
Dagan (1978)		✓
Hyder et al. (1994)/KGS Model		✓
Springer-Gelhar (1991)		✓
Slug Tests in Fractured Aquifers	Std	Pro
Barker-Black (1984) double-porosity slug test		✓

Figure Box 8-1 - Slug test methods available with the AQTESOLV 4.5 software. Methods available in the standard and pro version of the software are indicated. References for the methods are included in the reference section (of this book Section 19).

The slug test methods addressed in **AquiferTest 12** (Waterloo Hydrogeologic, 2021) are shown in Figure Box 8-2. The AquiferTest 12.0 User's Manual and software help menus provide information on the methods and their application waterloohydrogeologic.com/.

- [Hvorslev Slug Test](#) (Hvorslev, 1951)
- [Bouwer-Rice Slug Test](#) (Bouwer & Rice, 1976) (Bouwer, 1989)
- [Cooper-Bredehoeft-Papadopulos Slug Test](#) (Cooper et al., 1967)
- [High-K Butler](#) (Butler et al., 2000; Butler & Garnett, 2000)
- [Dagan Slug Test](#) (Dagan, 1978)
- [Binkhorst and Robbins effective radius](#) (Brinkhorst & Robbins, 1998)

Figure Box 8-2 - Slug test analytical methods supported by AquiferTest 12. References listed here are included in Section 19 of this book (modified from Waterloo Hydrogeologic, 2021).

Aquifer^{Win32} version 6 software includes the slug test analysis tools as shown in Figure Box 8-3 (Environmental Simulations, Inc., 2019) and can be accessed at groundwatermodels.com/. The Aquifer^{Win32} user’s manual provides more detail and support is available at this [link](#). Once the free trial version is downloaded and installed, a full user’s guide is available under the Help-Help Topics button.

Method	Reference
Hvorslev	Hvorslev, 1951 Time Lag and Soil Permeability in Ground-Water Observations
Bouwer and Rice	Bouwer & Rice, 1976 Slug test for determining hydraulic conductivity of unconfined aquifers with completely or partially penetrating wells
Black	Black, 1978 The use of the slug test in groundwater investigations (Modified Bouwer & Rice unconfined aquifer slug test analysis using an exponential type curve)
Cooper, Bredehoeft, Papadopulos	Cooper, Bredehoeft & Papadopulos, 1967 Response of a Finite-Diameter Well to an Instantaneous Charge of Water
Hyder, Butler, McElwee, Liu	Hyder, Butler, McElwee & Liu, 1994 Slug tests in partially penetrating wells (KGS Model including well skin and monitoring well response)
Kipp	Kipp, 1985 Type Curve Analysis of Inertial Effects in the Response of a Well to a Slug Test

Figure Box 8-3 - Slug test methods available in Aquifer^{Win32}. References cited here are available in Section 19 of this book (Environmental Simulations, Inc., 2019).

[Return to where text linked to Box 8](#) ↑

Box 9 Laboratory Methods used to Determine Hydraulic Properties of Aquitards and Low Permeability Formations

Small samples of aquitard and low permeability formations can be examined in the laboratory and estimates of the hydraulic conductivity and specific storage derived. Some transient field-scale testing results are stated in terms of diffusivity, K_h/S_s and K_v/S_s . Thus, measurements of specific storage are of value because they can be used to solve for hydraulic conductivity in transient settings.

As with any laboratory testing it is assumed that the sample is representative of the material under investigation. As previously mentioned, laboratory methods may appropriately represent field conditions when the confining unit is uniform and coarse-grained lenses or secondary permeability features are not present.

Methods discussed in this box include the falling head permeameter, triaxial cell, and consolidometer.

Box 9.1 Falling Head Permeameter (modified from Box 4.3 of Woessner and Poeter (2020))

The falling head permeameter was designed to determine hydraulic conductivity values of low permeability sediments. In this method the water levels and flow rates change over time. Data requirements include the dimensions of the sample and connected tube, and the change in water level over time as shown in Figure Box 9-1.

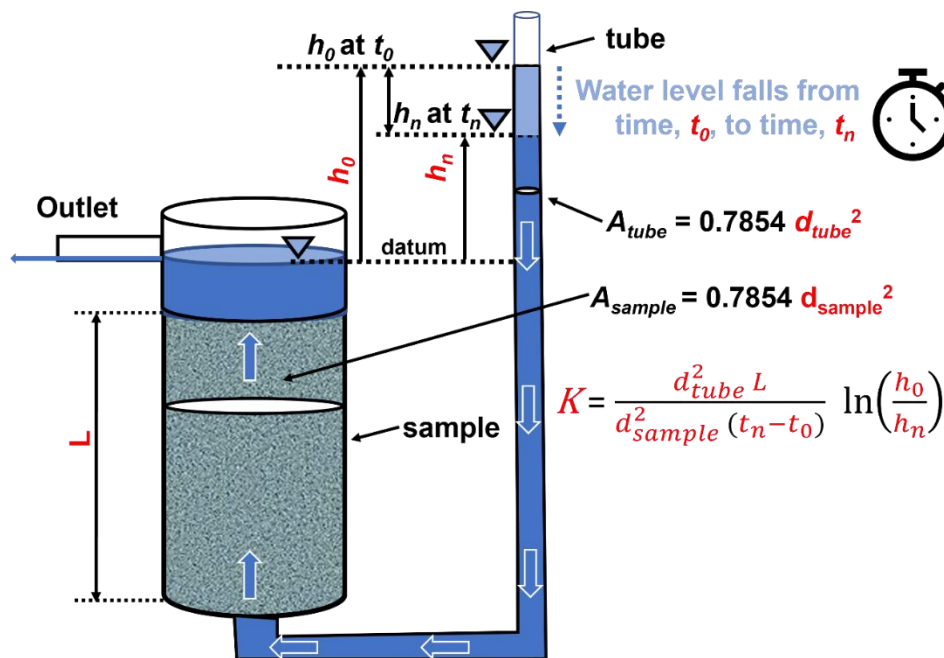


Figure Box 9-1 - Schematic of a falling head permeameter. The sample of length L is placed in a chamber of area A_{sample} , and saturated by adding water to the attached tube of area A_{tube} . Once the sample is saturated and water seeps from the outlet, the permeameter is ready to be used. At time t_0 the water level measurement above the sample outlet, h_0 is recorded. After an interval of time, $t_n - t_0$, a second measurement of the water level in the tube is made, h_n . These parameters are then used to compute the hydraulic conductivity of the sample as shown, where d_{tube} and d_{sample} are the diameters of the tube and sample, respectively (Woessner & Poeter, 2020).

The sample should first be saturated using de-aired water and then a vacuum is applied to the top of the sample chamber. Water is introduced at the base of the sample. If saturation cannot be achieved over about 24 hours, then it is recommended that the triaxial permeability test method as described in the next section should be applied. Woessner and Poeter (2020) present the derivation of the falling head equation and details on conducting the test as presented in Equation Box 9-1.

$$K = \frac{d_{tube}^2 L}{d_{sample}^2 t} \ln \left(\frac{h_0}{h_n} \right) \quad (\text{Box 9-1})$$

where:

- K = vertical hydraulic conductivity (LT^{-1})
- d_{tube} = diameter of the tube (L)
- d_{sample} = diameter of the sample (L)
- t = time interval between the measured heads (T)
- h_0 = head at the start of the measuring time (T)
- h_n = head at the end of the time interval (T)

Box 9.2 Triaxial Permeability Test

The operation of triaxial cells is described in a number of publications of the America Society of Testing and Materials (e.g., Carpenter & Stephenson, 1986, *Permeability Testing in the Triaxial Cell*). These publications describe standard methods used in sample preparation and equipment operation. Instructional videos are also available at sites such as coffeytesting.com.au/soil-permeability-testing/.

A cylindrical geological sample is placed in a flexible compressible membrane mounted inside a rigid triaxial chamber and the chamber is then filled with water (Figure Box 9-2). The sample is saturated using back pressure. The chamber is pressurized to represent user specified stress conditions of the sample in the field setting. Flow through the sample is accomplished by slightly increasing the water pressure at the base of the sample and slightly lowering it at the top of the sample (establishing a hydraulic gradient). Details on triaxial testing methods are provided by Das (1983). The volume change of water leaving the column is monitored until it reaches a steady state. Then using the dimensions of the column, gradient, and steady state discharge, K_v is calculated using Darcy's Law (Equation Box 9-2).



Figure Box 9-2 - Triaxial permeability cell. Valves and tubes shown connect to a control panel that supplies water, pressurization, vacuum, as well as methods to control gradients and measure flow rates. Water in the sample moves from the bottom to the top of the cell. A is the sample cross sectional area. The pressurized water in the rigid triaxial cell remains constant after being set by the user. The gradient is computed by subtracting the head at the top of the cell (h_{top} , lower) from the head at the bottom of the cell (h_{bottom} , higher), and dividing by the sample thickness, b . K_v is calculated after the flow rate reaches steady state (photograph modified from <https://www.geo-con.com.au/product/permeability-cells/>).

$$K_v = \frac{Q}{i A} \quad (\text{Box 9-2})$$

where:

- K_v = hydraulic conductivity (LT^{-1})
- Q = constant discharge rate (L^3T^{-1})
- i = hydraulic gradient, (head at the outlet – head at the inlet) / sample thickness, b , (negative value) (dimensionless)
- A = cross sectional area of the sample (L^2)

Box 9.3 Consolidometer

When designing and constructing foundations for buildings, one must account for settlement from lateral deformation of the soil and a gradual settling resulting from a

volume change if pore water drains from the soil. In the case of saturated clay deposits, one-dimensional compression is of concern. Consolidation considerations generally assume the particles themselves are incompressible such that changes in the volume of material are due to rearrangement of the particles in response to loading and drainage of fluid. It is generally assumed that drainage follows Darcy's Law.

The consolidometer (or oedometer) test is used to generate relationships between consolidation pressures, changes in the void ratio of the soil, and variations in the soil's coefficient of consolidation. Estimates of vertical hydraulic conductivity can also be derived for each loading increment as reported by Haneberg and others (1998). Components of the equipment are shown in Figure Box 9-3.



Figure Box 9-3 - Consolidometer set up and components. a) The chamber is fitted with a porous stone, filter paper, the saturated sample, filter paper and a second porous stone, and then secured with an outer ring. b) The chamber with the top compression piston installed. c) The chamber placed in an apparatus that applies varied consolidation pressures (black bar) using a lever and weights (not shown). The gauge measures the change in sample thickness. A saturated sample is allowed to drain and water discharge can be measured. (photographs from: a) <https://certifiedmtp.com/karol-warner-1240-d-2-42in-fixed-ring-consolidometer/>; b) <https://www.globalgilson.com/100mm-fixed-ring-consolidometer/>; c) <https://www.globalgilson.com/lever-loaded-consolidation-frame/>).

The coefficient of consolidation, C_v , is determined from testing and relates to the rate of consolidation in response to a change in pressure. It is derived from interpretation of sample condition changes and is often interpreted from graphical plots of where the time associated with changes in 50 percent or 90 percent of the sample thickness are identified (Wray, 1986). The saturated hydraulic conductivity can be computed for each load increment (Terzaghi, 1943; Das, 1983) as shown in Equations Box 9-3 and Box 9-4.

$$K_v = \frac{a_v \gamma}{1 - e} \quad (\text{Box 9-3})$$

$$a_v = \frac{e_1 - e_2}{(p_2 - p_1)} \quad (\text{Box 9-4})$$

where:

K_v = permeability at a specified time (LT^{-1})

C_v = coefficient of consolidation (L^2T^{-1})

- a_v = change in void ratio divided by the change in pressure at specified time increment (LT^2M^{-1})
 e_1 = void ratio at pressure p_1 (dimensionless)
 e_2 = void ratio at pressure p_2 (dimensionless)
 p_1 = compression pressure applied to the sample ($M(L^{-2}T^{-1})$)
 p_2 = compression pressure applied to the sample ($ML^{-2}T^{-1}$)
 γ = specific weight of water ($ML^{-2}T^{-2}$)

Petersen (1956) modified the consolidation testing apparatus to directly measure hydraulic conductivity at different pressure increments using a falling head permeameter. He found a good correlation with computed values of K_v and falling head derived values.

Olsen and others (1991) published innovations in measuring hydraulic conductivity using a one-dimensional consolidometers and triaxial cells. In both cases a flow pump creates a constant flow from the sample base that is established from a pressure-controlled reservoir (Figure Box 9-4). Pressure differences are measured, a gradient computed, and K_v is calculated using Darcy's Law (Equation Box 9-2).

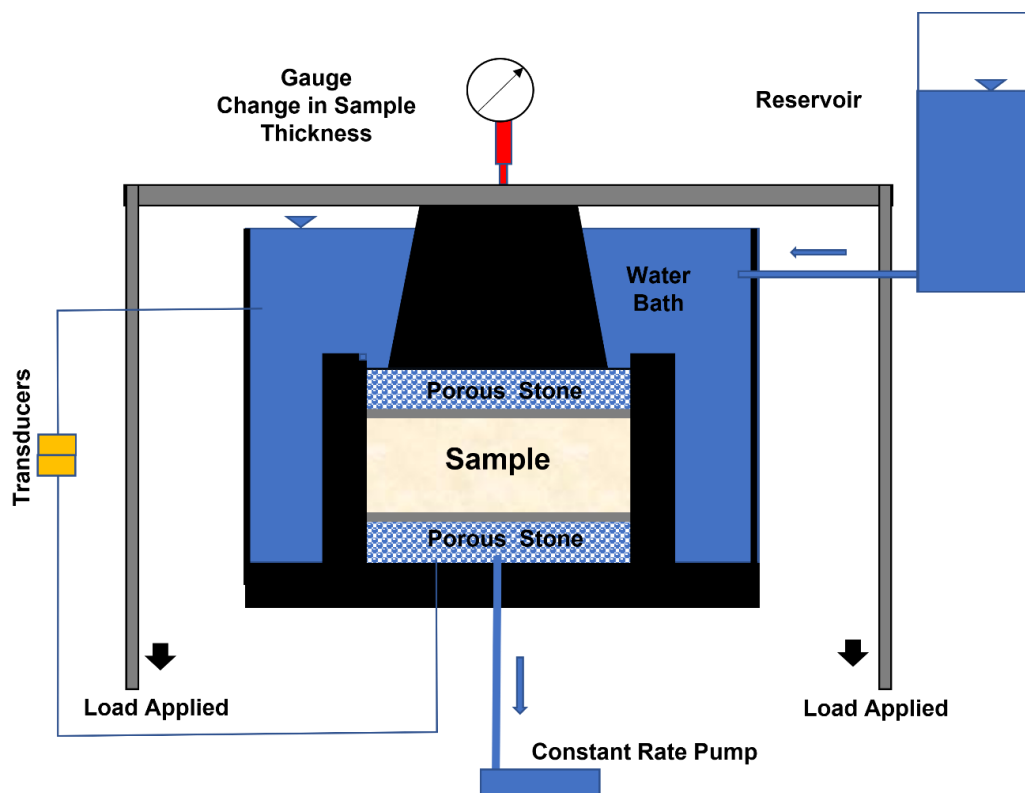
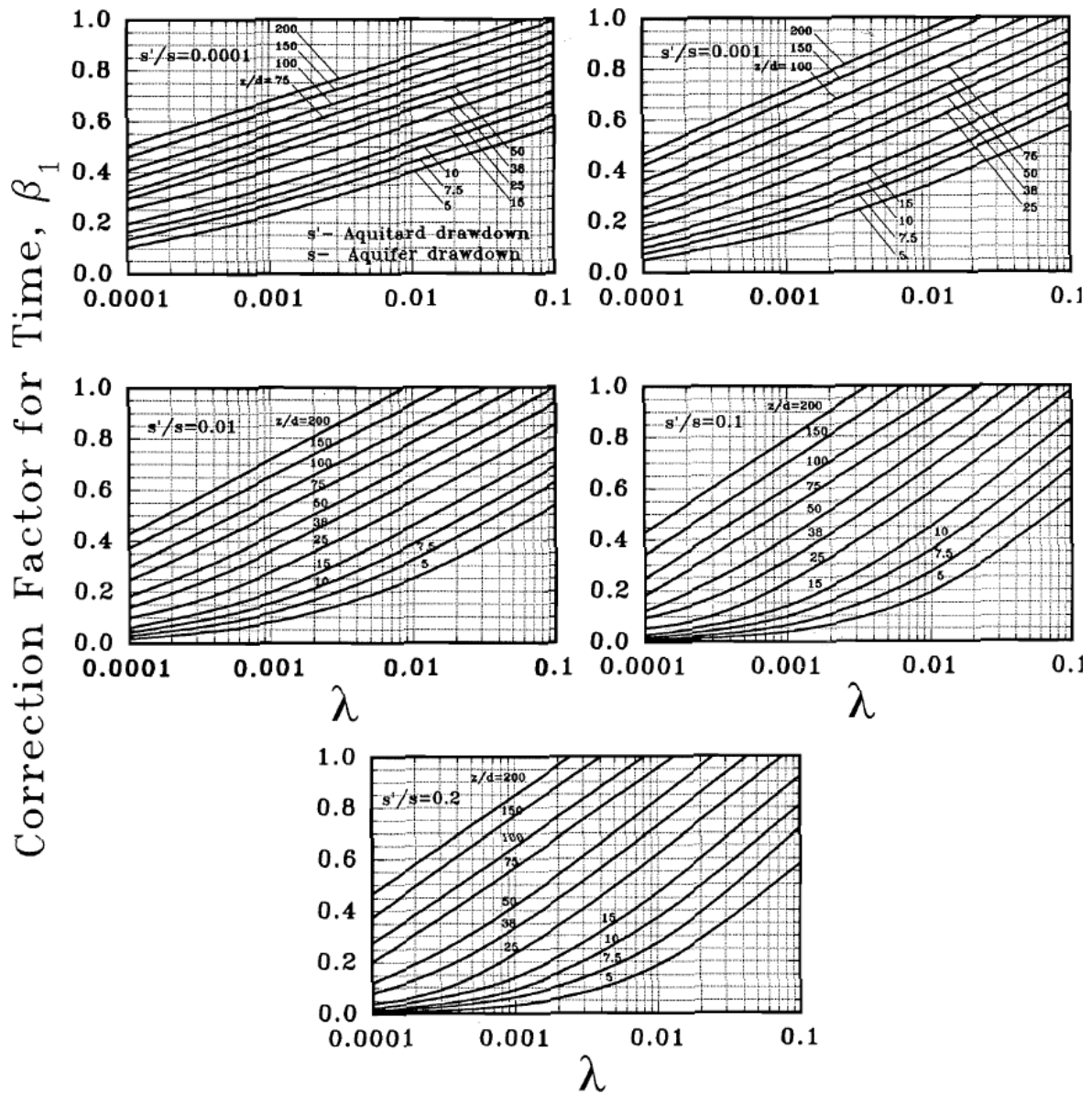


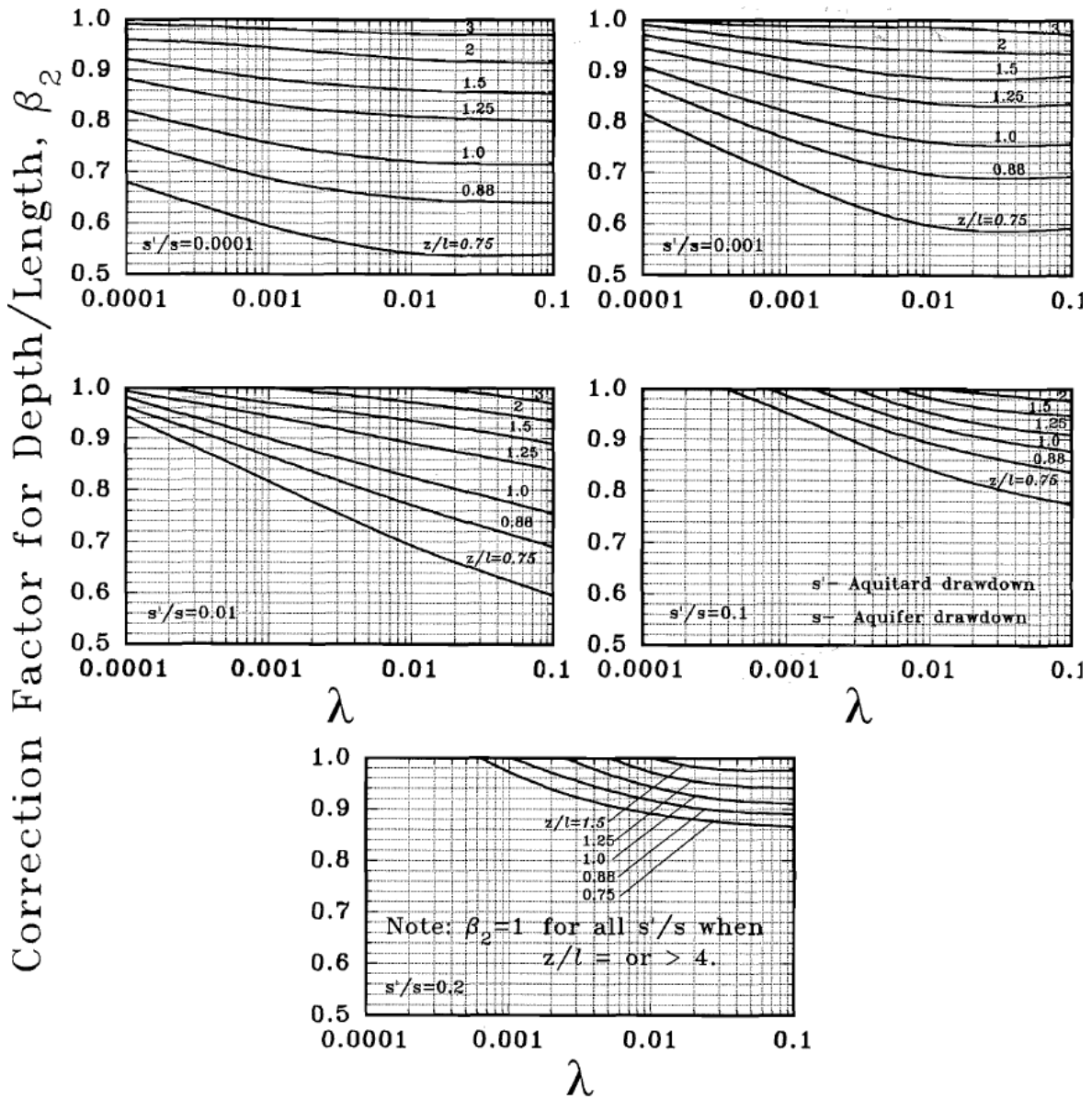
Figure Box 9-4 - Consolidometer set up with a constant rate pump. Gauge measures the change in sample thickness. Transducers measure the head at the base and top of the sample and the constant rate pump controls the flow rate through the sample. The reservoir provides a constant head to the water bath that is in communication with the sample.

[Return to where text linked to Box 9](#) ↗

Box 10 Reproduction of Figures from Rowe and Nadarajah (1993) Correction Factors



Reproduction of Figure 5 from Rowe and Nadarajah (1993) to facilitate education of Groundwater Project readers who do not have access to commercial journals. Correction factor for, β_1 , versus λ for drawdown ratios s'/s of 0.0001, 0.001, 0.01, 0.1, and 0.2.



Fair use reproduction of Figure 8 from Rowe and Nadarajah (1993) to facilitate education of Groundwater Project readers who do not have access to commercial journals. Correction factor for, β_2 , versus λ for drawdown ratios s'/s of 0.0001, 0.001, 0.01, 0.1, and 0.2.

[Return to where text linked to Box 10](#) ↑

Box 11 AQTESOLV Solutions to Exercises

This box provides solutions to Exercises 2, 3, 5, and 7 using a standard version of AQTESOLV. The manual curve match and user fitted lines to semi-log analyses presented in Section 21 “*Exercise Solutions*” are compared with the results for the same problems generated using AQTESOLV. Once again, the three leading software developers provide free demonstration or trial versions.

- AQTESLOV (aqtesolv.com)
- AquiferTest (waterloohydrogeologic.com/download-trial/)
- Aquiferwin32 (zip file that [will download when this link is clicked](#))

These programs can be used to solve most, if not all, of the pumping test and slug test Exercises 2, 3, 5, and 7.

In many agencies and businesses hydraulic test analyses are commonly completed using one or more of the three software packages discussed in this book (Section 13, Section 14.6, and Boxes 5, 6, and 7). The material presented in this box shows how the results of manual curve matching methods compare to analyses accomplished using AQTESOLV, as they are in the other two commercially available programs. When analyses of hydraulic test data sets are routinely required, it is suggested that one of the commercially available programs become part of your hydrogeologic toolbox.

Box 11.1 AQTESOLV Solution for Exercise 2

The manual solution for Exercise 2 involves matching field data to Theis type curves as delineated in Section 21. This box provides images of the Exercise 2 solutions for part a, c, and d, using AQTESOLV, followed by a table comparing the manual and AQTESOLV results.

The AQTESOLV image of match to the Theis solution for Observation well 1 at $r = 66$ m is shown in Figure Box 11-1.

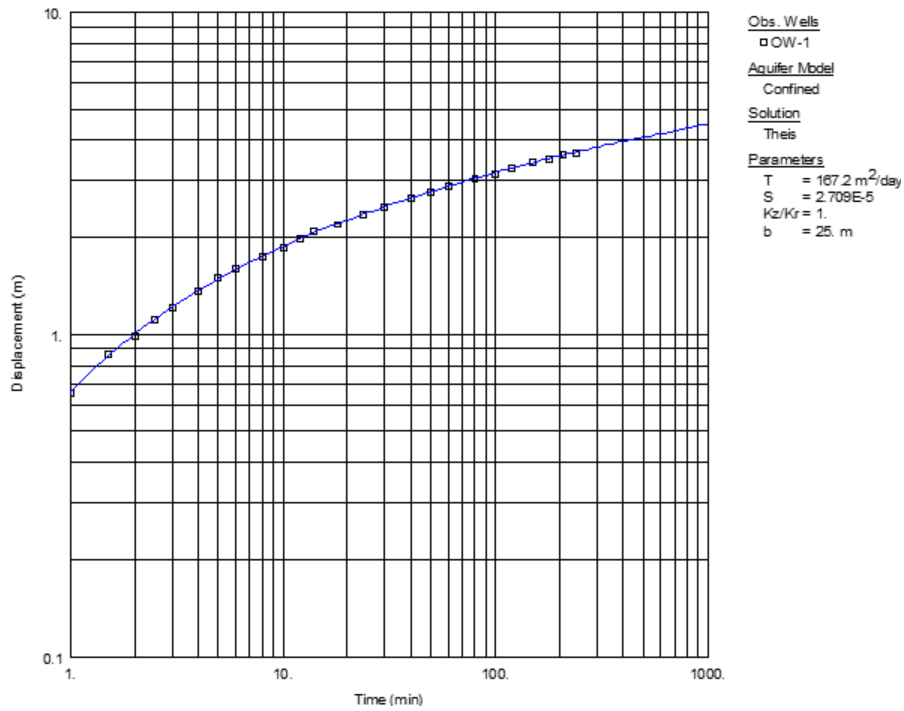


Figure Box 11-1 AQTESOLV Theis solution for OW1 $r = 66$ m.

The AQTESOLV image of match to the Theis solution for Observation well 2 at $r = 122$ m is shown in Figure Box 11-2.

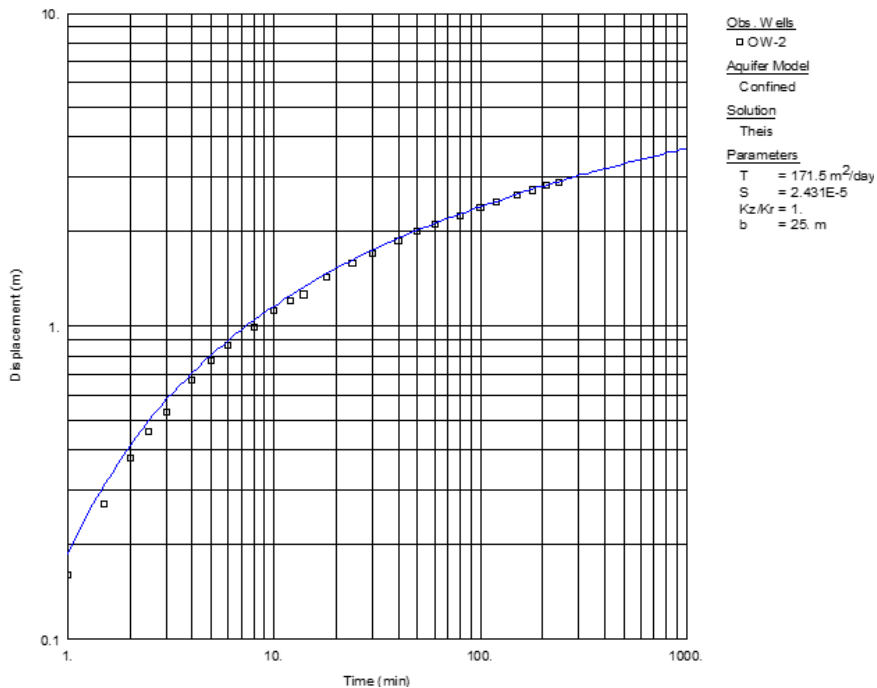


Figure Box 11-2 AQTESOLV Theis solution for OW2 $r = 122$ m.

The AQTESOLV image of match to the Theis solution for Observation well 3 at $r = 244$ m is shown in Figure Box 11-3.

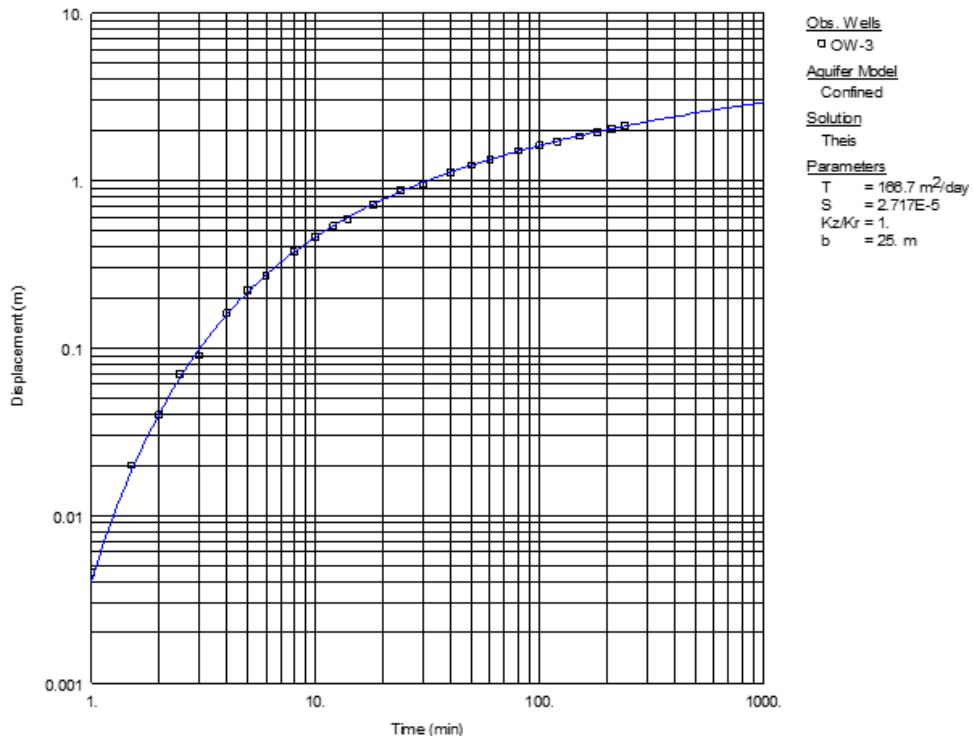


Figure Box 11-3 AQTESOLV Theis solution for OW3 $r = 244$ m.

The AQTESOLV image for match to Cooper-Jacob solution for Observation well 2 at $r = 122$ m is shown in Figure Box 11-4.

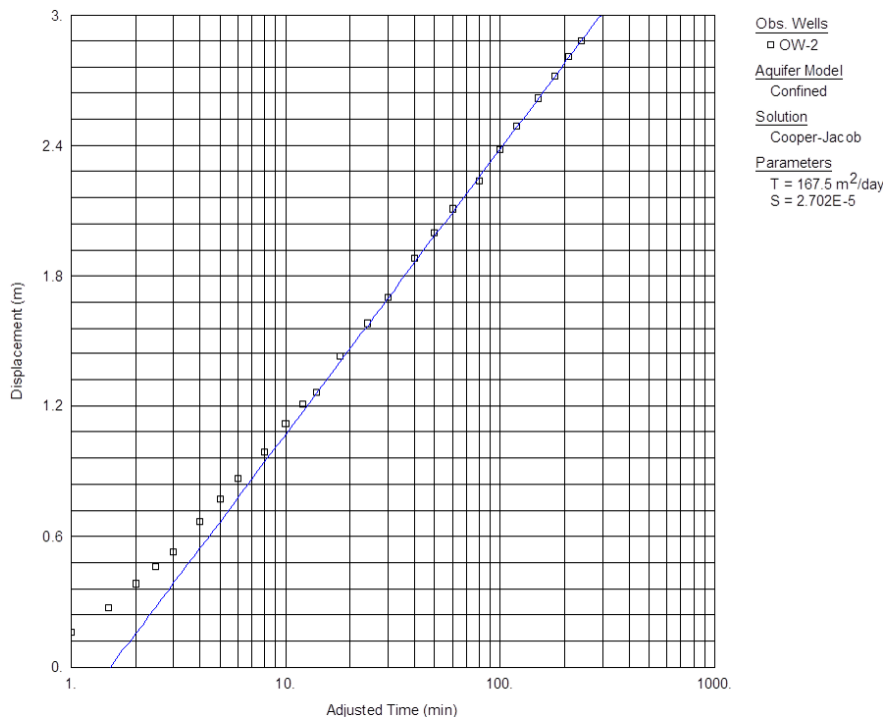


Figure Box 11-4 AQTESOLV Cooper-Jacob solution for OW2 $r = 122$ m.

The AQTESOLV image for a distance-drawdown solution at 100 minutes is shown in

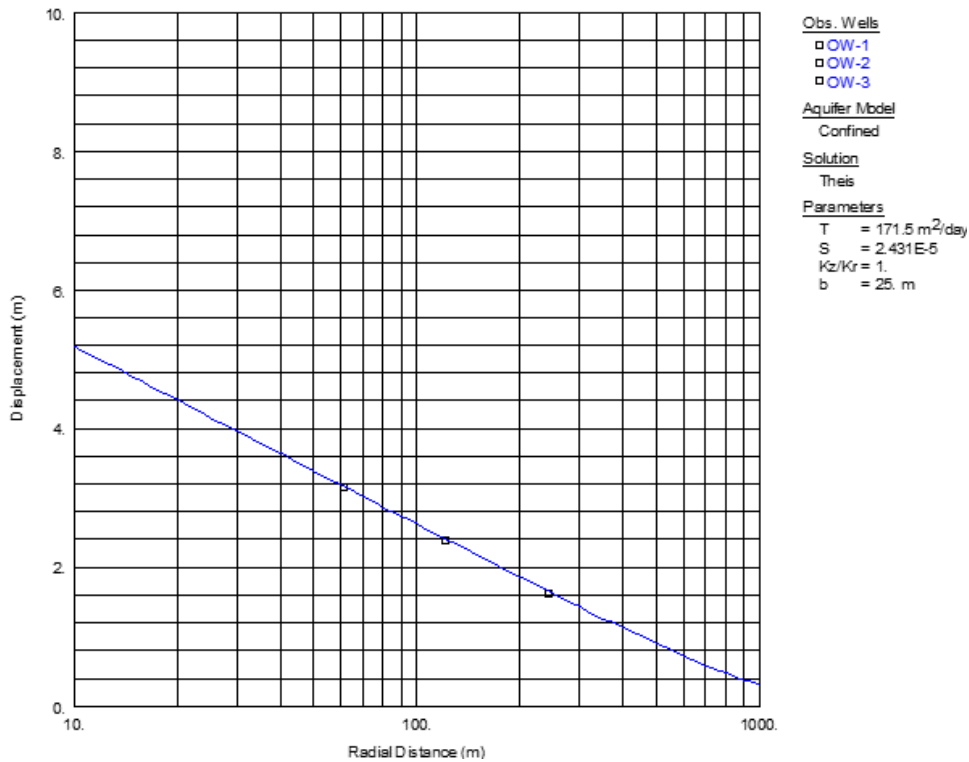


Figure Box 11-5 AQTESOLV confined distance-drawdown solution using OW1 $r = 66$ m., OW2 $r = 122$ m, OW3 $r = 244$ m at 100 minutes.

The results obtained by manual and automated fitting are compared in Table Box 11-1.

Table Box 11-1 - Comparison between results in *Solution Exercise 2* of Section 21 accomplished with hand-fitted curve matching and AQTESOLV results.

	Manual		Automated	
	$T \text{ m}^2 \text{ d}^{-1}$	S	$T \text{ m}^2 \text{ d}^{-1}$	S
Exercise 2				
Exercise 2a r = 66 m	165	3×10^{-5}	167	2.7×10^{-5}
Exercise 2a r = 122 m	159	3×10^{-5}	172	2.4×10^{-5}
Exercise 2a r = 244 m	165	2×10^{-5}	167	2.7×10^{-5}
Exercise 2c r = 122 m	164	6×10^{-6}	168	2.7×10^{-5}
Exercise 2d	163	3×10^{-5}	172	2.4×10^{-5}

Box 11.2 AQTESOLV Solution for Exercise 3 a and b

The manual solution for Exercise 3 involves matching field data to Hantush-Cooper leaky aquifer type curves as delineated in Section 21. This box provides images of the Exercise 3 solution using AQTESOLV, followed by a table comparing the manual and AQTESOLV results.

The AQTESOLV image of the Hantush-Cooper leaky aquifer solution match to the field data Figure Box 11-6.

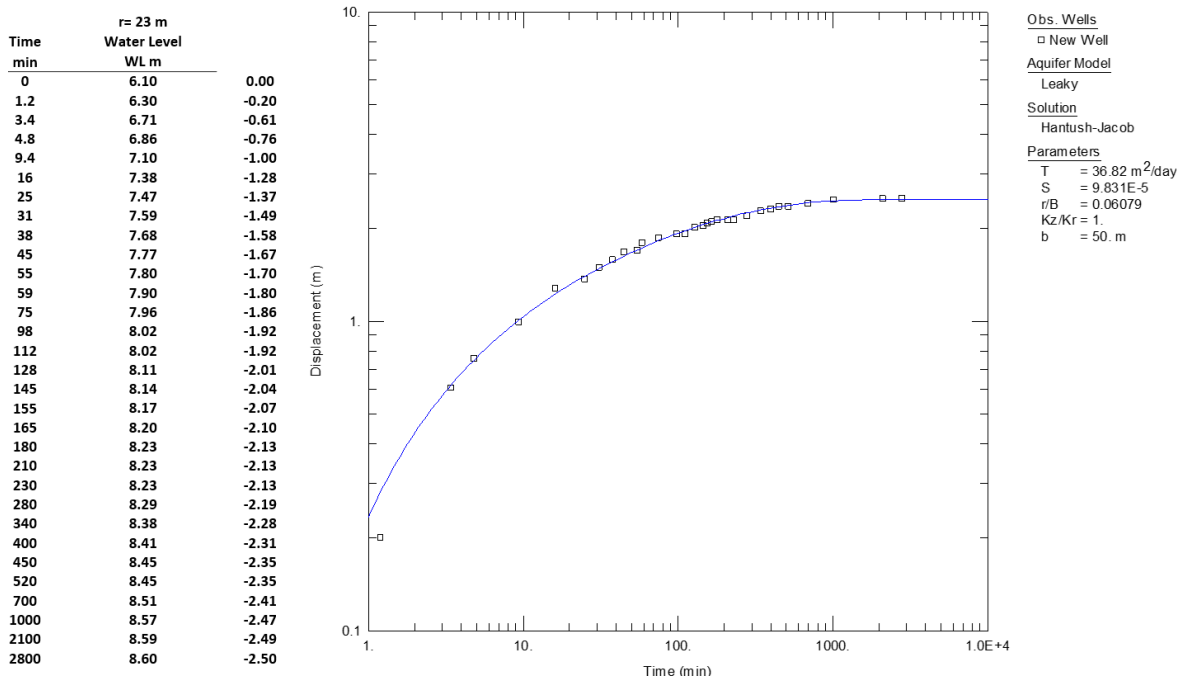


Figure Box 11-6 - AQTESOLV Hantush-Jacob solution for observation well data. Parameters calculated from the fit are shown in the upper right. Drawdown data computed and shown on left hand side of diagram.

Noting the discrepancy between the manual and automated results and knowing that it was difficult to read the r/B value for the manual solution, AQTESOLV was used to generate type curves for r/B from 0.02 to 3 and overlay the data on those curves as shown in Figure Box 11-7. This made it much easier to determine the r/B value.

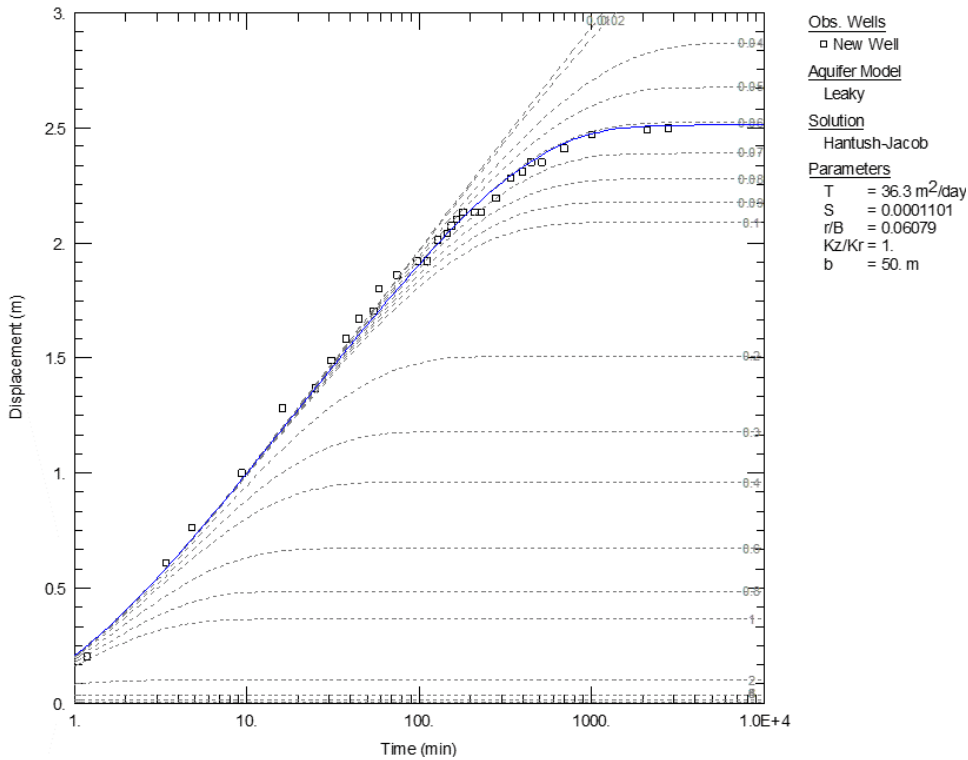


Figure Box 11-7 - AQTESOLV Hantush-Jacob solution for observation well data. In AQTESOLV an option to compute and show additional type curves for the chosen analysis method is available. Here values of r/B between 0.02 and 3 were generated from the analytical solution. The automated curve matched r/B value of 0.06069 is shown on this family of curves.

The results obtained by manual and automated fitting are compared in Table Box 11-2.

Table Box 11-2 - Comparison between results in *Solution Exercise 3* of Section 21 accomplished with hand-fitted curve matching and AQTESOLV results.

	Manual			Automated		
Exercise 3	$T \text{ m}^2/\text{d}$	S	$K' \text{ m/d}$	$T \text{ m}^2/\text{d}$	S	$K' \text{ m/d}$
OW = 23 m	32.5	1.2×10^{-4} $\approx 1 \times 10^{-4}$	0.0066	36.8	9.8×10^{-5} $\approx 1.0 \times 10^{-4}$	0.008*

*Computed outside of AQTESOLV using $r/B = 0.06$) as shown here.

$$K' = \frac{Tb' \left(\frac{r}{B}\right)^2}{r^2} = \frac{36.8 \frac{\text{m}^2}{\text{d}} (30 \text{ m})(0.06)^2}{(23 \text{ m})^2} = 0.008 \frac{\text{m}}{\text{d}}$$

The Hantush-Jacob visual curve matching and AQTESOLV results are similar. The application of either approach yields reasonable hydrogeologic values for this leaky confined aquifer data set.

Box 11.3 AQTESOLV Solution for Exercise 5

The manual solution for Exercise 5 involves analyzing a step drawdown test as delineated in Section 12. This box provides images of the Exercise 5 solution using AQTESOLV, followed by a table comparing the manual and AQTESOLV results. The AQTESOLV image of the analysis of the field data is presented in Figure Box 11-8.

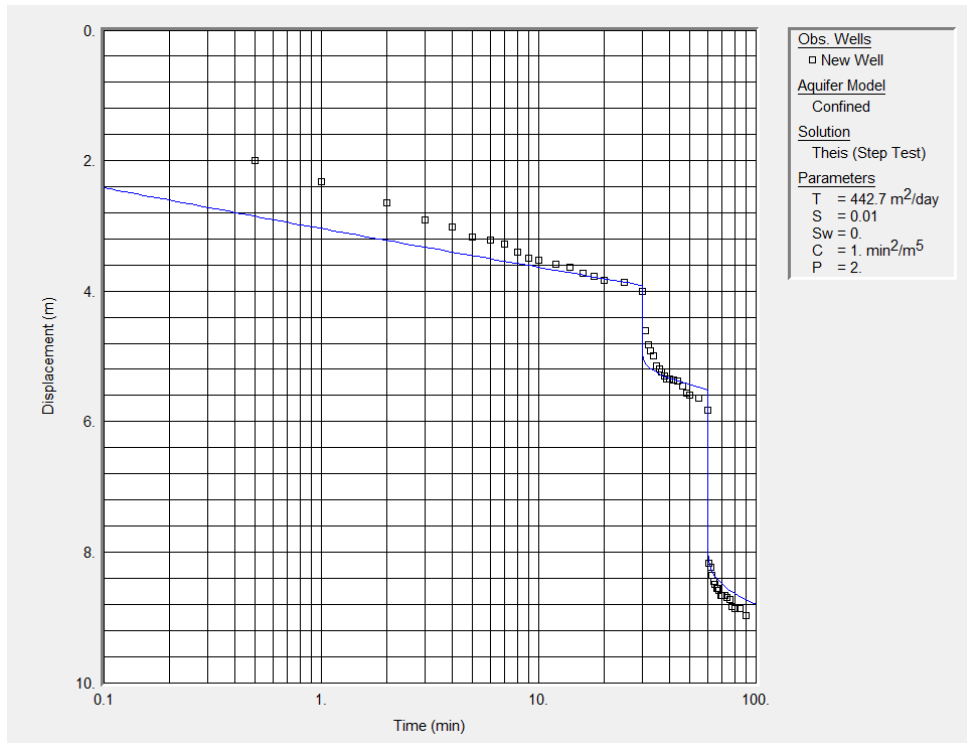


Figure Box 11-8 AQTESOLV Theis solution variable pumping rate slug test analyses for a step drawdown test.

The results obtained by manual and automated fitting are compared in Table Box 11-3.

Table Box 11-3 - Comparison between results in *Solution Exercise 5* of Section 21 accomplished with manual analysis and AQTESOLV results.

	Manual		Automated	
Exercise 5	$T \text{ m}^2/\text{d}$	$C \text{ d}^2/\text{m}^5$	$T \text{ m}^2/\text{d}$	$C \text{ d}^2/\text{m}^5$
	214	3.0×10^{-7}	443	$4.8 \times 10^{-7}^*$

*conversion: $(1.0 \text{ min}^2/\text{m}^5)(1 \text{ d} / 1440 \text{ min})^2 = 4.8 \times 10^{-7} \text{ d}^2/\text{m}^5$

The T value obtained using AQTESOLV is higher than that obtained using manual methods. The values of C are similar. Generally, in this case inputting the step drawdown data and letting AQTESOLV generate an estimate of C , P , S , and T yielded poor estimates. In order to obtain values of C similar to the manual solution of Exercise 5, the range of parameter values were constrained including setting P (exponent of C) to 2 and limiting the maximum S value to 0.01. The generated S value is unreasonably high for a confined

aquifer, however, constraining S to smaller values degraded the quality of fit to the data. In this case, careful analyses of model results are required to obtain reasonable values. It is recommended that manual analysis of step test data sets be performed before automated fitting. The manual analysis results serve as a check of the fitting program results.

Box 11.4 AQTESOLV Solution for Exercise 7

The manual solution for Exercise 7 involves analyzing a slug test as delineated in Section 14. This box provides images of the Exercise 7 solution using AQTESOLV, followed by a table comparing the manual and AQTESOLV results. The AQTESOLV image of the analysis of the field data is presented in Figure Box 11-9.

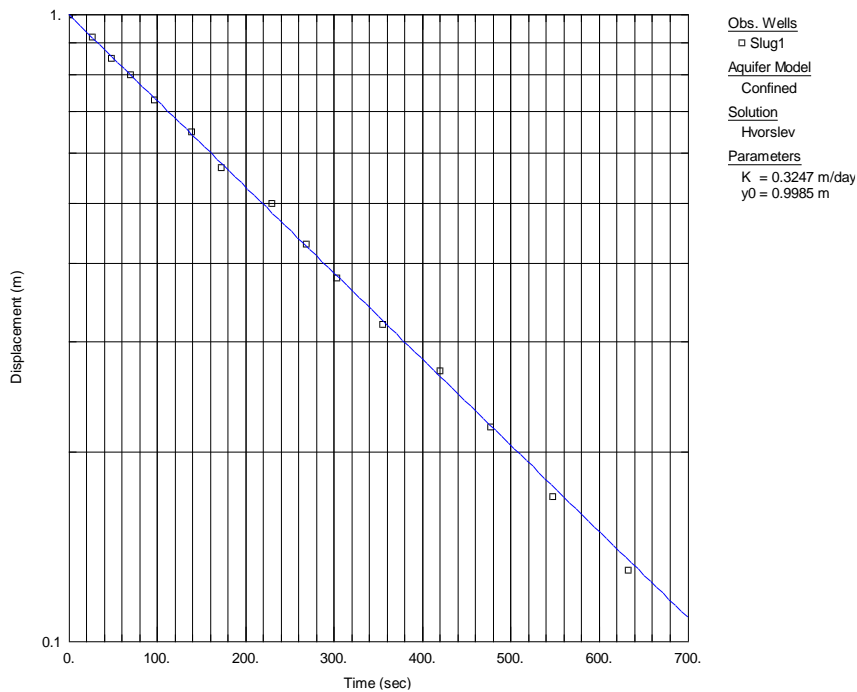


Figure Box 11-9 AQTESOLV slug test analysis .

The results obtained by manual and automated analysis are compared in Table Box 11-4.

Table Box 11-4 - Comparison between results in *Solution Exercise 5* of Section 21 accomplished with manual analysis and AQTESOLV results.

	Manual	Automated
Exercise 7	K m/d	K m/d
using Equation (107)	0.33	0.32
using Equation (108)	0.33	

The Hvorslev hand fitted curve matching and AQTESOLV results are very similar. The application of either approach yields reasonable hydrogeologic values for this unconfined slug test data set.

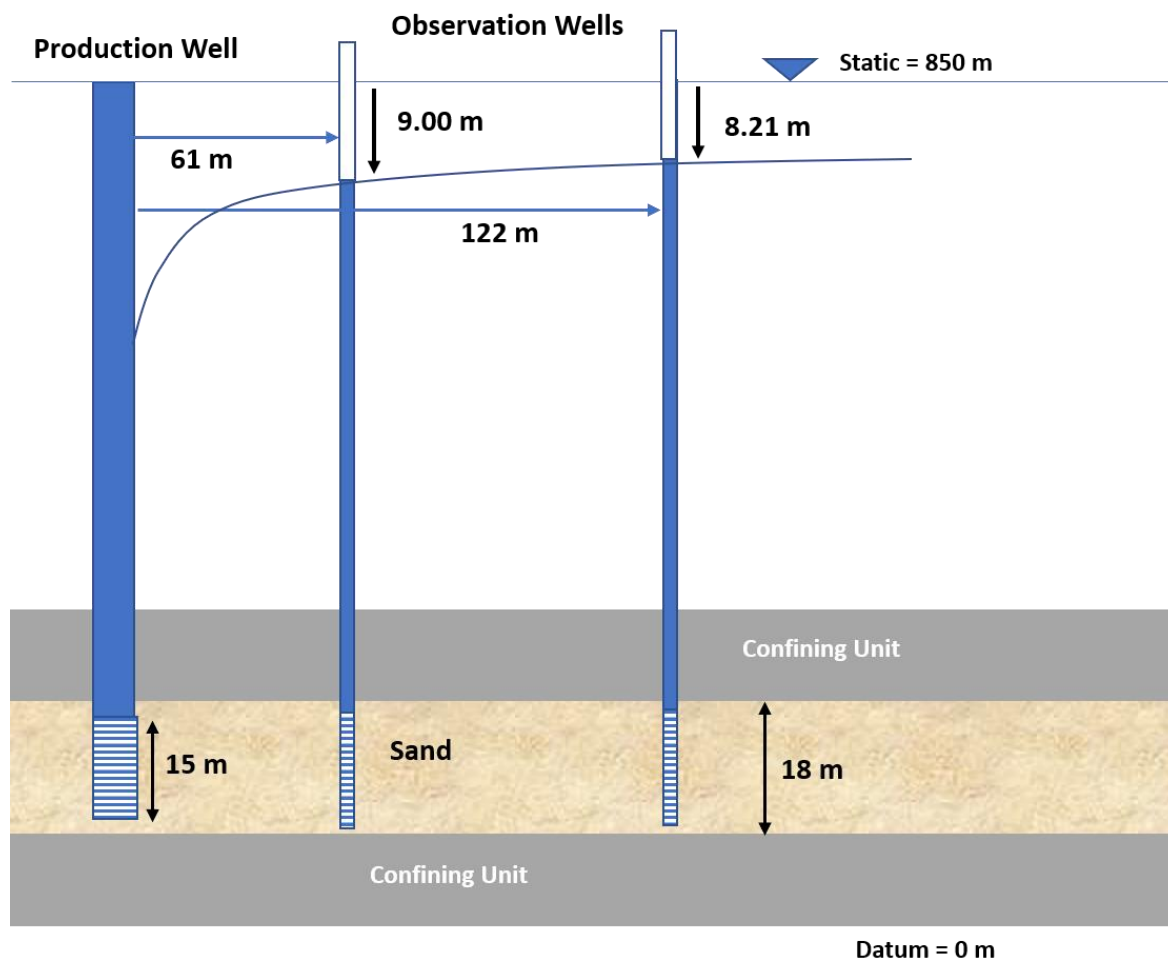
[Return to where text linked to Box 11](#) ↴

21 Exercise Solutions

Problem solutions are provided here. Curve matching is performed by visually matching type curves and slug test analyses from Excel® plots of data. Solutions using the commercially available software package AQTESOLV are also provided for comparison (Box 11). The original problems are restated here, and the solutions follow.

Solution Exercise 1

A 0.2 m diameter production well finished in a confined sand aquifer was pumped continuously at 300 L/minute for 10 hours. The water levels in the pumping well and two observation wells appeared to stabilize at about 6 hours as shown in this image.



Cross section of a sand water bearing unit. The production well is pumped at a constant rate of 300 L/min for 10 hours and the drawdown in two observation wells is observed under what appear to be steady state conditions. Drawdowns from the static pre-pumping water levels are shown along with the radial distances of wells from the production well.

- a) Assuming the pumping test reached steady state or pseudo steady state by 10 hours compute T and K .

The confined Thiem Equation (17) is applied to compute T under the stated conditions.

$$T = \frac{Q}{2\pi(h_2 - h_1)} \ln\left(\frac{r_2}{r_1}\right)$$

The values of h_1 and h_2 are equal to the static water level, 850 m, minus the reported steady state drawdown.

$$h_1 = 850 \text{ m} - 9.00 \text{ m} = 841.00 \text{ m}$$

$$h_2 = 850 \text{ m} - 8.21 \text{ m} = 841.79 \text{ m}$$

$$T = \frac{300 \frac{\text{L}}{\text{minute}} \frac{1 \text{ m}^3}{1000 \text{ L}} \frac{1440 \text{ minute}}{\text{d}}}{2 (3.14) (841.79 \text{ m} - 841.00 \text{ m})} \ln\left(\frac{122 \text{ m}}{61 \text{ m}}\right) = 60 \frac{\text{m}^2}{\text{d}}$$

$$T = Kb \text{ so } K = \frac{T}{b} = \frac{60 \frac{\text{m}^2}{\text{d}}}{18 \text{ m}} = 3.4 \frac{\text{m}}{\text{d}}$$

- b) Do you need to account for the effects of partial penetration on the observation well data? Why or why not?

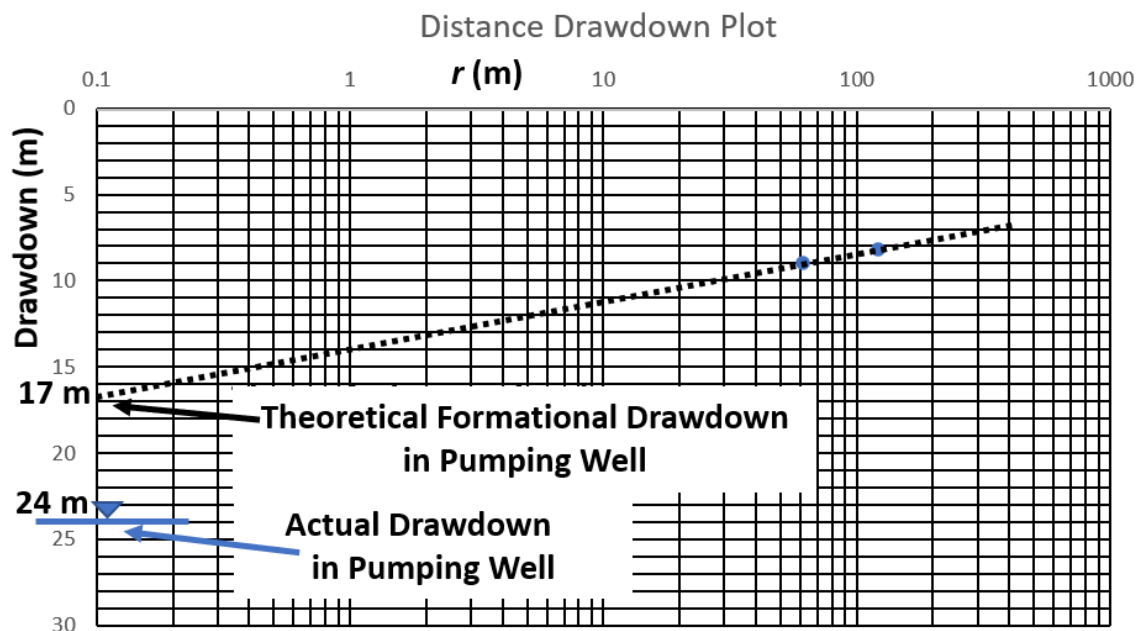
Pumping well partial penetration effects generally do not exceed a radial distance of $2b(K_h/K_v)^{0.5}$. Assuming the system is close to isotropic and homogeneous, then $K_h/K_v = 1$.

$$\text{extent of partial penetration effects} = 2b \left(\frac{K_v}{K_h}\right)^{0.5} = 2(18 \text{ m})(1)^{0.5} = 36 \text{ m}$$

Both observation wells are greater than 36 m from the pumping well, so partial penetration need not be accounted for.

- c) Assuming the production well radius is 0.1 m and the measured drawdown in the pumping well is 24 m, calculate the production well efficiency (i.e., measured drawdown divided by theoretical drawdown). A semi-log plot of the observation well data will be helpful.

A semi log plot of drawdown versus distance is prepared using $s=9.00$ m at $r=61$ m and $s=8.21$ m at $r=122$ m and shown below.



Drawdown at the two observation wells was plotted at the radial distance of each well. A straight line was fitted to the two data points (dashed black line), and extended back to the radius of the pumping well (0.1 m) where it is read from the graph as a theoretical drawdown of 17 m.

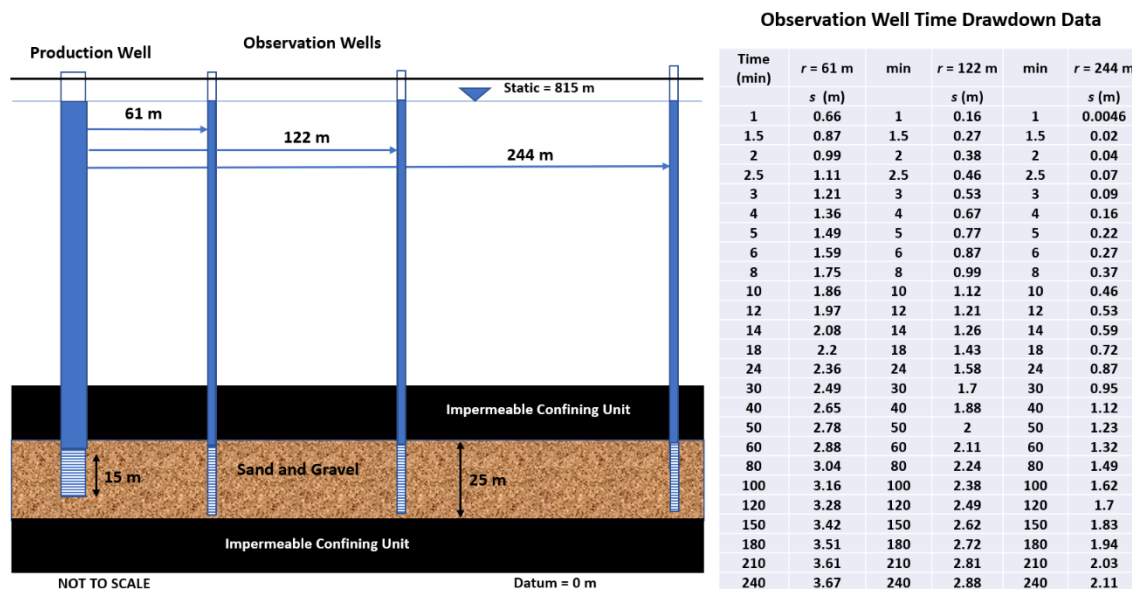
The well efficiency is computed as the theoretical drawdown (100 percent efficient) divided by the measured drawdown in the pumping well. Efficiency = $17 \text{ m} / 24 \text{ m} = 0.71$ or 71 percent efficient.

[Return to Exercise 1](#) ↑

[Return to where text linked to Exercise 1](#) ↑

Solution Exercise 2

A pumping test is conducted on a production well located in an extensive, isotropic, and homogeneous, 25-m thick, totally confined, sand and gravel aquifer. The production well has a 15 m screened interval. The well was pumped at a constant rate of 1,200 m³/d for 240 minutes. Time-drawdown data were collected at three observation wells located 61 m, 122 m, and 244 m from the pumping well as shown in the image below. An Excel® data base of the time-drawdown data is available on the [web page for this book](#).



Information related to Exercise 2. A production well is pumped at a constant rate in a totally confined isotropic and homogeneous aquifer that is infinite in lateral extent. Time-drawdown data are collected from three observation wells. Configuration of the pumping well location, screen length and location of the observation wells are shown in cross section. Time-drawdown data sets for the three observation wells are presented (modified from Lohman, 1972).

- a) Prepare log-log pots of the time-drawdown data for each of the observation wells. Using manual or automated curve matching, determine values of transmissivity and storativity for each data set.

The Theis equation and curve matching was applied to determine T and S using Equations (28) and (29) from Section 8.1.

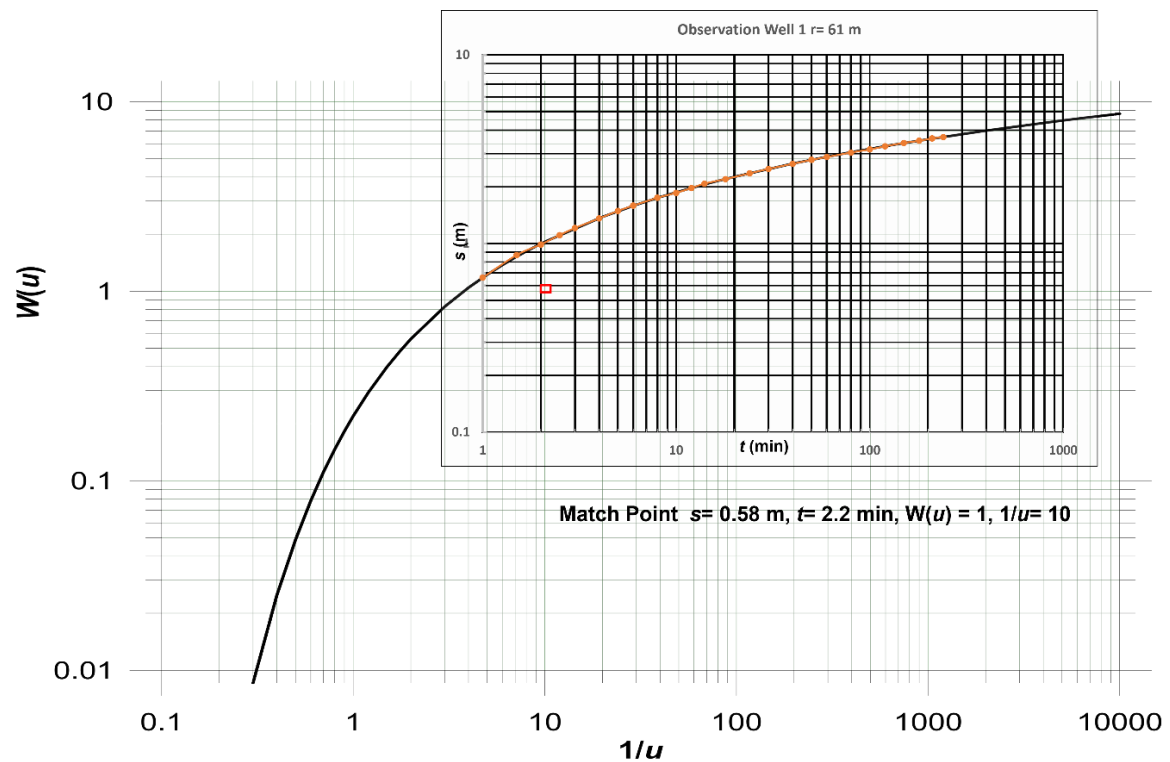
$$T = \frac{Q}{4\pi s} W(u)$$

$$S = \frac{u4Tt}{r^2}$$

Manual curve matching was applied. Observation well data sets were plotted as log-log plots in Excel®. The Excel® plot was copied into a slide in Microsoft PowerPoint®. The type curve for totally confined conditions, $W(u)$ versus $1/u$ (Figure 28 of Section 8) was copied and imported into PowerPoint. The Excel® time-drawdown data plot was made transparent by right clicking on the chart (log-log data plot) and then going to (Format

chart area). The transparency was then maximized. Next the x and y axes were stretched and adjusted to have the Excel® plot axes match the type curve axes (same area represented by each change in major axis (1 to 10, 10 to 100, etc.). Once the data plot was adjusted to the same scale as the type curve it was maneuvered to find the best fit of the data to the type curve while keeping the axes parallel. Next a match point in the overlapping plot area was selected and values of s , t , $W(u)$ and $1/u$ were determined.

An image resulting from the curve matching process is shown here for the observation well at $r = 61$ m with $Q = 1,200$ m³/d.



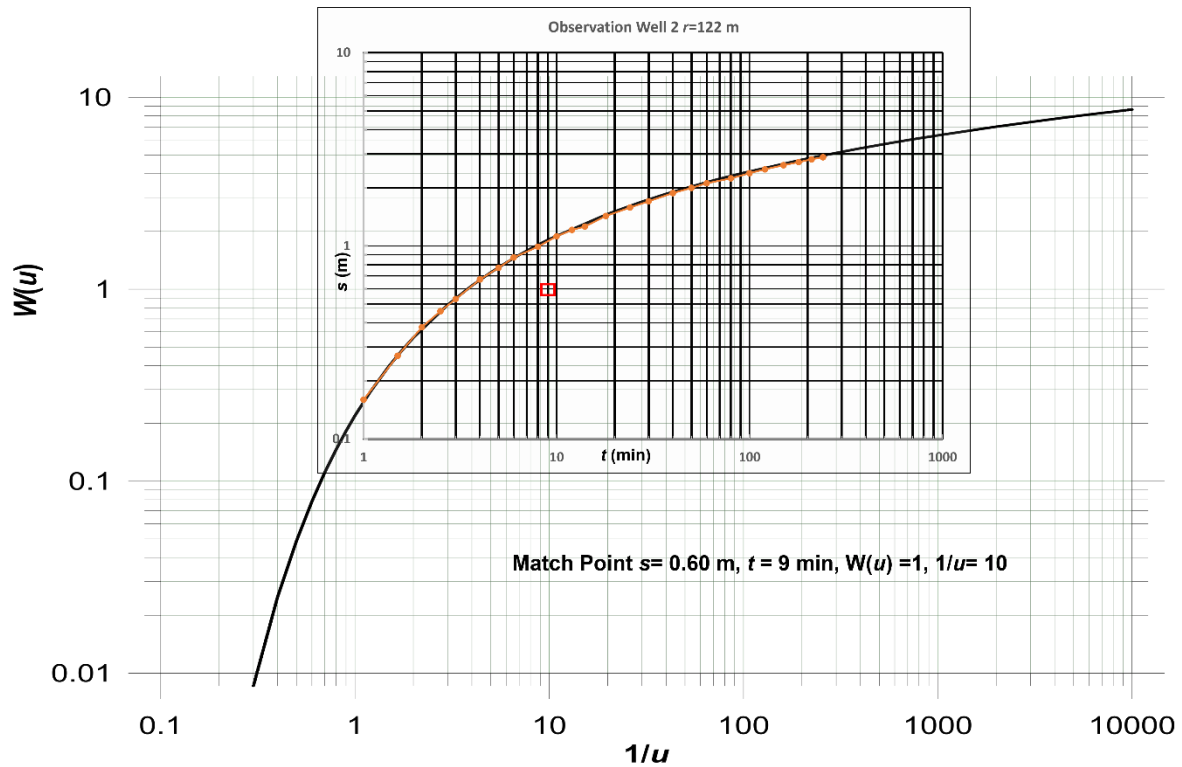
Curve matching for the observation well located at $r = 61$ m. The dark black line is the Theis type curve ($W(u)$ and $1/u$ axes). The orange dots and line represent the field data. The red square is the location of the match point.

Match point: $s = 0.58$ m, $t = 2.2$ min, $W(u) = 1$ and $1/u = 10$ ($u = 0.1$)

$$T = \frac{Q}{4\pi s} W(u) = \frac{1200 \frac{\text{m}^3}{\text{d}}}{4 (3.14) 0.58 \text{ m}} (1) = 165 \frac{\text{m}^2}{\text{d}}$$

$$S = \frac{u4Tt}{r^2} = \frac{0.1 (4) 165 \frac{\text{m}^2}{\text{d}} 2.2 \text{ min} \frac{1 \text{ d}}{1440 \text{ min}}}{(61 \text{ m})^2} = 0.00003 \text{ or } 3 \times 10^{-5}$$

An image resulting from the curve matching process is shown here for the observation well at $r = 122$ m with $Q = 1,200$ m³/d.



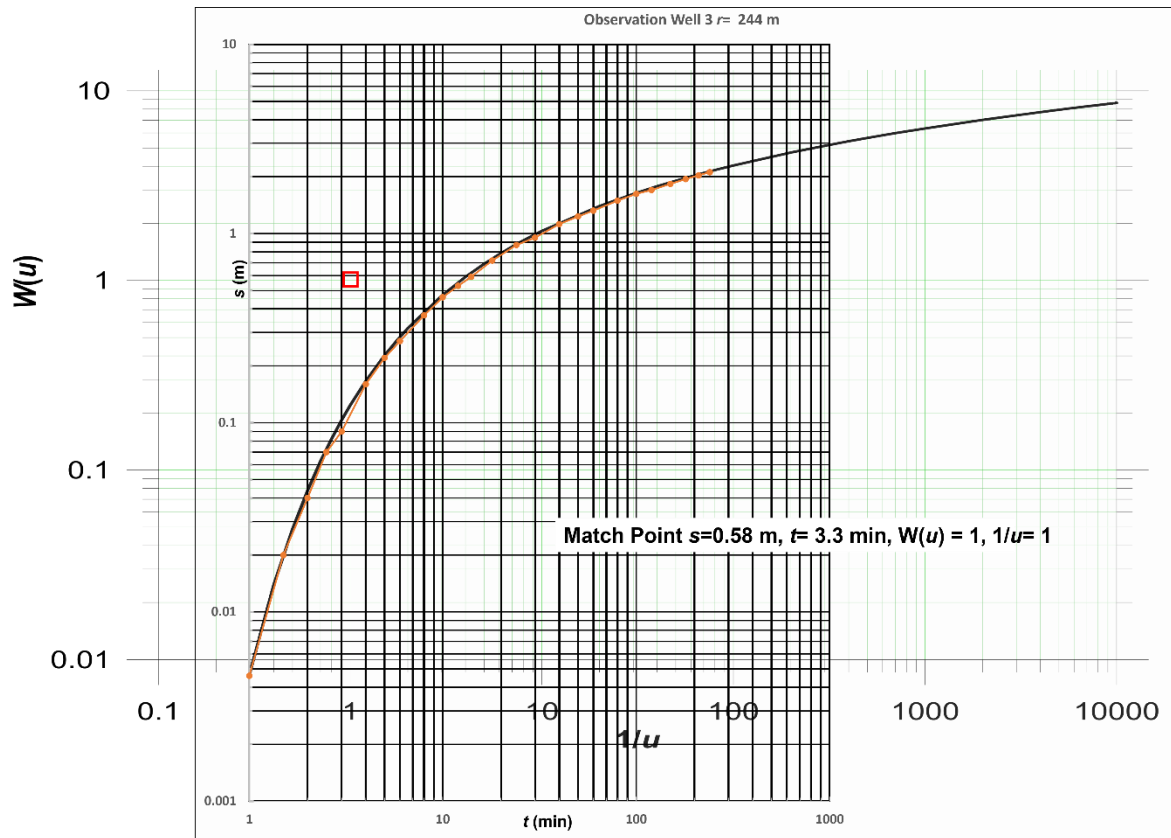
Curve matching for the observation well located at $r = 122$ m. The dark black line is the Theis type curve ($W(u)$ and $1/u$ axes) and the orange line represents the field data. The red square is the location of the match point.

Match point: $s = 0.6$ m, $t = 9.0$ min, $W(u) = 1$ and $1/u = 10$ ($u = 0.1$)

$$T = \frac{Q}{4\pi s} W(u) = \frac{1200 \frac{\text{m}^3}{\text{d}}}{4 (3.14) 0.6 \text{ m}} (1) = 159 \frac{\text{m}^2}{\text{d}}$$

$$S = \frac{u4Tt}{r^2} = \frac{0.1 (4) 159 \frac{\text{m}^2}{\text{d}} 9 \text{ min} \frac{1 \text{ d}}{1440 \text{ min}}}{(122 \text{ m})^2} = 0.00003 \text{ or } 3 \times 10^{-5}$$

An image resulting from the curve matching process is shown here for the observation well at $r = 244$ m, $Q = 1,200$ m³/d.



Curve matching for the observation well located at $r = 244$ m. The dark black line is the Theis type curve ($W(u)$ and $1/u$ axes) and the orange line represents the field data. The red square is the location of the match point.

Match point: $s = 0.58$ m, $t = 3.3$ min, $W(u) = 1$ and $1/u = 1$ ($u = 1$)

$$T = \frac{Q}{4\pi s} W(u) = \frac{1200 \frac{\text{m}^3}{\text{d}}}{4 (3.14) 0.58 \text{ m}} (1) = 165 \frac{\text{m}^2}{\text{d}}$$

$$S = \frac{u4Tt}{r^2} = \frac{1 (4) 165 \frac{\text{m}^2}{\text{d}} 3.3 \text{ min} \frac{1 \text{ d}}{1440 \text{ min}}}{(244 \text{ m})^2} = 0.00002 \text{ or } 2 \times 10^{-5}$$

- b) Compare and contrast the values computed. Should they all be the same? If not, how would you present the results to the well owner?

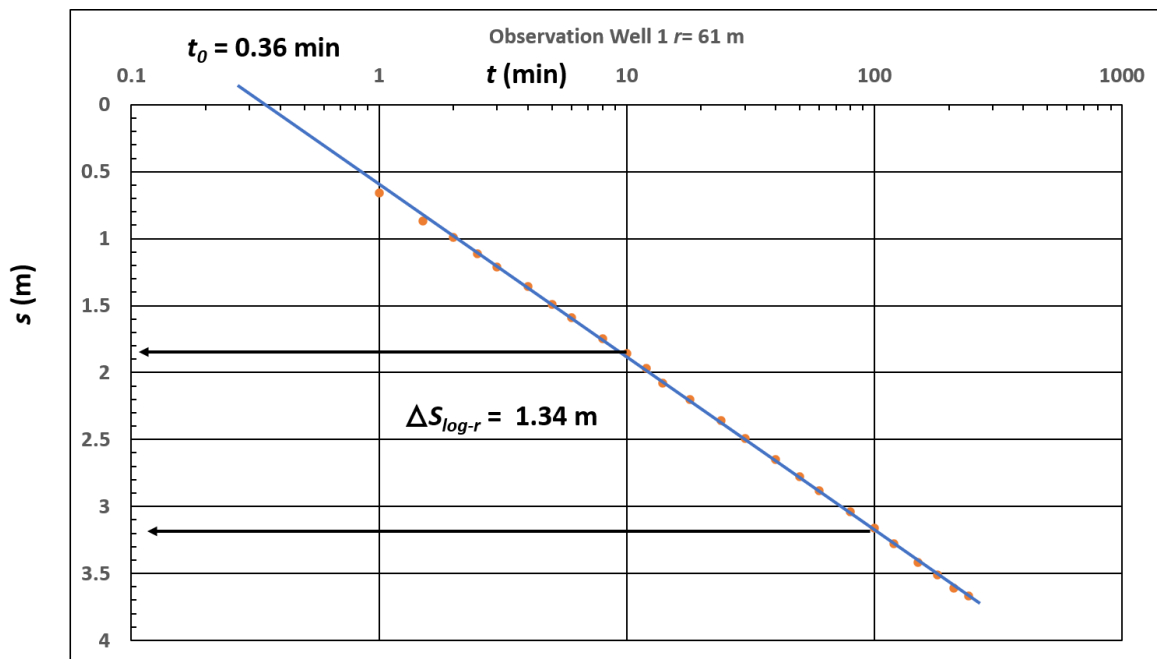
Given that the observation wells are more than two aquifer thicknesses from the pumping well there should not be any partial penetration effects, so if the aquifer is truly isotropic and homogeneous then the values should all be the same. For this example, they are all very close. Differences in computed values may have originated

from errors in field measurements of s , t , and Q , when constructing and matching the curves, and when selecting the match points.

The best way to present the results to the well owner would be to average and round the T and the S values, $T_{avg} = 163 \text{ m}^2/\text{d}$ rounded to $160 \text{ m}^2/\text{d}$; $S_{avg} = 0.000027$ rounded to 0.00003 .

- c) Analysis of pumping a confined aquifer can also be accomplished using the Cooper-Jacob straight line method. The process is to plot the time-drawdown data for the observation well located 122 m from the pumping well as a semi-log plot and determine T and S . Compare these results to the results from the part (a) type curve analyses, and comment on their similarity or differences.

The data set for the observation well located at $r = 122 \text{ m}$ is plotted as a semi-log graph in the image shown here.



Semi log plot of time-drawdown data for $r = 122 \text{ m}$. $\Delta s_{\log-t}$ was determined over one log cycle of time (10 to 100 minutes) and t_0 is derived from where the fitted line crosses the zero-drawdown line.

The applicable Cooper-Jacob approximation is given by Equations (34) and (35) from Section 8.3.2.

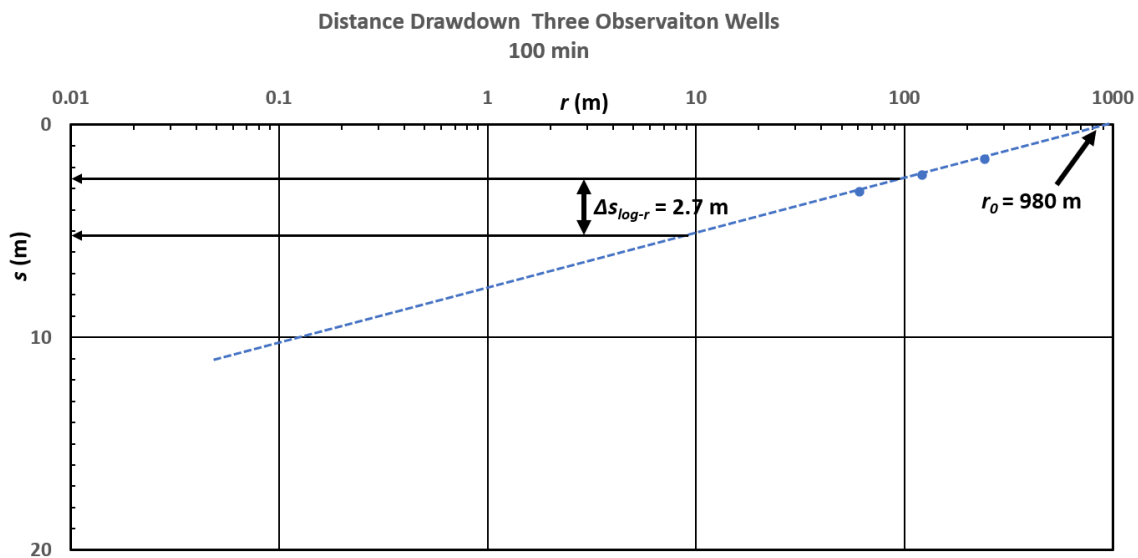
$$T = 2.3 \frac{Q}{4\pi\Delta s} = 2.3 \frac{1200 \frac{\text{m}^3}{\text{d}}}{4 (3.14) 1.34 \text{ m}} = 164 \frac{\text{m}^2}{\text{d}}$$

$$S = 2.25 \frac{Tt_0}{r^2} = 2.25 \frac{164 \frac{m^2}{d} \cdot 0.36 \text{ min} \cdot \frac{1 \text{ d}}{1440 \text{ min}}}{(122 \text{ m})^2} = 0.000006 \text{ or } 6 \times 10^{-6}$$

The T value is very similar to the values computed from curve matching. The storativity is lower than the values derived from the curve match. Both values can be represented by 0.00001.

- d) The confined time-drawdown data can also be interpreted using the distance-drawdown method. Make a semi-log plot of the distance-drawdown data at 100 minutes and calculate T and S. Compare these results to those derived from type curve and time-drawdown straight line analyses. Discuss why the values are similar or different.

A semi-log distance-drawdown plot at 100 min is presented in the image here.



A semi-log distance-drawdown plot of the observation well data at 100 minutes. $\Delta s_{\log-r}$ is computed over one log cycle of distance. A dashed trend line is added. r_0 is the radial distance where drawdown is zero.

The Cooper-Jacob equations used to analyze the distance-drawdown data are Equations (37) and (38) from Section 8.3.3.

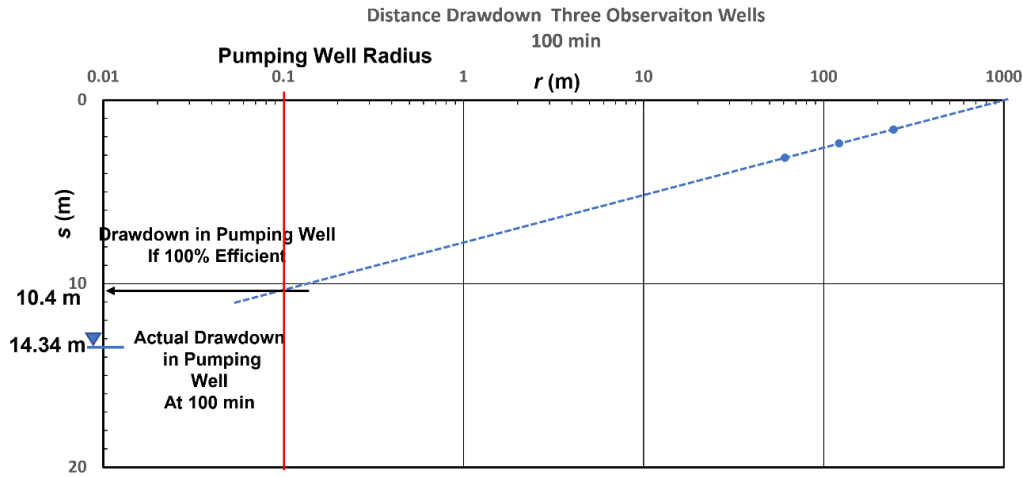
$$T = \frac{2.3 Q}{2 \pi \Delta s_{\log-r}} = \frac{2.3 \left(1200 \frac{m^3}{d}\right)}{2 (3.14) 2.7 \text{ m}} = 163 \frac{m^2}{d}$$

$$S = 2.25 \frac{Tt}{r_0^2} = 2.25 \frac{163 \frac{m^2}{d} \cdot 100 \text{ min} \cdot \frac{1 \text{ d}}{1440 \text{ min}}}{(980 \text{ m})^2} = 0.00003 \text{ or } 3 \times 10^{-5}$$

These values are very similar to those obtained from curve matching and the application of the time-drawdown semi-log plot. The storativity value interpreted from the semi-log, distance-drawdown plot was similar to curve matching results. All in all, the manual plotting and interpretations were very similar.

- e) Using the distance-drawdown plot examine the efficiency of the production well. If the production well diameter is 0.20 m and the drawdown at 100 minutes in the pumping well is 12.34 m, what is the efficiency of the pumping well (i.e., measured drawdown divided by theoretical drawdown)?

The straight trend line on the distance-drawdown plot can be extended to include the radius of the pumping well (0.1 m) as shown below.



Semi-log distance-drawdown plot at 100 minutes used to assess pumping well efficiency. The red line shows the pumping well radius. The corresponding theoretical drawdown (s_F) is 10.4 m.

The efficiency, E , of a pumping well is defined as the theoretical drawdown (s_F) at a fixed time divided by the observed drawdown or total drawdown, s_F/s_T . In this setting the well efficiency equals $10.4 \text{ m} / 14.34 \text{ m} = 0.72$ or 72 percent. The well efficiency represents conditions when the well is pumping at $1,200 \text{ m}^3/\text{d}$. In an inefficient well the amount of well loss that occurs (additional drawdown resulting from the hardware design and pumping rate) increases with the pumping rate. So, if the well yield is increased by 50 percent, a separate analysis would be required to determine the well efficiency at the higher pumping rate.

- f) The well is planned to be used to supplement the city water system. After a seasonal supply evaluation, it was decided to pump the well for 200 days at a constant rate of $1,000 \text{ m}^3/\text{d}$. There are other wells in the area and a regulatory agency wants to know if other wells would be affected when this well is pumped. Ignoring the effects of pumping in the other wells, what is the predicted drawdown 1000 m from the well at the end of the pumping period?

This new discharge rate and pumping schedule can be input into the Theis Equation (Equation (26)) to solve for the drawdown at 1,000 m from the pumping well. Based on the five testing results, using the mean, the transmissivity is set at $163 \text{ m}^2/\text{d}$ and the storativity at 2.3×10^{-5} . First, u , is calculated, then $W(u)$ is read from Figure 26 and drawdown is calculated using Equation (26).

$$u = \frac{r^2 S}{4Tt} = \frac{(1000 \text{ m})^2 0.000023}{4 \left(163 \frac{\text{m}^2}{\text{d}}\right) 200 \text{ d}} = 0.0002$$

Then using Figure 26 to look up, or WolframAlpha to solve $W(u) = -\text{Ei}(-u)$, $W(u)$ is 7.9402.

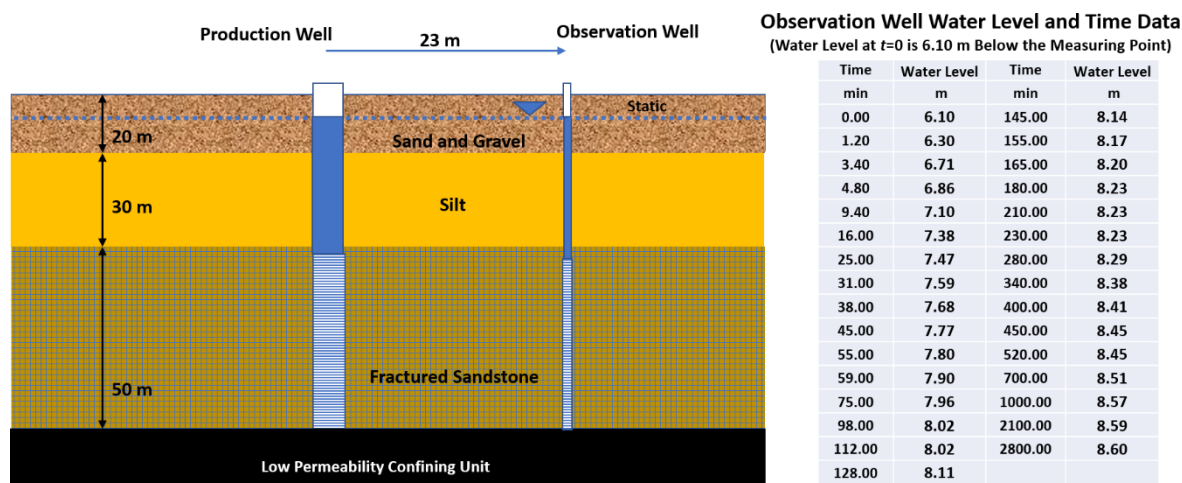
$$s(r, t) = \frac{Q}{4\pi T} W(u) = \frac{1200 \frac{\text{m}^3}{\text{d}}}{4 (3.14) 163 \frac{\text{m}^2}{\text{d}}} 7.9402 = 4.65 \text{ m}$$

[Return to Exercise 2](#) ↑

[Return to where text linked to Exercise 2](#) ↑

Solution Exercise 3

An irrigation well is designed and installed in a 50 m thick highly fractured sandstone that is overlain by 30 m of silt which is in turn overlain by 20 m of sand and gravel. The static water levels in the three units are similar, about 6 m below and surface. The production well is fully penetrating the water producing zone. A 6-cm diameter, fully penetrating, observation well was constructed in the highly fractured sandstone 23 m from the production well. A 1.9-day constant rate pumping test was conducted at a rate of 196 m³/d and the observation well water levels were monitored with an electric water level sensor. The test is illustrated in the image shown here.



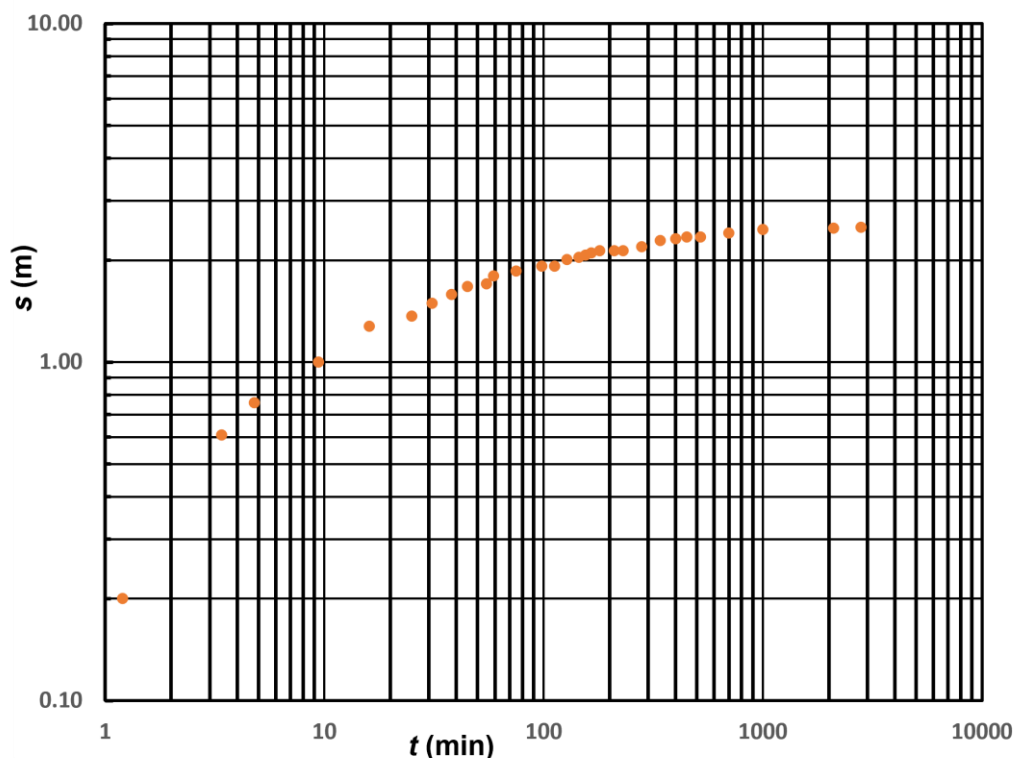
Cross section of hydrogeologic conditions associated with a pumping test. A fractured sandstone is the principal water bearing unit. Static water levels in each unit are about 6 m below land surface. The water level time data collected during the test are shown in the table.

An Excel® data base of the time-drawdown data is available on the [web page for this book](#).

a) Convert the water level data to drawdown and plot the data.

Water level data are converted to drawdown as shown here.

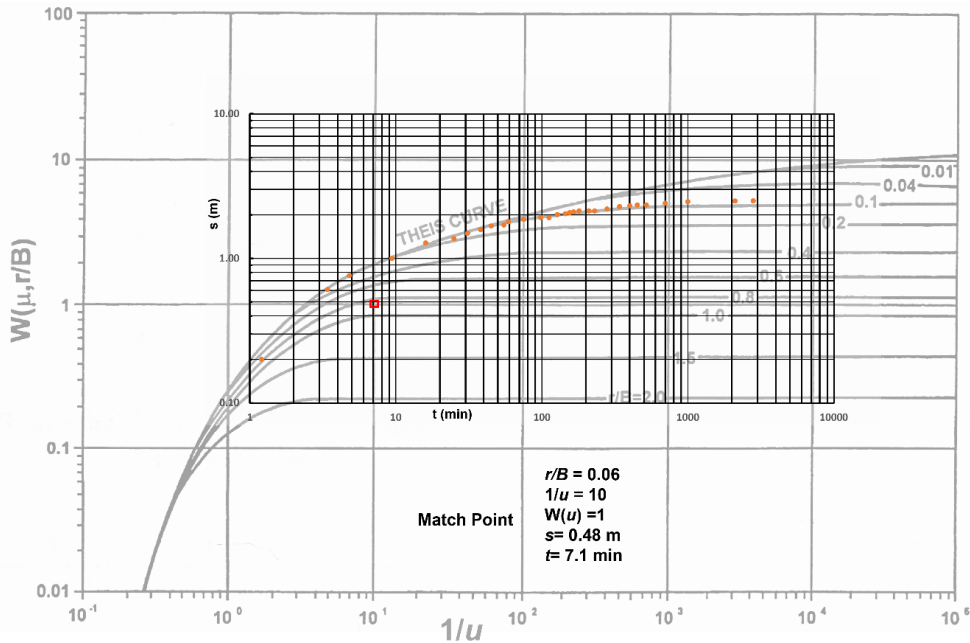
	<i>r</i> = 23 m	
Time	Water Level	Drawdown
min	m	m
0.00	6.10	0.00
1.20	6.30	0.20
3.40	6.71	0.61
4.80	6.86	0.76
9.40	7.10	1.00
16.00	7.38	1.28
25.00	7.47	1.37
31.00	7.59	1.49
38.00	7.68	1.58
45.00	7.77	1.67
55.00	7.80	1.70
59.00	7.90	1.80
75.00	7.96	1.86
98.00	8.02	1.92
112.00	8.02	1.92
128.00	8.11	2.01
145.00	8.14	2.04
155.00	8.17	2.07
165.00	8.20	2.10
180.00	8.23	2.13
210.00	8.23	2.13
230.00	8.23	2.13
280.00	8.29	2.19
340.00	8.38	2.28
400.00	8.41	2.31
450.00	8.45	2.35
520.00	8.45	2.35
700.00	8.51	2.41
1000.00	8.57	2.47
2100.00	8.59	2.49
2800.00	8.60	2.5



Log-log plot of drawdown time data (orange dots) for an observation well located 23 m from the pumping well.

- b) After reviewing the site data, select an analytical approach. Explain why you choose the analytical model used. Treat the highly fractured sandstone as an equivalent porous medium (Woessner & Poeter, 2020). Compute T and S for the highly fractured sandstone aquifer.

The log-log data plot looks like the response of a totally confined aquifer except it does not match the Theis type curve. The drawdown is behaving as if it is affected by an additional source of recharge, most-likely from leakage through the silt confining unit. The log-log plot matches the Hantush-Jacob family of type curves representing leaky conditions without water released from storage as it appears the drawdown is stabilizing over time.



Curve match using Hantush-Jacob type curves. Time-drawdown data are represented by orange dots. The match point is indicated by the red rectangle.

A match point is selected as the data appears to mostly fall along the $r/B = 0.1$ curve.

Equations (45) and (46) are used to compute T and S . Using the match point data shown on the graph.

$$T = \frac{Q}{4\pi s} W\left(u, \frac{r}{B}\right) = \frac{196 \frac{\text{m}^3}{\text{d}}}{4 (3.14) 0.48 \text{ m}} (1) = 32.5 \frac{\text{m}^2}{\text{d}}$$

$$S = \frac{u4Tt}{r^2} = \frac{(0.1) (4) 32.5 \frac{\text{m}^2}{\text{d}} 7.1 \text{ min} \frac{1 \text{ d}}{1440 \text{ min}}}{(23 \text{ m})^2} = 0.00012 \text{ or } 1.2 \times 10^{-4}$$

- c) Based on your analyses, estimate the vertical hydraulic conductivity of the confining silt layer.

Using the match point value of $r/B=0.06$ then

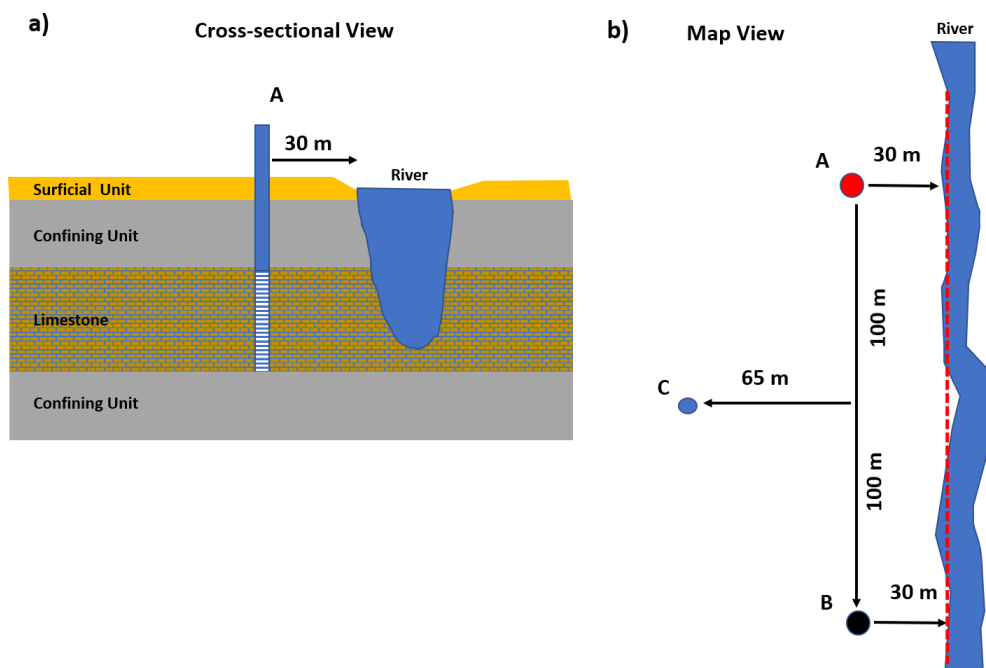
$$K' = \frac{Tb' \left(\frac{r}{B}\right)^2}{r^2} = \frac{32.5 \frac{\text{m}^2}{\text{d}} (30 \text{ m})(0.06)^2}{(23 \text{ m})^2} = 0.0066 \frac{\text{m}}{\text{d}}$$

[Return to Exercise 3 ↑](#)

[Return to where text linked to Exercise 3 ↑](#)

Solution Exercise 4

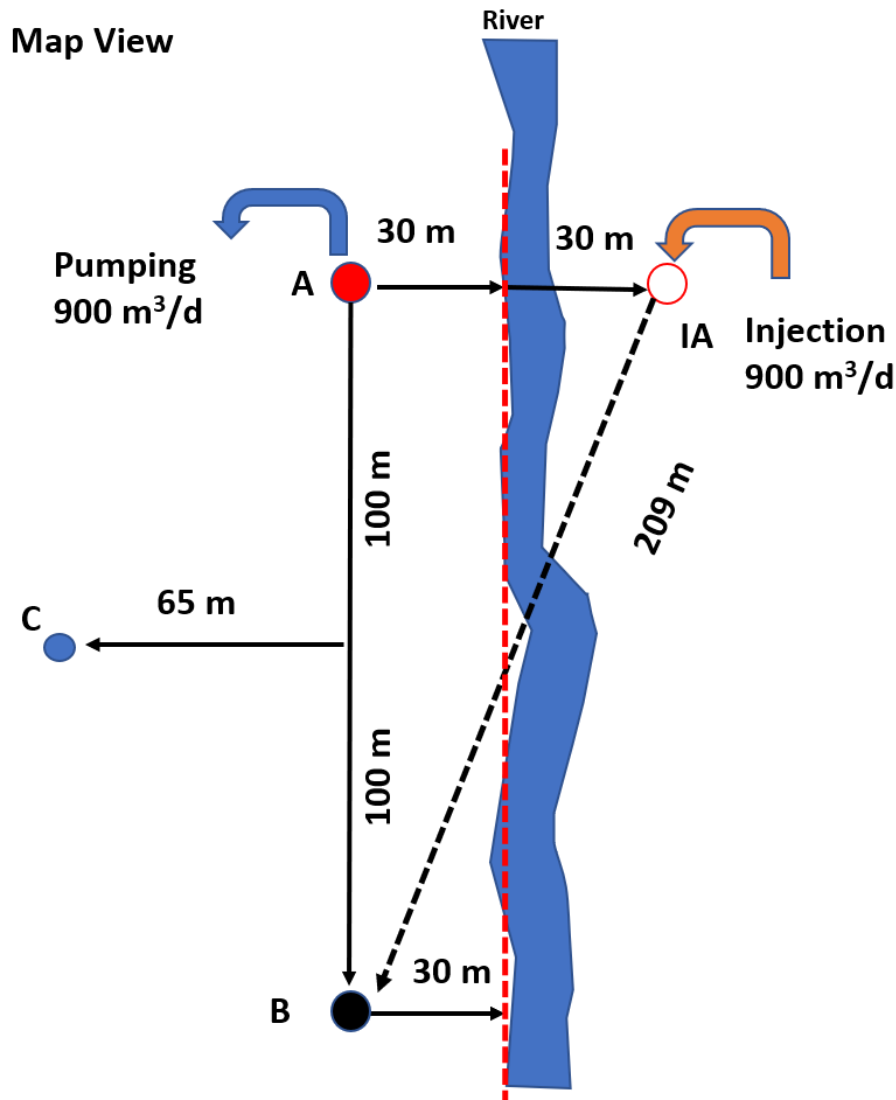
A well (A) pumping at $900 \text{ m}^3/\text{d}$ is located near a river as shown in the image below. The river penetrates a fractured, permeable, confined limestone. A second production well (B) is located 200 m from the first well. A previous pumping test of the formation at well A yielded a T of $75 \text{ m}^2/\text{d}$ and an S of 0.00003.



Production wells located near a fully penetrating river. On average, the distance to the river in the confined aquifer is 30 m from the pumping well as shown by the red dashed line. a) Cross section showing production well A and the lithology. b) Map view of the well locations relative to the river.

- a. Compute the well interference (drawdown) that would occur at B when well A is pumped at $900 \text{ m}^3/\text{d}$ for 50 days.

This problem deals with a linear recharge boundary where the river penetrates the confined aquifer. Using image well theory (Section 11), the river acts as an infinite source of water to the aquifer. To compute the drawdown at well location B the effect of the boundary must be represented by an image well (IA) located 30 m across the boundary from well A. As the image well represents the effects of a recharge boundary it becomes an injection well to mathematically create no drawdown at the boundary (i.e., an injection well has drawup, or negative drawdown) with an inflow of $900 \text{ m}^3/\text{d}$. The total drawdown at B from pumping A and the effects of the recharge boundary must be considered as shown in the image below.



Application of image well theory. Well IA is an image well representing the effect of the linear recharge boundary (river) when A is pumped. The image well is represented by an injection well (-900 m³/d). The figure also shows the radial distance from image well IA to location B.

$$s_T \text{ at } B = s_A + s_{IA}$$

Using the Theis Equation (26), the total drawdown at B can be computed. First, u is calculated, then $W(u)$ is read from Figure 26 and drawdown is calculated using Equation (26).

First, compute u for well A.

$$u_A = \frac{r^2 S}{4Tt} = \frac{(200 \text{ m})^2 \cdot 0.00003}{4 \left(75 \frac{\text{m}^2}{\text{d}}\right) 50 \text{ d}} = 0.00008 \cong 8 \times 10^{-5}$$

Then using Figure 26 to look up, or WolframAlpha to solve $W(u) = -\text{Ei}(-u)$, $W(u_A)$ is $\cong 8.8563$.

$$s_A = \frac{Q}{4\pi T} W(u) = \frac{900 \frac{\text{m}^3}{\text{d}}}{4 (3.14) 75 \frac{\text{m}^2}{\text{d}}} 8.8563 = 8.46 \text{ m}$$

Next, compute u for well IA.

$$u_{IA} = \frac{r^2 S}{4Tt} = \frac{(209 \text{ m})^2 0.00003}{4 \left(75 \frac{\text{m}^2}{\text{d}}\right) 50 \text{ d}} = 0.000087 \cong 8.7 \times 10^{-5}$$

Then using Figure 26, $W(u_{IA})$ is $\cong 8.7725$. As the image well represents a recharge boundary effect the pumping rate is input as $-900 \text{ m}^3/\text{d}$.

$$s_{IA} = \frac{Q}{4\pi T} W(u) = \frac{-900 \frac{\text{m}^3}{\text{d}}}{4 (3.14) 75 \frac{\text{m}^2}{\text{d}}} 8.7725 = -8.38 \text{ m}$$

The “drawdown” computed is negative because it is draw-up or a rise in water level in response to injection of water.

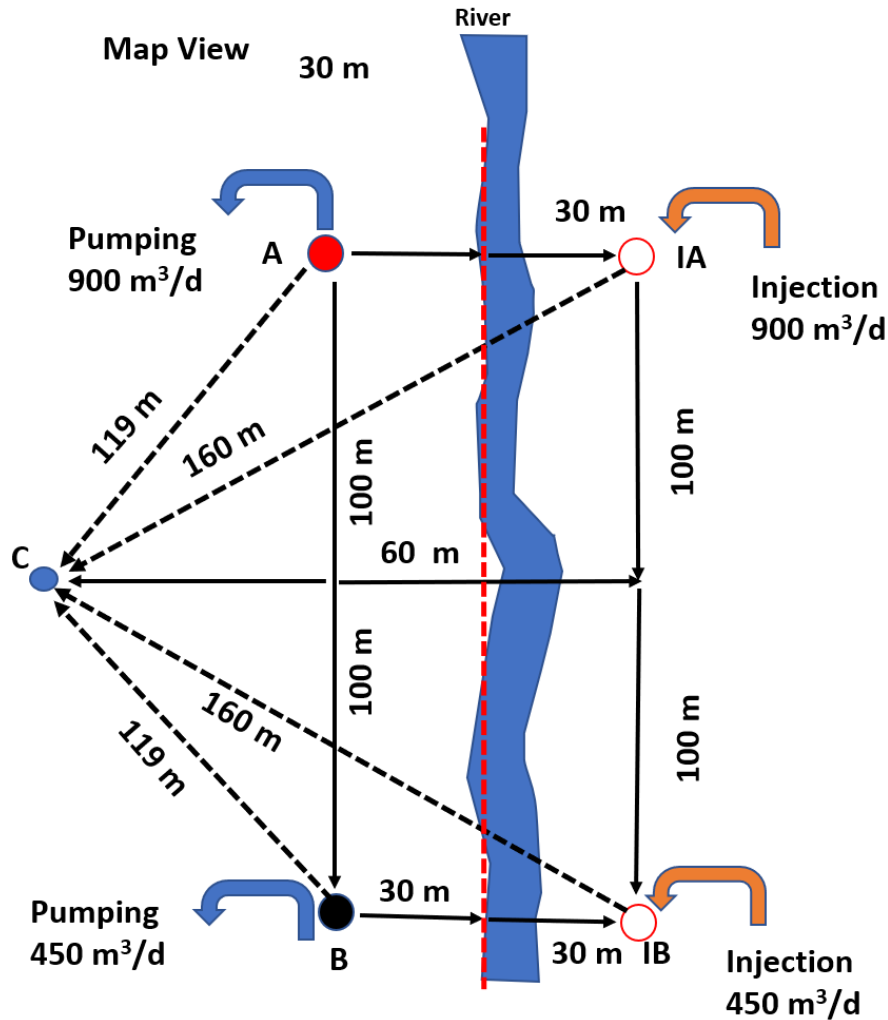
$$s_T \text{ at } B = 8.46 \text{ m} + (-8.38 \text{ m}) = 0.08 \text{ m}$$

- b) If during the same 50 days of pumping well A, the well at location B is pumped at $450 \text{ m}^3/\text{d}$, what would be the drawdown at unpumped observation well C at the end of the 50 days of pumping?

The total drawdown at C would be computed shown here.

$$s_T \text{ at } C = s_A + s_{IA} + s_B + s_{IB}$$

Drawdown at C is influenced by the two pumping wells and the two image wells that represent the recharge boundary. The image well locations and corresponding radial distances are shown in the following image.



Application of image well theory. Well IA is an image well representing the effect of the linear recharge boundary (river) on the drawdown at A and IB is the image well representing the effect of the boundary on the drawdown at B. To calculate the drawdown at the unpumped well located at C, the effect of all four wells must be considered. The calculated radial distances from pumping and image wells to well C are shown on the figure.

The first step is to compute the radial distances from the pumping and image wells to observation well C. Then values of u are computed for each of the 4 wells and corresponding values of $W(u)$ determined from the table shown in Figure 26 of Section 8. Q for the recharge boundary injection wells is input as a negative rate.

$$u_A = \frac{r^2 S}{4Tt} = \frac{(119 \text{ m})^2 \cdot 0.00003}{4 \left(75 \frac{\text{m}^2}{\text{d}}\right) 50 \text{ d}} = 0.000028 \cong 2.8 \times 10^{-5}$$

Then using Figure 26 to look up, or WolframAlpha to solve $W(u) = -\text{Ei}(-u)$, $W(u_A)$ is $\cong 9.9061$.

$$s_A = \frac{Q}{4\pi T} W(u) = \frac{900 \frac{\text{m}^3}{\text{d}}}{4 (3.14) 75 \frac{\text{m}^2}{\text{d}}} 9.9061 = \mathbf{9.46 \text{ m}}$$

$$u_{IA} = \frac{r^2 S}{4Tt} = \frac{(160 \text{ m})^2 0.00003}{4 \left(75 \frac{\text{m}^2}{\text{d}}\right) 50 \text{ d}} = 0.000051 \cong 5.1 \times 10^{-5}$$

Then using Figure 26, $W(u_{IA})$ is $\cong 9.3065$.

$$s_{IA} = \frac{Q}{4\pi T} W(u) = \frac{-900 \frac{\text{m}^3}{\text{d}}}{4 (3.14) 75 \frac{\text{m}^2}{\text{d}}} 9.3065 = \mathbf{-8.89 \text{ m}}$$

$$u_B = \frac{r^2 S}{4Tt} = \frac{(119 \text{ m})^2 0.00003}{4 \left(75 \frac{\text{m}^2}{\text{d}}\right) 50 \text{ d}} = 0.000028 \cong 2.8 \times 10^{-5}$$

Then using Figure 26, $W(u_B)$ is $\cong 9.9061$.

$$s_B = \frac{Q}{4\pi T} W(u) = \frac{450 \frac{\text{m}^3}{\text{d}}}{4 (3.14) 75 \frac{\text{m}^2}{\text{d}}} 9.9061 = \mathbf{4.73 \text{ m}}$$

$$u_{IB} = \frac{r^2 S}{4Tt} = \frac{(160 \text{ m})^2 0.00003}{4 \left(75 \frac{\text{m}^2}{\text{d}}\right) 50 \text{ d}} = 0.000051 \cong 5.1 \times 10^{-5}$$

Then using Figure 26, $W(u_{IB})$ is $\cong 9.3065$.

$$s_{IB} = \frac{Q}{4\pi T} W(u) = \frac{-450 \frac{\text{m}^3}{\text{d}}}{4 (3.14) 75 \frac{\text{m}^2}{\text{d}}} 9.3065 = \mathbf{-4.45 \text{ m}}$$

$$s_T \text{ at } C = s_A + s_{IA} + s_B + s_{IB} = 9.46 \text{ m} + (-8.89 \text{ m}) + 4.73 \text{ m} + (-4.45 \text{ m}) = \mathbf{0.85 \text{ m}}$$

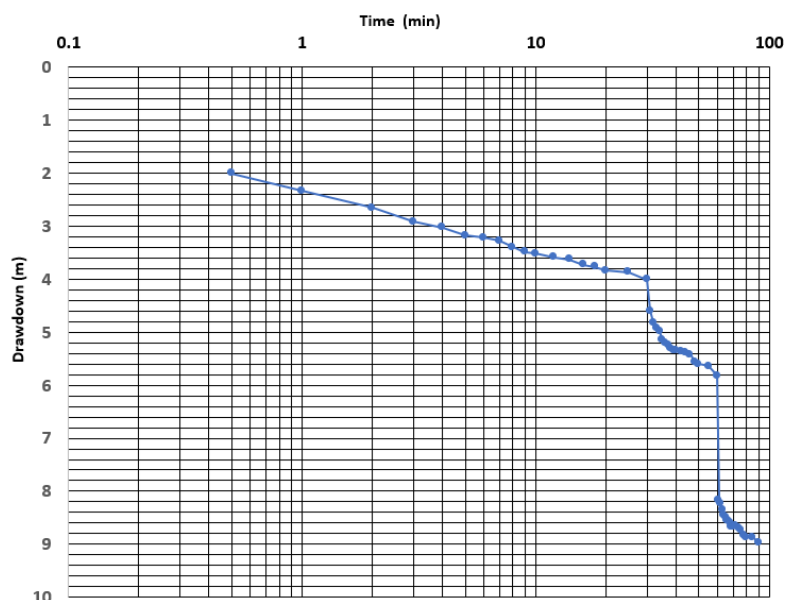
[Return to Exercise 4](#) ↑

[Return to where text linked to Exercise 4](#) ↑

Solution Exercise 5

A production well was designed to yield 2,000 m³/d from a 40 m thick confined gravel-rich aquifer. The well was 40 cm in diameter and screened over 35 m. Once the well was completed, a step test was conducted by pumping the well at 1,400 m³/d, 1,790 m³/d and then 2,520 m³/d for a total of 90 minutes with each step lasting 30 min. The time-drawdown data and a semi-log plot of the time-drawdown data are presented here.

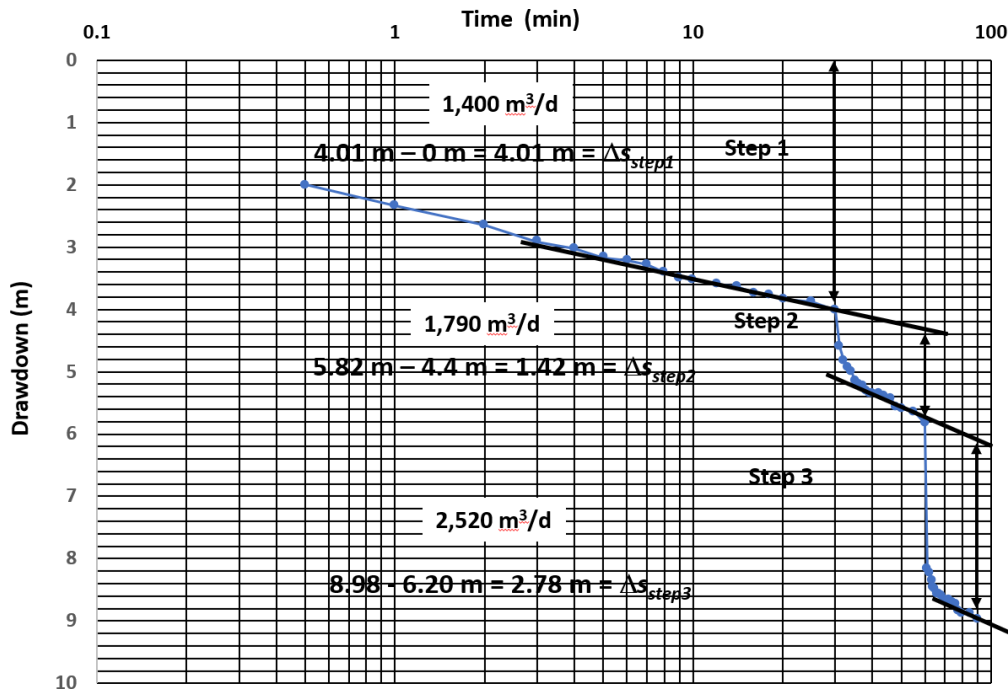
Total Time min	Drawdown m	Total Time min	Drawdown m
0.5	2.00	61	8.17
1	2.33	62	8.24
2	2.65	63	8.35
3	2.91	64	8.45
4	3.02	65	8.49
5	3.17	66	8.56
6	3.22	67	8.56
7	3.28	68	8.59
8	3.4	69	8.67
9	3.49	70	8.67
10	3.52	72	8.66
12	3.59	74	8.7
14	3.63	76	8.73
16	3.73	78	8.84
18	3.77	80	8.87
20	3.84	85	8.87
25	3.87	90	8.98
30	4.01		
31	4.6		
32	4.82		
33	4.92		
34	4.99		
35	5.15		
36	5.2		
37	5.24		
38	5.3		
39	5.35		
40	5.35		
42	5.36		
44	5.38		
46	5.42		
48	5.56		
50	5.6		
55	5.64		
--	--		



Step-drawdown test data for a production well. a) Time-drawdown data for three steps. b) Plot of the log of time versus drawdown.

An Excel® data base of the time-drawdown data is available on the [web page for this book](#).

- a) Calculate the value of C and B for this system. Compute the well loss expected when pumping the well at 2,000 m³/d.



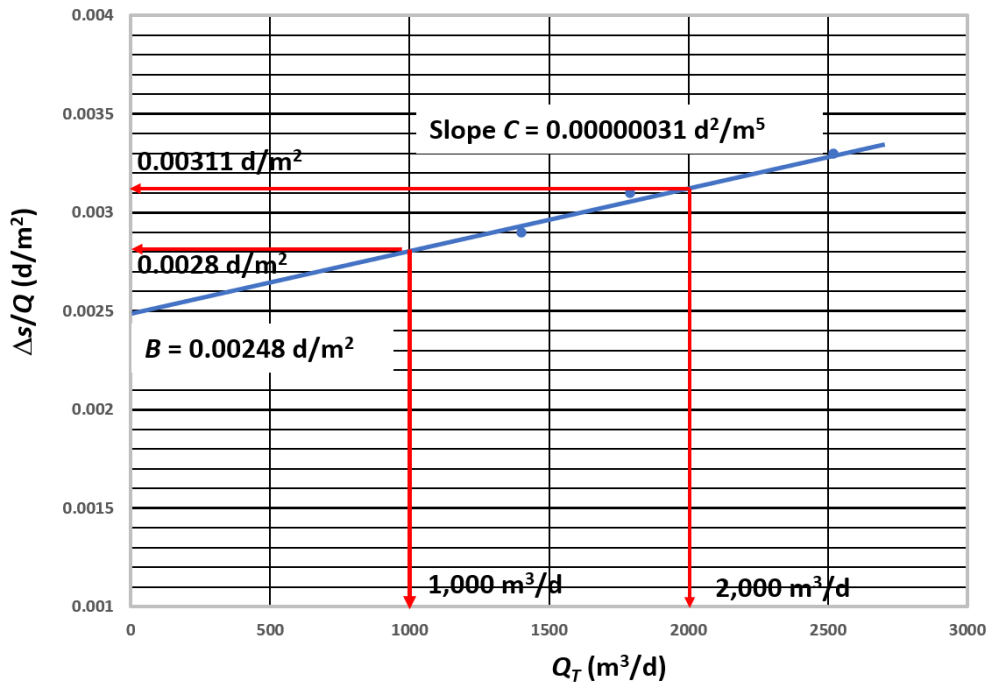
Plot of drawdown versus the log of time showing the calculation of Δs values. Δs_{Step1} for the first 30-minute step is computed as the difference from the drawdown at zero time and the drawdown at 30 min (double arrow). Δs_{Step2} is computed by subtracting the drawdown at 60 min from the extrapolated drawdown value from the first step (double arrow). Δs_{Step3} is computed in a similar fashion from the drawdown at 90 minutes.

A graph of s/Q_T versus total Q is prepared by computing the ratios of $\Delta s/Q$ and Q .

$$\frac{\Delta s_{Step1}}{Q_1} = \frac{4.1 \text{ m}}{1400 \frac{\text{m}^3}{\text{d}}} = 0.0029 \frac{\text{d}}{\text{m}^2}$$

$$\frac{\Delta s_{Step1} + \Delta s_{Step2}}{Q_2} = \frac{4.1 \text{ m} + 1.42 \text{ m}}{1790 \frac{\text{m}^3}{\text{d}}} = 0.003 \frac{\text{d}}{\text{m}^2}$$

$$\frac{\Delta s_{Step1} + \Delta s_{Step2} + \Delta s_{Step3}}{Q_3} = \frac{4.1 \text{ m} + 1.42 \text{ m} + 2.78 \text{ m}}{2520 \frac{\text{m}^3}{\text{d}}} = 0.0033 \frac{\text{d}}{\text{m}^2}$$



Plot of $\Delta s/Q$ versus the log of the corresponding total Q_T for each step. The slope of the line (C) is computed as the difference in the $\Delta s/Q$ values (e.g., horizontal red arrows) divided by the corresponding difference in pumping rate (vertical red arrows).

Reading values to define the slope from the graph, C is determined as follows.

$$C = \frac{0.0031 \frac{d}{m^2} - 0.0028 \frac{d}{m^2}}{2000 \frac{m^3}{d} - 1000 \frac{m^3}{d}} = 0.0000003 \text{ or } 3 \times 10^{-7} \frac{d^2}{m^5}$$

B is read from the graph as the y-intercept at $Q_T = 0$ as $B = 0.00248 \text{ d/m}^2$.

The well loss (CQ^2) when pumping at $2,000 \text{ m}^3/\text{d}$ would be computed as follows.

$$\text{well loss} = 0.0000003 \text{ d}^2/\text{m}^5 (2000 \text{ m}^3/\text{d})^2 = 1.2 \text{ m}$$

b) Estimate the total drawdown after pumping the well for 30 min at $2,000 \text{ m}^3/\text{d}$.

The total drawdown (formational drawdown + well loss) when pumping at $2,000 \text{ m}^3/\text{d}$ for 30 minutes is calculated as follows.

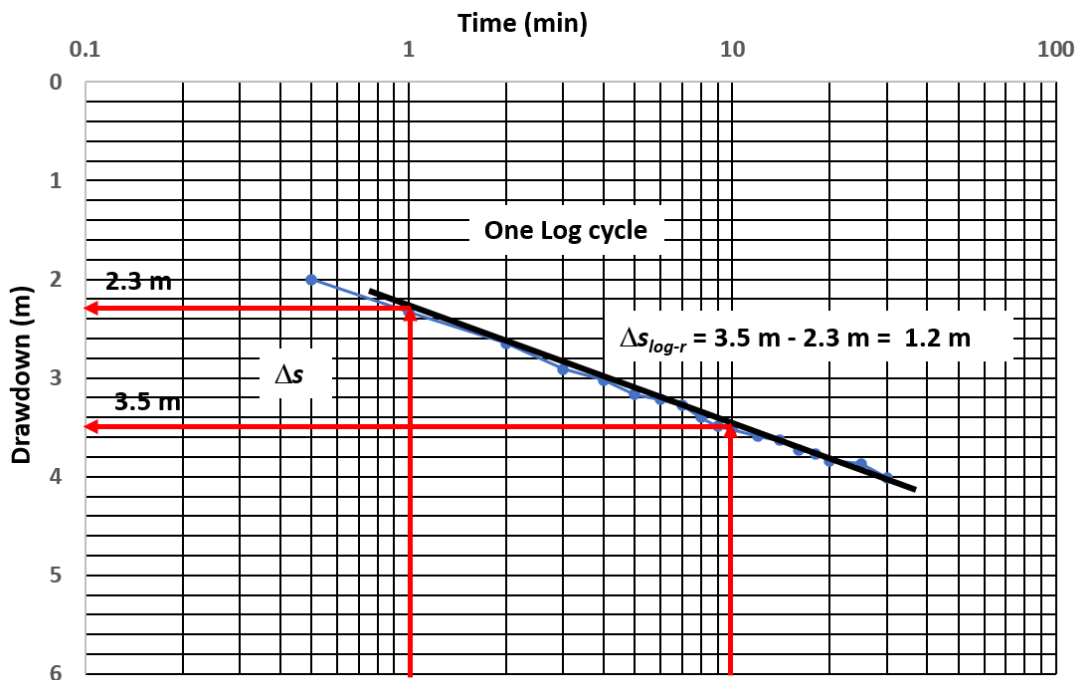
$$s_T = BQ + CQ^2$$

$$s_T = 0.0028 \frac{d}{m^2} \left(2000 \frac{m^3}{d} \right) + 3 \times 10^{-7} \frac{d^2}{m^5} \left(2000 \frac{m^3}{d} \right)^2$$

$$s_T = 5.6 \text{ m} + 1.2 \text{ m} = 6.8 \text{ m}$$

To compute total drawdowns at later times new values of B would need to be determined as B is time dependent. This would require inputting a value of T and S in the appropriate equation (e.g., Cooper-Jacob) and recomputing B for a prescribed period of pumping (t).

- c) Estimate transmissivity using the first 30 minutes of time-drawdown data (step 1) (use the Cooper-Jacob method).



Semi-log plot of the time drawdown data for step one. A straight-line fit is performed and a value of Δs_{log-t} determined. This value is then used in the Cooper-Jacob analysis to estimate a value of T . As the time drawdown data contains some well loss the storage coefficient is not computed.

The Cooper-Jacob solution found in Section 8.2.3.

$$T = 2.3 \frac{Q}{4\pi \Delta s \Delta s_{log-t}} = 2.3 \frac{1400 \frac{m^3}{d}}{4 (3.14) 1.2 \text{ m}} = 214 \frac{m^2}{d}$$

The time drawdown data in step one has some well loss so T can be determined but S is not estimated as the projected t_0 value would be too low (Section 12.1.4). If all the step 1 data were corrected for well loss ($s_T - CQ^2$) S could be computed from

a semi-log plot of the corrected data. For example, at 10 min the recorded drawdown is 3.52 m. The corrected drawdown (s) would be as follows.

$$s = 3.52 \text{ m} - 3 \times 10^{-7} \frac{\text{d}^2}{\text{m}^5} \left(1400 \frac{\text{m}^3}{\text{d}} \right)^2 = 2.93 \text{ m}$$

[Return to Exercise 5](#) ↑

[Return to where text linked to Exercise 5](#) ↑

Solution Exercise 6

A discussion of interpreting single well pumping tests methods used to evaluate a well performance test is presented (Section 12). Though performance test data has limitations (e.g., uncertainty related to: the nature and location of water bearing units in the well, pumping water levels, and well loss during pumping), approximations of T can be made. Most commonly, performance test data are found on driller’s logs when a well is constructed. Review the well log presented in the image below.

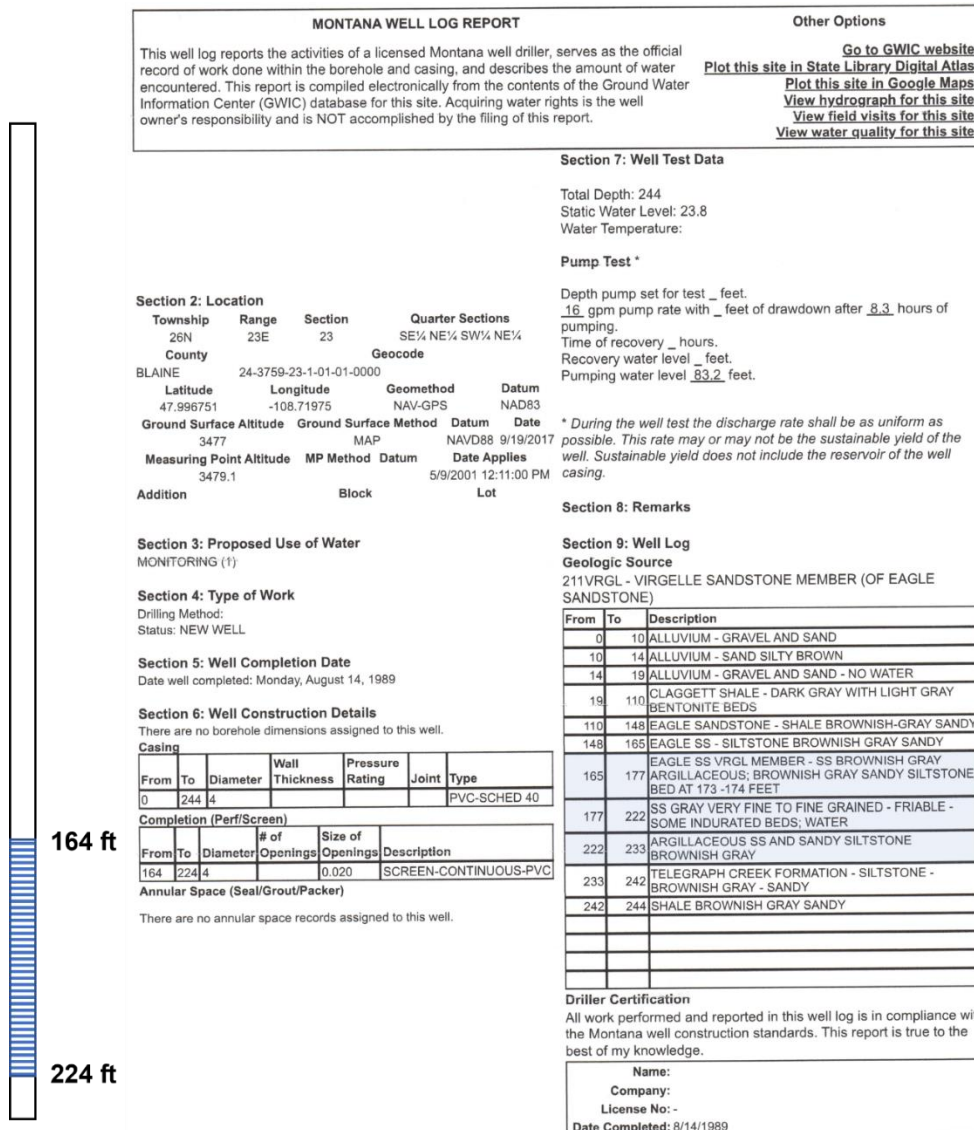
MONTANA WELL LOG REPORT						Other Options																																					
This well log reports the activities of a licensed Montana well driller, serves as the official record of work done within the borehole and casing, and describes the amount of water encountered. This report is compiled electronically from the contents of the Ground Water Information Center (GWIC) database for this site. Acquiring water rights is the well owner’s responsibility and is NOT accomplished by the filing of this report.						Go to GWIC website Plot this site in State Library Digital Atlas Plot this site in Google Maps View hydrograph for this site View field visits for this site View water quality for this site																																					
Section 2: Location						Section 7: Well Test Data																																					
Township	Range	Section	Quarter Sections			Total Depth: 244 Static Water Level: 23.8 Water Temperature: Pump Test * Depth pump set for test _ feet. .16 gpm pump rate with _ feet of drawdown after <u>8.3</u> hours of pumping. Time of recovery _ hours. Recovery water level _ feet. Pumping water level <u>83.2</u> feet.																																					
26N	23E	23	SE¼ NE¼ SW¼ NE¼																																								
County		Geocode																																									
BLAINE		24-3759-23-1-01-01-0000			* During the well test the discharge rate shall be as uniform as possible. This rate may or may not be the sustainable yield of the well. Sustainable yield does not include the reservoir of the well casing.																																						
Latitude	Longitude	Geomethod	Datum																																								
47.996751	-108.71975	NAV-GPS	NAD83																																								
Ground Surface Altitude		Ground Surface Method	Datum	Date		Section 8: Remarks																																					
3477		MAP	NAVD88	9/19/2017																																							
Measuring Point Altitude	MP Method	Datum	Date Applies																																								
3479.1			5/9/2001 12:11:00 PM		Section 9: Well Log																																						
Addition		Block	Lot				Geologic Source 211VRGL - VIRGELLE SANDSTONE MEMBER (OF EAGLE SANDSTONE)																																				
Section 3: Proposed Use of Water						<table border="1" style="width: 100%; border-collapse: collapse; font-size: x-small;"> <thead> <tr> <th>From</th> <th>To</th> <th>Description</th> </tr> </thead> <tbody> <tr><td>0</td><td>10</td><td>ALLUVIUM - GRAVEL AND SAND</td></tr> <tr><td>10</td><td>14</td><td>ALLUVIUM - SAND SILTY BROWN</td></tr> <tr><td>14</td><td>19</td><td>ALLUVIUM - GRAVEL AND SAND - NO WATER</td></tr> <tr><td>19</td><td>110</td><td>CLAGGETT SHALE - DARK GRAY WITH LIGHT GRAY BENTONITE BEDS</td></tr> <tr><td>110</td><td>148</td><td>EAGLE SANDSTONE - SHALE BROWNISH-GRAY SANDY</td></tr> <tr><td>148</td><td>165</td><td>EAGLE SS - SILTSTONE BROWNISH GRAY SANDY</td></tr> <tr><td>165</td><td>177</td><td>EAGLE SS VRGL MEMBER - SS BROWNISH GRAY ARGILLACEOUS; BROWNISH GRAY SANDY SILTSTONE BED AT 173 -174 FEET</td></tr> <tr><td>177</td><td>222</td><td>SS GRAY VERY FINE TO FINE GRAINED - FRIABLE - SOME INDURATED BEDS; WATER</td></tr> <tr><td>222</td><td>233</td><td>ARGILLACEOUS SS AND SANDY SILTSTONE BROWNISH GRAY</td></tr> <tr><td>233</td><td>242</td><td>TELEGRAPH CREEK FORMATION - SILTSTONE - BROWNISH GRAY - SANDY</td></tr> <tr><td>242</td><td>244</td><td>SHALE BROWNISH GRAY SANDY</td></tr> </tbody> </table>		From	To	Description	0	10	ALLUVIUM - GRAVEL AND SAND	10	14	ALLUVIUM - SAND SILTY BROWN	14	19	ALLUVIUM - GRAVEL AND SAND - NO WATER	19	110	CLAGGETT SHALE - DARK GRAY WITH LIGHT GRAY BENTONITE BEDS	110	148	EAGLE SANDSTONE - SHALE BROWNISH-GRAY SANDY	148	165	EAGLE SS - SILTSTONE BROWNISH GRAY SANDY	165	177	EAGLE SS VRGL MEMBER - SS BROWNISH GRAY ARGILLACEOUS; BROWNISH GRAY SANDY SILTSTONE BED AT 173 -174 FEET	177	222	SS GRAY VERY FINE TO FINE GRAINED - FRIABLE - SOME INDURATED BEDS; WATER	222	233	ARGILLACEOUS SS AND SANDY SILTSTONE BROWNISH GRAY	233	242	TELEGRAPH CREEK FORMATION - SILTSTONE - BROWNISH GRAY - SANDY	242	244	SHALE BROWNISH GRAY SANDY
From	To	Description																																									
0	10	ALLUVIUM - GRAVEL AND SAND																																									
10	14	ALLUVIUM - SAND SILTY BROWN																																									
14	19	ALLUVIUM - GRAVEL AND SAND - NO WATER																																									
19	110	CLAGGETT SHALE - DARK GRAY WITH LIGHT GRAY BENTONITE BEDS																																									
110	148	EAGLE SANDSTONE - SHALE BROWNISH-GRAY SANDY																																									
148	165	EAGLE SS - SILTSTONE BROWNISH GRAY SANDY																																									
165	177	EAGLE SS VRGL MEMBER - SS BROWNISH GRAY ARGILLACEOUS; BROWNISH GRAY SANDY SILTSTONE BED AT 173 -174 FEET																																									
177	222	SS GRAY VERY FINE TO FINE GRAINED - FRIABLE - SOME INDURATED BEDS; WATER																																									
222	233	ARGILLACEOUS SS AND SANDY SILTSTONE BROWNISH GRAY																																									
233	242	TELEGRAPH CREEK FORMATION - SILTSTONE - BROWNISH GRAY - SANDY																																									
242	244	SHALE BROWNISH GRAY SANDY																																									
MONITORING (1)																																											
Section 4: Type of Work						Driller Certification All work performed and reported in this well log is in compliance with the Montana well construction standards. This report is true to the best of my knowledge.																																					
Drilling Method:																																											
Status: NEW WELL																																											
Section 5: Well Completion Date						<table border="1" style="width: 100%; border-collapse: collapse; font-size: x-small;"> <thead> <tr> <th>From</th> <th>To</th> <th>Diameter</th> <th>Wall Thickness</th> <th>Pressure Rating</th> <th>Joint</th> <th>Type</th> </tr> </thead> <tbody> <tr> <td>0</td> <td>244</td> <td>4</td> <td></td> <td></td> <td></td> <td>PVC-SCHED 40</td> </tr> </tbody> </table>		From	To	Diameter	Wall Thickness	Pressure Rating	Joint	Type	0	244	4				PVC-SCHED 40																						
From	To	Diameter	Wall Thickness	Pressure Rating	Joint			Type																																			
0	244	4						PVC-SCHED 40																																			
Date well completed: Monday, August 14, 1989																																											
Section 6: Well Construction Details						Name: Company: License No: - Date Completed: 8/14/1989																																					
There are no borehole dimensions assigned to this well.																																											
Casing																																											
<table border="1" style="width: 100%; border-collapse: collapse; font-size: x-small;"> <thead> <tr> <th>From</th> <th>To</th> <th>Diameter</th> <th>Wall Thickness</th> <th>Pressure Rating</th> <th>Joint</th> <th>Type</th> </tr> </thead> <tbody> <tr> <td>0</td> <td>244</td> <td>4</td> <td></td> <td></td> <td></td> <td>PVC-SCHED 40</td> </tr> </tbody> </table>						From	To	Diameter	Wall Thickness	Pressure Rating	Joint	Type	0	244	4				PVC-SCHED 40																								
From	To	Diameter	Wall Thickness	Pressure Rating	Joint	Type																																					
0	244	4				PVC-SCHED 40																																					
Completion (Perf/Screen)						There are no annular space records assigned to this well.																																					
<table border="1" style="width: 100%; border-collapse: collapse; font-size: x-small;"> <thead> <tr> <th>From</th> <th>To</th> <th>Diameter</th> <th># of Openings</th> <th>Size of Openings</th> <th>Description</th> </tr> </thead> <tbody> <tr> <td>164</td> <td>224</td> <td>4</td> <td></td> <td>0.020</td> <td>SCREEN-CONTINUOUS-PVC</td> </tr> </tbody> </table>								From	To	Diameter	# of Openings	Size of Openings	Description	164	224	4		0.020	SCREEN-CONTINUOUS-PVC																								
From	To	Diameter	# of Openings	Size of Openings	Description																																						
164	224	4		0.020	SCREEN-CONTINUOUS-PVC																																						
Annular Space (Seal/Grout/Packer)																																											

Example of a driller’s well log report for the completion of a well in Montana, USA. All length units are reported in feet and pumping rate is in gallons per minute. This log provides information on the static water level at the time of drilling, performance testing data including a pumping rate, length of the test, and the pumping level at the end of the test. It also shows a geologic log of the borehole. The owner of the well has been deleted from the figure.

Using this driller’s log answer the following questions:

- a) What depth interval and geologic material did the driller perforate to produce water to the well?

As shown in the image below, the perforated interval is screened with a continuous screen between 164 and 224 feet (50-68 m). Geologically, this includes much of the Eagle Sandstone formation.



Well log showing the location of the screened interval and the corresponding geologic formations producing water (light blue shading). All units are in feet and discharge is in gallons per minute.

- b) Is this water producing unit likely confined or unconfined? Support your answer.

The water bearing zone is overlain by almost 100 feet (33 m) of shale and the static water level of the screened interval is above the top of the sandstone hydrogeologic unit (23.8 feet, 7.3 m). The presence of the confining shale and the position of the potentiometric surface supports that the water bearing unit is confined.

- c) Examine the static water level and performance test information, compute the specific capacity of the well.

The specific capacity is defined by Equation (99).

$$\text{Specific Capacity} = \frac{Q}{S_F}$$

In this case, the pumping rate is 16 gallons per minute (60.5 L/min), and the drawdown is 83.2 feet - 23.8 feet = 59.4 feet (18.1 m).

$$\text{Specific Capacity} = \frac{16 \frac{\text{gallons}}{\text{minute}}}{59.4 \text{ feet}} = \frac{0.27 \text{ gpm}}{\text{foot}}$$

$$\text{Specific Capacity} = \frac{60.5 \frac{\text{liters}}{\text{minute}} \frac{1 \text{ m}^3}{1000 \text{ liters}} \frac{1440 \text{ minute}}{1 \text{ d}}}{18.1 \text{ m}} = \frac{4.8 \frac{\text{m}^3}{\text{d}}}{\text{m}}$$

- d) Based on the pumping data recorded by the driller, estimate the transmissivity of the aquifer using two methods. When applying each method justify your approach.

- 1) Method 1: Assume the pumping has not proceeded to a steady state.

The Cooper-Jacob approximation method presented in Equation (101) can be used to estimate T in terms of the specific capacity.

$$\frac{Q}{s} = \frac{1}{\frac{1}{4\pi T} 2.30 \log \left(2.25 \frac{Tt}{r_w^2 S} \right)}$$

Well specific data include, $r_w = 4 \text{ inches}/2$, and $2 \text{ in} = 0.05 \text{ m}$, and $t = 8.3 \text{ h} = 0.125 \text{ d}$. The storativity is estimated for the sandstone (i.e., sound rock) based on concepts presented in Box 2 of Section 20 and using the data presented in Table Box 2-2 ($S_s = 3.24 \times 10^{-6} \text{ m}^{-1}$).

$$S = S_s b$$

The water bearing unit thickness, b , is assumed to be approximated by the screened interval, 224 feet - 164 feet = 60 feet (18.3 m).

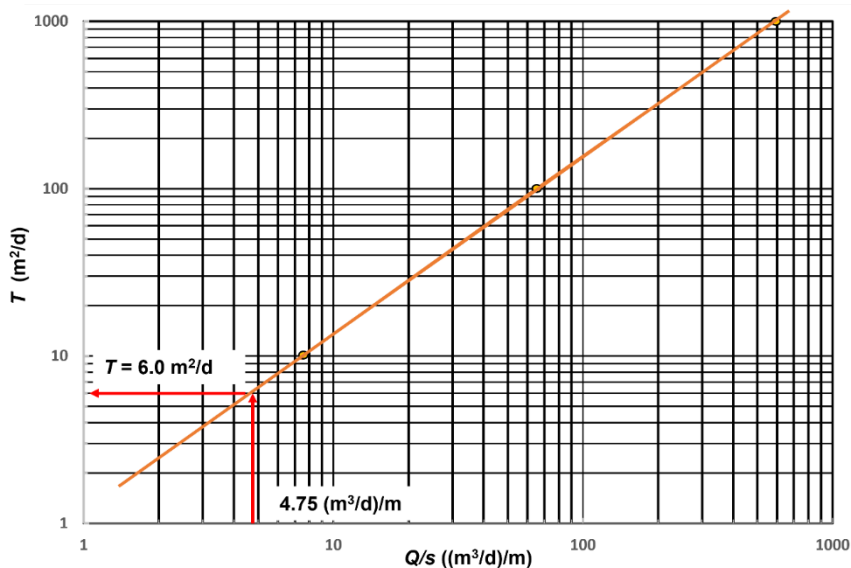
$$S = \frac{0.00000324}{m} (18.3 \text{ m}) = 0.00006$$

Then values of T are input and corresponding values of Q/s generated, then the results are plotted as a log-log plot of T versus Q/s in the image following the calculations.

$$\frac{Q}{s} = \frac{1}{\frac{1}{4(3.14)10 \frac{\text{m}^2}{\text{d}}} 2.30 \log \left\{ 2.25 \frac{10 \frac{\text{m}^2}{\text{d}} 0.125 \text{ d}}{(0.05 \text{ m})^2 (0.00006)} \right\}} = \frac{7.5 \frac{\text{m}^3}{\text{d}}}{\text{m}}$$

$$\frac{Q}{s} = \frac{1}{\frac{1}{4(3.14)100 \frac{\text{m}^2}{\text{d}}} 2.30 \log \left\{ 2.25 \frac{100 \frac{\text{m}^2}{\text{d}} 0.125 \text{ d}}{(0.05 \text{ m})^2 (0.00006)} \right\}} = \frac{66 \frac{\text{m}^3}{\text{d}}}{\text{m}}$$

$$\frac{Q}{s} = \frac{1}{\frac{1}{4(3.14)1000 \frac{\text{m}^2}{\text{d}}} 2.30 \log \left\{ 2.25 \frac{1000 \frac{\text{m}^2}{\text{d}} 0.125 \text{ d}}{(0.05 \text{ m})^2 (0.00006)} \right\}} = \frac{589 \frac{\text{m}^3}{\text{d}}}{\text{m}}$$



Log-log plot of T versus Q/s for the well presented on the driller's log. The Cooper-Jacob method was used to calculate values of Q/s for $T=10, 100,$ and $1,000 \text{ m}^2/\text{d}$. The values were plotted. The orange line is a straight-line fit to the data.

The specific capacity of the well is $4.75 \text{ (m}^3/\text{d)}/\text{m}$ and the value of T is read from the graph for that specific capacity as $T = 6.0 \text{ m}^2/\text{d}$.

- 2) Method 2: Assume the pumping has resulted in near steady state conditions (simple equation approximation).

As discussed in Section 12 and presented by Equation (102), T for confined conditions can be estimated as follows.

$$T = 1.39 \left(\frac{Q}{s} \right) = 1.39 \left(\frac{4.8 \frac{\text{m}^3}{\text{d}}}{\text{m}} \right) = 6.7 \frac{\text{m}^2}{\text{d}}$$

This equation assumes Q/s is a constant as it would be for steady state conditions. This value is close to the previous transient analyses, possibly because the pumping level was near steady state.

- e) When you only have performance data for a single pumping well do you anticipate the formational values of T will be greater or less than the values you computed? Why?

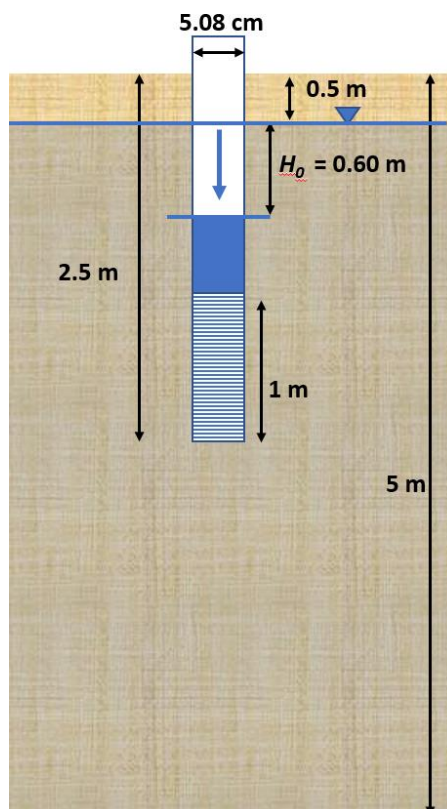
Generally, performance test data contain well loss and, depending on the well design, effects of partial penetration. One or both conditions would result in reported drawdown being greater than if the well was 100 percent efficient and fully penetrating (perforations greater than 80 to 85 percent of the unit thickness). This well would be considered fully penetrating. However, the effect of well loss is unknown. Thus, the drawdown likely includes well loss. Thus, an estimate of T is likely less than the formational T because Q/s would be smaller than if no well loss occurred.

[Return to Exercise 6 ↑](#)

[Return to where text linked to Exercise 6 ↑](#)

Solution Exercise 7

A monitoring well that is 5.08 cm in diameter was installed in an unconfined silt-rich formation that is 5 m thick. The base of the well screen is located 2.5 m below the land surface and is 1 m long. The water table is 0.5 m below land surface. A slug out test was performed on this well as illustrated in the image below.



Time	Lowered Water Level
s	m
0	0.6
27	0.55
48	0.51
70	0.48
97	0.44
139	0.39
172	0.34
230	0.3
268	0.26
303	0.23
355	0.19
420	0.16
477	0.13
547	0.1
633	0.08

Slug out test conducted in a silt-rich unconfined formation. a) Unpumped well design and location of screened interval. The slug test was conducted by lowering the water level by 0.6 m. This is the water level at the start of the test (H_0). b) After 10.5 minutes (633 s) the water level had recovered within 0.08 m of the static water elevation (modified from Todd and Mays, 2005).

An Excel® data base of the time-drawdown data is available on the [web page for this book](#).

- Select an appropriate method to analyze the slug test data. Explain your choice.
- Use this method to calculate K.

As the slug test results are overdamped, either the Hvorslev method or Bouwer and Rice method would be applicable as discussed in Section 14. They both can be applied to unconfined conditions. The Hvorslev method is used for this solution.

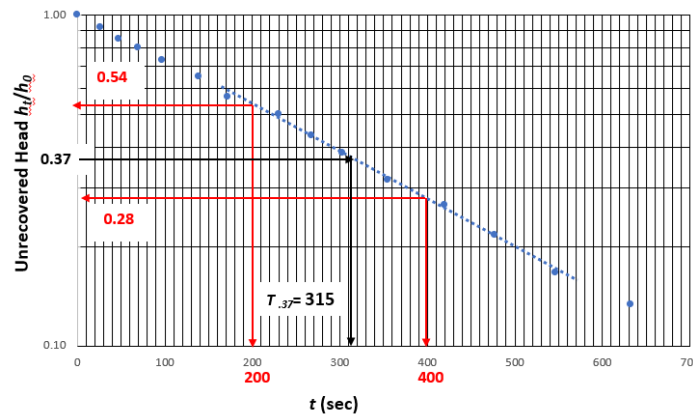
The Hvorslev method can be defined using the slope of the unrecovered data plot or the $T_{0.37}$ time as shown in Equations (107) and (108).

$$K = \frac{r_c^2 \ln\left(\frac{L_e}{r_s}\right)}{2 L_e (t_2 - t_1)} \ln\left(\frac{h_1}{h_2}\right)$$

$$K = \frac{r_c^2 \ln\left(\frac{L_e}{r_s}\right)}{2 L_e T_{.37}}$$

A plot of the unrecovered head data is plotted against time as shown here.

Time	h_t/h_0
Sec	
0	1.00
27	0.92
48	0.85
70	0.80
97	0.73
139	0.65
172	0.57
230	0.50
268	0.43
303	0.38
355	0.32
420	0.27
477	0.22
547	0.17
633	0.13



Slug test data and plot. a) Water level data converted to the ratio of unrecovered head ($H_0 = 0.6$ m). b) Semi-log plot of unrecovered head ratio versus time. The solid black line is fitted to the data.

Parameters for the Hvorslev equations are calculated and listed here.

$$r_c = r_s = \frac{5.08 \text{ cm}}{2} = 2.54 \text{ cm}$$

L_e is the length of the screen.

$$L_e = 1 \text{ m}$$

$$\frac{h_1}{h_2} = \frac{0.54 \text{ m}}{0.28 \text{ m}} = 1.9$$

$$t_2 - t_1 = 400 \text{ sec} - 200 \text{ sec} = 200 \text{ sec} \frac{1 \text{ d}}{86400 \text{ sec}} = 0.0023 \text{ d}$$

$$K = \frac{r_c^2 \ln\left(\frac{L_e}{r_s}\right)}{2 L_e (t_2 - t_1)} \ln\left(\frac{h_1}{h_2}\right) = \frac{(0.0254 \text{ m})^2 \ln\left(\frac{1}{0.0254 \text{ m}}\right)}{2 (1 \text{ m}) (0.0023 \text{ d})} \ln(1.9) = 0.33 \frac{\text{m}}{\text{d}}$$

Then computing K using $T_{0.37} = 309$ sec as read from the graph.

$$T_{.37} = 309 \text{ sec} \frac{1 \text{ d}}{86400 \text{ sec}} = 0.0036 \text{ d}$$

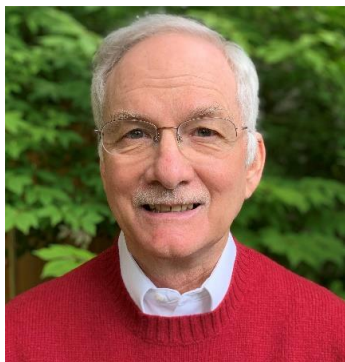
$$K = \frac{r_c^2 \ln\left(\frac{L_e}{r_s}\right)}{2 L_e T_{.37}} = \frac{(0.0254 \text{ m})^2 \ln\left(\frac{1}{0.0254 \text{ m}}\right)}{2 (1 \text{ m}) (0.0036 \text{ d})} = 0.33 \frac{\text{m}}{\text{d}}$$

In this example, the two approaches yield identical values of K.

[Return to Exercise 7](#) ↑

[Return to where text linked to Exercise 7](#) ↑

22 About the Authors



William W. Woessner, PhD, is a Montana University System Emeritus Regents' Professor of Hydrogeology. He taught introductory and graduate courses in the hydrogeological sciences including well design and hydraulic testing for over 30 years at the University of Montana, Missoula, USA. Professor Woessner is the Past Acting Director of the Center for Riverine Science and Stream Re-naturalization, and President of Woessner Hydrologic, LLC. He has mentored over 60 graduate students, many of whom have founded environmental consulting firms; worked for environmental non-profits; local, state, and federal agencies, and corporations. He has designed and installed production wells, hundreds of monitoring wells, and executed hydraulic testing of confined, leaky, and water table systems. Professor Woessner is well versed in field methods and application of modeling tools. He is the coauthor of two editions of *Applied Groundwater Modeling: Simulation of Flow and Advective Transport*. He served as a 2011 Fulbright Scholar-NAWI Austria. Professor Woessner is a Fellow of the Geological Society of America, served as the Geological Society of America Hydrogeology Division Birdsall-Dreiss Lecturer in 2005, and received the society's 2020 O. E. Meinzer Award. In addition, he is a Fellow and Life Member of the National Groundwater Association and was awarded the John Hem Excellence in Science and Engineering Award in 2008. He also authored two earlier Groundwater Project books: *Hydrogeologic Properties of Earth Materials and Principles of Groundwater Flow* (Woessner & Poeter, 2020) and *Groundwater - Surface Water Exchange* (Woessner, 2020).



A. Campbell Stringer, MS, PG, is a Principal Hydrogeologist with NewFields in Missoula, Montana, USA. Cam has over 30 years of consulting experience in hydrogeology; aquifer characterization; aquifer testing; water rights; public water supply development; remedial investigation; landfill permitting; mine permitting and remediation; corrective measure implementation; Comprehensive Environmental Response, Compensation and Liability Act (CERCLA); NEPA analysis; remedial investigation; and municipal water supply exploration, installation, and permitting. He has worked on projects across the USA and internationally on sites impacted by halogenated organic solvents, petroleum hydrocarbon fuels, radioactive elements, metals, and inorganic ions. Cam specializes in conceptual model development, 3-D groundwater modeling, groundwater-surface water interaction, multi-phase fluid flow, contaminant fate and transport theory, and natural attenuation of organic contaminants. He has developed numerical regional and local scale models for water rights applications, mines, electrical generation facilities, superfund sites, petroleum release sites,

350

uranium mill sites. Cam has extensive experience in the mining industry, providing services ranging from permitting new mines, developing water management and closure plans at active mines, and remediating legacy mines. He currently serves as a member of Independent Tailings Review Boards for mines in South America.



Eileen P. Poeter, P.E., is an Emeritus Professor of Geological Engineering at Colorado School of Mines where she taught groundwater courses and advised more than 40 graduate students who worked with her on groundwater system investigations and modeling research projects. She is also past director of the Integrated Groundwater Modeling Center and retired president of Poeter Engineering. With 40 years of experience modeling groundwater systems, she has consulted to attorneys, industries, engineering companies, government agencies, research labs, and citizen groups on groundwater modeling projects for aquifer storage and recovery; slurry wall performance; drainage at proposed nuclear power plant facilities; regional groundwater management; large-scale regional pumping; dam seepage; contaminant migration; impacts of dewatering; and stream-aquifer interaction. Dr. Poeter is an author of groundwater modeling software including evaluation of model sensitivity, assessment of data needs, model calibration, selection and ranking of models, and evaluation of predictive uncertainty. She was the National Groundwater Association (NGWA) Darcy Lecturer in 2006 and received their M. King Hubbert award in 2017 as well as being a NGWA Fellow and Life Member. She also authored three earlier Groundwater Project books: *Groundwater in Our Water Cycle* (Poeter et al., 2020), *Hydrogeologic Properties of Earth Materials and Principles of Groundwater Flow* (Woessner & Poeter, 2020), and *Graphical Construction of Groundwater Flow Nets* (Poeter & Hsieh, 2020).

Please consider signing up for the GW-Project mailing list to stay informed about new book releases, events, and ways to participate in the GW-Project. When you sign up for our email list, it helps us build a global groundwater community. [Sign up](#)[↗].



Modifications to Original Release

Changes from the Original Version to Version 2

Original Version: September 18, 2023, Version 2: October 30, 2023

Page numbers refer to the original PDF.

page ii, added doi

page xi, corrected 70 to 90

page 153, Figure 87 changed the denominator from 200 to 2000 in the third expression of part a)

page 196, changed $t_1 =$ time at head h_2 to $t_1 =$ time at head h_1

Changes from the Version 2 to Version 3

Version 3: March, 6, 2024

Page numbers refer to the PDF of Version 2.

page iii, corrected APA citation that was missing the third author's name

page 98, a number of changes were made:

The content of the first 3 paragraphs including table and equations were changed from the following as shown in gray:

Using the relationship $f(r/B) = 1.7 = \exp(r/B)K_0(r/B)$, then from Figure 48, the value between $X = 1.5$ and $X = 2.0$. The interpolation is shown below.

X	K₀(x)	exp (x) K₀(x)
1.5	0.21	0.96
1.7	0.17 (interpolated)	0.91 (interpolated)
2.0	0.11	0.84

Given that x in Figure 48 equals r/B , then $r/B=1.7$, with the observation well located 75 m from the pumping well, then $B = 75 \text{ m} / 1.7 = 44.1 \text{ m}$. Now using Equation (52).

A

$$T = \frac{4250 \frac{\text{m}^3}{\text{d}} 0.17}{2 (3.14) 3.7 \text{ m}} = 31.1 \frac{\text{m}^2}{\text{d}}$$

S is then computed from Equation (53).

$$S = \frac{4 \left(31.1 \frac{\text{m}^2}{\text{d}} \right) 0.011\text{d}}{2 (75 \text{ m}) (44.1)} = 0.0002 = 2 \times 10^{-4}$$

to:

Using the relationship $f(r/B) = 1.7 = \exp(r/B)K_0(r/B)$, then from Figure 48, the value is between $\exp(x)K_0(x) = 1.66$ and $\exp(x)K_0(x) = 1.75$. The interpolation is shown below.

x	$K_0(x)$	$\exp(x) K_0(x)$
0.40	1.11	1.66
0.37 (interpolated)	1.16 (interpolated)	1.7
0.35	1.23	1.75

Given that $x = 0.37 \text{ m}$, with the observation well located 75 m from the pumping well, then $B = 75 \text{ m} / 0.37 = 203 \text{ m}$. Now using Equation (52).

$$T = \frac{4250 \frac{\text{m}^3}{\text{d}} 1.16}{2 (3.14) 3.7 \text{ m}} = 212 \frac{\text{m}^2}{\text{d}}$$

S is then computed from Equation (53).

$$S = \frac{4 \left(212 \frac{\text{m}^2}{\text{d}} \right) 0.011\text{d}}{2 (75 \text{ m}) (203 \text{ m})} = 0.0003 = 3 \times 10^{-4}$$

In addition the calculation of K' was changed from the following as shown in gray:

$$K' = \frac{31.1 \frac{\text{m}^2}{\text{d}} 15 \text{ m}}{(44.1 \text{ m})^2} = 0.24 \frac{\text{m}}{\text{d}}$$

to:

$$K' = \frac{212 \frac{\text{m}^2}{\text{d}} 15 \text{ m}}{(203 \text{ m})^2} = 0.08 \frac{\text{m}}{\text{d}}$$

page 351, corrected format for Author's name and title